

Page is intentionally blank.

Program and Abstracts

2015

Atomic, Molecular, and Optical Sciences
Research PI Meeting

Gaithersburg Marriott Washingtonian Center
Gaithersburg, Maryland
October 25–28, 2015

Chemical Sciences, Geosciences, and Biosciences Division
Office of Basic Energy Sciences
Office of Science
U.S. Department of Energy

Cover Graphics: The input for the Wordle cover art is based on the titles of the abstracts for this year's meeting. The font is Teen.

The research grants and contracts described in this document are supported by the U.S. DOE Office of Science, Office of Basic Energy Sciences, Chemical Sciences, Geosciences and Biosciences Division

Page is intentionally blank.

FOREWARD

This volume summarizes the 35th annual Research Meeting of the Atomic, Molecular and Optical Sciences (AMOS) Program sponsored by the U. S. Department of Energy (DOE), Office of Basic Energy Sciences (BES), and comprises descriptions of the current research sponsored by the AMOS program. The participants of this meeting include the DOE laboratory and university principal investigators (PIs) within the BES AMOS Program. The purpose is to facilitate scientific interchange among the PIs and to promote a sense of program identity.

The BES/AMOS program is vigorous and innovative, and enjoys strong support within the Department of Energy. This is due entirely to our scientists, the outstanding research they perform, and the relevance of this research to DOE missions. The AMOS community continues to explore new scientific frontiers relevant to the DOE mission and the strategic challenges facing our nation and the world.

We are deeply indebted to the members of the scientific community who have contributed their valuable time toward the review of proposals and programs, either by mail review of grant applications, panel reviews, or on-site reviews of our multi-PI programs. These thorough and thoughtful reviews are central to the continued vitality of the AMOS program.

We are privileged to serve in the management of this research program. In performing these tasks, we learn from the achievements and share the excitement of the research of the scientists and students whose work is summarized in the abstracts published on the following pages.

Many thanks to the staff of the Oak Ridge Institute for Science and Education (ORISE), in particular Connie Lansdon and Tim Ledford, and to the Gaithersburg Marriott Washingtonian Center for assisting with the meeting. We also thank Diane Marceau, and Michaelena Kyler-Leon in the Chemical Sciences, Geosciences, and Biosciences Division for their indispensable behind-the-scenes efforts in support of the BES/AMOS program.

Thomas B. Settersten
Jeffrey L. Krause
Chemical Sciences, Geosciences, and Biosciences Division
Office of Basic Energy Sciences
Office of Science
US Department of Energy

Page is intentionally blank.

Agenda

Page is intentionally blank.

2015 Atomic, Molecular and Optical Sciences Research PI Meeting
Office of Basic Energy Sciences
U. S. Department of Energy

Gaithersburg Marriott Washingtonian Center, Gaithersburg, Maryland
October 25–28, 2015

Sunday, October 25

3:00 – 6:00 pm **** Registration ****
6:00 pm **** Reception (No Host, Lobby Lounge) ****
6:30 pm **** Dinner (Salon A-C) ****

Monday, October 26

7:30 am **** Breakfast (Salon A-C) ****

All presentations held in Salon D-F

8:00 am *Welcome and Introductory Remarks*
Tanja Pietraß and Thomas B. Settersten, BES/DOE

Session I Chair: **Nora Berrah**, University of Connecticut

8:30 am *Attosecond Atomic and Molecular Science*
Daniel M. Neumark, Lawrence Berkeley National Laboratory

9:00 am *Attosecond and Ultrafast X-ray Science*
Louis F. DiMauro, Ohio State University

9:30 am *Applications of Circularly-Polarized Attosecond Pulses*
Anthony F. Starace, University of Nebraska

10:00 am **** Break ****

10:30 am *Controlling Rotations of Asymmetric Top Molecules: Methods and Applications*
Vinod Kumarappan, Kansas State University

11:00 am *Ultrafast Electron Diffraction from Aligned Molecules*
Martin Centurion, University of Nebraska

11:30 am *Strong Field Coherent Dynamics and Control. From Alignment to High Harmonic Generation in Complex Systems*
Tamar Seideman, Northwestern University

12:00 pm **** Lunch (Salon A-C) ****

1:30 – 3:30 pm *Discussion: LCLS-II Science Opportunities and Instrumentation Planning*
Robert Schoenlein, LCLS Deputy for Science, SLAC National Accelerator Lab

- Session II** Chair: **Françoise Remacle**, University of Liège
- 4:30 pm *Combining High Level Ab Initio Calculations with Laser Control of Molecular Dynamics*
Spiridoula Matsika, Temple University
- 5:00 pm *Ultrafast Theory and Simulation*
Todd J. Martinez, SLAC National Accelerator Laboratory
- 5:30 pm *Physics of Correlated Systems*
Chris H. Greene, Purdue University
- 6:00 pm ***** Reception (No Host, Lobby Lounge) *****
- 6:30 pm ***** Dinner (Salon A-C) *****

Tuesday, October 27

- 7:30 am ***** Breakfast (Salon A-C) *****
- Session III** Chair: **Daniel S. Slaughter**, Lawrence Berkeley National Laboratory
- 8:30 am *Strong-Field Dynamics of Few-Body Atomic and Molecular Systems*
Brett D. Esry, Kansas State University
- 9:00 am *Understanding and Controlling Strong-Field Laser Interactions with Polyatomic Molecules*
Marcos Dantus, Michigan State University
- 9:30 am *First-Principles Strong-Field Ionization Rates and Dynamics: Towards High Harmonic Generation as a Probe of Charge Migration*
Kenneth Lopata, Louisiana State University
- 10:00 am ***** Break *****
- 10:30 am *Channel-Resolved Electron Momentum Correlation in Nonsequential Double Ionization*
Wen Li, Wayne State University
- 11:00 am *Quantum Nuclear Dynamics Following an Ultrafast Excitation of a Non-equilibrium Electronic State in Nitrogen*
Raphael D. Levine, University of California, Los Angeles
- 11:30 am *Electron- and Photon-Driven Processes*
Thorsten Weber, Lawrence Berkeley National Laboratory
- 12:00 pm ***** Lunch (Salon A-C) *****
- 1:00 – 4:00 pm Free/Discussion Time

- Session IV** Chair: **Daniel Rolles**, Kansas State University
- 4:00 pm *Nanoscale Dynamics Probed by Coherent Soft X-rays*
Margaret M. Murnane, University of Colorado
- 4:30 pm *Understanding Photochemistry using Extreme Ultraviolet and Soft X-Ray
Time Resolved Spectroscopy*
Markus Gühr, SLAC National Accelerator Laboratory and Universität Potsdam
- 5:00 pm *Imaging Ultrafast Dynamics with Multi-color Multi-pulse X-ray Schemes*
Christoph Bostedt, Argonne National Laboratory
- 5:30 pm *Illuminating Molecules from Within: Where do we go next?*
Allen L. Landers, Auburn University
- 6:00 pm ***** Reception (No Host, Lobby Lounge) *****
- 6:30 pm ***** Dinner (Salon A-C) *****

Wednesday, October 28

- 7:30 am ***** Breakfast (Salon A-C) *****
- Session V** Chair: **Phay J. Ho**, Argonne National Laboratory
- 8:30 am *Revealing Giant Internal Magnetic Fields due to Spin Fluctuations in
Magnetically-Doped Colloidal Nanocrystals*
Scott A. Crooker, Los Alamos National Laboratory
- 9:00 am *Harnessing Ultraintense X-rays to Probe Electronic and Nuclear Dynamics in
Complex Systems*
Linda Young, Argonne National Laboratory
- 9:30 am *Multispectral and Multipulse Studies of Phase Transitions at LCLS*
Claudiu A. Stan, SLAC National Accelerator Laboratory
- 10:00 am ***** Break *****
- 10:30 am *Dynamics of Molecular Dressed States*
Robin Côté, University of Connecticut
- 11:00 am *Experiments in Ultracold Molecules*
Phillip L. Gould, University of Connecticut
- 11:30 am *Closing Remarks*
Thomas B. Settersten, BES/DOE
- 12:00 pm Adjourn

Page is intentionally blank.

Table of Contents

Page is intentionally blank.

TABLE OF CONTENTS

Forward	iii
Agenda	v
Table of Contents	xi

Laboratory Research Summaries (by Institution)

Argonne National Laboratory

<i>AMO X-ray Physics at Argonne National Laboratory</i>	1
Christoph Bostedt, Gilles Doumy, Robert Dunford, Phay Ho, Elliot Kanter, Bertold Krässig, Anne Marie March, Steve Southworth, Linda Young	
<i>Ultraintense X-ray Interactions</i>	2
<i>Ultrafast X-Ray Inner-Shell Phenomena</i>	5
<i>X-Ray Probes of Laser Induced Dynamics</i>	12
<i>Optical Control and X-Ray Imaging of Nanoparticles</i>	19

J.R. Macdonald Laboratory

<i>J.R. Macdonald Laboratory Overview</i>	25
<i>Structure and Dynamics of Atoms, Ions, Molecules, and Surfaces: Molecular Dynamics with Ion and Laser Beams</i>	
Itzik Ben-Itzhak	27
<i>Strong-Field Dynamics of Few-Body Atomic and Molecular Systems</i>	
Brett Esry	31
<i>Controlling Rotations of Asymmetric Top Molecules: Methods and Applications</i>	
Vinod Kumarappan	35
<i>Strong Field Rescattering Physics and Attosecond Physics</i>	
Chii-Dong Lin	39
<i>Ultrafast Imaging of Molecular Dynamics with Lasers, Free-Electron Lasers, and Synchrotron Radiation</i>	
Daniel Rolles	43
<i>Electronic and Nuclear Dynamics Triggered by X-ray, XUV and Optical Excitations: Nonlinear Interactions and Ultrafast Imaging</i>	
Artem Rudenko	47
<i>Structure and Dynamics of Atoms, Ions, Molecules and Surfaces</i>	
Uwe Thumm	51
<i>Strong-Field Time-Dependent Spectroscopy</i>	
Carlos Trallero	55

Lawrence Berkeley National Laboratory

<i>Atomic, Molecular and Optical Sciences at LBNL</i>	59
C. William McCurdy (PI), Co-Investigators: Ali Belkacem, Oliver Gessner, Daniel J. Haxton, Martin Head-Gordon, Stephen R. Leone, Daniel M. Neumark, Thomas N. Rescigno, Robert W. Schoenlein, Daniel S. Slaughter, Thorsten Weber	
<i>Subtask 1: Photon and Electron Driven Processes in Atoms and Simple Molecules</i>	61
<i>Subtask 2: Photon and Electron Driven Processes in Complex Molecular Systems and Molecules in Complex Environments</i>	67
<i>Subtask 3: First-principles theory of dynamics and electronic structure</i>	75
<i>Early Career: Ultrafast X-ray Studies of Intramolecular and Interfacial Charge Migration</i> Oliver Gessner	91
<i>Early Career: The Multiconfiguration Time-Dependent Hartree-Fock Method for Interactions of Molecules with Ultrafast X-Ray and Strong Laser Pulses</i> Daniel J. Haxton	95

Los Alamos National Laboratory

<i>Engineered Electronic and Magnetic Interactions in Nanocrystal Quantum Dots</i> Victor I. Klimov	99
---	----

SLAC National Accelerator Laboratory

<i>PULSE Ultrafast Chemical Science Program</i>	103
<i>ATO: Attoscience</i> Philip H. Bucksbaum, Markus Gühr, and James Cryan	107
<i>Electron Dynamics on the Nanoscale</i> Tony F. Heinz	111
<i>NLX: Nonlinear X-ray Science</i> David Reis and Shambhu Ghimire	115
<i>NPI: Non-Periodic Imaging</i> Claudiu Stan	119
<i>SFA: Strong-Field Laser Matter Interactions</i> Philip H. Bucksbaum	123
<i>SPC: Solution Phase Chemical Dynamics</i> Kelly J. Gaffney	127
<i>UTS: Ultrafast Theory and Simulation</i> Todd J. Martínez	131

Early Career: Understanding Photochemistry using Extreme Ultraviolet and Soft X-ray Time Resolved Spectroscopy

Markus Gühr 135

Early Career: Strongly-Driven Attosecond Electron Dynamics in Periodic Media

Shambhu Ghimire 139

University Research Summaries (by PI)

Tracing and Controlling Ultrafast Dynamics in Molecules

Andreas Becker 143

Probing Complexity using the LCLS and the ALS

Nora Berrah 147

Ultrafast Electron Diffraction from Aligned Molecules

Martin Centurion 151

Atomic and Molecular Physics in Strong Fields

Shih-I Chu 155

Formation of Ultracold Molecules

Robin Côté 159

Optical Two-Dimensional Spectroscopy of Disordered Semiconductor Quantum Wells and Quantum Dots

Steven T. Cundiff 163

Understanding and Controlling Strong-Field Laser Interactions with Polyatomic Molecules

Marcos Dantus 167

Spatial-Temporal Imaging During Chemical Reactions

Louis F. DiMauro, Pierre Agostini, and Terry A. Miller 171

Attosecond and Ultra-Fast X-ray Science

Louis F. DiMauro and Pierre Agostini 175

High Intensity Femtosecond XUV Pulse Interactions with Atomic Clusters

Todd Ditmire and John Keto 179

Electron Correlation in Strong Radiation Fields

Joseph H. Eberly 183

Image Reconstruction Algorithms

Veit Elser 187

Collective Coulomb Excitations and Reaction Imaging

James M. Feagin 191

Studies of Autoionizing States Relevant to Dielectronic Recombination

Thomas F. Gallagher 195

<i>Experiments in Ultracold Molecules</i>	
Phillip L. Gould	199
<i>Physics of Correlated Systems</i>	
Chris H. Greene	203
<i>Using Strong Optical Fields to Manipulate and Probe Coherent Molecular Dynamics</i>	
Robert R. Jones	207
<i>Quantum Dynamics Probed by Coherent Soft X-Rays</i>	
Henry C. Kapteyn and Margaret M. Murnane	211
<i>Imaging Multi-particle Atomic and Molecular Dynamics</i>	
Allen Landers	215
<i>Exploiting Non-equilibrium Charge Dynamics in Polyatomic Molecules to Steer Chemical Reactions</i>	
Wen Li, Raphael D. Levine, Henry C. Kapteyn, H. Bernhard Schlegel, Françoise Remacle, and Margaret M. Murnane	219
<i>Probing Electron-Molecule Scattering with HHG: Theory and Experiment</i>	
Robert R. Lucchese and Erwin Poliakoff	223
<i>Photoabsorption by Free and Confined Atoms and Ions</i>	
Steven T. Manson	227
<i>Electron-Driven Processes in Polyatomic Molecules</i>	
Vincent McKoy	231
<i>Electron/Photon Interactions with Atoms/Ions</i>	
Alfred Z. Msezane	235
<i>Theory and Simulations of Nonlinear X-ray Spectroscopy of Molecules</i>	
Shaul Mukamel	239
<i>Revealing Nanoscale Energy Flow Using Ultrafast THz to X-ray Beams</i>	
Keith A. Nelson and Margaret M. Murnane	243
<i>Low-Energy Electron Interactions with Complex Molecules and Biological Targets</i>	
Thomas M. Orlando	247
<i>Structure from Fleeting Illumination of Faint Spinning Objects in Flight</i>	
Abbas Ourmazd	251
<i>Control of Molecular Dynamics: Algorithms for Design and Implementation</i>	
Herschel Rabitz and Tak-San Ho	255
<i>Atoms and Ions Interacting with Particles and Fields</i>	
Francis Robicheaux	259
<i>Generation of Bright Soft X-ray Laser Beams</i>	
Jorge J. Rocca	263
<i>Spatial Frequency X-ray Heterodyne Imaging and Ultrafast Nanochemistry</i>	
Christoph Rose-Petruck	267

<i>Transient Absorption and Reshaping of Ultrafast Radiation</i> Kenneth J. Schafer and Mette B. Gaarde	271
<i>Time-Resolved High Harmonic Spectroscopy: A Coherently Enhanced Probe of Charge Migration</i> Kenneth J. Schafer, Mette B. Gaarde, Kenneth Lopata, Louis F. DiMauro, Pierre Agostini, Robert R. Jones	275
<i>Strong-Field Control in Complex Systems</i> Tamar Seideman	281
<i>Inelastic X-ray Scattering under Extreme and Transitional Conditions</i> Gerald T. Seidler	285
<i>Dynamics of Few-Body Atomic Processes</i> Anthony F. Starace	289
<i>Femtosecond and Attosecond Laser-Pulse Energy Transformation and Concentration in Nanostructured Systems</i> Mark I. Stockman	293
<i>Laser-Produced Coherent X-ray Sources</i> Donald Umstadter	297
<i>Combining High Level Ab Initio Calculations with Laser Control of Molecular Dynamics</i> Thomas Weinacht and Spiridoula Matsika	301
Participants	305

Page is intentionally blank.

Laboratory Research Summaries
(by institution)

Page is intentionally blank.

AMO X-ray Physics at Argonne National Laboratory

Christoph Bostedt, Gilles Doumy, Robert Dunford, Phay Ho, Elliot Kanter,
Bertold Krässig, Anne Marie March, Steve Southworth, Linda Young
Argonne National Laboratory, Argonne, IL 60439
cbostedt@anl.gov, gdoumy@aps.anl.gov, dunford@anl.gov, pho@anl.gov, kanter@anl.gov,
kraessig@anl.gov, amarch@anl.gov, southworth@anl.gov, young@anl.gov

Norbert Scherer
Chemistry Department
University of Chicago, Chicago, IL 60637
nfschere@uchicago.edu

1 OVERVIEW

The Argonne AMO physics program has recently focused on four themes: (1) ultraintense x-ray interactions with atoms, molecules, clusters, and nanoparticles, (2) ultrafast x-ray phenomena using advancing XFEL capabilities to visualize inner-shell processes, (3) x-ray probes of laser-induced dynamics in solvated molecules, and (4) optical control and x-ray imaging of nanoparticles. Theory, computation and experiment are strongly interlinked in our program.

The intense, femtosecond x-ray pulses generated at the LCLS and SACLA XFELs represent a new regime for x-ray interaction with matter, where nonlinear and multiphoton x-ray processes are prominent, in stark contrast to the situation at synchrotrons. Our program aims to establish a fundamental understanding of ultraintense x-ray interactions in increasingly complex systems from atoms and molecules to clusters and nanoparticles. We use XFEL pulses to study ionization mechanisms in atoms and molecules and to record ultrafast x-ray images of transient structures of clusters induced by intense lasers or x-rays. The many-particle interactions probed experimentally are simulated with highly parallelized codes at the Argonne Leadership Computing Facility. These codes are also used to simulate evolving electronic structures of nanoparticles in intense x-ray pulses.

XFELs also represent a frontier for short-wavelength, ultrashort timescale probes. Recently, it has become possible to generate two femtosecond x-ray pulses with two colors for x-ray-pump/x-ray-probe experiments. Seeding techniques generate intense, narrow-bandwidth x-ray pulses with increased temporal coherence compared with SASE pulses. We exploit these enhanced capabilities to study inner-shell processes in the time domain and anticipate further improvements in XFELs such as planned for LCLS-II and other FELs. Our theoretical work includes demonstrating applications of temporal coherence, narrow bandwidths, and few-femtosecond pulse durations in anticipation of future experiments.

The Advanced Photon Source (APS) provides stable, tunable, polarized x-ray beams that we couple with high-repetition-rate optical lasers for time-resolved x-ray absorption and x-ray emission studies of the photophysics and photochemistry of molecules in the solution phase. Optical lasers can trap, orient, and order nanoparticles, providing a new route towards manipulation and assembly of nanomaterials. Advanced techniques to optically trap nanoparticles and measure their spectroscopic properties and interactions are being developed in the laboratory of Professor Norbert Scherer at the University of Chicago. We have exploited that expertise to develop optical traps for x-ray diffraction and coherent imaging of nanoparticles at the APS.

2 ULTRAINTENSE X-RAY INTERACTIONS

Resonance-mediated atomic ionization dynamics within intense XFEL pulses

(L. Young, P. J. Ho, E. P. Kanter, C. Bostedt, S. H. Southworth, B. Krässig, A. Rudenko², D. Rolles² & other collaborators)

Early experiments at LCLS established that multiphoton x-ray ionization via sequential single photon absorption is the dominant interaction mechanism at intensities approaching 10^{18} W/cm² for the 10-electron neon atom [39], that, at these intensities, the direct two-photon absorption channel was minimal [40], and that “hidden” inner-shell resonances could vastly alter the ionization dynamics [41]. Subsequent experiments on heavier atoms, Kr and Xe [42, 43], demonstrated an ultraefficient ionization mechanism proceeding via resonances between inner and outer shells. During the past year, we developed Monte-Carlo rate equation (MCRE) approach [17], which for the first time successfully demonstrated the role of both “hidden resonances” [41] and also identified the responsible resonance-enhanced x-ray multiple ionization (REXMI) pathways that lead to unexpectedly high charge states in Ar, Kr and Xe. The computational challenge is considerable as the number of potential electronic configurations for all resonances up to the 10g orbital in the Xe atom exceeds 10^{23} . We extend the application of this MCRE approach to explore the bandwidth and

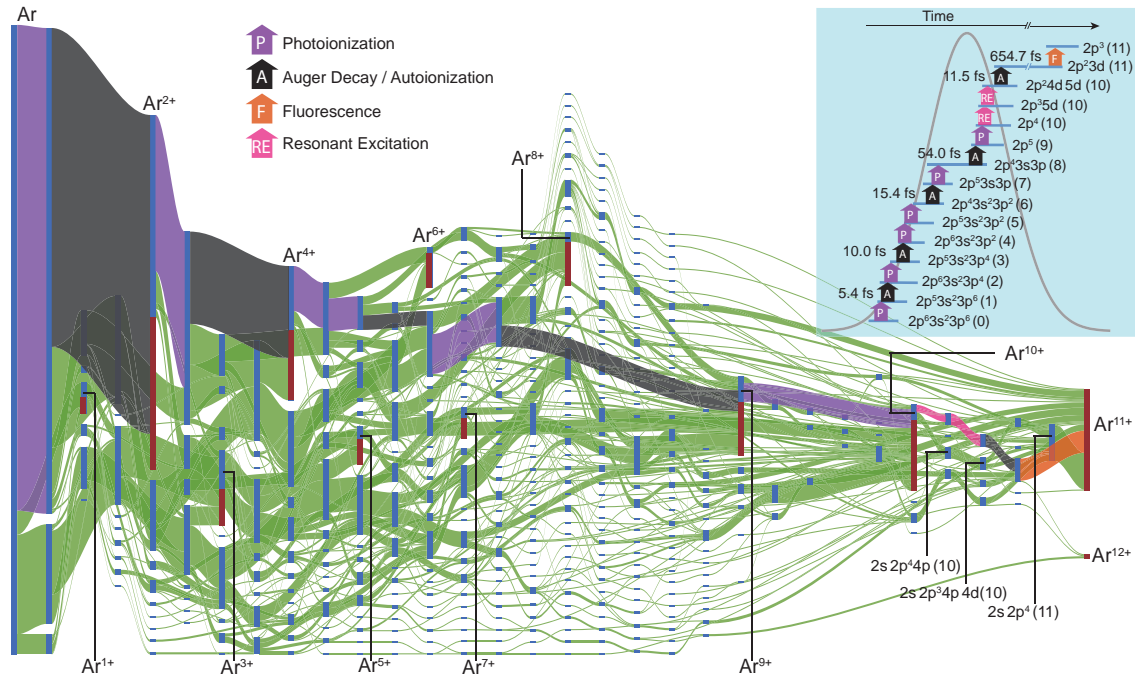


Figure 1: A Sankey diagram illustrating transition probabilities between the accessible electron configurations of an Ar atom exposed to an intense XFEL pulse at 480 eV. Ar¹¹⁺ is not expected from the sequential single photon model, and is largely produced by the single pathway that is not painted green. From [17]

pulse duration dependence for multiphoton ionization dynamics of Xe and Kr atoms and predict the behavior for both the standard SASE and the narrow-bandwidth seeded XFEL pulses [55] for a range of photon fluences and x-ray photon energies that overlap those used in experiments. Hot spots in the parameter space of photon energy vs fluence are identified where resonance effects, i.e. the difference between seeded and SASE pulses, are magnified. A manuscript has been prepared for submission [34]. A recent experiment performed in collaboration with the Kansas State University

group (see A. Rudenko’s abstract for details) at the CXI imaging beamline at LCLS allowed study of the response of Ar, Kr, Xe and simple molecules (CH_3I and $\text{C}_6\text{H}_5\text{I}$) to hard x-ray ($\sim 5 - 8$ keV) irradiation at extreme intensities approaching $10^{20}\text{W}/\text{cm}^2$ with both SASE and seeded pulses. For atoms, observations of the maximal charge state followed the basic sequential single photon ionization model, but detailed charge state distributions exhibit resonance effects. For CH_3I a reversed effect, where narrower bandwidth pulses induce higher charge state production, is observed.

Impact of high-intensity XFEL pulses on diffractive imaging of nano-sized systems

(P. J. Ho, C. Knight,¹ and L. Young)

We have developed a large-scale atomistic computational method based on a combined Monte Carlo [17] and Molecular Dynamics (MC/MD) method to simulate XFEL-induced radiation damage dynamics of complex materials, including homogeneous and heterogeneous nanomaterials and biomolecules. The molecular dynamics algorithm is used to propagate the trajectories of electrons, ions and atoms forward in time and the quantum nature of interactions with an XFEL pulse is accounted for by a Monte Carlo method to calculate probabilities of electronic transitions. Our model goes beyond the early particle approaches [44, 45] by tracking the electronic configuration of each charged particle explicitly throughout the x-ray pulse. Having this capability is important because sequential, multiple valence/core-shell ionization/excitation and relaxation are shown to be dominant in materials exposed to intense, femtosecond XFEL pulses. In addition, we account for three-body ion-electron recombination processes, which have not been included in previous studies [46]. The numerical code of MC/MD is highly parallelized with MPI/OpenMP implementation. It has been adapted to run on Mira, a Blue Gene/Q high performing computer at Argonne Leadership Computing Facilities, for systems with more than 50 million particles (ions + electrons), which exceed the capability in previous study by more than 4 orders of magnitude in particle number [44].

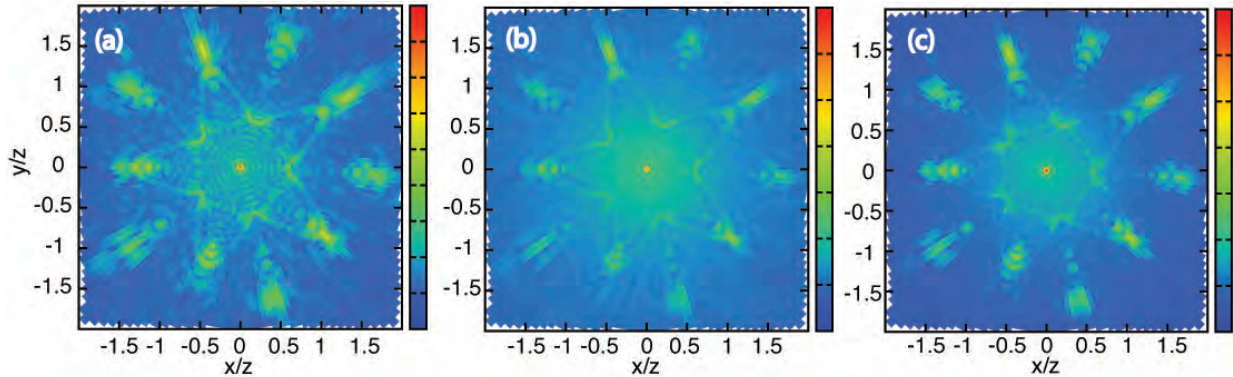


Figure 2: X-ray scattering pattern of a single Argon cluster calculated using 8 keV pulses with (a) 30 fs and 10^{10} photons/ μm^2 , (b) 30 fs and 10^{11} photons/ μm^2 , and (c) 2 fs and 10^{11} photons/ μm^2 showing clear signal dependence on the sample ionization and nanoplasma formation.

With this MC/MD model, rich datasets are generated and they will allow us to image the impact of both transient core-hole states and delocalized electrons in various experimental observables, which include coherent x-ray diffraction, ion, electron and fluorescence spectra. To show the impact, we investigate the x-ray diffraction patterns (XDP) of a 5.2-nm, 7-shell argon cluster with 1415 nuclei + 25470 electrons in 8-keV XFEL pulses with various pulse energies and durations (see Fig. 2). The x-ray focus is $1.6 \mu\text{m}$ in all cases. The XDP in panel (a), which is calculated for a 30-fs pulse with a pulse energy of 0.0015 mJ, shows clear fringes and five-fold symmetry as the low-intensity

pulse only ionizes $<2\%$ of the atoms. Such a 30-fs pulse, however, might not be able produce enough scattering events in one shot. For single-pulse diffractive imaging, a higher pulse fluence is needed. In panel (b), we show the XDP obtained in a 30-fs pulse but at a pulse energy that is 10 times higher than that in panel (a). These pulse parameters are currently accessible at LCLS. It is clear that many fringes are being washed out in the XDP captured in this high-fluence pulse. This is due to the fact that intense XFEL pulse can efficiently strip off electrons from atoms/ions and lead to significant rearrangement of electrons, ions/atoms during the pulse. Thus, the incoming XFEL pulse probes a non-static electronic and lattice structure. As expected, the XDP from a 2-fs, 0.015-mJ XFEL pulse shows a better resemblance of panel (a) since this pulse can largely freeze out atoms/ions motion. However, this 2-fs XDP gives lower contrast and displays evidence of diffuse scattering due to the presence of delocalized electrons and core-hole ion states and plasma formation.

To further analyze the potential of using XFEL pulses as a structural imaging tool, we calculate the diffraction signals in 3-D Fourier space and perform 3-D phase retrieval analysis to reconstruct 3-D electronic density for different XFEL pulse fluences at 8 keV. The maximum Q value in each dimension of the Fourier space is 3.24 \AA^{-1} to give a real space resolution of 1.9 \AA , which is smaller than the bond distance in the Argon cluster. There are many advanced phase retrieval algorithms available, like the EMC algorithm [47], but we adopt a commonly used phase retrieval method that combines three algorithms: error reduction, hybrid input-output and shrinkwrap algorithms [48, 49]. The reconstructed 3-D electronic density from these patterns suggests that the structure of the argon cluster with atomic resolution can be recovered despite the presence diffuse scattering. We are currently preparing a manuscript on the obtained results.

Ultrafast imaging of complex systems

(C. Bostedt, P. J. Ho, S. H. Southworth, L. Young, M. Bucher,¹¹ K. Ferguson,¹¹ T. Gorkhover¹¹ and other collaborators)

Free-electron lasers deliver extremely intense, coherent x-ray flashes with femtosecond pulse length, allowing to image single nanometer sized objects with single shots. The coherent image of the particles contains information about their geometric structure and transient electronic configuration. We have employed single-shot imaging for spatially and time resolved investigations of clusters droplets, and core-shell systems. Combining the imaging approach with optical and x-ray pump – x-ray probe techniques allows imaging the structural and electronic evolution of highly excited clusters and nanoplasmas far from equilibrium. Optically pumped clusters show a rapid expansion starting from their surface on the hundred femtoseconds time scale [35]. The surface melting leaves distinct fingerprints in the coherent scattering image. Fitting routines based on the Guinier approach yield a detailed density profile through the nanoplasma and allow reconstructing the original cluster size. Imaging of xenon clusters in helium droplets shows evidence for fast charge transfer processes from the helium shell to the cluster core. Hard x-ray scattering experiments of isochorically heated xenon clusters indicate a bond contraction prior to the nanoplasma expansion which is attributed to ultrafast changes in the potential energy landscape in the nanoplasma compared to the neutral van-der-Waals systems [36]. Our future work is aimed at imaging the electron dynamics in the highly excited nanoplasma systems, studying bond-hardening and phase transitions in clusters at the solid-plasma interface, and investigating the role of the quasi-free electrons in the deep nanoplasma Coulomb potential to the imaging process. Two manuscripts based on results of this research have been submitted for publication [36, 35].

High-resolution electron spectroscopy with the LCLS-AMO electron time-of-flight spectrometers

(B. Krässig)

This work concerns measurements of the Auger spectrum from neon double core hole (KK) decay performed at the Linac Coherent Light Source (LCLS) at SLAC National Accelerator Laboratory using five identical electron time-of-flight (ETOF) spectrometers mounted at strategic angles. The goal is the spectroscopic determination of transition energies, branching ratios, and line shapes of the neon KK - KLL hypersatellite lines. Time-of-flight spectrometry is the method of choice for electron spectroscopy applications with low-repetition rate pulsed ionization sources such as the LCLS. Unlike electrostatic energy analyzers, which at a given time and spectrometer voltage collect electrons only within a small energy range, ETOFs can register all electrons emitted into the analyzer acceptance. The downside of spectroscopy with ETOFs is the reciprocal dependence of electron kinetic energy and energy resolution on the electron time-of-flight. The addition of electron optics to a time-of-flight spectrometer renders the mathematical conversion of electron flight times to electron kinetic energies non-analytic. Here we use interpolation between entries in a database assembled from ray tracing results to associate experimental times-of-flight with kinetic energies. The ray tracing was performed as Monte Carlo simulations for the the nominal geometry and configuration of the LCLS ETOFs used during the experiments described in [9]. Time resolution in the measurements, determined by the uncertainty of the start time, different trajectory paths, and detector response, imposes the ultimate limit on the energy resolution of ETOFs. The combination of these effects in the temporal response, distorted by the nonlinear conversion to kinetic energy, is imprinted on the spectroscopic features in the kinetic energy spectra. The absolute energies of the observed features depend critically on how well the actual conditions in the experiment can be reconstructed. A substantial effort in this work went into characterizing the detector response, spectrometer transmission, and reconciling differences in the results from the five ETOFs using the well-characterized neon K - LL part of the Auger spectrum recorded simultaneously. A thorough analysis was enabled by the fact that the ETOF detector signals were recorded and stored as digitized waveforms for every LCLS shot during the measurements. In the off-line processing of the data it was therefore possible to detect and correct for, e.g., the diurnal ± 500 -ps drift of the start signal for the transient digitizer, or the delayed pulsing of the micro-channel plate detectors. If not corrected, such effects directly broaden or distort the spectral lines shapes of the Auger spectrum.

3 ULTRAFAST X-RAY INNER-SHELL PHENOMENA

Hetero-site-specific ultrafast intramolecular dynamics

(A. Picón, C. S. Lehmann, S. H. Southworth, C. Bostedt, G. Doumy, P. J. Ho, E. P. Kanter, B. Krässig, A. M. March, D. Moonshiram, L. Young, S. T. Pratt, A. Rudenko,² D. Rolles,² R. Wehlitz,⁶ L. Cheng,⁷ J. F. Stanton,⁷ and other collaborators)

The intramolecular flow of charge, energy and nuclear motion is widely encountered in molecular dynamics and underlies chemical reactivity and biological processes. The intramolecular flow may start at one atomic site and propagate to another site. A good example is the response of molecules, nanoparticles, and condensed matter to the absorption of an x-ray photon. An inner-shell hole is created that is localized around a specific atomic site. The relaxation of the inner-shell hole involves both electronic and nuclear motion, and induces ultrafast flow of charge and energy. As Auger electrons are emitted, the system becomes positively charged and Coulomb repulsion induces dissociation into atomic and molecular fragment ions. The dynamics triggered by the inner-shell hole decay plays an important role in x-ray damage and is a major limiting factor in macromolecular crystallography using synchrotron x rays and XFELs.

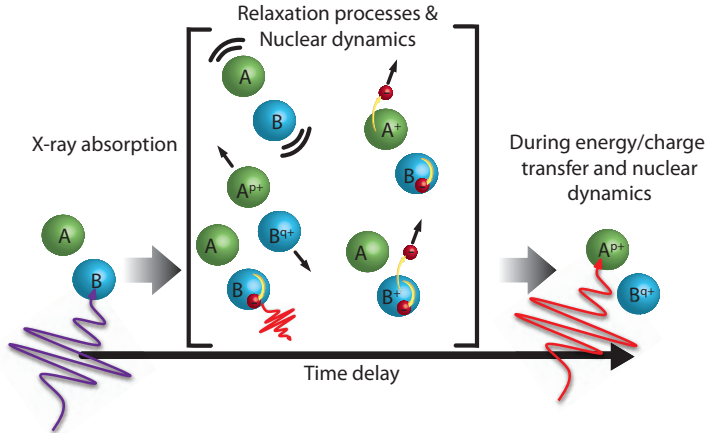


Figure 3: Illustration of a two-color x-ray-pump/x-ray-probe experiment. The x-ray absorbed by B induces inner-shell electronic excitation, ionization, fluorescence, Auger-electron emission, and charge redistribution to site A. Nuclear dynamics is also induced - dissociation, isomerization, and vibrational excitation. The site-to-site intramolecular dynamics is explored by absorbing a second x ray at site A after a controlled delay.

The LCLS and other XFELs can generate two intense, femtosecond x-ray pulses with two colors and controlled delay [50]. This opens the opportunity to perform hetero-site-specific x-ray-pump/x-ray-probe experiments, as sketched in Fig. 3. We performed such an experiment on XeF_2 molecules at the LCLS. A 690-eV pump pulse excites the $\text{Xe } 3d \rightarrow \epsilon f$ shape resonance and triggers core-hole decay and nuclear dynamics. The $\text{Xe } 3d$ hole decays by sequential emission of several Auger electrons. In XeF_2 , charge is redistributed from the Xe site to the F sites, and the system dissociates into three atomic ions. After time delays of 4, 29, and 54 fs, a 683-eV probe pulse excites the $1s \rightarrow 2p$ resonances of F^+ and F^{2+} ions that are emerging during the breakup process. This increases the charge on one of the F ions, transferring the event to another three-ion breakup channel. We measured the three ions in coincidence by ion time-of-flight with a multi-hit, position-sensitive detector. Time-dependent features are thereby observed in the kinetic-energy-release (KER) spectra and in the momentum distributions of the three-ion breakup channels. The time-dependent features in the KER spectra are simulated with a classical model that simply accounts for the Coulomb repulsion as a function of internuclear separations and pump-probe delay. A manuscript on the results has been prepared to submit for publication [31].

In preparation for the LCLS experiments, the photoionization cross sections and partial ion yields of Xe and XeF_2 were measured over the 660–740 eV range at Wisconsin’s Synchrotron Radiation Center. This energy range encompasses the ionization thresholds and near-edge regions of $\text{Xe } 3d_{5/2}$, $\text{Xe } 3d_{3/2}$, and $\text{F } 1s$ electrons. Particularly interesting are strong resonant features in the XeF_2 data from excitation of the lowest unoccupied molecular orbital (LUMO). The theorists in our collaboration used Equation of Motion Coupled Cluster calculations to predict the resonant energies and oscillator strengths. The results were published in Ref. [26]. The synchrotron measurements and corresponding calculations were very useful in planning and conducting the LCLS experiments. The absorption cross sections of the transient states of the x-ray-pumped molecule are not known and are quite difficult to calculate because they involve high charge states and ultra-fast nuclear motion. Although these states have some molecular character, we estimated the cross sections by a combination of atomic cross sections of the Xe and F ions. Additional theoretical work that incorporates inner-shell transitions in molecular quantum chemical codes is needed to further explore core-hole decay dynamics.

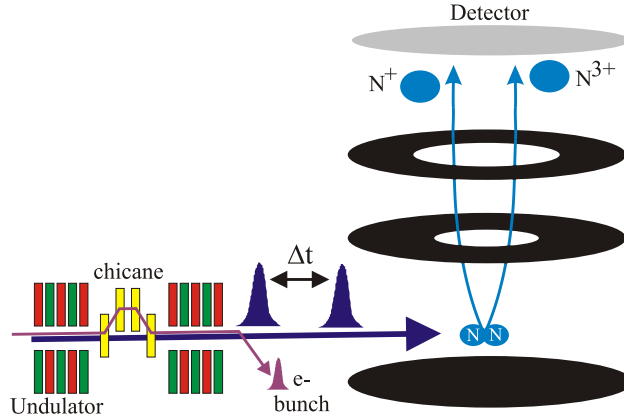


Figure 4: Sketch of the setup used for an x-ray-pump/x-ray-probe experiment on N_2 molecules. The first pulse triggers K -shell ionization and Auger decay of N_2 , mainly producing the N^+ - N^+ breakup channel. After a delay of 4, 29, or 54 fs, K -shell ionization and Auger decay of one of the N^+ ions by the probe pulse converts it to N^{3+} . The ions are recorded in coincidence with a position-sensitive detector and the kinetic energy release (KER) is measured. Time-dependent features are observed in the KER scans of the N^+ - N^{3+} breakup channel.

Ultrafast measurements of molecular nuclear dynamics using two x-ray pulses

(C. S. Lehmann, A. Picón, S. H. Southworth, C. Bostedt, G. Doumy, P. J. Ho, E. P. Kanter, B. Krässig, A. M. March, D. Moonshiram, L. Young, S. T. Pratt, A. Rudenko,² D. Rolles,² and other collaborators)

Recent capabilities at x-ray free-electron lasers (XFELs) allow the production of two intense x-ray pulses with controlled delay. That opens the opportunity to track x-ray induced dynamics in matter on the femtosecond time scale. In the same LCLS beamtime in which we made x-ray-pump/x-ray-probe measurements on XeF_2 , we also observed time-dependent kinetic energy release (KER) spectra for the two-ion breakup channels of N_2 and O_2 molecules. A sketch of the N_2 experiment is shown in Fig. 4. The x-ray energies of the pump and probe pulses were both in the 683-702 eV range, which is far above the K -shell ionization thresholds of N_2 (~ 410 eV) and O_2 (~ 540 eV). Our analysis focuses on N_2 , although similar dynamics are involved for O_2 . The pump pulse induced K -shell ionization and Auger decay of N_2 that leaves it in manifolds of transient intermediate states (primarily N_2^{2+} states with two valence-shell holes) that continue to evolve. The manifold of intermediate states includes both dissociative states that break apart promptly into N^+ - N^+ channels and long-lived quasi-bound states that are detected as molecular ions. For the dissociative states, the probe pulse can K -shell ionize one of the N^+ ions and convert it to N^{3+} after Auger decay. That transfers the breakup event from N^+ - N^+ to the N^+ - N^{3+} channel that we observe as time-dependent structure in the KER, i.e., as a function of internuclear distance between the two N^+ ions. The probe pulse can also convert quasi-bound N_2^{2+} states to the N^+ - N^{3+} channel, but in that case the structure produced in the KER is fixed in energy without time dependence.

In contrast with the XeF_2 molecule that involves a complex set of Auger decay and charge redistribution steps, N_2 involves a single Auger decay and a set of N_2^{2+} transient states that have been extensively studied experimentally and their potential curves calculated [51]. To simulate the time-dependent structure measured in the KER scans, we developed a theoretical model that accounts for K -shell ionization, Auger decay, and the time evolution of the nuclear wavepackets populated on

the manifold of dissociative and quasi-bound N_2^{2+} states. Our simulated KER scans account for the time-dependent feature observed at lower energy that is attributed to the dissociative intermediate states. The simulation also displays structure at fixed energy due to the quasi-bound states, but this structure is difficult to discern in the measured KER scans. This is due in part to the use of ion spectrometer potentials that ensured detection of high-energy F ions for the XeF_2 experiments, but at reduced resolution for the N_2 and O_2 measurements. We have submitted an LCLS proposal to follow up on our N_2 results with new measurements in which the spectrometer potentials and other experimental parameters will be optimized for each molecule studied. This x-ray-pump/x-ray-probe technique takes advantage of presently available two-pulse generation at XFELs and provides a novel method of imaging nuclear wavepackets as a function of time using ion-ion coincidence spectroscopy. A manuscript on the results has been prepared to submit for publication [32].

Time-resolved inner-shell spectroscopy for ultrafast molecular dynamics

(C. Bostedt, G. Doumy, A. Picon, S. Southworth, L. Young, M. Bucher,¹¹ K. Ferguson,¹¹ T. Gorkhover,¹¹ P. Stefan,¹¹ Y. Feng,¹¹ and other collaborators)

Inner-shell spectroscopy and in particular x-ray absorption and photoemission spectroscopy have been essential for understanding the electronic structure of matter. At free-electron laser sources, however, their implementation has been difficult because of the fluctuating nature and wide bandwidth of the SASE source. Recent improvements in free-electron laser technology such as the implementation of self-seeding and development of multi-pulse and multi-color techniques have enabled new possibilities for inner-shell spectroscopy but their implementation is still lacking. We have developed a technique to characterize the central energy and quality of seeded free-electron laser pulses on a shot by shot basis, opening the door to record ultrafast x-ray absorption measurements. Further, we have established the experimental and theoretical framework for ultrafast photoemission spectroscopy with a two-color, two-pulse approach. We plan on pumping CO molecules efficiently at the O 1s \rightarrow π^* resonance and monitor the electronic structure changes during molecular break-up with C 1s photoemission in the time window between 5-50 fs. The data will be complemented with time-dependent core-level binding energy calculations that are currently being developed in our group. Through the combination of photoemission spectroscopy with the novel narrow-bandwidth x-ray-pump/x-ray-probe technique we can directly and site-specifically follow the electronic structure changes on a few femtosecond time scale. In the future, we will be able to extend this first step to shorter time-scales, opening the door to follow electronic relaxation on time scales of Auger decay, as well as to larger molecules, allowing to follow charge flow in complex systems with site-specificity. We have submitted a proposal for an LCLS experiment to explore this approach to ultrafast molecular dynamics.

Molecular response to x-ray absorption and vacancy cascades

(R. W. Dunford, S. H. Southworth, G. Doumy, E. P. Kanter, B. Krässig, L. Young)

We are carrying out experiments at APS to study decay processes in molecules following the inner shell excitation of one of the atoms. Our experiments study cascade decay and Coulomb explosion following ionization of atoms in the studied molecules. The availability of high energy x-rays from the APS provides the opportunity to study the relatively unexplored regime in which the initial molecular excitation occurs in a deep inner-shell of a heavy atom. So we study molecules which contain a heavy component such as Xe, I, or Br. In earlier studies of molecular effects in vacancy cascades of the molecule XeF_2 , we found evidence that the total charge produced in the XeF_2 molecule was larger than that produced in an isolated Xe atom [52]. This led to theoretical work in which the cascade decay from Xe following *K*-shell ionization was simulated, taking into account Auger and Coster-Kronig rates, fluorescence rates, and shake-off branching ratios. It was

found that the appearance of 5p electrons signals the time scale for participation of the molecular orbitals and when ionization of F atoms is expected. The results of this analysis indicated that the F atoms participate in the decay cascade during the fragmentation process and this lowers the kinetic energy release (KER) in comparison to a model in which the KER is estimated based on the ground state Xe-F intermolecular distance. This reduction in KER is in qualitative agreement with experimental observations [52].

Following the initial experiments, an improved apparatus with a position-sensitive ion detector was built. This allowed a complete reconstruction of each ion fragmentation event. This apparatus has been used in a series of experiments; first doing a more detailed study of the XeF₂ molecule and then moving on to other species such as IBr, and CH₂BrI. For IBr, *K* holes can be created in either the Br atom at 13 keV or on the I atom at 33 keV. These data allow us to study these molecules for two different excitation modes and compare with theoretical calculations based on atomic theory. We used similar techniques to study the molecule CH₂BrI to explore the effect of changing the separation between the I and Br atoms in a molecule.

Recent efforts have concentrated on determining the probabilities for the various breakup modes of XeF₂. One of the challenges to the analysis is that the highly charged ions produced in these experiments have large cross sections for electron pickup in the target or from background gas in the chamber. The effects of this charge exchange can be seen in the molecular data as well as the data from atomic Xe. These effects distort the observed ion distributions following photoionization and add additional ions (from background gas) unrelated to the ions from the molecular breakup we are studying. Further complications include the variation of detection efficiency with charge state and dead time in the coincidence electronics. To understand these issues and be able to make corrections and more reliably estimate uncertainties, we have developed a Monte-Carlo code to model these experiments. The code accounts for the cross sections for charge exchange of the different species on the background gas and the variation of detection efficiency of the different ions as a function of their charge states. In addition, the effect of a variable dead time can be simulated. The code not only allows us to quantify systematic effects in our current data, but will be useful in guiding the choice of future experiments. One recent result of the Monte-Carlo simulation is that pressure effects have a strong influence on the fraction of symmetric-fluorine-ion events in the XeF₂ data. A symmetric fluorine ion event is one in which the charge states are the same on both fluorine ions. Such symmetric events are favored by theoretical considerations and we are trying to check this prediction. The Monte-Carlo simulation indicates that charge exchange tends to reduce this effect, so that a correction is needed in order to obtain a reliable value for the fraction of symmetric events.

Pulse duration measurements at LCLS

(G. Doumy, C. Bostedt, W. Helml,⁴ A. L. Cavalieri³ and other collaborators)

The LCLS x-ray free electron laser is capable of producing very intense x-ray pulses believed to be as short as a few tens of femtoseconds, with a special mode where <5 fs pulses are expected. Those properties have already revolutionized the field of ultrafast time resolved x-ray science, in spite of the current lack of exact determination of the pulse duration characteristics. Any measuring scheme is rendered even more challenging by the operating mode of LCLS, called SASE (Self Amplified Spontaneous Emission), which makes it a purely chaotic source and ultimately requires a single shot measurement of every shot to get a full characterization of the source properties. In addition, the SASE operation produces an inherent temporal jitter between the x-ray pulses and any other laser source operating in parallel, which limits greatly the resolution of pump-probe techniques commonly used in timeresolved measurements. Our large collaboration has been using the technique known as laser streaking to get a handle on those pulse properties, which are translated to electron wave-packets produced during ionization of a gas target. The simultaneous presence

of a strong laser field (operating in the visible, IR or THz region) modifies the energy spectrum of those electrons' wave-packets in a deterministic way. It is then possible to extract from the measured final energy distribution some of the properties of the x-ray pulses, as well as the jitter between the x-rays and the strong laser field. Several attempts have been made, most recently using single cycle THz pulses, which allowed for measurement of the jitter and the pulse duration simultaneously. However, the achieved temporal resolution is still much larger than the individual SASE spike expected in the temporal domain. Our latest attempt focused on the shortest pulses possible to generate in the soft x-ray regime (around 1 keV). A strong mid-IR field provided by 6 μm laser pulses, corresponding to a half-cycle duration of 10 fs, is ideal to be able to extract the temporal substructure of the SASE pulses. We were able to make sure that we were operating the measurement in adequate conditions by taking advantage of the newly installed XTCAV measurement, which uses RF deflection to measure precisely the temporal properties of the electron bunch after going through the undulators. Crucial information on the pulse duration and pulse temporal properties at the exit of the undulator region can then be extracted, and used for tuning the machine and ensuring that the streaking measurement operates with pulses shorter than the half period of the laser. By stretching the laser pulse temporally to a few ps, we were also able to limit the influence of the jitter between x-rays and IR. Preliminary analysis of the data during the beamtime was very encouraging, but further analysis is ongoing.

Self-referencing time domain measurements of femtosecond inner shell dynamics

(G. Doumy, C. Bostedt, A. L. Cavalieri,³ L. F. DiMauro⁵ and other collaborators)

The streaking technique used in pulse duration measurements can be extended to make use of the determination of the timing of direct photoionization by the x-ray pulse in the same experimental conditions where a time dependent feature of interest is measured. In a sense, measuring the photoionization event allows one to create, on a shot by shot basis, an absolute reference for the timeline of events being triggered by that pulse. Because this timing is extracted for every shot, even events with low statistics could then be correctly added up to yield high quality data in the time domain.

The objective is to measure, for every shot, the streaked energy spectra of both the photoelectron and the other electrons of interest. A streaked photoelectron spectrum collected with good statistics allows determining, for this particular shot, the relative position inside the streaking ramp. Then, determining the amount of streaking experienced by the other electrons that are detected can directly indicate their emission time inside the ramp, and relative to the x-ray pulse. Data from several pulses can then in principle be added with the correct time axis.

For this concept to work well, the absolute electric field responsible for the streaking needs to be known, including the phase. This is very difficult when dealing with non-CEP stable sources like the OPA available at LCLS currently. A clever solution was found when we first attempted to detect both the photoelectrons and Auger electrons following *K*-shell ionization of Neon atoms. The spectrometer that measured the streaked photoelectron spectrum with good resolution also measured the Auger streaked spectrum, albeit with limited resolution. In spite of this limitation, we are able to observe a correlation between the positions of the centers of the streaked spectra, which exhibits the signature of the delay of peak emission of the Auger electrons relative to the photoelectrons due to the Auger lifetime. This in turn allows for identifying both the slope and the phase of the streaking field, allowing for selecting the shots that overlapped with streaking field conditions providing optimum temporal resolution.

In our latest attempt, we were able to operate successfully two such spectrometers simultaneously, with a streaking laser wavelength of 17 μm . We not only reproduced our early result, but also demonstrated an even more powerful method of operation. Because the IR laser pulses have

to be focused in order to obtain sufficiently strong electric fields to produce a significant streaking effect, an additional, geometric phase is accumulated along the laser propagation direction as one goes through the focus (this is called the Gouy phase). As a consequence, if the two spectrometers are collecting electrons originating from different regions along the propagation axis, they will essentially see a different phase of the electric field. When looking at the correlation map, the effect of any delay between the emission times of the two types of electrons becomes much more obvious. And the geometric phase effect can be calibrated by having both spectrometers look at the photoelectrons simultaneously. Our study was limited to Neon atoms, and established the need for a good characterization of the laser properties along the propagation direction, which was lacking and is likely responsible for some unexplained behavior as the position of the two spectrometers was varied. This is however very encouraging as far as the potential of the method is concerned, and we hope to be able to extend it to electron dynamics in molecules.

Stimulated Raman adiabatic passage with two-color x-ray pulses

(A. Picón, J. Mompert,⁸ S. H. Southworth)

Seeding techniques for x-ray free electron lasers (XFELs) allow the generation of highly coherent, intense x-ray pulses with time lengths on the order of femtoseconds. Here we explore the possibilities of using such x-ray pulses to control matter based on coherence. First experiments using XFEL pulses interacting with atoms, molecules, and clusters [39, 53, 54] show a complex multiphoton response driven by strong electron correlation. Absorption by matter of an x-ray photon excites an inner-shell hole state that rapidly decays on the timescale of a few femtoseconds to hundreds of attoseconds either by an Auger process or by a fluorescent process. When matter is illuminated by high-fluence XFEL pulses, the inner-shell hole-decay processes proceed concurrently with the absorption of additional x-ray photons. Hence, the typical response to XFEL pulses is to produce highly charged final states, and the extension of coherent quantum control techniques to the x-ray regime is not trivial.

Recent developments in seeding techniques at XFELs [55, 56] have significantly increased the quality of the pulse temporal coherence. In the optical regime, in which lasers have achieved a high-degree of spatio-temporal coherence several decades ago, we find many quantum control techniques for atoms and molecules based on coherence.

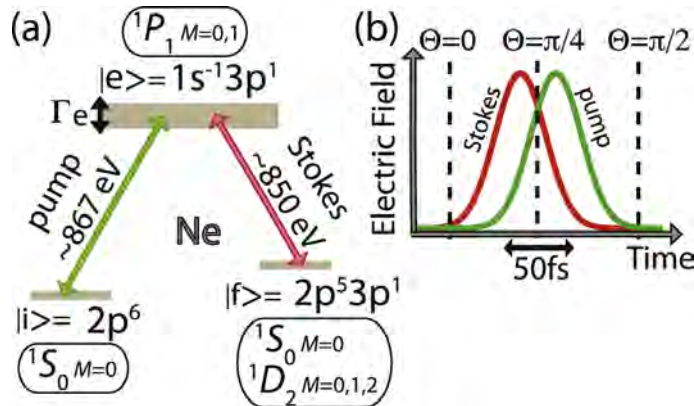


Figure 5: (a) STIRAP scheme for Ne using an 867-eV pump pulse between the ground state and $1s^{-1}3p$ core-excited state and an 850-eV Stokes pulse that connects the core-excited state to the $2p^5 3p$ valence-excited final states. (b) Numerical simulations show efficient population transfers with the pulses partially overlapped and the Stokes pulse preceding the pump.

Quantum control techniques have not yet been exploited in the x-ray regime. The extension of quantum control techniques to high photon energies allows the combination of powerful techniques to control population with the characteristic site-specificity of the x rays. We recently proposed a theoretical scheme to perform stimulated Raman adiabatic passage in the x-ray regime by using inner-hole excited states, and a paper on this research was published [27]. Numerical results in two well-known systems, the neon atom and the carbon monoxide molecule, show a robust control of population transfer. In the molecule, vibrational selectivity is achieved with femtosecond x-ray pulses. This work supports the possibility of using two-color x-ray pulses for coherent control.

Figure 5 presents a three-level-lambda system for a Ne atom in which the lower state $|i\rangle$ is the ground state, the intermediate state $|e\rangle$ is the $1s \rightarrow 3p$ core-excited state, and the final states $|f\rangle$ are the valence-excited states $2p^5 3p \ ^1S_0$ and $\ ^1D_2$. In our numerical simulations, both pulses were modeled with 83-fs Gaussian line shapes and FWHM intensities of $1 \times 10^{16} \text{ W cm}^{-2}$ (pump) and $1 \times 10^{14} \text{ W cm}^{-2}$ (Stokes). We observe large population transfers, $\sim 30\%$, and separation of the two final state populations by tuning the x-ray energy of the Stokes pulse. We also observe strong suppression of the Auger decay yield despite the short lifetime (2.4 fs) of the core-excited state. This illustrates an advantage of STIRAP using x rays - population in the inner-shell intermediate state is suppressed and avoids radiation damage.

4 X-RAY PROBES OF LASER INDUCED DYNAMICS

Time resolved spectroscopy of solution phase polycarbonyl ligated Mn complexes

(A. M. March, G. Doumy, S. H. Southworth, E. P. Kanter, L. Young, H. Cho,⁹ N. Huse,¹⁰ R. Schoenlein,¹¹ T. Assefa,¹² Z. Németh,¹³ C. Bressler,¹² G. Vankó,¹³ and W. Gawelda¹²)

Using our high-repetition-rate pump-probe setup at beamline 7ID-D at the APS we have explored the photoexcitation of $[\text{Mn}(\text{CO})_5]_2$ (dimanganese decacarbonyl) in isopropanol. Along with being an important reagent in organic synthesis, $[\text{Mn}(\text{CO})_5]_2$ is an important model system in the photochemistry of metal-metal bonds. From ultrafast visible and infrared spectroscopy, it is known that upon photoexcitation two dissociation channels open up: 1) the photodetachment of one of the CO ligands producing $\text{Mn}_2(\text{CO})_9$ and 2) the formation of two identical radicals in their doublet ground state, $\text{Mn}(\text{CO})_5$, which remain stable in solution until nongeminate recombination occurs. The individual yields are wavelength dependent and for wavelengths $>300 \text{ nm}$ the Mn-Mn cleavage is strongly favored. We carried out x-ray absorption spectroscopy measurements at the Mn K-edge and x-ray emission spectroscopy measurements after excitation with both 266 nm and 355 nm optical pump wavelengths. At these two pump wavelengths both photoproducts are present but in different weights. Analysis is ongoing, exploring ways to determine the quantum yields of these photoproducts from our x-ray measurements. The yields can then be used as input to extract the transient structures of both species.

Visualizing transient electronic and structural changes of an iridium-based photosensitizer for photocatalytic hydrogen generation

(A. M. March, G. Doumy, S. H. Southworth, L. Young, T. Assefa,¹² A. Britz,¹² Z. Németh,¹³ C. Bressler,¹² G. Vankó,¹³ and W. Gawelda¹²)

The catalytic splitting of water into hydrogen and oxygen with the aid of visible light is a desirable approach for generating hydrogen fuel. A typical homogeneous photocatalytic system used for hydrogen generation consists of a photosensitizer that absorbs visible light, a water reduction catalyst, and a sacrificial reductant. The role of the photosensitizer is to provide a photo-induced, long-lived, charge-separated excited state. This state typically undergoes a reductive quenching due to the sacrificial reductant and the reduced photosensitizer can then transfer an electron further to

the water reduction catalyst. The water reduction catalyst then transfers electrons onto aqueous protons to give hydrogen. A key challenge is the design of new photosensitizer complexes that can more efficiently harvest solar light and act as electron donor sources. Using our high-repetition-rate laser-pump, x-ray-probe setup at 7ID-D we have studied a new iridium-based photosensitizer complex synthesized by M. Beller and H. Junge from the Leibniz Institute for Catalysis. It is known from femtosecond transient absorption spectroscopy that this complex undergoes an intersystem crossing and relaxation into the lowest triplet state in less than 30 ps. The longer lived $^3\text{MLCT}$ state was probed using HERFD XAS (High Energy Resolution Fluorescence Detected X-ray Absorption Spectroscopy) at the Ir L_3 edge which allowed for observation of spectral features with sharpness greater than that due to core-hole lifetime broadening. This allowed for a precise deconvolution of the absorption spectrum into the bound-bound transitions, and the ionization edge. In turn, an absolute determination of the excited state fraction (10%) was obtained, allowing for reconstructing the exact excited state absorption spectrum. We also confirmed that the photosensitizer reacts identically alone or in the presence of the water reduction catalyst and the sacrificial reductant, albeit with the expected lifetime quenching. A manuscript is in preparation.

Elucidating the transient structure of a novel polypyridyl Fe(II) compound for solar energy conversion

(A. M. March, G. Doumy, S. H. Southworth, E. P. Kanter, L. Young, H. Cho,⁹ N. Huse,¹⁰ R. Schoenlein,¹¹ J. McCusker,¹⁴ E. Jakubikova,¹⁵ A. Britz,¹² T. Assefa,¹² Z. Németh,¹³ C. Bressler,¹² G. Vankó,¹³ and W. Gawelda¹²)

Analysis of our x-ray absorption and x-ray emission measurements of laser excited $[\text{Fe}(\text{dcp})_2]^{2+}$ has continued and revealed intriguing results. $[\text{Fe}(\text{dcp})_2]^{2+}$ is a novel polypyridyl Fe(II) complex with a slightly modified structure to yield perfect octahedral symmetry. The complex seems to exhibit very different energetics as compared to other intensely studied polypyridyl iron complexes such as $[\text{Fe}(\text{bpy})_3]^{2+}$ or $[\text{Fe}(\text{terpy})_2]^{2+}$. While O_h symmetry permits both the $^3\text{T}_1$ and the $^5\text{T}_2$ states to form the lowest excited states for sufficiently high ligand-field splitting (favoring paired electrons at the expense of spin pairing energy in the $^1\text{A}_1$ ground state), only Fe(II) compounds with a $^5\text{T}_2$ state as the lowest excited state have been observed so far. Electrochemical and excited-state lifetime measurements indicated that $[\text{Fe}(\text{dcp})_2]^{2+}$ may indeed be the first of a novel class of Fe(II) compounds and if so, could have an impact in synthesized molecular systems for light harvesting and catalytic conversion. Using our high-repetition-rate pump-probe setup at beamline 7ID-D at the APS we collected high quality time-resolved EXAFS measurements at the Fe K -edge and $K\alpha$ x-ray emission measurements after 532 nm laser excitation. The laser triggers a sequence of ultrafast photophysical processes, including a metal-to-ligand charge transfer (MLCT) and a subsequent spin crossover (SCO) process. The resulting high spin state is that probed by the x-rays. Analysis of the $K\alpha$ emission spectrum revealed that the high spin state is a quintet state, similar to $[\text{Fe}(\text{bpy})_3]^{2+}$ or $[\text{Fe}(\text{terpy})_2]^{2+}$. Using this knowledge, the excited state fraction present during our measurement could be extracted from the emission data. This value, 78%, was then used as input for the EXAFS analysis. The EXAFS analysis revealed a rather asymmetric excited state structure with $R(\text{Fe}-\text{N}_{ax}) \sim 2.05\text{\AA}$ and $R(\text{Fe}-\text{N}_{eq}) \sim 2.21\text{\AA}$ which is not in agreement with DFT calculations for $[\text{Fe}(\text{dcp})_2]^{2+}$ but is similar to the excited state structure of $[\text{Fe}(\text{terpy})_2]^{2+}$. Yet, the excited state lifetime of $[\text{Fe}(\text{dcp})_2]^{2+}$ is an order of magnitude shorter than that of $[\text{Fe}(\text{terpy})_2]^{2+}$. Further measurements to explore these discrepancies will be carried out with optical techniques by the McCusker group.

Tracking ligand exchange in solution phase ferrocyanide ions with x-ray spectroscopies

(A. M. March, G. Doumy, D. Moonshiram, S. H. Southworth, E. P. Kanter, L. Young, G. Vankó,¹³ W. Gawelda¹² and other collaborators)

We have continued studies of the model system $[\text{Fe}(\text{II})(\text{CN})_6]^{4-}$ (ferrocyanide) in an aqueous solution after laser excitation using x-ray absorption spectroscopy (XAS) and x-ray emission spectroscopy (XES). We studied the system with 10 ps laser pulses at 355 nm, where the photoexcited state is believed to evolve into the pentacyano-aquo complex $[\text{Fe}(\text{II})(\text{CN})_5\text{H}_2\text{O}]^{3-}$ via ligand dissociation, and also at 266 nm where the excited state can also lead to photo-injection of an electron into the solvent, concomitant to the oxidation state change of the iron center, yielding $[\text{Fe}(\text{III})(\text{CN})_6]^{3-}$. Previously, we collected XANES data and XES $K\beta_{1,3}$ (1s-3p) data at both wavelengths as well EXAFS data at 355 nm with good statistics. Initial analysis of the XANES and XES data indicated that the spectra at 266 nm excitation are due to the presence of both $[\text{Fe}(\text{II})(\text{CN})_5\text{H}_2\text{O}]^{3-}$ and $[\text{Fe}(\text{III})(\text{CN})_6]^{3-}$. By comparison of the spectra at the two excitation wavelengths, we were able to quantify the contributions from each species and thus reconstruct the absorption spectrum of the pentacyano-aquo complex intermediate. Further analysis has suggested that the reconstructed pentacyano-aquo spectrum contains contributions from pentacyanide, which lacks the water ligand.

Continuing to take advantage of our high-repetition-rate pump-probe setup at APS 7ID-D, we performed additional measurements tracking the time dependence of particular spectral features following laser excitation in order to confirm our hypothesis that both $[\text{Fe}(\text{II})(\text{CN})_5\text{H}_2\text{O}]^{3-}$ and $[\text{Fe}(\text{II})(\text{CN})_5]^{3-}$ were present. We have also measured the evolution of the strength of the transient signal as a function of incident laser fluence, in order to establish the linearity of the processes we are observing. Preliminary results from these studies indicate that there are indeed at least two species produced, with one decaying into the other over a few nanoseconds, and that there is a good probability that two photons contributions represent part of the detected signal, especially for the pentacyanide species. Further studies using a laser pump-repump, x-ray probe scheme are planned to better understand those complex dynamics.

In addition, we have had the opportunity to study the process happening at 355 nm on a faster time scale using the SACLA XFEL in Japan. We measured XAS, $K\beta_{1,3}$ XES and XDS in the first 20 ps following laser excitation. In the laser conditions present for the experiment, we confirmed the immediate presence of the two photoproducts detected at APS. In addition, a XES transient strongly suggestive of a spin change was observed. This is largely expected for the pentacyanide product, even if DFT calculations are currently presenting difficulties in establishing the most likely geometric and electronic configuration. Additional input from the diffuse scattering should help in identifying the correct geometry. Further analysis is ongoing.

Observation of high-valent iron nitride catalyst formation using time-resolved x-ray spectroscopies

(A. M. March, G. Doumy, S. H. Southworth, L. Young, G. Vankó,¹³ W. Gawelda¹² and other collaborators)

High-valent iron complexes, i.e. species containing the metal center at an oxidation state +IV and higher, belong to a fascinating class of chemical compounds involved in numerous biochemically and technologically relevant catalytic processes, including the biocatalytic activity involving heme and non-heme metalloenzymes. In general, these are extraordinarily reactive and therefore very difficult to detect during their catalytic action. Particularly intriguing are high-valent Fe complexes featuring a terminal Fe-N multiple bond, the so-called nitridoiron complexes, which are considered as prototypical surface binding motifs involved in industrial N fixation on metallic surface catalysts. At the oxidation state +IV, the Fe-N multiple bond can be stabilized in trigonal-pyramidal coordination geometry providing thermally stable samples to allow for a full crystallographic anal-

ysis. In contrast, structures containing Fe(IV) and Fe(V) centers have never been detected under biochemically and technologically relevant conditions, e.g. in liquid solution under ambient conditions, until just last year, when a stable high-valent nitridoiron(V) complex has been reported in trans-[(cyclam)Fe(III)(N3)₂]PF₆ following UV photoexcitation. The formation of the high-valent species was inferred from time-resolved IR detection of a vibrational label that was introduced in trans-position to the photolabile azido ligand. Comparing the time-resolved IR spectra with predictions from DFT indicated the high-valent nature of the fleeting nitridoiron species.

However, an independent and unambiguous determination of the oxidation state had not been achieved. We have used time-resolved XAS and $K\beta_{1,3}$ XES following excitation at 266 and 355 nm wavelengths to capture the electronic and geometric structure around the Fe ion. The advantage of using two different laser wavelengths is that it allows to better separate the expected contribution of the high valent state from other competing processes, that include ligand substitution or even ligand detachment. Strong transients have been observed, and are being compared with DFT derived calculated XAS spectra. In particular, at 266nm, where the formation of the high valent state is expected to be prevalent, a strong pre-edge feature is observed, in agreement with calculations. The results obtained at the APS were the basis of a successful proposal at the SACLA XFEL, where we were able to study the onset of formation of the high valent state during the first few picosecond after 266 nm excitation, with a resolution around 100 fs after correction with a timing tool recently implemented at SACLA.

Probing Ultrafast Electron (De)localization Dynamics in Mixed Valence Complexes Using Time-Resolved X-ray Spectroscopies

(A. M. March, G. Doumy, S. H. Southworth, M. Khalil, R. Schoenlein, A. Cordones-Hahn, J. H. Lee, T. Kim and other collaborators)

Cyanide-bridged transition metal mixed-valence complexes are a class of molecules, which exhibit unique redox, spectroscopic, and charge transfer properties by virtue of bearing oxidizing and reducing moieties. They are widely studied for their applications in magnetism and photochemical energy conversion, and serve as model systems to probe the coupling between electronic and vibrational motions during photoinduced ultrafast electron transfer reactions using equilibrium and transient spectroscopic techniques. A central question in the field of transition metal mixed-valence complexes is the precise nature and extent of electron delocalization. XAS and XES (including RIXS maps) can probe changes in the local electronic structure following metal-to-metal charge transfer (MMCT) excitation with atomic specificity, tracking time-evolving spin-orbit couplings, solvent rearrangement and metal-ligand interactions. Using crystal optics for a von Hamos dispersive geometry developed in house by the APS optical group, we measured simultaneously the $K\alpha$ and $K\beta$ portions of the emission spectrum (including the Valence-to-Core) at both the Fe K -edge and the Cr K -edge. For the two Fe-containing complexes, only static measurements were performed since the back electron transfer rates are known to be too fast (100 fs) to be followed at a synchrotron, but represent crucial building block for an upcoming XFEL time resolved measurement. In contrast, the covalently linked electron acceptor Cr(III) in a Ru-Cr-Ru mixed valence complex leads to remarkably long-lived charge-separated intermediates, attributed to the existence of electronic states of different spin multiplicity that effectively inhibit back electron transfer. Transient XAS measurements identified the production of a unique photoproduct with a lifetime around 35 ns. Time-resolved XES spectra were recorded at a repetition rate of 1.3 MHz, and the $K\beta$ exhibits a small transient signal consistent with the spin change associated with the MMCT. DFT calculations, including molecular dynamics to take into account the effect of the solvent, are in progress to complete the interpretation.

Preliminary studies of light induced magnetic transitions in solid state samples

(A. M. March, G. Doumy, J. Freeland, D. Keavney and V. Stoica)

Sector 4ID-C at the APS is a soft x-ray beamline operating between 500 and 2000 eV, with great polarization control. The opportunity exists to extend our time resolved x-ray spectroscopies to the L-edges of first row transition metals, which are more readily sensitive to the valence electrons, especially the $3d$ orbitals involved in the ligand field of transition metal complexes. Operating at 4ID-C involves bringing our own laser system and gated data acquisition system, and as a test of capabilities, we brought the Duetto laser system and some of our FPGA based electronics to perform some time resolved x-ray scattering measurements on magnetic materials that exhibit an insulator to metal transition above a critical temperature. Using the laser to create a local, temporary temperature increase can drive the systems across the transition, and x-ray measurements can be used to probe the dynamics and the properties of the transient phases. The sample used for this first test was a Nickelate (NdNiO_3) thin film. Performing x-ray reflectivity at the Ni L-edge after excitation with the laser at the fundamental wavelength (1064 nm), we observed a distinct transient signal in the absorption spectrum. This first attempt demonstrated the successful transport of the laser system, therefore opening more opportunities for experiments at the APS.

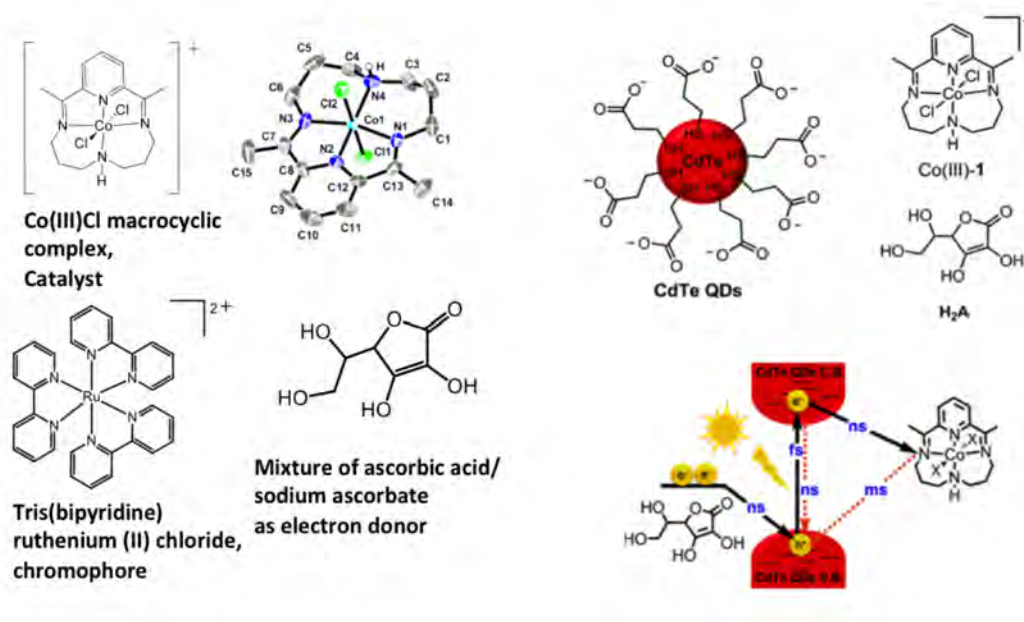


Figure 6: The multimolecular hydrogen evolution system studied consisting of the macrocyclic cobalt complex Co(III), an equimolar mixture of ascorbic acid/sodium ascorbate as buffer, and electron donor and photosensitizers $\text{Ru}[\text{bpy}_3]^{2+}$ as well as water solution cadmium telluride quantum dots.

Time-resolved x-ray absorption and emission spectroscopy of a cobalt-based hydrogen evolution system for artificial photosynthesis

(D. Moonshiram, C. Gimbert-Suriñach,¹⁶ A. Guda,¹⁷ C. S. Lehmann, S. H. Southworth, A. Picón, X. Zhang, G. Doumy, A. M. March, L. Young, and A. Llobet¹⁶)

Production of cost-effective hydrogen gas through solar power is an important challenge of the Department of Energy among other global industry initiatives. In natural photosynthesis, the oxygen evolving complex (OEC) can carry out the four-electron water splitting reaction to hydrogen

with an efficiency of around 60%. Although much progress has been carried out in determining mechanistic pathways of the OEC, biomimetic approaches have not duplicated Nature’s efficiency in function. Over the past years, we have witnessed progress in developments of light harvesting modules, so called chromophore/catalytic assemblies. In spite of reportedly high catalytic activity of these systems, quantum yields of hydrogen production are below 40% when using monochromatic light. Proper understanding of kinetics and bond making/breaking steps has to be achieved to improve efficiency of hydrogen evolution systems. This project uses the timing implementation of ultrafast x-ray absorption (XAS) and x-ray emission spectroscopies (XES) to visualize in “real time” the photo-induced kinetics accompanying a sequence of redox reactions in a macrocyclic cobalt complex. This complex was shown to have superior catalytic activity to that of the cobaloxime-type catalyst that has also been used as a proton reduction catalyst in water [57]. Time-resolved XAS and XES in parallel with laser transient absorption spectroscopy of the cobalt molecular catalyst (see Fig. 6) and $[\text{Ru}(\text{bpy})_3]^{2+}$ as well as CdTe quantum dots photosensitizers allowed us to identify two key intermediates. The intermediates are a reduced Co(II) species with a bound water molecule and spin 1/2 as well as a square-planar Co(I) intermediate with spin 0. XANES, XES and EXAFS analysis together with TD-DFT XANES calculations helped to ascertain the oxidation states, the spin states of the species, and their coordination sphere. A manuscript on the results of this research is in preparation [37].

X-ray absorption spectroscopy and density functional theory characterization of the $\text{Ru}(\text{bpy})_3\text{-Ni}(\text{P}^{Ph_2}\text{N}^{Ph_2})_2(\text{CH}_3\text{CN})]^{2+}$ multimolecular system

(D. Moonshiram, A. Guda,¹⁷ L. Kohler, C. S. Lehmann, S. H. Southworth, X. Zhang, A. Picon, G. Doumy, A. M. March, L. Young, and K. Mulfort)

Production of carbon neutral fuels through solar energy is one of the most important global challenges. One efficient way to store solar energy is to convert it into chemical energy by fuel-forming reactions such as water splitting into hydrogen and oxygen ($2 \text{H}_2\text{O} + 4h\nu = \text{O}_2 + 2 \text{H}_2$) and/or reduction of CO_2 to methanol or other carbon based fuels ($2 \text{H}_2\text{O} + \text{CO}_2 + 6 h\nu = \text{CH}_3\text{OH} + 3/2 \text{O}_2$). The idea of using molecular hydrogen as a renewable fuel has motivated considerable research in the development of cheap, abundant and first-row transition metals. Recently, Du Bois, Bullock and co-workers pioneered the synthesis of a highly efficient and active nickel-phosphine water reduction catalyst of the general form $\text{Ni}(\text{P}^{Ph_2}\text{N}^{Ph_2})_2(\text{CH}_3\text{CN})]^{2+}$ [58]. Although there is an abundance of information on the spectroscopic characterization of the nickel catalyst through electrochemistry, UV-Vis spectroscopy, mass spectrometry and electron paramagnetic resonance, these techniques are not sensitive to the formal oxidation state, coordination chemistry and the unoccupied electronic states and spins of atoms surrounding the specific element. As such, there is no clear understanding between performance and stability of the complex to its structure and ligand geometry. This project combined the analysis of time-resolved x-ray absorption and laser transient absorption of a chromophore/catalytic multimolecular assembly consisting of the $\text{Ni}(\text{P}^{Ph_2}\text{N}^{Ph_2})_2(\text{CH}_3\text{CN})]^{2+}$ catalyst, $[\text{Ru}(\text{bpy})_3]^{2+}$ photosensitizer and ascorbic acid as electron donor. Time-resolved pump-flow probe experiments showed formation of a Ni(I) reduced state active in the water reduction process with a long lifetime of around 263 μs . Interestingly from TD-DFT calculations, the Ni(II) ground state complex was found to bind to the ascorbate in solution over time leading to deactivation of the complex and reduction of the transient signal corresponding to formation of Ni(I). TD-DFT calculations point towards a change of the XANES structure from a Ni(II) octahedral structure with water bound to it to a trigonal pyramidal Ni(I) species with no bound water molecule. A manuscript on the results of this research is in preparation [38].

Development of efficient, high-resolution x-ray emission spectrometers

(S. H. Southworth, D. Moonshiram, C. S. Lehmann, G. Doumy, A. M. March, L. Young, A. Kastengren, X. Shi, D. Casa, X. Huang, E. Kasman, M. Wieczorek, L. Assoufid)

X-ray emission spectroscopy (XES) is a powerful method for studying electronic structure, e.g., molecules with 3d transition metal centers. Understanding the photophysics and photochemistry of such molecules is of high interest due to their roles in light gathering, intramolecular transfer of charge, energy and spin, photocatalysis, and biological processes. High-resolution XES uses crystal spectrometers with small acceptance solid angles that require high x-ray flux, particularly the weaker valence-to-core transitions that are most sensitive to the oxidation state and chemical environment of the transition metal center or ligand sites. Our high-repetition-rate laser at beamline 7ID-D allows us to use ~5-20% of the available x-ray flux for pump-probe experiments, which makes time-resolved XES feasible but still challenging to conduct with high precision. To improve our capability to perform time-resolved XES experiments, we are working with the APS Optics Group to design and fabricate efficient x-ray analyzers. We have developed three types of analyzers - cylindrically shaped for use with position-sensitive detectors in von Hamos geometry, spherical analyzers in Johann geometry in which the Bragg angle and point detector are scanned, and a prototype design that approximates the Wittry geometry. A stepped Wittry analyzer has been fabricated that is expected to provide 4x larger solid angle with resolution similar to that of a spherical analyzer.

Analyzer tests have been conducted at beamline 7BM that provides an intense, microfocused beam that is ideal for creating point sources of x-ray fluorescence on samples. Several spherical and cylindrical analyzers have been tested at 7BM, and we recently tested the stepped Wittry analyzer. Using a 1D array as the detector, we demonstrated that some imprecisions in the assembly of the optic are resulting in different areas of the crystal diffracting at different spots on the detector, but that the measurement can be corrected to retrieve an optimal resolution comparable to the simple spherical analyzer with larger radius of curvature. Further measurements, including using monochromatic beam, are planned in the near future, and this success is encouraging us to develop a geometry using two or more such crystals simultaneously for efficient time-resolved measurements. Meanwhile we have used both Johann and von Hamos analyzers for selected time-resolved pump-probe measurements at 7ID-D. The measurements made include studies of low-spin to high-spin transitions, resonant inelastic x-ray scattering (RIXS) in which the XES is measured vs. absorbed x-ray energy near threshold, and a first measurement of valence-to-core XES of a laser-excited transient [23]. Finally, we used another design with two wafers on the same cylindrical surface to collect at the same time, on the same detector, both the $K\alpha$ and $K\beta$ XES.

Design of a high x-ray flux microprobe optical system

(R. Reininger, Z. Liu, G. Doumy and L. Young)

An extension of our high repetition rate laser pump/x-ray probe setup implemented at 7ID-D, specifically aimed at x-ray emission spectroscopy, which requires high x-ray flux but only limited energy resolution such as offered with pink beams, is being developed. The x-ray microprobe geometry is essential, since it allows completely clearing a fresh spot in the liquid jet at repetition rates around 300 kHz. The small x-ray beam probes only the center of the laser spot where excitation is maximal and uniform and yields high excitation fractions with modest laser pulse energies. Conserving the microprobe concept with pink beam is essential, as is the ability to tune the central photon energy and reject higher harmonics from the undulator radiation. Tunability in the 5 to 10 keV range, where all 4 K -edges of first-row transition metals fall, separated by 500-600 eV, is necessary to keep the element specificity of hard x-ray spectroscopies that allow for local probing around an active center. Harmonic rejection is also essential for the element

specificity and to eliminate higher-order electronic excitations that would contaminate the signal. The requirements of this experiment can be fulfilled with a relatively simple optical system based on two cooled elliptical mirrors in a Kirkpatrick-Baez configuration.

One of the issues with this configuration is maintaining the focal spot dimension as the energy of the undulator is varied, since this changes the heat load absorbed by the first optical element. Finite element analyses of the power absorbed by a side water-cooled mirror exposed to the radiation emitted by an undulator at the Advanced Photon Source (APS) and at the APS after the proposed upgrade (APS-U) reveals that the mirror deformation is very close to a convex cylinder creating a virtual source closer to the mirror than the undulator source. Ray tracing calculations show that a simple pitch correction is able to recover the small focus spot size with limited aberrations, and with only a minor translation in the focal plane, easily recoverable by our experimental setup. A report on this design study was recently published [24].

5 OPTICAL CONTROL AND X-RAY IMAGING OF NANOPARTICLES

X-ray diffraction from optically trapped nanoparticles

(Y. Gao, R. Harder, S. H. Southworth, J. Guest, N. F. Scherer,¹⁸ Z. Yan,¹⁸ L. Ocola, M. Pelton,¹⁹ and L. Young)

Coherent x-ray diffraction imaging (CXDI) is a sensitive microscopic method for imaging crystalline and noncrystalline objects at high spatial resolution. CXDI is particularly useful for measuring strain patterns in nanoparticles that arise due to the large ratio of surface area to bulk volume [59]. CXDI is highly developed for imaging the 3D structures of samples with micrometer and sub-micrometer sizes. In order to acquire a clear coherent diffraction pattern, the sample must be held and aligned at sub-micron and milli-degree accuracy. A major barrier to applying CXDI to free-standing micro- and nano-scale objects is their tendency to freely move within the intense beam of synchrotron x rays. Typically such objects must be securely bonded to a substrate, which can alter their internal structures. While the forces moving such particles are not completely understood, we believe optical tweezers may be a solution to this problem.

Optical tweezers provide a unique method to control small particles, ranging from several microns to tens of nanometers. Using optical techniques, these laser trapped particles can be manipulated and forces on the objects in the trap can be measured. By utilizing phase modulation techniques, optical traps with different geometries and polarization can be generated, resulting in accurate orientation of anisotropic particles [60, 61].

We have designed an apparatus of dynamic holographic optical tweezers which is compatible with the CXDI beamline 34-ID-C at the APS. Our optical tweezers utilizes a 1064 nm CW laser to manipulate micron-scale particles. The phase of the beam is modified by a liquid-crystal spatial light modulator to generate various trapping geometries, such as a line of trapping sites to hold and rotate a ZnO nano-rod ($\sim 0.5 \mu\text{m}$ diameter, $\sim 4 \mu\text{m}$ long). In order to achieve highly stable optical trapping, we use two types of trapping geometries to compensate the scattering force from the laser: trapping against the internal surface of the sample cell and dual-beam counterpropagating trap. We use microfluidic sample cells fabricated by bonding a 100- μm Si wafer between two 150- μm thick Pyrex cover slips. Anodic bonding and etching procedures are used to achieve the desired geometry and bonding of the materials. The sample cell can then be held between the microscope objectives of the optical tweezers for viewing the particles with a CCD camera while positioning them in the x-ray beam for diffraction measurements.

We have trapped both ZnO tetrapods and single rods formed by broken arms of tetrapods. We observed two Bragg peaks: the (002) peak from the ZnO rod and the (110) peak from one arm of the tetrapod. Coherent 11-keV x rays were focused by Kirkpatrick-Baez mirrors to a 2- μm x

1- μm spot. Coherent fringes were recorded in the diffraction images, but higher trapping stability is needed to record images that can be analyzed to extract detailed structural information on the nanoparticles. For future experiments, we are developing a better trapping geometry that utilizes the interference between counter-propagating beams to improve the trapping stability. A progress report on this project has been submitted for publication [29].

Meso-scale magnetic dipolar resonances excited by optical vector beams

(U. Manna,¹⁸ Z. Yan,¹⁸ Y. Bao,¹⁸ J-H. Lee,¹⁸ Y. Weizmann,¹⁸ and N. F. Scherer¹⁸)

In addition to participating in the optical trapping/x-ray diffraction experiments being conducted by Drs. Yuan Gao and Stephen Southworth, Dr. Manna is creating and using focused optical vector beams to conduct novel spectroscopic experimental studies of nano-meta materials. Optical beams with azimuthally polarized light (this is entirely different than circularly polarized light), where each part of the beams cross-section is polarized in a direction tangential to that angular portion of the cross-section, results in focused light that has a tightly focused magnetic field (B-field) with the E-field surrounding it as a halo. Such a beam has a curl in the E-field and correspondingly the B-field is polarized along the optical propagation direction. By Faradays law, the electro-dynamically coupled electric dipoles of (plasmonic) metal nanoparticles arranged on the surface of a dielectric core can be driven by a beam with a curl that results in a (collective) magnetic dipole mode. The “nano-meta-material” and the scattering spectra from a single such object are shown in Fig. 7. The longest wavelength feature is strongly enhanced by the focused azimuthally polarized beam relative to the spectra of the identical nanostructure obtained with a focused linearly polarized or radially polarized light. The spectra and enhancements also agree. Such vector beams also have enhanced focusing and hence optical trapping capabilities that could be employed in the optical trapping/x-ray diffraction experiments just described.

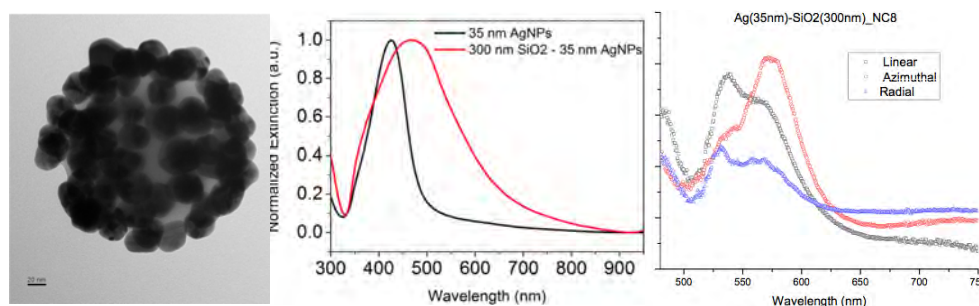


Figure 7: Spectroscopic study of single nano-meta-materials. (left) TEM image of a single nano-meta-particle consisting of 35-nm dia. Au nanoparticles chemically attached to a 300-nm dia SiO_2 core. (scale bar = 20 nm). (center) Spectra of 35-nm dia. Au nanoparticles in solution and spectra of an ensemble of Au-based nano-meta-particles in solution (red curve). (right) Scattering spectra from the same identical single nano-meta-particle obtained using linearly (black points), radially (blue points) and azimuthally (red points) polarized light.

Femtosecond laser pulse driven melting in gold nanorod aqueous colloidal suspension: identification of a transition from stretched to exponential kinetics

(Y. Li, Z. Jiang, X.-M. Lin, H. Wen, D. A. Walko, S. A. Deshmukh, R. Subbaraman, S. K. R. S. Sankaranarayanan, S. K. Gray and P. J. Ho)

Many potential industrial, medical, and environmental applications of metal nanoparticles rely on the physics and resultant kinetics and dynamics of the interaction of these particles with light.

This is because these particles have strong optical interactions that depend on the size and shape of the particles. The energy deposition process is dominated by the surface plasmon resonance (SPR), which is a collective excitation of conduction electrons. In order to gain a better understanding of the interaction of light with gold nanoparticles, a series of melting experiments were performed at different peak laser fluences at APS. An aqueous colloidal suspension of nanorods 4560 nm long and aspect ratio of 34.5 were exposed to laser pulses with peak fluence ranging from 14 to 116 mJ/cm², with an accumulated laser fluence in each sample of up to 20 J/cm². In situ small angle x-ray scattering (SAXS) was used to track the rod-to-sphere morphological transformation of the nanoparticles as the laser melting progresses. The experiments showed a surprising kinetics transition in the global melting of femtosecond laser-driven gold nanorod aqueous colloidal suspensions. At low laser intensity, the melting exhibits a stretched exponential kinetics, which abruptly transforms into a compressed exponential kinetics when the laser intensity is raised. It is found that the relative formation and reduction rate of intermediate shapes play a key role in the transition.

Our theoretical effort confirmed the effectiveness of SAXS for monitoring the ensemble change. Using atomic form factors obtained from the Hartree-Fock-Slater model, we calculated the x-ray scattering patterns of an ensemble of gold nanoparticles, in which each nanoparticle is assumed to be a collection of independent gold atoms. The ensemble was treated as a bimodal mixture of spherical nanoparticles and nanorods with aspect ratio of about 3. We showed that the signals from the SAXS depend sensitively on the actual fractions of the spherical nanoparticles and nanorods. This predicted sensitivity was observed in experimental SAXS and confirmed in TEM images.

6 Affiliations of collaborators

¹Argonne Leadership Computing Facility, Argonne National Laboratory, Argonne, IL

²Kansas State University, Manhattan, KS

³Center for Free-Electron Laser Science, DESY, Hamburg, Germany

⁴MPQ, Garching, Munich, Germany

⁵Ohio State University, Columbus, OH

⁶University of Wisconsin, Madison, WI

⁷The University of Texas at Austin, Austin, TX

⁸Universitat Autònoma de Barcelona

⁹Lawrence Berkeley National Laboratory, Berkeley, CA

¹⁰Universität Hamburg, Hamburg, Germany

¹¹Linac Coherent Light Source, SLAC National Accelerator Laboratory, Menlo Park, CA

¹²European XFEL, Hamburg, Germany

¹³Wigner Research Centre for Physics, Hungarian Academy Sciences, Budapest, Hungary

¹⁴Michigan State University, East Lansing, MI

¹⁵North Carolina State University, Raleigh, NC

¹⁶Institute of Chemical Research of Catalonia, Tarragona, Spain

¹⁷Southern Federal University, Rostov, Russia

¹⁸University of Chicago, Chicago, IL

¹⁹University of Maryland, Baltimore County, MD

References

Publications 2013–2015

- [1] A. Picón, C. Buth, G. Doumy, B. Krässig, L. Young, and S. H. Southworth, “Optical control of resonant Auger processes,” *Phys. Rev. A* **87**, 013432 (2013).

- [2] G. Vankó, A. Bordage, P. Glatzel, E. Gallo, M. Rovezzi, W. Gawelda, A. Galler, C. Bressler, G. Doumy, A. M. March, E. P. Kanter, L. Young, S. H. Southworth, S. E. Canton, J. Uhlig, V. Sundström, K. Haldrup, T. Brandt van Driel, M. M. Nielsen, K. S. Kjaer, and H. T. Lemke, “Spin-state studies with XES and RIXS: From static to ultrafast,” *J. Electron. Spectrosc. Relat. Phenom.* **188**, 166 (2013).
- [3] C. Buth, F. He, J. Ullrich, C. H. Keitel, and K. Z. Hatsagortsyan, “Attosecond pulses at kiloelectronvolt photon energies from high-order-harmonic generation with core electrons,” *Phys. Rev. A* **88**, 033848 (2013).
- [4] B. W. Adams, C. Buth, S. M. Cavaletto, J. Evers, Z. Harman, C. H. Keitel, A. Pálffy, A. Picón, R. Röhlberger, Y. Rostovtsev, and K. Tamasaku, “X-ray quantum optics,” *J. Mod. Opt.* **60**, 2 (2013).
- [5] R. Reininger, E. M. Dufresne, M. Borland, M. A. Beno, L. Young, K.-J. Kim, and P. G. Evans, “Optical design of the short pulse x-ray imaging and microscopy time-angle correlated diffraction beamline at the Advanced Photon Source,” *Rev. Sci. Instrum.* **84**, 053013 (2013).
- [6] R. Reininger, D. Keavney, M. Borland and L. Young, “Optical design of the Short Pulse Soft X-Ray Spectroscopy beamline at the Advanced Photon Source, *J. Synch. Rad.* **20**, 654 (2013).
- [7] A. Picón, P. J. Ho, G. Doumy, and S. H. Southworth, “Optically-dressed resonant Auger processes induced by high-intensity x rays,” *New J. Phys.* **15**, 083057 (2013).
- [8] C. Hernández-García, A. Picón, J. San Román, and L. Plaja, “Attosecond extreme ultraviolet vortices from high-order harmonic generation,” *Phys. Rev. Lett.* **111**, 083602 (2013).
- [9] C. Bostedt, J.D. Bozek, P.H. Bucksbaum, R.N. Coffee, J.B. Hastings, Y. Huang, R.W. Lee, S. Schorb, J.N. Corlett, P. Denes, P. Emma, R.W. Falcone, R.W. Schoenlein, G. Doumy, E. Kanter, B. Krässig, S. Southworth, L. Young, L. Fang, M. Hoener, N. Berrah, C. Roedig, L.F. DiMauro, “Ultra-fast and ultra-intense x-ray sciences: first results from the Linac Coherent Light Source free-electron laser,” *J. Phys. B* **46**, 1 (2013).
- [10] T. Osipov, L. Fang, B. Murphy, F. Tarantelli, E. R. Hosler, E. Kukk, J. D. Bozek, C. Bostedt, E. P. Kanter, and N. Berrah, “Sequential multiple ionization and fragmentation of SF₆ induced by an intense free electron laser pulse,” *J. Phys. B* **46**, 164032 (2013).
- [11] Z. Yan, Y. Bao, U. Manna, R. A. Shah, N. F. Scherer, “Enhancing nano particle electrodynamics with gold nanoplate mirrors, Supporting Information,” *Nano Lett.* **14**, 2436 (2014).
- [12] L. Young, “Ultra-intense X-ray interactions at the Linac Coherent Light Source,” Chapter 15, 529-556. In *Attosecond and XUV Physics*, Editors: Thomas Schultz and Marc Vrakking, Wiley (2014).
- [13] R. Reininger, E. M. Dufresne, M. Borland, M. Beno, L. Young, P. G. Evans, “A short-pulse X-ray beamline for spectroscopy and scattering,” *J. Synchrotron Rad.* **21**, 1194 (2014).
- [14] L. Young, “Understanding ultra-intense x-ray interactions with matter,” *Advances in Chemical Physics*, Volume 157: Proceedings of the 240 Conference: Science’s Great Challenges, First Edition, p. 183-194 (2015).
- [15] C. Bressler, W. Gawelda, A. Galler, M. M. Nielsen, V. Sundström, G. Doumy, A. M. March, S. H. Southworth, L. Young, and G. Vankó, “Solvation dynamics monitored by combined X-ray spectroscopies and scattering: photoinduced spin transition in aqueous [Fe(bpy)₃]²⁺,” *Faraday Discuss.* **171**, 169 (2014).
- [16] Y. Pushkar, D. Moonshiram, V. Purohit, L. Yan, and I. Alperovich, “Spectroscopic analysis of catalytic water oxidation by [Ru^{II}(bpy)(tpy)H₂O]²⁺ suggests that Ru^V=O is not a rate-limiting intermediate,” *J. Am. Chem. Soc.* **136**, 11938 (2014).
- [17] P. J. Ho, C. Bostedt, S. Schorb, and L. Young, “Theoretical tracking of resonance-enhanced multiple ionization pathways in x-ray free-electron laser pulses,” *Phys. Rev. Lett.* **113**, 253001 (2014).
- [18] Z. Yan, M. Sajjin, N. F. Scherer, “Tailoring nano particle dynamics with optical phase,” in preparation (2014).
- [19] U. Manna, Z. Yan, Y. Bao, J. Jureller, N. F. Scherer, “Meso-scale dipolar interactions in synthetic photonic metal nanoparticle lattices,” in preparation (2014).
- [20] W. Helml, A. R. Maier, W. Schweinberger, I. Grguras, P. Radcliffe, G. Doumy, C. Roedig, J. Gagnon, M. Messerschmidt, S. Schorb, C. Bostedt, G. Grüner, L. F. DiMauro, D. Cubaynes, J. D. Bozek, Th. Tschentscher, J. T. Costello, M. Meyer, R. Coffee, S. Düsterer, A. L. Cavalieri, and R. Kienberger, “Measuring the temporal structure of few-femtosecond free-electron laser x-ray pulses directly in the time domain,” *Nature Photon.* **8**, 950 (2014).
- [21] Y. Li, Z. Jiang, X.-M. Lin, H. Wen, D. A. Walko, S. A. Deshmukh, R. Subbaraman, S. K. R. S. Sankaranarayanan, S. K. Gray, and P. J. Ho, “Femtosecond laser pulse driven melting in gold nanorod aqueous colloidal suspension: identification of a transition from stretched to exponential kinetics,” *Scientific Reports* **5**, 8146 (2015).
- [22] G. Vankó, A. Bordage, M. Pápai, K. Haldrup, P. Glatzel, A. M. March, G. Doumy, A. Britz, A. Galler, T. Assefa, D. Cabaret, A. Juhin, T. B. van Driel, K. S. Kjær, A. Dohn, K. B. Møller, H. T. Lemke, E. Gallo, M. Rovezzi, Z. Németh, E. Rozsályi, T. Rozgonyi, J. Uhlig, V. Sundström, M. M. Nielsen, L. Young, S. H. Southworth, C. Bressler, and W. Gawelda, “Detailed characterization of a nanosecond-lived excited state: x-ray and theoretical investigation of the quintet state in photoexcited [Fe(terpy)₂]²⁺,” *J. Phys. Chem C* **119**, 5888 (2015).
- [23] A. M. March, T. A. Assefa, C. Bressler, G. Doumy, A. Galler, W. Gawelda, E. P. Kanter, Z. Németh, M. Pápai, S. H. Southworth, L. Young, and G. Vankó, “Feasibility of valence-to-core x-ray emission spectroscopy for tracking transient species,” *J. Phys. Chem. C* **119**, 14571 (2015).

- [24] R. Reininger, Z. Liu, G. Doumy, and L. Young, “A simple optical system delivering a tunable micrometer pink beam that can compensate for heat-induced deformations,” *J. Synchrotron Rad.* **22**, 930 (2015).
- [25] B. Zimmermann, V. McKoy, S. H. Southworth, E. P. Kanter, B. Krässig, and R. Wehlitz, “Dipole and nondipole photoionization of molecular hydrogen,” *Phys. Rev. A* **91**, 053410 (2015).
- [26] S. H. Southworth, R. Wehlitz, A. Picón, C. S. Lehmann, L. Cheng, and J. F. Stanton, “Inner-shell photoionization and core-hole decay of Xe and XeF₂,” *J. Chem. Phys.* **142**, 224302 (2015).
- [27] A. Picón, J. Mompert, and S. H. Southworth, “Stimulated Raman adiabatic passage with two-color x-ray pulses,” *New J. Phys.* **17**, 083038 (2015).
- [28] L. Young, “A stable narrow-band X-ray laser,” (Invited News & Views article for Nature), *Nature* **524**, 424 (2015).
- [29] Y. Gao, R. Harder, S. Southworth, J. Guest, N. Scherer, Z. Yan, L. Ocola, M. Pelton, and L. Young, “Bragg diffraction from sub-micron particles isolated by optical tweezers,” *Proceedings of the 12th International Conference on Synchrotron Radiation Instrumentation*, American Institute of Physics Conference Proceedings, submitted (2015).
- [30] R. Santra and L. Young, “Interaction of intense X-ray beams with atoms,” in “Synchrotron Light Sources and Free-Electron Lasers: Accelerator Physics, Instrumentation and Science Applications,” Editors: E. Jaeschke, S. Khan, J.R. Schneider, and J.B. Hastings (Springer, Heidelberg) in press.
- [31] A. Picón, C. S. Lehmann, C. Bostedt, A. Rudenko, A. Marinelli, T. Osipov, D. Rolles, N. Berrah, C. Bomme, M. Bucher, G. Doumy, B. Erk, K. Ferguson, T. Gorkhover, P. J. Ho, E. P. Kanter, B. Krässig, J. Krzywinski, A. A. Lutman, A. M. March, D. Moonshiram, D. Ray, L. Young, S. T. Pratt, and S. H. Southworth, “Heterosite-specific ultrafast intramolecular dynamics,” to be submitted (2015).
- [32] C. S. Lehmann, A. Picón, C. Bostedt, A. Rudenko, A. Marinelli, D. Moonshiram, T. Osipov, D. Rolles, N. Berrah, C. Bomme, M. Bucher, G. Doumy, B. Erk, K. Ferguson, T. Gorkhover, P. J. Ho, E. P. Kanter, B. Krässig, J. Krzywinski, A. A. Lutman, A. M. March, D. Ray, L. Young, S. T. Pratt, and S. H. Southworth, “Ultrafast measurements of molecular nuclear dynamics using two x-ray pulses,” to be submitted (2015).
- [33] C. Bostedt, S. Boutet, D. M. Fritz, Z. Huang, H. J. Lee, H. T. Lemke, A. Robert, W. F. Schlotter, J. J. Turner, and G. J. Williams, “The Linac Coherent Light Source: The First Five Years,” *Rev. Mod. Phys.*, submitted.
- [34] P. J. Ho, E. P. Kanter, and L. Young, “Resonance mediated atomic ionization dynamics in femtosecond XFEL pulses,” to be submitted (2015).
- [35] T. Gorkhover, S. Schorb, R. Coffee, M. Adolph, L. Foucar, D. Rupp, A. Aquila, J. D. Bozek, S. W. Epp, B. Erk, L. Gumprecht, L. Holmegaard, A. Hartmann, R. Hartmann, G. Hauser, P. Holl, A. Hömke, N. Kimmel, K.-U. Kühnel, P. Johnsson, M. Messerschmidt, C. Reich, A. Rouzée, B. Rudek, C. Schmidt, J. Schulz, H. Soltau, S. Stern, G. Weidenspointner, B. White, J. Küpper, L. Strüder, I. Schlichting, J. Ullrich, D. Rolles, A. Rudenko, T. Möller, and C. Bostedt, “Femtosecond and nanometer visualisation of structural dynamics in superheated nanoparticles,” submitted (2015).
- [36] K. R. Ferguson, M. Bucher, T. Gorkhover, S. Boutet, H. Fukuzawa, J. E. Koglin, Y. Kumagai, A. Lutman, A. Marinelli, M. Messerschmidt, K. Nagaya, J. Turner, K. Ueda, G. J. Williams, P. H. Bucksbaum, and C. Bostedt, “Transient lattice compression in the solid-to-plasma transition,” submitted (2015).
- [37] D. Moonshiram, C. Gimbert-Suriñach, A. Guda, C. S. Lehmann, S. H. Southworth, A. Picón, X. Zhang, G. Doumy, A. M. March, L. Young, and A. Lobet, “Tracking the structural and electronic dynamics of a cobalt-based hydrogen evolution system,” to be submitted (2015).
- [38] D. Moonshiram, A. Guda, L. Kohler, C. S. Lehmann, S. H. Southworth, A. Picón, G. Doumy, A. M. March, L. Young, and K. Mulfort, “Time-resolved x-ray absorption spectroscopy of a highly stable nickel catalyst for artificial photosynthesis,” to be submitted (2015).

Other cited references

- [39] L. Young, E. P. Kanter, B. Krässig, Y. Li, A. M. March, S. T. Pratt, R. Santra, S. H. Southworth, N. Rohringer, L. F. DiMauro, G. Doumy, C. A. Roedig, N. Berrah, L. Fang, M. Hoener, P. H. Bucksbaum, J. P. Cryan, S. Ghimire, J. M. Glowina, D. A. Reis, J. D. Bozek, C. Bostedt, and M. Messerschmidt, “Femtosecond electronic response of atoms to ultra-intense x-rays,” *Nature* **466**, 56 (2010).
- [40] G. Doumy, C. Roedig, S.-K. Son, C. I. Blaga, A. D. Chiara, R. Santra, N. Berrah, C. Bostedt, J. D. Bozek, P. H. Bucksbaum, J. Cryan, L. Fang, S. Ghimire, J. M. Glowina, M. Hoener, E. P. Kanter, B. Krässig, M. Kuebel, M. Messerschmidt, G. G. Paulus, D. A. Reis, N. Rohringer, L. Young, P. Agostini, and L. F. DiMauro, “Nonlinear atomic response to intense ultrashort x rays,” *Phys. Rev. Lett.* **106**, 083002 (2011).
- [41] E. P. Kanter, B. Krässig, Y. Li, A. M. March, P. Ho, N. Rohringer, R. Santra, S. H. Southworth, L. F. DiMauro, G. Doumy, C. A. Roedig, N. Berrah, L. Fang, M. Hoener, P. H. Bucksbaum, S. Ghimire, D. A. Reis, J. D. Bozek, C. Bostedt, M. Messerschmidt, and L. Young, “Unveiling and driving hidden resonances with high-fluence, high-intensity x-ray pulses,” *Phys. Rev. Lett.* **107**, 233001 (2011).
- [42] B. Rudek, S.-K. Son, L. Foucar, S. W. Epp, B. Erk, *et al.*, “Ultra-efficient ionization of heavy atoms by intense X-ray free-electron laser pulses,” *Nat. Photon.* **6**, 858 (2012).

- [43] B. Rudek, D. Rolles, S.-K. Son, L. Foucar, B. Erk *et al.*, “Resonance-enhanced multiple ionization of krypton at an x-ray free-electron laser, *Phys. Rev. A* **87**, 023413 (2013).
- [44] Z. Jurek, G. Faigel, and M. Tegze, “Dynamics in a cluster under the influence of intense femtosecond hard X-ray pulses,” *Eur. Phys. J. D* **29**, 217 (2004).
- [45] U. Saalmann and J.-M. Rost, “Ionization of Clusters in Strong X-Ray Laser Pulses,” *Phys. Rev. Lett.* **89**, 143401 (2002).
- [46] C. Caleman *et al.*, “On the Feasibility of Nanocrystal Imaging Using Intense and Ultrashort X-ray Pulses,” *ACS Nano* **5**, 139 (2011).
- [47] N.-T. Loh and V. Elser, “Reconstruction algorithm for single-particle diffraction imaging experiments,” *Phys. Rev. E* **80**, 026705 (2009).
- [48] J. R. Fienup, “Phase retrieval algorithms - a comparison” *Appl. Opt.* **21**, 2758 (1982).
- [49] S. Marchesini, H. He, H. N. Chapman, S. P. Hau-Riege, A. Noy, M. R. Howells, U. Weierstall, and J. C. H. Spence, “X-ray image reconstruction from a diffraction pattern alone,” *Phys. Rev. B* **68**, 140101(R) (2003).
- [50] A. A. Lutman, R. Coffee, Y. Ding, Z. Huang, J. Krzywinski, T. Maxwell, M. Messerschmidt, and H.-D. Nuhn, “Experimental demonstration of femtosecond two-color x-ray free-electron lasers,” *Phys. Rev. Lett.* **110**, 134801 (2013).
- [51] A. Pandey, B. Bapat, and K. R. Shamasundar, “Charge symmetric dissociation of doubly ionized N₂ and CO molecules,” *J. Chem. Phys.* **140**, 034319 (2014).
- [52] R. W. Dunford, S. H. Southworth, D. Ray, E. P. Kanter, B. Krässig, L. Young, D. A. Arms, E. M. Dufresne, D. A. Walko, O. Vendrell, S.-K. Son, and R. Santra, “Evidence for interatomic Coulombic decay in Xe *K*-shell-vacancy decay of XeF₂,” *Phys. Rev. A* **86**, 033401 (2012).
- [53] M. Hoener, L. Fang, O. Kornilov, O. Gessner, S. T. Pratt, M. Gühr, E. P. Kanter, C. Blaga, C. Bostedt, J. D. Bozek, P. H. Bucksbaum, C. Buth, M. Chen, R. Coffee, J. Cryan, L. DiMauro, M. Glowia, E. Hosler, E. Kukk, S. R. Leone, B. McFarland, M. Messerschmidt, B. Murphy, V. Petrovic, D. Rolles, and N. Berrah, “Ultra-intense x-ray induced ionization, dissociation, and frustrated absorption in molecular nitrogen,” *Phys. Rev. Lett.* **104**, 253002 (2010).
- [54] S. Schorb, D. Rupp, M. L. Swiggers, R. N. Coffee, M. Messerschmidt, G. Williams, J. D. Bozek, S.-I. Wada, O. Kornilov, T. Möller, and C. Bostedt, “Size-dependent ultrafast ionization dynamics of nanoscale samples in intense femtosecond x-ray free-electron-laser pulses,” *Phys. Rev. Lett.* **108**, 233401 (2012).
- [55] J. Amann *et al.*, “Demonstration of self-seeding in a hard-x-ray free-electron laser,” *Nature Photonics* **6**, 693 (2012).
- [56] E. Hemsing, G. Stupakov, D. Xiang, and A. Zholents, “Beam by design: laser manipulation of electrons in modern accelerators,” *Rev. Mod. Phys.* **86**, 897 (2014).
- [57] C. Gimbert-Suriñach, J. Albero, T. Stoll, J. Fortage, M.-N. Collomb, A. Deronzier, E. Palomares, and A. Llobet, “Efficient and limiting reactions in aqueous light-induced hydrogen evolution systems using molecular catalysts and quantum dots,” *J. Am. Chem. Soc.* **136**, 7655 (2014).
- [58] M. A. Gross, A. Reynal, J. R. Durrant, and E. Reisner, “Versatile photocatalytic systems for H₂ generation in water based on an efficient DuBois-type nickel catalyst,” *J. Am. Chem. Soc.* **136**, 356 (2014).
- [59] M. A. Pfeifer, G. J. Williams, I. A. Vartanyants, R. Harder, and I. K. Robinson, “Three-dimensional mapping of a deformation field inside a nanocrystal,” *Nature* **442**, 63 (2006).
- [60] Z. Yan, J. Sweet, J. E. Jureller, M. J. Guffey, M. Pelton, and N. F. Scherer, “Controlling the position and orientation of single silver nanowires on a surface using structured optical fields,” *ACS Nano* **6**, 8144 (2012).
- [61] Z. Yan, J. E. Jureller, J. Sweet, M. J. Guffey, M. Pelton, and N. F. Scherer, “Three-dimensional optical trapping and manipulation of single silver nanowires,” *Nano Lett.* **12**, 5155 (2012).

J.R. Macdonald Laboratory Overview

The J.R. Macdonald Laboratory focuses on the interaction of intense laser pulses with matter for the purpose of understanding and even controlling the resulting ultrafast dynamics. The timescales involved range from attoseconds, necessary for studying electronic motion in matter, to femtoseconds and picoseconds for molecular vibration and rotation, respectively. We continue to harness the multi-timescale expertise within the Lab to further our progress in both understanding and control. The synergy afforded by the close interaction of theory and experiment within the Lab serves as a significant multiplier for this effort. To achieve our goals, we are advancing theoretical modeling and computational approaches as well as experimental techniques, for example by taking advantage of our expertise in particle imaging (using COLTRIMS, VMI, MDI, etc.).

Most of our research projects have been associated with one of two themes: “Attosecond Physics” and “Control”. These themes serve as broad outlines only, as the boundary between them is not always well defined. A few examples from each are briefly mentioned below, while further details are provided in the individual abstracts of the PIs: I. Ben-Itzhak, B.D. Esry, V. Kumarappan, C.D. Lin, D. Rolles, A. Rudenko, U. Thumm, and C.A. Trallero.

Attosecond physics: Attosecond science is motivated by the idea of observing electronic motion in atoms and molecules on its natural timescale. Light pulses whose durations approach this timescale are a necessary component of this work, and we continued our efforts to produce and characterize them. In addition to studies of electronic motion, attosecond-scale pulses can also serve as very precise triggers or probes of the femtosecond-scale nuclear motion in molecules. Moreover, the underlying high-harmonic generation (HHG) mechanism, used to create attosecond pulses, provides essential information about the target and has been the focus of some of our theoretical and experimental studies. Theoretical work from the Lab has shown, for instance, that optimizing the waveform of the driving infrared pulse can improve HHG by orders of magnitude. To that end, we continue to develop an intense light synthesizer. High harmonics from aligned molecules have also been used to experimentally uncover information about the orbitals involved in the process. Pump-probe measurements using EUV-pump pulses to initiate molecular dynamics in ions have been extended to neutral molecules.

Control: Methods for controlling the motion of heavy particles in small molecules continue to be developed. Theoretically, our work has shown that carrier-envelope phase (CEP) effects arise from interference between different multiphoton pathways. We have conducted extensive measurements of the CEP dependence of D^* production in strong-field dissociation of D_2 and have extracted quantitative information from these measurements, such as the difference in photon number between interfering pathways, which allows us to detect the presence of higher-order effects. Work in the Lab has also led to the imaging of structural rearrangement in small polyatomic molecules and to theoretical treatment of nuclear-dynamics imaging. Related work on charge transfer following multiphoton ionization by X-rays has been conducted at the LCLS. Significant steps to improve impulsive alignment of symmetric, and even asymmetric, top molecules have been made in the Lab. Our ability to align molecules has also enabled molecular-frame studies of ionization and fragmentation, as well as studies of rotational and electronic wave packets in molecules.

Some of this ultrafast-laser research at JRML involves very productive collaborations, such as with E. Wells from Augustana College and E. Poliakoff from Louisiana State University. In

addition to our laser-related research, we have conducted some studies using our low-energy ECR ion source in collaboration with visiting scientists, specifically the group of S. Lundeen, which recently terminated their research project.

Like the visitors benefiting from the use of our facilities, we pursue several outside collaborations at other facilities and with other groups (*e.g.*, ALS, Århus, FLASH, University of Frankfurt, University of Jena, LBNL, LCLS, Max-Planck Institutes for Quantum Optics and Kernphysik, the Ohio State University, Texas A&M, Tokyo, Weizmann Institute, and others).

On the personnel side, Daniel Rolles, who was hired from FLASH, Germany, last year, joined us as an Assistant Professor in January 2015. His first measurements at JRML have focused on ultrafast nuclear wavepacket dynamics in CH₃I molecules. The results were presented at DAMOP soon after the data were taken.

Finally, it is worth mentioning the improved laser facilities available to researchers at JRML. Our high-repetition rate laser, PULSAR, became the main laser system, while the old workhorse laser, KLS, is still yielding high-quality results. The newest laser system, HITS, features high-power pulses at tunable long wavelengths (6 mJ output combined signal and idler). The CEP of HITS can be locked for extended periods – over 9 hours – thus enabling long measurements with a locked CEP, a key ingredient for the synthesis of intense optical waveforms. The university-funded renovation of one of our old experimental rooms contributed significantly to the stability of the new laser system. Combining the experimental and theoretical expertise within the Lab with the capabilities becoming available with the new laser facilities continues to produce exciting physics.

**Structure and Dynamics of Atoms, Ions, Molecules, and Surfaces:
Molecular Dynamics with Ion and Laser Beams**

*Itzik Ben-Itzhak, J. R. Macdonald Laboratory, Physics Department, Kansas State University,
Manhattan, KS 66506; ibi@phys.ksu.edu*

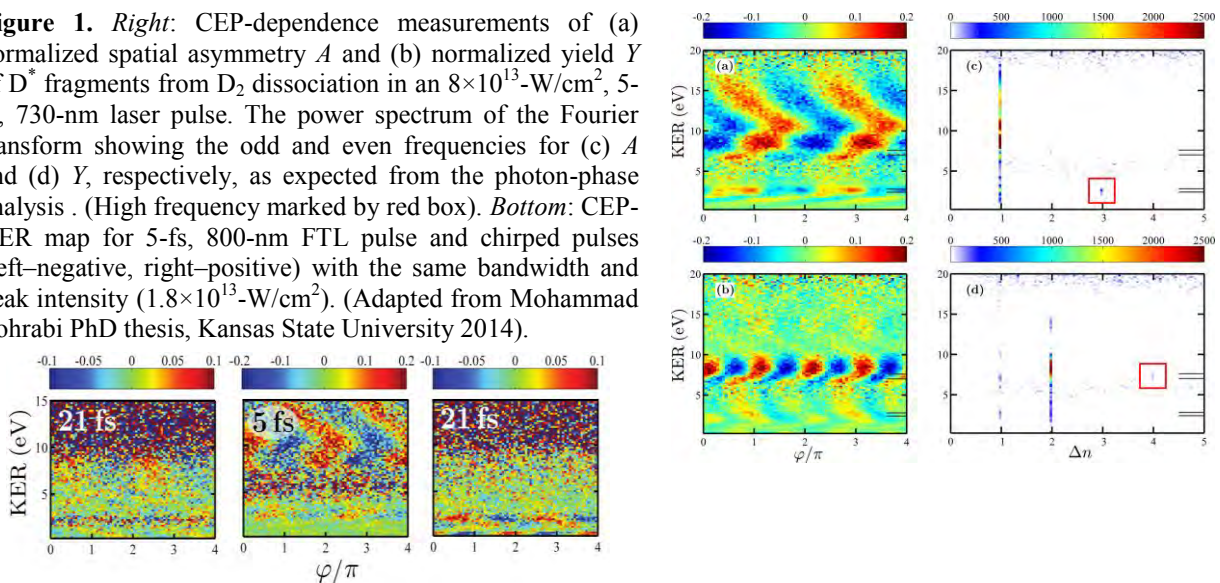
Scope: The goal of this part of the JRML program is to study and control molecular dynamics under the influence of ultrashort intense laser pulses. To this end, we typically study molecular ion beams and have a close collaboration between theory and experiment.¹

Carrier-envelope phase (CEP) control over molecular dynamics, *M. Zohrabi, B. Berry, U. Ablikim, Nora G. Kling, T. Severt, Bethany Jochim, K.D. Carnes, Y. Wang, J.V. Hernández, S. Zeng, B.D. Esry, and I. Ben-Itzhak* – The phase between the carrier and the pulse envelope has been used in recent years to control, for example, photoionization (Refs. [1,2] and Pub. [8,13]) and molecular dissociation (Refs. [4-5] and Pubs. [5,9,17]). In the latter case, studies have focused mainly on spatial asymmetries along the laser polarization – a symmetry broken by the CEP, φ , in broadband FTL (Fourier Transform Limited) pulses approaching single cycle.

Taking advantage of technology advancements – CEP-tagging [2,6] of sub-5-fs FTL pulses from our 10 kHz PULSAR laser – we were able to perform demanding CEP-dependent measurements on an H_2^+ beam (see Pub. [9] and B.D. Esry’s abstract). In addition, we have measured the CEP dependence of D^* (i.e. $D(nl)$ with $n \gg 1$) formation upon dissociation of D_2 in intense broadband laser pulses. With its high density of Rydberg states, it is practically impossible to treat this process from first principles. Therefore, it is an excellent test of the general predictions of the photon-phase CEP formalism of Esry’s group, which requires no computation. A Fourier transform of the measured data reveals the predicted [7,8] odd and even frequencies associated, respectively, with asymmetry and yield oscillations with CEP, as shown in Fig. 1. Note the contributions of high-order interfering paths, also shown in the figure.

The CEP-dependence of D^* production vanishes, as expected, when the pulse duration is long. The question is why – is it because of the pulse duration or the associated broad bandwidth? The framework of Esry’s theory predicts that it is the latter, as a broader bandwidth leads to increased interference between dissociation paths involving different photon numbers. As predicted, our measured CEP oscillations in asymmetry and yield, shown in Fig. 1 (*bottom*), persist in pulses chirped up to 21 fs (all with the same bandwidth).

Figure 1. *Right:* CEP-dependence measurements of (a) normalized spatial asymmetry A and (b) normalized yield Y of D^* fragments from D_2 dissociation in an 8×10^{13} -W/cm², 5-fs, 730-nm laser pulse. The power spectrum of the Fourier transform showing the odd and even frequencies for (c) A and (d) Y , respectively, as expected from the photon-phase analysis. (High frequency marked by red box). *Bottom:* CEP-KER map for 5-fs, 800-nm FTL pulse and chirped pulses (left–negative, right–positive) with the same bandwidth and peak intensity (1.8×10^{13} -W/cm²). (Adapted from Mohammad Zohrabi PhD thesis, Kansas State University 2014).

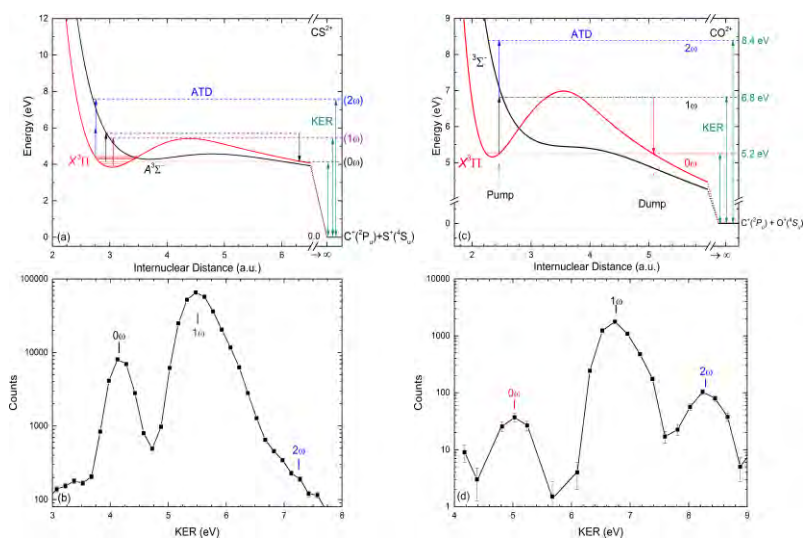


Strong-field dissociation of CO^{2+} and CS^{2+} driven by a pump-dump-like mechanism, T. Severt, M. Zohrabi, U. Ablikim, K.J. Betsch, Bethany Jochim, B. Berry, K.D. Carnes, Tereza Uhlíková, B.D. Esry, and I. Ben-Itzhak – The target CS^{2+} beam “cools” vibrationally in flight to the interaction region, since states above $v=7$ in the $X^3\Pi$ ground state predissociate. A single photon absorption may excite the CS^{2+} to the $A^3\Sigma^-$ state as depicted in Fig. 2(a), leading to dissociation into $\text{C}^+ + \text{S}^+$ with KER values centered around 5.6 eV – the dominant peak, labeled 1ω , in Fig. 2(b). The KER of the peak labeled 0ω matches the expected values for unimolecular dissociation of the metastable $v=0-7$ vibrational levels. However, the tunneling rates of these states are much too small to produce a peak of this magnitude, as are the rates of predissociation caused by the X–A spin-orbit coupling. A two-photon process resulting in a net zero photon absorption, namely absorption followed by stimulated emission, depicted by the up and down arrows on Fig. 2(a), provides a better explanation of the observed data.

This two-photon process is somewhat similar to the pump-dump control scheme suggested by Tannor and Rice [9], where a first pulse excites the system and the second de-excites it to the desired final state. In our case, a single pulse is used, and soon after the CS^{2+} is excited to the vibrational continuum of the $A^3\Sigma^-$ and stretches, stimulated emission becomes energetically forbidden because of the shape of the $X^3\Pi$ potential. However, stimulated emission is allowed beyond the Condon point. Alternatively, one can think of this two-photon process as a delayed Raman transition [10], where the deexcitation transition is delayed during the motion above the wide potential barrier for the reasons describe above until the Condon point is reached or passed. Both views suggest that the KER is given by the energy difference between the initial vibrational state and the dissociation limit with shifts constrained by the laser bandwidth.

Our measured CO^{2+} KER spectrum, shown in Fig. 2(d), exhibits a similar 0ω peak, which indicates that this two-photon mechanism is due to the shape of the metastable potential and not to the shape of the excited state, as the latter is repulsive for CO^{2+} and metastable for CS^{2+} [see Fig. 2(a,c)]. Therefore, we expect this two-photon process to be common in many molecules having similar metastable potentials. Finally, we note that the magnitude of the 0ω and 2ω -ATD peaks relative to the main 1ω peak seem to depend on the properties of each molecule – an observation calling for further work.

Figure 2. The lowest two triplet potentials (a) of CS^{2+} [this work and Šedivcová *et al.* J. Chem. Phys. **125**, 164308 (2006)], and (c) of CO^{2+} [from Šedivcová *et al.* J. Chem. Phys. **124**, 214303 (2006)]. The measured KER spectrum (b) of CS^{2+} dissociation into $\text{C}^+ + \text{S}^+$ in a 25-fs, 790-nm, 1×10^{14} -W/cm² pulse, and (d) of CO^{2+} dissociation into $\text{C}^+ + \text{O}^+$ in a 40-fs, 790-nm, 1.4×10^{15} -W/cm² pulse.



Future plans: We will continue to probe molecular-ion beams in a strong laser field, specifically exploring challenging two-color, pump-probe and CEP-dependence experiments. We will carry

on our studies of more complex systems, including simple polyatomic molecules. In addition, we are upgrading our setup to enable measurements of negative and neutral molecular beams.

References:

1. G.G. Paulus *et al.*, Nature (London) **414**, 182 (2001)
2. N.G. Johnson *et al.*, Phys. Rev. A **83**, 013412 (2011)
3. B. Bergues *et al.*, Nature Comm. **3**, 813 (2012)
4. M.F. Kling *et al.*, Science **312**, 246 (2006)
5. M. Kremer *et al.*, Phys. Rev. Lett. **103**, 213003 (2009)
6. T. Rathje *et al.*, J. Phys. B **45**, 074003 (2012)
7. V. Roudnev and B.D. Esry, Phys. Rev. Lett. **99**, 220406 (2007)
8. J.J. Hua and B.D. Esry, J. Phys. B **42**, 085601 (2009)
9. D. J. Tannor and S. A. Rice, J. Chem. Phys. **83**, 5013 (1985)
10. B. Hartke *et al.*, J. Chem. Phys. **96**, 5636 (1992)

Publications of DOE sponsored research in the last 3 years:

29. “Long term carrier-envelope-phase stabilization of a terawatt-class Ti:Sapphire laser”, Adam M. Summers, Benjamin Langdon, Jonathan Garlick, Xiaoming Ren, Derrek J. Wilson, Stefan Zigo, Matthias F. Kling, Shuting Lei, Christopher G. Elles, Eric Wells, Erwin D. Poliakoff, Kevin D. Carnes, Vinod Kumarappan, Itzik Ben-Itzhak, and Carlos A. Trallero-Herrero, FIO – *accepted*.
28. “[Quantum control of photodissociation using intense, femtosecond pulses shaped with third order dispersion](#)”, Uri Lev, L. Graham, C.B. Madsen, I. Ben-Itzhak, B.D. Bruner, B.D. Esry, H. Frostig, O. Heber, A. Natan, V.S. Prabhudesai, D. Schwalm, Y. Silberberg, D. Strasser, I.D. Williams, and D. Zajfman, J. Phys. B **48**, 201001 (2015) – Fast Track Communication – IOP Select.
27. “[Auger decay and subsequent fragmentation pathways of ethylene following K-shell ionization](#)” B. Gaire, D.J. Haxton, F.P. Sturm, J. Williams, A. Gatton, I. Bocharova, N. Gehrken, M. Schöffler, H. Gassert, S. Zeller, J. Voigtsberger, T. Jahnke, M. Zohrabi, D. Reedy, C. Nook, A.L. Landers, A. Belkacem, C.L. Cocke, I. Ben-Itzhak, R. Dörner, and Th. Weber, Phys. Rev. A **92**, 013408 (2015).
26. “[Note: Determining the detection efficiency of excited neutral atoms by a microchannel plate detector](#)”, Ben Berry, M. Zohrabi, D. Hayes, U. Ablikim, Bethany Jochim, T. Severt, K.D. Carnes, and I. Ben-Itzhak, Rev. Sci. Instrum. **86**, 046103 (2015).
25. “[Coherent electronic wave packet motion in C₆₀ controlled by the waveform and polarization of few-cycle laser fields](#)”, H. Li, B. Mignolet, G. Wachter, S. Skruszewicz, S. Zherebtsov, F. Süßmann, A. Kessel, S.A. Trushin, Nora G. Kling, M. Kübel, B. Ahn, D. Kim, I. Ben-Itzhak, C.L. Cocke, T. Fennel, J. Tiggesbäumker, K.-H. Meiwes-Broer, C. Lemell, J. Burgdörfer, R.D. Levine, F. Remacle, and M.F. Kling, Phys. Rev. Lett. **114**, 123004 (2015).
24. “[Identification of a previously unobserved dissociative ionization pathway in time-resolved photospectroscopy of the deuterium molecule](#)”, Wei Cao, Guillaume Laurent, Itzik Ben-Itzhak and C. Lewis Cocke, Phys. Rev. Lett., **114**, 113001 (2015) – *Editors’ Suggestion*.
23. “[A carrier-envelope-phase stabilized terawatt class laser at 1 kHz with a wavelength tunable option](#)”, Benjamin Langdon, Jonathan Garlick, Xiaoming Ren, Derrek J. Wilson, Adam M. Summers, Stefan Zigo, Matthias F. Kling, Shuting Lei, Christopher G. Elles, Eric Wells, Erwin D. Poliakoff, Kevin D. Carnes, Vinod Kumarappan, Itzik Ben-Itzhak, and Carlos A. Trallero-Herrero, Opt. Exp. **23**, 4563 (2015). *Featured in Nature Photonics* <http://www.nature.com/nphoton/journal/v9/n4/pdf/nphoton.2015.47.pdf>.
22. “[Fragmentation of CD⁺ induced by intense ultrashort laser pulses](#)”, L. Graham, M. Zohrabi, B. Gaire, U. Ablikim, B. Jochim, B. Berry, T. Severt, A.M. Summers, U. Lev, O. Heber, D. Zajfman, I.D. Williams, K.D. Carnes, B.D. Esry, and I. Ben-Itzhak, Phys. Rev. A **91**, 023414 (2015).
21. “[Attosecond control of electron emission in two-color ionization of atoms](#)”, G. Laurent, W. Cao, I. Ben-Itzhak, and C.L. Cocke, *Ultrafast Phenomena XIX* – Proceedings of the 19th International Conference, Okinawa, Japan, July 2014, edited by Kaoru Yamanouchi, Steven Cundiff, Regina de Vivie-Riedle, Makoto Kuwata-Gonokami, and Louis DiMauro, Springer Proceedings in Physics, Vol. **162** (2015) p. 3.
20. “[Note: Position dependence of time signals picked of a microchannel plate detector](#)”, U. Ablikim, M. Zohrabi, Bethany Jochim, B. Berry, T. Severt, K.D. Carnes, and I. Ben-Itzhak, Rev. Sci. Instrum. **86**, 016111 (2015).
19. “[Incorporating real time velocity map image reconstruction into closed-loop coherent control](#)”, C.E. Rallis, T.G. Burwitz, P.R. Andrews, M. Zohrabi, R. Averin, S. De, B. Bergues, Bethany Jochim, A.V. Voznyuk, Neal Gregerson, B. Gaire, I. Znakovskaya, J. Mckenna, K.D. Carnes, M.F. Kling, I. Ben-Itzhak, and E. Wells, Rev. Sci. Instrum. **85**, 113105 (2014).
18. “[Thick-lens velocity-map imaging spectrometer with high resolution for high-energy charged particles](#)”, N.G. Kling, D. Paul, A. Gura, G. Laurent, S. De, H. Li, Z. Wang, B. Ahn, C.H. Kim, T.K. Kim, I.V. Litvinyuk, C.L. Cocke, I. Ben-Itzhak, D. Kim, and M.F. Kling, Journal of Instrumentation **9**, P05005 (2014).

17. "[Subfemtosecond steering of hydrocarbon deprotonation through superposition of vibrational modes](#)", A.S. Alnaser, M. Kübel, R. Siemering, B. Bergues, Nora G. Kling, K.J. Betsch, Y. Deng, J. Schmidt, Z.A. Alahmed, A.M. Azzeer, J. Ullrich, I. Ben-Itzhak, R. Moshhammer, U. Kleineberg, F. Krausz, R. de Vivie-Riedle, and M.F. Kling, *Nature Communications* **5**, 3800 (2014).
16. "[Multielectron effects in strong-field dissociative ionization of molecules](#)", X. Gong, M. Kunitski, K.J. Betsch, Q. Song, L.Ph.H. Schmidt, T. Jahnke, Nora G. Kling, O. Herrwerth, B. Bergues, A. Senfleben, J. Ullrich, R. Moshhammer, G.G. Paulus, I. Ben-Itzhak, M. Lezius, M.F. Kling, H. Zeng, R.R. Jones, and J. Wu, *Phys. Rev. A* **89**, 043429 (2014).
15. "[Hydrogen and fluorine migration in photo-double-ionization of 1,1-difluoroethylene \(1,1-C₂H₂F₂\) near and above threshold](#)", B. Gaire, I. Bocharova, F.P. Sturm, N. Gehrken, J. Rist, H. Sann, M. Kunitski, J. Williams, M.S. Schöffler, T. Jahnke, B. Berry, M. Zohrabi, M. Keiling, A. Moradmand, A.L. Landers, A. Belkacem, R. Dörner, I. Ben-Itzhak, and Th. Weber, *Phys. Rev. A* **89**, 043423 (2014).
14. "[Attosecond Control of electron emission from atoms](#)", G. Laurent, W. Cao, I. Ben-Itzhak, and C.L. Cocke, *Journal of Physics: Conference Series* **488**, 012008 (2014) – ICPEAC 2013 proceedings – invited talk
13. "[Non-sequential double ionization of Ar: from the single- to the many-cycle regime](#)", M. Kübel, K.J. Betsch, Nora G. Kling, A.S. Alnaser, J. Schmidt, U. Kleineberg, Y. Deng, I. Ben-Itzhak, G.G. Paulus, T. Pfeifer, J. Ullrich, R. Moshhammer, M.F. Kling, and B. Bergues, *New J. Phys.* **16**, 033008 (2014).
12. "[Elucidating isotopic effects in intense ultrafast laser-driven D₂H⁺ fragmentation](#)", A.M. Sayler, J. McKenna, B. Gaire, Nora G. Johnson, K.D. Carnes, B.D. Esry, and I. Ben-Itzhak, *J. Phys. B: At. Mol. Opt. Phys.* **47**, 031001 (2014) – Fast Track Communication – IOP Select (see also [LabTalk](#)).
11. "[Photo-double-ionization of ethylene and acetylene near threshold](#)", B. Gaire, S.Y. Lee, D. J. Haxton, P.M. Pelz, I. Bocharova, F.P. Sturm, N. Gehrken, M. Honig, M. Pitzer, D. Metz, H-K. Kim, M. Schöffler, R. Dörner, H. Gassert, S. Zeller, J. Voigtsberger, W. Cao, M. Zohrabi, J. Williams, A. Gatton, D. Reedy, C. Nook, Thomas Müller, A.L. Landers, C.L. Cocke, I. Ben-Itzhak, T. Jahnke, A. Belkacem, and Th. Weber, *Phys. Rev. A* **89**, 013403 (2014) – Editors' suggestion.
10. "[Adaptive strong-field control of chemical dynamics guided by three-dimensional momentum imaging](#)", E. Wells, C.E. Rallis, M. Zohrabi, R. Siemering, B. Jochim, P.R. Andrews, U. Ablikim, B. Gaire, S. De, K.D. Carnes, B. Bergues, R. de Vivie-Riedle, M.F. Kling, and I. Ben-Itzhak, *Nature Communications* **4**, 2895 (2013).
9. "[Carrier-envelope phase control over pathway interference in strong-field dissociation of H₂⁺](#)", Nora G. Kling, K.J. Betsch, M. Zohrabi, S. Zeng, F. Anis, U. Ablikim, Bethany Jochim, Z. Wang, M. Kübel, M.F. Kling, K.D. Carnes, B.D. Esry, and I. Ben-Itzhak, *Phys. Rev. Lett.* **111**, 163004 (2013).
8. "[Nonsequential double ionization of N₂ in a near-single-cycle laser pulse](#)", M. Kübel, Nora G. Kling, K.J. Betsch, N. Camus, A. Kaldun, U. Kleineberg, I. Ben-Itzhak, R.R. Jones, G.G. Paulus, T. Pfeifer, J. Ullrich, R. Moshhammer, M.F. Kling, and B. Bergues, *Phys. Rev. A* **88**, 023418 (2013).
7. "[Attosecond pulse characterization](#)", G. Laurent, W. Cao, I. Ben-Itzhak, and C.L. Cocke, *Opt. Exp.* **21**, 16914 (2013).
6. "[Charge asymmetric dissociation of CO⁺ molecular ion beams induced by strong laser fields](#)", Nora G. Kling, J. McKenna, A.M. Sayler, B. Gaire, M. Zohrabi, U. Ablikim, K.D. Carnes, and I. Ben-Itzhak, *Phys. Rev. A* **87**, 013418 (2013).
5. "[Controlled directional ion emission from several fragmentation channels of CO driven by a few-cycle laser field](#)", K.J. Betsch, Nora G. Johnson, B. Bergues, M. Kübel, O. Herrwerth, A. Senfleben, I. Ben-Itzhak, G.G. Paulus, R. Moshhammer, J. Ullrich, M.F. Kling, and R.R. Jones, *Phys. Rev. A* **86**, 063403 (2012).
4. "[Frustrated tunneling ionization during strong-field fragmentation of D₃⁺](#)", J. McKenna, A.M. Sayler, B. Gaire, Nora G. Johnson, B.D. Esry, K.D. Carnes, and I. Ben-Itzhak, *New J. Phys.* **14**, 103029 (2012).
3. "[Quantum control of photodissociation by manipulation of bond softening](#)", Adi Natan, Uri Lev, Vaibhav S. Prabhudesai, Barry D. Bruner, Daniel Strasser, Dirk Schwalm, Itzik Ben-Itzhak, Oded Heber, Daniel Zajfman, and Yaron Silberberg, *Phys. Rev. A* **86**, 043418 (2012).
2. "[Measurements of intense ultrafast laser-driven D₃⁺ dynamics](#)", A.M. Sayler, J. McKenna, B. Gaire, Nora G. Johnson, K.D. Carnes, and I. Ben-Itzhak, *Phys. Rev. A* **86**, 033425 (2012).
1. "[Fragmentation of molecular-ion beams in intense ultrashort laser pulses](#)", Itzik Ben-Itzhak, *Fragmentation Processes - Topics in Atomic and Molecular Physics*, edited by Colm T. Whelan (Cambridge University Press, 2013) p. 72 – *Invited*.

ⁱ In addition to the close collaboration with the theory group of *Brett Esry*, some of our studies are done in collaboration with others at JRML and elsewhere.

Strong-field dynamics of few-body atomic and molecular systems

B.D. Esry

J. R. Macdonald Laboratory, Kansas State University, Manhattan, KS 66506

esry@phys.ksu.edu

Program Scope

A main component of my program is to quantitatively understand the behavior of simple benchmark systems in ultrashort, intense laser pulses. As we gain this understanding, we will work to transfer it to more complicated systems. The other main component of my program is to develop novel analytical and numerical tools to more efficiently and more generally treat these systems and to provide rigorous, self-consistent pictures within which their non-perturbative dynamics can be understood. The ultimate goal is to uncover the simplest picture that can explain the most — ideally, without heavy computation being necessary.

Carrier-envelope phase control over pathway interference in strong-field dissociation of H_2^+

Recent progress

As part of our effort to achieve quantitatively good agreement between theory and experiment, we investigated the carrier-envelope phase (CEP) dependence of dissociation of H_2^+ . For this benchmark system, dissociation can be calculated nearly exactly [R1] — as long as ionization is negligible — and kinematically complete momentum imaging measurements can be performed [R2]. While there was general agreement between the time-dependent Schrödinger equation (TDSE) calculations and the measurements, the agreement was not nearly as good as it should be for this supposedly simple system.

These results appeared in Pub. [P4] slightly after a similar measurement from Paulus' group in Jena appeared in Pub. [P5]. Our group provided theory support for both the experimental efforts involved in this friendly rivalry. In fact, both of the experimental groups will be joining the theory group in a longer follow-up paper [R3] that, in part, seeks to uncover the sources of the remaining disagreement. Unfortunately, many of our improvements to the calculations actually tend to worsen the agreement, leaving the path to better agreement somewhat unclear.

The theoretical calculations included in Pub. [P4] were performed for a 5-fs Gaussian laser pulse and included Franck-Condon and intensity averaging. The peak intensity, however, was limited to $1 \times 10^{14} \text{ W/cm}^2$ to avoid incurring large errors due to our neglect of ionization (see Refs. [R1,R4] for details of the calculation). The trivial 2π -periodicity [R5,R6] of the normalized spatial asymmetry

$$\mathcal{A} = \frac{P_{\text{up}} - P_{\text{down}}}{P_{\text{up}} + P_{\text{down}}}$$

was, of course, reproduced. Remarkably, the relative phases of the low- and high-energy sinusoids shown in Fig. 1(b) were also well reproduced. The magnitude

of \mathcal{A} at these two energies, however, was not — theory underestimated it in both cases.

Although the level of agreement we obtained meets or exceeds most any found in the strong-field literature, we wanted to resolve these discrepancies and obtain truly good quantitative agreement — as should be possible for this simple system. In our follow-up paper [R3], we seek to address the biggest remaining differences between the theoretical and experimental conditions: (i) the greater intensity used in the experiment and (ii) the deviation of the experimental pulse from Gaussian.

Figure 2(a) shows the magnitude of \mathcal{A} calculated for a Gaussian pulse to higher peak intensities than in Pub. [P4]. Since including ionization in a code that already treats nuclear vibration and rotation is a challenge not yet met by anyone, we put our effort into including more electronic channels and estimat-

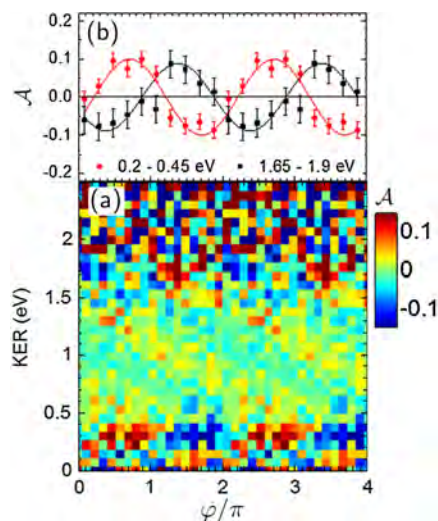


Figure 1: (a) The normalized asymmetry $\mathcal{A}(E, \varphi)$. (b) The asymmetry parameter integrated over the indicated energy regions, fit to sinusoidal curves (see the text). (From Pub. [P4].)

ing the theoretical error bars at these higher intensities [R3]. It is clear from the figure that the error bars grow rapidly, but it is also clear that the degree of asymmetry does not grow monotonically with intensity. Therefore, while performing the calculation at the correct intensity is important, it does not explain the greater asymmetry seen in the experiment and actually makes the agreement worse. The full energy-dependent \mathcal{A} in Fig. 2(b), however, shows definite qualitative agreement with the experiment (up to an overall constant shift in the CEP φ).

To address the second point above, we used a more realistic pulse in the TDSE. Unfortunately, only the experimental pulse’s power spectrum was available. Assuming a flat spectral phase, we computed the time-dependent field $\mathcal{E}(t)$ to use in the TDSE.

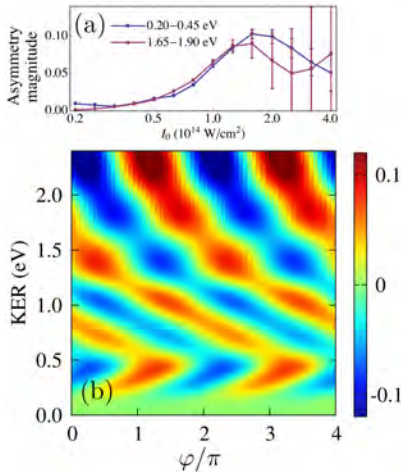


Figure 2: (a) The calculated magnitude of \mathcal{A} as a function of the peak intensity I_0 of a Gaussian laser pulse under the conditions of the experiment in Fig. 1. The two curves denote KER integrations to match Fig. 1. The error bars represent the estimated theoretical errors [R3]. (b) The full energy dependence of \mathcal{A} at $I_0=4\times 10^{14}$ W/cm². (Adapted from Ref. [R3].)

Figure 3(c) shows that the pulse was indeed not Gaussian. The other panels in the figure show the theoretical observables for this pulse. The significant changes seen in Figs. 3(b) and 3(d) upon comparison with Fig. 2 reveal that \mathcal{A} is very sensitive to the exact shape of the laser pulse. The intensity dependence of the magnitude of \mathcal{A} is still not monotonic, but the error bars are smaller. In the end, though, we cannot escape the fact that making the theory more faithful to the conditions of the experiment has, in fact, made the agreement with experiment worse.

Future plans

Obviously, substantial gaps in our understanding of even this simple system remain and more work is required to fill them in. We will work with the experimentalists to obtain better characterizations of the experimental conditions, and we will work to improve the calculations themselves.

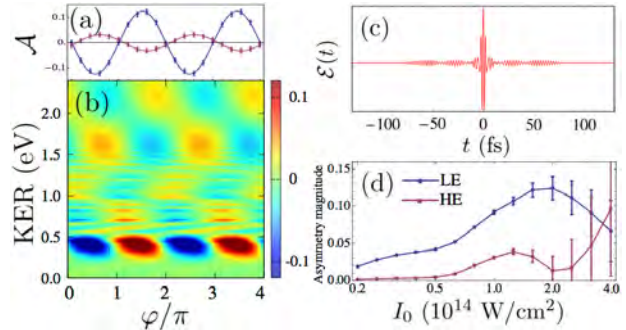


Figure 3: Calculations using a more realistic pulse. (a) \mathcal{A} at $I_0=1.6\times 10^{14}$ W/cm² for the low-energy (LE) and high-energy (HE) KER cuts to match experiment (same as in Fig. 2). (b) The full energy dependence of \mathcal{A} at the same I_0 as (a). (c) The pulse’s electric field $\mathcal{E}(t)$ calculated from the measured power spectrum assuming a flat spectral phase and $\varphi=0$. (d) The I_0 dependence of the magnitude of \mathcal{A} in the two energy cuts. (Adapted from Ref. [R3].)

Post-pulse alignment and the axial recoil approximation

Recent Progress

In understanding the fragmentation dynamics of molecules in strong fields, it is very often assumed that the fragmenting nuclei do not rotate about their common center of mass. This approximation, the axial recoil approximation, is valid when the radial kinetic energy is much higher than the rotational kinetic energy. In many strong-field processes, however, this condition is not fulfilled or only marginally met. Given its widespread use, it is therefore important to test its limits more quantitatively.

We had investigated the axial recoil approximation previously [R7] for $H_2^+ + n\omega \rightarrow p + H$ in 800-nm

pulses, concluding that it can indeed fail as quantified by the change in $\langle \cos^2 \theta \rangle(t)$ from the end of the pulse to $t \rightarrow \infty$ — *i.e.* $\Delta \langle \cos^2 \theta \rangle$. The failure was especially acute for short pulses due to impulsive alignment of the dissociating fragments.

We recently revisited this question [R4] to see whether the conclusions change for longer wavelengths. We found, for example, that for $H_2^+(v=9, J=0)$ in a 1600-nm, 3-cycle (~ 15 -fs) pulse, that post-pulse rotation is significant with a nearly 15% relative change in $\Delta \langle \cos^2 \theta \rangle$. Of course, H_2^+ is the lightest molecule and thus rotates most easily. To test the impact of mass on the results, we increased

the mass in the calculations while keeping the electronic structure fixed to isolate the effect of mass. We also chose the initial vibrational state to keep the initial energy as constant as possible. We found that the relative change in $\Delta\langle\cos^2\theta\rangle$ actually increased with mass through the three physical isotopes before slowly decreasing through the unphysical isotopes—not until the mass increases $35\times$ to the “Cl₂” case does $\Delta\langle\cos^2\theta\rangle$ drop to 10%.

Given that $\langle\cos^2\theta\rangle$ is an average quantity, however, its change does not give the whole story. We thus show in Fig. 4 the angular distributions of the fragments in a few cases at the end of the pulse ($t = t_f$) and at the detector ($t \rightarrow \infty$). While there is correlation between $\Delta\langle\cos^2\theta\rangle$ and the change in the angular distribution, the angular distribution can show even more dramatic changes, especially for 1600 nm where strongly directional features both appear and disappear in time after the pulse. Thus, applying the axial recoil approximation in these cases could certainly lead to incorrect conclusions.

Future Plans

We will continue to explore the limits of the axial recoil approximation in strong-field processes—how

it depends on the electronic structure, whether there are any experimentally measurable signatures of its breakdown, and how we can more accurately predict its breakdown in general. This is not a high-priority project for us, however, but it does serve as a good warm-up project for a new group member.

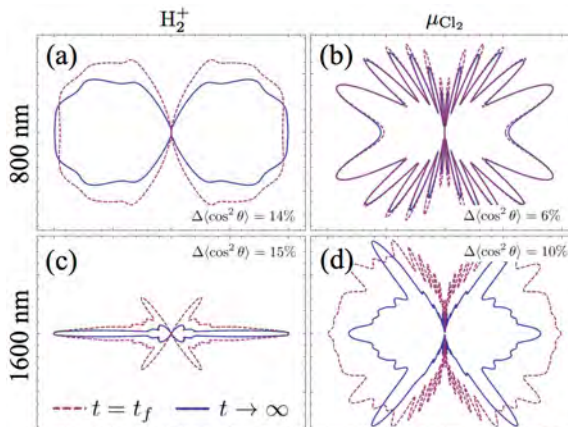


Figure 4: Angular distributions at the end of the pulse ($t = t_f$) and at the detector ($t \rightarrow \infty$) of the p +H fragments produced from H_2^+ by 3-cycle pulses at 800 nm and 1600 nm at the intensity $5 \times 10^{13} \text{ W/cm}^2$. (Adapted from Ref. [R4].)

Strong-field coherent control over charge exchange

Recent Progress

Alkali-halides have long been studied in ultrafast chemistry [R8] in large part because they have a simple—but intriguing—structure. For most IR-driven coherent control purposes, only their lowest two Born-Oppenheimer potentials need be considered. But, as shown in Fig. 5(a) for LiF, these potentials have a characteristic avoided crossing at relatively large distances between the ionic and covalent channels that is ideal for controlling the non-Born-Oppenheimer transitions—and thus the branching ratio of the products.

We have carried out pump-probe calculations for LiF with precisely this goal in mind [R9]. In these exploratory calculations, we solved the TDSE neglecting rotation, but including the full non-Born-Oppenheimer coupling between the channels. Our 14.1-fs, 8.2-eV, Gaussian pump pulse promoted the ground vibrational state to the excited electronic channel via a one-photon transition. The resulting wavepacket passed through the avoided crossing at ~ 13.5 a.u. after ~ 66 fs, leading to 86% returning to Li+F with the remaining 14% as $\text{Li}^+ + \text{F}^-$. Most of the wavepacket thus underwent a nonradiative transition at the crossing.

We probe the dissociating wavepacket with a two-

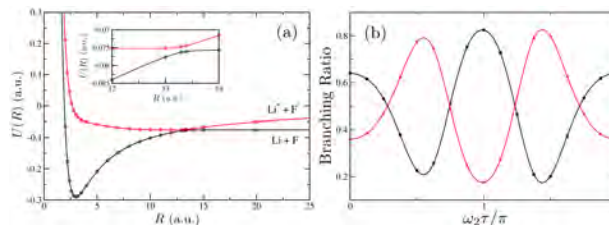


Figure 5: (a) Lowest two adiabatic potential energy curves for LiF. Symbols: values calculated by Werner and Meyer [R10]; solid lines: the fit we constructed. (b) Branching ratios of dissociation into Li+F (black) and $\text{Li}^+ + \text{F}^-$ (red) as a function of the delay τ between the two colors (789 nm and 811 nm) of the probe pulse which arrives 66 fs after the pump pulse. (Adapted from Ref. [R9].)

color, 14.1-fs, 1×10^{12} -W/cm², Gaussian pulse 66 fs after the pump while the wavepacket is at the crossing. Since calculations with a single-color probe pulse convinced us that Raman transitions were primarily responsible for controlling the branching ratio, we chose the two colors to be $\lambda_1 = 789$ nm and $\lambda_2 = 811$ nm since their difference would then lie within the pump-pulse bandwidth—and thus within the energy distribution of the wavepacket—providing ample opportunity for interference between quantum pathways. Moreover, the delay τ between the two colors provided the means to control their relative phase. The

results, shown in Fig. 5(b), are that we can indeed exert significant control over the branching ratio. Specifically, we can effectively reverse the branching ratio from the no-probe case and force the system to favor the $\text{Li}^+ + \text{F}^-$ channel more than 80% of the time. We can thus control charge exchange in the strong-field regime.

Future Plans

We will repeat these calculations with nuclear ro-

tation included to confirm that the degree of control we obtained is not an artifact of the reduced dimensionality. To gauge whether this control will be possible experimentally, we will also need to average over intensity and possibly over the initial rotational distribution for this relatively heavy system. We will also work with Ben-Itzhak's experimental group—since they can potentially perform a kinematically complete measurement of this process—to identify experimentally convenient pulse parameters.

References

- [R1] F. Anis and B. D. Esry, *Phys. Rev. A* **77**, 033416 (2008).
- [R2] I. Ben-Itzhak, P. Q. Wang, J. F. Xia, A. M. Sayler, M. A. Smith, K. D. Carnes, and B. D. Esry, *Phys. Rev. Lett.* **95**, 073002 (2005).
- [R3] S. Zeng, N. G. Kling, T. Rathje, A. M. Sayler, K. J. Betsch, M. Zohrabi, F. Anis, U. Ablikim, B. Jochim, Z. Wang, M. Kübel, P. Wustelt, H. Figger, G. G. Paulus, M. F. Kling, K. D. Carnes, I. Ben-Itzhak, and B. D. Esry (in preparation).
- [R4] S. Zeng, Ph.D. thesis, Kansas State University (2015).
- [R5] V. Roudnev and B. D. Esry, *Phys. Rev. Lett.* **99**, 220406 (2007).
- [R6] J. J. Hua and B. D. Esry, *J. Phys. B* **42**, 085601 (2009).
- [R7] F. Anis, T. Cackowski, and B. D. Esry, *J. Phys. B* **42**, 091001 (2009).
- [R8] A. H. Zewail, *J. Phys. Chem. A* **104**, 5660 (2000).
- [R9] B. Rigsbee, Master's thesis, Kansas State University (2015).
- [R10] H.-J. Werner and W. Meyer, *J. Chem. Phys.* **74**, 5802 (1981).

Publications of DOE-sponsored research in the last 3 years

- [P1] F. Anis and B. D. Esry, “Enhancing the intense field control of molecular fragmentation,” *Phys. Rev. Lett.* **109**, 133001 (2012).
- [P2] C. B. Madsen, F. Anis, L. B. Madsen, and B. D. Esry, “Multiphoton above threshold effects in strong-field fragmentation,” *Phys. Rev. Lett.* **109**, 163003 (2012).
- [P3] J. McKenna, A. M. Sayler, B. Gaire, N. G. Kling, B. D. Esry, K. D. Carnes, and I. Ben-Itzhak, “Frustrated tunnelling ionization during strong-field fragmentation of D_3^+ ,” *New J. Phys.* **14**, 103029 (2012).
- [P4] N. G. Kling, K. J. Betsch, M. Zohrabi, S. Zeng, F. Anis, U. Ablikim, B. Jochim, Z. Wang, M. Kübel, M. F. Kling, K. D. Carnes, B. D. Esry, and I. Ben-Itzhak, “Carrier-envelope phase control over pathway interference in strong-field dissociation of H_2^+ ,” *Phys. Rev. Lett.* **111**, 163004 (2013).
- [P5] T. Rathje, A. M. Sayler, S. Zeng, P. Wustelt, H. Figger, B. D. Esry, and G. G. Paulus, “Coherent control at its most fundamental: Carrier-envelope-phase-dependent electron localization in photodissociation of a H_2^+ molecular ion beam target,” *Phys. Rev. Lett.* **111**, 093002 (2013).
- [P6] J. Wu, M. Kunitski, M. Pitzer, F. Trinter, L. P. H. Schmidt, T. Jahnke, M. Magrakvelidze, C. B. Madsen, L. B. Madsen, U. Thumm, and R. Dörner, “Electron-nuclear energy sharing in above-threshold multiphoton dissociative ionization of H_2 ,” *Phys. Rev. Lett.* **111**, 023002 (2013), although my name does not appear, C.B. Madsen was a postdoc in my group.
- [P7] A. M. Sayler, J. McKenna, B. Gaire, N. G. Kling, K. D. Carnes, B. D. Esry, and I. Ben-Itzhak, “Elucidating isotopic effects in intense ultrafast laser-driven D_2H^+ fragmentation,” *J. Phys. B* **47**, 031001(FTC) (2014).
- [P8] L. Graham, M. Zohrabi, B. Gaire, U. Ablikim, B. Jochim, B. Berry, T. Severt, K. J. Betsch, A. M. Summers, U. Lev, O. Heber, D. Zajfman, I. D. Williams, K. Carnes, B. D. Esry, and I. Ben-Itzhak, “Fragmentation of CD^+ induced by intense ultrashort laser pulses,” *Phys. Rev. A* **91**, 023414 (2015).
- [P9] U. Lev, L. Graham, C. B. Madsen, I. Ben-Itzhak, B. D. Bruner, B. D. Esry, H. Frostig, O. Heber, A. Natan, V. S. Prabhudesai, D. Schwalm, Y. Silberberg, D. Strasser, I. D. Williams, and D. Zajfman, “Quantum control of photodissociation using intense, femtosecond pulses shaped with third order dispersion,” *J. Phys. B* **48**, 201001(FTC) (2015).

Controlling rotations of asymmetric top molecules: methods and applications

Vinod Kumarappan

James R. Macdonald Laboratory, Department of Physics

Kansas State University, Manhattan, KS 66506

vinod@phys.ksu.edu

Program Scope

The goal of this program is to improve molecular alignment methods, especially for asymmetric top molecules, and then use well-aligned molecules for further experiments in ultrafast molecular physics. We use multi-pulse sequences for 1D alignment and orientation and 3D alignment of molecules. We have identified a single metric for 3D alignment of molecules and used it to experimentally demonstrate a multi-pulse scheme for 3D alignment of asymmetric top molecules [P3]. By using two-pulse alignment and cold molecules for high harmonic generation, we have shown that a Cooper minimum and shape resonance in nitrogen can clearly be identified in the HHG spectrum of nitrogen [P1, P2]. In this experiment we were able to extract the complete angle-dependence of the photo-ionization cross section of the molecule over a range of ~ 20 -65 eV. We have also demonstrated experimentally a multi-pulse technique (proposed by Zhang *et al.* [1]) for orienting polar molecules [P4]. Our main focus now is to further develop our method for extracting orientation-resolved information from rotational wavepacket dynamics, particularly for asymmetric top molecules.

Recent progress

Orientation-resolved measurements with asymmetric top molecules:

Traditionally, two broad classes of methods are used to make orientation resolved measurements for asymmetric top molecules. In the first, molecules are aligned using external fields so that their orientation in space is preselected before the measurement is made. These pre-selection techniques have been widely used in the ultrafast AMO community with both impulsive and adiabatic alignment of molecules using intense, non-resonant laser fields. The second type of measurement involves determining the orientation of every individual molecule after the fact using the momentum distribution of molecular fragments. Such measurements require coincident detection of fragments and, in many cases, electrons. Both techniques have been used extensively, especially for linear molecules.

For asymmetric top molecules, both pre-selection and post-selection techniques have significant limitations. Alignment of asymmetric tops, particularly under field-free conditions, is still difficult. Moreover, even 3D alignment only allows the variation of only one Euler angle because the molecules can only be rotated in the polarization plane of the laser pulses. Coincidence techniques, on the other hand require multi-particle measurements and reliance on the axial recoil approximation to determine the orientation a molecule completely. These requirements are often not met—high harmonic generation and non-dissociative ionization are important examples.

We have recently developed a third method for orientation resolved measurements that exploits the evolution of a rotational wavepacket and is particularly useful for asymmetric top molecules. We first applied this technique to characterizing HHG from a linear molecule [P2]. Mikosch *et al.* [2] and Spector *et al.* [3] have used closed related approaches for analyzing

strong-field ionization and HHG, respectively. Briefly, a short pulse launches an impulsive rotational wavepacket in rotationally cold molecules, which causes the molecular axis distribution to evolve with time after the alignment pulse is gone. A probe pulse then drives an orientation dependent process and the delay-dependent yield of a product (the molecular ion yield in the case of non-dissociative ionization by the probe, for instance) is measured. The measured signal is a convolution of the orientation dependence of the process and the time-dependent molecular axis distribution. By expanding the orientation dependence in a basis of Wigner functions, and evaluating the expectation values of these basis function using a rigid-rotor TDSE code, we construct a basis for the delay dependent signal. A least-squares fit to the data then provides us with the coefficients that determine the orientation dependence of the probe process. By varying the experimental parameters in the TDSE calculation (laser intensity, pulse duration and gas temperature), we determine the time-dependent molecular axis distribution as well. An outline of the algorithm is shown in Fig. 1.

This technique has several unique advantages. First, it provides the complete orientation dependence of the probe process in two Euler angles without requiring 3D alignment. Second, there is no need to break up the molecules; the axial recoil approximation is not required. Finally, the molecular axis distribution is fully characterized in the same experiment. We have used this technique to characterize the orientation dependence of harmonic generation from nitrogen and of strong -field ionization and fragmentation of ethylene. The experimental HHG and strong field ionization rates can be used with the qualitative re-scattering theory to obtain angle and energy resolved photoionization cross sections.

Orientation-resolved high-order harmonic spectroscopy:

(in collaboration with Carlos Trallero)

Our first application of the rotational wavepacket method was an HHG experiment, in which we aligned nitrogen molecules with a two-pulse sequence and then generated harmonics with a well-aligned target (at peak alignment, $\langle \cos^2 \theta \rangle$ was estimated to be 0.83) [P2]. The analysis of the delay dependent HHG signal agreed well with angle-dependent measurements in which the pump polarization was rotated with respect to probe polarization. The experiment showed clear signatures of both the shape resonance (at ~ 30 eV and a Cooper-like minimum at ~ 55 eV in the energy and angle resolved HHG spectrum. One limitation of this measurement was that it was necessary to assume that the phase of the harmonics did not depend on the angle. This assumption

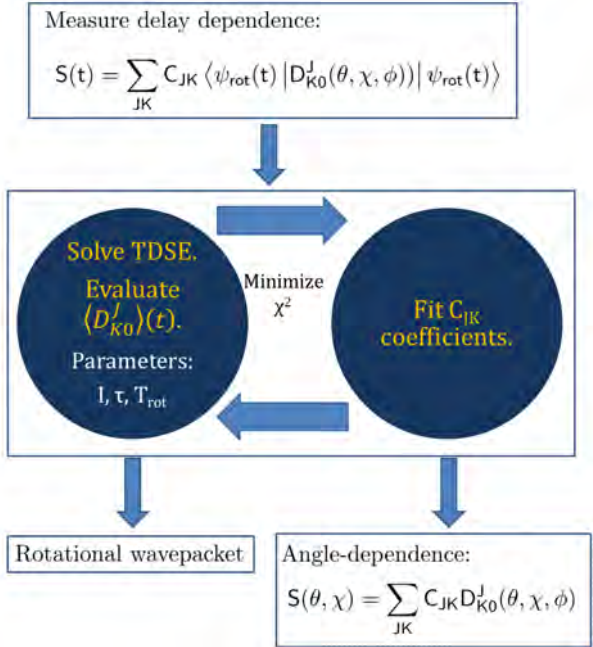


Figure 1: The algorithm for extracting the the angle dependence of an observable S from a pump-probe measurement following a non-resonant pump that launches a rotational wavepacket. The wavepacket itself is determined by the pump pulse duration and intensity, and the rotational temperature. The angle dependence of S is expanded in a Wigner function basis, and the expansion coefficients are determined by a least-squares fit to the delay-dependent data $S(t)$.

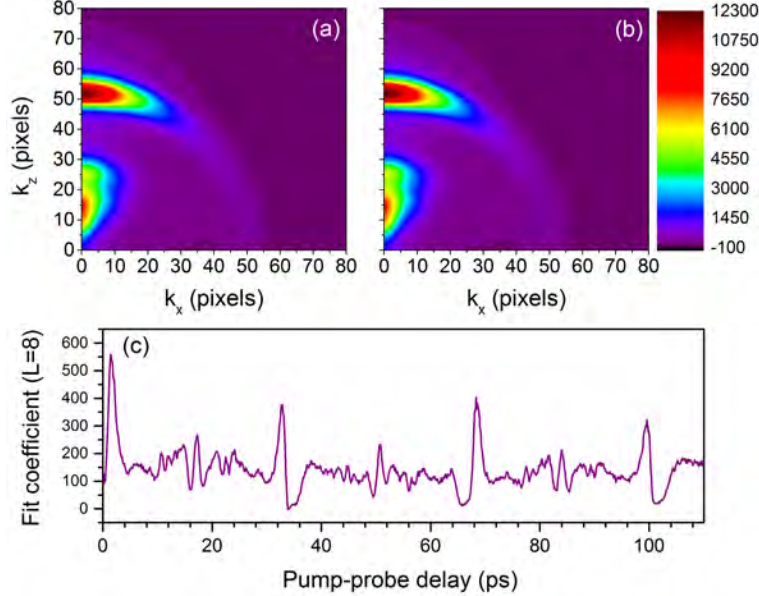


Figure 2: (a) Momentum distribution of I^+ ions measured with a VMI spectrometer. (b) pBasex fit to the data shown in (a). (c) The delay dependence of the $L = 8$ in the Legendre polynomial expansion of the angular of the high energy channel.

is not unreasonable for HHG from the HOMO in nitrogen, but is expected to be a limitation in general.

In order to overcome this limitation, a two-source experiment that measures both phase and amplitude of the harmonics is in progress. Initial results for HHG from ethylene are promising, and we expect that we will be able to extract both angle-dependent phase and amplitude from the data. HHG measurements from ethylene without phase information yield either a poor fit (when a uniform phase is assumed) or do not provide a unique solution (when phase is included in the fitting).

Momentum distributions in the molecular frame:

A more complex and information-rich application of the wavepacket method would be to analyze the momentum spectra of ions or electrons. With photoelectron momentum spectra measured as a function of delay after a pump pulse, we aim to extract molecular frame photoelectron angular distributions from such measurements. We have developed an algorithm for analyzing the data and carried out preliminary experiments for both electron and ion momentum spectra using a velocity map imaging spectrometer. The electron measurements for nitrogen molecules used either an 800 nm or a 1300 nm pulse for ionization. The ion momentum measurements were done with methyl iodide, where the momentum distribution of I^+ fragments was recorded.

In both cases we Abel-invert the 2D momentum spectra and reconstruct the axially-symmetric 3D momentum spectrum using the pBasex algorithm [4], which uses a radial and angular basis set for the 3D momentum distribution. Each coefficient in this expansion can then be analyzed using the same fitting procedure we use for the ionization measurement. An example is shown in Fig. 2. The top panels show measured momentum spectrum of I^+ ions from methyl iodide and the pBasex fit. The bottom panel shows delay dependence of the $L = 8$ coefficient of the Legendre polynomial expansion of the high energy channel in the image (at $k = 50-65$ pixels). By analyzing

such data using the algorithm shown in Fig. 2, we expect to be able to extract molecular frame angular distributions of ions as well as electrons.

Future plans:

We believe that extracting angular information from rotational wave packets is a powerful new tool, particularly when applied to asymmetric tops. We plan to continue our efforts to apply this technique to a wider range of experiments, including molecular frame photoelectron angular distribution measurements. These experiments have the potential to provide us fully orientation resolved measurements of photoelectrons from asymmetric tops.

Publications from DOE-funded research:

- [P1] X. Ren, V. Makhija, A.-T. Le, J. Tross, S. Mondal, C. Jin, C. Trallero and V. Kumarappan, “Shape Resonance and Cooper Minimum in High Harmonic Generation from Strongly Aligned Nitrogen”, In CLEO: 2013, JTh2A.11. San Jose, California: Optical Society of America, 2013.
- [P2] X. Ren, V. Makhija, A.-T. Le, J. Troß, S. Mondal, C. Jin, V. Kumarappan and C. Trallero-Herrero, “Measuring the angle-dependent photoionization cross section of nitrogen using high-harmonic generation”, *Physical Review A* 88, 043421 (2013).
- [P3] X. Ren, V. Makhija, V. Kumarappan, “Multipulse Three-Dimensional Alignment of Asymmetric Top Molecules”, *Physical Review Letters* 112, 173602 (2014).
- [P4] X. Ren, V. Makhija, H. Li, M. F. Kling, V. Kumarappan, “Alignment-assisted field-free orientation of rotationally cold CO molecules”, *Physical Review A* 90, 013419 (2014).
- [P5] J. Yang, V. Makhija, V. Kumarappan, M. Centurion, “Reconstruction of three-dimensional molecular structure from diffraction of laser-aligned molecules”, *Structural Dynamics* 1, 044101 (2014).
- [P6] Benjamin Langdon, Jonathan Garlick, Xiaoming Ren, Derrek J. Wilson, Adam M. Summers, Stefan Zigo, Matthias F. Kling, Shuting Lei, Christopher G. Elles, Eric Wells, Erwin D. Poliakov, Kevin D. Carnes, Vinod Kumarappan, Itzik Ben-Itzhak, and Carlos A. Trallero-Herrero, “Carrier-envelope-phase stabilized terawatt class laser at 1 kHz with a wavelength tunable option,” *Opt. Express* 23, 4563-4572 (2015).

References:

- [1] S. Zhang *et al.*, *Phys. Rev. A* **83**, 043410 (2011).
- [2] J. Mikosch *et al.*, *J. Chem. Phys.* **139**, 024304 (2013).
- [3] L. S. Spector *et al.* *Nature Communications* **5**, 3190 (2014).
- [4] G. A. Garcia, L. Nahon and I. Powis, *Rev. Sci. Instrum.* 75, 4989 (2004).

Strong field rescattering physics and attosecond physics

C. D. Lin

J. R. Macdonald Laboratory, Kansas State University
Manhattan, KS 66506
e-mail: cdlin@phys.ksu.edu

Program Scope:

We investigate the interaction of ultrafast intense laser pulses, and of attosecond pulses, with atoms and molecules. Most notable accomplishments in the past year are: (1) Waveform synthesis for optimizing high-order harmonic generation towards the water-window region; (2) Imaging polyatomic molecules using laser-induced electron diffraction; (3) Benchmark attosecond pulses characterization. Additional results and plans for the coming year will be summarized.

Introduction

When an atom or molecule is exposed to an intense infrared laser pulse, an electron which was released earlier may be driven back by the laser field to recollide with the parent ion. The recollision of electrons with the ion can be described by the quantitative rescattering theory (QRS) established in 2009 under this program. The QRS theory has been the backbone of our theoretical tools for studying rescattering phenomena in strong field physics. Below are specific progress made in the last year.

1. Waveform synthesis for optimizing high-order harmonic generation

Recent progress

Bright, coherent light sources over a broad electromagnetic spectrum are always in great demand for physical sciences. Today such sources are available only at large synchrotron and free-electron X-ray lasers facilities. Through high-order harmonics generation (HHG), a broadband coherent light can be generated with intense infrared or mid-infrared lasers, but the conversion efficiency of HHG is quite small. In the last two years we have devoted great effort at addressing efficient ways to enhance high-harmonic yields as well as extending harmonics towards the water-window region. The harmonics are enhanced by using two- or three-color lasers where the intensity and phase of each color are optimized to achieve highest yields for a predetermined spectral range. The optimization method was first introduced in a paper in Nature Communications (Pub. A10) where it was shown that proper choices of laser parameters would allow the enhancement of harmonics by two orders. As a follow-up, in a report in Sci. Rept. [Pub. A5], we addressed the optimal route to achieve highest harmonic yields by using an intense long-wavelength laser and a small amount of its third harmonic. We have also investigated conditions for optimizing phase-matching of harmonics inside a gas-filled hollow fiber, in a paper published in Phys. Rev. Lett. [Pub. A2], such that harmonics generated are well-focused along the propagation direction. Such harmonics are useful directly for experiments since no refocusing is needed. In this paper, we also illustrated how phase matching is achieved in a delicate way through diffraction and dispersion compensations.

We have also demonstrated that waveform synthesis is an extreme example of coherent control where harmonics can be dramatically manipulated by changing the electric field of the laser pulse. We demonstrated in Pub. A7 that it is possible to adjust the relative phase, the chirp and the relative intensity of each color in a three-color synthesized pulse consisting of 800nm laser and its second and third harmonics, such that only one single harmonic is primarily generated. This has applications when a table-top, near-monochromatic intense high harmonic is needed for applications.

Ongoing projects and future plan

Efficient waveform synthesis requires lasers with very stable phases. A number of experimental groups are making good progress on this front, including the one at JRM. We will work closely with experimental groups to provide optimal parameters for their experiments. In the coming year, we will optimize the generation of single attosecond pulses with two- or three-color pulses. In Pub. A9 we have already shown that longer pulses can be used to generate single attosecond pulses. This would reduce the demand for experimentalists to use extreme short pulses and enable them to generate stronger single attosecond pulses. Another possible method to generate intense single attosecond pulses is to use high pressure gas with high laser intensities. While plasma defocusing may reduce the cutoff energies, the plateau harmonics yields are increased and harmonics are greatly blue-shifted. This may lead to continuum spectra that would appear as single attosecond pulses.

2. Laser-induced electron diffraction from aligned polyatomic molecules*Recent progress*

The basic theory of laser-induced electron diffraction (LIED) was established in our earlier paper [Xu et al., Phys. Rev. A82, 033403 (2010)] where we have established the condition for self-imaging interatomic separations of a molecule with mid-infrared lasers. The first proof-of-principle experiment was reported in 2012 [Blaga et al, Nature 483, 194 (2012)] for diatomic N₂ and O₂ molecules using 2 μm lasers at Ohio State University. For larger molecules where the ionization potential is smaller, even longer wavelength lasers are needed to fulfill the condition. In the last year and half, we have been collaborating with the experimental group of Professor Jens Biegert in Barcelona. Using 160 kHz, 3.1 μm laser and COLTRIM, they have been able to generate high-energy photoelectron spectra of acetylene (C₂H₂) which are prealigned or anti-aligned. The COLTRIM allows them to measure high-energy photoelectron spectra in coincidence with the molecular ions. Based on the coincidence data of C₂H₂⁺, the bond lengths of C-C and of C-H have been extracted which are in good agreement with the known equilibrium distances. It is interesting to mention that the scattering data were accurate enough to retrieve the C-H distance, a unique feature of LIED since lower-energy backscattered electrons are used to take the diffraction image. This work has been published in Nature Comms. [Ref. A3].

The recent success of LIED from aligned polyatomic molecules motivated us to place greater emphasis on developing better tools for retrieving molecular structures from aligned complex molecules. During this period, working with a visiting graduate student Chao Yu from China, a method similar to what was used by Martin Centurion's group for retrieving molecular bond lengths from partially 1D aligned molecules in conventional electron diffraction (CED) was developed. With this method, 2D information about the molecules can be obtained from 1D aligned symmetric polyatomic molecules. The method has been tested based on diffraction images generated from theoretical calculations. A manuscript submitted to Sci. Report has been accepted for publication [Pub. A1].

Ongoing projects and future plan

We are waiting for LIED experiments from 1D aligned symmetric polyatomic molecules and our collaborators in Barcelona definitely will get into it. At this stage, the collaboration has been devoted to analyzing additional data from previous C₂H₂ experiments that result in C₂H⁺+ H⁺. Analysis so far supports a stretched C-H bond but with the C-C bond remains nearly the same. Additional molecules such as CS₂ have also been taken and analysis of these data are still going on. More LIED experiments are coming out. In fact, we are collaborating with Professor Ueda's group in Japan on benzene targets now.

3. Benchmarking methods of attosecond pulses characterization

Recent progress

Last year we began to examine methods of characterizing single attosecond pulses (SAP) that are in use today. The methods are typically based on measuring photoelectron spectra (by the XUV attosecond pulses), called spectrogram, of atoms in the presence of a delayed IR or NIR laser pulse. The often-used one is called FROG-CRAB, which is a generalization of FROG used for ultrashort femtosecond lasers. However, the FROG-CRAB is based on the assumption that the spectrogram can be described by the strong field approximation (SFA) for describing laser-dressed photoionization. However, it is well-known that SFA fails to describe photoelectron momentum spectra. In addition, in FROG-CRAB, photoionization cross sections are assumed to be constant within the spectral range of the SAP. An alternative method called PROOF was proposed by Zenghu Chang's group. This method is also started with SFA, and was supposed to be applied to shorter attosecond pulses (or broadband). For PROOF the IR intensity is assumed to be weak such that only the first-order correction from the IR is considered. Both FROG-CRAB and PROOF intrinsically are approximate theories, thus the retrieved SAP pulses, including phase and amplitude, have errors that have never been evaluated.

Our conclusion on FROG-CRAB is that the method is reasonable accurate if the dipole matrix element in the spectral region of the SAP is relatively smooth, such as in Ne, and the pulse is not highly chirped. The method cannot be applied to regions where the photoelectron energy is a few eV's above the ionization threshold. The PROOF method does not work well in general, but a scattering wave based PROOF, called swPROOF works well, if the IR intensity is held below 10^{12} W/cm², see Pub. A4.

Ongoing projects and future plan

If the phase of the SAP is accurately retrieved, then both FROG-CRAB and sw-PROOF in principle can be used to extract the phase of the transition dipole moment. This is the underlying method for extracting the so-called time delays in photoionization. We have examined the accuracy of this procedure. The conclusion so far shows that the accuracy of such retrievals is limited, causing the so-called time delays reported in experiments so far questionable. Further investigations are underway to see if we can find another method such that atomic dipole phase can be accurately retrieved. If this is possible, the method may be generalized to extract the phase of a wave packet. The phase retrieval so far has been limited to XUV photons with energies below 100 eV. In view of attosecond pulses with photon energies in the 200-400 eV region are coming out, we will test the retrieval methods for such pulses in the coming year.

Publications

A. Published and accepted papers (2014- present)

A1. Chao Yu, Hui Wei, Xu Wang Anh Thu Le, Ruifeng Lu, and C. D. Lin, "Reconstruction of two-dimensional molecular structure with laser-induced electron diffraction from laser-aligned polyatomic molecules", Sci. Repts. (accepted)

A2. Cheng Jin, Gregory J. Stein, Kyung-Han Hong and C. D. Lin, "Generation of Bright, Spatially Coherent Soft X-Ray High Harmonics in a Hollow Waveguide Using Two-Color Synthesized Laser Pulses", Phys. Rev. Lett. 115, 043901 (2015).

A3. Michael Pullen, Benjamin Wolter, Anh-Thu Le, Matthias Baudisch, Michaël Hemmer, Arne Senftleben, Claus Dieter Schröter, Joachim Ullrich, Robert Moshhammer, C. D. Lin, Jens Biegert,

“Imaging an aligned polyatomic molecule with laser-induced electron diffraction”, *Nature Comms.* 6, 7262 (2015).

A4. Hui Wei, Anh-Thu Le, Toru Morishita, Chao Yu, and C. D. Lin ” Benchmarking accurate spectral phase retrieval of single attosecond pulses” , *Phys. Rev. A* 91, 023407 (2015).

A5. Cheng Jin, Guoli Wang, A. T. Le and C. D. Lin, “Route to Optimal Generation of keV High-Order Harmonics with Synthesized Two-Color Laser Fields”, *Sci. Repts*, 4, 7067 (2014).

A6. Qianguang Li, Xiao-Min Tong , Toru Morishita , Cheng Jin , Hui Wei , and C. D. Lin, “Rydberg states in strong field ionization of hydrogen by 800, 1200 and 1600 nm lasers”, *J. Phys. B* 47, 204019 (2014).

A7. Xu Wang, Cheng Jin and C. D. Lin, “Coherent control of high-harmonic generation using waveform synthesized chirped laser fields”, *Phys. Rev. A* 90, 023416 (2014).

A8. A.T. Le, Hui Wei, Cheng Jin, Vu Ngoc Tuoc, Toru Morishita and C. D. Lin, “Universality of returning electron wave packet in high-order harmonic generation with mid-infrared laser pulses “, *Phys. Rev. Lett.* 113, 033001 (2014).

A9. Junliang Xu, Cosmin Blaga, K. K. Zhang, Y. H. Lai, C. D. Lin, T. Miller, P. A. Agostini and L. F. DiMauro, “ Diffraction using laser-driver broadband electron wave packets”, *Nature. Comms.* 5, 5635 (2014).

A10. Cheng Jin , Guoli Wang, Hui Wei, Anh-Thu Le, C. D. Lin , “Waveforms for Optimal sub-keV High-Order Harmonics with Synthesized Two- or Three-Color Laser Fields”, *Nature Comms.* 5, 4003 (2014).

A11. Wei-Chun Chu, Toru Morishita, and C. D. Lin, “Probing dipole-forbidden autoionizing states by isolated attosecond pulses”, *Phys. Rev. A* 89, 033427 (2014).

A12. Wei-Chun Chu, Toru Morishita and C. D. Lin, ” Probing and controlling autoionization dynamics with attosecond light pulses in a strong dressing laser field”, *Chin. J. Phys.* 52, 301 (2014).

A13. Qianguang Li, Xiao-Min Tong, Toru Morishita, Hui Wei, and C. D. Lin, “Fine structures in the intensity dependence of excitation and ionization probabilities of hydrogen atom in intense 800 nm laser pulses”, *Phys. Rev. A* 89, 023421 (2014).

B. Papers submitted for Publications

B1. Anh-Thu Le, Hui Wei, Cheng Jin, and C. D. Lin, “ Strong field approximation in high-order harmonic generation with mid-infrared lasers”, Submitted to *J. Phys. B* (Tutorial article).

B2. M. Reduzzi, W.-C. Chu, C. Feng, A. Dubrouil, F. Calegari, F. Frassetto, L. Poletto, M. Nisoli, C.-D. Lin, G. Sansone, “Attosecond control of quantum beating in electronic molecular wave packets”, submitted to *New J. Phys.*

Ultrafast Imaging of Molecular Dynamics with Lasers, Free-Electron Lasers, and Synchrotron Radiation

Daniel Rolles

J.R. Macdonald Laboratory, Physics Department, Kansas State University,
Manhattan, KS 66506, rolles@phys.ksu.edu

Program Scope: This program focuses on imaging nuclear and electronic dynamics during photochemical reactions by means of femtosecond pump-probe experiments with laboratory-based laser sources complemented by experiments with free-electron lasers and 3rd generation synchrotrons. The aim of these experiments is to study exemplary reactions in gas-phase molecules with the goal of clarifying their reaction mechanisms and pathways.

Recent Progress: Since joining the Physics Department at Kansas State University as a new assistant professor at the beginning of this year, my newly founded research group has concentrated on three main projects. We have set up and performed a pump-probe experiment with ~25 fs IR pulses in a COLTRIMS setup to investigate ultrafast nuclear wave-packet dynamics in CH₃I molecules. We have studied the UV-induced dissociation of halogenated benzenes in a time-resolved experiment at the FLASH free-electron laser in Hamburg. And we have investigated the fragmentation dynamics of halomethanes after inner-shell ionization by performing photoelectron-ion coincidence experiments at the Advanced Light Source (ALS) in Berkeley. All of these projects were performed in close collaboration with other experimentalists at JRML and, in the case of the FLASH and ALS experiments, also with a number of outside collaborators.

1) Ultrafast nuclear wave-packet dynamics in CH₃I molecules, Y. Malakar, B. Kaderiya, F. Ziaee, W.L. Pearson, K.R. Pandiri, M. Zohrabi, I. Ben-Itzhak, A. Rudenko, and D. Rolles.

Using an interferometric pump-probe scheme at JRML's 10-kHz PULSAR femtosecond laser system combined with a COLTRIMS ion momentum imaging setup, we studied the dynamics of bound and dissociating nuclear wave packets in strong-field ionized CH₃I molecules via time-resolved Coulomb explosion imaging. The evolution of different dissociation pathways was observed by measuring the kinetic energies and emission angles of coincident ionic fragments as a function of time delay between two 25-fs, 800-nm pump and probe pulses.

Figure 1 shows the delay-dependent kinetic energy release (KER) spectrum for CH₃⁺ + I⁺ ion-ion coincidences, where both bound and dissociating nuclear wave packets can be clearly distinguished. A delay-dependent structure that moves towards lower KER at longer delays originates from the Coulomb explosion of dissociating molecules with increasing internuclear dis-

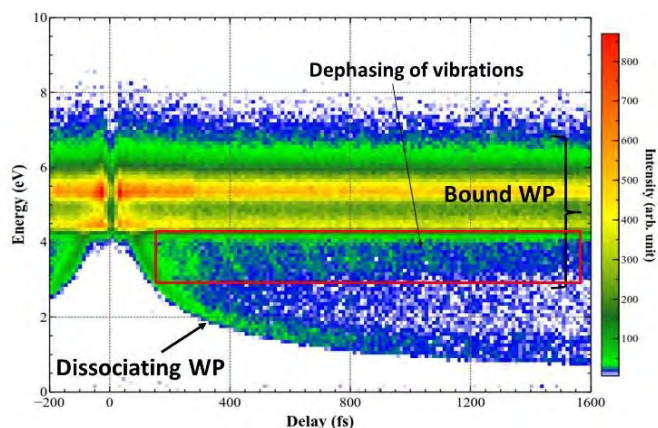


Fig. 1: Delay-dependent KER spectrum recorded for the CH₃⁺ + I⁺ channel. The intensity was 1.5×10^{14} W/cm² for both, pump and probe pulses. In addition to the descending curve corresponding to the dissociating wave packet (WP), an oscillatory structure (highlighted by the red box) is seen that corresponds to vibrational motion of the bound wave packet.

tance. In addition, an oscillatory feature in the bound wave packet is observed that slowly fades with increasing delays [1]. The frequency of the oscillation corresponds to C-I stretching vibrations in the lowest cationic state. Interestingly, the oscillation shows a dephasing at larger delays, possibly due to coupling to different degrees of freedom (e.g. the “umbrella mode”) or due to frequency differences within the vibrational wave packet.

We have since employed the same experimental technique to study nuclear wave-packet dynamics in diiodomethane (CH_2I_2), and are currently setting up for an new measurement on CH_3I , where we will use the third harmonic of the PULSAR laser beam at 266 nm as a pump in order to excite the molecules into a neutral dissociative state which we will then probe with an intense 800-nm pulse as described above.

2) Three-color pump-probe experiments at the FLASH free-electron laser, E. Savelyev¹, R. Boll¹, C. Bomme¹, B. Erk¹, S. Techert¹, J. Küpper¹, M. Brouard², A. Rouzee³, N. Berrah⁴, R. Moshhammer⁵, H. Stapelfeldt⁶, A. Rudenko, and D. Rolles; ¹DESY, Hamburg, Germany; ²Oxford University, UK; ³Max-Born-Institut, Berlin, Germany; ⁴University of Connecticut; ⁵Max Planck Institute for Nuclear Physics, Heidelberg, Germany; ⁶Arhus University, Denmark.

Combining time-resolved photoelectron and ion imaging with an adiabatic molecular alignment technique, we have studied the UV-induced dissociation of 2,6-difluoriodobenzene (DFIB) using the FLASH free-electron laser (FEL). The goal of the experiment was to observe the iodine-carbon bond cleavage by recording fragment ion momentum images and inner-shell photoelectron angular distributions in the frame of the aligned molecules as a function of pump-probe delay between the 266-nm UV-pump and the 11-nm FEL-probe pulse.

The DFIB molecules were introduced into the vacuum as a pulsed molecular beam, adiabatically aligned with nanosecond Nd:YAG laser pulses, dissociated with femtosecond UV pulses, and then ionized with the 11-nm FEL pulses from FLASH. The photoelectrons and fragment ions produced by the FEL pulse were measured in a double-sided velocity map imaging (VMI) spectrometer as sketched in Fig. 2.

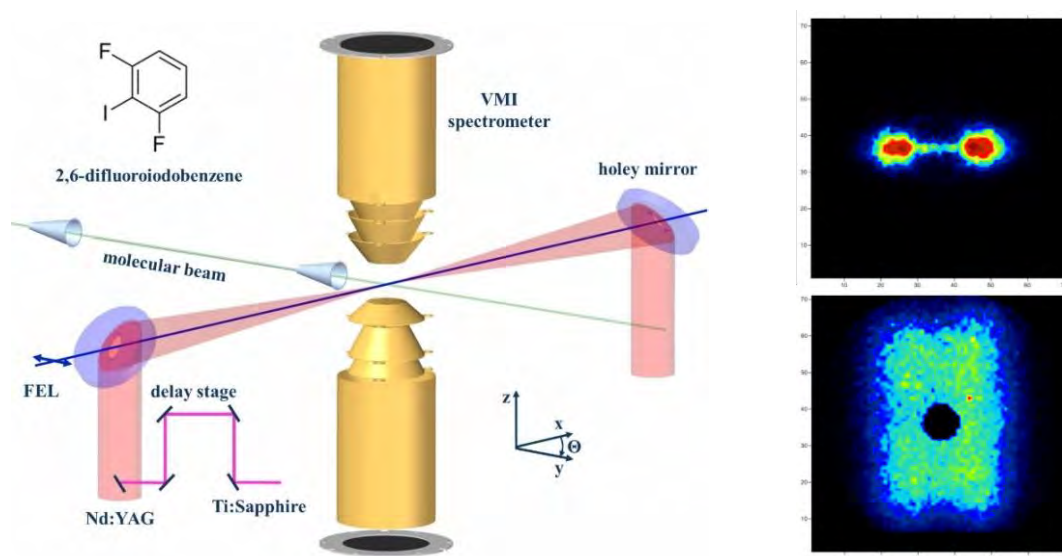


Fig. 2: Left panel: Experimental setup for our time-resolved photoelectron fragment-ion imaging experiment at FLASH. Right panels: I^+ (top) and F^+ (bottom) fragment ion images for 1-D aligned DFIB molecules. The polarization direction of the alignment laser pulse is horizontal.

When the DFIB molecules are aligned, the iodine-carbon axis is fixed along the polarization direction of the Nd:YAG laser pulses, and the I^+ fragments produced by the FEL pulse are thus emitted along this axis and can be used as a diagnostics for the degree of alignment that was obtained in the experiment [2]. Since the second molecular axis, i.e. the plane of the benzene ring, is not aligned when using linear Nd:YAG laser pulses, the F^+ fragments are emitted into two doughnut shaped distributions around the iodine-carbon axis [3].

We are currently analyzing the $I(4d)$ photoelectron angular distributions that were measured simultaneously with the ion images shown in Fig. 2 with the goal to retrieve structural information on the changing molecular geometry during the UV-induced dissociation via femtosecond photoelectron diffraction [4,5].

3) Investigating the fragmentation dynamics of halomethanes after inner-shell ionization, *U. Ablikim, B. Kaderiya, A. Rudenko, V. Kumarappan, C. Bomme¹, E. Savelyev¹, T. Osipov², H. Xiong³, N. Berrah³, and D. Rolles; ¹DESY, Hamburg, Germany; ²LCLS, SLAC National Laboratory; ³University of Connecticut.*

We have studied the fragmentation dynamics of halomethanes after inner-shell ionization by conducting photoelectron-photoion coincidence experiments with synchrotron radiation at the ALS. For this purpose, we have developed an instrument based on a double-sided velocity map imaging spectrometer equipped with two delay-line detectors that allows us to perform photoelectron-photoion coincidence experiments in the ALS multi-bunch operation mode.

From the momentum correlations between the ionic fragments that are detected in coincidence (see Fig. 3), we can draw conclusions about the sequence of the bond breaking. For the case of a concerted fragmentation, we can then link the measured angles to the initial geometry of the molecule with the help of Coulomb explosion simulations assuming pure Coulomb repulsion between point-like charges [6]. The dependence of the recoil-frame photoelectron angular distributions, which are recorded simultaneously, on the molecular geometry is currently under investigation.

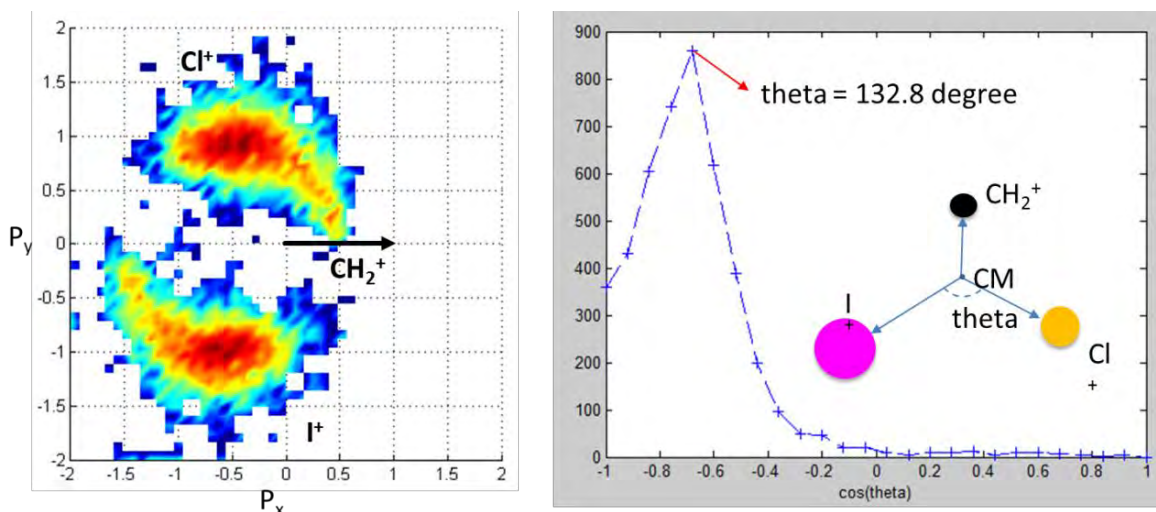


Fig 3: Left panel: Newton diagram for $CH_2^+ - I^+ - Cl^+$ triple coincidences recorded after $I(4d)$ photoionization of CH_2ICl at 107 eV photon energy. Right panel: The corresponding angle between the momentum vectors of I^+ and Cl^+ ions (right).

Future Plans:

With the light sources and techniques that we now have at our disposal, we can study the reaction dynamics of gas-phase molecules with an unprecedented spatial and temporal resolution. We will further exploit these possibilities to investigate various exemplary reactions of chemical relevance, while continuing to improve existing methods and to develop new schemes for imaging molecular dynamics with femtosecond and sub-femtosecond resolution. To this end, we are planning further pump-probe experiments with PULSAR using both, 800 and 266 nm pulses as a pump and 800 nm pulses as a probe in order to study isomerization reactions in halomethanes and haloethanes. In parallel, we will set up the instrumentation and explore the possibilities for using JRML's high-repetition rate XUV source, XUUS, for similar pump-probe studies. We will also continue our FLASH, LCLS, and ALS experiments and have approved beamtime scheduled at all three facilities in the coming year. These experiments also aim at investigating ultrafast reaction dynamics but focus on utilizing the complementary capabilities of the X-rays provided by these facilities as compared to the ultrafast laser sources available at JRML.

References:

- [1] Y. Malakar, B. Kaderiya, W.L. Pearson, K.R. Pandiri, F. Ziaee, M. Zohrabi, I. Ben-Itzhak, A. Rudenko, D. Rolles, *Nuclear Wave-Packet Dynamics in Strong-Field Ionized Iodomethane Studied by Coincident Ion Momentum Imaging*, in preparation.
- [2] R. Boll, A. Rouzée, M. Adolph, ..., D. Rolles, *Farad. Discuss.* **171**, 57-80 (2014).
- [3] I. Nevo, L. Holmegaard, J. H. Nielsen, J. L. Hansen, H. Stapelfeldt, F. Filsinger, G. Meijer, J. Küpper, *Phys. Chem. Chem. Phys.* **11**, 9912–9918 (2009).
- [4] R. Boll, D. Anielski, C. Bostedt, ..., D. Rolles, *Phys. Rev. A* **88**, 061402(R) (2013).
- [5] D. Rolles, R. Boll, M. Adolph et al., *J. Phys. B* **47**, 124035 (2014).
- [6] U. Ablikim, C. Bomme, E. Savelyev, B. Kaderiya, T. Osipov, H. Xiong, A. Rudenko, V. Kumarappan, N. Berrah, and D. Rolles, *Investigating the fragmentation dynamics of CH₂ICl after inner-shell ionization*, in preparation.

Publications from DOE sponsored research since joining the program in 2015:

1. A. Rudenko and D. Rolles, *Time-resolved studies with FELs*, *J. Electron Spectrosc. Relat. Phenom.* (in press).
2. K. Schnorr, ..., A. Rudenko, ..., D. Rolles, ..., R. Moshhammer, *Time-Resolved Study of ICD in Ne Dimers Using FEL Radiation*, *J. Electron Spectrosc. Relat. Phenom.* (in press).
3. T. Kierspel, ..., D. Rolles, A. Rudenko, ..., J. Küpper, *Strongly aligned gas-phase molecules at Free-Electron Lasers*, *J. Phys. B: At. Mol. Opt. Phys.* (in press, 2015). <http://arxiv.org/abs/1506.03650>
4. C.E. Liekhus-Schmaltz, ..., D. Rolles, A. Rudenko, ..., P.H. Bucksbaum, V.S. Petrovic, *Ultrafast Isomerization Initiated by X-Ray Core Ionization*, *Nat. Commun.* **6**, 8199 (2015).
5. T. Ekeberg, ..., D. Rolles, A. Rudenko, ..., J. Hajdu, *Three-dimensional reconstruction of the giant mimivirus particle with an X-ray free-electron laser*, *Phys. Rev. Lett.* **114**, 098102 (2015).

Electronic and Nuclear Dynamics Triggered by X-ray, XUV and Optical Excitations: Nonlinear Interactions and Ultrafast Imaging

Artem Rudenko

J. R. Macdonald Laboratory, Department of Physics, Kansas State University, Manhattan, KS 66506

rudenko@phys.ksu.edu

Program scope: The main goals of this research are (i) to understand basic physics of (non-linear) light-matter interactions in a broad span of wavelengths, from terahertz and infrared (IR) to XUV and X-ray domains, and (ii) to apply the knowledge gained for real-time imaging of ultrafast photo-induced reactions. These goals are being pursued using both, lab-based laser and high-harmonic sources, and external free-electron laser facilities. The program aims at studying light-induced phenomena in systems of increasing complexity, from isolated atoms to small and mid-size molecules, recently extending to the nanoscale particles

Recent progress:

1. X-ray interactions with matter: multiphoton ionization and charge transfer phenomena
(in collaboration with D. Rolles and Argonne National Lab group)

The development of high-intensity, short-pulsed XUV and X-ray radiation sources promises revolutionary new imaging techniques in diverse scientific fields, approaching angstrom spatial and femtosecond (or even sub-femtosecond) temporal resolution. The basic prerequisite for designing these experiments is understanding the response of individual atoms, and tracing electronic and nuclear dynamics in the vicinity of the atom that absorbed X-ray photon(s). In extended systems this sheds light on basic mechanisms of local radiation damage, and is also vital for novel phase retrieval methods at high intensities. Addressing these issues, we have recently performed a series of experiments comparing multiphoton multiple ionization of isolated atoms and similar atoms in molecular systems by intense soft X-ray (1.5-2 keV) radiation. We found that intermediate resonant excitations are crucial for our understanding of extremely high charge states observed at certain wavelengths [P2-4,15]. Applying the technique of coincident ion momentum imaging, we observed the signatures of efficient ultrafast charge redistribution from the absorbing atom to its neighbours in molecular systems [P5,6]. Since then, we performed a series of dedicated laser-pump – X-ray probe [P12,13] and XUV pump –XUV-probe [P14,P20] experiments aimed at studying the mechanisms of this charge rearrangement, in particular, electron transfer. Main developments within the last year focused on extending similar single pulse experiments into hard X-ray domain and ultra-high intensities, and on employing novel pump-probe schemes, including time-resolved photo- and Auger electron spectroscopy, and X-ray pump – X-ray probe schemes.

Since XFEL imaging experiments mentioned above ideally require angstrom wavelengths and extreme intensities ($> 10^{20}$ W/cm²) to reach atomic resolution, there is a strong need to extend basic experiments on individual atom / small molecule response into this parameter regime. Recently we have accomplished first steps in this direction by studying ionization of rare gas atoms and small polyatomic molecules by ultra-intense X-ray radiation at 5-8 keV photon energy range. The experiments were performed using the nanofocus of the coherent imaging beamline (CXI) at LCLS. Focusing few mJ, 40 fs hard X-ray LCLS pulses to a spot size less than 250 nm in diameter, we were able to reach the intensities exceeding 10^{20} W/cm², unprecedented for this photon energy range. Under these conditions we were able to strip all electrons from argon atoms, all but two 1s electrons from krypton, and reached the record 48+ charge state for xenon ionization at 8.3 keV. Even though the highest charge states is reached at the highest photon energy (8.3 keV), the wavelength dependence of the spectra shows significant overall enhancement in the production of charge states from Xe³⁰⁺ to Xe⁴⁰⁺ at the intermediate photon energies (~ 6.5 keV). Comparing the data with the simulation based on the XATOM model of R. Santra's group, we conclude that the simple sequential ionization picture needs to be modified to include resonant excitations to explain the obtained results, although the resonant effects are not as extreme as in the soft X-ray regime [P2,3].

Following the approach we developed earlier for the XUV and the soft-X-ray domains, we compared the ionization of isolated xenon atoms and iodine atoms embedded into molecular systems, and obtained first experimental results on ultrafast charge rearrangement in small and medium-size molecules. In contrast to our results in the soft X-ray regime [P5,6], the presence of molecular partners does not significantly reduce the highest charge state observed for high-Z elements in small systems. We observed I⁴⁷⁺ ions from iodomethane (CH₃I) at 8.3 keV (compared to Xe⁴⁸⁺). The most likely reason for this is a limited amount of electrons available from the neighbouring atoms, and very large photon density allowing for further ionization of partially neutralized iodine. To verify this, we collaborated on similar experiments on Xe / CH₃I at the Japanese XFEL facility SACLA, which were also performed at hard X-ray photon energies, but at much lower intensities [P18]. There, the outcome was rather similar to earlier results in the soft-X-ray domain, confirming that this is the high photon densities on target

which results in higher ionization of molecules. However, for larger systems like iodobenzene (C_6H_5I), the maximum charge state observed even at highest intensities is $\sim I^{30+}$, indicating that the charge transfer from the neighbouring atoms still plays an important role if enough electrons are present. The highest charge state of carbon, which does not directly absorb X-ray photons (C^{4+}) is in good agreement with the prediction of our charge transfer model developed in [P12,14].

Furthermore, in order to reveal the effect of the spectral and temporal shape of the X-ray pulses on X-ray induced multiphoton processes, we compared the results obtained with the regular LCLS pulses generated by the SASE scheme and with the self-seeded X-ray pulses. Whereas for isolated atoms (Xe) we observe reduced production of the highest charge states for seeded pulses, which we attribute to the suppression of resonant effects, the results on CH_3I molecules demonstrate the opposite trend (higher charge states of I), most likely because of different charge transfer dynamics resulting from narrower temporal profile of the seeded pulses.

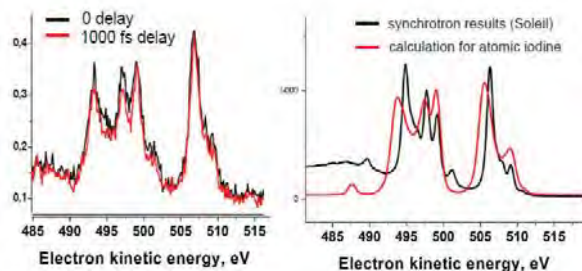


Figure 1. Iodine M-shell Auger electron spectra at 730 eV photon energy. Left: the results from the LCLS experiment on CH_3I for two different delays between the UV pump and X-ray probe pulses. Right: Measured synchrotron spectrum for CH_3I (courtesy of T. Marchenko and M. Simon, UPMC Paris) compared to the calculated distribution for the atomic iodine Performed by M. Pattanen (Synchrotron Soleil)

Whereas the ion measurements described above and employed in recent pump-probe measurements [P12-14,20] yield direct information on the distance dependence of the electronic rearrangement processes, they do not allow one to disentangle local Auger decay followed by the valence charge transfer from interatomic Auger-type processes. This would require measuring the channel-selective Auger electron spectra. As a first step in this direction, we measured molecular Auger spectra in CH_3I and CH_3F molecules dissociated by a 266 nm pulses as a function of the internuclear distance, which can be reconstructed from the ion measurements similar to earlier experiments. Fig. 1 displays the measured Auger electron spectra for iodine M-shell ionization. As can be seen from the right panel of the figure, the Auger spectrum of the CH_3I molecule clearly differs from the distribution simulated for the isolated iodine atom (slightly shifted peak positions, different relative intensities of the peaks). The LCLS CH_3I pump-probe spectrum at zero UV / X-ray delay (black line in the left panel of Fig. 1) closely resembles the synchrotron data, i.e., the spectra for the intact molecule. If, however, the molecule is dissociated by the 266 nm pulse (1000 fs delay, red line in Fig. 1 left), the branching ratio of different peaks changes towards the ones simulated for the atomic iodine, reflecting the transition towards the ionization of the isolated iodine atom.

As a next step in this direction, we performed 266 nm pump – XUV probe experiments at FLASH employing photoelectrons from I 4d ionization as an observable (effort led by D. Rolles). Furthermore, in order to get more insight into the dynamics following the inner-shell absorption in the X-ray domain, we participated in a recent two-colour X-ray pump – X-ray probe experiments at LCLS led by the Argonne National Lab group.

2. Imaging of nuclear wave packets and structural rearrangement dynamics triggered by single-photon and strong-field ionization (in collaboration with V. Kumarappan, D. Rolles and I. Ben-Itzhak)

This part of the program aims at visualizing, understanding and controlling fundamental photo-induced nuclear dynamics in small molecules, with the focus on the comparison between strong-field-induced and single photon-induced dynamics. These studies rely on coincident momentum imaging of ionic fragments combined with channel-selective Fourier spectroscopy, and employ both, IR-IR and VUV-IR pump-probe schemes. A detailed understanding of the nuclear wave packet motion gained in such experiments are also an essential prerequisite of the studies employing X-ray probes described above.

An illustrative example of such laser-triggered wave packet dynamics is given by the so-called scissors motion of halomethanes. An outcome of a pump-probe experiment revealing the details of the scissors motion in CH_2I_2 molecule is shown in Fig. 2. In Fig. 2a the delay-dependent yield of I_2^+ elimination is shown, which exhibits a pronounced oscillation of ~ 300 fs period, which approximately corresponds to the period of the scissors motion. The fast Fourier transform of this yield plotted in Fig. 2b reveals a pronounced peak at the corresponding frequency (~ 120 cm^{-1}). It appears natural that the new I-I bond is more likely formed for the minimum distance between the two I atoms. However, a second, less pronounced peak appears at 4 times higher frequency, matching well the known spectroscopic value for the frequency of the $C-I_2$ symmetric stretch.

As an example of single-photon induced nuclear wave packet dynamics, we study the dissociative ionization of molecular oxygen employing the 11th harmonic of 800 nm as a pump. The molecule excited into the the $a^4\Pi_u$ ionic state was dissociated by the IR pulse, and the reaction was probed by measuring the yield and kinetic energy

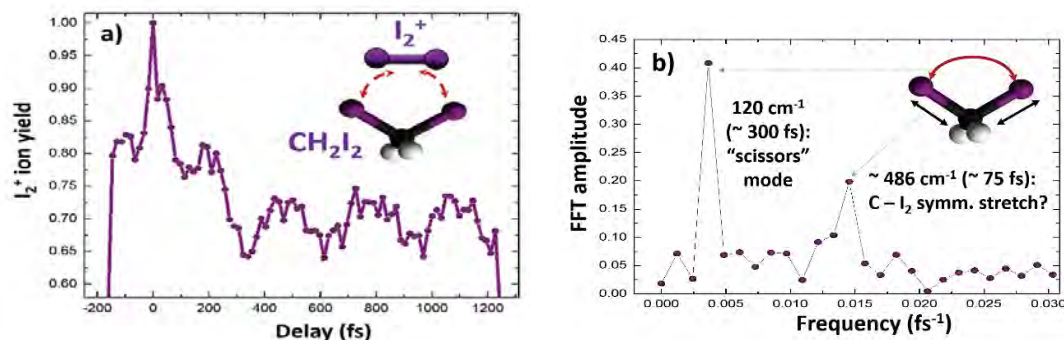


Figure 2: (a) The yield of the I_2^+ molecular ion produced from the CH_2I_2 molecule as a function of the delay between the two 800 nm, 25 fs laser pulses. (b) Fast Fourier transform (FFT) of the yield shown in (a).

spectrum of the created O^+ ions as a function of the VUV-IR delay. The results are summarized in Fig. 3, where the delay-dependent KER spectrum of O^+ ions (a) and the delay dependence of the yields of individual channels (b) are plotted. The low-energy channel results from the absorption of a single IR photon. However, the one-photon coupling between the $a^4\Pi_u$ and the dissociative $f^4\Pi_g$ states occurs at rather large R, hence a slower rise time for this channel in Fig. 3b. The high-energy channel results from the net two-photon absorption. However, the direct two-photon transition between the $a^4\Pi_u$ and $f^4\Pi_g$ states is forbidden by the dipole selection rules. Thus, this channel results from the three-photon transition and subsequent stimulated emission of one photon, similar to well-known 1ω and 2ω in H_2^+ dissociation. As the three-photon coupling occurs nearly at the Franck-Condon region of the neutral O_2 , resulting in a faster rise time of this channel. However, at larger VUV-IR delays, most of the wave packet propagates towards larger R and does not return to the region of 3-photon coupling near Franck-Condon region of VUV absorption, explaining subsequent decrease of the high KER O^+ yield.

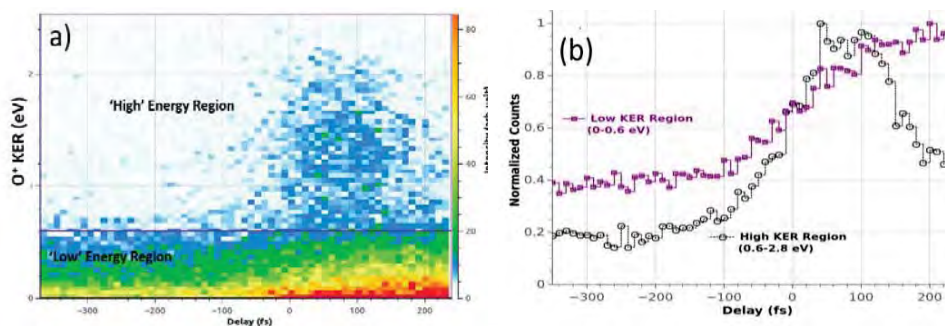


Figure 3: a) The KER spectrum of O^+ measured as a function of the VUV-IR delay. b) The measured delay-dependent yields of the low- and high-energy channels (KER below and above 0.6 eV, respectively).

Future plans

We plan to continue the research activities in both areas outlined above, and increase the internal cross-links between them. In particular, the HHG setup capable of ionizing iodine 4d shell has been built up at JRML, and will be used for the pump-probe experiments on charge transfer following the 4d absorption, which can be performed at high rep. rates and with much better time resolution compared to the FEL-based experiments. Moreover, based on the outcome of the laser-only measurements described in the previous section, we also proposed a series of experiments aimed to study the correlation between the electronic rearrangement / charge transfer processes and the bound wave packet motions. The experiments at FLASH and SACLA facilities are scheduled for the end of 2015 / beginning of 2016, and the corresponding LCLS proposal has been submitted.

Publications from the DOE-funded research (in the last 3 years):

[P1] "Single-particle structure determination by correlations of snapshot X-ray diffraction patterns", D. Starodub, A. Aquila, S. Bajt, M. Barthelmeß, A. Barty, C. Bostedt, J. D. Bozek, N. Coppola, R.B. Doak, S.W. Epp, B. Erk, L. Foucar, L. Gumprecht, C.Y. Hampton, A. Hartmann, R. Hartmann, P. Holl, S. Kassemeyer, N. Kimmel, H. Laksmono, M. Liang, N. D. Loh, L. Lomb, A. V. Martin, K. Nass, C. Reich, D. Rolles, B. Rudek, A. Rudenko, J. Schulz, R. L. Shoeman, R.G. Sierra, H. Soltau, J. Steinbrener, F. Stellato, S. Stern, G. Weidenspointner, M. Frank, J. Ullrich, L. Strüder, I. Schlichting, H. N. Chapman, J.C.H. Spence, M. J. Bogan, *Nature Communications*, 3 1276 (2012).

[P2] "Ultra-efficient ionization of heavy atoms by intense X-Rays", B. Rudek, S.-K. Son, L. M. Foucar, S. W. Epp, B. Erk, R. Hartmann, M. Adolph, R. Andritschke, A. Aquila, N. Berrah, C. Bostedt, J. Bozek, N. Coppola, F. Filsinger, H. Gorke, T. Gorkhover, H. Graafsma, L. Gumprecht, A. Hartmann, G. Hauser, S. Herrmann, H. Hirsemann, P. Holl, A. Hömke, L. Journel, C. Kaiser, N. Kimmel, F. Krasniqi, K.-U. Kühnel, M. Matysek, M. Messerschmidt, D. Miesner, T. Möller, R. Moshhammer, K. Nagaya, B. Nilsson, G. Potdevin, D. Pietschner, C. Reich,

- D. Rupp, G. Schaller, I. Schlichting, C. Schmidt, F. Schopper, S. Schorb, C.-D. Schröter, J. Schulz, M. Simon, H. Soltau, L. Strüder, K. Ueda, G. Weidenspointner, R. Santra, J. Ullrich, A. Rudenko, and D. Rolles, *Nature Photonics*, 6 858 (2012).
- [P3] “Resonance-enhanced multiple ionization of krypton at an x-ray free-electron laser”, B. Rudek, D. Rolles, S.-K. Son, L. Foucar, B. Erk, S.W. Epp, R. Boll, D. Anielski, C. Bostedt, S. Schorb, R. Coffee, J. Bozek, S. Trippel, T. Marchenko, M. Simon, L. Christensen, S. De, S. Wada, K. Ueda, I. Schlichting, R. Santra, J. Ullrich and A. Rudenko, *Phys. Rev. A.*, 87, 023413 (2013).
- [P4] “Strong-field interactions at EUV and X-ray wavelengths”, A. Rudenko, Chapter 15 in “Attosecond and Free-Electron Laser Physics”, T. Schultz and M.J.J. Vrakking, Editors, Wiley (2013).
- [P5] “Ultrafast charge rearrangement and nuclear dynamics upon inner-shell multiple ionization of small polyatomic molecules”, B. Erk, D. Rolles, L. Foucar, B. Rudek, S.W. Epp, M. Cryle, C. Bostedt, S. Schorb, J. Bozek, A. Rouzee, T. Marchenko, M. Simon, F. Filsinger, L. Christensen, S. De, S. Trippel, J. Küpper, H. Stapelfeldt, S. Wada, K. Ueda, M. Swiggers, M. Messerschmidt, C.D. Schröter, R. Moshhammer, I. Schlichting, J. Ullrich and A. Rudenko, *Phys. Rev. Lett.*, 110, 053003 (2013).
- [P6] “Inner-shell multiple ionization of polyatomic molecules with an intense x-ray free-electron laser studied by coincident ion momentum imaging”, B. Erk, D. Rolles, L. Foucar, B. Rudek, S. W. Epp, M. Cryle, C. Bostedt, S. Schorb, J. Bozek, A. Rouzee, T. Marchenko, M. Simon, L. Christensen, S. De, S. Trippel, J. Küpper, H. Stapelfeldt, S. Wada, K. Ueda, M. Swiggers, M. Messerschmidt, C. D. Schröter, R. Moshhammer, I. Schlichting, J. Ullrich and A. Rudenko, *J. Phys. B: At. Mol. Opt. Phys.*, 46, 164031 (2013).
- [P7] “Time-Resolved Measurement of Interatomic Coulombic Decay in Ne₂”, K. Schnorr, A. Senfleben, M. Kurka, A. Rudenko, L. Foucar, G. Schmid, T. Pfeifer, D. Meyer, D. Anielski, R. Boll, D. Rolles, M. Kubel, M.F. Kling, Y.H. Jiang, S. Mondal, K. Ueda, T. Marchenko, M. Simon, G. Brenner, R. Treusch, S. Scheit, V. Averbukh, J. Ullrich, C.D. Schröter, R. Moshhammer, *Phys. Rev. Lett.*, 111, 093402 (2013).
- [P8] “Ultrafast dynamics in acetylene clocked in a femtosecond XUV stopwatch”, Y H Jiang, A Senfleben, M Kurka, A Rudenko, L Foucar, O Herrwerth, M F Kling, M Lezius, J V Tilborg, A Belkacem, K Ueda, D Rolles, R Treusch, Y Z Zhang, Y F Liu, C D Schröter, J Ullrich and R Moshhammer, *J. Phys. B: At. Mol. Opt. Phys.*, 46 164027 (2013).
- [P9] “Femtosecond photoelectron diffraction on laser-aligned molecules: Towards time-resolved imaging of molecular structure”, R. Boll, D. Anielski, C. Bostedt, J. D. Bozek, L. Christensen, R. Coffee, S. De, P. Declava, S. W. Epp, B. Erk, L. Foucar, F. Krasniqi, J. Küpper, A. Rouzee, B. Rudek, A. Rudenko, S. Schorb, H. Stapelfeldt, M. Stener, S. Stern, S. Techert, S. Trippel, M.J.J. Vrakking, J. Ullrich and D. Rolles, *Phys. Rev. A.*, 8, 061402(R) (2013).
- [P10] “X-Ray diffraction from isolated and strongly aligned gas-phase molecules with a free-electron laser”, J. Küpper, S. Stern, L. Holmegaard, F. Filsinger, A. Rouzee, D. Rolles, A. Rudenko, P. Johnsson, A. V. Martin, M. Adolph, A. Aquila, S. Bajt, A. Barty, C. Bostedt, J. D. Bozek, R. Coffee, N. Coppola, T. Delmas, S. Epp, B. Erk, L. Foucar, Tais Gorkhover, L. Gumprecht, A. Hartmann, R. Hartmann, G. Hauser, P. Holl, N. Kimmel, K.-U. Kühnel, J. Maurer, M. Messerschmidt, R. Moshhammer, C. Reich, B. Rudek, R. Santra, I. Schlichting, C. Schmidt, S. Schorb, J. Schulz, H. Soltau, L. Strueder, T. Jan, M. J. J. Vrakking, G. Weidenspointner, T. A. White, C. Wunderer, G. Meijer, J. Ullrich, H. Stapelfeldt and H. N. Chapman, *Phys. Rev. Lett.*, 112, 083002 (2014).
- [P11] “Towards atomic resolution diffractive imaging of isolated molecules with X-ray free-electron lasers”, S. Stern, L. Holmegaard, F. Filsinger, A. Rouzee, A. Rudenko, P. Johnsson, A. V. Martin, A. Barty, C. Bostedt, J. Bozek, R. Coffee, S. Epp, B. Erk, L. Foucar, R. Hartmann, N. Kimmel, K.-U. Kühnel, J. Maurer, M. Messerschmidt, B. Rudek, D. Starodub, J. Thøgersen, G. Weidenspointner, T. A. White, H. Stapelfeldt, D. Rolles, H. N. Chapman and J. Küpper, *Faraday Discussions*, 171, 393 (2014).
- [P12] “Imaging charge transfer in iodomethane upon x-ray photoabsorption”, B. Erk, R. Boll, S. Trippel, D. Anielski, L. Foucar, B. Rudek, S.W. Epp, R. Coffee, S. Carron, S. Schorb, K.R. Ferguson, M. Swiggers, J.D. Bozek, M. Simon, T. Marchenko, J. Küpper, I. Schlichting, J. Ullrich, C. Bostedt, D. Rolles, A. Rudenko, *Science* 345, 288 (2014).
- [P13] “Multiple ionization and fragmentation dynamics of molecular iodine studied in IR-XUV pump-probe experiments”, K. Schnorr, A. Senfleben, G. Schmid, A. Rudenko, M. Kurka, K. Meyer, L. Foucar, M. Kübel, M.F. Kling, Y.H. Jiang, S. Düsterer, R. Treusch, C. D. Schröter, J. Ullrich, T. Pfeifer, R. Moshhammer, *Faraday Discussions*, 171, 41 (2014).
- [P14] “Electron Rearrangement Dynamics in Dissociating I₂⁺ Molecules Accessed by Extreme Ultraviolet Pump-Probe Experiments”, K. Schnorr, A. Senfleben, M. Kurka, A. Rudenko, G. Schmid, T. Pfeifer, K. Meyer, M.F. Kling, Y.H. Jiang, R. Treusch, S. Düsterer, B. Siemer, H. Zacharias, R. Mitzner, T. J. M. Zouros, T. J. Ullrich, C. D. Schröter and R. Moshhammer, *Physical Review Letters*, 113, 073001 (2014).
- [P15] “Probing ultrafast molecular dynamics with free-electron lasers”, L. Fang, T. Osipov, B.F. Murphy, A. Rudenko, D. Rolles, V.S. Petrovic, C. Bostedt, J.D. Bozek, P.H. Bucksbaum, N. Berrah, *J. Phys. B: At. Mol. Opt. Phys.*, 47, 124006 (2014).
- [P16] “Femtosecond x-ray photoelectron diffraction on gas-phase dibromobenzene molecules”, D. Rolles, R. Boll, M. Adolph, A. Aquila, C. Bostedt, J.D. Bozek, H.N. Chapman, R. Coffee, N. Coppola, P. Declava, T. Delmas, S.W. Epp, B. Erk, F. Filsinger, L. Foucar, L. Gumprecht, A. Homke, T. Gorkhover, L. Holmegaard, P. Johnsson, C. Kaiser, F. Krasniqi, K.-U. Kühnel, J. Maurer, M. Messerschmidt, R. Moshhammer, W. Quevedo, A. Rouzee, B. Rudek, I. Schlichting, C. Schmidt, S. Schorb, C.D. Schröter, J. Schulz, H. Stapelfeldt, M. Stener, S. Stern, S. Techert, J. Thøgersen, M.J.J. Vrakking, A. Rudenko, J. Küpper, J. Ullrich, *J. Phys. B: At. Mol. Opt. Phys.*, 47, 124035 (2014).
- [P17] “Imaging molecular structure through femtosecond photoelectron diffraction on aligned and oriented gas-phase molecules”, R. Boll, A. Rouzee, M. Adolf, D. Anielski, A. Aquila, S. Bari, C. Bomme, C. Bostedt, J. D. Bozek, H.N. Chapman, L. Christensen, R. Coffee, N. Coppola, S. De, P. Declava, S. W. Epp, B. Erk, F. Filsinger, L. Foucar, T. Gorkhover, L. Gumprecht, A. Homke, L. Holmegaard, P. Johnsson, J.S. Kienitz, T. Kierspel, F. Krasniqi, K.-U. Kühnel, J. Maurer, M. Messerschmidt, R. Moshhammer, N.L.M. Müller, B. Rudek, E. Savelyev, I. Schlichting, C. Schmidt, F. Scholz, S. Schorb, J. Schulz, J. Seltmann, M. Stener, S. Stern, S. Techert, J. Thøgersen S. Trippel, J. Viefhaus, M.J.J. Vrakking, H. Stapelfeldt, J. Küpper, J. Ullrich, A. Rudenko, and D. Rolles, *Faraday Discussions*, 171, 57 (2014).
- [P18] “Charge transfer and nuclear dynamics following deep inner-shell multiphoton ionization of CH₃I molecules by X-ray free-electron laser pulses”, K. Motomura, E. Kukk, H. Fukuzawa, S. Wada, K. Nagaya, S. Ohmura, S. Mondal, T. Tachibana, Y. Ito, R. Koga, T. Sakai, K. Matsunami, A. Rudenko, C. Nicolas, X.-J. Liu, C. Miron, Y. Zhang, Y. Jiang, J. Chen, M. Anand, D. Kim, K. Tono, M. Yabashi, M. Yao, and K. Ueda, *J. Phys. Chem. Lett.*, 6, 2944 (2015).
- [P19] “Ultrafast Isomerization Initiated by X-Ray Core Ionization”, C. Liekhus-Schmaltz, I. Tenney, T. Osipov, A. Sanchez-Gonzalez, N. Berrah, R. Boll, C. Bomme, C. Bostedt, J. Bozek, S. Carron, R. Coffee, J. Devin, B. Erk, K. Ferguson, R. Field, L. Foucar, L. Frasninski, J. Glownia, M. Gühr, J. Krzywinski, H. Li, J. Marangos, T. Martinez, B. McFarland, S. Miyabe, B. Murphy, A. Wang, D. Rolles, A. Rudenko, M. Siano, E. Simpson, L. Spector, M. Swiggers, D. Walke, S. Wang, T. Weber, P. Bucksbaum, and V. Petrovic, *Nature Commun.* 6, 8199 (2015).
- [P20] “Time-resolved studies with FELs”, A. Rudenko and D. Rolles, *J. Electr. Spectr. Rel. Phen.*, in press (2015).
- [P21] “Time-resolved study of ICD in Ne dimers using FEL radiation”, K. Schnorr, A. Senfleben, G. Schmid, S. Augustin, M. Kurka, A. Rudenko, L. Foucar, K. Meyer, D. Anielski, R. Boll, D. Rolles, M. Kubel, M. F. Kling, Y. Jiang, K. Ueda, T. Marchenko, M. Simon, G. Brenner, R. Treusch, V. Averbukh, J. Ullrich, T. Pfeifer, C. Schroter, and R. Moshhammer, *J. Electr. Spectr. Rel. Phen.*, in press (2015).
- [P22] “Strongly aligned gas-phase molecules at Free-Electron Lasers”, T. Kierspel, J. Wiese, T. Mullins, J. Robinson, A. Aquila, A. Barty, R. Bean, R. Boll, S. Boutet, P. Bucksbaum, H.N. Chapman, L. Christensen, A. Fry, M. Hunter, J.E. Koglin, M. Liang, V. Mariani, A. Morgan, A. Natan, V. Petrovic, D. Rolles, A. Rudenko, K. Schnorr, H. Stapelfeldt, S. Stern, J. Thøgersen, C. H. Yoon, F. Wang, S. Trippel, J. Küpper, *J. Phys. B: At. Mol. Opt. Phys.*, in press (2015).

Structure and Dynamics of Atoms, Ions, Molecules and Surfaces

Uwe Thumm

J.R. Macdonald Laboratory, Kansas State University, Manhattan, KS 66506, thumm@phys.ksu.edu

A. XUV double ionization (DI) of He

Project scope: To examine - with atomic resolution in time - correlation effects, photoexcitation, and photoemission mechanisms during the ionization of He atoms and H₂ molecules exposed to intense short XUV and IR pulses.

Recent progress: Photo-DI of helium is a convoluted process where photon-electron, electron-nucleus, and electronic interactions compete. Accordingly, the detailed scrutiny of measured and calculated double-ionization data requires highly differential emission probabilities (or cross sections). We therefore focussed on specific values of the energy sharing between the two emitted electrons and investigated joint angular distributions (JADs) in coplanar emission geometry [1,2]. We considered XUV pulses with photon energies between 30 and 99 eV, covering the non-sequential and sequential DI regimes, and examined DI in ultrashort XUV pulses that spectrally overlap both regimes [3].

Example 1: Single-photon XUV DI. We continued to validate our new finite-element discrete-variable-representation code [1] for solving in full dimensionality the TDSE for two-electron atoms exposed to time-dependent external electric fields. We applied this *ab initio* code to the time-propagated calculation of DI of helium by up to three XUV photons and compared our numerical results with published experimental and theoretical triply differential cross sections (TDCSs) for single-XUV-photon DI data [2] (Fig. 1).

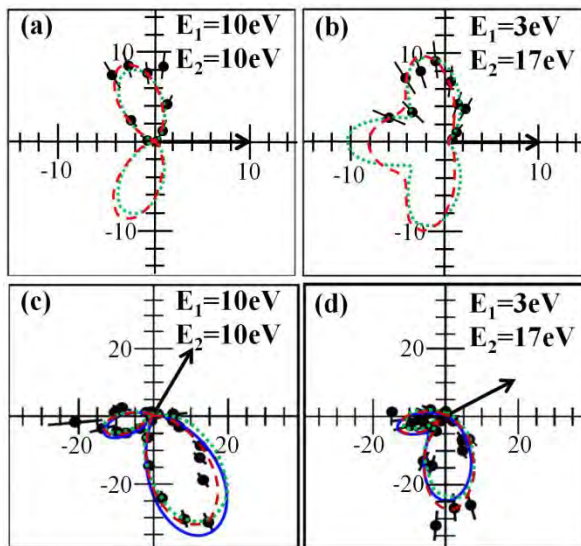


Fig. 1: TDCSs for single 99-eV-photon DI of He and fixed detection angles of one electron (a,b) $\Theta_1=0^\circ$, (c) 60° , and (d) 30° , indicated by the back arrows.

The black dots with error bars are absolute experimental TDCSs from Bräuning *et al.* [R1]. E_1 and E_2 denote asymptotic electron energies. Our calculated results (red dashed lines) are normalized to the experimental data.

(a,c) Equal ($E_1=E_2$) and (b,d) unequal energy sharing.

The green dotted lines show theoretical results of (a) Huetz *et al.* [R2] and (b-d) Kheifets and Bray (as given in [R1]). (c,d) The solid blue lines show TDCSs calculated by Palacios *et al.* [R3].

Example 2: Few-photon XUV DI. Figure 2a shows our calculated JAD for DI as a result of the absorption of two 45 eV photons. The four distinct peaks correspond to back-to-back emission. Selection-rule-prohibited features in single-photon sequential DI (back-to-back and conic emission) are dominant for two-photon DI [1]. The JAD for three-photon DI in Fig. 2b is similar to the single-photon JAD, with the same dominant nodal lines. In either case, back-to-back, conic, and side-by-side emission are prohibited, all in compliance with known selection rules.

Example 3: Sequential contributions to two-photon DI in ultrashort XUV pulses. For long XUV pulses, sequential and non-sequential two-photon DI are distinguishable by the central XUV photon energy $\hbar\omega_X$. If $\hbar\omega_X$ is above the second ionization potential (54.4 eV), DI proceeds sequentially, otherwise non-sequentially [1]. For ultrashort XUV pulses, this distinction becomes less obvious if their spectrum overlaps the sequential and non-sequential regimes [3]. We therefore introduced the emission asymmetry in JADs (ranging from -1 to 1 for

emission into opposite and the same hemispheres), as a measure that allows us to quantify "sequential" and "non-sequential" contributions to DI in linearly polarized ultrashort XUV pulses that spectrally overlap both regimes. Figure 3 displays the "effective sequential DI (SDI) yield" and DI emission-asymmetry dependence on the XUV-pulse duration. Comparison with our *ab initio* calculation (stars) confirms that the effective SDI yield (blue solid line) factorises into the effective interaction time (proportional to the pulse duration) and the integrated XUV-pulse spectral intensity for $\hbar\omega_X > 54.4$ eV [3]. The SDI contribution reaches a maximum value at 650 as pulse duration, due to the competition between increasing temporal and decreasing spectral pulse widths.

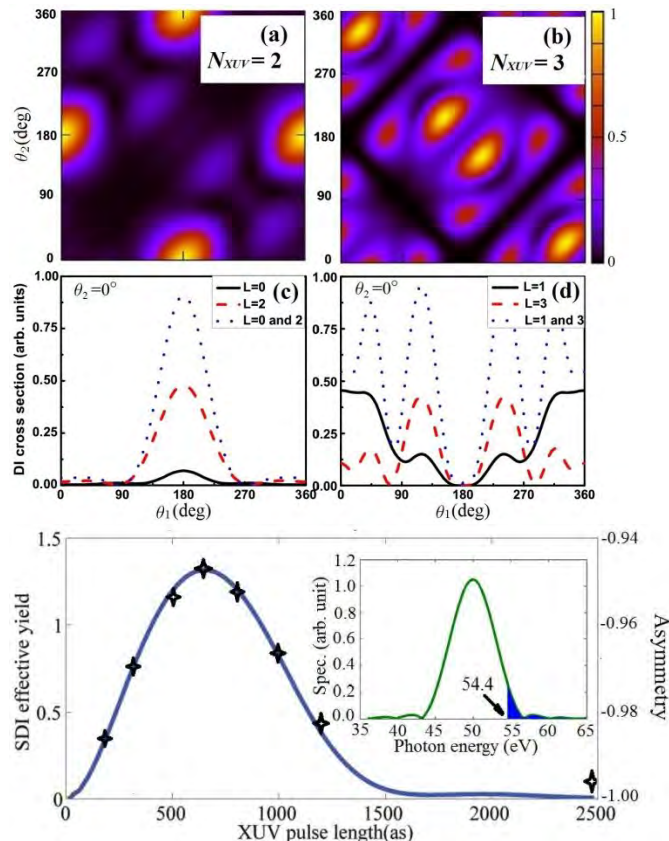


Fig. 2: (a,b) Calculated normalized JADs at equal energy sharing by (a) two 45 and (b) three 30 eV photons in 1 fs, 10^{14} W/cm² XUV pulses.

(c,d) Corresponding conditional DI angular distributions for the emission of one electron along the XUV polarization direction ($\theta_2=0^\circ$) by (c) two 45 and (d) three 30 eV photons.

Contributions to the DI yields from individual allowed total angular momenta L are shown as dashed and dotted lines.

Fig. 3: Heuristic effective SDI yield for 10^{14} W/cm² XUV pulses centered at 50 eV as a function of the XUV pulse duration. The stars are results of our *ab initio* TDSE calculation of the emission asymmetry at extremely unequal energy sharing.

The inset displays a typical XUV-spectral intensity, the blue area indicating the spectrum above the second ionization potential.

Future plans: (i) We plan to extend these studies to laser-assisted DI with variable delays between ultrashort XUV and IR pulses in order to resolve in time DI by sequential and non-sequential emission mechanisms. We further intend to (ii) calculate time-resolved IR Stark shifts for He, for comparison with recent and emerging transient absorption measurements, and (iii) search for ideal laser parameters for the observation, with sub-IR-cycle resolution, of IR level shifts in delay-dependent DI. We envision (iv) to compute the laser-dressed autoionization of He and to compare our *ab initio* results with our heuristic model for the decay of laser-coupled autoionizing states [R4,R5] and (v) to extend this line of work to H₂ (in fixed-ion approximation).

B. Complementary imaging of the nuclear dynamics in molecular ions

Project scope: To develop conceptual, analytical, and numerical tools to (i) predict the effects of strong IR-laser, XUV, and X-ray fields on the bound and free electronic and nuclear dynamics in small molecules and (ii) image their laser-controlled nuclear and electronic dynamics.

Recent progress: When photoionizing heavy diatomic molecules, intense pump pulses tend to populate several intermediate excited electronic states of the molecular ion. By comparing characteristic features of simulated kinetic-energy release (KER) spectra (vibrational periods, wave-packet revivals, and quantum-beat frequencies), that result from the nuclear motion on individual adiabatic potential curves of the molecular ion, with measured spectra, we developed a scheme for identifying intermediate ionic states that are relevant for the dissociation process [4]. We recently applied this method to examine van-der-Waals-bound noble-gas dimers [5,6] and (ii) test the accuracy of O₂ molecular potential curves [7].

Example: Scrutinizing molecular potential curves with XUV-pump - IR-probe experiments. We simulated the dissociative photoionization of O_2 in support of a kinematically complete XUV-IR pump-probe experiment in which charged fragments and photoelectrons were detected in coincidence [7]. The experiment employed 30 fs, 760 nm, $3 \times 10^{12} \text{W/cm}^2$ IR pulses that were split to generate higher harmonics with energies between 17 and 40 eV to compose XUV pulses. Experiment and numerical simulation revealed a pump-probe delay-dependent yield of very low energetic O^+ ions with an oscillation period of 40 fs (Fig. 4).

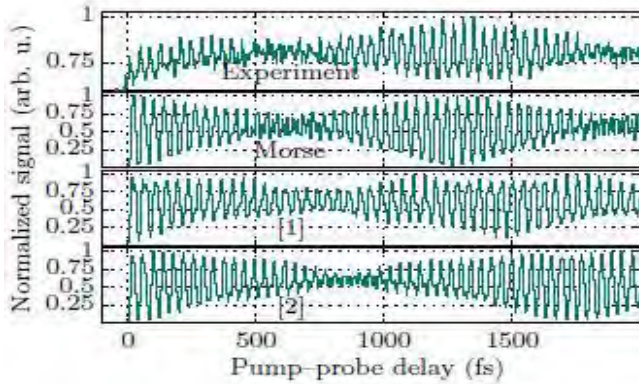


Fig. 4: O^+ yield as a function of the pump-probe delay. Probed by resonant absorption of a single IR photon to the weakly repulsive $O_2^+(f^4\Pi_g)$ state, this yield images the motion of a vibrational wave packet in the binding $O_2^+(a^4\Pi_u)$ state.

Experimental data (top) and simulated spectra using a Morse potential as well as the potential-energy curves calculated in [R6] (here labeled as “[1]”) and [R7] (“[2]”).

By comparison of the experimental KER and quantum-beat spectra with numerical simulations, we could distinguish published adiabatic O_2^+ potential-energy curves from different authors (Fig. 4), finding, in general, good agreement between experimental and simulated KER and quantum-beat spectra. However, using these potential curves, our calculations did not reproduce all features in the experimental data. In contrast, adjusting a Morse potential to the experimental data, most characteristics of the experimental spectra could be well reproduced by our simulation. This comparison demonstrates the sensitivity of the used pump-probe coincidence experimental method to small changes in the shape of the binding potential.

Future plans: We plan to (i) refine the simultaneous analysis of measured and simulated KER spectra in both, time and energy domains in order to better understand the ro-vibrational nuclear dynamics following the ionization of diatomic molecules by short laser and XUV pulses and to (ii) apply this method to larger molecules (e.g., dissociation along valence coordinates of CO_2 [R8] and the CH_3 -I stretch mode in CH_3I [R9]).

C. Time-resolved photoelectron (PE) spectroscopy

Project scope: To numerically model and understand IR-streaked (and IR side-banded) XUV PE emission and Auger decay in pump-probe experiments with atoms, molecules, and more complex targets.

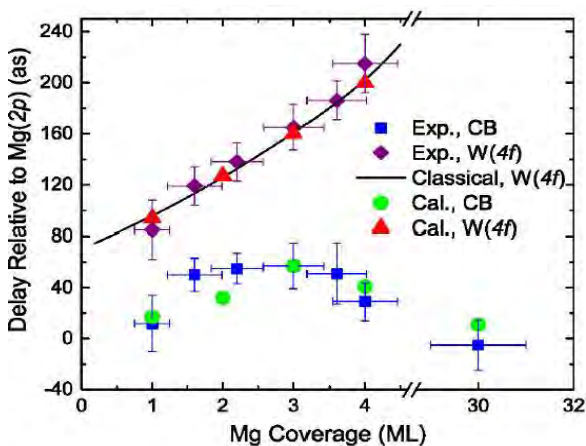


Fig. 5: Measured [R10], classically [R10], and quantum-mechanically [10] calculated streaking time delays relative to $Mg(2p)$ emission for CB and $W(4f)$ photoelectrons as a function of the Mg coverage on a $W(110)$ substrate for 118 eV XUV pulses.

We employ measured and calculated MFPs and an IR skin depth of 2 Å [8]. We describe the dispersion of CB electrons inside the substrate by adjusting the effective electron mass (0.86 a.u.). We assume free propagation of CB electrons in the adsorbate and for electrons released from $Mg(2p)$ and $W(4f)$ CLs, to match the measured photoemission delay between CB and $W(4f)$ PEs for the *adsorbate-free* $W(110)$ surface.

Recent progress: We developed a quantum model to simulate streaked PE emission from adsorbate-covered metal surfaces, incorporating the effects of energy-dependent electron mean-free paths (MFPs), properties of initial states, photoelectron energy dispersion, and screening of the streaking field [8,9]. Our simulations [10] reproduce recently measured streaked photoemission spectra with ultrathin Mg adsorbate films on a $W(110)$ substrate [R10] that revealed a monotonic dependence on the adsorbate thickness of the relative photoemission

time delay between W(4f) and Mg(2p) core-level (CL) PEs and a non-monotonic dependence of the relative photoemission time delay between conduction-band (CB) and Mg(2p) CL PEs (Fig. 5).

Future plans: We intend to further improve our modeling of (i) photoemission from atoms and (ii) the transport of photoreleased electrons inside complex targets. We will collaborate with experimental groups to explore the feasibility of and ideal parameters for the observation of dielectric response (plasmonic) effects during and after the XUV-pulse-triggered release of PEs from metal surfaces and nanoparticles.

Publications and manuscripts acknowledging DOE support addressed in this abstract

- [1] *Laser-assisted XUV few-photon double ionization of helium: joint angular distributions*, A. Liu, U. Thumm, Phys. Rev. A **89**, 063423 (2014).
- [2] *Laser-assisted XUV double ionization of helium: energy-sharing dependence of joint angular distributions*, A. Liu, U. Thumm, Phys. Rev. A **91**, 043416 (2015).
- [3] *A criterion for distinguishing sequential from non-sequential contributions to two-photon double ionization of helium in ultrashort XUV pulses*, A. Liu, U. Thumm, Phys. Rev. Lett., submitted.
- [4] *Complementary imaging of the nuclear dynamics in laser-excited diatomic molecular ions in the time and frequency domains*, M. Magrakvelidze, A. Kramer, K. Bartschat, U. Thumm, J. Phys. B **47**, 124003 (2014).
- [5] *Steering the nuclear motion in singly ionized argon dimers with mutually detuned laser pulses*, J. Wu, M. Magrakvelidze, A. Vredenburg, L. Ph. H. Schmidt, T. Jahnke, A. Czasch, R. Dörner, U. Thumm, Phys. Rev. Lett. **110**, 033005 (2013).
- [6] *Dissociation dynamics of noble-gas dimers in intense two-color IR laser fields*, M. Magrakvelidze, U. Thumm, Phys. Rev. A **88**, 013413 (2013).
- [7] *Probing O_2^+ potential-energy curves with an XUV – IR pump – probe experiment*, P. Cörlin, A. Fischer, M. Schönwald, A. Sperl, T. Mizuno, U. Thumm, T. Pfeifer, R. Moshhammer, Phys. Rev. A **91**, 043415 (2015).
- [8] *Attosecond time-resolved photoelectron dispersion and photoemission time delays*, Q. Liao, U. Thumm, Phys. Rev. Lett. **112**, 023602 (2014).
- [9] *Initial-state, mean-free-path, and skin-depth dependence of attosecond time-resolved IR-streaked XUV photoemission from single-crystal magnesium*, Q. Liao, U. Thumm, Phys. Rev. A **89**, 033849 (2014).
- [10] *Attosecond time-resolved streaked photoemission from Mg-covered W(110) surfaces*, Q. Liao, U. Thumm, Phys. Rev. A., Rapid Comm., accepted.

Other recent publications and manuscripts acknowledging DOE support (2013-15)

- [11] *Attosecond Physics: attosecond streaking spectroscopy of atoms and solids*, U. Thumm, Q. Liao, E. M. Bothschafter, F. Süßmann, M. F. Kling, R. Kienberger, p. 387, Handbook of Photonics, Vol. **1**, Chap. XIII (Wiley, 2015).
- [12] *Attosecond science – What will it take to observe processes in real time*, S. R. Leone, C. W. McCurdy, J. Burgdörfer, L. Cederbaum, Z. Chang, N. Dudovich, J. Feist, C. Greene, M. Ivanov, R. Kienberger, U. Keller, M. Kling, Z.-H. Loh, T. Pfeifer, A. Pfeiffer, R. Santra, K. Schafer, A. Stolow, U. Thumm, M. Vrakking, Nature Photonics **8**,162 (2014).
- [13] *Understanding the role of phase in chemical bond breaking with coincidence angular streaking*, J. Wu, M. Magrakvelidze, L. Ph. H. Schmidt, M. Kunitski, T. Pfeifer, M. Schöffler, M. Pitzer, M. Richter, S. Voss, H. Sann, H. Kim, J. Lower, T. Jahnke, A. Czasch, U. Thumm, R. Dörner, Nat. Commun. **4**, 2177 (2013).
- [14] *Electron-nuclear energy sharing in above-threshold multiphoton dissociative ionization of H_2* , J. Wu, M. Kunitski, M. Pitzer, F. Trinter, L. Ph. H. Schmidt, T. Jahnke, M. Magrakvelidze, C. B. Madsen, L. B. Madsen, U. Thumm, R. Dörner, Phys. Rev. Lett. **111**, 023002 (2013).
- [15] *H formation by electron capture in collision of H with an Al(100) surface*, B. Obreshkov, U. Thumm, Phys. Rev. A **87**, 022903 (2013).

References: [R1] H. Bräuning *et al.*, J. Phys. B **31**, 5149 (1998). [R2] A. Huetz *et al.*, J. Phys. B **24**, 1917 (1991). [R3] A. Palacios *et al.*, J. Phys. B **77**, 032716 (2008). [R4] H. Wang *et al.*, Phys. Rev. Lett. **105**, 143002 (2010). [R5] F. He *et al.*, J. Phys. B **44**, 211001 (2011). [R6] C. M. Marian *et al.*, Mol. Phys. **46**, 779 (1982). [R7] M. Magrakvelidze *et al.*, Phys. Rev. A **86**, 023402 (2012). [R8] H. Timmers *et al.*, Phys. Rev. Lett. **113**, 113003 (2014). [R9] B. Erk *et al.*, Science **345**, 288 (2014). [R10] S. Neppl *et al.*, Nature **517**, 342 (2015).

Strong-Field Time-Dependent Spectroscopy

Carlos A. Trallero

J. R. Macdonald Laboratory, Kansas State University, Manhattan, KS 66506
 trallero@phys.ksu.edu

Scope

The main scope of my research is to measure time dependent molecular structure with ultrafast time resolution. As a complement of this goal I'm developing novel ultrafast optical sources.

1 High harmonic generation spectroscopy

1.1 Towards a photoionization experiment with high harmonic generation spectroscopy *with A. Starace*

Experimentally, it is easy to measure the harmonic yield with elliptically polarized field when the ellipticity η is small. The harmonic yield as a function of ellipticity in Ar is shown in Fig. 1. The yield for each harmonic is shown normalized to the yield at linearly polarized light. From the figure it is very easy to see that the harmonic yield decreases with ellipticity in the same manner for all harmonics in the plateau except for harmonics that are in the vicinity of the Cooper minimum of Ar which occurs at around harmonic 33 or 51 eV. We measured the harmonic yield as a function of η for various macroscopic conditions by changing the focus position of the laser respect to the gas jet and at different laser intensities. A major challenge however is to theoretically describe the generation of harmonics with elliptically polarized light. We show here how the harmonic generation can be parametrized in similar equation as that used for weak field XUV photoionization.

These experiments and the collaboration with Frolov and Starace was facilitated by an EPSCoR grant. The DOE JRML grant supported the laser and infrastructure.

From the theoretical point of view the most important result is that we were able to parametrize the harmonic yield generated with an elliptically polarized field in a form similar to that used in photoionization spectroscopy. In particular, for an atomic system with p -state optical electron gives access to the whole parameters which describe the photoionization cross section:

$$Y_{\text{HHG}}^{(\text{tot})} \propto e^{-\alpha\eta^2} \sigma(E_\Omega, 0^\circ) \left(1 + f(\eta^2) \frac{1 - \beta/2}{1 + \beta} \right), \quad (1)$$

where $f(\eta^2) \propto \eta^2$ for small η , $\alpha = F_0 \mathcal{E}_0 / (F I_p)$, and $\sigma(E, \theta = 0)$ is the PICS as a function of energy along the field polarization. The exponential decreasing of HHG yield as laser ellipticity increases was predicted before based on the semiclassical model.

This last expression Eq. 1 is extremely important as it provides a parametrization that is very similar in functional form to the well know photoionization equation in terms of the β parameter. This equation can further be decomposed to arrive to the following equation relating the harmonic yield, cross section and β parameter,

$$Y(E_\Omega, \eta = 0) \propto EWP \times \sigma(E_\Omega) [1 + \beta(E_\Omega)]. \quad (2)$$

1.2 Interferometric studies with higher order harmonic generation *with V. Kumarap-pan*

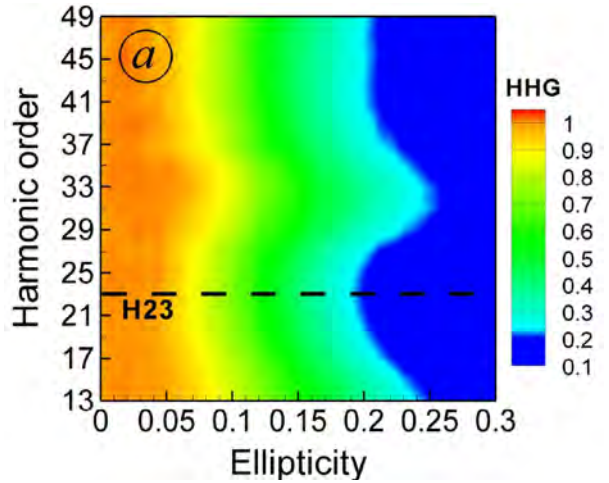


Figure 1: Normalized harmonic yield as a function of ellipticity and harmonic order ($\hbar\nu = 1.55\text{eV}$). The yield of each harmonic is normalized to its respective yield for linearly polarized light ($\eta = 0$).

One of the main benefits of using HHG as a spectroscopic tool is the possibility of providing heterodyne measurements. Therefore, one of our goals is to extract, not only the absolute value of the photoionization dipole moment but also its phase. We make use of an interferometric setup to extract the phase of different harmonics relative to a reference. In particular, we attempt to extract the phase of each harmonic as a function of molecular alignment angle relative to an unaligned sample. Experimentally, we generate harmonics from two sources that are close to each other but without overlap (S1 and S2 in the figure). The experimental setup is shown in Fig. 2. Harmonics emerging from each focus position interfere in the far field (the detector plane) creating an interference pattern similar to the one shown in the figure. We then rotate the molecular alignment angle by changing the polarization of the pump beam in S2 and record the interference pattern as a function of angle. Afterwards, we perform a Fourier transform of the interference pattern for each harmonic. The phase of the first Fourier component is the relative phase between harmonic emerging from S1 and S2.

As a check we first performed measurements in N₂. In this case, the delay between the pump and probe in S2 was 8.2 ps, the delay at which we reach maximum alignment. A comparison between the experimentally measured theoretically calculated relative phases for harmonics 13, 15 and 17 is shown in Fig. 3. While the agreement between the experiment and theory is not extremely good, they both agree in the trends. We also performed several scans around the first J-type revival in C₂H₄, corresponding to a delay between pump and probe of 7 to 12 ps.

2 Strong field ionization of molecular isomers *with A. T. Le*

Recent results of HHG from isomer molecules indicate show large differences in the harmonic yield for different isomers of the the same molecular specie. In particular, studies of the isomers cis- and trans-1,2-dichloroethylene (DCE) and cis- and trans-2-butene suggest that the difference in the ionization yields for the cis-1,2-DCE is 7-9 times higher than for the trans-1,2-DCE, and a factor of 5 higher for the cis-2-butene compared to the trans-2-butene. Later results claim that the difference in ionization is only a factor of 2 between the cis and trans isomers. Besides the implications for HHG-based spectroscopic, such hypothesis are important because it also involves a comparison between polar (cis) and non-polar molecules. Our goal is to test the Keldysh interpretation of strong field ionization by comparing ionization yields from polar and non-polar which are isomers from each other and therefore have the same ionization potential. Since our last report we have improved our experimental setup and now have access to single-shot measurements of the ionization yield and the laser power fluctuation. This improvements have allowed us to decrease the error in the measurements, in particular at lower intensities.

The ratio, trans / cis, of the normalized ionization yield as a function of intensity for the first ion of 1,2-DCE can be seen in figure 4. Error bars in the graphs were calculated by the standard deviation over fifty plus scans. The range of intensities shown here are at the low end, where there the appear-

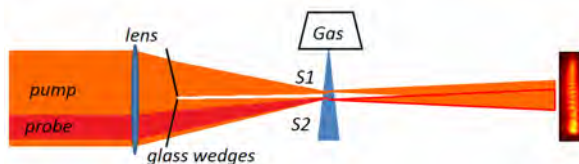


Figure 2: Interferometric HHG setup. S1 is a source of unaligned harmonics while S2 is source of harmonics that are aligned. Harmonics emerging from S1 and S2 overlap in the far field creating and interference pattern.

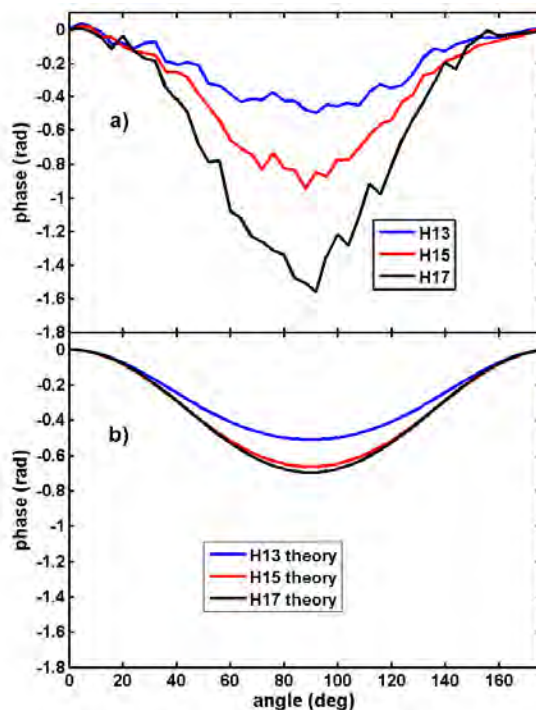


Figure 3: a) Relative phase of harmonics 13, 15, and 17 as a function of delay for N₂ retrieved from experiment. b) Theoretically calculated relative phases for the same harmonics.

ance of secondary fragments is negligible. This range of intensities is also far from the saturation regime, which is observed at two to three times the shown values. The first feature observed in the data is that both ratios remain almost constant for the shown range of pulse energies. Closer to saturation intensities, this trend changes. More relevant to this study is the fact that the ratio between isomers is very close to 1. It should be noted that we are not suggesting that the ionization ratios are constant. It is clear that they change gradually with intensity and molecular orientation respect to the laser polarization.

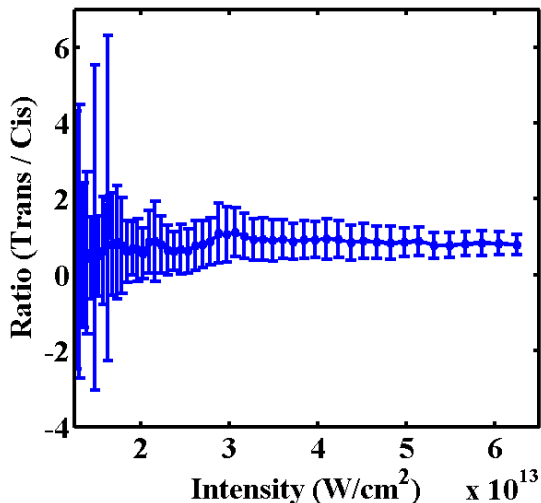


Figure 4: The ratio of trans-1,2- and cis-1,2-dichloroethylene using the ionization yields of the first ion of each sample at low intensities.

ment were running as needed in true experimental conditions. Parts of the CEP development was done jointly between KMLabs and the JRML and continue to be developed.

The laser is used to pump a high energy, white-light-seeded high energy optical parametric amplifier (OPA) with 18 mJ of the 20 mJ available from HITS, producing a maximum of 6 mJ of energy in the signal plus idler. It should be noted that even at the extremes of the tuning curve (1100 nm for the signal and 2550 nm for the idler) the energy per pulse is still in excess of 1 mJ at 1KHz repetition rate. Thus this HE-OPA is perfectly suited for strong field physics experiments in a wide range of wavelengths.

3.1 Towards the synthesis of intense optical waveforms

The synthesis of ultrabroadband optical pulses will allow for arbitrary control of sub-cycle features at the fs time scales. Achieving this however requires the generation of multiple octaves of bandwidth as well as very fine control of the CEP over the entire spectral range. As discussed above the OPA is white light seeded and thus the relationship between the signal, idler and pump is well defined. We devised a method to use the depleted pump emerging from the OPA to generate few-cycle pulses from all three beams simultaneously. Because pulse broadening occurs via self-phase-modulation (SPM), which is also a parametric process, the relative CEP between all pulses is maintained.

In order to have sub-cycle laser pulses, the pump beam (800 nm) and the 6 mJ S+I beam need to be spectrally broadened and then synthesized. Any

The relatively low differences might indicate that molecular ionization has only a small dependence on atomic configuration with the same atomic composition. Such observations lead to the conclusion that for randomly aligned molecules, the Keldysh parameter is still the characteristic parameter for strong field ionization.

3 Optics development

The most recent laser installed in the lab (HITS) was purchased from KMLabs through an NSF-MRI grant and its specifications were reported last year. It is to date one of the highest energy-per-pulse CEP stable systems worldwide. Besides the high energy per pulse the CEP noise represents one of the best to date in terms of long term stability [1]. Because the laser will be used in atomic and molecular experiments the environment for this scans was not controlled. All the turbo pumps and other equip-

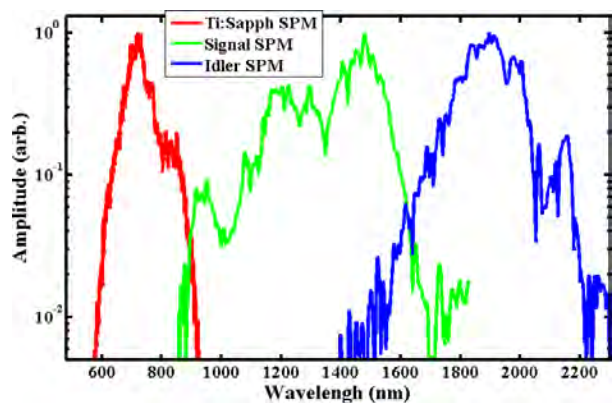


Figure 5: The broadened spectrum of pump, signal and idler. The sum of the three pulses yields more than 2.5 mJ of energy per pulse and 2.4 octaves of bandwidth.

small CEP drifts can also be corrected by rotating a pair of glass plates in the OPA with a piezo motor. Furthermore, the idler output is known to have passive CEP stability. Therefore, if the time separation of all three pulses can further be precisely stabilized and delayed, mJ level sub-cycle synthesized laser pulses could be realized. In our case this stabilization should be realizable since we are using the depleted pump out of the OPA together with the signal and idler. Only in the last step of recombining the three pulses is where we should be concerned about the interferometric stability of all frequency components. Usually the depleted pump of the OPA was discarded as the spatial mode is not a Gaussian but rather resembles a bagel in the sense that it is depleted in the center. However we demonstrated that SPM to broaden the depleted pump simultaneously with the signal is possible to generate few-cycle pulses. Since then we have also demonstrated that the same can be achieved with the signal and idler.

Using this technique, we were able to obtain more than 2.5 mJ of energy per pulse in the broadened pump, signal and idler [1]. By adding all three broadened spectra, we obtained the multi-octave spectrum shown in Fig. 5. Both the energy per pulse and the broadening represent lower limits of what is possibly achievable, yet we have been able to achieve almost three octaves of bandwidth and multi-mJ energies. Such achievements emphasize the strength of our method. We need to point out that at this stage we haven't compressed the broadened pulses at the same time, nor recombined them.

DOE Supported Publications

- “A carrier-envelope-phase stabilized terawatt class laser at 1 kHz with a wavelength tunable option”, Benjamin Langdon, Jonathan Garlick, Xiaoming Ren, Derrek J. Wilson, Adam M. Summers, Stefan Zigo, Matthias F. Kling, Shuting Lei, Christopher G. Elles, Eric Wells, Erwin D. Poliakoff, Kevin D. Carnes, Vinod Kumarappan, Itzik Ben-Itzhak and Carlos A. Trallero-Herrero, *Optics Express*, **23** 4563 (2015)
- “An Atomic Photoionization Experiment by Harmonic Generation Spectroscopy”, M. V. Frolov, T. S. Sarantseva, N. L. Manakov, K. D. Fulfer, B. D. Wilson, J. Troß, X. Ren, E. Poliakoff, A. A. Silaev, N. V. Vvedenskii, Anthony F. Starace, C. A. Trallero-Herrero, *Physical Review Letters*, (submitted), (2015)
- “Direct measurement of multi-orbital angular contributions in N₂ using high harmonic generation”, Jan Troß, Xiaoming Ren, Varun Makhija, Sudipta Mondal, V. Kumarappan and C. A. Trallero-Herrero, *Physical Review A*, (submitted) (2015)
- “Materials processing with superposed Bessel beams”, Xiaoming Yu, Carlos A. Trallero-Herrero and Shuting Lei, *Applied Surface Science*, (submitted), (2015)
- “Long term carrier-envelope-phase stabilization of a terawatt-class Ti:Sapphire laser”, Adam M. Summers, Benjamin Langdon, Jonathan Garlick, Xiaoming Ren, Derrek J. Wilson, Stefan Zigo, M. F. Kling, Shuting Lei, Christopher G. Elles, Eric Wells, Erwin D. Poliakoff, K. D. Carnes, V. Kumarappan, I. Ben-Itzhak and C. A. Trallero-Herrero, *Proceedings of Frontiers in Optics* (to appear) (2015)
- “A 260 MW light source at 7 μm center wavelength as a path to strong field science in the far infrared”, Derrek J. Wilson, Adam M. Summers and C. A. Trallero-Herrero”, *Frontiers in Optics*, (to appear) (2015)

Atomic, Molecular and Optical Sciences at the Lawrence Berkeley National Laboratory

C. William McCurdy (PI), Co-Investigators: Ali Belkacem, Oliver Gessner, Daniel J. Haxton, Martin Head-Gordon, Stephen R. Leone, Daniel M. Neumark, Thomas N. Rescigno, Robert W. Schoenlein, Daniel S. Slaughter, Thorsten Weber

Chemical Sciences, Lawrence Berkeley National Laboratory, Berkeley, CA 94720

CWMcCurdy@lbl.gov, ABelkacem@lbl.gov, OGessner@lbl.gov, DJHaxton@lbl.gov, MHead-Gordon@lbl.gov, SRLeone@lbl.gov, DMNeumark@lbl.gov, TNRescigno@lbl.gov, RWSchoenlein@lbl.gov, DSSlaughter@lbl.gov, TWeber@lbl.gov

Objective and Scope: The AMOS program at LBNL seeks to answer fundamental questions in atomic, molecular and chemical sciences that are central to the mission of the Department of Energy's Office of Science. The essential strategy is to apply a broad span of existing and currently emerging tools such as synchrotron radiation, lasers, laboratory-based extreme ultraviolet sources, and low-energy electron beams together with state-of-the-art experimental techniques including momentum imaging, coincidence techniques, electron and x-ray absorption spectroscopy, scattering, and transient absorption, in combination with the development of advanced theoretical methodologies, to studies across a broad range of time scales and systems. This approach will provide deep insight into the chemistry and physics of the fundamental interactions that drive key chemical processes in simple molecules, complex molecular systems and molecules in complex environments. The current emphasis of the program is in three major areas with important connections and overlap: inner-shell photo-ionization and multiple-ionization and dissociation dynamics of small molecules; time-resolved studies of charge dynamics involving molecules in the gas phase, in condensed phase and at interfaces using a combination of attosecond to picosecond x-rays and laser pulses; and low-energy electron impact and dissociative electron attachment of molecules. The theory component of the program focuses on the development of new methods for solving from first-principle complex multi-atom and multi-electron processes that play a key role in these systems. The theory and experimental parts of the program are closely coupled. They are designed to work together to tackle problems of scale that are otherwise inaccessible without a strong and continuous collaboration and interaction.

The program at LBNL, recently reorganized to combine the former activities of the AMO base program and those of the former Ultrafast X-ray Sciences Laboratory into a single, integrated, AMOS program, consists of three subtasks:

- 1. Photon and electron driven processes in atoms and simple molecules.**
- 2. Photon and electron driven processes in complex molecular systems and molecules in complex environments.**
- 3. First-principles theory of dynamics and electronic structure.**

The co-investigators participate in multiple subtasks, collaborating and using common techniques in an effort in which experiment and theory are tightly integrated.

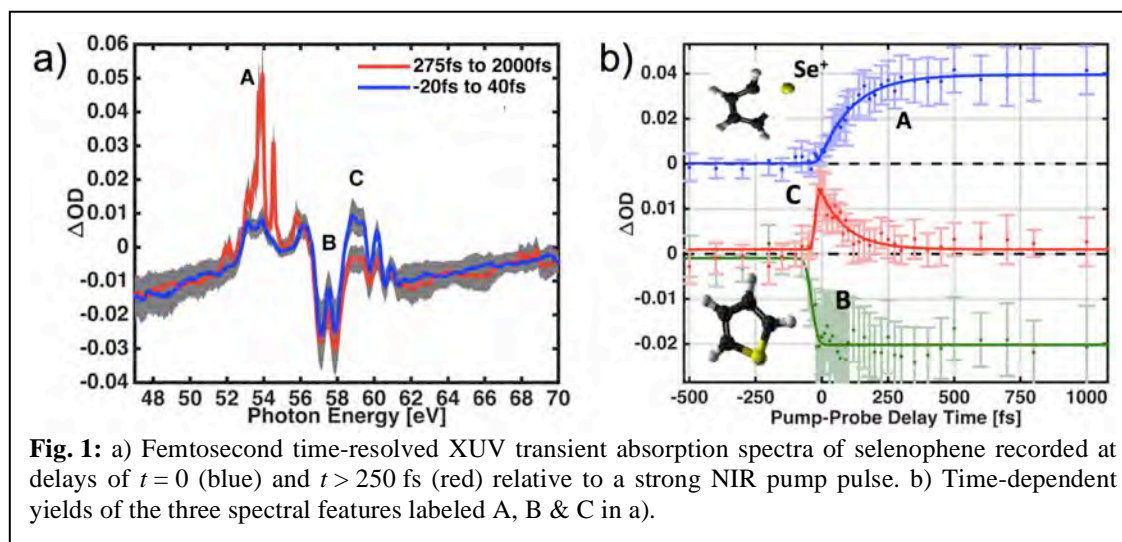
Subtask 1: Photon and electron driven processes in atoms and simple molecules.

Thrust 1: Photon driven processes in atoms and small molecules.

A. Belkacem, O. Gessner, D. J. Haxton, C.W. McCurdy, D. M. Neumark, S. R. Leone, T. N. Rescigno, D. S. Slaughter, and Th. Weber.

Femtosecond extreme ultraviolet (XUV) transient absorption spectroscopy (*O. Gessner, S.R. Leone, D.M. Neumark*)

Femtosecond extreme ultraviolet (XUV) transient absorption spectroscopy is used to explore ultrafast dynamics in molecular systems in the gas phase. XUV transitions are element specific, which is exploited to monitor molecular dynamics from the viewpoints of specific reporter atoms. Several technical improvements enabled the extension of previous experimental campaigns on atoms and small molecules toward more complex systems and, in particular, aromatic compounds. Three molecules have been explored: selenophene, ferrocene, and 1,2-dibromoethane (DBE). In a first series of experiments on these systems, strong field ionization (SFI) by an intense near infrared (NIR) pump pulse initiated molecular dynamics that were probed by femtosecond XUV absorption at variable time delays.



Selenophene is a selenium analogue of thiophene and furan with the selenium atom providing readily accessible 3d inner-shell orbitals for probing molecular dynamics. Photo-induced dynamics in these heterocyclic aromatic molecules are of particular interest with respect to the mechanisms that underlie ring-opening reactions. Fig. 1a shows XUV absorption spectra at pump-probe delays $t = 0$ fs (blue), and $t > 250$ fs (red). Three spectral features A, B, and C are clearly visible. Their spectral fingerprints in combination with their distinct temporal evolutions as shown in Fig. 1b provide an atomic-scale view of the molecular dissociation process: The depletion of the molecular ground state (feature B) marks the moment of ionization at zero pump-probe delay. Simultaneously, a new, transient species appears (feature C) corresponding to excited

selenophene ions whose yield decays on a 100-150 fs timescale. Decomposition of the molecule leads to the elimination of bare Se^+ ions, which give the sharp atomic lines of feature A and which appear on a very similar timescale as the parent ion decays. Interestingly, no signature of an intermediate configuration between the parent ion and the free Se^+ ion is detected, indicating that cleavage of two bonds occurs essentially simultaneously within only ~ 150 fs.

Another very fast dissociation is detected for the classic organometallic sandwich compound ferrocene. This molecule is composed of a central iron atom located between two aromatic hydrocarbon rings. XUV transitions involving the 3p orbitals of the central iron are used to monitor the dissociation dynamics. We find that following SFI, complete dissociation occurs to give free Fe^+ ions in only 250 fs. Intriguingly, only double ring loss is observed, and no evidence for a fragment with only one ring detached is recorded. As the molecules are excited by very strong laser fields, and therefore the amount of deposited energy may be large, it is perhaps not too surprising that decomposition occurs all the way to atomic ions and that intermediate species are not observed. However, in contrast to the direct, single-step dissociation observed for aromatic compounds, the seemingly less complex model system 1,2-dibromoethane (DBE) exhibits apparently richer dissociation dynamics. Using transient XUV absorption at the Br 3d edge, the release of a Br^+ fragment by the excited DBE parent ion is detected within 40 fs after SFI. The remaining monobromoethane radical, however, is unstable and decomposes to give a neutral bromine atom and an ethylene co-fragment within 220 fs. The femtosecond XUV transient absorption technique provides the unique possibility to track this 2-step dissociation reaction through its simultaneous sensitivity to both neutral and ionic reaction products.

Attosecond dynamics (*S.R. Leone, D.M. Neumark*)

The attosecond dynamics subgroup uses the exceptional time and energy resolution characteristic of attosecond transient absorption to study electronic dynamics directly in the time domain. In this effort, tunable isolated attosecond pulses are synchronized with a moderately intense few-cycle near infrared (NIR) pulse to study time-resolved changes in coherent electronic superpositions of states excited by the attosecond pulse.

Recent experiments obtained XUV pulses in the 11 to 17 eV energy range to study the dynamics of valence electrons in atoms and small molecules. In contrast to previous work on the $n=3$ states of neon, larger n Rydberg states can be addressed in argon close to the first ionization potential (15.75 eV) and more complicated dynamics arise from the high state density and large polarizability near the ionization limit. In addition to substantial level shifting and broadening, periodic modulations are observed in the absorption of various states as a function of XUV-NIR time delay; a 1.3 fs oscillation in the unresolved $[^2\text{P}^{\circ}_{1/2}]6s/4d$ states at 15 eV (circled in fig.2(b)) and 5-10 fs oscillations in the Rydberg states near the ionization limit (dashed line in fig.2(b)) are observed. These quantum beats correspond to two distinct population transfer pathways that occur in this system, lambda and ladder type transitions. An analytical model has been developed to describe the relative contributions of perturbative energy shifts and resonant population transfer processes in the observed dynamics.

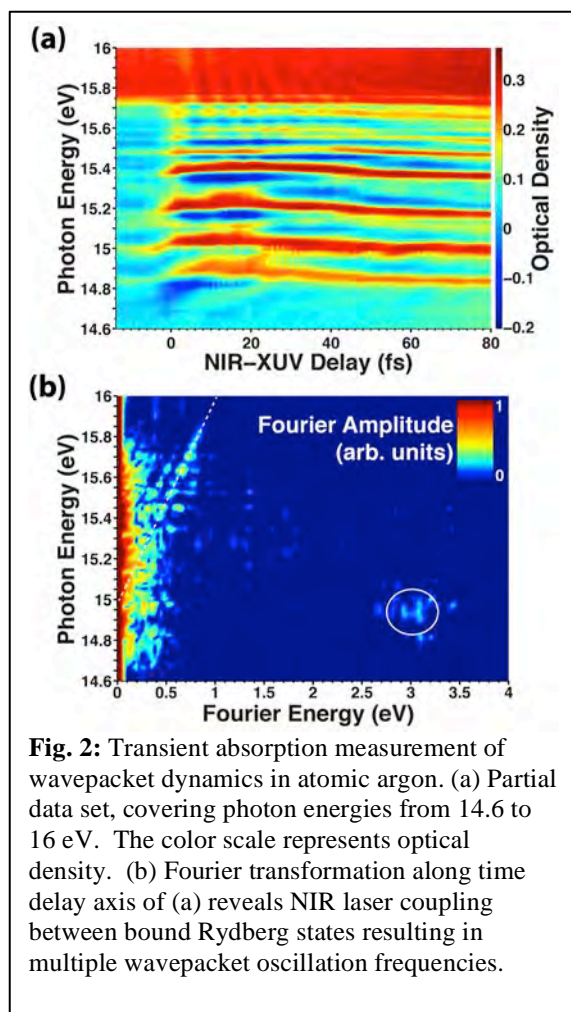


Fig. 2: Transient absorption measurement of wavepacket dynamics in atomic argon. (a) Partial data set, covering photon energies from 14.6 to 16 eV. The color scale represents optical density. (b) Fourier transformation along time delay axis of (a) reveals NIR laser coupling between bound Rydberg states resulting in multiple wavepacket oscillation frequencies.

In a related experiment, a coherent superposition is created in krypton near the first ionization potential at 14 eV, and this wavepacket also includes spin-orbit autoionizing states that are spectrally resolvable due to the large spin-orbit splitting. Few-femtosecond quantum beats are observed in these states despite the short (<100 fs) autoionization lifetimes of some of the states, and the unique decaying contributions to the wavepacket dynamics are the subject of investigation. In addition, the magnitude of the observed quantum beating is dependent on the NIR polarization, offering the possibility to determine the specific coupling pathway, as well as the potential for coherent control of population transfer processes.

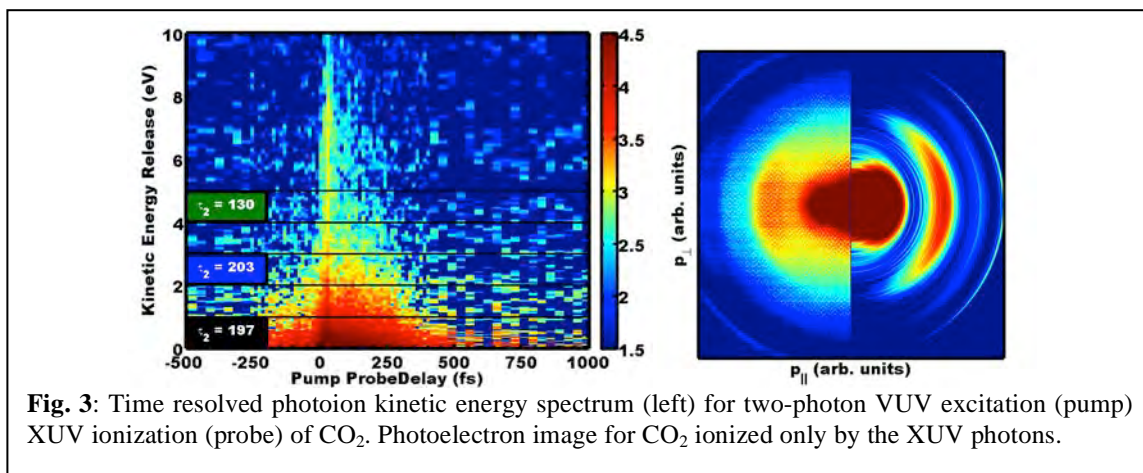
Future work will focus on applying the knowledge gained from the atomic systems to the study of small molecules such as oxygen and nitrogen. Preliminary results in nitrogen show wavepacket behavior that is strikingly similar to atomic argon for the high n Rydberg states built on the A state ion core, and complicated vibrational-electronic

coherences in the b' valence state. The current technique holds promise for revealing dynamics induced by nuclear-electronic coupling, such as vibrationally-resolved predissociation and autoionization, in molecular excited states.

Non-Born-Oppenheimer dynamics in molecules studied by few-femtosecond XUV pulses (A. Belkacem)

This effort aims to follow electronic excitations with state specificity to look at model molecular systems exhibiting non-adiabatic dynamics. The role of low-lying Rydberg states in ultrafast dynamics of valence excited molecular systems has been a growing topic of both theoretical study and experimental work. Embedded in the valence structure of molecule, such states can be transiently populated on ultrafast time-scales following valence electronic excitation. In ethylene, population of the $\pi 3s$ Rydberg state following excitation to the $\pi\pi^*$ state has been predicted theoretically. UV light generated via High Harmonic Generation is used to both pump to the valence state and subsequently ionize the system. Using velocity map photoelectron imaging we measured the resultant photoelectron kinetic energy spectrum, which reveals transient population of this low-lying Rydberg state.

We have performed the first experimental time resolved study on the lowest lying electronically excited states of carbon dioxide (Fig. 3). In this experiment we use a two photon 4.77 eV pump to excite to a neutral manifold containing many degeneracies, and probe using a combination of the 14.3 eV and 11.1 eV photons. This set up reveals two primary channels. The first is the direct dissociation of the state pumped by the two 4.77 eV photons. We measure this to be less than our pulse resolution and it represents over half the signal. The second effect is a longer lived channel measuring over 200 fs in duration. By analogy to previous experiments performed in the isoelectronic molecule carbon disulfide, and from the theoretical predictions about the multiple degeneracies in the vicinity of the pumped state, we conclude that this long lived channel is the mixing of other states with the optically pumped state creating a delay in the dissociation. One of the previous studies on carbon disulfide also revealed vibrational wave packet dynamics with a period of about 80 fs. In the higher kinetic energy release CO^+ fragments we measure oscillations with a period of 133 fs and a characteristic decay time of 160 fs.



Reaction Microscopy (*Th. Weber, A. Belkacem, C. W. McCurdy, T. N. Rescigno*)

In this branch we investigated and controlled the mechanisms and dynamics of photochemistry at the atomic and molecular level of small systems by combining microscopy and spectroscopy to visualize and understand their kinematics and dynamics in fragmentation processes.

We have studied the molecular-frame photoelectron angular distributions (MFPADs) for carbon K-edge photoionization of C_2H_6 , CF_4 and $\text{C}_2\text{H}_2\text{F}_2$ at photoelectron energies below 10 eV applying our COLTRIMS technique. The measurements agree rather well overall with the predictions of our theory group (Trevisan, McCurdy, and Rescigno) using complex Kohn calculations. The MFPADs, when integrated over all directions of the photon polarization, yield shapes consistent with the symmetry point group of the target molecule. For C_2H_6 , that shape also images the shape of the molecule, with lobes showing preferential ejection along the C-H bonds. For CF_4 a contrasting “anti-imaging” effect is found, with photoelectrons preferentially ejected in directions between the C-F bonds. A set of measurements and theoretical investigations for $\text{C}_2\text{H}_2\text{F}_2$ was also carried

out. As this molecule comprises two energetically non-degenerate carbon K-edges, the emission center of the photoelectron can be chosen by considering the photoelectron kinetic energy, yielding distinct differences in the MFPADs. Consistent with what we saw for ethane and carbon tetrafluoride, the MFPADs for $C_2H_2F_2$ shows a combination of both behaviors. A “simple man’s” picture for this important bond imaging/anti-imaging effect (first seen in our work in *Phys. Rev. Lett.* **108**, 233002 (2012) and *J. Phys. B* **45**, 194002 (2012)) remains elusive.

In the second project we isolated conical intersections and investigated their influence on the electron and ion dynamics in the fragmentation process of hydrocarbon molecules. Exploiting our coincident recoil-ion and Auger electron 3D-momentum imaging scheme we were able to probe the multi-dimensional potential energy surfaces of the ethylene dication after K-shell ionization followed by subsequent Auger decay. The PIPICO spectra helped us to distinguish three different fragmentation channels

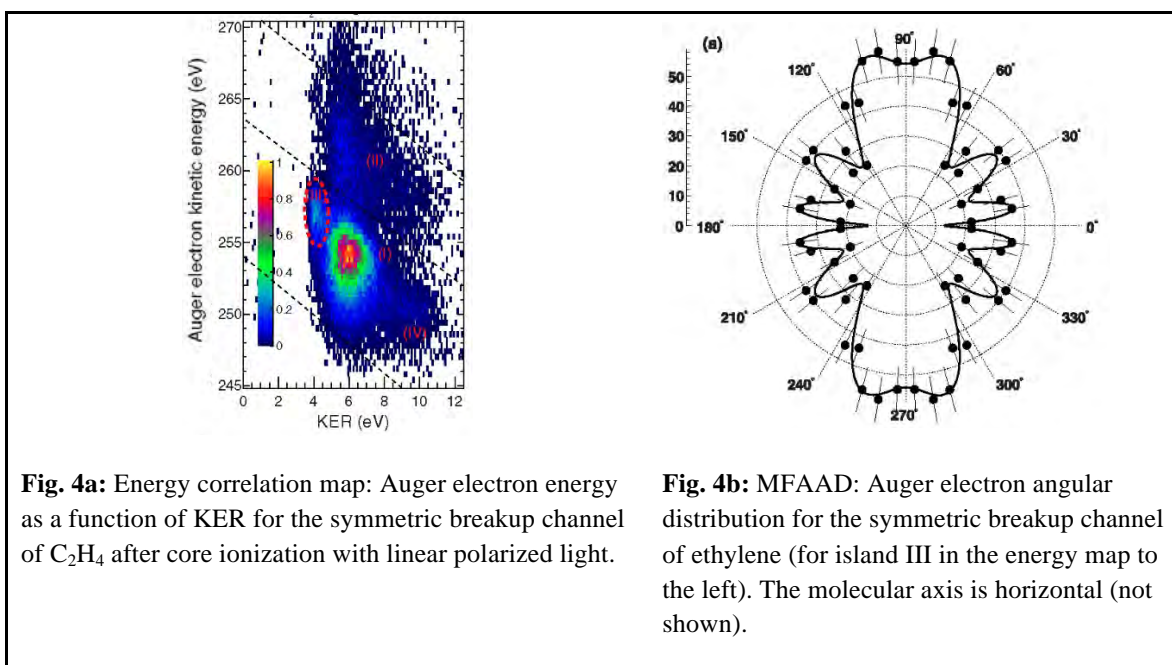


Fig. 4a: Energy correlation map: Auger electron energy as a function of KER for the symmetric breakup channel of C_2H_4 after core ionization with linear polarized light.

Fig. 4b: MFAAD: Auger electron angular distribution for the symmetric breakup channel of ethylene (for island III in the energy map to the left). The molecular axis is horizontal (not shown).

(deprotonation, symmetric breakup, and molecular hydrogen ion elimination). The branching ratios allowed us to classify the most probable double ionization decay mechanisms. Moreover, energy correlation maps representing the kinetic energies of the Auger electrons as a function of the KER (see fig. 4) in combination with the PESs from our theory group (D. Haxton) using the multi-configuration self-consistent field method enabled us to identify the most likely electronic states involved in the fragmentation pathways. We found no hints of core-hole localization or diffraction in the deprotonation channel; all molecular frame Auger electron angular distributions (MFAADs) showed a symmetric emission pattern. However, in case of the symmetric channel, we find strong evidence of multiple scattering of the outgoing Auger electron. For very low kinetic energy release of the symmetric breakup we found a highly structured Auger electron angular distribution (see fig. 4) similar to the Auger decay of N_2 which suggests an entangled Auger and photoelectron pair facilitated by two conical intersections. The conical intersections between the two excited states and the ground states (i.e. S_3 - S_2 and

S_2 - S_1) result in degenerate electronic states which give rise to the mix of interference patterns of Auger electrons emitted from gerade and ungerade orbitals.

To further understand conformation changes we studied the non-dissociative and dissociative photo-double-ionization of 1,1-difluoroethylene using single photons of energies ranging from 40 to 70 eV applying our COLTRIMS technique. We could isolate the branching ratios of the six reaction channels identified in the experiment. We also could study the influence of selection and propensity rules and precise threshold energies of double ionization could be extracted, which hint to the involvement of different manifolds of states. Electron-ion energy maps and relative electron emission angles are used to distinguish between direct and indirect photo-double-ionization mechanisms. Our measurements suggest direct (TS1) and indirect (molecular Auger) ionization processes responsible for the production of metastable dications, while additional contribution from the autoionization in the dissociation is possible only for the direct ionization channels. In some of these direct ionization channels, namely, $\text{HF}^+ + \text{C}_2\text{HF}^+$ and $\text{CF}^+ + \text{CH}_2\text{F}^+$, we have observed intriguing phenomena of bond rearrangement involving the migration of constituent hydrogen and fluorine atoms. To our surprise the hydrogen elimination channel $\text{C}_2\text{F}_2^+ + \text{H}_2^+$ was very much suppressed (1%) compared to the H_2^+ emission in C_2H_4 which we studied earlier and which suggested a concerted scissoring and stretching motion of the two protons at one end of the molecule, circumventing a potential barrier to direct dissociation while finding a conical intersection which facilitated this conformation change on an ultrafast time scale.

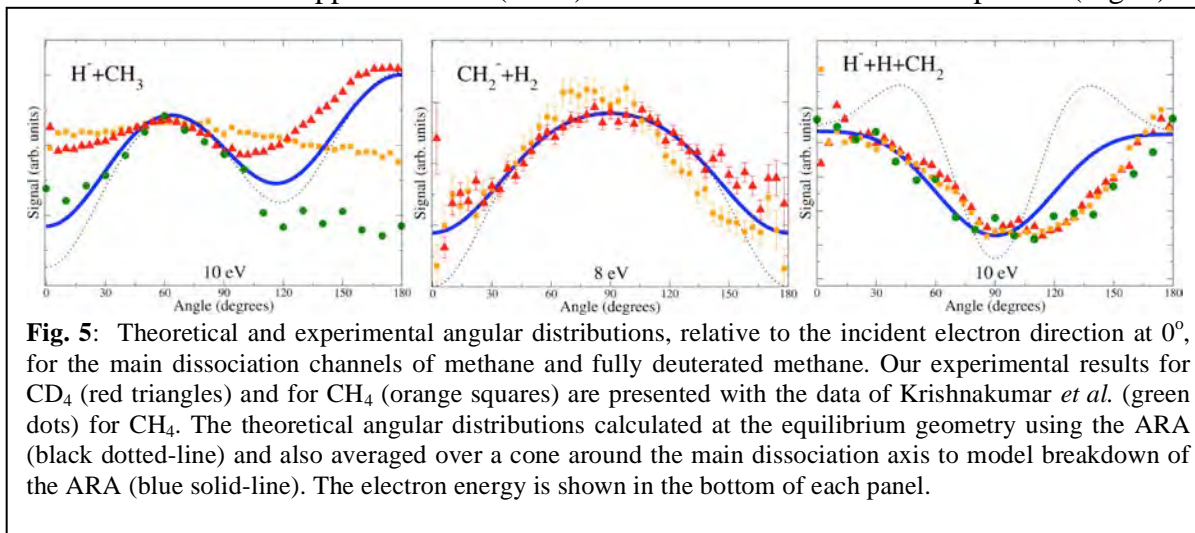
Thrust 2: Electron driven processes in atoms and small molecules.

A. Belkacem, D. J. Haxton, C. W. McCurdy, T. N. Rescigno, D. S. Slaughter, and Th. Weber.

Detailed investigation of dissociative electron attachment dynamics in fundamental systems (*D. S. Slaughter, A. Belkacem, D. J. Haxton, C. W. McCurdy, T. N. Rescigno, Th. Weber*)

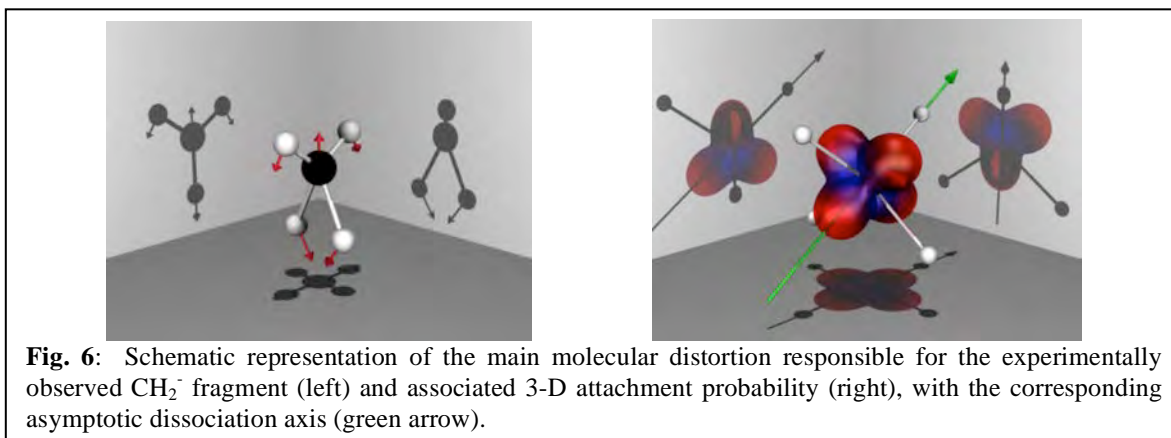
Understanding dissociative electron attachment (DEA) dynamics in gas phase systems is essential to understanding the chemistry of various diffuse media, such as interstellar clouds, planetary atmospheres and plasmas. With Ann Orel and Nicolas Douguet at University of California, Davis, we recently studied the anion dynamics of three competing dissociation pathways of a doubly-excited 2T_2 Feshbach resonance in methane. Molecular-frame scattering calculations using the complex Kohn variational method were used to determine the electron attachment entrance amplitude, giving the 3D angular dependence of electron attachment in the molecular frame. These calculations were compared with the results of momentum imaging experiments using the dissociative electron attachment reaction microscope, through which we could distinguish each of the different fragmentation channels, their kinetic energy release and angular distributions.

We found that this broad anion resonance exhibits both dissociation and bond formation dynamics in the production of CH_2^- and H_2 at 8 eV electron attachment energy, where 3-body breakup is energetically forbidden. We found good the agreement between the measurements and predicted angular distributions of the CH_2^- fragment and the 3-body breakup channel $\text{H}^- + \text{H} + \text{CH}_2$ (Fig. 5), where the latter were calculated using a modified axial recoil approximation (ARA) derived from the entrance amplitude (Fig. 6).



For the $\text{H}^- + \text{CH}_3$ channel the agreement was less satisfactory and a clear isotope effect was apparent between experiments on methane and its isotopologue CD_4 . In both cases a breakdown in the ARA is apparent, leading to a nearly isotropic broadening of the dissociating nuclear wavepacket that is somewhat suppressed in CD_4 . In this case a more detailed calculations of the excited state potential energy surfaces are needed for a complete understanding of the non Born-Oppenheimer anion dynamics.

We are currently investigating detailed dynamics in small model systems such as



ammonia, formamide, methanol and formic acid. These molecules have immediate relevance to atmospheric and interstellar chemistry and possess key functional groups that play important roles in larger systems.

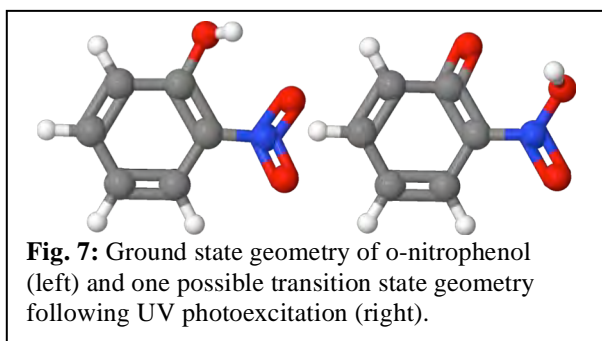
Subtask 2: Photon and electron driven processes in complex molecular systems and molecules in complex environments.

Thrust 1: Photon driven processes in complex molecular systems and molecules in complex environments.

A. Belkacem, O. Gessner, M. Head-Gordon, S. R. Leone, D. M. Neumark, and R. W. Schoenlein.

Non-Born-Oppenheimer excited state dynamics in multielectronic systems following resonant photoexcitation (*A. Belkacem*)

Aromatic molecules like nitro-phenols play an important role in atmospheric chemistry and are good model systems to study photochemical dynamics in relatively large molecules. They have a high absorption cross section in the ultraviolet (UV) where excitations lead to a variety of fragmentation pathways involving non-radiative internal relaxation processes. These pathways lead to elimination of the hydroxyl and nitro groups, isomerization and even formation of new bonds between the different functional groups before elimination. Very few studies have looked at these systems, especially in the time domain.



Very few studies have looked at these systems, especially in the time domain.

We are investigating these complex processes by time-resolving them on femtosecond time scales. We use 25 fs Ultraviolet (~ 4.7 eV) and Vacuum

Ultraviolet (~ 8 eV) pulses obtained from high harmonic generation to pump and probe neutral excited states in o-Nitrophenol (Fig. 7). Measurements from time-resolved photoion and photoelectron spectroscopy are combined to develop an understanding of the different processes at play in this system. We plan to further explore this system by introducing an additional wavelength tunable femtosecond laser pulse in a ‘pump - re-pump - probe’ scheme, focusing on the role of doubly excited states near the ionization threshold in breaking bonds that eventually results in the opening of the ring and fragmentation of the chain.

Control of Intermolecular Coulombic Decay in small hetero-nuclear clusters (*Th. Weber*)

The recently observed Interatomic Coulomb Decay (ICD) between atomic or molecular neighbors is one of the most effective ones chemical key processes associated with radiation chemistry, environmental chemistry, and chemical synthesis. The decisive next step is to go from observation of ICD to control of this decay process and its consequences for the environment. Controllability through environmental changes can make this inter-molecular decay even more significant for life sustaining applications.

The goal of our project in this subtask was hence to demonstrate control of ICD for the first time experimentally by changing the pH value of the environment. ICD strongly depends on the energy levels in the cluster and on the internuclear distance of the atoms participating in the decay. Thus the composition and structure of the cluster have a direct influence on relatively general quantities, such as the fragmentation rates, the energy spectrum of the emitted ICD electrons and the kinetic energy release of the ionic fragments.

We chose to examine the decay of ammonia clusters in a water environment. This system is of particular interest because of the possibility to protonate/deprotonate ammonia clusters to allow investigating the response of ICD to changes of pH value on a fundamental level. After the removal of an inner-valence electron, an isolated NH_3 molecule, like many other molecules, cannot relax by emitting another electron for energetic reasons. In contrast, both the H-donor and H-acceptor molecules in the ammonia dimer can decay electronically after inner-valence ionization. One can expect that much less effort is needed to detach electrons from the deprotonated systems. That is because the single- and double-ionization potentials of the deprotonated dimers (and trimers) are noticeably lower than those of the normal clusters. That way the inner-valence vacancy of any ammonia molecule in the deprotonated clusters now has plenty of new open decay channels at its disposal so that electronic decay of this vacancy speeds up considerably compared to the normal clusters. Protonation is expected to have the opposite effect on the ammonia clusters than deprotonation; it switches ICD off because the single- and double-ionization potentials of the protonated clusters are higher than those of the normal ones.

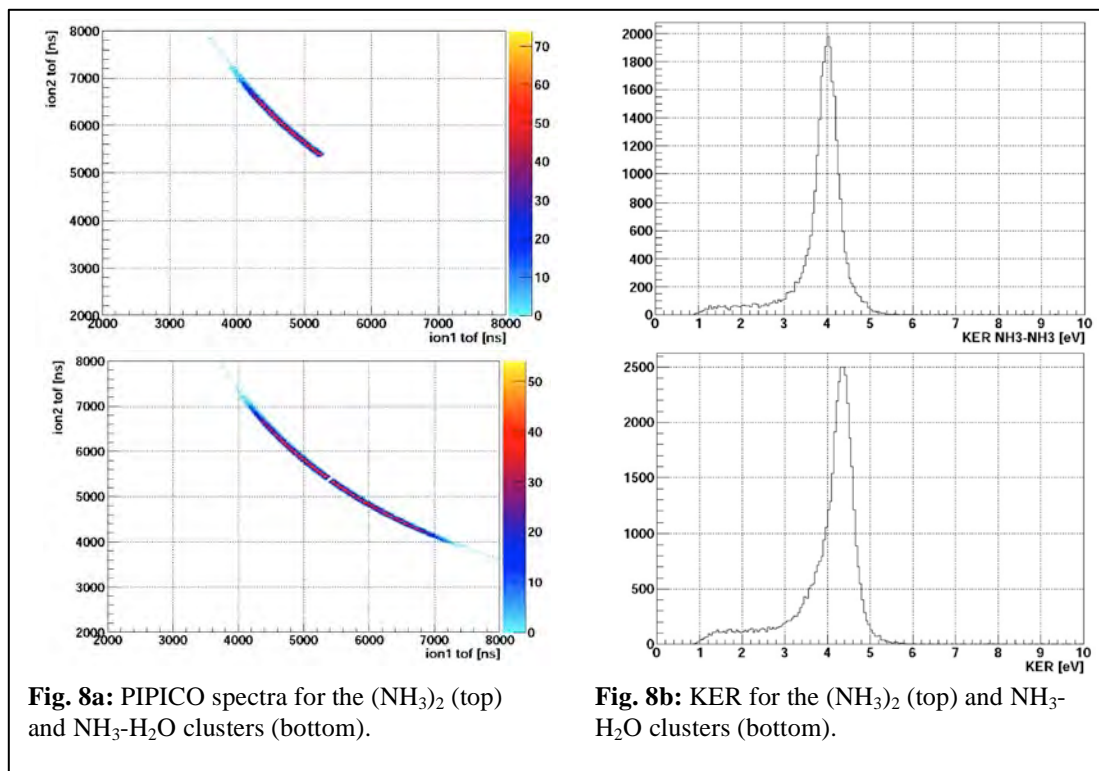


Fig. 8a: PIPICO spectra for the $(\text{NH}_3)_2$ (top) and $\text{NH}_3\text{-H}_2\text{O}$ clusters (bottom).

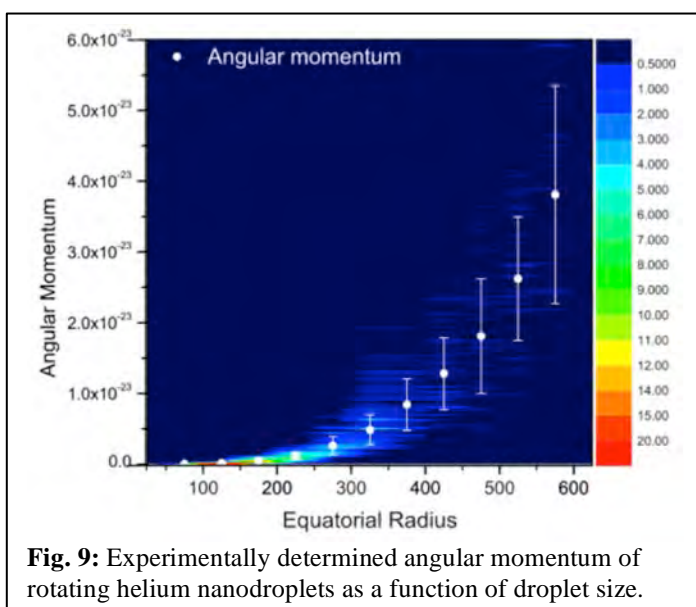
Fig. 8b: KER for the $(\text{NH}_3)_2$ (top) and $\text{NH}_3\text{-H}_2\text{O}$ clusters (bottom).

In our ongoing project we isolate and investigate ICD processes of pure ammonia dimers and compare them to water-ammonia clusters (i.e. ammonium hydroxide) for different concentrations of the solution. We have performed four particle coincidence experiments where we measure the 3D-momenta of the photo- and ICD electron and two fragment ions of the cluster simultaneously. We isolated the ICD process in $(\text{NH}_3)_2$ and $\text{NH}_3\text{-H}_2\text{O}$ clusters via PhotoIon PhotoIon Coincidence (PIPICO) spectra and we able to derive the respective KER's (Fig. 8).

In the next step we will demonstrate its control by protonation/deprotonation for different compositions and concentrations of the clusters. Moreover, the measured photo electron energies will be analyzed as a function of the KERs in particle energy correlation maps, which will effectively probe the potential energy surfaces and give insight to the dynamics of the fragmentation pathways.

Ultrafast EUV and X-ray studies of dynamics in clusters (*O. Gessner, S. R. Leone, and D. M. Neumark*)

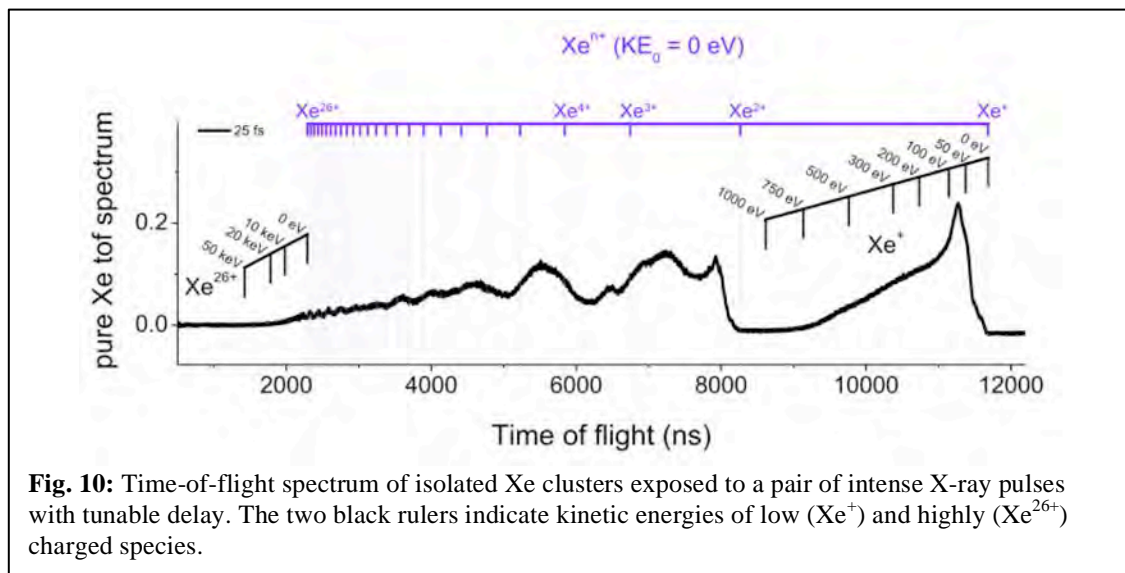
Helium nanodroplets are unique systems that exhibit quantum behavior on length scales between the few-atom and macroscopic limits and are widely used as cryogenic spectroscopy matrices. Our research explores the fundamental properties of these systems on two different fronts using laboratory- and accelerator-based ultrafast X-ray light sources. High harmonic generation (HHG) based experiments employ ultrafast extreme ultraviolet (EUV) photoelectron and ion imaging to study the electronic dynamics of both pure and doped helium nanodroplets. These experiments in the weak field limit are complemented by free electron laser (FEL) based experimental campaigns that exploit extreme X-ray peak powers available at light sources such as the Linac Coherent Light Source (LCLS). Ground state droplet dynamics are imaged through coherent scattering and extreme non-equilibrium dynamics of embedded nanoplasmas are studied by both scattering and time-resolved ion mass spectrometry.



The diffraction patterns of isolated helium droplets provide direct access to the sizes and shapes of the superfluid systems. In particular, shape distortions that correspond to rotation-induced flattening of the (ideally) spherical droplets are a measure of the droplets' rotational excitation. The detection of this phenomenon has been one of the highlights of this project and the subject of considerable interest due to the quantum nature of the nano- to micrometer sized rotors. A detailed modeling, however, of the mechanisms that *induce* the

rotation of the isolated droplets, is still outstanding. We are currently developing tools to perform an automated statistical analysis of the extensive image data sets in an effort to understand the origin of the droplets' vorticity and how it correlates with the hydrodynamics that govern the droplet generation processes in the breakup of a liquid helium jet. Fig. 9 shows a preliminary result from these efforts. The histogram displays total angular momentum distributions (vertical axis) of droplets with different sizes (horizontal axis). The color patterns represent the statistical distribution of angular momenta as a function of droplet size. The white markers and error bars indicate the respective means and standard deviations. A clear systematic trend is apparent that may provide a first steppingstone to connect the isolated superfluid droplet dynamics with the normal fluid dynamics in the droplet generation region of the experimental setup.

In our most recent LCLS experiment, isolated Xe clusters and Xe clusters embedded in He droplets were exposed to a pair of intense X-ray pulses separated by a tunable time delay. In addition to the diffraction pattern, time-delay dependent ion time-of-flight (TOF) spectra were recorded that give access to the kinetic energies released in the ejection of ions as illustrated for pure Xe cluster targets in Fig. 10. A series of TOF spectra recorded for the mixed He/Xe systems for different X-ray pulse delays indicate unexpectedly complex dynamics beyond existing standard models for the interaction of homogeneous noble gas clusters with intense X-ray pulses. The quantitative interpretation of these results will provide new insight into the dynamics of core-shell hybrid systems in intense X-ray fields and, potentially, the application of helium droplets as tamper materials to mediate Coulomb explosion effects during FEL imaging experiments.

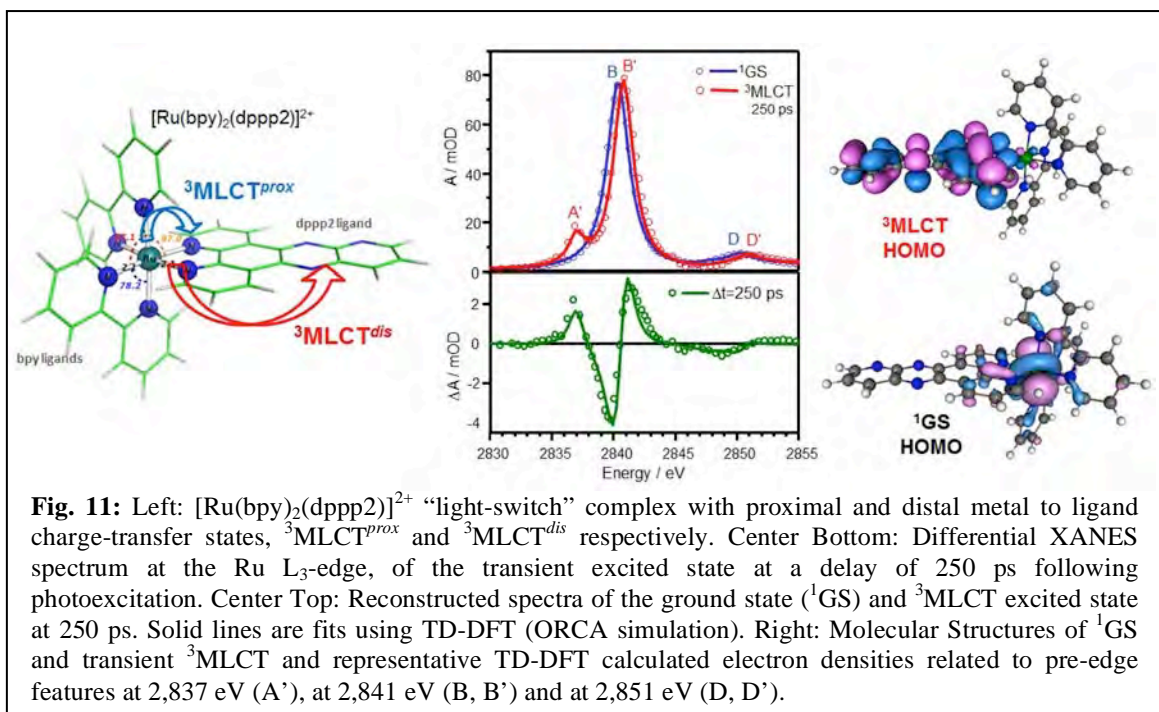


Great strides have been made in extending the laboratory-based experiments on ultrafast electronic dynamics in pure helium nanodroplets toward the study of energy- and charge-transfer mechanisms such as Penning ionization in doped droplets. Experimentally, this required a significantly increased sensitivity of the HHG setup and the addition of a new beam path in order to generate the 14th harmonic of the 800nm

driver pulse that can directly access the prominent droplet 1s2p absorption band centered at 21.6 eV. Nanodroplets containing 10^4 to 10^6 helium atoms doped with small contributions ($< 10^{-3}$) of noble gas atoms (Xe, Kr, Ne) have been excited to the 1s2p Rydberg band and several transient photoelectron images have been recorded. Preliminary results indicate that energy transfer processes between the droplets and Kr dopants may be reflected in the photoelectron spectra. The experiments will be further improved to enable time-resolved measurements that will provide new information about the dynamic timescales and relaxation channels that govern solvent-solute interaction in the superfluid environment.

Ultrafast X-ray studies of condensed phase molecular dynamics (*Robert W. Schoenlein*)

The objective of this subtask is to advance our understanding of solution-phase molecular dynamics using ultrafast X-rays as time-resolved probes of the evolving electronic and atomic structure of solvated molecules. Time-resolved XANES provide detailed information about dynamics of the valence charge structure, while time-dependent EXAFS provides information about changes in the local atomic structure. X-ray measurements thereby reveal important new information about reactions including: charge transfer processes, changes in oxidation states, formation/dissolution of bonds, and conformational changes. This subtask exploits picosecond time-resolved X-ray beamlines at the ALS (soft X-rays BL 6.0.2, hard X-ray BL6.0.2), beamlines 7-ID and 11-ID at the APS, and ultrafast instruments SXR and XPP at the LCLS X-ray free electron laser, complemented by table-top ultrafast optical spectroscopy studies.



One area of present focus is on solvated transition-metal complexes exhibiting strong coupling between molecular structure, charge transfer, and electronic properties arising from the ligand field and solvent environment. These include transition-metal polypyridyl

compounds, metal-porphyrins, metal-carbonyls, and bridged heteronuclear metal-metal compounds. Understanding the fundamental dynamics in these classes of compounds is relevant for solar energy conversion schemes, photo-catalysis, and related processes.

Charge-transfer Dynamics in Ru- polypyridyl Complexes: We have initiated new studies in a Ru- polypyridyl complex with extended ligands (Fig. 11), the so-called “light-switch” complex $[\text{Ru}(\text{bpy})_2(\text{dppp2})]^{2+}$ which exhibits photo-induced charge-transfer processes that are poorly understood, and yet are central for solar energy conversion (e.g. dye sensitized solar cells) and photo-catalysis. Ru-dppp2 exhibits two triplet excited states *proximal* and *distal* to the Ru center, and the branching and charge localization are highly dependent on the solvent environment. Time-resolved XAS at the Ru L-edge (ALS BL6.0.1) captures these transient excited states, and detailed comparison with TD-DFT analysis provides quantitative information on the transient excited intermediate valence charge distributions ($^3\text{MLCT HOMO}$). Complementary studies at APS 11-ID have focused on EXAFS at the Ru K-edge, and studies at ALS BL6.0.2 provide a “ligand-view” of the charge dynamics via time-resolved XANES at the N K-edge.

We are conducting related studies of the photochromic Ru-complex $[\text{Ru}(\text{bpy})_2(\text{pyESO})]^{2+}$ which exhibits photo-driven isomerization that is predicted to be mediated by conical intersections. Time-resolved XAS at the Ru L-edge and S K-edges (ALS BL6.0.1) provide complimentary views of the isomerization dynamics, and yield the first experimental evidence of a metal-centered intermediate state.

Porphyrin-based Donor- π -Acceptor Complexes based on 3d transition metals employ a “push-pull” architecture to facilitate e-h separation, and are new candidates for efficient dye-sensitized solar cells. Collaborating with F. Himpsel and co-workers, we have initiated time-resolved XAS studies, combined with TD-DFT simulations, in order to visualize the initial photo-excited valence charge distribution and its evolution. Picosecond soft X-ray studies at ALS will provide a foundation for future femtosecond studies (e.g. of the electron-hole separation) using the SXR instrument at LCLS.

Thrust 2: Electron driven processes in complex molecular systems and molecules in complex environments.

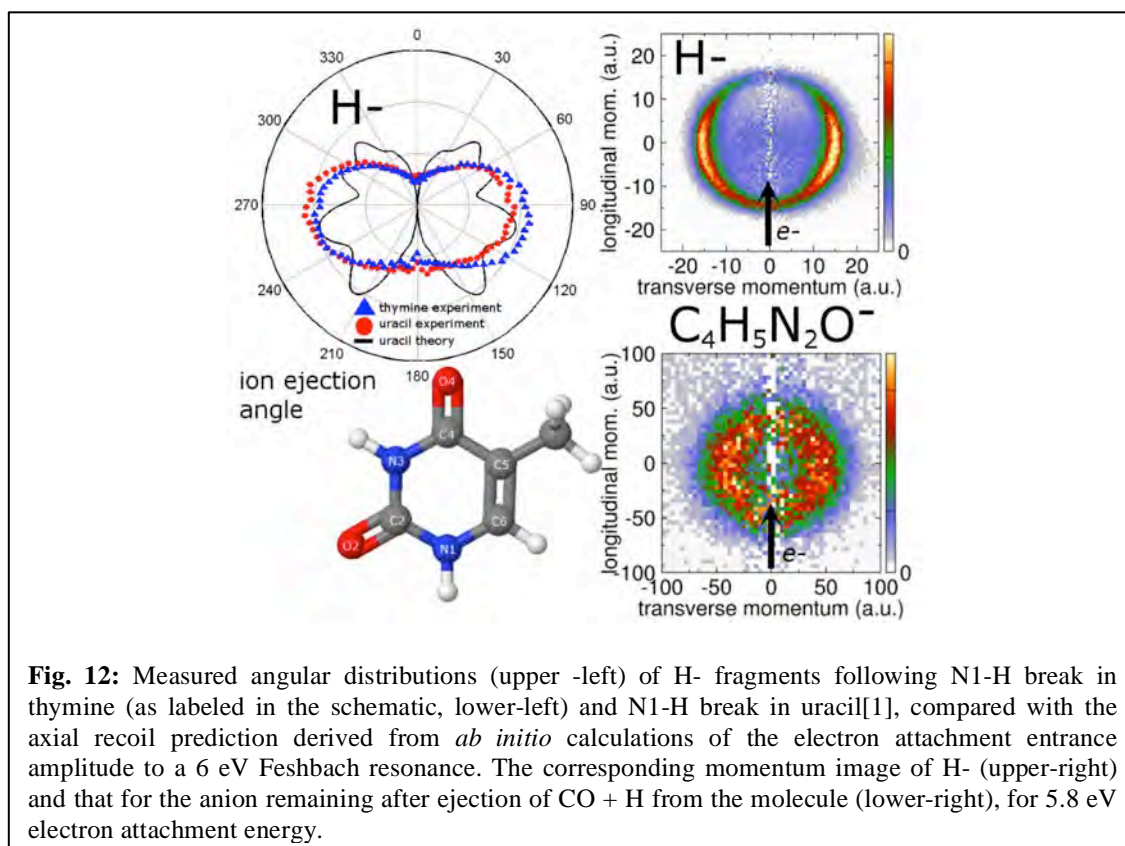
A. Belkacem, D. J. Haxton, C. W. McCurdy, T. N. Rescigno, D. S. Slaughter, and Th. Weber.

Investigation of dissociative electron attachment dynamics in biologically relevant molecules (D. S. Slaughter, A. Belkacem)

Low energy free electrons have presented unique capabilities to break covalent bonds at sub-ionization and sub-excitation energies via the formation of transient anion resonances. Resonant anion states decay by electron autodetachment and/or dissociation while typically exhibiting strong coupling between the electronic and nuclear degrees of freedom. The bond- and site-specificity of these resonant processes play a significant role

in understanding and modeling radiation damage and ultimately could be exploited to control chemical processes with exquisite precision and high energy efficiency.

In a combined experimental and theoretical study with Vince McKoy and Carl Winstead at Cal Tech, we determined that dissociative electron attachment (DEA) in the gaseous RNA base uracil at 6 eV electron collision energy leads to ring-breaking and loss of CO + H with a total translational kinetic energy release greater than 1-2 eV.[1] The experiments employed anion fragment momentum imaging consisting of a tunable low-energy electron gun, an effusive molecular beam from a hot oven, a COLTRIMS-type ion momentum imaging spectrometer and a time- and position sensitive ion detector. In the laboratory frame defined by the incident electron direction, the angular dependence of the fragments from this fragmentation channel is isotropic, in contrast to the competing N-H breaking channel at the same resonant electron energy, which broadly resembles the axial recoil prediction. The latter was determined by single-excitation configuration interaction electronic structure and Schwinger multichannel scattering calculations. Recent experiments on the DNA base thymine (5-methyl-uracil) show that the addition of the methyl group has little if any influence on the DEA dynamics; preliminary results from these experiments are presented in Fig. 12.



Prospects for future work on dissociative electron attachment dynamics in systems of biological and technological importance We will investigate correlations between the bond- and site-specific fragmentation in DEA and the dynamics of the dissociating anion for the molecular subunits of DNA and other systems that will help improve our

understanding of radiation damage in biological systems. This work will be extended to investigate solvation effects on the DEA dynamics of these molecules when they are incorporated in clusters with water or other solvents.

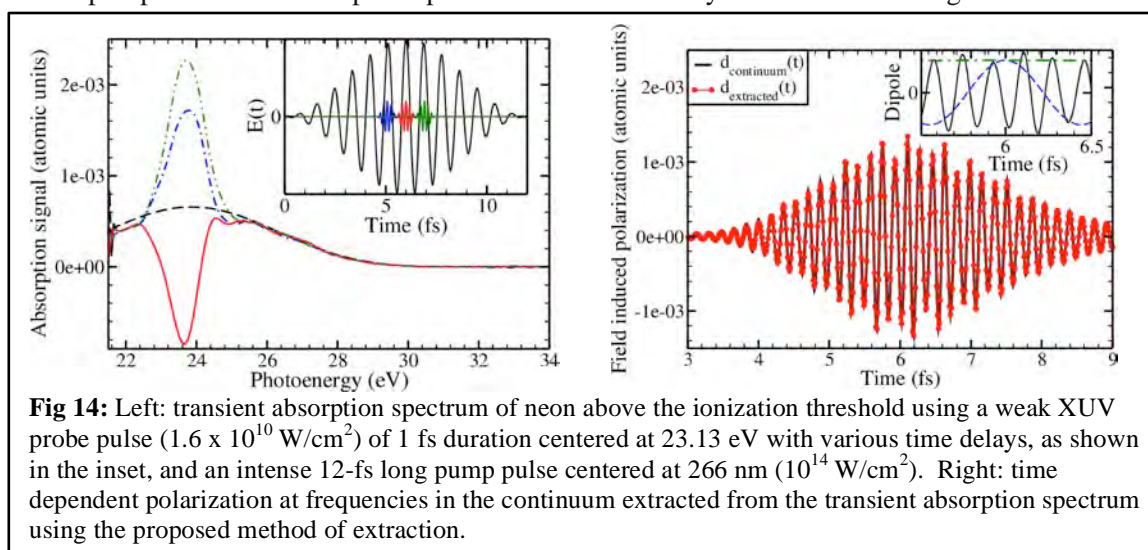
We will examine the role that functional groups such as OH, NO_x, NH_x and CH_x play electron driven processes in relatively large multielectronic systems such as biomolecules, alcohols and acids. This will lead us to understand and ultimately control the dynamics in transient anions for other systems of interest to existing and emerging technologies. Some current examples include dimethyl carbonate, dimethyl sulfoxide, diethyl carbonate used in battery technologies and cobalt tricarbonyl nitrosyl used in focused electron/ion beam induced processing.

Subtask 3: First-principles theory of dynamics and electronic structure.

D. J. Haxton, M. Head-Gordon, C. W. McCurdy, T. N. Rescigno

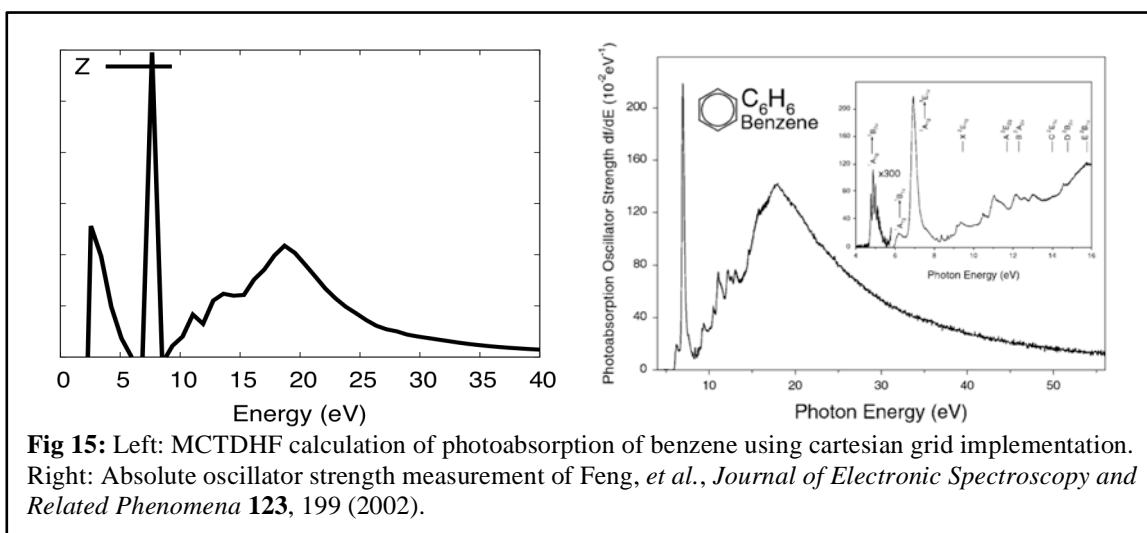
MCTDHF Calculations on Atomic Transient Absorption (*C. W. McCurdy, D. J. Haxton*)

Using the LBNL Multiconfiguration Time-Dependent Hartree Fock (MCTDHF) capability developed by Dan Haxton, we performed a study on transient absorption of neon at photon energies above the ionization potential. These calculations allowed us to suggest a method for using transient absorption spectroscopy above the ionization threshold to directly measure the polarization of the continuum induced by an intense optical pulse as shown in Fig. 14. In this way transient absorption measurement can be used to probe sub-femtosecond intense field dynamics in atoms and molecules. The method is based on an approximation to the dependence of these spectra on time-delay between an attosecond XUV probe pulse and an intense pump pulse that is tested over a wide range of intensities and time delays by all-electrons-active calculations using the MCTDHF method. The basis of this approximation is the observation that the polarizations at frequencies corresponding to energies in the continuum induced by the intense pump and weak XUV probe pulses are almost exactly additive over a range of intensities.



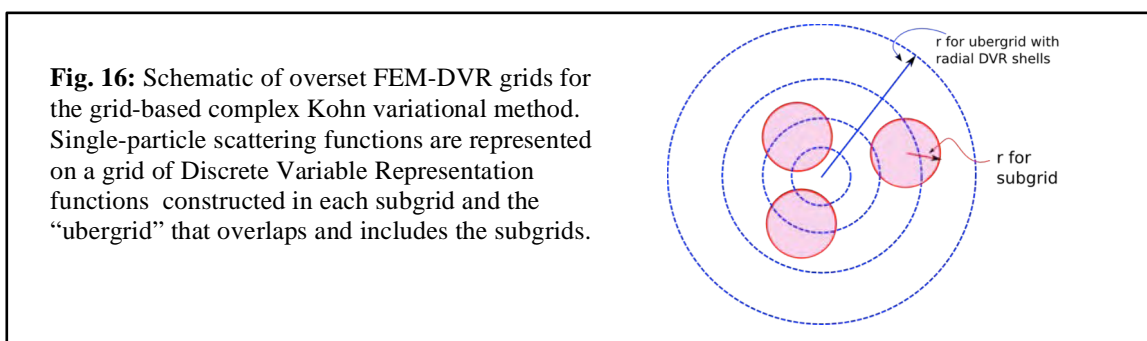
MCTDHF calculation of absorption signals for polyatomic molecules (*D. J. Haxton*)

An extension to the LBNL MCTDHF capability based on Cartesian DVR grids (as opposed to the prolate spheroidal grids we used for diatomics) has been developed and preliminary results using it have been obtained. We have demonstrated that the LBNL-MCTDHF code is capable of calculating all-active electron dynamics of polyatomic molecules and have begun to calculate absorption signals for applications including transient absorption. A preliminary result for the benzene photoabsorption cross section (with a configuration interaction representation capable of double core hole physics) is shown in Fig 15. Also shown is an experimental result [Feng et al, *Journal of Electronic Spectroscopy and Related Phenomena* **123**, 199 (2002)]. The comparison at this preliminary stage is favorable except for the spurious peak below 5eV. The immediate



goal is to use this capability to calculate transient absorption signals for polyatomic molecules.

Development of a New Grid-based Complex Kohn Computational Method (*C. W. McCurdy, T. N. Rescigno*)



In collaboration with Prof. Robert Lucchese of Texas A&M University, also funded by the DOE AMOS program, we have begun the development of a new Complex Kohn Variational method for electron-polyatomic molecule scattering and photoionization problems. The Complex Kohn variational method developed over decades by the LBNL group solves for the scattering wave function and scattering amplitudes in a close-coupling expansion over channels, Γ , of the full many-electron solution, $\Psi^{(+)} = \sum_{\Gamma} \psi_{\Gamma}(\mathbf{r}_1, \dots, \mathbf{r}_N) \phi_{\Gamma}(\mathbf{r}_{N+1})$. This new implementation will eliminate the use of Gaussian basis functions and spherical Bessel functions to represent the single particle scattering solutions, $\phi_{\Gamma}(\mathbf{r}_{N+1})$, with outgoing scattering boundary conditions that appear in the close-coupling expansion. The key to method is the representation of the scattering orbitals on a Discrete Variable Representation (DVR) grid over points using “overset grids” as shown schematically in Fig. 16. In early work this year we have discovered that very rapid convergence by making use of a particular Krylov series of functions in the Arnoldi solution of the Kohn linear equations for the values of $\phi_{\Gamma}(\mathbf{r}_{N+1})$ on the grid that involves repeated application of the known free-particle Green’s function on the grid.

The long-range objective is the development and application of new complex Kohn computer codes for the study of electron-molecule collisions and molecular photoionization. The proposed theoretical and computational developments will lead to a modern, easy-to-use, and general electron-molecule collision code, parallelized with OpenMPI that will be made available to other users and will support experiments planned at LBNL in dissociative electron attachment, X-ray photoionization, and high harmonic generation.

Dissociative Electron Attachment (*T. N. Rescigno, C. W. McCurdy*)

The fundamental importance of dissociative electron attachment in electron-driven chemistry as well as the chemistry of various diffuse media, such as interstellar clouds, planetary atmospheres, and plasmas, provides an impetus for understanding the mechanism of DEA. Our work in this area has focused on the study of ion fragment angular distributions; in the favorable case of prompt dissociation, characterized by the existence of predominant dissociation pathways, electron-molecule scattering calculations can tie the observed angular distributions to specific dissociation mechanisms. We have found that the combination of electronic structure calculations on the relevant diabatic resonant anion states and electron scattering calculations to compute the entrance amplitudes (attachment probabilities) offers a useful and practical alternative to a complete dynamical treatment of DEA involving time-dependent wave-packet propagation on complex potential energy surfaces, which becomes prohibitive for complex polyatomic targets.

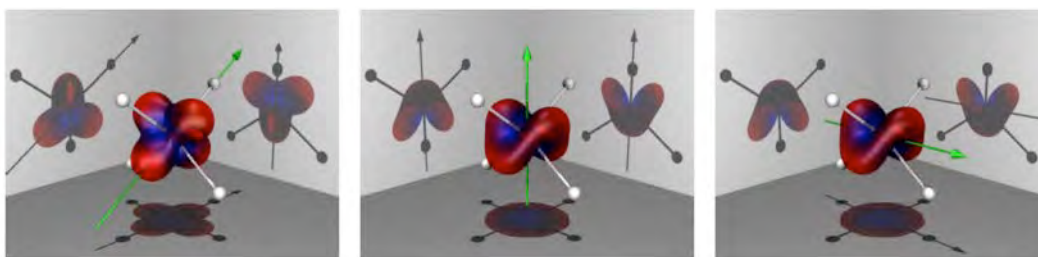
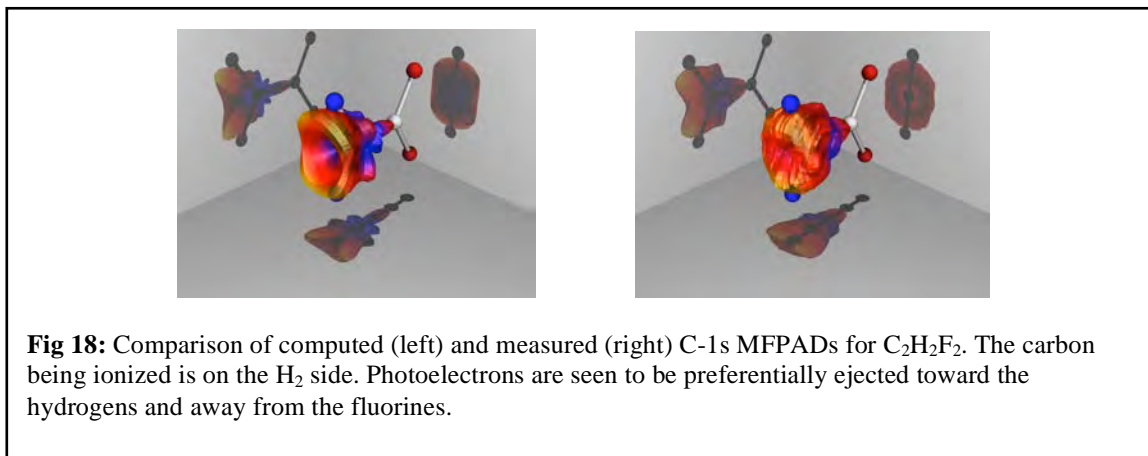


Fig. 17: 3-D electron attachment probabilities for the principal dissociation channels in methane: (left to right) $\text{H}^- + \text{CH}_3$, $\text{H}_2 + \text{CH}_2^-$, $\text{H}^- + \text{H} + \text{CH}_2$ with the corresponding asymptotic dissociation axes (green arrows).

We have focused our efforts over the past year on two systems: methane and ammonia. Methane's dissociation mechanisms presented something of a mystery. DEA to methane is characterized by a broad dissociation peak centered near 10 eV which gives rise to three principal dissociation channels, namely, $\text{H}^- + \text{CH}_3$, $\text{H}_2 + \text{CH}_2^-$, $\text{H}^- + \text{H} + \text{CH}_2$. Our calculations have shown that DEA proceeds through a single, triply degenerate $^2\text{T}_2$ Feshbach resonance and that Jahn-Teller splitting through molecular distortions in this $^2\text{T}_2$ state induce dissociation into the three different break-up channels. Entrance amplitudes obtained from theoretical electron-methane scattering calculations, shown in Fig. 17, along with reasonable assumptions about the dissociation dynamics deduced from structure calculations, gave angular distributions in good agreement with experiment. In the case of ammonia, experiment shows two broad peaks near 6 and 10

eV. The lower peak feeds both $\text{H}^- + \text{NH}_2$ and $\text{NH}_2^- + \text{H}$, while the upper resonance produces predominantly $\text{H}^- + \text{NH}_2$. The ground state $\text{H}^- + \text{NH}_2$ and $\text{NH}_2^- + \text{H}$ asymptotes are quasi-degenerate, differing in energy by only 0.02 eV. The conventional view is that the 6 eV peak is associated with a non-degenerate $^2\text{A}_1$ resonance that can only correlate with $\text{H}^- + \text{NH}_2$ ($^2\text{B}_1$), while the upper 10 eV resonance state can cross the lower state at large distances and correlates with NH_2^- production. Our calculations confirm that the 6 eV resonance is a doubly excited Feshbach state that does indeed correlate with $\text{H}^- + \text{NH}_2$ ($^2\text{B}_1$) and give angular distributions close to what has been measured for that channel. The lowest $\text{NH}_2^- + \text{H}$ asymptote, on the other hand, does not correspond to resonance but rather becomes an NH_3^- virtual state at small N—H internuclear separation. At large N—H separations, it parallels the $^2\text{A}_1$ resonance and thus NH_2^- can be formed by charge exchange with the resonance state. Our calculations also show that the 10 eV resonance is in fact a doubly excited ^2E state which splits into dissociative and non-dissociative components and that the dissociative component correlates diabatically with $\text{H}^- + \text{NH}_2^*$ ($^2\text{A}_1$). Our computed angular distributions again confirm this assignment.

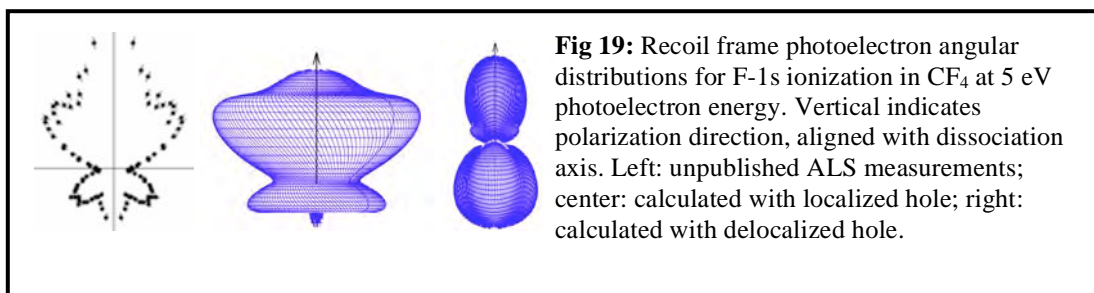
Molecular-Frame Photo-Electron Angular Distributions (MFPADs) (*T. N. Rescigno, C. W. McCurdy*)



MFPADs are sensitive probes of molecular structure and initial electronic state, but observing them at high resolution requires accurate orientation in the gas phase of the molecule from which the electron is ejected. The most accurate orientation has been accomplished in the cases of core or inner-shell ionization by detecting the photoelectron in coincidence with positively charged fragments that emerge following prompt Auger decay and dissociation of the molecule. Our unexpected discovery that, for a class of molecules containing a single heavy atom and several hydrogen atoms (CH_4 , H_2O , NH_3), the K-shell MFPADs at relatively low photoelectron energies, when averaged over all photon polarization directions, effectively image the geometry of the molecule has prompted us to study this phenomenon in molecules with two or more equivalent heavy atoms. In particular, we wished to investigate whether the imaging effect was specific to hydrogen-containing molecules, since we had earlier seen an anti-imaging effect in carbon 1s ionization of CF_4 . In a collaborative theoretical/experimental effort involving calculations by Prof. Cynthia Trevisan of the California Maritime and a series of ALS

experiments by Thorsten Weber of LBNL and the research group of Prof. Reinhard Dörner in Frankfurt, we showed, using C-1s ionization from $C_2H_2F_2$ as an example, that imaging and anti-imaging effects could be seen in the same molecule as shown in Fig. 18.

Studies were also undertaken to see if imaging effects could be used to detect the creation of localized core-holes in molecules with symmetry-equivalent atoms. Typically, such localization effects are rather small, as evidenced by asymmetry in the MFPADs on the order of a few percent. Our studies revealed two striking exceptions to this finding. Using acetylene (HCCH) as an example, we showed that by first using an X-ray photon to excite a carbon 1s electron to a discrete π^* level below the carbon K-edge, the core-vacancy created would rapidly localize on one of the carbon atoms, so that subsequent ionization of the π^* state by a second photon would produce an MFPAD with a pronounced asymmetry. In another study on *flourine* K-shell ionization of CF_4 , we discovered an interesting phenomenon. An attempt to reproduce a measured MFPAD at 5 eV photoelectron energy with delocalized orbitals failed to reproduce the measured angular distribution. When the calculation was repeated assuming a localized F 1s orbital, the agreement with experiment was excellent, as shown in Fig 19. Our finding was that, although the probability of ionizing a F 1s electron is the same for all four fluorine sites, the atomic site where the hole is created corresponds to the C-F bond that breaks. As that bond is broken, the dissociating F ion, because of its large electronegativity, withdraws an electron from the CF_3 fragment to form a CF_3^+ ion and a F atom with a filled 2p shell and the subsequent Auger decay is from the core-excited F atom ($1s2s^22p^6$). Our calculations predict that effect should be observable in other molecules with symmetry-equivalent halogens, such as C_2F_2 or CCl_4 .



Atomic Two-Photon Double Ionization (*T. N. Rescigno, C. W. McCurdy*)

The group 2a atoms offer an interesting contrast to the much studied case of two-photon double ionization of helium. The threshold for sequential 2-photon double ionization actually proceeds through excitation-ionization of the mono-cation as the first step ($h\nu + A(ns^2) \rightarrow A^+(np) + e^-$), reflecting the importance of the correlating configuration np^2 in these atoms. In contrast to helium, the window where non-sequential double ionization alone can occur is very small (0.44 eV in the case of Be). The consequence is that, for finite pulses, sequential double ionization produces two continuum electrons with very closely spaced energies in a single broad peak via excitation-ionization, and more widely spaced energies when proceeding through ground-

state single ionization. We have completed a theoretical study of this process in the case of Be in collaboration with Frank Yip of the California Maritime Academy. An interesting feature we find is that the electrons produced by sequential double ionization via excitation-ionization are still highly correlated, as reflected by a back-to-back angular ejection pattern for equal-energy sharing, while those produced via ground-state sequential ionization show a more characteristic uncorrelated behavior as found in helium.

Molecular Double Ionization (*T. N. Rescigno, C. W. McCurdy*)

We have made progress in our efforts to develop a robust, hybrid numerical method that combines Gaussian molecular orbital technology with grid-based, exterior complex scaled finite-element DVR methodology to overcome the computational obstacles involved in treating photo-double and electron-impact ionization studies to complex molecular targets. This work is being done in collaboration with Prof. Frank Yip of California Maritime Academy. The viability of the approach was demonstrated last year in a study that showed how the hybrid methodology could be used to efficiently calculate singly ionized continuum states for the cases of NO and O₂⁺, an essential step toward application to problems involving a double continuum. Our planned efforts will be directed at carrying out the first calculations of DPI on O₂ and N₂.

Electron-Molecule Scattering (*T. N. Rescigno*)

In a follow-up to our recent study of non-resonant dissociative excitation of water, we extended our study to electron collisions with methanol. This study was done in collaboration with Prof. Ann Orel and the Caltech/CSU Fullerton group under Profs. Morty Khakoo and Vincent McKoy.

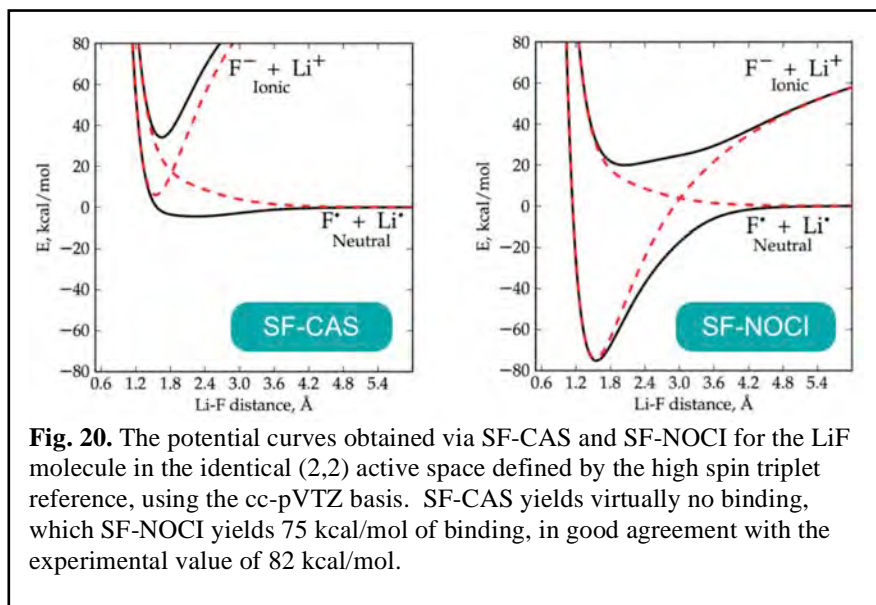
As was the case with water, the analysis of the electron energy loss spectra is complicated by the fact that the low-lying electronic states of methanol are dissociative and the profiles of the individual states are broad and strongly overlapped, making it difficult to extract a unique set of cross sections. In the case of water, the overlapping singlet and triplet transitions could be reliably separated by using photoabsorption profiles to characterize the corresponding singlet excitation profiles. This procedure was less successful in the case of methanol, because the corresponding transition dipoles are much weaker. On the whole, the trends we found are similar to what we found for water, although the theoretical results (our complex Kohn and the Schwinger variational results from the Caltech group) were in better agreement with each other than either were with experiment.

Molecular Excited States and Applications to Multielectronic Excitations. (*M. Head-Gordon*)

Multi-electron excited states are an area where standard electronic structure methods perform poorly and there is a need for new approaches. They are important in ultra-fast electron dynamics, the probing of valence electron dynamics by core excitations, and also the often poorly characterized low-lying excited states of systems that exhibit strong electron correlations. Under this program, we pioneered a new and very promising class of methods that combine the well-known active space approach (as in the Complete Active Space methods) for describing strongly correlated methods, and the spin-flip method. We have applied the resulting method to the very topical problem of singlet fission (the generation of two triplet excitations from absorption of a single photon) in solid pentacene, using a pentacene dimer model embedded in a molecular mechanics model of the extended crystal. This research identified a new singlet fission mechanism based on surface hopping between bright one-electron and dark two-electron excited states.

Our recent focus has been development of a new tool for multi-electron excited states that we first considered several years ago: non-orthogonal configuration interaction (NOCI) for excited states. Our very recent work on this problem has yielded a very general implementation of NOCI that for the first time can treat either real or complex or general orbitals as required for spin-frustrated systems, and other molecules that exhibit strong correlations. The important advantage of NOCI is that applications to multielectron excited states in very large molecules are possible. The main limitations are that it is not obvious other than by physical understanding of the states desired how many and which configurations should be included. To illustrate that the advantage is real, and that the limitations are not critical, we have treated excited states of long polyenes, including beta carotene itself, with very promising results.

We have completed a particularly important extension of the general NOCI method, which is to combine it with our spin-flip complete active space (SF-CAS) approach, to



define the SF-NOCI method. The point of the combination is that a high spin single reference defines an active space whose orbitals can be localized and then frozen. Each configuration of the resulting SF-CAS can then have its doubly occupied core relaxed

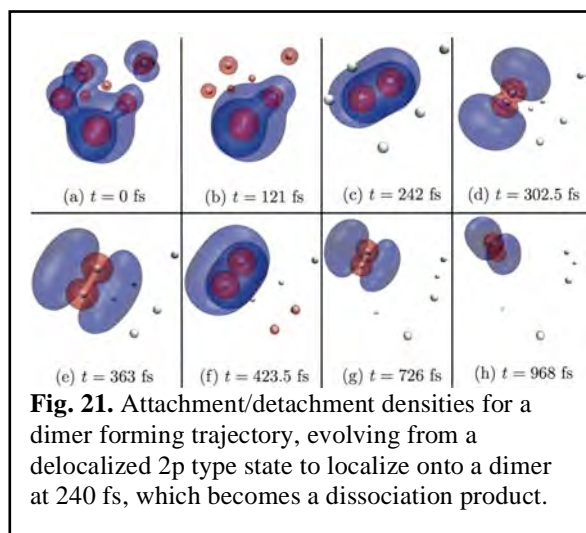
independently to define the SF-NOCI method. The power of the SF-NOCI approach comes from several factors. First, whilst relaxing the core only may sound limited (and, in a variational sense it is), those relaxations allow ionic configurations to be lowered in energy relative to the covalent configurations which are energetically favored by the (covalent) orbitals of the high spin single reference configuration. The great improvement of SF-NOCI relative to SF-CAS is shown in Fig. 20 for the ionic-covalent interaction that yields the LiF molecule. Second, the individual core relaxations are well-conditioned because the active orbitals are frozen, and therefore the omnipresent NOCI threat of variational collapse is rendered null and void. This is probably the first really usable NOCI method, and is a feasible way to generate qualitatively correct wavefunctions for multielectron excited states as well as ground states.

We are in the process of developing second order perturbation theory corrections to NOCI reference functions to include the dynamic correlation effects necessary to achieve quantitative accuracy. This poses interesting theoretical challenges because there is no well-defined partition of the orbital space into doubly occupied and virtual subspaces after the NOCI relaxation.

Simulations of Helium Cluster Dynamics in Excited States and a New Approach for Larger Clusters. (*M. Head-Gordon*)

To complement recent experimental studies of helium cluster dynamics in excited states, we have conducted ab initio trajectory studies exploring the dynamics of photoinduced dissociation. Using small He_7 clusters for computational tractability, we have investigated their fate by ab initio molecular dynamics after excitation into the $n = 2$ manifold. On the 1 ps timescale of the simulation a large majority (90%) of the trajectories exhibit full dissociation to 6 ground state atoms and 1 excited atom, with kinetic energy release commensurate with the blue shift discussed above. A small fraction (3%) of the trajectories yield bound excited dimers, as $(\text{He}_2)^*$ is bound and acts as a $(\text{He}_2)^+$ core and an outer Rydberg electron, as is evident in the trajectory visualization shown in Fig. 21. An even smaller fraction ($< 0.5\%$) of trajectories result in trimers. In addition, the dissociation timescale, the kinetic energy release, and the range of products all bear interesting and suggestive similarities to the experimental results for $n = 3,4$ excitations in clusters 4 orders of magnitude larger.

To lay the groundwork for future studies of much larger clusters, we have also formulated an excited state method that retains a number of amplitudes that scales only linearly with the size of the cluster. This method employs absolutely localized molecular orbital (ALMO) with single excitation configuration interaction method using non-



orthogonal occupied and virtual orbitals. In contrast to NOCI above, ALMO-CIS uses the same orbitals for all configurations to enable the Hamiltonian to be explicitly constructed and directly diagonalized to yield the large numbers of states necessary to describe absorption and dynamics in large clusters.

A first production version of the implementation has been completed and applied to clusters as large as 485 atoms, to yield 4850 excited states, which is about 10 times larger than we could previously simulate. This is made possible because the method scales as the cube of the number of atoms in the cluster, whilst giving a representation of a cluster band of states whose number increases linearly with the cluster size. We are currently working on new theory to correct the ALMO-CIS model for neglected charge transfer contributions (which are small but not negligible in the He cluster $n=2$ excitations), as well as to interface the approach with a semi-classical method for propagating nonadiabatic dynamics.

HHG Simulations in Atoms and Molecules. (*M. Head-Gordon*)

There has been a large gap between the methods of bound state quantum chemistry, and numerical approaches used to simulate high harmonic generation spectra. We have begun to bridge this gap with the first calculations of molecular HHG spectra using bound state quantum chemistry methods. We have also obtained insights into both the advantages and limitations of this approach by carefully analyzing the HHG spectrum of the H atom, and H₂ molecule, and assessing the contribution of both bound and continuum levels to the HHG signal.

Publications of the LBNL AMOS program (2013-2015)

1. M.S. Schoeffler, C. Stuck, M. Waitz, F. Trinter, T. Jahnke, U. Lenz, M. Jones, A. Belkacem, A. Landers, C. L. Cocke, J. Colgan, A. Kheifets, I. Bray, H. Schmidt-Boecking, R. Doerner, and Th. Weber, "Ejection of quasi free electron pairs from the helium atom ground state by a single Photon", *Phys. Rev. Lett.* **111**, 013003, (2013).
2. F. Trinter, M. Schoeffler, H.K. Kim, F. Sturm, K. Cole, N. Neumann, A. Vredenburg, J. Williams, I. Bocharova, R. Guillemin, M. Simon, A. Belkacem, A. Landers, Th. Weber, H. Schmidt-Boecking, R. Doerner, and T. Jahnke, "Resonant Auger decay driven intermolecular Coulombic decay as a tool for site-selective creation of low energy electrons in biological systems", *Nature*, Vol. **505**, 664 (2013).
3. M. S. Schöffler, T. Jahnke, M. Waitz, F. Trinter, U. Lenz, C. Stuck, M. Jones, M. S. Pindzola, A. Belkacem, C. L. Cocke, A. Landers, J. Colgan, A. Kheifets, I. Bray, H. Schmidt-Böcking, R. Dörner and Th. Weber, "Single photon double ionization of Helium at 800 eV – observation of the Quasi Free Mechanism", *Journal of Physics: Conference Series*, **488**, 022007 (2014).
4. B. Gaire, D.J. Haxton, P. Braun, S.Y. Lee, I. Bocharova, F.P. Sturm, N. Gehrken, M. Honig, M. Pitzer, D. Metz, H-K. Kim, T. Jahnke, H. Gassert, S. Zeller, J. Voigtsberger, W. Cao, M. Zohrabi, J. Williams, A. Gatton, D. Reedy, C. Nook, Th. Mueller, A. Landers, C. L. Cocke, I. Ben-Itzhak, R. Doerner, A. Belkacem, and Th. Weber, "Photo double ionization of ethylene and acetylene near threshold", *Phys. Rev. A* **89**, 013403, (2014). (*featured in "Editors' Suggestion"*)
5. B. Gaire, I. Bocharova, F.P. Sturm, N. Gehrken, J. Rist, H. Sann, M. Kunitski, J. Williams, M.S. Schoeffler, T. Jahnke, B. Berry, M. Zohrabi, M. Keiling, A. Moradmand, A.L. Landers, A. Belkacem, R. Doerner, I. Ben-Itzhak, R. Doerner, and Th. Weber, Hydrogen and fluorine migration in photo double ionization of 1,1-difluoroethylene (C₂H₂F₂) near and above threshold, *Phys. Rev. A* **89**, 043423 (2014).
6. B. Gaire, I. Bocharova, F.P. Sturm, N. Gehrken, J. Rist, H. Sann, M. Kunitski, J. Williams, M.S. Schoeffler, T. Jahnke, B. Berry, M. Zohrabi, M. Keiling, A. Moradmand, A.L. Landers, A. Belkacem,, I. Ben-Itzhak, R. Doerner, and Th. Weber, "Auger decay and subsequent fragmentation pathways of ethylene following K-shell ionization", *Phys. Rev. A* **92**, 013408 (2015).
7. M. Waitz, D. Aslituerk, N. Wechselberger, H.K. Gill, J. Rist, F. Wiegandt, C. Goihl, G. Kastirke, M. Weller, T. Bauer, D. Metz, F.P. Sturm, J. Voigtsberger, S. Zeller, F. Trinter, G. Schiwietz, T. Weber, J.B. Williams, M.S. Schoeffler, L.Ph.H. Schmidt, T. Jahnke, and R. Doerner, "Electron localization in dissociating H₂⁺ by retroaction of a photoelectron onto its source," *Submitted to Phys. Rev. Lett.* (June 2015)
8. A. Menssen, C.S. Trevisan, M.S. Schöffler, T. Jahnke, I. Bocharova, F. Sturm, N. Gehrken, B. Gaire, H. Gassert, S. Zeller, J. Voigtsberger, A. Kuhlins, A. Gatton, J. Sartor, D. Reedy, C. Nook, B. Berry, M. Zohrabi, A. Kalinin, A. Belkacem, R. Dörner, Th. Weber, A.L. Landers, T.N. Rescigno, C.W. McCurdy, J.B. Williams, "Molecular frame photoelectron angular distributions for core ionization of ethane, carbon tetrafluoride and 1,1-difluoroethylene," *Submitted to J. Phys. B: At. Mol. Opt. Phys.*, August (2015).
9. M-F. Lin, D. M. Neumark, O. Gessner, and S. R. Leone, "Ionization and Dissociation Dynamics of Vinyl Bromide Probed by Femtosecond Extreme Ultraviolet Transient Absorption Spectroscopy", *J. Chem. Phys.* **140**, 064311 (2014).
10. M. J. Bell, A. R. Beck, H. Mashiko, D. M. Neumark, and S. R. Leone, "Intensity dependence of light induced states in transient absorption of laser dressed helium measured with isolated attosecond pulses", *J. Mod. Opt.* **60**, 1506 (2013).
11. A. N. Pfeiffer, M. J. Bell, A. R. Beck, H. Mashiko, D. M. Neumark, and S. R. Leone, "Alternating absorption features during attosecond pulse propagation in a laser-controlled gaseous medium, *Phys. Rev. A* **88**, 051402(R) (2013).

12. H. Mashiko, M. J. Bell, A. R. Beck, D. M. Neumark, and S. R. Leone, "Frequency Tunable Attosecond Apparatus, in *Progress in Ultrafast Intense Laser Science*" X, K. Yamanouchi, G. Paulus, D. Mathur, eds., Springer Science+Business Media, Inc. (2014).
13. B. Bernhardt, A. R. Beck, X. Li, E. R. Warrick, M. J. Bell, D. J. Haxton, C. W. McCurdy, D. M. Neumark, and S. R. Leone, "High-spectral-resolution attosecond absorption spectroscopy of autoionization in xenon", *Phys. Rev. A* **89**, 023408 (2014).
14. A.R. Beck, B. Bernhardt, E.R. Warrick, M. Wu, S. Chen, M. Gaarde, K. Schafer, D.M. Neumark, and S.R. Leone, "Attosecond transient absorption probing of electronic superpositions of bound states in neon: detection of quantum beats", *New J. Phys.* **16**, 113016 (2014).
15. A. R. Beck, D. M. Neumark, and S. R. Leone, "Probing ultrafast dynamics with attosecond transient absorption", *Chem. Phys. Lett.* **624**, 119 (2015).
16. X. Li, B. Bernhardt, A. R. Beck, E. Warrick, A. Pfeiffer, M. J. Bell, D. Haxton, C. McCurdy, D. M. Neumark, and S. R. Leone, "Investigation of coupling mechanisms in attosecond transient absorption of autoionizing states: comparison of theory and experiment in xenon", *J. Phys. B: At. Mol. Opt. Phys.* **48**, 125601 (2015).
17. K. Ramasesha, S. R. Leone, and D. M. Neumark, "Real-time probing of electron dynamics using attosecond time-resolved spectroscopy", *Annu. Rev. Phys. Chem.* (*submitted*) (2015).
18. E. G. Champenois, N. H. Shivaram, T. W. Wright, C.-S. Yang, A. Belkacem, J. P. Cryan, "Involvement of a Low-Lying Rydberg State in the Ultrafast Relaxation Dynamics of Ethylene", *submitted to J. Chem. Phys.* (2015).
19. A. Moradmand, D.S. Slaughter, D.J. Haxton, T.N. Rescigno, C.W. McCurdy, Th. Weber, S. Matsika, A.L. Landers, A. Belkacem, and M. Fogle, "Dissociative electron attachment to carbon dioxide via the $^2\Pi_u$ shape resonance", *Phys. Rev. A* **88**, 032703 (2013).
20. D.S. Slaughter, D.J. Haxton, H. Adaniya, T. Weber, T.N. Rescigno, C.W. McCurdy, and A. Belkacem, "Ion momentum imaging of dissociative electron attachment dynamics in methanol", *Phys. Rev. A* **87**, 052711 (2013).
21. A. Moradmand, D.S. Slaughter, A.L. Landers, and M. Fogle, "Dissociative-electron-attachment dynamics near the 8-eV Feshbach resonance of CO_2 ", *Phys. Rev. A* **88**, 022711 (2013).
22. S. Kosugi, M. Iizawa, Y. Kawarai, Y. Kuriyama, A. L. D. Kilcoyne, F. Koike, N. Kuze, D. S. Slaughter, Y. Azuma, "PCI effects and the gradual formation of Rydberg series due to photoelectron recapture, in the Auger satellite lines upon Xe $4d^{1}_{5/2}$ photoionization", *J. Phys. B: At. Mol. Opt. Phys.* **48**, 115003 (2015).
23. T. N. Rescigno, N. Douguet, D. S. Slaughter, H. Adaniya, A. Belkacem and A. Orel, "Signatures of bond formation and bond scission dynamics in dissociative electron attachment to methane", *Phys. Chem. Chem. Phys.* *Accepted* (2015).
24. B. Van Kuiken, M. Valiev, S. Daifuku, C. Bannan, M. Strader, H. Cho, N. Huse, R. Schoenlein, N. Govind, M. Khalil, "Simulating Ru L_3 -edge X-ray Absorption Spectroscopy with Time-Dependent Density Functional Theory: Model Complexes and Electron Localization in Mixed-Valence Metal Dimers," *J. Phys. Chem. A*, **117**, 4444 (2013).
25. O. Smirnova and O. Gessner, "Attosecond Spectroscopy," *Chem. Phys.* **414**, 1 (2013).
26. A. Shavorskiy, A. Cordones, J. Vura-Weis, K. Siefertmann, D. Slaughter, F. Sturm, F. Weise, M. Strader, H. Cho, M.-F. Lin, C. Bacellar, C. Khurmi, M. Hertlein, J. Guo, H. Bluhm, T. Tylliszczak, D. Prendergast, G. Coslovich, J. Robinson, R. Kaindl, R. W. Schoenlein, A. Belkacem, Th. Weber, D. M. Neumark, S. R. Leone, D. Nordlund, H. Ogasawara, A. R. Nilsson, O. Krupin, J. J. Turner, W. F. Schlotter, M. R. Holmes, P. A. Heimann, M. Messerschmidt, M. P. Minitti, M. Beye, S. Gul, J. Zhang, N. Huse, and O. Gessner, "Time-Resolved X-Ray Photoelectron Spectroscopy Techniques for Real-Time Studies of Interfacial Charge Transfer Dynamics," *Application of Accelerators in Research and Industry*, AIP Conf. Proc. **1525**, 475 (2013).

27. K. D. Closser, O. Gessner, and M. Head-Gordon, "Simulations of the dissociation of small helium clusters with ab initio molecular dynamics in electronically excited states," *J. Chem. Phys.* **140**, 134306 (2014).
28. L. F. Gomez, K. R. Ferguson, J. P. Cryan, C. Bacellar, R. M. P. Tanyag, C. Jones, S. Schorb, D. Anielski, A. Belkacem, C. Bernando, R. Boll, J. Bozek, S. Carron, G. Chen, T. Delmas, L. Englert, S. W. Epp, B. Erk, L. Foucar, R. Hartmann, A. Hexemer, M. Huth, J. Kwok, S. R. Leone, J. H.S. Ma, F. R. N. C. Maia, E. Malmerberg, S. Marchesini, D. M. Neumark, B. Poon, J. Prell, D. Rolles, B. Rudek, A. Rudenko, M. Seifrid, K. R. Siefertmann, F. P. Sturm, M. Swiggers, J. Ullrich, F. Weise, P. Zwart, C. Bostedt, O. Gessner, A. F. Vilesov, "Shapes and Vorticities of Superfluid Helium Nanodroplets," *Science* **345**, 906 (2014).
29. K.R. Siefertmann, C.D. Pemmaraju, S. Nepl, A. Shavorskiy, A.A. Cordones, J. Vura-Weis, D.S. Slaughter, F.P. Sturm, F. Weise, H. Bluhm, M.L. Strader, H. Cho, M.-F. Lin, C. Bacellar, C. Khurmi, J. Guo, G. Coslovich, J.S. Robinson, R.A. Kaindl, R.W. Schoenlein, A. Belkacem, D.M. Neumark, S.R. Leone, D. Nordlund, H. Ogasawara, O. Krupin, J.J. Turner, W.F. Schlotter, M.R. Holmes, M. Messerschmidt, M.P. Minitti, S. Gul, J.Z. Zhang, N. Huse, D. Prendergast, and O. Gessner, "Atomic-Scale Perspective of Ultrafast Charge Transfer at a Dye-Semiconductor Interface," *J. Phys. Chem. Lett.*, **5**, 2753 (2014).
30. M. P. Ziemkiewicz, C. Bacellar, K. Siefertmann, S. R. Leone, D. M. Neumark, and O. Gessner, "Femtosecond time-resolved XUV + UV photoelectron imaging of pure helium nanodroplets," *J. Chem. Phys.* **141**, 174306 (2014).
31. A. Shavorskiy, S. Nepl, D. Slaughter, J. Cryan, K. Siefertmann, F. Weise, M.-F. Lin, C. Bacellar, M. Ziemkiewicz, I. Zegkinoglou, M. Fraund, C. Khurmi, M. Hertlein, T. Wright, N. Huse, R. Schoenlein, T. Tylliszczak, G. Coslovich, J. Robinson, R. Kaindl, B. Rude, A. Oelsner, S. Maehl, H. Bluhm, and O. Gessner, "Sub-Nanosecond Time-Resolved Ambient-Pressure X-ray Photoelectron Spectroscopy Setup for Pulsed and Constant Wave X-ray Light Sources," *Rev. Sci. Inst.* **85**, 093102 (2014).
32. S. Nepl, A. Shavorskiy, I. Zegkinoglou, M. Fraund, D. S. Slaughter, T. Troy, M. P. Ziemkiewicz, M. Ahmed, S. Gul, B. Rude, J. Z. Zhang, A. S. Tremsin, P.-A. Glans, Y.-S. Liu, C. H. Wu, J. Guo, M. Salmeron, H. Bluhm, and O. Gessner, "Capturing interfacial photo-electrochemical dynamics with picosecond time-resolved X-ray photoelectron spectroscopy," *Faraday Discuss.* **171**, 219 (2014).
33. M. P. Ziemkiewicz, D. M. Neumark, and O. Gessner, "Ultrafast electronic dynamics in helium nanodroplets," *Int. Rev. Phys. Chem.* **34**, 239 (2015).
34. S. Nepl, Y.-S. Liu, C.-H. Wu, A. Shavorskiy, I. Zegkinoglou, T. Troy, D. S. Slaughter, M. Ahmed, A. S. Tremsin, J.-H. Guo, P.-A. Glans, M. Salmeron, H. Bluhm, and O. Gessner, "Toward Ultrafast In Situ X-Ray Studies of Interfacial Photoelectrochemistry," in *Ultrafast Phenomena XIX*, Kaoru Yamanouchi, Steven Cundiff, Regina de Vivie-Riedle, Makoto Kuwata-Gonokami, Louis DiMauro, Eds., Springer (2015).
35. K. Hong, H. Cho, R.W. Schoenlein, T.-K. Kim, and N. Huse, "Element-Specific Characterization of Transient Electronic Structure of Solvated Fe(II) Complexes with Time-Resolved Soft X-ray Absorption Spectroscopy," *Acc. Chem. Res.*, *in press* (2015).
36. B.E. van Kuiken, H.Cho, K. Hong, M. Khalil, R.W. Schoenlein, T.K. Kim, and N. Huse, "Time-Resolved X-ray Spectroscopy in the Water Window: Elucidating Transient Valence Charge Distributions in Aqueous Fe(II) Complexes," *J. Am. Chem. Soc.*, *submitted* (2015).
37. C. F. Jones, C. Bernando, R. M. P. Tanyag, C. Bacellar, K. R. Ferguson, L. F. Gomez, D. Anielski, A. Belkacem, R. Boll, J. Bozek, S. Carron, J. Cryan, L. Englert, S. W. Epp, B. Erk, L. Foucar, R. Hartmann, D. Neumark, D. Rolles, A. Rudenko, K. Siefertmann, F. Weise, B. Rudek, F. P. Sturm, J. Ullrich, C. Bostedt, O. Gessner, A. F. Vilesov, "Coupled motion of Xe clusters and quantum vortices in He nanodroplets," *Phys. Rev. Lett.* *submitted* (2015).
38. R. M. P. Tanyag, C. Bernando, C. Jones, C. Bacellar, K. R. Ferguson, D. Anielski, R. Boll, J. Bozek, S. Carron, J. P. Cryan, L. Englert, S. W. Epp, B. Erk, L. Foucar, L. F. Gomez, R. Hartmann, D. M. Neumark, D. Rolles, B. Rudek, A. Rudenko, S. Schorb, K. R. Siefertmann, J. Ullrich, F. Weise, C.

- Bostedt, O. Gessner, A. F. Vilesov, "X-ray microscopy by immersion in nanodroplets," *Struct. Dyn.*, submitted (2015).
39. Y. Kawarai, T. Weber, Y. Azuma, C. Winstead, V. McKoy, A. Belkacem, and D.S. Slaughter, "Dynamics of the Dissociating Uracil Anion Following Resonant Electron Attachment," *J. Phys. Chem. Lett.* **5**, 3854 (2014).
 40. F. L. Yip, T. N. Rescigno, C. W. McCurdy and F. Martín, "Fully Differential Single-Photon Double Ionization of Neon and Argon", *Phys. Rev. Lett.* **110**, 173001 (2013).
 41. N. Douguet, T. N. Rescigno and A. E. Orel, "Time-resolved molecular-frame photoelectron angular distributions: Snapshots of acetylene-vinylidene cationic isomerisation", *Phys. Rev. A* **86**, 013425 (2013).
 42. T. N. Rescigno and A. E. Orel, "A Theoretical Study of Excitation of the Low-Lying Electronic States of Water by Electron Impact", *Phys. Rev. A* **88**, 012703 (2013).
 43. N. Douguet T. N. Rescigno and A. E. Orel, "Carbon K-shell molecular-frame photoelectron angular distribution in the photoisomerization of neutral ethylene", *Phys. Rev. A* **88**, 013425 (2013).
 44. D. J. Haxton, "Breakup of H_2^+ by Photon Impact", *Phys. Rev. A* **88**, 013415 (2013).
 45. Chih-Yuan Lin, C. W. McCurdy and T. N. Rescigno, "Complex Kohn Approach to Molecular Ionization by High-Energy Electrons: Application to H_2O ", *Phys. Rev. A* **89**, 012703 (2014).
 46. J. Jose, R. R. Lucchese and T. N. Rescigno, "Interchannel coupling effects in the valence photoionization of SF_6 ", *J. Chem. Phys.* **140**, 204305 (2014).
 47. S. M. Poullain, C. Elkharrat, W. B. Li, K. Veyrinas, J. C. Houver, C. Cornaggia, T. N. Rescigno, R. K. Lucchese and D. Doweck, "Recoil frame photoemission in multiphoton ionization of small polyatomic molecules: photodynamics of NO_2 probed by 400 nm fs pulses", *J. Phys. B* **47**, 124024 (2014).
 48. Chih-Yuan Lin, C. W. McCurdy and T. N. Rescigno, "Theoretical study of $(e/2e)$ from outer- and inner-valence orbitals of CH_4 : A complex Kohn treatment" *Phys. Rev. A* **89**, 052718 (2014).
 49. M. Fogle, D. J. Haxton, A. L. Landers, A. E. Orel and T. N. Rescigno, "Ion-momentum imaging of dissociative electron attachment dynamics in acetylene", *Phys. Rev. A* **90**, 042712 (2014).
 50. F. L. Yip, C. W. McCurdy and T. N. Rescigno, "Hybrid Gaussian-discrete variable representation for one- and two-active electron continuum calculations in molecules", *Phys. Rev. A* **90**, 063421 (2014).
 51. S. Fonseca dos Santos, N. Douguet, A. E. Orel and T. N. Rescigno, "Ligand effects in carbon K-shell photoionization of small linear molecules", *Phys. Rev. A* **91**, 023408 (2015).
 52. K. Varela, L. R. Hargreaves, K. Ralphs, M. A. Khakoo, C. Winstead, V. McKoy, T. N. Rescigno and A. E. Orel, "Excitation of the 4 Lowest Electronic Transitions in Methanol by Low-Energy Electrons", *J. Phys. B* **48**, 115208 (2015).
 53. T. N. Rescigno, C. S. Trevisan and C. W. McCurdy, "Tracking hole localization in K -shell and core-valence-excited acetylene photoionization via body-frame photoelectron angular distributions", *Phys. Rev. A* **91**, 023429 (2015).
 54. F. L. Yip, A. Palacios, F. Martín, T. N. Rescigno and C. W. McCurdy, "Two-photon double ionization of atomic beryllium with ultrashort laser pulses", *Phys. Rev. A* *Submitted (2015)*.
 55. X. Li, D. J. Haxton, M. Gaarde, K. J. Schafer, C. W. McCurdy, "Direct extraction of intense-field induced polarization in the continuum on the attosecond time scale from transient absorption," *Phys. Rev. A* *Submitted, August (2015)*.
 56. D. J. Haxton, K. V. Lawler, and C. W. McCurdy, "Qualitative failure of a multiconfiguration method in prolate spheroidal coordinates in calculating dissociative photoionization of H_2^+ ," *Phys. Rev. A* **91**, 062502 (2015).
 57. D. J. Haxton and C. W. McCurdy, "Two methods for restricted configuration spaces within the multiconfiguration time-dependent Hartree-Fock method," *Phys. Rev. A* **91**, 012509 (2015).

58. D. J. Haxton and C. W. McCurdy, "Ultrafast population transfer to excited valence levels of a molecule driven by x-ray pulses," *Phys. Rev. A* **90**, 053426 (2014).
59. X. Li, C. W. McCurdy, and D. J. Haxton, "Population transfer between valence states via autoionizing states using two-color ultrafast π pulses in XUV and the limitations of adiabatic passage" *Phys. Rev. A* **89**, 031404(R) (2014).
60. P.M. Zimmerman, C.B. Musgrave, and M. Head-Gordon, "A Correlated Electron View of Singlet Fission", *Acc. Chem. Res.* **46**, 1339-1347 (2013).
61. E. Luppi and M. Head-Gordon, "The role of Rydberg and continuum levels in computing high harmonic generation spectra of the hydrogen atom using time-dependent configuration interaction", *J. Chem. Phys.* **139**, 164121 (2013).
62. E.J. Sundstrom and M. Head-Gordon, "Non-Orthogonal Configuration Interaction for the Calculation of Multi-electron Excited States", *J. Chem. Phys.* **140**, 114103 (2014).
63. K. D. Closser, O. Gessner, and M. Head-Gordon, "Ab initio molecular dynamics simulations of the photodissociation of small helium clusters", *J. Chem. Phys.* **140**, 134306 (2014).
64. D. Zuev, T.-C. Jagau, K.B. Bravaya, E. Epifanovsky, Y. Shao, E. Sundstrom, M. Head-Gordon and A.I. Krylov, "Complex absorbing potentials within EOM-CC family of methods: Theory, implementation, and benchmarks", *J. Chem. Phys.* **141**, 024102 (2014).
65. N.J. Mayhall, P.R. Horn, E.J. Sundstrom, and M. Head-Gordon, "Spin-flip non-orthogonal configuration interaction: A variational and almost black-box method for describing strongly correlated electrons", *PCCP* **16**, 22694-22705 (2014).
66. Y. Shao, Z. Gan, E. Epifanovsky, A.T.B. Gilbert, M. Wormit, J. Kussmann, A.W. Lange, A. Behn, J. Deng, X. Feng, D. Ghosh, M. Goldey, P.R. Horn, L.D. Jacobson, I. Kaliman, R.Z. Khaliullin, T. Kus, A. Landau, J. Liu, E.I. Proynov, Y.M. Rhee, R.M. Richard, M.A. Rohrdanz, R.P. Steele, E.J. Sundstrom, H.L. Woodcock, P.M. Zimmerman, D. Zuev, B. Albrecht, E. Alguire, B. Austin, G.J.O. Beran, Y.A. Bernard, E. Berquist, K. Brandhorst, K.B. Bravaya, S.T. Brown, D. Casanova, C.-M. Chang, Y. Chen, S.H. Chien, K.D. Closser, D.L. Crittenden, M. Diedenhofen, R.A. DiStasio Jr., H. Do, A.D. Dutoi, R.G. Edgar, S. Fatehi, L. Fusti-Molnar, A. Ghysels, A. Golubeva-Zadorozhnaya, J. Gomes, M.W.D. Hanson-Heine, P.H.P. Harbach, A.W. Hauser, E.G. Hohenstein, Z.C. Holden, T.-C. Jagau, H. Ji, B. Kaduk, K. Khistyayev, J. Kim, J. Kim, R.A. King, P. Klunzinger, D. Kosenkov, T. Kowalczyk, C.M. Krauter, K.U. Lao, A. Laurent, K.V. Lawler, S.V. Levchenko, C.Y. Lin, F. Liu, E. Livshits, R.C. Lochan, A. Luenser, P. Manohar, S.F. Manzer, S.-P. Mao, N. Mardirossian, A.V. Marenich, S.A. Maurer, N.J. Mayhall, E. Neuscammann, C.M. Oana, R. Olivares-Amaya, D.P. O'Neill, J.A. Parkhill, T.M. Perrine, R. Peverati, A. Prociuk, D.R. Rehn, E. Rosta, N.J. Russ, S.M. Sharada, S. Sharma, D.W. Small, A. Sodt, T. Stein, D. Stück, Y.-C. Su, A.J.W. Thom, T. Tsuchimochi, V. Vanovschi, L. Vogt, O. Vydrov, T. Wang, M.A. Watson, J. Wenzel, A. White, C.F. Williams, J. Yang, S. Yeganeh, S.R. Yost, Z.-Q. You, I. Y. Zhang, X. Zhang, Y. Zhao, B.R. Brooks, G.K.L. Chan, D.M. Chipman, C.J. Cramer, W.A. Goddard III, M.S. Gordon, W.J. Hehre, A. Klamt, H.F. Schaefer III, M.W. Schmidt, C.D. Sherrill, D.G. Truhlar, A. Warshel, X. Xu, A. Aspuru-Guzik, R. Baer, A.T. Bell, N.A. Besley, J.-D. Chai, A. Dreuw, B.D. Dunietz, T.R. Furlani, S.R. Gwaltney, C.-P. Hsu, Y. Jung, J. Kong, D.S. Lambrecht, W.-Z. Liang, C. Ochsenfeld, V.A. Rassolov, L.V. Slipchenko, J.E. Subotnik, T. Van Voorhis, J.M. Herbert, A.I. Krylov, P.M.W. Gill and M. Head-Gordon, "Advances in molecular quantum chemistry contained in the Q-Chem 4 program package", *Mol. Phys.* **113**, 184–215 (2015).
67. D.W. Small, E.J. Sundstrom, and M. Head-Gordon, "A simple way to test for collinearity in spin symmetry broken wave functions: Theory and application to Generalized Hartree-Fock", *J. Chem. Phys.* **142**, 094112 (2015); (9 pages) <http://dx.doi.org/10.1063/1.4913740>
68. K.D. Closser, Q. Ge, Y. Mao, Y. Shao, and M. Head-Gordon, "A local excited state method using single substitutions in the absolutely localized molecular orbital basis with application to spectra of large helium clusters", *J. Chem. Theory Comput.* (submitted, July 2015).

69. D. Stuck and M. Head-Gordon, "Regularized CC2: Parameter Transferability To Excited States", Chem. Phys. Lett. (submitted, August 2015).
70. A. White, C. Heide, P. Saalfrank, M. Head-Gordon, and E. Luppi."Computation of high-harmonic generation spectra of the hydrogen molecule using time-dependent configuration-interaction", Mol. Phys. (submitted, August 2015)

Page is intentionally blank.

Early Career: Ultrafast X-ray Studies of Intramolecular and Interfacial Charge Migration

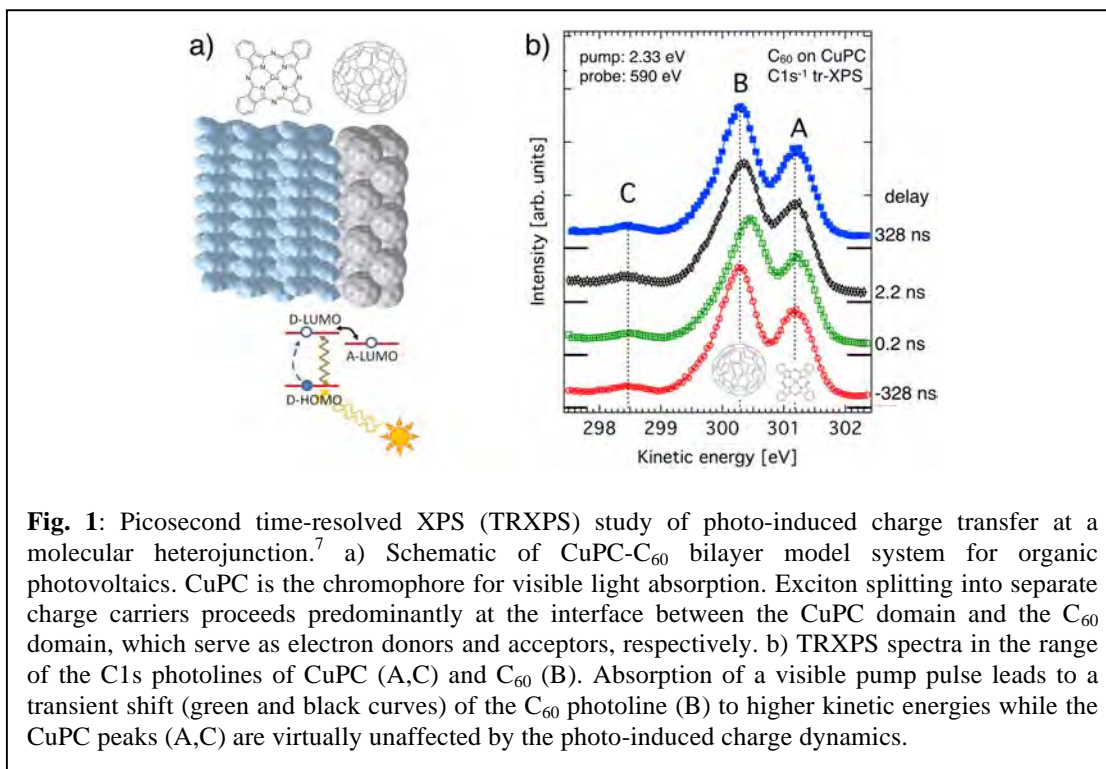
Oliver Gessner

Chemical Sciences Division, Lawrence Berkeley National Laboratory, Berkeley, CA 94720

OGessner@lbl.gov

Program Scope: At the heart of many emerging sunlight-to-fuel and molecular photovoltaic concepts are interfacial processes that require an optimized, concerted flow of charge and energy on a molecular level. This program is focused at developing and applying time-domain X-ray spectroscopy techniques that enable an atomic-scale understanding of the fundamental mechanisms underlying interfacial electronic and chemical dynamics. In particular, ultrafast dynamics at interfaces between molecules, molecular domains, and semiconductors are studied by time-resolved X-ray photoelectron spectroscopy (TRXPS) and time-resolved X-ray absorption spectroscopy (TRXAS) techniques, which are deployed at the Linac Coherent Light Source (LCLS) and the Advanced Light Source (ALS).

Recent Progress and Future Plans: Picosecond TRXPS has been used to monitor photo-induced electronic dynamics in a variety of systems of interest for next generation energy solutions. Experiments have been performed on thin films of transition metal complexes, semiconductor nanocrystals, molecular heterojunctions, molecule-semiconductor interfaces, as well as buried molecule-semiconductor and semiconductor-semiconductor interfaces.²⁻⁹ The ALS based studies complement our femtosecond



TRXPS efforts at the Linac Coherent Light Source.^{2,3} A particularly successful study demonstrated the site-specific probing of photo-induced charge-transfer dynamics in a model system for organic photovoltaic devices (Fig. 1).⁷ The system consists of a bilayer of C₆₀ electron acceptors deposited on top of a multilayer of copper phthalocyanine (CuPC) chromophores (Fig. 1a). Optical excitation of the CuPC domain leads to a clear time-dependent shift of the C1s inner-shell photoline associated with the C₆₀ domain relative to the C1s photoline of the CuPC domain at optical pump / X-ray probe time delays of 200 ps and beyond (Fig. 1b).

The proof-of-principle experiment has important technological and scientific implications. To the best of our knowledge, it represents the first demonstration of the feasibility of ultrafast X-ray spectroscopy studies on a “soft” condensed phase sample consisting of two molecular domains rather than, for example, “hard” samples such as bulk semiconductor crystals or replenishing liquid and gas phase samples. The careful characterization and mediation of sample damage effects developed within this project is a critical enabling factor that opens the route toward the study of a large range of technologically pertinent interfacial systems that have long been considered too radiation sensitive for ultrafast X-ray studies. Scientifically, the clear site-specific fingerprint enabled by the exquisite element specificity and chemical sensitivity of time-domain X-ray spectroscopy techniques opens the route for a better understanding of the fundamentals of photo-induced intramolecular and interfacial charge dynamics that form the basis for chemically engineered photovoltaic and photocatalytic devices.

A major effort has been initiated to complement the time-resolved XPS studies with ultrafast transient X-ray absorption spectroscopy (TRXAS) studies. A new TRXAS setup for the study of “soft” condensed phase samples has been designed, constructed, and commissioned at the ALS. It employs a similar picosecond time-stamping principle as the TRXPS setup and enables TRXAS studies with >100 kHz optical and 500 MHz X-ray pulse repetition rates, making it applicable in both two-bunch and multi-bunch operating mode of the ALS. The scientific driver for this activity is to complement the excellent sensitivity of XPS to surface dynamics and transient electronic band structures with the bulk sensitivity of X-ray absorption techniques, which are particularly well suited to advance experimental techniques toward in operando studies. First results strongly indicate the capability of the new technique to enable picosecond TRXAS studies in complex interfacial systems including operating photoelectrochemical devices.

Publications 2013-2015

1. Olga Smirnova and Oliver Gessner, “Attosecond Spectroscopy”, *Chem. Phys.* **414**, 1 (2013).
2. Andrey Shavorskiy, Amy Cordones, Josh Vura-Weis, Katrin Siefermann, Daniel Slaughter, Felix Sturm, Fabian Weise, Matthew Strader, Hana Cho, Ming-Fu Lin, Camila Bacellar, Champak Khurmi, Marcus Hertlein, Jinghua Guo, Hendrik Bluhm, Tolek Tyliczszak, David Prendergast, Giacomo Coslovich, Joseph Robinson, Robert A. Kaindl, Robert W. Schoenlein, Ali Belkacem, Thorsten Weber, Daniel M. Neumark, Stephen R. Leone, Dennis Nordlund, Hirohito Ogasawara, Anders R. Nilsson, Oleg Krupin, Joshua J. Turner, William F. Schlotter, Michael R. Holmes, Philip A. Heimann, Marc Messerschmidt, Michael P. Minitti, Martin Beye, Sheraz Gul, Jin Z. Zhang, Nils Huse, and Oliver Gessner, “Time-Resolved X-Ray Photoelectron Spectroscopy Techniques for Real-Time Studies of Interfacial Charge Transfer Dynamics”, *Application of Accelerators in Research and Industry*, AIP Conf. Proc. **1525**, 475 (2013).
3. K. R. Siefermann, C. D. Pemmaraju, S. Neppel, A. Shavorskiy, A. A. Cordones, J. Vura-Weis, D. S. Slaughter, F. P. Sturm, F. Weise, H. Bluhm, M. L. Strader, H. Cho, M.-F. Lin, C. Bacellar, C. Khurmi,

- J. Guo, G. Coslovich, J. S. Robinson, R. A. Kaindl, R. W. Schoenlein, A. Belkacem, D. M. Neumark, S. R. Leone, D. Nordlund, H. Ogasawara, O. Krupin, J. J. Turner, W. F. Schlotter, M. R. Holmes, M. Messerschmidt, M. P. Minitti, S. Gul, J. Z. Zhang, N. Huse, D. Prendergast, and O. Gessner, "Atomic Scale Perspective of Ultrafast Charge Transfer at a Dye-Semiconductor Interface", *J. Phys. Chem. Lett.* **5**, 2753 (2014).
4. Andrey Shavorskiy, Stefan Neppel, Daniel S. Slaughter, James P. Cryan, Katrin R. Siefertmann, Fabian Weise, Ming-Fu Lin, Camila Bacellar, Michael P. Ziemkiewicz, Ioannis Zegkinoglou, Matthew W. Fraund, Champak Khurmi, Marcus P. Hertlein, Travis W. Wright, Nils Huse, Robert W. Schoenlein, Tolek Tyliczszak, Giacomo Coslovich, Joseph Robinson, Robert A. Kaindl, Bruce S. Rude, Andreas Ölsner, Sven Mähle, Hendrik Bluhm, and Oliver Gessner, "Sub-Nanosecond Time-Resolved Ambient-Pressure X-ray Photoelectron Spectroscopy Setup for Pulsed and Constant Wave X-ray Light Sources", *Rev. Sci. Instrum.* **85**, 093102 (2014).
 5. Stefan Neppel, Andrey Shavorskiy, Ioannis Zegkinoglou, Matthew Fraund, Daniel S. Slaughter, Tyler Troy, Michael P. Ziemkiewicz, Musahid Ahmed, Sheraz Gul, Bruce Rude, Jin Z. Zhang, Anton S. Tremsin, Per-Anders Glans, Yi-Sheng Liu, Cheng Hao Wu, Jinghua Guo, Miquel Salmeron, Hendrik Bluhm, and Oliver Gessner, "Capturing interfacial photo-electrochemical dynamics with picosecond time-resolved X-ray photoelectron spectroscopy", *Faraday Discuss.* **171**, 219 (2014).
 6. S. Neppel, Y.-S. Liu, C.-H. Wu, A. Shavorskiy, I. Zegkinoglou, T. Troy, D. S. Slaughter, M. Ahmed, A. S. Tremsin, J.-H. Guo, P.-A. Glans, M. Salmeron, H. Bluhm, and O. Gessner, "Toward Ultrafast In Situ X-Ray Studies of Interfacial Photoelectrochemistry", in *Ultrafast Phenomena XIX*, Kaoru Yamanouchi, Steven Cundiff, Regina de Vivie-Riedle, Makoto Kuwata-Gonokami, Louis DiMauro, Eds., Springer (2015).
 7. Tiberiu Arion, Stefan Neppel, Friedrich Roth, Andrey Shavorskiy, Hendrik Bluhm, Zahid Hussain, Oliver Gessner, and Wolfgang Eberhardt, "Site-specific probing of charge transfer dynamics in organic photovoltaics", *Appl. Phys. Lett.* **106**, 121602 (2015).
 8. Stefan Neppel and Oliver Gessner, "Time-resolved X-ray Photoelectron Spectroscopy Techniques for the Study of Interfacial Charge Dynamics", *J. Electron Spectrosc. Relat. Phenom.*, *in press*, DOI: 10.1016/j.elspec.2015.03.002.
 9. Oliver Gessner and Markus Gühr, "Monitoring Ultrafast Chemical Dynamics by Time-Domain X-Ray Photo- and Auger-Electron Spectroscopy", *Acc. Chem. Res.*, *submitted*.

Page is intentionally blank.

Early Career Project: **The Multiconfiguration Time-Dependent Hartree-Fock Method for Interactions of Molecules with Ultrafast X-Ray and Strong Laser Pulses**

Daniel J. Haxton
Lawrence Berkeley National Laboratory
1 Cyclotron Road, MS 2R0100
Berkeley, CA 94720
djhaxton@lbl.gov

Program scope / definition

The mission of Basic Energy Sciences (BES) is to support fundamental research to understand, predict, and ultimately control matter and energy at the level of electrons, atoms, and molecules. DOE is investing considerable resources into the development of ultrafast, coherent X-ray lasers and high harmonic generation in order to excite and probe electronic excitations in molecules and materials.

To accompany these experiments, we need the ability to calculate arbitrary, nonperturbative, many-body electronic and nuclear dynamics of molecules and other quantum systems. This project directly addresses this need. It is based upon the development, implementation, and distribution of an open-source computer code for solving the nonrelativistic Schrodinger equation for atoms, diatoms, and polyatomic molecules, subject to arbitrarily strong laser fields. It is a first-principles implementation, including correlated wave functions.

The final goal of the project is a fully nonadiabatic treatment of polyatomic molecules, including electronic and nuclear degrees of freedom.

Recent progress

The polyatomic method with fixed nuclei is now implemented including parallelization of both the Slater determinant all-electron representation and the single-electron orbital representation, and ionization. We are now calculating all-electrons-active time-dependent wave functions for polyatomic molecules in intense laser fields, using millions of Slater determinants and millions of basis functions for the time-dependent orbitals.

1) With major help from the SciDAC (Scientific Discovery through Advanced Computing) initiative of the DOE, we have parallelized the representation of the orbitals using a Cartesian product sinc functions. Using a cube of points n on a side, the number of basis functions $N=n^3$.

A linear algebraic method using fast Fourier transforms accelerates the matrix-vector multiplication operation that is required to construct mean fields and two-electron matrix elements. The task of parallelizing the construction of mean fields and two-electron matrix elements consists of parallelizing a three-dimensional fast Fourier transform. Using this linear algebraic method, the operation takes order- $(N \log N)$ time, not order- N^2 . We have performed LBNL-AMO-MCTDHF calculations using a number of primitive sinc basis functions N greater than 100 million. A paper on the method has been submitted for publication and can be seen at

<http://arxiv.org/abs/1507.03324>

- 2) The implementation allowing restricted configuration spaces – that is, not full configuration interaction, spaces of Slater determinants like those used in quantum chemistry such as configuration interaction with singles and doubles (CISD) – has been published in Ref. (3) below. Explicit working equations for MCTDHF with restricted configuration spaces, for the MacLachlan and Lagrangian stationary principles as well as an ad-hoc method based on the single-electron density matrix, were derived and presented for the first time. Conditions under which the stationary principles are inequivalent were specified for the first time.
- 3) We have published a paper on two-color stimulated X-ray Raman within the NO molecule; this is Ref. (1) below. We demonstrated 40% population transfer to valence excited states, using this two-color setup.
- 4) Rational software development and distribution of the code to the public using git and GitHub.com

<https://commons.lbl.gov/display/csd/LBNL-AMO-MCTDHF>
<https://github.com/LBNL-AMO-MCTDHF/>
<http://danhax.us/Research/LBNL-AMO-MCTDHF.html>

These websites were created in the past year. They provide the public space through which we are distributing this code for solving the time-dependent Schrodinger equation for a polyatomic molecule to the AMO physics community and beyond. Also, git and GitHub.com provide a tool for code development and version control, for our team of software developers.

5) Treatment of ionization for polyatomics

Coordinate scaling, or more specifically smooth exterior complex coordinate scaling and stretching, permits the accurate treatment of ionization. Rigorous complex coordinate scaling is already part of the atomic and diatomic codes. This allows us to accurately represent AC stark shifts in the continuum, decay of metastable states such as Auger decay, and other continuum physics. There is now a polyatomic implementation of coordinate scaling that is more primitive, and incomplete, but it gives what look to be good results, at a preliminary stage. A result calculated for absorption of benzene, above the ionization potential, is shown below. Although this result is caused by valence excitation and ionization, it was calculated using a representation capable of double-core-hole physics.

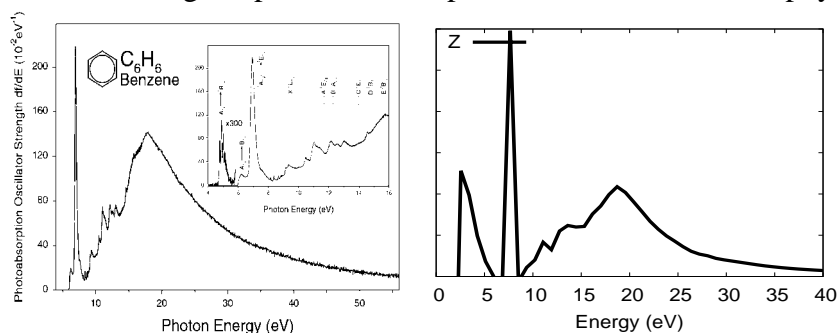


Figure: absorption cross section of Benzene. Left: experimental result [R. Feng et al., *J. Electron Spectroscopy and Related Phenomena* **123**, 199 (2002)]; right, first result from polyatomic code, giving good overall agreement except for spurious low-energy peak.

6) Example directories available to the AMO community

In the distribution package available on GitHub.com, we have several examples that can be used by members of the AMO community to perform interesting calculations. We have a Diels-Alder example, a Helium-Neon interatomic Coulombic decay example, and others.

7) Study of dissociative photoionization using diatomic code with nonadiabatic nuclear motion

To test the implementation for diatomics with nuclear motion, we attempted to calculate a difficult problem for the simplest molecule: dissociative ionization of H_2^+ . We published the results in Ref. (2) below. The results are generally accurate except in the region of onset. For photon energies near onset, the method produces spurious steps in the cross section.

Future plans

1) The proposal “Advanced Computational Methods for the Quantum Mechanical Many-Body Problem in Physics and Chemistry” has been funded by the Peder Sather institute, which provides funding for scientists to travel between Berkeley, USA and Oslo, Norway. One of the main goals of this proposal is to implement S. Kvaal’s method

Simen Kvaal. **Multiconfigurational time-dependent Hartree method to describe particle loss due to absorbing boundary conditions.** Phys. Rev. A **84**, 022512 (2011)

within LBNL-AMO-MCTDHF. With this method, we will be able to rigorously calculate multiple ionization physics. For instance, we can calculate the dipole response of an atom undergoing total photoionization.

2) Calculating nonlinear optical signals the primary priority at this time. We want to chart the paths through which energy flows in a molecule, in terms of time, frequency, and symmetry.

In general, we want to decompose the signal from a nonlinear laser experiment into its contributions from different numbers of photons absorbed and emitted from each laser used in the experiment.

We are focusing on interpreting the results of transient absorption experiments.

We have developed a generalization of the method of Domcke and coworkers [L. Seidner, G. Stock, and W. Domcke. J. Chem. Phys. **103**, 3998 (1995)] for calculating phase matched signals for nonlinear wave mixing experiments. With this generalized method we may distinguish the signal due to absorption of two photons and emission of one, from that due to absorption of one photon alone, for instance. Using this method, we will be able to provide new insight into nonlinear laser experiments.

Below the transient absorption spectrum of helium, left, calculated with LBNL-AMO-MCTDHF is partially decomposed. The total XUV transient absorption signal, left, is separated into its components due to different numbers of IR photons absorbed and emitted. The right panel shows the component due to zero IR photons absorbed and zero IR photons emitted. It is featureless, equal to the IR-free result, as desired. Additional programming is required to rigorously obtain the other components, but preliminary results are promising.

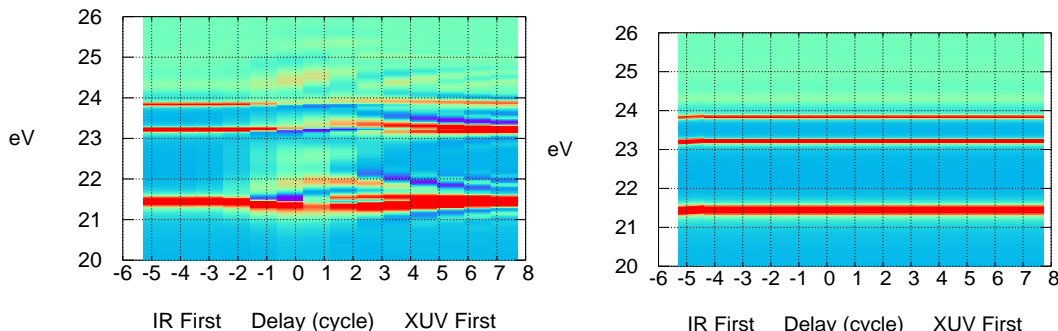
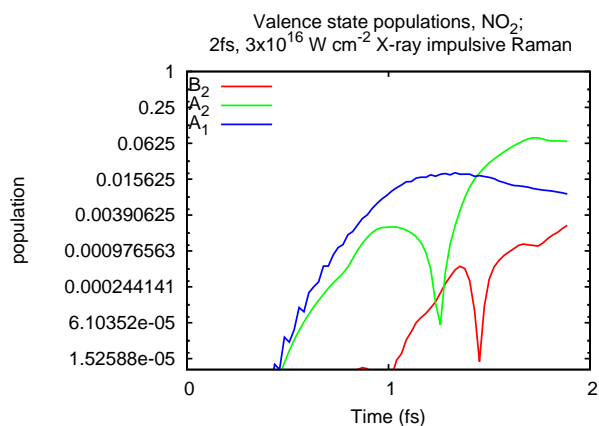


Figure: preliminary results from “complex Domcke method.” Left: total transient absorption signal. Right: component due to absorption of zero IR photons and emission of zero IR photons.

3) Calculations on population transfer due to X-ray impulsive Raman transitions in the NO_2 molecule. We are supporting a proposal for work at LCLS under J. Cryan et al. We are trying to optimize population transfer due into excited valence electronic states due to the Raman transition. A very preliminary result, showing 6% population transfer at $3 \times 10^{16} \text{ W cm}^{-2}$ into the low-lying A_2 state, is shown at right.



References

3) D. J. Haxton and C. W. McCurdy. **Two methods for restricted configuration spaces within the multiconfiguration time-dependent Hartree-Fock method.** *Phys. Rev. A* **91**, 012509 (2015).

2) D. J. Haxton, K. V. Lawler, and C. W. McCurdy. **Qualitative failure of a multiconfiguration method in prolate spheroidal coordinates in calculating dissociative photoionization of H_2^+ .** *Phys. Rev. A* **91**, 062502 (2015).

1) D. J. Haxton and C. W. McCurdy. **Ultrafast population transfer to excited valence levels of a molecule driven by x-ray pulses.** *Phys. Rev. A* **90**, 053426 (2014).

Engineered Electronic and Magnetic Interactions in Nanocrystal Quantum Dots

Victor I. Klimov

Chemistry Division, C-PCS, MS-J567, Los Alamos National Laboratory
Los Alamos, New Mexico 87545, klimov@lanl.gov, <http://quantumdot.lanl.gov>

1. Program Scope

Chemically synthesized semiconductor nanocrystals (NCs), known also as nanocrystal quantum dots (QDs), have been extensively studied as both a test bed for exploring the physics of strong quantum confinement as well as a highly flexible materials platform for the realization of a new generation of solution-processed optical, electronic and optoelectronic devices. Due to readily size-tunable emission, colloidal NCs are especially attractive for applications in light-emitting diode (LED) displays, solid-state lighting, lasing, and single-photon sources. It is universally recognized that the realization of these and other prospective applications of NCs requires a detailed understanding of carrier-carrier interactions in these structures, as they have a strong effect on both recombination dynamics of charge carriers and spectral properties of emitted light. A unifying theme of this project is fundamental physics of electronic and magnetic interactions involving strongly confined carriers/spins with focus on control of these interactions via size/shape manipulation, doping/heterostructuring, and “interface engineering.” Our goals in this project include: the development of high-efficiency NC-based LEDs free from detrimental effects of Auger recombination such as efficiency “roll-off” at high currents; realization of electrically pumped single-NC light sources; the achievement of NC lasing under continuous-wave (*cw*) excitation; and control over the magneto-optical properties of NCs doped with magnetic atoms.

2. Recent Progress

During the past year, our research has focused in three main areas: (1) We have continued the exploration of ideas of “Auger-decay engineering” in application to problems of QD lasing; (2) We have evaluated the potential of a new class of QDs based on inorganic perovskites for applications as room-temperature single-photon sources; (3) Finally, we have used newly developed Mn-doped CdSe QDs with strong excitonic emission to demonstrate “giant” magnetic field fluctuations detected *via* ultrafast Faraday rotation measurements. Below, we provide a more detailed description of our accomplishments in these three areas.

2.1 Effect of Auger recombination on lasing in heterostructured QDs with engineered core/shell interfaces.

Since the first demonstration of optical amplification in colloidal QDs (Klimov *et al.*, *Science* **290**, 2000), these structures have been extensively studied as prospective materials for the realization of solution-processed lasing media with broadly tunable emission wavelengths. Despite their favorable light emitting properties, application of QDs in lasing is complicated by extremely short optical gain lifetimes limited by nonradiative multicarrier Auger decay (Klimov *et al.*, *Science* **287**, 2000), the process wherein the energy released during electron-hole recombination is transferred to a third carrier. It was realized already at early stages of QD research, that Auger decay represents a major complication for both generating population inversion and maintaining it long enough for the development of lasing. However, the effect of Auger recombination on lasing characteristics such as lasing threshold has never been analyzed in quantitative terms either theoretically or experimentally.

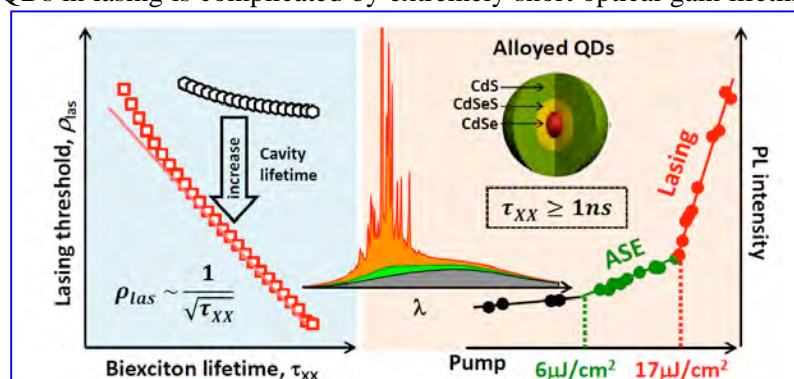


Figure 1. Left (modeling): Lasing threshold evaluated in terms of critical population inversion (ρ_{las}) as a function of biexciton lifetime (τ_{XX}) for high- (black) and low- (red) loss cavities (1 ps and 1 ns cavity photon lifetimes, respectively). Right (experiment): By incorporating an alloyed layer at the core/shell interface, we achieve a ca. 3-fold reduction in the Auger decay rate, which translates into the reduced ASE and lasing thresholds; the demonstrated threshold values establish a new record for colloidal QDs.

As part of this project’s effort on “engineered multiexciton interactions”, we have conducted coordinated theoretical and experimental studies of optical amplification in colloidal QDs with a goal to elucidate the role of Auger recombination in the regimes of both pulsed and *cw* excitation.

As part of this project’s effort on “engineered multiexciton interactions”, we have conducted coordinated theoretical and experimental studies of optical amplification

in colloidal QDs with a goal to elucidate the role of Auger recombination in the regimes of both pulsed and *cw* excitation.

First, we have developed a model, which explicitly accounts for the multiexciton nature of optical gain in QDs, and used it to analyze the competition between stimulated emission from multiexcitons and their decay *via* Auger recombination. According to our calculations, in the limit of the lossless cavity, the critical population inversion required for the lasing action (ρ_{las}) scales inversely with the biexciton lifetime (τ_{XX}) as $\rho_{\text{las}} \propto (\tau_{\text{XX}})^{-1/2}$ (Fig. 1, left). While under pulsed excitation this scaling leads to only modest dependence of the lasing threshold on the rate of Auger decay, the effect of τ_{XX} becomes much more dramatic under *cw* excitation when carrier generation directly competes with Auger recombination at the pumping stage. For example, the increase of τ_{XX} from 50 ps to 1 ns leads to the reduction of the *cw* lasing threshold by 3 orders of magnitude.

To experimentally evaluate the role of Auger recombination in lasing, we have synthesized and studied two types of CdSe/CdS core/shell QDs, engineered to have the same volumes (and hence, same absorption cross-sections) but different Auger lifetimes. The first (reference) sample represents core/shell (C/S) QDs with a sharp core/shell interface while in the second sample, the core and the shell are separated by a CdSe_{0.5}S_{0.5} alloy layer (C/A/S QDs). As we have demonstrated previously, the C/A/S QDs feature strong suppression of Auger decay resulting from the grading of the confinement potential. For both samples, we observe a transition to amplified spontaneous emission (ASE) and then lasing with increasing pump fluence (Fig. 1, right). Importantly, the lasing thresholds are consistently lower for the alloyed QDs *vs.* reference samples. Since the two types of dots are characterized by identical absorption cross-sections, the observed improvement can be unambiguously attributed to suppression of Auger decay, which validates the results of our modeling and re-emphasizes the importance of Auger-decay control for the realization of *cw* lasing. Furthermore, this study offers practical strategies for suppression of Auger recombination via “interface engineering” in core/shell structures.

2.2 Room-temperature single-photon emission from inorganic perovskite QDs. Perovskite materials have become the subject of intense recent interest due to rapid advances in perovskite solar cell efficiencies that skyrocketed from 3-4% in 2009 to ~20% in recent years. In addition, perovskites have high emission efficiencies and composition-tunable emission wavelengths.

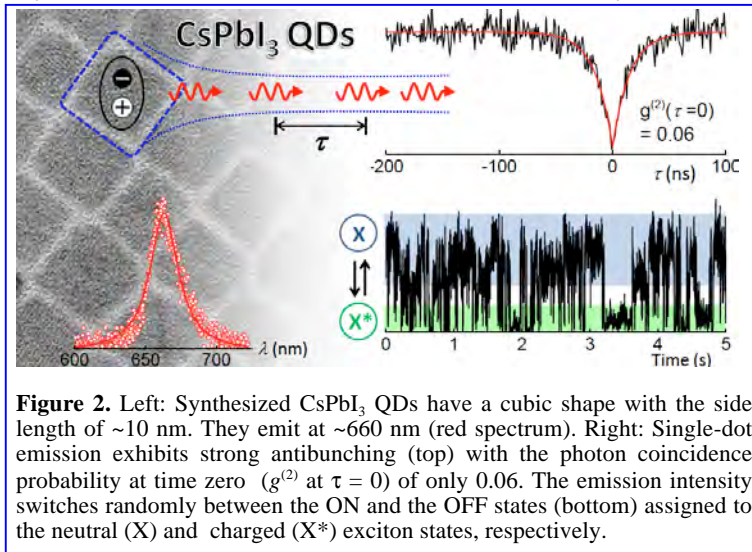


Figure 2. Left: Synthesized CsPbI₃ QDs have a cubic shape with the side length of ~10 nm. They emit at ~660 nm (red spectrum). Right: Single-dot emission exhibits strong antibunching (top) with the photon coincidence probability at time zero ($g^{(2)}(\tau=0)$) of only 0.06. The emission intensity switches randomly between the ON and the OFF states (bottom) assigned to the neutral (X) and charged (X*) exciton states, respectively.

These properties have been explored in the context of applications in LEDs and lasing. Use of nanostructured forms of these materials can potentially provide additional flexibility in tailoring their electronic and optical spectra, and also allows for the realization of principally new applications that explicitly rely on quantum-confined electronic excitations.

As part of this project’s “nanoscale emitter” effort, we have conducted single-QD studies of inorganic CsPbX₃ perovskite (X = I or Br); Fig. 2 (left). Our measurements indicate that these QDs behave as quantum emitters at room temperature, *i.e.*, show strong photon antibunching in the emitted light (Fig. 2, top right). We also observed strong fluctuations in

the photoluminescence (PL) intensity that correlate with the variation of the PL lifetime (Fig. 2, bottom right). This behavior is typical of blinking due to fluctuations of the QD charge when the high- (ON) and low (OFF) emissivity states are ascribed to a neutral and a charged exciton, respectively (Galland *et al.*, *Nature* **479**, 2011). The analysis of blinking trajectories as a function of excitation intensity suggests that charging is driven by photoionization due to a combination of both linear and nonlinear processes.

Interestingly, the PL blinking behaviors observed in the present study are notably different from those reported previously for larger-size perovskite nanostructures. However, if we analyze them in the context of previous work on more traditional colloidal QDs (based, *e.g.*, on II-VI semiconductors), we find many similarities. This provides yet another example of generality of many physical phenomena across colloidal nanocrystals of different compositions. In addition to PL blinking, colloidal QDs exhibit remarkably similar trends in intra-band relaxation, Auger recombination, magneto-optical properties, *etc.* One might expect that at least some of these trends will also be found in the emerging class of QDs based on perovskite materials.

2.3 Giant internal magnetic fields due to spin fluctuations in magnetically doped QDs. The past decade has witnessed a resurgent interest in magnetically doped semiconductors, motivated in large part by the ability to tailor, via quantum confinement and wavefunction engineering, the spin interactions between embedded magnetic atoms (such as Mn) and band carriers (electrons and holes). New materials for spin-based electronic and photonic applications include Mn²⁺-doped nanoribbons, nanowires, epitaxially grown quantum dots, and colloidal nanocrystals. The very strong quantum confinement that exists in colloidal nanocrystals can compress the wavefunctions of band electrons and holes to nanometer-scale volumes, significantly enhancing interactions between themselves and individual Mn²⁺ dopants. In magnetically-doped semiconductors, where paramagnetic dopants (*e.g.*, Mn²⁺) couple to band carriers via strong sp-d spin exchange, giant magneto-optical effects can therefore be realized in confined geometries using few or even single Mn²⁺ spins.

Importantly, however, thermodynamic spin fluctuations become increasingly relevant in this few-spin limit. In nanoscale volumes, the statistical $(N)^{1/2}$ fluctuations of N spins are expected to generate giant *effective* magnetic fields \mathbf{B}_{eff} , which should dramatically impact carrier spin dynamics, even in the absence of any external field. Over the past year we have developed new capabilities for measuring spin and magnetization dynamics on ultrafast timescales using time-resolved Faraday rotation. We have used this new capability to directly and unambiguously reveal the huge effective fields \mathbf{B}_{eff} that exist – *even at zero applied magnetic field* – in a new class of Mn²⁺-doped CdSe colloidal nanocrystals. At zero applied magnetic field, extremely rapid (300-600GHz) spin precession of photoinjected electrons is observed, indicating \mathbf{B}_{eff} of 15-to-30T for electrons. Precession frequencies exceed 2 THz in applied magnetic fields. These signals arise from electron precession about the random fields due to statistically-incomplete cancellation of the embedded Mn²⁺ moments, thereby revealing the initial coherent dynamics of magnetic polaron formation, and highlighting the importance of magnetization fluctuations in carrier spin dynamics in nanomaterials.

3. Future work

3.1 Auger-decay engineering for positive and negative trions. So far, we have studied the ideas of “interface engineering” for suppression of Auger recombination using CdSe/CdS QDs. However, while allowing for a considerable suppression of Auger decay rates for positive trions, these nanostructures do not allow for effective control of Auger recombination of negative trions. On the other hand, the optical-gain lifetime is defined by biexciton Auger recombination, which occurs via both positive- and negative-trion pathways. In order to achieve effective suppression of both of these decay channels, we will develop and study structures in which not only a hole but also an electron experiences a graded confinement potential. We will explore two distinct approaches, which we will refer to as dual-graded and single-graded structures. Dual-graded QDs will provide smooth potential gradients for each carrier in separate shell regions. This concept can be exemplified, within the material class of either CdSe/CdS/ZnS or CdSe/ZnSe/ZnS heterostructures featuring corresponding ternary alloys between each layer. On the other hand, the single-graded motif will feature a smooth potential gradient for both carriers in the same shell region. This can be achieved in CdSe/Cd_{1-x}Zn_xSe_{1-y}S_y/ZnS QDs, in which both cation and anion ratios are continuous varied throughout the interfacial quaternary alloy region. The synthetic work on these structures and their optimization will be conducted based on feedback from ensemble and single-dot spectroscopic studies. The optimized structures will be tested for their lasing performance with an ultimate goal of demonstrating *cw* lasing under standard blue-LED excitation.

3.2 New types of LEDs based on heavy-metal-free QDs. Up to now, all record-performance QD-LEDs have used materials comprising the toxic metal Cd, which seriously complicates their applications in real-life technologies. To address this problem, we will explore the replacement of Cd-based structures with QDs of I-III-VI₂ (*e.g.*, CuInSe_xS_{2-x}) compounds. Presently, progress towards making heavy metal-free electroluminescent devices with I-III-VI₂ QDs has been slow due various non-radiative exciton decay pathways such as Auger recombination and charge trapping at surface imperfections. In this project, we will explore the possibility of overcoming these problems by growing a very thick ZnS shell (more than 10 monolayers) around the emissive CuInSe_xS_{2-x} core, thus realizing the “giant-QD” strategy within the I-III-VI₂ material’s system. This strategy has been successfully applied by us previously to CdSe/CdS QDs and we anticipate it will also help us resolve Auger recombination and surface trapping issues in the case of CuInSe_xS_{2-x} materials. This study will involve a range of capabilities across the entire team from synthesis and various optical spectroscopies to device design, development and

characterization. Our target in the first round of these coordinated studies conducted in FY16 will be to demonstrate CuInSe_xS_{2-x} QD-based LEDs with more than 1% external quantum efficiency.

3.3 Magnetic polarons in magnetically-doped QDs. To date, we have applied our new capabilities for ultrafast spin and magnetization dynamics only to CdSe nanocrystals uniformly doped with magnetic Mn²⁺ ions. In such nanocrystals, the *s-d* (electron-Mn) and *p-d* (hole-Mn) exchange interactions are averaged over the entire nanocrystal, and moreover, the individual *s-d/p-d* contributions cannot be measured independently. Our future studies will therefore focus on the development of magnetically doped nanocrystals wherein the embedded magnetic dopants are *controllably positioned* radially within the nanocrystal, allowing to tune the spin interactions by engineering the overlap of the magnetic dopants with the carrier wavefunction(s). Moreover, we will explore the use of core-shell heterostructures to spatially separate the electron and hole wavefunctions, thereby permitting magnetic dopants to interact with either electrons *or* holes. The ability to engineer these parameters will directly influence the formation dynamics and stability of *magnetic polarons* in these colloidal nanocrystals, *i.e.*, the collective ferromagnetic alignment of the embedded magnetic spins by a single optically excited exciton. Whether the strong confinement in colloidal nanocrystals can stabilize magnetic polarons up to room temperature remains an important and outstanding question in this field.

4. Publications (2013 - 2015)

1. Y.-S. Park, W.-K. Bae, T. Baker, J. Lim, and V. I. Klimov, *Effect of Auger Recombination on Lasing in Heterostructured Quantum Dots with Engineered Core/Shell Interfaces*, Nano Lett. in press (2015)
2. Y. S. Park, S. Guo, N. S. Makarov, V. I. Klimov, *Room Temperature Single-Photon Emission from Individual Perovskite Quantum Dots*, ACS Nano, in press (2015)
3. I. Robel, A. Shabaev, D. C. Lee, R. D. Schaller, J. M. Pietryga, S. A. Crooker, Al. L. Efros, V. I. Klimov, *Temperature and Magnetic-Field Dependence of Radiative Decay in Colloidal Germanium Quantum Dot*, Nano Lett. **15**, 2685-2692 (2015)
4. M. V. Kovalenko, L. Manna, A. Cabot, Z. Hens, D. V. Talapin, C. R. Kagan, V. I. Klimov, A. L. Rogach, P. Reiss, D. J. Milliron, P. Guyot-Sionnest, G. Konstantatos, W. J. Parak, T. Hyeon, B. A. Korgel, C. B. Murray, W. Heiss, *Prospects of Nanoscience with Nanocrystals*, ACS Nano **9**, 1012-1057 (2015)
5. W. D. Rice, H. McDaniel, V. I. Klimov, S. A. Crooker, *Magneto-Optical Properties of CuInS₂ Nanocrystals*, J. Phys. Chem. Lett. **5**, 4105-4109 (2014)
6. J. Lim, B. G. Jeong, M. Park, J. K. Kim, J. M. Pietryga, Y.-S. Park, V. I. Klimov, C. Lee, D.C. Lee, W.K. Bae, *Influence of shell thickness on the performance of light emitting devices based on CdSe/Zn_{1-x}Cd_xS core/shell quantum dots*, Adv. Mater. **26**, 8034 (2014)
7. Y.-S. Park, W. K. Bae, J. M. Pietryga, V. I. Klimov, *Auger recombination of biexcitons and negative and positive trions in individual quantum dots*, ACS Nano **8**, 7288 (2014).
8. S. Brovelli, W. K. Bae, F. Meinardi, M. Lorenzon, C. Galland, V. I. Klimov, *Electrochemical control of two-color emission from colloidal dot-in-bulk nanocrystals*, Nano Lett. **5**, 3855 (2014).
9. V. I. Klimov, *Multicarrier interactions in semiconductor nanocrystals in relation to the phenomena of Auger recombination and carrier multiplication*, Annu. Rev. Condens. Matter Phys. **5**, 13.1 (2014).
10. S. Brovelli, W. K. Bae, C. Galland, U. Giovanella, F. Meinardi, V. I. Klimov, *Dual-color electroluminescence from dot-in-bulk nanocrystals*, Nano Lett. **14**, 486 (2014).
11. Y.-S. Park, W. K. Bae, L. A. Padilha, J. M. Pietryga, V. I. Klimov, *Effect of the core/shell interface on Auger recombination evaluated by single-quantum dot spectroscopy*, Nano Lett. **13**, 396 (2013)
12. W. K. Bae, S. Brovelli, V. I. Klimov, *Spectroscopic insights into the performance of quantum dot light-emitting diodes*, MRS Bulletin **38**, 721 (2013).
13. C. Galland, S. Brovelli, W.K. Bae, L.A. Padilha, F. Meinardi, V.I. Klimov, *Dynamic hole blockade yields two-color quantum and classical light from 'dot-in-bulk' nanocrystals*, Nano Lett. **13**, 321 (2013)
14. L.A. Padilha, W.K. Bae, V.I. Klimov, J.M. Pietryga, R.D. Schaller, *Response of semiconductor nanocrystals to extremely energetic excitation*, Nano Lett. **13**, 925 (2013).
15. Y.-S. Park, Y. Ghosh, Y. Chen, A. Piryatinski, P. Xu, N. H. Mack, H. -L. Wang, V. I. Klimov, J. A. Hollingsworth, H. Htoon, *Super-Poissonian statistics of photon emission from single core/shell nanocrystals coupled to metal nanostructures*, Phys. Rev. Lett. **110**, 117401 (2013).

PULSE Ultrafast Chemical Science

*P.H. Bucksbaum, D.A. Reis, K. Gaffney, T. Heinz, T. Martinez, T. Wolf, M. Guehr, C. Stan, J. Cryan, S. Ghimire, SLAC National Accelerator Laboratory, 2575 Sand Hill Rd. MS 59, Menlo Park, CA 94025.
Email michelley@slac.stanford.edu*

Overarching science goal: The PULSE Ultrafast Chemical Science program focuses on ultrafast chemical physics research at SLAC that is enabled by SLAC's x-ray and relativistic electron facilities, including LCLS, SSRL, Ultrafast Electron Diffraction (UED) and in the future, LCLS-II. Our research at SLAC makes optimal use of these unique tools for fundamental discoveries and new insights in ultrafast science. The two distinguishing advantages of this program are the on-site presence of the LCLS; and our connection to Stanford University. These help to keep us competitive on an international level.

Major Themes: In its February 2015 meeting, BESAC approved a list of "Transformational Opportunities," meant to bring the 2007 Grand Challenges up to date. The Ultrafast Chemical Science program has connections to many of the themes in these documents. We have particular emphasis on the transformation opportunities of "Imaging Matter across Scales", "Harnessing Coherence in Light and Matter". We also have high relevance to the Grand Challenges in the areas of "Energy and Information on the Nanoscale" and "Control at the Level of Electrons."

Imaging matter across scales: The nanoscale in space and the femtoscale in time. Microscopy at its most essential level in both space and time is paramount to the BES mission to control matter. Non-periodic nano-structures and ultrafast timescales dominate the workings of biology and chemistry. To understand and control function we therefore must first observe structure and motion on these scales.

X-ray lasers are revolutionary sources of short wavelength coherent radiation for investigations on the nanoscale, and one of our subtasks is devoted to developing science using coherent x-ray imaging techniques x-ray free electron lasers. This work includes serial femtosecond nanocrystal imaging on the few-Angstrom scale; nonperiodic imaging of single biomolecules; and imaging structure and dynamics in a number of systems, from electrons inside small molecules to micron-scale shocks and phase transitions.

We also image smaller structures such as small molecules using other techniques, such as particle fragment velocity maps, and electron holography. Here we are exploring fundamental energy-relevant processes such as photo-induced isomerization, dissociation, and x-ray damage, using optical and x-ray probes, and a combination of linear and nonlinear spectroscopic methods.

Much of chemistry happens at the femtosecond scale, and it is necessary to develop new methods to simultaneously achieve this level of temporal resolution with simultaneous chemical and structural sensitivity. FEL and laser-based sources of x-ray and extreme ultraviolet radiation afford the opportunity for atomic specificity combined with femtosecond resolution. To realize this opportunity, pump-probe spectroscopy at visible and infrared wavelengths must be extended to the soft and hard x-ray range, and to new sources such as FELs. Much of our efforts are devoted to developing new methods and advancing ultrafast science in this area, including impulsive stimulated Raman and other nonlinear x-ray scattering methods.

Energy and Information: The architecture of light conversion chemistry. Light from the sun is the primary source of energy on earth, and so we are exploring light conversion to electron motion and then to chemical bonds. Some molecules are particularly adept at this conversion and we would like to understand how they work. For example, how does non-adiabatic dynamics affect the process of photocatalysis within coordination complexes and similar materials.

Energy conversion is initiated by charge separation, and we know that the charge distribution of the electron and hole, as well as the presence of low-energy ligand field excited states greatly influence the lifetime of optically generated charge transfer excited states. The detailed mechanism for the excited state

quenching remains unclear. New methods of linear and nonlinear spectroscopy, and especially x-ray spectroscopy involving short-pulse FELs, can help provide the answer.

An equally important problem is the protection of some chemical bonds, particularly in biology, from destruction in the presence of ultraviolet sunlight. Photoprotection is also an ultrafast process involving charge transfer, and so these new techniques such as ultrafast x-ray absorption and Auger emission can show how critical bonds are protected.

The incorporation of theory within this FWP is critical for rapid progress in light conversion chemistry, and helps us to focus our efforts in areas of greatest impact.

Harnessing coherence on the eV scale in time, space, and field strength. This is the fundamental scale that determines structure and dynamics of electrons in molecules, and motivates advances in sub-femtosecond time-resolution and Angstrom spatial resolution in theory and experiments. To achieve an adequate view of the molecular realm with at this level, we must interrogate atoms with fields comparable to Coulomb binding fields, and on time scales set by the electronic energy splittings in atoms.

One method to reach this scale is through nonlinear frequency conversion, known as high harmonic generation (HHG). We are constructing new intense sources of attosecond pulsed vacuum ultraviolet radiation based on HHG, and will use it to develop new spectroscopies that can detect the motion of electrons within molecules.

We are particularly interested in the response of atoms to fields strong enough to ionize them multiple times. It has long been known that the ionization thresholds are greatly suppressed for multiple ionization, and a number of theories about this will be tested during the next contract period. This is an example of coupled motion among multiple electrons, which goes beyond the single active electron approximation that has dominated thinking about strong field laser-atom physics. New theoretical approaches are also required for this, and we are tackling these as well.

LCLS is also capable of sub-femtosecond or few femtosecond pulses, and these have the unique property of wavelengths short enough to reach the most deeply bound electrons in first through third row atoms. We will use LCLS to image the strong-field electronic response during HHG in solids at the atomic-scale in length and time, and to explore nonlinear x-ray Compton scattering as a means to achieve simultaneous chemical and structural sensitivity. Through the use of novel methods such as low bunch charge, double-slotted spoilers, strong laser fields, and novel data sorting methods, as well as future methods such as self-seeding, we will incorporate LCLS fully as a tool for sub-femtosecond spectroscopy.

Management Structure: This Ultrafast Chemical Science research program resides within the Chemical Science Division within the SLAC Science Directorate. The current CS Director is Tony Heinz. SLAC Director Chi-Chang Kao presently leads the Science Directorate.

Space allocations: Most of our research activities take place in laboratories in SLAC Building 40a. SLAC currently provides office space for our research groups, and also allocates approximately 8000 square feet to research laboratories and a computer room for this FWP. The co-location of most of our program within Building 40 and 40a is a distinct advantage, but is not entirely sufficient for the space requirements of this program, and so we also perform some of this research in PULSE Institute space within the Varian Physics Lab and the Mudd Chemistry Lab on the Stanford campus (approximately 1000 square feet, including offices and labs, in each building). Further details are in the Facilities and Resources Section 11 of this document.

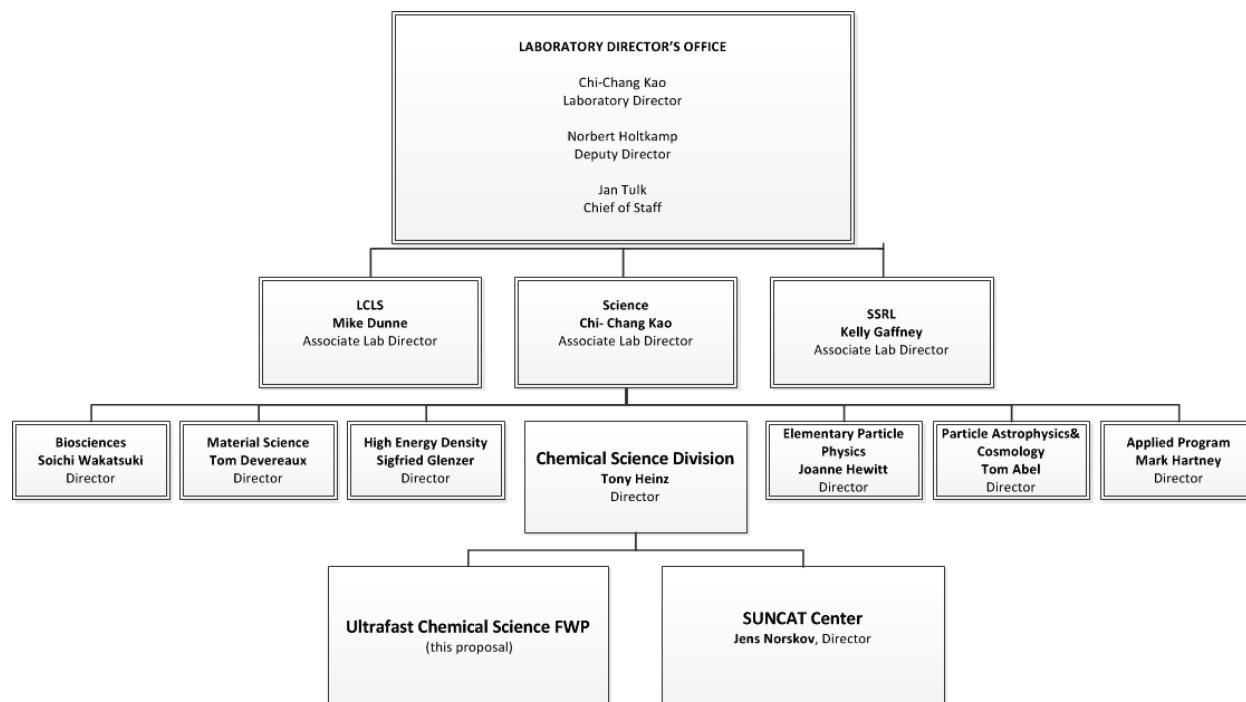


Figure 1. Partial organization chart for SLAC, showing the relation of the Ultrafast Chemical Science FWP to other units with close research ties.

Subtasks and allocations: Seven key personnel are responsible for six subtasks, which represent six different areas of expertise:

1. UTS: Ultrafast Theory and Simulation (Martinez)
2. ATO: Attoscience (Bucksbaum, Gühr, Cryan)
3. SPC: Solution Phase Chemistry (Gaffney)
4. NPI: Non-periodic X-ray Imaging (Stan)
5. SFA: Strong Field AMO Physics (Bucksbaum)
6. NLX: Nonlinear X-ray Science (Reis, Ghimire)
7. EDN: Electron Dynamics on the Nanoscale (Heinz)
8. EIM: Excitations in Molecules (Guehr, Wolf)

Support operations (finance, HR, safety, purchasing, travel) are directed by the Associate Laboratory Director for Science and the Chemical Sciences Director and their staff. They provide oversight and delegate the work to appropriate offices in the SLAC Operations Directorate or to the staff of the Stanford PULSE Institute.

Connections to other units within the SLAC organizational structure: Close collaborations are maintained with the Science R&D Division within the LCLS Directorate; the Materials Science Division (SIMES) within the Science Directorate; SSRL; and the SUNCAT Center within our own Chemical Sciences Division, as shown in figure 4.1. Our location near these facilities and research organizations at SLAC greatly aids collaboration.

Other important connections: The PIs have affiliations with other Stanford University research and academic units: All members of this FWP are members of the Stanford PULSE Institute, and several are affiliated with the SIMES Institute, Bio-X, the Ginzton Laboratory, and the Departments of Chemistry, Physics, and Applied Physics.

We also have collaborative connections to other outside research labs, including DESY, the Lawrence Berkeley Laboratory, the Center for Free Electron Lasers (CFEL) in Hamburg, and BES funded groups at

the University of Michigan, the Ohio State University, the University of Connecticut, Louisiana State University, and Northwestern University.

Knowledge transfer to LCLS: LCLS does not grant any preferred status to research proposals from this FWP, nor for any program in the SLAC Science Division. This is considered an important principle to maintain fairness in the international research community. Nonetheless, the transfer of knowledge to and from LCLS is extremely fluid and critical to our success. Much of our research creates benefits for LCLS by providing new research methods and research results, and in addition there are several more direct transfers of our research product to help LCLS:

- We continue to help to commission several LCLS instruments and setup space, particularly for the LAMP chamber and the X-ray Split and Delay for the AMO beam line (AMO), and infrastructure for CXI experiments.
- Some of our graduate students provide user support through to LCLS users, particularly in cooperation with CXI, AMO, and the Laser Division, and they receive salary supplements for this work. This activity has been endorsed by review panels and is supported by the Associate Laboratory Directors and the SLAC Director.
- We have assisted in the development of timing tools currently in use at LCLS.
- Several of our postdocs and students have transferred to permanent staff positions at LCLS.
- Several LCLS Scientists and Staff have become members of the PULSE Institute, and this provides a connection to the larger research community of Stanford.
- Some LCLS Instrument Scientists have a direct connection to the research activities of this FWP. In the previous funding cycle this included Christoph Bostedt and Ryan Coffee, who participated in the NPI and SFA subtasks, respectively. In this renewal proposal, Sebastian Boutet participates in the NPI subtask.
- PULSE has helped LCLS to institute a Graduate Fellowship program, and PULSE manages several LCLS graduate student campus appointments.
- PULSE conducts an annual Ultrafast X-ray Summer School to train students and postdocs about LCLS science opportunities.

Advisory committee. The SLAC Science Policy Committee advises SLAC and the Stanford Provost on all science activities at the laboratory. Neither the SLAC Chemical Sciences Division nor the SLAC Science Directorate has their own standing science advisory committee at present. The PULSE External Advisory Board advises us on our DOE activities. This board meets annually and reports to the PULSE Director and to the Stanford Dean of Research. The reports are also forwarded to the SLAC Director, the ALD for Science, and to the SLAC Science Policy Committee.

Educational programs and outreach activities. We have an extremely active outreach and visitors program supported by Stanford through the PULSE Institute. Each year one or more scientists receive sabbatical travel supplements to permit them to be in residence in PULSE. This year, Jan-Michael had a partial sabbatical here. This visitors program also helps postdocs with fellowships or from other institutes to work at PULSE and collaborate with us.

PULSE also maintains an annual Ultrafast X-ray Summer School (Figure 4.2). This school, which was founded by the PIs of this FWP in 2006, continues to be a main mechanism for expanding the research community interested in using x-ray free electron lasers for their research. In 2011 we began a cooperative activity with CFEL in Hamburg to rotate the school between DESY and SLAC in alternate years. The school has received continued strong support from BES, Stanford, and from CFEL. The school will be held at SLAC in 2016 and 2018.

ATO: Attosecond Science

Philip H. Bucksbaum, Markus Guehr, James Cryan, SLAC National Accelerator Laboratory, 2575 Sand Hill Rd MS 59, Menlo Park, CA 94025. Email phb@slac.stanford.edu

Objective and Scope: Electron motion is a key ingredient of all chemical reactions. It is also the means by which light energy is harnessed in photochemistry. Our goal is to track the evolution of electrons on their natural time scales, to understand the earliest processes involved in chemical change.

Recent Progress:

Transient Impulsive Electronic Raman Redistribution: Last year we reported on our preliminary calculations of impulsive stimulated Raman scattering (ISRS), which will result in a superposition of valence-excited electronic states. This process exploits the large absorption

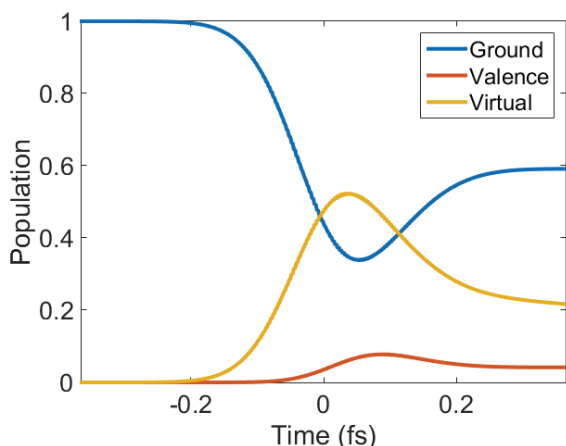


Figure 1 – Population of ground, valence, and autoionizing (virtual) states as a function of time inside the x-ray pulse. This calculation uses our 3-state model to calculate ISRS for CO molecules exposed to 530 eV x-ray pulses with an intensity near 10^{18} W/cm²

cross-section of auto-ionizing resonances and the large coherent bandwidth obtainable with XUV pulses created in strong-field driven high-order harmonic generation (HHG). In collaboration with Shungo Miyabe, we developed an effective 3-state model for the system that includes the auto-ionizing continuum. This year we have started collaboration with Daniel Haxton (LBNL) in order to verify the results obtained with our simple model by comparing to full simulation performed with Haxton's MCTDHF approach.

Our initial calculations, reported last year, focused on atomic sodium targets and XUV pulses [1]. Atomic sodium is attractive because there are many excited states within 3 eV of the ground state, which is approximately the bandwidth of a 500 as pulse. We are working to employ this same effective 3-state model to other systems such as NO and CN and NO₂, which also have low-lying valence-excited states. We have also used this model to make predictions for other wavelength ranges, such as the soft x-ray regime, which is accessible with FEL facilities, as shown in Figure 1. Following impulsive excitation of low-lying electronic states in molecular systems, interesting charge dynamics should develop, similar to the charge migration phenomena proposed by Cederbaum et al. [2] We are working to simulate the observables related to this ultrafast charge dynamics.

HHG in oriented water: The presence of hydrogen atoms in molecular systems greatly complicates the HHG process, since the protons can move significantly in the time between ionization and recombination. We have shown that water is a good candidate to study these types of complications. The first two ionic states of water are the ¹B₁ ground state, which closely resembles the neutral molecule ground state, and the ¹A₁ state, which has a potential minimum near a linear geometry. We have shown that strong-field ionization leads to a superposition of these two states [3], and that nuclear motion on the ¹A₁ surface leads to a

suppression of the overall HHG yield. Recently we have used THz radiation to impulsively excite rotational coherences in water molecules and we are working towards measurements of the HHG from oriented H₂O targets. Molecular orientation should provide a method to control the relative population of the ¹A₁ and ¹B₁ states, similar to what was observed in N₂ [4].

HHG in Vibrationally Excited Molecules:

We have continued our previous work of HHG from vibrationally-excited molecules. We have found that following impulsive vibrational excitation the HHG spectrum produced in SO₂ is modulated, not only in amplitude, but the individual harmonics are also modulated in frequency. This modulation is shown in Figure 3. Immediately following the impulsive excitation the

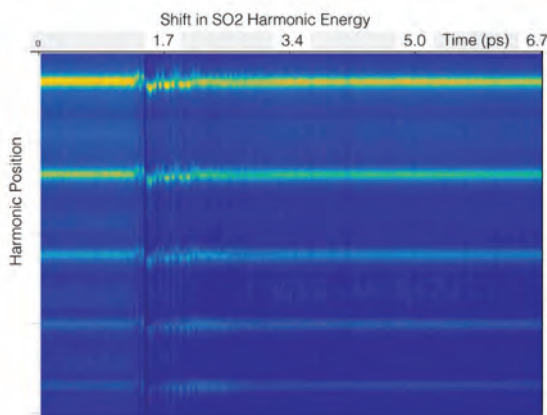


Figure 3 – High harmonic spectrum from SO₂ as a function of delay between impulsive Raman excitation and HHG probe pulse. Overlap between the pump and probe pulses occurs near 1.5 ps. Longer time delays are pump pulse preceding probe pulse.

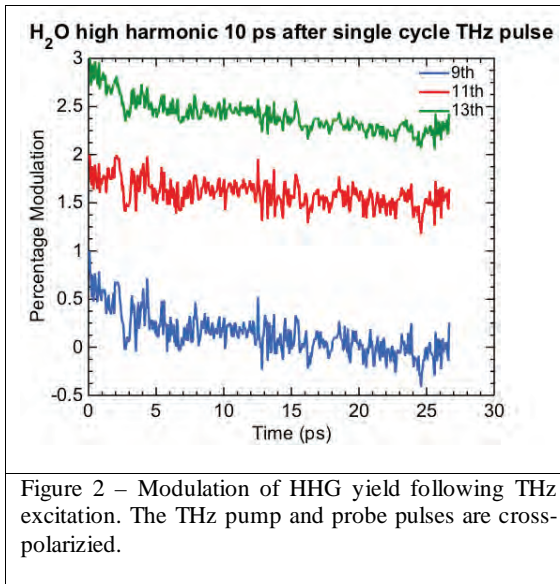


Figure 2 – Modulation of HHG yield following THz excitation. The THz pump and probe pulses are cross-polarized.

following the impulsive excitation the harmonic spectrum immediately blue shifts and oscillates with a ~50 fs period. There is also an overall frequency offset which decays on a longer, ~1 ps time scale.

High Intensity Attosecond Bursts: In the past year we have been developing a new beam line for producing intense trains of attosecond pulses with adjustable delays. Our method relies on the non-collinear optical gating (NOG) scheme developed by the L'Hullier group [5], [6]. This schemes produce angularly separated attosecond bursts that can be individually manipulated and then refocused using a set of XUV mirrors.

Future Projects:

Attosecond Pulses: We plan to commission use a new attosecond beam that incorporates attosecond lighthouse methods combined with a novel device to stack attosecond pulses. This beam line is especially designed to look at impulse induced electronic coherence in small molecular systems. We can use our variable train to provide a pair of intense attosecond pulses for pump/probe spectroscopy, we can also combine the entire train to produce one intense burst capable of driving impulsive Raman redistribution as described above. We will investigate the possibility of controlling the electron dynamics through precision tailoring of the attosecond pulse train.

Connecting our work to LCLS and LCLS-II: We have submitted an LCLS proposal, which proposes to use x-ray pulses from the LCLS, to drive Stimulated Raman Scattering in order

to create a coherent superposition of electronic states in NO₂. We plan to use a second time-delayed x-ray pulse in order to probe this coherence. This type of experiment is necessary in order to verify much of the AMO science case for LCLS-II [7].

- [1] S. Miyabe and P. Bucksbaum, “Transient Impulsive Electronic Raman Redistribution,” *Phys. Rev. Lett.*, vol. 114, no. 14, p. 143005, Apr. 2015.
- [2] A. I. Kuleff and L. S. Cederbaum, “Ultrafast correlation-driven electron dynamics,” *J. Phys. B At. Mol. Opt. Phys.*, vol. 47, no. 12, p. 124002, Jun. 2014.
- [3] J. P. Farrell, S. Petretti, J. Förster, B. K. McFarland, L. S. Spector, Y. V. Vanne, P. Decleva, P. H. Bucksbaum, A. Saenz, and M. Gühr, “Strong Field Ionization to Multiple Electronic States in Water,” *Phys. Rev. Lett.*, vol. 107, no. 8, p. 083001, Aug. 2011.
- [4] B. K. McFarland, J. P. Farrell, P. H. Bucksbaum, and M. Gühr, “High Harmonic Generation from Multiple Orbitals in N₂,” *Science*, vol. 322, no. 5905, pp. 1232–1235, Nov. 2008.
- [5] C. M. Heyl, S. N. Bengtsson, S. Carlström, J. Mauritsson, C. L. Arnold, and A. L’Huillier, “Noncollinear optical gating,” *New J. Phys.*, vol. 16, no. 5, p. 052001, May 2014.
- [6] M. Louisy, C. L. Arnold, M. Miranda, E. W. Larsen, S. N. Bengtsson, D. Kroon, M. Kotur, D. Guénot, L. Rading, P. Rudawski, F. Brizuela, F. Campi, B. Kim, A. Jarnac, A. Houard, J. Mauritsson, P. Johnsson, A. L’Huillier, and C. M. Heyl, “Gating attosecond pulses in a noncollinear geometry,” *Optica*, vol. 2, no. 6, p. 563, Jun. 2015.
- [7] R. Schoenlein, “New Science Opportunities Enabled by LCLS-II X-ray Lasers.” SLAC National Accelerator Laboratory, 01-Jun-2015.

Publications:

Publications based on research that was primarily supported by this FWP in 2013-2015.

- Bucksbaum, Philip. 2014. “Molecular Dissociation Dynamics Driven by Strong-Field Multiple Ionization.” *Bulletin of the American Physical Society* 59.
- Bucksbaum, Philip H. 2013. “Ultrafast Quantum Control in Atoms and Molecules.” In *Ultrafast Nonlinear Optics*, 105–28. Springer. http://dx.doi.org/10.1007/978-3-319-00017-6_5.
- Guehr, Markus, Brian McFarland, Joseph Farrell, Shungo Miyabe, Francesco Tarantelli, Alejandro Aguilar, Nora Berrah, Christoph Bostedt, John Bozek, and Phillip H Bucksbaum, others. 2013. “Delayed Ultrafast X-Ray Induced Auger Probing.” In *Laser Science*, LW5H–3. Optical Society of America.
- McFarland, BK, N Berrah, C Bostedt, J Bozek, PH Bucksbaum, JC Castagna, RN Coffee, JP Cryan, L Fang, and JP Farrell, others. 2014. “Experimental Strategies for Optical Pump–soft X-Ray Probe Experiments at the LCLS.” *Journal of Physics: Conference Series* 488 (1): 12015–22.
- McFarland, BK, JP Farrell, N Berrah, C Bostedt, J Bozek, PH Bucksbaum, R Coffee, J Cryan, L Fang, and R Feifel. 2013. “Probing Nucleobase Photoprotection with Soft X-Rays.” In *EPJ Web of Conferences* 41, 07004 (2013), 41:07004. doi:10.1051/epjconf/20134107004.
- McFarland, B. K., J. P. Farrell, S. Miyabe, F. Tarantelli, A. Aguilar, N. Berrah, C. Bostedt, et al. 2014. “Ultrafast X-Ray Auger Probing of Photoexcited Molecular Dynamics.” *Nature Communications* 5 (June): 4235. doi:10.1038/ncomms5235.
- S. Miyabe and P. H. Bucksbaum, “Transient Impulsive Electronic Raman Redistribution,” *Phys. Rev. Lett.* 114 143005 (2015)
- Spector, Limor S, Maxim Artamonov, Shungo Miyabe, Todd Martinez, Tamar Seideman, Markus Guehr, and Philip H Bucksbaum. 2014. “Axis-Dependence of Molecular High Harmonic

Emission in Three Dimensions.” *Nature Communications* 5: 3190.
doi:10.1038/ncomms4190.

Spector, Limor S, Shungo Miyabe, Alvaro Magana, Simon Petretti, Piero Decleva, Todd Martinez, Alejandro Saenz, Markus Guehr, and Philip H Bucksbaum. 2013. “Multiple Orbital Contributions to Molecular High-Harmonic Generation in an Asymmetric Top.” <http://arxiv.org/abs/1308.3733>.

Spector, L.S., M. Artamonov, S. Miyabe, T. Martinez, T. Seideman, M. Guehr, and P.H. Bucksbaum. 2014. “Quantified Angular Contributions for High Harmonic Emission of Molecules in Three Dimensions.” arXiv:1207.2517.

Electron Dynamics on the Nanoscale, Tony Heinz, PI

SLAC National Accelerator Laboratory, 2575 Sand Hill Road MS 59, Menlo Park, CA 94025

theinz@slac.stanford.edu

Program Scope

This research program, recently initiated at SLAC, seeks to obtain fundamental understanding of the dynamics of electronic excitations in nanostructures. The research addresses central issues for photoexcited electrons in atomically thin two-dimensional (2D) layers of van-der-Waals crystals and heterostructures, with particular emphasis on monolayers of transition metal dichalcogenide crystals. The investigations make use of complementary experimental techniques based on ultrafast spectroscopy to probe radiative and non-radiative relaxation pathways after photoexcitation, addressing the role of Coulomb and vibrational interactions as manifest in exciton formation, exciton-exciton and exciton-carrier interactions, intervalley scattering, and exciton radiative decay. The research also examines electron dynamics in heterostructures composed of atomically thin 2D van der Waals layers combined with other 2D layers and with 0D structures, such as quantum dots. Because of the unreactive character of 2D van der Waals layers, combinations of a wide variety of structures can be prepared by mechanical assembly, as well as by chemical deposition techniques. The research program addresses the dynamics of both charge and energy transfer processes for these heterostructures using ultrafast spectroscopy techniques.

Progress Report

Our recent research has investigated exciton states and dynamics in the monolayer and ultrathin layers of transition metal dichalcogenide materials in the class of MX_2 ($M = \text{Mo}, \text{W}$ and $X = \text{S}, \text{Se}, \text{Te}$). The measurements have included both spectroscopy measurements to determine the excited excitonic states and excitonic binding and dynamical studies in which exciton-exciton interactions lead to biexciton states and an optically induced Mott transition. We have also applied experimental methodologies based on time-domain terahertz spectroscopy to examine the dynamics of photoinduced charge transfer at the model system of C_{60} adsorbed on a monolayer of graphene. Below we briefly summarize progress in these area.

Exciton Rydberg series and exciton binding energy in 2D TMDC systems

Atomically thin semiconductors in the TMDC family have been predicted to have unusually strong Coulomb interactions. This situation arises from the reduced dimensionality and the reduced dielectric screening. In this study, we applied photoluminescence excitation (PLE) spectroscopy to identify the ground state and excited states in the Rydberg series of excitons in monolayers of MoS_2 and WS_2 . In Fig. 1 we present the PLE spectra from the MoS_2 monolayer. In addition to the strong ground-state excitonic

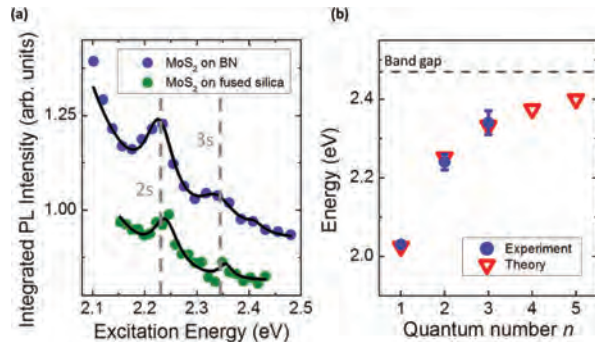


Fig. 1: Exciton Rydberg series in monolayer MoS_2 . (a) PLE spectrum exhibiting the peaks corresponding to creation of the first ($2s$) and second ($3s$) excited states for MoS_2 monolayers on two different substrates. (b) Energies of the first three excitonic levels from experiment (dots) and from theory (triangles) based on the usual effective mass treatment, but with a non-locally screened Coulomb interaction between the electron and hole.

peak, at 2.02 eV, the PLE spectra reveal additional higher lying excitonic transitions, as indicated. The disposition of the levels in this system deviates strongly from the predictions of a 2D hydrogenic model. The data can, however, be modeled by a theory that accounts for the inhomogeneous nature of the dielectric screening: charges are strongly screened at small separations, but experience weaker screening at separations greater than the layer thickness. This study reveals the strength of the Coulomb interaction and the deviation from the standard $1/r$ effective potential through the non-hydrogenic spectrum and an exciton binding energy as large as 440 meV. Similar results are obtained for the excitons in WS_2 monolayers, which were previously investigated by direct absorption spectroscopy.

Observation of biexciton states in WSe_2 monolayers

The strong Coulomb interactions that give rise to very high exciton binding energies in the atomically thin TMDC semiconductor nanosheets suggest that higher-order excitonic states may also be significant under photoexcitation. Indeed, earlier work by the Heinz group and others revealed that stable charged excitons also form when a doped material is optically excited. These three-body states or trions consist of two electrons and a hole in an electron-doped layer and, unlike excitons, carry a net charge. They can be considered as the excitonic analog of the hydrogen anion. The binding energy of the additional electron (trion binding energy) is found to be in the range of ~ 30 meV.

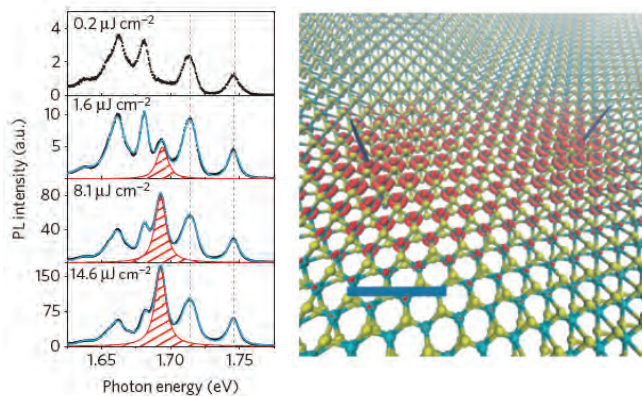


Fig. 2: Biexcitons in monolayer WSe_2 . (a) PL spectra from low to high exciton concentration, as controlled by the pump laser fluence. In addition to the exciton, trion, and defect peaks, a new feature appears at 1.68 eV, becoming the strongest peak at high excitation density. (b) Representation of the biexciton or exciton molecule. The spikes are the most probable separation for the two holes and the red shading represents the electron density. The theory is based on a variational calculation with the same non-locally screened potential as the one successfully used to describe the ground and excited excitonic states.

In recent work, the Heinz group has identified a clear signature of biexcitons or excitonic molecules. These four-body correlated quantum states are analogous to the hydrogen molecule. They were identified by a PL peak lying below the exciton emission energy and exhibiting a strongly superlinear dependence on exciton concentration (Fig. 2). The binding energy of the biexciton, *i.e.*, the energy required to separate it into two individual excitons, is determined from the spectra shift to be ~ 50 meV, a value considerably greater than the binding energy of the exciton itself in conventional semiconductors.

Exciton screening and Mott transition at high densities in atomically thin WS_2

In a recent investigation, the Heinz group identified a transition in the behavior of photoexcited layers of atomically thin WS_2 . In the regime of low exciton density, the optically excited state consists of isolated excitons (and potentially higher-order trions in the presence of free charges). At somewhat higher exciton density, biexcitons are formed. However, as the exciton density is further increased, the system undergoes a phase change, the so-called Mott transition. In this limit, the excited carriers form a plasma of free electrons and holes, which act to screen on another and prevent the formation of tightly bound excitons. In this regime, the system behaves more like a conventional semiconductor with free carriers.

The transition from the excitonic to the free-carrier regime is accompanied by a large change in the band-gap (band-gap renormalization) of the material: Just as for the excitonic (attractive) interactions, the repulsive electron-electron interactions affecting the quasi-particle band structure are also screened.

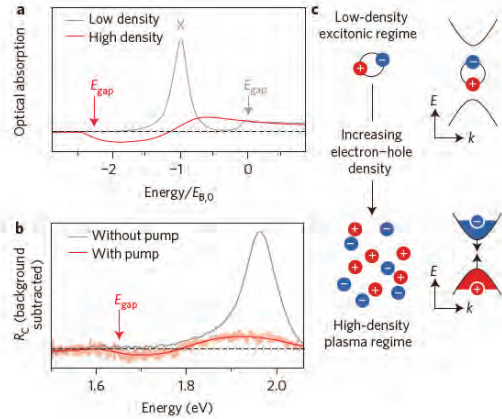


Fig. 3: Mott transition in atomically thin WS_2 crystals. (a) The expected change in the optical response from a material with a strong excitonic transition to one with free carrier transitions, a renormalized band gap, and population inversion. This representation is based on existing theory for quantum-well systems. (b) The corresponding transient absorption spectra before and just after excitation by an intense 100 fs pump pulse for WS_2 . (c) A schematic representation of the Mott transition from excitonic excited states to a free carrier plasma of electrons and holes.

Importantly, at high excitation density, the experiment also reveals that population inversion is created. In the absence of other loss channels, this will give rise to optical gain.

These results (Fig. 3) were obtained by strong photoexcitation of the WS_2 layers with a femtosecond laser pulse. A time synchronized broadband continuum pulse was used to probe the optical state of the system as a function of delay time. The excitonic absorption peak vanishes within a few 100 fs, corresponding to the time resolution of the measurement. At the same time, spectroscopic signatures of population inversion and band-gap renormalization appear. The system recovered its original optical response after ~ 100 ps. The vdW layer was found to be extremely robust, allowing for excitation densities in excess of 1 carrier per nanometer.

Photoinduced charge transfer for C_{60} /graphene system

As a model of an important interface of a vdW layered material with a localized chromophore, we have investigated charge transfer processes for a layer of solid C_{60} molecules deposited on a monolayer of graphene. These materials are both of fundamental interest and have also attracted attention for use in organic photovoltaic devices. Our investigations have examined charge transfer following photoexcitation, as well as charge transfer in the ground state. For static measurements, we determined levels of charge transfer by applying Raman and time-domain THz spectroscopy. For the former, we made use of shifts of the Raman G-mode as a measure of charge density; for the latter, we analyzed the complex, frequency-dependent conductivity to determine the graphene charge density. More distinctively, we also applied time-domain THz spectroscopy to monitor the graphene conductivity spectrum as a function of delay after photoexcitation.

Measurement of the transient THz response for the individual components of the hybrid material and the composite system revealed that photoexcitation with 4-eV photons gave rise to hole injection into the graphene. The process was relatively efficient for the C_{60} molecules adjacent to graphene and produced a transient increase in conductivity lasting ~ 100 ps before the charge in graphene returned to its equilibrium state in the C_{60} layer. This experiment established THz time-domain spectroscopy as a new method to quantitatively evaluate photoinduced charge transfer in 2D layers and to follow the dynamics of this process with ultrafast time resolution.

Future Plans

Our planned experiments will be directed towards establishing the dynamics for the elementary processes in both individual 2D layers, as well as in tailored nanostructures composed of 2D layers combined with other 2D layers and with 0D quantum dot structures. Through the application of diverse ultrafast spectroscopy techniques, we will examine in individual layers the rates of exciton formation, radiative decay of excitons, and inter-valley scattering and dephasing processes. We will make use of different

heterostructures, including those with spacer layers of varying thickness, to develop an understanding of the processes of interfacial energy and charge transfer for the model heterostructures systems.

Publications Acknowledging AMOS Support

1. H. M. Hill, A. F. Rigosi, C. Roquelet, A. Chernikov, T. C. Berkelbach, D. R. Reichman, M. S. Hybertsen, L. E. Brus, and T. F. Heinz, "Observation of Excitonic Rydberg State in Monolayer MoS₂ and WS₂ by Photoluminescence Excitation Spectroscopy," *Nano Lett.* **15**, 2992 - 2997 (2015).
2. Y. You, X. X. Zhang, T. C. Berkelbach, M. S. Hybertsen, D. R. Reichman, and T. F. Heinz, "Observation of Biexcitons in Monolayer WSe₂," *Nature Phys.* **11**, 477-481 (2015).
3. A. F. Rigosi, H. M. Hill, Y. Li, A. Chernikov, T. F. Heinz, "Probing Interlayer Interactions in Transition Metal Dichalcogenide Heterostructures by Optical Spectroscopy: MoS₂/WS₂ and MoSe₂/WSe₂," *Nano Lett.* **15**, 5033–5038 (2015).
4. A. Chernikov, C. Ruppert, H.M. Hill, A.F. Rigosi, T.F. Heinz, "Population inversion and giant bandgap renormalization in atomically thin WS₂ layers," *Nature Photon.* **9**, 466-470 (2015).
5. G. Jnawali, Y. Rao, J.H. Beck, N. Petrone, I. Kymissis, J. Hone, T.F. Heinz, "Observation of Ground- and Excited-State Charge Transfer at the C₆₀/Graphene Interface," *ACS Nano* **9**, 7175-7185 (2015).
6. O. Yaffe, A. Chernikov, Z. M. Norman, Y. Zhong, A. Velauthapillai, A. van der Zande, J. S. Owen, and T. F. Heinz, "Excitons in Ultrathin Organic-Inorganic Perovskite Crystals," *Phys. Rev. B* **92** 045414 (2015).
7. A. Chernikov, A. M. van der Zande, H. M. Hill, A. F. Rigosi, A. Velauthapillai, J. Hone, and T. F. Heinz, "Electrical Tuning of Exciton Binding Energies in Monolayer WS₂," *Phys. Rev. Lett.* **115**, 126802 (2015).

NLX: Nonlinear X-ray Science

David A. Reis*, Shambhu Ghimire

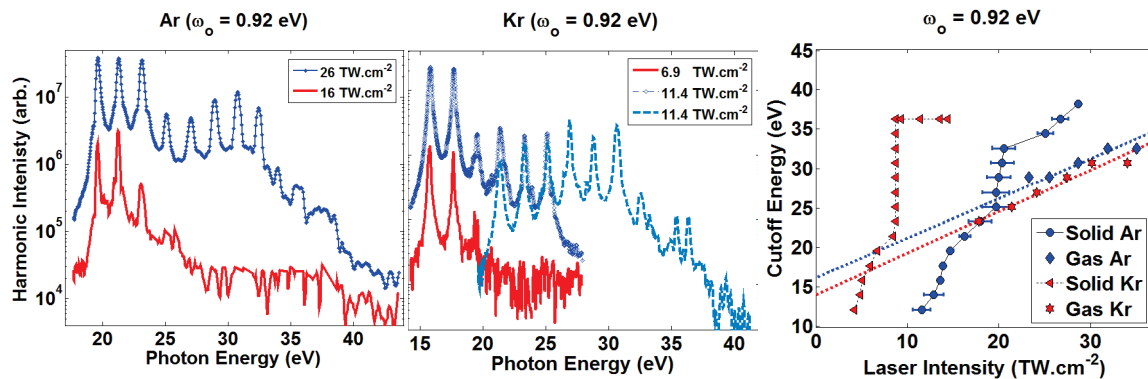
Stanford PULSE Institute
 SLAC National Accelerator Laboratory, MS 59
 2575 Sand Hill Rd.
 Menlo Park, CA 94025

[*dreis@slac.stanford.edu](mailto:dreis@slac.stanford.edu)

Program Scope:

In the NLX program, we are focused on the nonlinear optics of short-wavelength, ultrafast coherent radiation. We seek to understand strong-field and multi-photon interactions and exploit them to probe electronic structure at the atomic-scale in space and time. We are interested in fundamental interactions, with a primary focus on coherent non-sequential processes such as wave-mixing and two-photon Compton scattering using hard x rays. In the upcoming funding period, we propose experiments on x-ray and optical wave-mixing to image the strong-field-driven attosecond electronic dynamics responsible for solid-state high-harmonic generation. We will also explore the bound-state contribution to two-photon Compton scattering. The new scattering mechanism holds promise as a nonlinear photons-in/photon-out method of achieving simultaneous chemical specificity and atomic-scale structure in low Z materials. Our program is synergistic with other strong-field investigations in PULSE and makes use of the unprecedented intensities at hard x-ray wavelengths of LCLS and SACLA free-electron lasers. The results could have a profound impact on future light sources such as the LCLS-II.

Progress Report

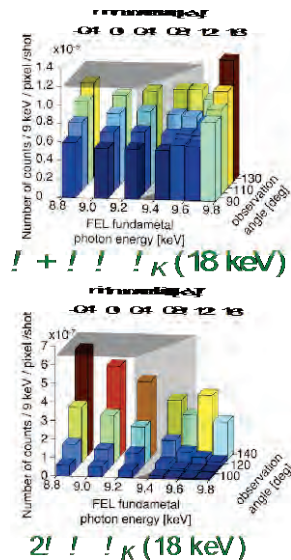


Following our discovery of nonperturbative high harmonics in solids, there has been much recent experimental and theoretical work trying to understand the physical mechanism and how it differs from typical gas phase harmonics. Under AMOS funding, we have studied HHG in rare gas solids as compared them directly to the dilute gas. Rare gas solids are a near ideal platform for studying the differences between gas and solid harmonics: they are weakly bound by van der Waals interactions and thus at some level they best approximate a dense atomic solid. Thickness dependent studies show that cascaded harmonic mixing can become important for crystals thicker than the coherence length of the third-harmonics, so the measurements need to be performed on thin films where propagation effects are measured to be negligible. Unlike the ZnO and other covalently bonded materials, the cutoff does not show a simple linear relationship with field. Notably, it exhibits a secondary plateau and a subsequent high-energy cut-off that extends well

beyond that of Ar gas (measured with the same apparatus). Qualitatively similar results are obtained for Kr, although the details appear to be material dependent. Also unlike the ZnO results, the ellipticity dependence is similar to the gas phase for both Ar and Kr. This suggests the importance of coherent single-site recombination. We have begun a collaboration with the theory group of Mette Gaarde and Ken Schafer to try and understand the role of multiple bands in the harmonic generation process. Preliminary results show that a four-band model can at least qualitatively give rise to the features seen in the rare gas solids.

We have also explored several fundamental nonlinear x-ray processes on the LCLS and SACLA x-ray free-electron lasers (FEL)s, most recently in the hard x-ray regime, including x-ray and optical wave-mixing, phase-matched x-ray second harmonic generation and anomalous nonlinear Compton scattering. In general, these experiments involve especially careful design to separate the signal from backgrounds, particularly in the scattering experiments where background from the undulator harmonics and parasitic scattering of the fundamental can easily overwhelm the signals.

Far from resonance, the linear x-ray matter interaction can be well approximated by the scattering off a collection of free-electrons. Before our experiments, the expectation was that the nonlinear scattering in this limit would also be well approximated by a free-electron-like nonlinearity for both the elastic and inelastic channels. Indeed we find that models that treat the solid as a collection of free-electrons are successful at describing both the x-ray second-harmonic generation and the (optically modulated) x-ray susceptibility in x-ray-optical sum frequency generation. However we found that in nonlinear two-photon Compton scattering, the free-electron model breaks down. We detected an anomaly in the scattered photon spectrum that suggests a new type of bound-state nonlinearity involving simultaneous scattering and photoionization. The scattering rate for producing high-energy photons varies quadratically with the FEL intensity as expected for a second-order perturbative process, follows a non-dipolar pattern, and produces a signal well above the measured background. However, the spectrum shows an anomalously large broadening and redshift as compared to both the free-electron theory and to the simultaneously measured linear scattering from the weak residual FEL second harmonic generated by the undulators. Our observations are incompatible with kinematics for the ground state electron distribution in the usual impulse approximation (IA). These anomalies are consistent with a novel nonlinear scattering mechanism involving bound-state electrons, despite an X-ray energy of approximately two orders of magnitude above the 1s binding energy.



18 keV photons from nonlinear Compton scattering of the 12 keV photons (top) and linear scattering from the FEL second harmonic background (bottom).

The next three years:

We will concentrate our efforts on two main areas. In the first focus area we will use x-ray-optical wave mixing to image the attosecond, subcycle motion of electrons within a single unit cell driven by a strong optical field. To achieve this, we will measure the dynamical x-ray structure factors corresponding to the high-order optical side-bands about several different reciprocal lattice vectors. We will use this unprecedented information, in combination with first-

principles calculations, to elucidate the microscopic mechanism behind high-harmonic generation in solids. In the second focus area, we will investigate more thoroughly the fundamental physics of two-photon Compton scattering. Here we have designed experiments that can separate hot plasma effects from the bound-state nonlinearity (awarded LCLS beamtime in February 2016). A consequence of the bound-state nonlinearity is that it is possible to phase-match in a single crystal. Here we have proposed an experiment (awarded SACLA beamtime also in February 2016) that should allow for its observation at a tunable red-shift (determined by geometry) and at intensities where the crystal is not damaged. Finally, we will explore the use of two-color Compton scattering as a simultaneous spectroscopic and structural tool.

References to publications of DOE sponsored research

2015

- [1] M. Fuchs, M. Trigo, J. Chen, S. Ghimire, S. Shwartz, M. Kozina, M. Jiang, T. Henighan, C. Bray, G. Ndabashimiye, P. H. Bucksbaum, Y. Feng, S. Herrmann, G. A. Carini, J. Pines, P. Hart, C. Kenney, S. Guillet, S. Boutet, G. J. Williams, M. Messerschmidt, M. M. Seibert, S. Moeller, J. B. Hastings, and D. A. Reis. Anomalous nonlinear x-ray Compton scattering. *Nat Phys*, advance online publication:–, 08 2015.
- [2] D. Reis. High harmonic generation in rare gas solids. *Bulletin of the American Physical Society*, 60, DAMOP, 2015.
- [3] M. Wu, S. Ghimire, D. A. Reis, K. J. Schafer, and M. B. Gaarde. High-harmonic generation from Bloch electrons in solids. *Physical Review A*, 91(4):043839, 2015.

2014

- [1] S. Ghimire, G. Ndabashimiye, A. D. DiChiara, E. Sistrunk, M. I. Stockman, P. Agostini, L. F. DiMauro, and D. A. Reis. Strong-field and attosecond physics in solids. *Journal of Physics B: Atomic, Molecular and Optical Physics*, 47(20):204030, 2014.
- [2] J. Goodfellow, M. Fuchs, D. Daranciang, S. Ghimire, F. Chen, H. Loos, D. A. Reis, A. S. Fisher, and A. M. Lindenberg. Below gap optical absorption in GaAs driven by intense, single-cycle coherent transition radiation. *Optics Express*, 22(14):17423–17429, 2014.
- [3] S. Shwartz, M. Fuchs, J. B. Hastings, Y. Inubushi, T. Ishikawa, T. Katayama, D. A. Reis, T. Sato, K. Tono, M. Yabashi, S. Yudovich, and S. E. Harris. X-ray second harmonic generation. *Phys. Rev. Lett.*, 112:163901, 2014.
- [4] G. Ndabashimiye, S. Ghimire, and D. Reis. High harmonic mixing in solid argon. *Bulletin of the American Physical Society*, 59, P5.00005 DAMOP, 2014.

2013

- [1] M. Trigo, M. Fuchs, J. Chen, M. P. Jiang, M. Cammarata, S. Fahy, D. M. Fritz, K. Gaffney, S. Ghimire, A. Higginbotham, S. L. Johnson, M. E. Kozina, J. Larsson, H. Lemke, A. M. Lindenberg, G. Ndabashimiye, F. Quirin, K. Sokolowski-Tinten, C. Uher, G. Wang, J. S. Wark, D. Zhu, and D. A. Reis. Fourier-transform inelastic x-ray scattering from time- and momentum-dependent phonon-phonon correlations. *Nat Phys*, 9(12):790–794, 12 2013. [Ghimire contribution]

- [2] S. Shwartz, M. Fuchs, J. B. Hastings, Y. Inubushi, D. A. Reis, M. Yabashi, and S. E. Harris. Second harmonic generation at x-ray wavelengths. In *Nonlinear Optics*. Optical Society of America, 2013.
- [3] A. D. DiChiara, S. Ghimire, D. A. Reis, L. F. DiMauro, and P. Agostini. Strong-field and attosecond physics with mid-infrared lasers. In *Attosecond Physics*, pages 81–98. Springer, 2013.
- [4] G. Ndabashimiye, S. Ghimire, D. Reis, and D. Nicholson. Measurement of coherence lengths of below threshold harmonics in solid argon. In *CLEO: 2013*, page QW1A.7. Optical Society of America, 2013.
- [5] T. Glover, D. Fritz, M. Cammarata, T. Allison, S. Coh, J. Feldkamp, H. Lemke, D. Zhu, Y. Feng, R. Coffee, M. Fuchs, S. Ghimire, J. Chen, S. Shwartz, D. Reis, S. Harris, and J. Hastings. X-ray / optical sum frequency generation. In *2013 Conference on Lasers and Electro-Optics (CLEO 2013)*.

NPI: Non-Periodic Imaging

Claudiu A. Stan, Raymond G. Sierra, Hasan Demirci, E. Han Dao
 Stanford PULSE Institute for Ultrafast Energy Science
 SLAC National Accelerator Laboratory, Menlo Park, CA 94025
 Email: cstan@slac.stanford.edu

PROGRAM SCOPE

The main goal of the Non-Periodic Imaging Task of the Ultrafast Chemical Science field work proposal is the determination of the dynamics and structure of matter that cannot be investigated with standard atomic-resolution techniques—disordered and biological systems, and materials undergoing fast structural transformations—taking advantage of the brilliance, time resolution, and coherence of X-ray free-electron laser (XFEL) light sources such as the Linac Coherent Light Source (LCLS) at SLAC. To realize the full potential of XFELs for these tasks, it is critical (i) to identify important scientific systems and processes that can be investigated with X-ray lasers, and (ii) to develop a range of new techniques that are necessary for these experiments. The NPI group works in both areas, supporting DOE's mission of understanding and controlling matter through in-house science and the development of techniques useful to the XFEL user community.

Our recent work focuses on developing femtosecond X-ray scattering methods at LCLS to investigate two classes of phenomena whose atomic-scale dynamics are invisible to other scattering methods: the structure and phase transitions of water, and structural changes in biological macromolecules. The work on phase transitions used hard X-ray scattering to investigate the nonequilibrium solidification of ice from supercooled water, and the vaporization of liquid water under tension (*i.e.*, at negative pressures). For these studies we developed multiscale and multiscale probing techniques at LCLS, in which we either probed the system simultaneously at a molecular scale with hard X-rays and at micron scale with optical imaging (freezing studies), or we used XFEL pump and probe methods to initiate the phase transition (vaporization studies). Our XFEL-based pumping methods are based on the application of pressure pulses generated by the XFEL radiation, which we couple with XFEL probing at nanosecond delays using a new mode of operation at LCLS. Our recent experimental work using XFEL pump and probe investigated an amorphous system (liquid water), and we are planning to extend the method of XFEL pressure-based pumping to induce and study fast structural changes in biomolecules, either dispersed in solution, or assembled in microcrystals.

This program's near-term goals include analysis of data collected in recent experiments to determine the structure of ice formed during nonequilibrium solidification and the structure of liquid water under tension, continuing the development of sample delivery and optical imaging systems at LCLS, and solving time-resolved protein structures at atomic resolution using serial femtosecond crystallography.

RECENT PROGRESS

Our group's activities focused on analysis and modeling of XFEL-induced explosions, developing sample delivery techniques, and running experiments at SLAC's Linac Coherent Light Source (LCLS). In FY 14–15 we led 2 LCLS full beamtimes and 2 protein screening beamtimes, and had major contributions in 5 other LCLS beamtimes and in-house experiments. The section below describes work performed during FY 15 in which our lab had a leading role.

Modeling the dynamics of XFEL-induced explosions for high-repetition rate XFELs. The absorption of XFEL pulses in the micron-sized drops and jets that are used to deliver samples leads to sequence of energy deposition and release phenomena with timescales ranging from femtosecond X-ray absorption to long-lived, microsecond flows of liquid and vapor that affect the delivery of samples. We recorded the damage phenomena occurring on nanosecond to microsecond time scales using time-resolved imaging. Explosions in jets create large gaps that are refilled by fresh liquid only after microseconds after the XFEL pulse, and also generate shock waves that may damage the samples. Explosions of single drops displace neighboring drops when samples are delivered as a train of drops, impairing the synchronization of drops with XFEL pulses. This explosion dynamics can already affect LCLS experiments that use slow jets, and their impact on experiments is expected to be more severe in experiments at future high-repetition rate XFELs such as LCLS-II.

We modeled the hydrodynamic effects of explosions that can affect the delivery of samples, on the timescales that are relevant to experiments at high-repetition-rate XFELs. These models predict the pressures, velocities, and liquid displacements that characterize XFEL-induced explosions in jets and drops. For example, Fig. 1 shows how the experimentally measured gap growth curves are characterized by the same scaling on the jet diameter for up to hundreds of nanoseconds after the pulse, and can thus be predicted. This data set includes both jets of pure water and jets containing microcrystals, showing that our models can be applied to actual serial femtosecond crystallography experiments. According to our models, the jets and the trains of drops compatible with high-repetition-rate XFELs must flow at high velocities (~ 100 m/s) and have sizes bounded by threshold values given by the properties of the liquid and the parameters of the XFEL pulse. Our measurements also indicate that samples delivered with jets may be affected by shock waves generated in the explosions.

Determination of the structural dynamics of ice formed during non-equilibrium solidification. The solidification of liquids in nature is predominantly a nonequilibrium process. Environmentally and technologically important cases of solidification occur far from equilibrium starting from a deeply supercooled liquid, such as the freezing of water in clouds or the production of metal shapes by casting. Under these conditions, metastable solids may form, but the structural dynamics of these metastable intermediates cannot be investigated with standard X-ray probing techniques due to their short lifetimes and to the stochasticity of nucleation.

We have probed, using single-shot X-ray diffraction at LCLS, the freezing of supercooled water drops, during the first ~ 1 ms after the nucleation of ice. To identify the rare cases (hit rates on the order of 10^{-4}) in which the drops froze just before the XFEL probe, we simultaneously recorded high-resolution optical images of the drops. (The micron-scale morphology of the freezing drops evolves through several characteristic stages on a submillisecond timescale, providing a measure of the time elapsed after the nucleation of ice.) We found that during the first millisecond after freezing, the ice is metastable. The dominant deviation from equilibrium is not a different crystalline structure, but imperfections in the stable hexagonal structure of ice, characterized by small crystallite sizes and large strains. We have also observed that this metastable ice anneals on a microsecond to millisecond timescale, evolving to larger and less strained grains. These are the first time-resolved structural investigations of the evolution of metastability in rapidly solidified materials on microsecond timescales, and show that the transformation from a liquid to a solid state can involve a rich sequence of structural transformations at both the molecular and the mesoscopic scales.

Producing and investigating liquid water under tension at LCLS. We observed that XFEL-induced explosions in drops of water lead to the generation of shock waves and of a dilatational motion the liquid. After the shock wave passes through the drop, the dilatational motion continues, stretching the liquid, which is thus subjected to negative pressures and eventually ruptures. We investigated this process using time-resolved imaging, for a range of conditions including different XFEL pulse energies, X-ray photon energy, drop sizes, and drop temperatures. Compared to other methods that have been used to produce liquids at negative pressures, XFEL explosions represent an extreme case of dynamic decompression, in which stretching forces comparable to those that would break

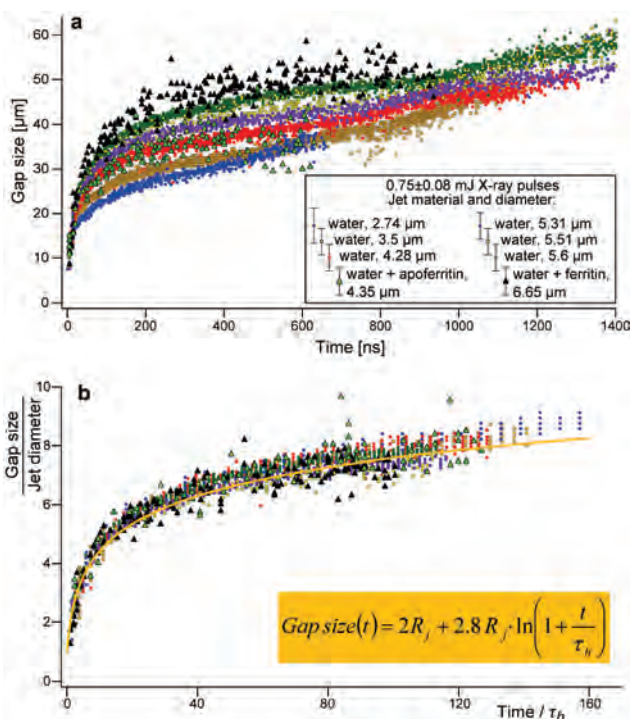


Fig. 1. a) XFEL pulses generate explosions in liquid jets carrying samples, creating gaps which must be filled by the jets before the next XFEL pulse. The growth of the gap has a multistage dynamics which depends on the jet diameter. b) The early stage of gap dynamics can be modeled with a simple logarithmic function of the jet diameter and of a characteristic timescale that depends on the properties of the jet and of the XFEL pulse. All experimental data can be collapsed to a master curve, which can be used to predict the time that elapses before the jet returns to the interaction region, and to design jets for new XFEL facilities.

intermolecular forces are applied on nanosecond timescales. The preliminary analysis of explosion dynamics from optical images indicates that we generated negative pressures that exceed those achieved previously.

Two other unique features of the XFEL-induced dynamic decompression of liquid drops are the absence of a container, and the formation of gradients in density and pressure that lead to a well-defined and narrow region at which the rupture of water occurs. Both of these features open the way to probe far-from-equilibrium stretched water and its transition to a vapor phase with spectroscopic and scattering techniques, including XFEL probing. We used a two-pulse, two-color mode of operation of LCLS to probe the molecular structure of decompressing drops via X-ray scattering. Employing, for the first time in a LCLS user experiment, two XFEL pulses with nanosecond separation and different photon energies, we induced explosions with the first pulse and we recorded the small-angle and wide-angle scattering signal generated by the second pulse. The XFEL probe passed through the exploding drop while it was still liquid, but stretched to negative pressures. The scattering patterns are significantly different from those characteristic of water at ambient or high pressures, and are consistent with a dilation of water while also indicating a possible residual heating caused by the passage of shock waves.

Sample delivery and preparation for serial femtosecond crystallography at LCLS. We developed an electrospun jet that delivers an additional liquid coating around a core jet carrying the samples. This liquid coat protects the sample from drying and freezing, and enabled the study of new samples at LCLS through serial femtosecond crystallography. We used this jet to deliver crystals of ribosome-antibiotic complexes grown in our lab in a protein crystal screening beamtime at LCLS, and we determined the molecular structure of these complexes at ambient temperature. The ambient-temperature structure has significant differences from the same structure determined at a synchrotron under cryogenic conditions, suggesting that cryogenic crystallography of complex biomolecules may not reveal certain details of their structure and dynamics. We have also participated in a CXI in-house commissioning beamtime for a new chamber for tandem SFX studies, providing dual electrospun injectors and synthesizing protein crystal samples for Se phasing.

FUTURE PLANS

Data analysis for the LCLS data on metastable water and its phase transitions. Our two recent beamtimes produced both X-ray scattering data and auxiliary optical imaging data. We plan to approach the analysis of X-ray diffraction on metastable ice in two stages, starting with the generation of virtual powder patterns to quantify the average proportions of stable and metastable crystalline phases of ice, and then continuing with the analysis of single-shot patterns to determine crystal sizes, strains, and shapes. For water under tension, we plan to determine its structure factor from X-ray scattering patterns. In parallel with the analysis of X-ray scattering data, we plan to analyze optical images to determine (i) the relation between images of freezing drops and the time elapsed from nucleation, and (ii) the detailed hydrodynamics of the rupture process. Additional work will be directed at refining (i) the evaporation models that give us the temperature of water drops in vacuum, and (ii) our hydrodynamic model of dynamic decompression, to provide an independent measure of the negative pressure in water when it was probed.

Determining the structural properties of double metastable water. We have submitted an LCLS proposal to produce water which is simultaneously supercooled and at negative pressure. Among the metastable phases of water, this doubly metastable regime is the least explored, and was not accessible to X-ray probing techniques. Using XFEL pump and probe techniques, we plan to determine the structure and phase transition dynamics in doubly metastable water. This direction of research could lead unique applications of XFELs in investigating transient and very far from equilibrium states of condensed matter that are not accessible experimentally at the present time.

New methods for imaging biomolecular dynamics in LCLS experiments. Pressure is a thermodynamic variable that can be used to induce fast changes, including structural changes in biomolecules. To study protein folding on fast time scales, pressure cells are used at synchrotrons to initiate the folding with an accuracy of hundreds of microseconds. We have submitted an LCLS proposal to extend the pressure jump technique of studying protein folding on nanosecond time scales, by using XFEL-induced shock waves.

COLLABORATIONS: This work was done with colleagues from SLAC, LCLS, Stanford, LBNL, the Paul Scherrer Institute, the Max Planck Institute, Arizona State University, UCLA, Brown University, and others.

PUBLICATIONS WHICH NPI WAS PRIMARY AUTHOR

- Bogan, M. J. (2013). "X-ray Free Electron Lasers Motivate Bioanalytical Characterization of Protein Nanocrystals: Serial Femtosecond Crystallography.", *Anal. Chem.* **85**, 3464.
- Dao, E. H. , *et al.* (2015). "Goniometer-based femtosecond X-ray diffraction of mutant 30S ribosomal subunit crystals.", *Struct. Dyn.* **2**, 041706.
- Demirci, H., *et al.* (2013). "Serial femtosecond X-ray diffraction of 30S ribosomal subunit microcrystals in liquid suspension at ambient temperature using an X-ray free-electron laser." *Acta Crystallog.* **F69**, 1066.
- Laksmono, H., *et al.* (2015). "Anomalous behavior of the homogeneous ice nucleation rate in "No-man's land." ", *J. Phys. Chem. Lett.* **6**, 2826.
- Loh, N. D., *et al.* (2013). "Sensing the wavefront of x-ray free-electron lasers using aerosol spheres." *Opt. Express* **21**, 12385.
- Pedersoli, E., *et al.* (2013) "Mesoscale morphology of airborne core-shell nanoparticle clusters: x-ray laser coherent diffraction imaging." *J. Phys. B At. Mol. Opt. Phys.* **46**, 164033.
- Sierra, R. G., *et al.* (2012). "Nanoflow electrospinning serial femtosecond crystallography." *Acta Crystallog.* **D68**, 1584.
- Starodub, D., *et al.* (2012). "Single-particle structure determination by correlations of snapshot X-ray diffraction patterns" *Nat. Commun.* **3**, 1276.

PUBLICATIONS IN WHICH NPI WAS A COLLABORATOR

- Alonso-Mori, R., *et al.* (2012). "Energy-dispersive X-ray emission spectroscopy using an X-ray free-electron laser in a shot-by-shot mode." *Proc. Natl. Acad. Sci. USA* **109**, 19103.
- Deckert, F.-J., *et al.* (2015). "Two bunches with ns-separation with LCLS." *Proceedings of the 2015 Free Electron Laser Conference, Daejeon Korea, in press.*
- Hattne, J., *et al.* (2014). "Accurate macromolecular structures using minimal measurements from X-ray free-electron lasers." *Nat. Methods* **11**, 545.
- Johansson, L. C., *et al.* (2013). "Structure of a photosynthetic reaction centre determined by serial femtosecond crystallography." *Nat. Commun.* **4**, 3911.
- Kern, J., *et al.* (2013). "Simultaneous Femtosecond X-ray Spectroscopy and Diffraction of Photosystem II at Room Temperature." *Science* **340**, 491.
- Kern, J., *et al.* (2014). "Methods development for diffraction and spectroscopy studies of metalloenzymes at X-ray free-electron lasers." *Phil. Trans. R. Soc. B* **369**, 20130590
- Kern, J., *et al.* (2014). "Taking snapshots of photosynthetic water oxidation using femtosecond X-ray diffraction and spectroscopy." *Nat. Comm.* **5**, 4371.
- Kupitz, C., *et al.* (2014). "Serial time-resolved crystallography of photosystem II using a femtosecond X-ray laser.", *Nature* **513**, 261.
- Mitzner, R., *et al.* (2013). "L-Edge X-ray Absorption Spectroscopy of Dilute Systems Relevant to Metalloproteins Using an X-ray Free-Electron Laser.", *J. Phys. Chem. Lett.* **4**, 3641.
- Park, H. J., *et al.* (2013). "Toward unsupervised single-shot diffractive imaging of heterogeneous particles using X-ray free-electron lasers." *Opt. Express* **21**, 28729.
- Redecke, L., *et al.* (2013). "Natively Inhibited Trypanosoma brucei Cathepsin B Structure Determined by Using an X-ray Laser." *Science* **339**, 227.
- Schreck, S., *et al.* (2014). "Reabsorption of Soft X-Ray Emission at High X-Ray Free-Electron Laser Fluences." *Phys. Rev. Lett.* **113**, 153002.
- Sellberg, J. A., *et al.* (2014). "Ultrafast X-ray probing of water structure below the homogenous ice nucleation temperature" *Nature*, **510**, 381.
- Sellberg, J. A., *et al.* (2014) "X-ray Emission Spectroscopy of Bulk Liquid Water in 'No-man's Land", *J. Chem. Phys.* **142**, 044505.

SFA: Strong-field laser matter interactions

PI: P. Bucksbaum; Research Associate: Adi Natan; Staff Scientist: Ryan Coffee; Graduate Students: Matthew Ware, Lucas Zipp, Andrei Kamalov

PULSE Ultrafast Chemical Science Program, SLAC National Accelerator Laboratory, Menlo Park, CA 94025. Email: phb@slac.stanford.edu

Program Scope: The SFA task investigates *strong field interactions* in small molecules and atoms. We have recently developed two-color velocity map imaging methods that allow us to probe dynamics of strong field and multiphoton ionization and have observed several new ultrafast phenomena from sub-picosecond quantum beats to photoelectron delays of a tens of attoseconds.

Recent Progress and Future Work:

Angle-Resolved Attosecond dynamics in strong field ionization: Attosecond delay measurements utilizing interference of an infrared (IR) reference with short ionizing pulses of extreme ultraviolet (XUV) radiation have attracted considerable attention recently. This measurement technique allows the observation of ultrafast dynamics during photoionization. We have now extended these methods to ATI in the strong field regime by measuring the relative phase of different momentum components of the ATI spectra using a weak probe at *twice* the fundamental ionization field frequency. By analyzing each photoelectron momentum component we are able to observe different momentum distributions for different ionization mechanisms present in harmonics of the fundamental ionization field. This opens the way to deconvolve different strong field ionization mechanisms that overlap in momentum space. For example, we observe that the signal amplitude from the Fourier components that were at the second harmonic of the weak probe is more spherically symmetric (Fig 1b) than for the fundamental frequency (Fig 1a). This indicates that this filter captures ionization from rescattering processes. Analyzing the phase component of these Fourier coefficient (Fig 1c-d) shows that there is a $\pi/2$ phase delay for population that ionizes in the polarization direction of the laser, supporting the picture of direct vs rescattering times in the optical cycle. **Future work:** we will expand these observations and build a theoretical framework to understand and simulate the nature of the distributions and delays for different Fourier components and how their angular and phase signature can be used in order to isolate various mechanisms of ionization.

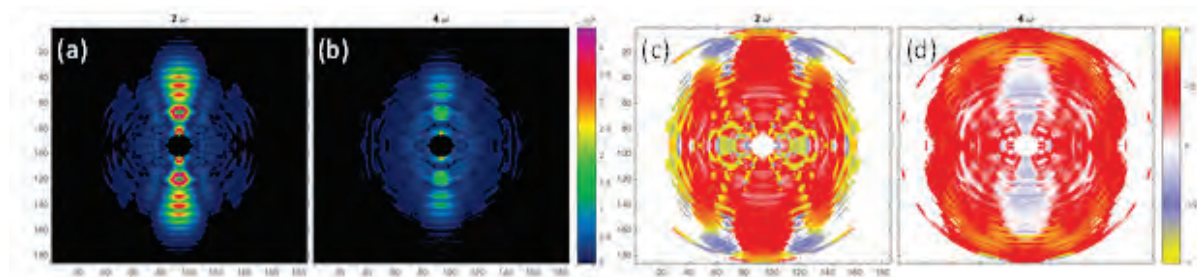


Fig 1. Amplitudes of the 2D momentum maps of photoelectrons emitted from strong field ionization of Argon (10^{14} W/cm²) filtered by the (a) first and (b) second Fourier components as a result of a weak second field at twice the frequency. The phases of these components (c) and (d) show shifts of $\pi/2$ in the main ionization direction.

Attosecond delays through transient resonances in above threshold ionization: Building upon previous work in our group measuring delays in above-threshold ionization (ATI), we have measured the attosecond delays as electrons are ionized through transient ac-Stark shifted Rydberg states in a strong field. This extends previous work performed by Swoboda et al. that measured the phase shift occurring during resonant two photon ionization in a weak XUV field. Our technique uses a weak probe field at half

the frequency of the strong laser field to create sidebands in the ATI spectrum which interfere adjacent ATI pathways. This enables us to probe the intrinsic phase accumulated by the electron during above-threshold ionization with a relative precision of a few attoseconds in the corresponding time domain. We find that electrons ionized through these resonances exhibit large phase shifts (~ 1 rad), for peaks that are closely spaced in energy (< 0.2 eV). This could be indicative of large Coulomb phase shifts due to low energy continuum transitions near the ionization threshold, providing a sensitive measure of the time-dependent atomic core potential in a strong laser field.

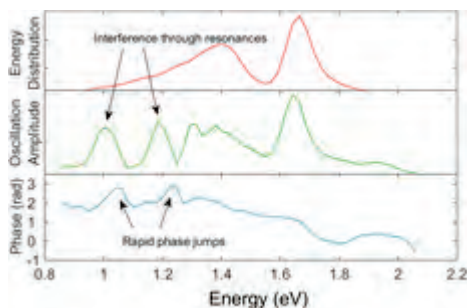


Fig 2. ATI spectrum of Ar in a 400nm field of $\sim 10^{14}$ W/cm 2 , with an 800nm probe field at 1% intensity. (top) the energy distribution angle-integrated over a half plane in the direction of the laser polarization, and averaged over all optical delays. (middle) The amplitude and (bottom) The “phase jumps” in the measured oscillations which occur near resonances.

Angle Resolved Attosecond dynamics in multiphoton ionization Following our recent study regarding attosecond delays between adjacent ATI peaks in the multiphoton regime using multi-path interference of adjacent ATI peaks by a weak probe field at *half* the frequency we have observed large attosecond delays between main ATI peaks. We now have evidence that these shifts are due to contributions of different partial waves at final momentum states that contribute different delays at specific angles. The delays that were previously measured for a specific ATI peaks are averages of these partial waves over all angles. **Future work:** In the future we will apply this technique to cold molecular samples, to explore angle resolved attosecond delays that arise from molecular degrees of freedom. For example, we expect to detect an asymmetry in the ionization delay from CO depending due to the asymmetry of the HOMO structure.

Very low energy structure in Argon: Recollision of an electron with its parent ion under a linearly polarized strong laser field has been shown to be the basis of phenomena in atoms and molecules. Using the 3-step model this process can be described by a single degree of freedom along the laser polarization axis. The bound electron is released, then it accelerates and is driven back to the ion. It can then either recombine and create HHG or scatter and induce high-energy above-threshold ionization (ATI). Recently, an unexpected “low-energy structure” (LES) was observed in the photoelectron spectrum of atoms in strong infrared (a few μm wavelength) laser pulses, and discussed in a semiclassical approach. It has eluded observation in previous experiments and theoretical studies at 800 nm wavelength. We have found very low energy structures (< 0.1 eV) that are due to longer-lived doubly-excited Argon atoms (Fig 3) trapped during strong field ionization. We observed narrow (< 5 meV) resonances at energies below 0.1 eV when a strong laser ionizes Argon atoms. These rings width makes them much longer lived than the driving field. **Future work:** We plan to investigate the mechanism by which these states are created.

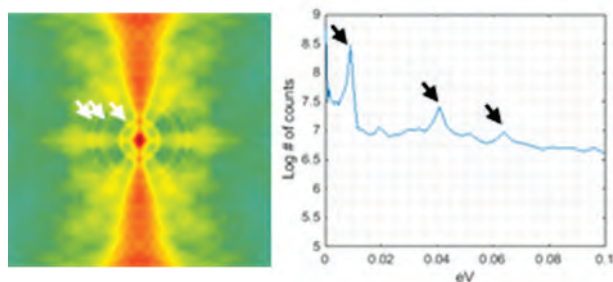


Fig. 3 Raw momentum map of strong field ionization of Argon atoms at 800nm with $\sim 10^{14}$ W/cm 2 . Zooming into very low energies reveal distinct narrow ring structures, which have energies consistent with Rydberg states correlated with the $P_{1/2}$ cation core.

Quantum Beats in Molecular Rydberg States: We observe angular beating in the photoelectron angular distribution resulting from single photon ionization of a superposition of Rydberg states in molecular nitrogen. The wave packet is prepared with an intense 400nm pulse which sweeps several Rydberg states into resonance due to intensity-dependent ac-Stark shifts. Although a large portion of the population in these Rydberg states is ionized during the pulse, some population survives and can be probed at a later time. The resulting photoelectron angular distribution (PAD) shows a distinct beating with a period of ~650 fs. Preliminary analysis suggests that it arises from a superposition of $5f\sigma$ and $4f\pi$ molecular Rydberg states accompanied by a predissociative decay of one of the states. The influence of the rotating core on these Rydberg states is of particular interest, since they approach a regime of “L-uncoupling”, where the projection of the electronic angular orbital momentum onto the internuclear axis is no longer a good quantum number. **Future Work:** We will probe these L-uncoupling effects by altering the angle between the polarizations of the pump and probe pulses and also the initial rotational temperature, in order to disentangle the effects of the molecular frame alignment on the electron angular distribution in the lab frame, in this L-uncoupling regime.

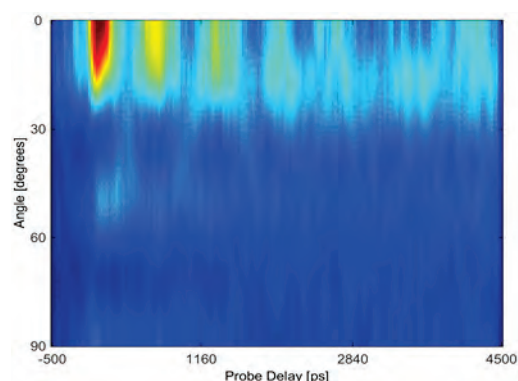


Fig 4. Photoelectron angular distribution from single photon ionization of a superposition of the $5f$ and $4f$ states in N_2 as a function of pump-probe delay. The beating in the angular distribution can be seen near zero degrees (along the polarization direction).

References:

- Berrah, N. and P. H. Bucksbaum (2013). *Scientific American* **310**(1): 64-71.
- Bostedt, C., J. Bozek, P. Bucksbaum, R. Coffee, J. Hastings, Z. Huang, R. Lee, S. Schorb, J. Corlett and P. Denes (2013). *Journal of Physics B: Atomic, Molecular and Optical Physics* **46**(16): 164003.
- Bucksbaum, P. (2012). "Atomic and molecular physics at the LCLS x-ray laser." *Mexican Optics and Photonics Meeting*.
- Bucksbaum, P. (2014). "Molecular dissociation dynamics driven by strong-field multiple ionization." *Bulletin of the American Physical Society* **59**.
- Bucksbaum, P. H., and Glowonia, J. M. (2013). "Ultrafast AMO physics at the LCLS x-ray FEL.", EPJ Web of Conferences (Vol. 57, p. 04001). EDP Sciences.
- Bucksbaum, P., T. Möller and K. Ueda (2012). *Journal of Physics B: Atomic, Molecular and Optical Physics* **45**(16): 160101.
- Bucksbaum, P. H. (2011). "Observing Structure and Motion in Molecules with Ultrafast Strong Field and Short Wavelength Laser Radiation". ANL (Argonne National Laboratory (ANL), Argonne, IL (United States)).
- Bucksbaum, P. H. (2013). *Ultrafast nonlinear optics*, Springer: 105-128.
- Bucksbaum, P. H., R. Coffee and N. Berrah (2011). *Advances in Atomic Molecular and Optical Physics* **60**: 239-289.
- Cryan, J., J. Glowonia, J. Andreasson, A. Belkacem, N. Berrah, C. Blaga, C. Bostedt, J. Bozek, N. Cherepkov and L. DiMauro (2012). *Journal of Physics B: Atomic, Molecular and Optical Physics* **45**(5): 055601.
- Cryan, J., Glowonia, J., Cherepkov, N. A., Bucksbaum, P. H., & Coffee, R. N. (2011, June). Angular Dependence of Auger electrons from N_2 . In APS Division of Atomic, Molecular and Optical Physics Meeting Abstracts (Vol. 1, p. L1144).
- Cryan, J. P., J. M. Glowonia, D. W. Broege, Y. Ma and P. H. Bucksbaum (2011). *Physical Review X* **1**(1): 011002.
- Doumy, G., C. Roedig, S.-K. Son, C. I. Blaga, A. DiChiara, R. Santra, N. Berrah, C. Bostedt, J. Bozek and P. Bucksbaum (2011). *Physical Review Letters* **106**(8): 083002.

14. Fang, L., T. Osipov, B. Murphy, A. Rudenko, D. Rolles, V. Petrovic, C. Bostedt, J. Bozek, P. Bucksbaum and N. Berrah (2014). *Journal of Physics B: Atomic, Molecular and Optical Physics* **47**(12): 124006.
15. Fang, L., T. Osipov, B. Murphy, F. Tarantelli, E. Kukk, J. Cryan, M. Glownia, P. Bucksbaum, R. Coffee and M. Chen (2012). *Physical Review Letters* **109**(26): 263001.
16. Farrell, J., et al (2012). “Ultrafast X-ray probe of nucleobase photoprotection.” Quantum Electronics and Laser Science Conference (pp. QW1F-4). Optical Society of America.
17. Fung, R., J. Glownia, J. Cryan, A. Natan, P. Bucksbaum and A. Ourmazd (2012). *Signal* **1**: i2.
18. Glownia, J. M., Ourmazd, A., Fung, R., Cryan, J., Natan, A., Coffee, R., & Bucksbaum, P. (2012). “Sub-cycle strong-field influences in x-ray photoionization”, Quantum Electronics and Laser Science Conference (pp. QW1F-3). Optical Society of America.
19. Kanter, E., B. Krässig, Y. Li, A. March, P. Ho, N. Rohringer, R. Santra, S. Southworth, L. DiMauro and G. Doumy (2011). *Physical Review Letters* **107**(23): 233001.
20. Li, H., Chen, L. J., Cheng, H. P. H., May, J. E., Smith, S., Muehlig, K., A. Uttamadoss, J. C. Frisch, A. R. Fry, F. X. Kärtner, and Bucksbaum, P. H. (2014). *Optics letters*, **39**(18), 5325-5328.
21. McFarland, B., et al (2014). *Journal of Physics: Conference Series* **488**: 012015.
22. McFarland B., et al (2013). *EPJ Web of Conferences* **41**, 07004 (2013) **41**: 07004.
23. McFarland, B., et al. (2012). “Ultrafast nucleobase photoprotection probed by soft x-rays.”, Laser Science (pp. LTu2H-1). Optical Society of America.
24. Natan, A., Ware, M. R., & Bucksbaum, P. H. (2014). “Experimental Evidence of Light Induced Conical Intersections in Dissociation of Diatomic Molecules.” International Conference on Ultrafast Phenomena (pp. 09-Wed). Optical Society of America.
25. Natan, A., Ware, M. R., & Bucksbaum, P. H. (2014). “Experimental Observation of Light Induced Conical Intersections in a Diatomic Molecule.”, CLEO: QELS_Fundamental Science (pp. FTu1D-2). Optical Society of America.
26. Natan, A., Ware, M. R., and Bucksbaum, P. H. (2015). “Experimental Signature of Light Induced Conical Intersections in Diatomics.”, Ultrafast Phenomena XIX (pp. 122-125). Springer International Publishing.
27. Natan, A. L. Zipp and P. H. Bucksbaum (2015). “Angle Resolved Photoelectron Phase Shifts in Above Threshold Ionization”, *Frontiers in Optics* (FTh4A.4), Optical Society of America.
28. Petrovic, V. S., S. Schorb, J. Kim, J. White, J. P. Cryan, J. M. Glownia, L. Zipp, D. Broege, S. Miyabe and H. Tao (2012) *arXiv preprint arXiv:1212.3728*.
29. Petrovic, V. S., S. Schorb, J. Kim, J. White, J. P. Cryan, J. M. Glownia, L. Zipp, D. Broege, S. Miyabe and H. Tao (2013). *The Journal of chemical physics* **139**(18): 184309.
30. Petrović, V. S., M. Siano, J. L. White, N. Berrah, C. Bostedt, J. D. Bozek, D. Broege, M. Chalfin, R. N. Coffee and J. Cryan (2012). *Physical Review Letters* **108**(25): 253006.
31. Roedig, C., G. Doumy, S.-K. Son, C. Blaga, A. DiChiara, R. Santra, N. Berrah, C. Bosteadt, J. Bozek and P. H. Bucksbaum (2011). *Laser Science*, Optical Society of America.
32. Zipp, L., A. Natan and P. H. Bucksbaum (2014). *Optica*, **1**, 361-364 (2014)
33. Zipp, L., Natan, A., & Bucksbaum, P. H. (2014). “Two Color Interferences and Quantum Phase Shifts in Above Threshold Ionization.” CLEO: QELS_Fundamental Science (pp. FTu1D-3). Optical Society of America.
34. Zipp, L., A. Natan and P. Bucksbaum (2014). “Quantum Phase Measurements in Two Color Above Threshold Ionization”, *Bulletin of the American Physical Society* **59**.
35. Zipp, L., A. Natan and P. Bucksbaum (2015). “Excited State Molecular Dynamics in Intense Laser Fields”, *Bulletin of the American Physical Society* **60**.

Solution Phase Chemical Dynamics, Kelly Gaffney PI

SLAC National Accelerator Laboratory, 2575 Sand Hill Rd MS 59, Menlo Park, CA 94025

Email: kgaffney@slac.stanford.edu

Program Scope: Electronic excited state phenomena provide a compelling intersection of fundamental and applied research interests in inorganic chemistry. Harnessing the strong optical absorption and photocatalytic activity of compounds depends on our ability to control fundamental physical and chemical phenomena associated with the non-adiabatic dynamics of electronic excited states. The central events of excited state chemistry can all critically influence the dynamics of electronic excited states, including internal conversion and intersystem crossing events governed by non-adiabatic interactions between electronic states in close proximity to conical intersections, as well as solvation and electron transfer. (Chergui 2012)

The research opportunities enabled by LCLS direct both the scientific and technical focus of the Solution Phase Chemistry (SPC) sub-task. Scientifically, this sub-task focuses on two critical aspects of electronic excited state dynamics emphasizing the fundamental understanding of phenomena relevant to solar energy applications:

- (1) We use ultrafast time resolution measurements, simple ligand exchange reactions, and simulation to understand the molecular properties that control excited state relaxation dynamics in coordination compounds.
- (2) We use photo-excitation to change the electronic structure and reactivity of inorganic complexes and track site specific changes in metal solvation and coordination dynamics with ultrafast time-resolved measurements and molecular simulation.

Technically, the SPC sub-task focuses on developing and exploiting femtosecond resolution x-ray scattering and spectroscopy methods and complementing them with established femtosecond resolution optical spectroscopy methods. We rely on collaboration for synthesis and simulation efforts beyond the routine.

Recent Progress and Future Plans

The presence of metal-centered excited states with varying spin and charge distributions significantly impact the excited state dynamics and chemical reactivity of transition metal complexes. The characterization of the coupled dynamics of charge, spin, and inner shell coordination geometry in transition metal complexes benefits greatly from the atomic specificity of x-ray spectroscopy. We have developed both soft x-ray resonant inelastic x-ray scattering (RIXS) and hard x-ray K β fluorescence spectroscopy to characterize these ultrafast changes in molecular electronic structure.

Excited State Charge Transfer in Coordination Chemistry

X-ray spectroscopy, particularly hard x-ray fluorescence and soft x-ray absorption spectroscopy for 3d transition metals, provide sensitive measures of the metal spin state. Ionization of the Fe 1s orbital with a hard x-ray photon above the Fe 1s ionization potential of 7,120 eV, leads to x-ray fluorescence. Fe K β fluorescence involves 3p filling of the 1s hole. The strong exchange interaction between the 3d electrons and the hole in the 3p level created by fluorescence makes the K β fluorescence spectrum sensitive to the 3d spin moment.

We have used K β fluorescence to study photo-induced spin crossover in poly-pyridal Fe(II) complexes. For these molecular systems, the spin dynamics prove to be of particular importance because of the interest in using spin crossover materials in light triggered data storage and iron based dyes as earth

abundant light harvesters in dye sensitized solar cells. In both cases the rate of photo-induced spin crossover proves critical, since this rate controls the switching time on the one hand and competes with charge injection on the other. Our initial studies of $[\text{Fe}(\text{2,2}'\text{-bipyridine})_3]^{2+}$, an archetypical spin crossover complex, has demonstrated the value of this experimental approach. The sensitivity of the $K\beta$ fluorescence spectra to the iron spin moment enables the spin crossover mechanism to be monitored. Based on these measurements, we have concluded that photo-induced spin crossover in $[\text{Fe}(\text{2,2}'\text{-bipyridine})_3]^{2+}$ occurs sequentially through a triplet (^3T) transient state. Our future work focuses on mechanistic understanding of the electronic states and nuclear coordinates involved in charge transfer state relaxation in metal complexes with the goal of understanding how to extend the lifetime from 0.1 ps to a nanosecond or beyond.

We have developed RIXS as a molecular-orbital specific probe of photochemistry and photocatalysis. RIXS, the x-ray analogue of resonance Raman, provides atom specific information about both unoccupied and occupied frontier orbitals. RIXS has been widely used to characterize the properties of the electronic ground state of materials. Recently, we demonstrated the power of RIXS for characterizing the electronic structure of excited states. We used femtosecond resolution Fe L_3 -edge RIXS to study the archetypical photodissociation of CO from $\text{Fe}(\text{CO})_5$ and the generation of the catalytically active $\text{Fe}(\text{CO})_4$. Our investigation demonstrated that singlet and triplet reaction channels proceed in parallel for $\text{Fe}(\text{CO})_4$. Prior studies have emphasized the significance of one channel versus another, but we have clearly demonstrated that both triplet and singlet forms of $\text{Fe}(\text{CO})_4$ occur with appreciable concentration on the sub-picosecond time scale. The ability to track the spin state of metal center excited states also provides the opportunity to investigate the role of spin in catalytic mechanisms.

Site-specific solvation and coordination dynamics in model photo-catalysts

Femtosecond resolution x-ray scattering provides a powerful means of measuring solvation dynamics that will enable the solute-solvent dynamics to be decomposed into site-specific contributions for the heavy atom scatters in the solute. This enables site-specific solvation to be characterized in inorganic chemistry where the metal centers in the complexes can be the strongest scattering centers and also sets the stage for using x-ray scattering to study photocatalysis since substrate bonding to the metal center represents an initial step in any photocatalytic cycle.

We have been using the photocatalyst, $[\text{Ir}_2(\text{dimen})_4]^{2+}$, where dimen = diisocyano-*p*-menthane, in acetonitrile as a model system for demonstrating the efficacy of diffuse x-ray scattering for investigating the dynamics of site-specific solvation. Our femtosecond resolution x-ray scattering measurements of excited state dynamics in $[\text{Ir}_2(\text{dimen})_4]^{2+}$ accentuate the advantages of x-ray scattering as a probe of structural dynamics. Two critical distinction between optical and x-ray scattering studies of dynamics need to be emphasized. Ultrafast optical measurements observe structural dynamics via the vibrational period and only provide a robust characterization of Franck-Condon active vibrational motions. X-ray scattering directly measures the anisotropic pair distribution function, so it does not rely on normal mode analysis to assign motion nor does it require the motion to be Franck-Condon active to be observable.

Our ultrafast x-ray scattering experiments have directly measured this time dependent Ir-Ir bond length, but more importantly they have characterized the delayed reorganization of the coordinating ligands and the dynamics of the acetonitrile-Ir interaction. Our current analysis, based on comparison of mixed quantum-classical simulations lead by the Klaus Møller research group, indicates that we have been seen the delayed twisting of the diisocyano-*p*-menthane ligands about the Ir-Ir bond following Ir-Ir bond contraction. In optical measurements this appeared as an exponential shift in the spectrum of the excited state stimulated emission, but

assignment of the structural origin of the dynamics could not be discerned from the measurement. The comparison of measurement and simulation also provides a compelling picture for the distinct solvation of the Ir atoms in the ground and excited states. Simulation shows that the methyl groups of the acetonitrile preferentially solvate the Ir atoms in the electronic ground state, while the N of the cyano group preferentially solvates the excited state. Furthermore, the comparison of simulated time dependent scattering and measurement shows the critical importance of site-specific solvation and significant deviation from linear response. The response of the solvent to the significant contraction in Ir-Ir bond length and change in charge distribution about the Ir atoms requires significant translational and reorientational motion outside the realm of linear response.

Publications Supported by AMOS Program

- Gaffney, K. J., M. B. Ji, M. Odellius, S. Park, et al. (2011). H-bond switching and ligand exchange dynamics in aqueous ionic solution. *Chem. Phys. Lett.* **504**: 1.
- Hartsock, R. W., W. K. Zhang, M. G. Hill, B. Sabat, et al. (2011). Characterizing the Deformational Isomers of Bimetallic $[\text{Ir}_2(\text{dimen})_4]^{2+}$ (dimen=1,8-diisocyanop-menthane) with Vibrational Wavepacket Dynamics. *J. Phys. Chem. A* **115**: 2920.
- Jha, S. K., M. B. Ji, K. J. Gaffney and S. G. Boxer (2011). Direct measurement of the protein response to an electrostatic perturbation that mimics the catalytic cycle in ketosteroid isomerase. *Proc. Natl. Acad. Sci. U. S. A.* **108**: 16612.
- Ji, M. B. and K. J. Gaffney (2011). Orientational relaxation dynamics in aqueous ionic solution: Polarization-selective two-dimensional infrared study of angular jump-exchange dynamics in aqueous 6M NaClO₄. *J. Chem. Phys.* **134**: 044516.
- Ji, M. B., R. W. Hartsock, Z. Sun and K. J. Gaffney (2011). Interdependence of Conformational and Chemical Reaction Dynamics during Ion Assembly in Polar Solvents *J. Phys. Chem. B* **115**: 11399.
- Chergui, M. (2012). On the interplay between charge, spin and structural dynamics in transition metal complexes. *Dalton Trans.* **41**: 13022.
- Jha, S. K., M. B. Ji, K. J. Gaffney and S. G. Boxer (2012). Site-Specific Measurement of Water Dynamics in the Substrate Pocket of Ketosteroid Isomerase Using Time-Resolved Vibrational Spectroscopy. *J. Phys. Chem. B* **116**: 11414.
- Ji, M. B., R. W. Hartsock, Z. Sun and K. J. Gaffney (2012). Influence of solute-solvent coordination on the orientational relaxation of ion assemblies in polar solvents. *J. Chem. Phys.* **136**: 014501.
- Kunnus, K., I. Rajkovic, S. Schreck, W. Quevedo, et al. (2012). A setup for resonant inelastic soft x-ray scattering on liquids at free electron laser light sources. *Rev. Sci. Instr.* **83**.
- Zhang, W. K., M. B. Ji, Z. Sun and K. J. Gaffney (2012). Dynamics of Solvent-Mediated Electron Localization in Electronically Excited Hexacyanoferrate(III). *J. Am. Chem. Soc.* **134**: 2581.
- Zhang, W. K., Z. G. Lan, Z. Sun and K. J. Gaffney (2012). Resolving Photo-Induced Twisted Intramolecular Charge Transfer with Vibrational Anisotropy and TDDFT. *J. Phys. Chem. B* **116**: 11527.
- Lemke, H. T., C. Bressler, L. X. Chen, D. M. Fritz, et al. (2013). Femtosecond X-ray Absorption Spectroscopy at a Hard X-ray Free Electron Laser: Application to Spin Crossover Dynamics. *J. Phys. Chem. A* **117**: 735.
- Sun, Z., W. K. Zhang, M. B. Ji, R. W. Hartsock, et al. (2013). Aqueous Mg^{2+} and Ca^{2+} Ligand Exchange Mechanisms Identified with 2DIR Spectroscopy. *J. Phys. Chem. B*: accepted.
- Sun, Z., W. K. Zhang, M. B. Ji, R. W. Hartsock, et al. (2013). Contact Ion Pair Formation between Hard Acids and Soft Bases in Aqueous Solutions Observed with 2DIR Spectroscopy. *J. Phys. Chem. B*: accepted.
- Trigo, M., M. Fuchs, J. Chen, M. P. Jiang, et al. (2013). Fourier-transform inelastic X-ray scattering from time- and momentum-dependent phonon-phonon correlations. *Nature Phys.* **9**: 790.
- McFarland, B. K., J. P. Farrell, S. Miyabe, F. Tarantelli, et al. (2014). Ultrafast X-ray Auger probing of photoexcited molecular dynamics. *Nature Comm.* **5**.
- Zhang, W. K., R. Alonso-Mori, U. Bergmann, C. Bressler, et al. (2014). Tracking Excited State Charge and Spin Dynamics in Iron Coordination Complexes *Nature* **509**: 345.
- Wernet, P., K. Kunnus, I. Josefsson, I. Rajkovic, et al. (2015). Orbital-specific mapping of the ligand exchange dynamics of $\text{Fe}(\text{CO})_5$ in solution. *Nature* **520**: 78.
- Zhang, W. K. and K. J. Gaffney (2015). Mechanistic Studies of Photoinduced Spin Crossover and Electron Transfer in Inorganic Complexes. *Acc. Chem. Res.* **48**: 1140.

Page is intentionally blank.

Ultrafast Theory and Simulation, Todd J. Martínez PI

SLAC National Accelerator Laboratory, 2575 Sand Hill Rd. MS 59, Menlo Park, CA 94025

Email: toddmtz@slac.stanford.edu

Program Scope: This program is focused on developing and applying new methods for describing molecular dynamics on electronically excited states, as well as the interaction of molecules with radiation fields. We continue to develop and apply the *ab initio* multiple spawning (AIMS) method that solves the electronic and nuclear Schrodinger equations simultaneously from first principles, including the treatment of cases where the Born-Oppenheimer approximation breaks down (e.g. around conical intersections where two or more electronic states are exactly degenerate). We are working to extend this methodology to incorporate the effects of novel pump and probe pulses using high energy photons, including those obtained from modern x-ray sources such as LCLS. We also focus on understanding the behavior of molecular excited states in paradigmatic phenomena such as light-induced isomerization, excited state proton transfer, and excitation energy transfer.

Recent Progress and Future Plans

Characterizing the space of conical intersections:

Conical intersections are not isolated points, but rather high-dimensional seams. This high dimensionality makes it difficult to map out the space of conical intersections and also to determine their connectivity (i.e. are two conical intersection geometries part of the same seam?). One way of characterizing high-dimensional surfaces is to locate stationary points on the surface, such as local minima that have been termed minimal energy conical intersections (MECIs). In many cases, the MECIs are not dynamically dominant (largely because of the strongly nonequilibrium nature of many excited state processes). Nevertheless, the MECIs serve as valuable “signposts” on the potential energy surfaces – hallmarks of areas in configuration space that might lead to efficient nonadiabatic transitions. Viewed in this light, one realizes that a key objective should be broader characterization of the set of molecular geometries that are part of the conical intersection space. Thus, we introduced a new method (Mori and Martinez 2013) – seam-space nudged elastic band or SS-NEB – that finds pathways that connect MECIs within the space of conical intersections. These are minimal energy paths and thus represent the lowest energy way to distort the molecule from one MECI to another while maintaining the electronic degeneracy. Using SS-NEB, we were able to show that all the known S_0/S_1 MECIs in ethylene are part of the same seam (see Figure 1).

GPU-Based Electronic Structure For Nonadiabatic Dynamics: We have extended our graphical processing unit (GPU)-based electronic structure theory efforts (principally ground state and TDDFT in the past) to include multireference electronic structure theory – specifically the floating occupation molecular orbital – complete active space configuration interaction (FOMO-CASCI) method. (Hohenstein, Bouduban, Song, Luehr, Ufimtsev and Martinez 2015) In FOMO-CASCI, the orbitals are determined using an ensemble averaging method and a CASCI within a chosen active space is then performed to describe the ground and excited electronic states. We were able to show that using a new method based on atomic orbitals (and hence exploiting spatial locality) and implemented on GPUs, we

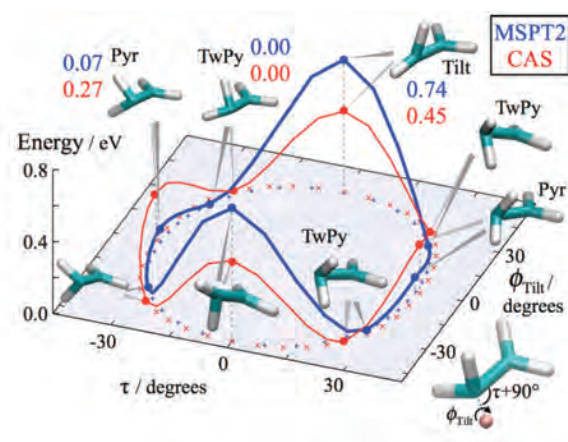


Figure 1. SS-NEB minimum energy path connecting the symmetry-equivalent twisted-pyramidalized S_0/S_1 MECIs in ethylene.

could accelerate this method by 1-2 orders of magnitude compared to conventional CPU-based approaches. The FOMO-CASCI method is an efficient approximation to the fully self-consistent state-averaged CASSCF method, and its accuracy has been previously demonstrated. Using the GPU-accelerated FOMO-CASCI method, we were able to carry out excited state dynamics for photoinitiated proton transfer in methyl salicylate using up to 1000 initial conditions. These calculations significantly exceed what has been previously possible, but perhaps more importantly, they were carried out in a matter of less than a week on a single desktop computer costing less than \$2000. Figure 2 shows results for the average proton transfer after photoexcitation in methyl salicylate.

Exciton Dynamics: We showed that one could devise an electronic structure model based on an exciton Hamiltonian, where all the components of the model were generated by solving the electronic structure problem “on the fly.” (Sisto, Glowacki and Martinez 2014) This is advantageous because each of the chromophores is much smaller than the aggregate system. Because the scaling of the electronic structure methods (such as time-dependent density functional theory, TDDFT, which we used here) is cubic, it is much faster to solve many small problems as opposed to a single large problem. We were able to show that one could differentiate the exciton model directly (using quantities computed for the individual chromophores) and thus carry out dynamics for large chromophoric assemblies such as the LH2 photosynthetic apparatus.

Future Plans: We have begun application of our *ab initio* exciton model to the LH2 complex. We are implementing AIMS dynamics within this context to describe nonadiabatic effects and explore the role of electronic coherence in this system. We are also planning to devote effort to the modeling of excited state dynamics in coordination complexes containing transition metals. This is now feasible with the GPU-accelerated FOMO-CASCI method and the effective core potentials we have implemented on GPUs. (Song, Wang, Sachse, Preiss, Presselt and Martinez 2015) It remains to extend the AIMS method to include intersystem crossing phenomena and to implement a Breit-Pauli Hamiltonian (and the required integrals) to compute spin-orbit couplings within our GPU-accelerated framework. This will allow us to investigate excited state dynamics of paradigmatic inorganic photochemical systems such as $\text{Fe}(\text{CO})_5$, as well as energy-relevant complexes like $\text{Ru}(\text{bpy})_3$ and Fe-containing analogs.

Publications Supported by the AMOS Program

Evenhuis, C. and T. J. Martinez (2011). "A scheme to interpolate potential energy surfaces and derivative coupling vectors without performing a global diabaticization." *J. Chem. Phys.* **135**: 224110.

Tao, H., T. K. Allison, T. W. Wright, A. M. Stooke, C. Khurmi, J. van Tilborg, Y. Liu, R. W. Falcone, A. Belkacem and T. J. Martinez (2011). "Ultrafast internal conversion in ethylene. I. The excited state lifetime." *J. Chem. Phys.* **134**: 244306.

Tao, H., L. Shen, M. H. Kim, A. G. Suits and T. J. Martinez (2011). "Conformationally selective photodissociation dynamics of propanal cation." *J. Chem. Phys.* **134**: 054313.

Thompson, A. L. and T. J. Martinez (2011). "Time-resolved photoelectron spectroscopy from first principles: Excited state dynamics of benzene." *Faraday Disc.* **150**: 293-311.

Yang, S. and T. J. Martinez (2011). *Ab initio multiple spawning: First principles dynamics around conical intersections. Conical Intersections: Theory, Computation and Experiment.* W. Domcke and H. Koppel. Singapore, World Scientific.

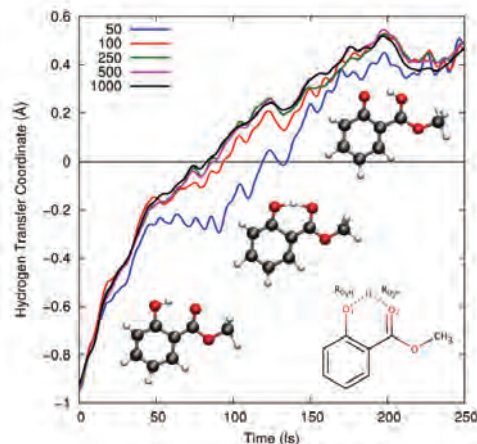


Figure 2. Demonstration of convergence of excited state dynamics for proton hopping time after photoexcitation using FOMO-CASCI on a single node with GPUs.

- Allison, T. K., H. Tao, W. J. Glover, T. W. Wright, A. M. Stooke, C. Khurmi, J. van Tilborg, Y. Liu, R. W. Falcone, T. J. Martinez and A. Belkacem (2012). "Ultrafast internal conversion in ethylene. II. Mechanisms and pathways for quenching and hydrogen elimination." *J. Chem. Phys.* **136**: 124317.
- Kim, J., H. Tao, J. L. White, V. S. Petrovic, T. J. Martinez and P. H. Bucksbaum (2012). "Control of 1,3-cyclohexadiene photoisomerization using light-induced conical intersections." *J. Phys. Chem. A* **116**: 2758-2763.
- Kuhlman, T. S., W. J. Glover, T. Mori, K. B. Moller and T. J. Martinez (2012). "Between ethylene and polyenes - the nonadiabatic dynamics of cis-dienes." *Faraday Disc.* **157**: 193-212.
- Mori, T., W. J. Glover, M. S. Schuurman and T. J. Martinez (2012). "Role of Rydberg States in the Photochemical Dynamics of Ethylene." *J. Phys. Chem. A* **116**: 2808-2818.
- Petrovic, V. S., M. Siano, J. L. White, N. Berrah, C. Bostedt, J. D. Bozek, D. Beroege, M. Chalfin, R. N. Coffee, J. P. Cryan, L. Fang, J. P. Farrell, L. J. Frasinski, J. M. Glowonia, M. Guehr, M. Hoener, D. M. P. Holland, J. Kim, J. P. Marangos, T. Martinez, B. K. McFarland, R. S. Minns, S. Miyabe, S. Schorb, R. J. Sension, L. S. Spector, R. Squibb, H. Tao, J. G. Underwood and P. H. Bucksbaum (2012). "Transient X-Ray fragmentation; Probing a prototypical photoinduced ring-opening." *Phys. Rev. Lett.* **108**: 253006.
- Mori, T. and T. J. Martinez (2013). "Exploring the Conical Intersection Seam: The Seam Space Nudged Elastic Band Method." *J. Chem. Theo. Comp.* **9**: 1155-1163.
- Petrovic, V. S., S. Schorb, J. Kim, J. L. White, J. P. Cryan, J. M. Glowonia, L. Zipp, D. Broege, S. Miyabe, H. Tao, T. Martinez and P. H. Bucksbaum (2013). "Enhancement of strong-field multiple ionization in the vicinity of the conical intersection in 1,3-cyclohexadiene ring-opening." *J. Chem. Phys.* **139**: 184309.
- Glover, W. J. (2014). "Smoothing out excited-state dynamics: Analytical gradients for dynamically weighted complete active space self-consistent field." *J. Chem. Phys.* **141**: 171102.
- Joalland, B., T. Mori, T. J. Martinez and A. G. Suits (2014). "Photochemical dynamics of ethylene cation C₂H₄⁺." *J. Phys. Chem. Lett.* **5**: 1467-1471.
- McFarland, B. K., J. P. Farrell, S. Miyabe, F. Tarantelli, A. Aguilar, N. Berrah, C. Bostedt, J. D. Bozek, P. H. Bucksbaum, J. C. Castagna, R. N. Coffee, J. P. Cryan, L. Fang, R. Feifel, K. J. Gaffney, J. M. Glowonia, T. J. Martinez, M. Mucke, B. Murphy, A. Natan, T. Osipov, V. S. Petrovic, S. Schorb, T. Schultz, L. S. Spector, M. Swiggers, I. Tenney, S. Wang, J. L. White, W. White and M. Guehr (2014). "Ultrafast X-Ray Auger probing of photoexcited molecular dynamics." *Nature Comm.* **5**: 4235.
- Punwong, C., T. J. Martinez and S. Hannongbua (2014). "Direct QM/MM simulation of photoexcitation dynamics in bacteriorhodopsin and halorhodopsin." *Chem. Phys. Lett.* **610-611**: 213-218.
- Sisto, A., D. R. Glowacki and T. J. Martinez (2014). "Ab initio nonadiabatic dynamics of multichromophore complexes: A scalable graphical-processing-unit-accelerated exciton framework." *Acc. Chem. Res.* **47**: 2857-2866.
- Spector, L. S., M. Artamonov, S. Miyabe, T. Martinez, T. Seideman, M. Guehr and P. H. Bucksbaum (2014). "Axis-dependence of molecular high harmonic emission in three dimensions." *Nature Comm.* **5**: 3190.
- Wolf, T. J. A., T. S. Kuhlman, O. Schalk, T. J. Martinez, K. B. Moller, A. Stolow and A.-N. Unterreiner (2014). "Hexamethylcyclopentadiene: time-resolved photoelectron spectroscopy and ab initio multiple spawning simulations." *Phys. Chem. Chem. Phys.* **16**: 11770-11779.
- Hohenstein, E. G., M. E. F. Bouduban, C. Song, N. Luehr, I. S. Ufimtsev and T. J. Martinez (2015). "Analytic first derivatives of floating occupation molecular orbital-complete active space configuration interaction on graphical processing units." *J. Chem. Phys.* **143**: 014111.
- Song, C., L.-P. Wang, T. Sachse, J. Preiss, M. Presselt and T. J. Martinez (2015). "Efficient implementation of effective core potential integrals and gradients on graphical processing units." *J. Chem. Phys.* **143**: 014114.

Page is intentionally blank.

Understanding Photochemistry using Extreme Ultraviolet and Soft X-ray Time Resolved Spectroscopy

Markus Gühr and Thomas Wolf, SLAC National Accelerator Laboratory, 2575 Sand Hill Road, Menlo Park, CA 94025
mguehr@slac.stanford.edu

Scope of the program

The scientific scope of this early career program is the site specific probing of chemical processes. For this purpose, we use light in the extreme ultraviolet (EUV) and soft x-ray (SXR) spectral range providing the site specificity due to the distinct absorption and emission features of core electrons. We are especially interested in non-Born-Oppenheimer approximation (non-BOA) dynamics, because of its importance for light harvesting, atmospheric chemistry and DNA nucleobases photoprotection. We use three different technical approaches for our studies: Laboratory based high harmonic generation (HHG) sources in the range of 10-100 eV delivering pulses with a few femtoseconds duration, synchrotrons with a wide spectral range from the EUV to the high SXR and the Linac Coherent Light Source (LCLS) providing high pulse energy femtoseconds pulses in the soft and hard x-ray range.

Progress in 2013/2014

Spectroscopy with EUV light (T. Wolf, A. Battistoni, M. Gühr, Jakob Grilj (now at EPFL), M. Koch (now at TU Graz), E. Sistrunk (now at LLNL))

Gasphase Photoelectron Spectroscopy

Our laser laboratory at SLAC houses a fully operational high harmonic source and photoelectron spectrometer for molecules in the gasphase. First experiments with this source have given us insight on the differences of single- vs multiphoton ultrafast probing. We used perylene, a polyaromatic hydrocarbon for this study. Perylene can be excited by 400 nm UV light (3 eV photon energy) to the S_1 state, which then undergoes fluorescence decay in a few nanoseconds. Probing the excited state with infrared multi-photon absorption exhibits a decay in the integrated ion signal with a time constant of ~ 1 ps. The single photon probing with 14 eV EUV probes however exhibits a photoelectron spectrum that hardly changes over this timescale. The two transitions are sensitive to different states of the molecule. The EUV probe directly leads from the S_1 to the cationic states; the multi-photon probe process involves several neutral resonant states in between the S_1 and cationic states, as we know from signal vs. IR intensity measurements. The energy-difference of S_1 and cationic states is constant along the nuclear geometry change induced by the 400 nm excitation, which leads to no or little modulation in the one photon probed photoelectron signal. The intermediate states in the multi-photon probe are getting shifted out of resonance on this path, explaining the signal decay.

Multi-photon infrared probing is a very popular tool due to its simplicity, but the role of intermediate states has never been investigated directly. Perylene does not undergo any intersystem crossing (ISC) or internal conversion (IC). It is ideal to show how signal decay, which might be interpreted as a signature IC or ISC in more complex systems, is purely due to shifting intermediate resonances.

Using the 14 eV probe pulse, we have recorded time resolved photoelectron spectra of the nucleobase thymine. We clearly identify the signatures of the photoexcited state via the kinetic energy of the features. While we are working on the exact interpretation of the results, we are certain that the 14 eV probing shows remarkable new features when comparing the results to literature spectra with highest probe photon energy at about 6 eV. Our probe pulses follow the relaxing photoexcited molecular population over a much longer time interval and we see a long living feature still shifting in kinetic energy on the picosecond timescale. We do not expect that these observations are specific for thymine and will continue our experimental work on other nucleobases.

Transient Grating Spectroscopy

X-ray nonlinear methods will play an important role for the upcoming generation of free electron lasers, operating at high repetition rates up to 1MHz. We have done very recent work which demonstrates a nonlinear scheme (transient grating) using one extreme ultraviolet pulse at an inner shell resonance. Our work

shows features of a pure electronic response measured at the M-edge of vanadium inside VO₂. We used two 800 nm beams in TG geometry) to excite the insulator-to-metal transition in VO₂ and a third extreme ultraviolet (EUV) beam produced by strong field high harmonic generation of 800 nm light to probe the sample. The inset in Figure 1a shows the first diffraction order on the CCD detector on the left and the different spots show harmonics 21-13 (32-20 eV), all having photon energy different by 3eV. The line spacing in this experiment was ~15µm, smaller periods can be regularly achieved using diffractive optics. Figure 1a shows the transient FWM signal for two of the harmonics as a function of delay between the simultaneous 800 nm pulses and the EUV pulse. For a sample temperature below the insulator to metal transition, the signal rises on a 10 ps time scale and decays in about 150 ps (not shown). The diffraction at 38.8 eV shows a faster transient, which is the electronic response of the sample smeared out by our time resolution (~3 ps) due to non-matched excitation wavefronts.

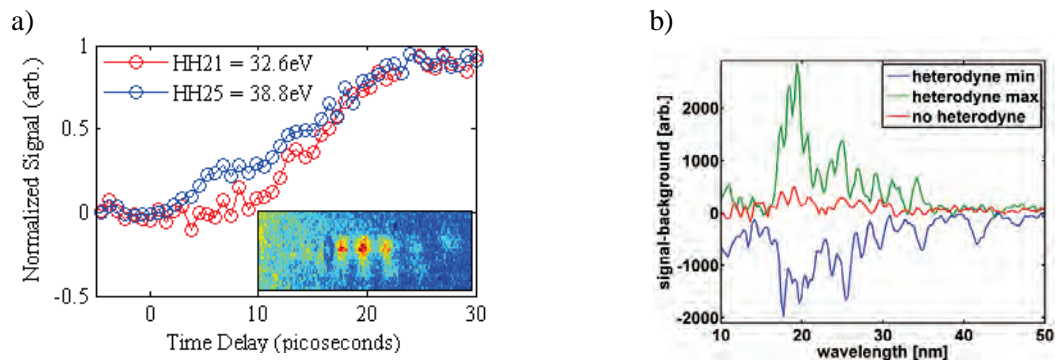


Figure 1a) Time resolved transient grating signal for two different EUV photon energies (32.6 (off resonance) and 38.8 eV (close to resonance/on resonance)). The higher photon energy detects an electronic effect in the first few picoseconds, which is smeared out by our apparatus limited resolution of ~3 ps. The inset shows the diffracted harmonics on the CCD. b) First indication for heterodyning. A permanent grating was interfering with the transient response leading to an increase (green) or decrease (blue) depending on the relative phase between the gratings. A measurement without permanent grating serves as a reference (red).

Heterodyning by a phase stable reference electric field is a well known technique to amplify weak nonlinear signals. For short wavelength at FEL sources, the generation of a reference field in front of the sample is challenging because of a lack of suitable beamsplitters. Figure 1b shows new results that indicate a pioneering TG heterodyning experiment in our lab. We show the diffracted extreme ultraviolet spectrum at one fixed delay. The non-heterodyne experiment shows a positive signal. After writing a permanent grating on the sample (by temporarily increasing the intensity to the damage threshold), we observe its interference with the transient grating signal (green: constructive, blue: destructive interference). We have demonstrated a new self-referencing technique for heterodyning transient grating signals

The enormous advantage in this technique is that controlling the phase of a few nanometer wavelength pulses is accomplished by translating a grating by parts of its grating constants, which can be well into the 100 nm to micron range. This scheme makes use of the available technology to overcome the much harder technological problem of beamsplitters for soft x-rays as posed by multidimensional x-ray spectroscopy.

Soft x-ray probing of nucleobase photoprotection (together with the nucleobase photoprotection collaboration)

In our first experiment on nucleobase photoprotection in 2011, we discovered that the Auger spectrum as a function of photoexcitation – X-ray -probe delay contains valuable information about crucial bond distances. For the nucleobase thymine, the oxygen Auger spectrum shifts towards high kinetic energies, resulting from a particular C-O bond stretch of only 0.1 Å in the $\pi\pi^*$ photoexcited state. A subsequent shift of the Auger spectrum towards lower kinetic energies displays the electronic relaxation of the initial photoexcited state within 200 fs.

A very recent LCLS beamtime on the same topic was devoted to finding the product channels of the $\pi\pi^*$ decay. We implemented ultrafast near edge absorption fine structure (NEXAFS) spectroscopy for the gas at the LCLS to accomplish our goal. Using the monochromator in the SXR hutch together with femtosecond UV excitation and Auger yield detection, we obtained NEXAFS spectra of the excited state with a time resolution of 100 fs.

Two remarkable features are clearly visible in the data. First, the π^* NEXAFS peak associated with the π^* orbital active in the UV excitation is bleached. This effect can be attributed to the UV induced increased occupation of an initially completely unfilled orbital. In addition, a remarkably strong peak shifted about 4.5 eV towards lower excitation energies is visible after UV excitation. This peak shows a delayed onset and is visible over several picoseconds time delay. Due to these features, the new spectral signature must reflect a transiently filled and emptied state of thymine.

Ultrafast Electron Diffraction (*together with Centurion group University Nebraska*)

In 2015, SLAC has started a new initiative to determine the transient structure of isolated molecules via scattering of relativistic MeV electron pulses from an RF photocathode gun. Our task has been responsible for the realization of the first gas phase experiment together with the group of Martin Centurion at University of Nebraska. The work was performed in close collaboration with the accelerator directorate and the LCLS laser group. Relativistic electrons are ideally suited for this task because their velocity is close to the group velocity of a laser pulse traversing a gas phase target. Thus the technique does not suffer the typical degeneration of time resolution observed with keV electrons. The great promise of this technique, elaborated further below, is the identification of important nuclear geometries for ultrafast energy conversion in molecules, such as potential minima and regions on the way to conical intersections. Electrons interact with the photoexcited molecule mostly via elastic scattering. The transient molecular structure is encoded in terms its Fourier transform intensity in the electron scattering image.

The nitrogen molecules used in this study were cooled by expansion out of a pulsed nozzle. A first (alignment) laser pulse (~ 50 fs, 800 nm, $\sim 10^{13}$ W/cm²) excited a rotational wavepacket in the molecules through a nonresonant Raman interaction. The relativistic electrons were scattered from the transient ensemble. The simulation of the anisotropy using the calculated diffraction images with identical regions of interest reflects the data well. From the comparison of the experimental alignment traces and simulations of the traces, we conclude that the time resolution of the new SUED machine is about 200 fs FWHM.

Plans

- 1) Photoelectron/Photoion EUV spectroscopy: We plan to observe the dynamics of nucleobases other than thymine
- 2) TG spectroscopy: we are working on covering the full M-edge of 3d transition metals and on a better time-resolution using tilted excitation wavefronts.
- 3) SLACs ultrafast electron diffraction initiative: this task is supporting this initiative in collaboration with M. Centurions group from the University of Nebraska. We will perform ultrafast electron diffraction on photoexcited isolated molecules in the gas phase.

References of this task (or with participation of this task) during the last three years:

1. Ultrafast Isomerization Initiated by X-Ray Core Ionization, C. Liekhus-Schmaltz, et al. Nature Comm. accepted (2015) (this task not lead)
2. Probing Molecular Photoexcited Dynamics by Soft X-Rays, M. Gühr in: Ultrafast Dynamics Driven by Intense Light Pulses, eds.: M. Kitzler S. Graefe (Springer, Heidelberg, 2016)
3. MeV Ultrafast Electron Diffraction at SLAC, S. P. Weathersby, et al., Rev. Sci. Instr. 86, 073702 (2015)
4. Femtosecond X-ray-induced fragmentation of fullerenes, N. Berrah, et al. J. Mod. Opt. (2015) (this task not lead)
5. The linac coherent light source single particle imaging road map, A. Aquila, et al. Struct. Dyn. 2, 041701 (2015) (this task not lead)

6. Self referencing heterodyne transient grating spectroscopy with short wavelength, J. Grilj, E. Sistrunk, J. Jeong, M. G. Samant, A. X. Gray, H. A. Dürr, S. S. P. Parkin, M. Gühr, *Photonics* 2, 392 (2015)
7. Understanding the modulation mechanism in resonance-enhanced multi-photon probing of molecular dynamics, M. Koch, T. J. A. Wolf, M. Gühr, *Phys. Rev. A* 91, 031403 (2015)
8. Extreme Ultraviolet Probing of Transient Grating Measurement of the Insulator to Metal Transition Dynamics in VO₂
E. Sistrunk, J. Grilj, J. Jeong, M. G. Samant, A. X. Gray, H. A. Dürr, S. S. P. Parkin, M. Gühr, in: *Ultrafast Phenomena XIX*, p. 64 (Springer, 2015)
9. Direct comparison of multi-photon and EUV single-photon probing of molecular relaxation processes, T. J. A. Wolf, M. Koch, E. Sistrunk, J. Grilj, M. Gühr in: *Ultrafast Phenomena XIX*, p. 46 (Springer, 2015)
10. Broadband Extreme Ultraviolet Probing of Transient Gratings in Vanadium Dioxide, E. Sistrunk, J. Grilj, J. Jeong, M. G. Samant, A. X. Gray, H. A. Dürr, S. S. P. Parkin, M. Gühr, *Optics Express* 24, 4340 (2015)
11. A low-cost mirror mount control system for optics setups, M. Gopalakrishnan and M. Gühr, *Amer. J. Phys.* 83, 186 (2015)
12. Extreme ultraviolet spectrometer based on a transmission electron microscopy grid, E. Sistrunk and M. Gühr, *Journal of Optics* 17, 015502 (2015)
13. Femtosecond photoelectron and photoion spectrometer with vacuum ultraviolet probe pulses, M. Koch, T. J. A. Wolf, J. Grilj, E. Sistrunk, M. Gühr, *J. Electr. Spectr. Rel. Phenom.* 197, 22 (2014)
14. Femtosecond X-ray Induced Explosion of C₆₀ at Extreme Intensity, B. Murphy, et al., *Nature Comm.* 5, 4281 (2014) (this task not lead)
15. Ultrafast X-ray Auger Probing of photoexcited molecular dynamics, B. K. McFarland, J. P. Farrell, S. Miyabe, F. Tarantelli, A. Aguilar, N. Berrah, C. Bostedt, J. D. Bozek, P.H. Bucksbaum, J. C. Castagna, R. N. Coffee, J. P. Cryan, L. Fang, R. Feifel, K. J. Gaffney, J. M. Glowonia, T.J. Martinez, M. Mucke, B. Murphy, A. Natan, T. Osipov, V. S. Petrovic, S. Schorb, Th. Schultz, L. S. Spector, M. Swiggers, I. Tenney, S. Wang, J. L. White, W. White, and M. Gühr, *Nature Comm.* 5, 4235 (2014)
16. Experimental strategies for optical pump – soft x-ray probe experiments at the LCLS, B. K. McFarland, N. Berrah, C. Bostedt, J. Bozek, P.H. Bucksbaum, J. C. Castagna, R. N. Coffee, J. Cryan, L. Fang, J. P. Farrell, R. Feifel, K. Gaffney, J. Glowonia, T. Martinez, M. Mucke, B. Murphy, S. Miyabe, A. Natan, T. Osipov, V. Petrovic, S. Schorb, Th. Schultz, M. Swiggers, L. Spector, F. Tarantelli, I. Tenney, S. Wang, W. White, J. White, M. Gühr, *J. Phys.: Conf. Ser.* 488, 012015 (2014)
17. A beamline for time-resolved extreme ultraviolet and soft x-ray spectroscopy, J. Grilj, E. Sistrunk, M. Koch, M. Gühr, *J. Anal. Bioanal. Tech.* S12:005 (2014)
18. Quantified angular contributions for high harmonic emission of molecules in three dimensions, L. S. Spector, M. Artamonov, S. Miyabe, T. Martinez, T. Seideman, M. Guehr, and P. H. Bucksbaum, *Nature Comm.* 5, 3190 (2014) (this task not lead)
19. Resonant photoemission at the iron M-edge of Fe(CO)₅, E. Sistrunk, J. Grilj, B. K. McFarland, J. Rohlen, A. Aguilar, and M. Gühr, *J. Chem. Phys.*, 139, 164318 (2013)
20. Probing Nucleobase Photoprotection with soft x-rays, B. K. McFarland, J. P. Farrell, N. Berrah, C. Bostedt, J. Bozek, P.H. Bucksbaum, R. N. Coffee, J. Cryan, L. Fang, R. Feifel, K. Gaffney, J. Glowonia, T. Martinez, M. Mucke, B. Murphy, S. Miyabe, A. Natan, T. Osipov, V. Petrovic, S. Schorb, Th. Schultz, L. Spector, F. Tarantelli, I. Tenney, S. Wang, W. White, J. White, M. Gühr, *EDP Web of Conferences*, 41, 07004 (2013)

Early Career: Strongly-driven attosecond electron-dynamics in periodic media

Shambhu Ghimire, SLAC National Accelerator Laboratory
2575 Sand Hill Rd, Menlo Park, CA, 94025
shambhu@slac.stanford.edu

Scope of the program

This program is focused on strongly-driven electron dynamics in bulk crystals subjected to intense infrared laser fields. This regime is known to produce ultra-short wavelength high harmonic radiation, similar to the gas phase atomic and molecular high harmonic generation (HHG). The gas phase HHG has been very well studied, and that knowledge has been the foundation of current Attosecond Science and Technology. It is tempting to say that solid-state HHG physics could take a similar path. However, the generation mechanism for the solid-state harmonics is a matter of intense debate. Two distinct solid-state electronic processes can contribute: inter-band electron dynamics and intra-band electron dynamics. The difficulty in disentangling their individual contribution is mainly because both mechanisms predict the same linearly scaled high-energy cutoff (with the electric field). In this project, we are pursuing a series of experiments and theoretical studies aimed to disentangle these roles quantitatively. Thus the objective of this project is to advance our understanding of strong-field physics in the condensed phase with direct implications in XUV source technology. Because of the high density target the solid-state harmonics could lead to a compact attosecond XUV source. Such a light source could be an alternative to the existing gas phase sources since they typically require fairly complex setup including the use of high power pump lasers due to low conversion efficiency.

Recent Progress

Two-color HHG for measuring harmonics in time domain: We investigated the time-frequency profile of solid-state harmonics theoretically considering a model solid [1]. The results predict two distinct characteristics corresponding to the inter-band and intra-band nonlinear currents. In the case of intra-band emission, harmonics do not exhibit chirp as all harmonics are emitted at the peak of the electric field. However, inter-band emission exhibits atto-chirp, similar to the atomic HHG along with some important differences, for example here the near cutoff harmonic are emitted at the zero crossing of the field. We are considering two-color HHG approach to deduce the time-frequency profile in the experiments. The theoretical work is ongoing in collaboration with *Gaarde* and *Schafer* group at LSU. In the experimental side, preliminary results are obtained in the single crystal MgO, which indeed show atto-chirp. We are currently analyzing that data.

Role of periodicity in high harmonic generation from solids: Understanding the role of long range periodicity of the target in generating harmonics is important for fundamental physics point of view as well as for potential applications in future XUV photonics. Particularly, if amorphous targets support the XUV generation it would have a substantial implication in the fiber laser technology in terms of developing high repetition rate XUV source. In this project, we compare harmonic generation in crystal quartz with amorphous fused silica because of their same band-gap. We have started by looking at the angular distribution of 5th and 7th harmonics for a linearly polarized 2 μm laser. Crystal quartz showed clear 6-fold symmetry consistent to the crystal structure. In contrast, fused silica showed an isotropic angular distribution, as expected in isotropic medium. We plan on extending these measurements to higher order harmonics.

Ellipticity dependence of high harmonics from solids: We are investigating the ellipticity dependence of harmonics from MgO crystals. In the gas phase, it is well known that once the harmonics are of high enough photon energy compared to the ponderomotive energy they show strong ellipticity dependence. In the case of solids, the ellipticity dependence seems more complex. In the original ZnO experiments, we reported a very weak dependence but in a recent experiment performed in collaboration with *Reis* group we measured a strong dependence in rare gas solid target. Our preliminary results in MgO indicate the possibility of using harmonics to study crystal bonding.

Construction of XUV spectrometer: We have completed the construction of a XUV spectrometer that covers the spectral range from ~ 10 eV to ~ 50 eV. The chamber encloses focusing optics, kinematics for mounting samples, a diffraction grating and a MCP detection system. The chamber was commissioned using harmonics produced in single crystal MgO[2].

Development of mid-IR Laser system: Earlier this year, we installed a Ti:sapphire laser amplifier that produces 8 mJ, 35 fs, 800 nm pulses at 1kHz. Also, we installed a high energy OPA, which allowed us to reach the $2 \mu\text{m}$ wavelength with ~ 50 fs pulses at the mJ level. Currently, we are working on extending the wavelength to $4 \mu\text{m}$ by employing the difference frequency generation technique.

Planned Research

We are working with the LSU group on the issue of how to extract harmonic phase information from the two-color data. From this study, we expect to distinguish the contribution from inter- and intra-band nonlinear current. We plan to use the newly built XUV spectrometer for atto-chirp and ellipticity dependence measurements. We continue to collaborate with the *Reis* group at PULSE Institute on finishing up rare gas solids experiments and in new nonlinear x-ray physics experiments at the LCLS.

In the laboratory, within next year, we expect to complete the mid-infrared laser system. Long wavelength and ultra-short laser pulses are crucial for achieving high damage threshold. Currently, we are working on a nonlinear pulse compressor technique for obtaining few cycle laser pulses near $2 \mu\text{m}$ wavelength. A difference frequency generation setup is being developed to reach the $4 \mu\text{m}$ wavelength range, which will allow us to study a wide range of optical medium with different band-gap and band structures.

In the longer term we will perform photoemission experiments, where we will measure electrons from strongly driven solid surface.

Publication directly supported by this project

[1] M. Wu, S. Ghimire, D. A. Reis, K. J. Schafer, and M. B. Gaarde. High-harmonic generation from bloch electrons in solids. *Physical Review A*, 91(4):043839, 2015.

Other related publication

[2] S. Ghimire, G. Ndabashimiye, A. D. DiChiara, E. Sistrunk, M. I. Stockman, P. Agostini, L. F. DiMauro, and D. A. Reis. Strong-field and attosecond physics in solids. *Journal of Physics B: Atomic, Molecular and Optical Physics*, 47(20):204030, 2014.

University Research Summaries
(by PI)

Page is intentionally blank.

Tracing and Controlling Ultrafast Dynamics in Molecules

Principal Investigator: Andreas Becker

JILA and Department of Physics, University of Colorado at Boulder,
440 UCB, Boulder, CO 80309-0440

andreas.becker@colorado.edu

Program Scope

The emergence of attosecond technology has shifted our perspective in ultrafast science from the time scales intrinsic to nuclear dynamics to that of electron dynamics. With our projects we seek to provide theoretical support to establish new ultrafast concepts and optical techniques to obtain an advanced understanding and interpretation of electron dynamics in atoms and molecules.

Recent Progress and Future Goals

Our activities in the project over the last year can be summarized in the following sub-projects.

A. Time delays in single and two-photon ionization

Observing the time-resolved behavior of electrons is among the primary challenges at the frontier of attosecond science. One of the key methods for time-resolved measurements is the attosecond streak camera technique [1]. It is based on the observation of the momentum (or energy) of a photoelectron, ionized by an ultrashort XUV pulse from a target and streaked by an additional laser pulse, usually a near-infrared pulse. The final electron momentum depends on the vector potential of the streaking field at the time instant of the transition of the electron into the continuum. By scanning the relative delay between the two pulses, time information is mapped onto the streaking trace, i.e., the final electron momentum as a function of the relative delay between the two pulses. In streaking experiments on the photoionization of atoms [2] and solids [3], temporal shifts between different streaking traces have been observed. We have recently shown [DOE10] that the shifts, when compared with the vector potential of the streaking pulse, can be interpreted as due to two contributions, namely a time delay acquired during the transition in the continuum (absorption time delay) and a time delay accumulated by the photoelectron in the continuum (continuum time delay).

We have studied both contributions in different scenarios, involving single-photon and two-photon ionization. For ionization due to single photon absorption or a nonresonant two-photon transition, the transition from the bound state to the continuum is found to occur without time delay and the observed streaking time delay does arise from the interaction of the photoelectron with the Coulomb potential of the residual ion and the field of the streaking pulse [DOE4, DOE6]. In contrast, for a resonant two-photon ionization a substantial absorption time delay is found, which scales linearly with the duration of the ionizing pulse [DOE10]. The latter can be related to the phase acquired during the transition of the electron from the initial ground state to the continuum and the influence of the streaking field on the resonant structure of the atom. Furthermore, we were able to establish the existence of such an absorption time delay via an independent analysis of photoelectron trajectories following two-photon ionization.

The continuum time delay is often considered to involve contributions from the WS time delay [4,5] and the coupling between the streaking field and the Coulomb field. Alternatively, we have interpreted it as solely due to the interaction with the *combined* Coulomb and streaking fields

[DOE4, DOE6]. Very recently, we were able to show that the former split in a field-free and a field-induced time delay can be derived as an approximation from our theoretical interpretation. This has further led us to a simple model formula which allows for the efficient calculation of continuum time delays. As a first approximation of this new model formula we have studied the influence of the attochirp of the ionizing XUV pulse on the streaking time delays.

Currently, we extend our streaking time delay studies to molecules, involving single-photon as well as resonant and non-resonant two photon ionization.

B. High harmonic spectroscopy of nonadiabatic electron dynamics

Another way to achieve attosecond temporal resolution of electron dynamics is given via high harmonic generation through the interaction of atoms and molecules with intense femtosecond lasers [6]. The harmonic radiation with photon energies extending from the VUV to the soft-X-ray region is generated upon recombination of the electron with the parent ion and serves as a natural probe of the nuclear and electronic structure or dynamics of molecular targets [7]. Each of the three steps in harmonic generation [8,9], namely emission, propagation and recombination of the electron wavepacket, occurs on a femto- or sub-femtosecond time span. HHG is therefore a spectroscopic tool offering temporal resolution on the time scale of electron dynamics.

Based on the results of numerical simulations we have explored a new mechanism resulting in a minimum in the high harmonic spectrum of a hydrogen molecular ion driven at extended internuclear distances by a mid-infrared laser source of moderate intensity [10]. Our analysis identifies this minimum to be a signature of the transient localization of the electron upon alternating nuclear centers, which we have previously studied in this program [11]. Surprisingly, this dynamics, which exclusively occurs at the time of ionization, transfers into a suppression of harmonic generation at specific orders. We have further demonstrated the sensitivity of this spectroscopic feature to driving field parameters as well as its robustness to distributions of laser field intensities and internuclear distances in an attempt to explore the experimental feasibility to observe the present theoretical findings. It is also shown how variations in the nonadiabatic dynamics induced by the ramping driving field can be imaged through changes in the number and locations of minima in the spectra. This leads to a temporal resolution of the transition from adiabatic to nonadiabatic dynamics over the course of the driving laser pulse.

In future, we plan to extend our studies towards an analysis of propagation effects regarding the spectroscopic feature in harmonic emission and the investigation of the signatures of nonadiabatic dynamics in photoelectron energy spectra.

C. High harmonic and isolated attosecond pulse generation at long driver wavelengths

In collaboration with the experimental groups of Margaret Murnane and Henry Kapteyn we have examined the generation of isolated ultrashort pulses by multi-cycle driving laser pulses at midinfrared wavelengths. Our calculations are based on an extension of the strong-field approximation at the microscopic level and the assumption to discretize the medium into elementary radiators. The radiation via harmonic emission by each of these sources is then propagated to the detector and calculated as coherent sum. Our results indicate, in support of corresponding experimental observations, that a temporal gating of the harmonic emission down to one optical cycle can be achieved via macroscopic phase matching [DOE8].

More recently, as continuation of this project we have analyzed the important role of group velocity matching in the macroscopic build up of the high-harmonic signal generated in gas

targets at high pressures. The non-perturbative nature of high-harmonic generation required a new definition of the walk-off length associated with group velocity matching [12]. Predictions based on this definition are in excellent agreement with full quantum simulations. It is shown that group velocity matching is a relevant factor in the isolation of attosecond pulses and leads to the selection of the contributions from the short quantum path to harmonic emission. We have also demonstrated that the effects due to group velocity matching become most relevant for pulses with long driver wavelengths and short durations.

D. Noncollinear generation of angularly circularly polarized high harmonics

Finally, in collaboration with the groups of Margaret Murnane and Henry Kapteyn and other experimental groups we have shown that angularly separated pulses of circularly polarized high harmonics can be generated through a noncollinear set-up with circularly polarized driving lasers [DOE11]. This new technique offers advantages over previous methods, including the generation of higher photon energies, the separation of the harmonics from the pump beam, the production of both left and right circularly polarized harmonics at the same wavelength, and the capability of separating the harmonics without using a spectrometer. We have supported the pioneering experimental efforts in this direction by numerical simulations. In particular, we were able to show that the technique is applicable at a variety of driver wavelengths. Furthermore, our calculations provide insights in the temporal structure of the generated light pulses, showing that the pulses, in general, emerge as single long pulses, which however in the case of a few-cycle driver can lead to an isolated circularly polarized attosecond pulse.

References

- [1] J. Itatani et al., Phys. Rev. Lett. **88**, 173903 (2002).
- [2] M. Schultze et al., Science **328**, 1658 (2010).
- [3] A.L. Cavalieri et al., Nature **449**, 1029 (2007).
- [4] E. P. Wigner, Phys. Rev. **98**, 145 (1955).
- [5] F. T. Smith, Phys. Rev. **118**, 349 (1960).
- [6] T. Popmintchev, M.C. Chen, P. Arpin, M.M. Murnane, and H.C. Kapteyn, Nat. Photon. **4**, 822 (2010).
- [7] M. Lein, J. Phys. B **40**, R135 (2007).
- [8] P.B. Corkum, Phys. Rev. Lett. **71**, 1994 (1993).
- [9] K.J. Schafer, B. Yang, L.F. Di Mauro, and K.C. Kulander, Phys. Rev. Lett. **70**, 1599 (1993).
- [10] M.R. Miller, A. Jaron-Becker and A. Becker, submitted for publication.
- [11] N. Takemoto and A. Becker, Phys. Rev. Lett. **105**, 203004 (2010).
- [12] C. Hernandez-Garcia et al., submitted for publication.

Publications of DOE sponsored research (since 2012)

- [DOE1] A. Picon, A. Jaron-Becker and A. Becker, *Enhancement of vibrational excitation and dissociation of H_2^+ in infrared laser pulses*, Physical Review Letters **109**, 163002-1-4 (2012)
- [DOE2] J. Su, H. Ni, A. Becker and A. Jaron-Becker, *Numerical simulation of time delays in light induced ionization*, Physical Review A **87**, 0334201-9 (2013)
- [DOE3] A. Becker, F. He, A. Picon, C. Ruiz, N. Takemoto and A. Jaron-Becker, *Observation and control of electron dynamics in molecules*, in *Attosecond Physics: Attosecond Measurements and Control of Physical Systems*, Eds. L. Plaja, R. Torres and A. Zair, Springer Series in Optical Sciences, Vol. 177 (Springer, Berlin - Heidelberg, 2013) p. 207-229
- [DOE4] J. Su, H. Ni, A. Becker and A. Jaron-Becker, *Finite-range time delay in numerical streaking experiments*, Physical Review A **88**, 023413-1-6 (2013)
- [DOE5] J. Su, H. Ni, A. Becker and A. Jaron-Becker, *Theoretical analysis of time delays and streaking effects in XUV photoionization*, Journal of Modern Optics **60**, 1484-1491 (2013)
- [DOE6] J. Su, H. Ni, A. Becker and A. Jaron-Becker, *Attosecond streaking time delays: Finite-range property and comparison of classical and quantum approaches*, Physical Review A **89**, 013404 (2014)
- [DOE7] J. Su, H. Ni, A. Becker and A. Jaron-Becker, *Numerical simulations of attosecond streaking time delays in photoionization (invited paper)*, Chinese Journal of Physics **52**, 404 (2014)
- [DOE8] M.-C. Chen, C. Mancuso, C. Hernández-García, F. Dollar, B. Galloway, D. Popmintchev, P.-C. Huang, B. Walker, L. Plaja, A. A. Jaro -Becker, A. Becker, M. M. Murnane, H. C. Kapteyn, and T. Popmintchev, *Generation of bright isolated attosecond soft X-ray pulses driven by multicycle midinfrared lasers*, Proceedings of the National Academy of Sciences of the United States of America **111**, E2361 (2014)
- [DOE9] M.R. Miller, C. Hernandez-Garcia, A. Jaron-Becker, and A. Becker, *Targeting multiple rescatterings through VUV-controlled high-harmonic generation*, Physical Review A **90**, 053409 (2014)
- [DOE10] J. Su, H. Ni, A. Jaro -Becker and A. Becker, *Time delays in two-photon ionization*, Physical Review Letters **113**, 263002 (2014)
- [DOE11] D.D. Hickstein, F.J. Dollar, P. Grychtol, J.L. Ellis, R. Knut, C. Hernández-García, D. Zusin, C. Gentry, J.M. Shaw, T. Fan, K.M. Dorney, A. Becker, A. Jaro -Becker, H.C. Kapteyn, M.M. Murnane, and C.G. Durfee, *Noncollinear generation of angularly isolated circularly polarized high harmonics*, Nature Photonics (accepted for publication).

Probing Complexity using the LCLS and the ALS

Nora Berrah

Physics Department, University of Connecticut, Storrs, CT 06268

e-mail:nora.berrah@uconn.edu

Program Scope

The goal of our research program is to investigate *fundamental interactions between photons and molecular systems* to advance our quantitative understanding of electron correlations, charge transfer and many body phenomena. Our research investigations focus on probing on femtosecond time-scale multi-electron interactions and tracing nuclear motion in order to understand and ultimately control energy and charge transfer processes from electromagnetic radiation to matter. Most of our work is carried out in a strong partnership with theorists.

Our current interests include: **1)** The study of non linear and strong field phenomena in the x-ray regime using free electron lasers (FELs), and in particular, the ultrafast linac coherent light source (LCLS) x-ray FEL facility at the SLAC National Laboratory. **2)** Time-resolved molecular dynamics investigations using pump-probe techniques. Our experiments probe physical and chemical processes that happen on femtosecond time scales. This is achieved by measuring and examining both electronic and nuclear dynamics subsequent to the interaction of molecules and clusters with LCLS pulses of various (4-500 fs) pulse duration. **3)** The study of dynamics and correlated processes in select molecules as well as anions with vuv-soft x-rays from the Advanced Light Source (ALS) at Lawrence Berkeley Laboratory.

We present below results completed and in progress this past year and plans for the immediate future.

Recent Progress

1) Fragmentation Dynamics of Endohedral Fullerene $\text{Ho}_3\text{N}@C_{80}$ Ionized with Intense and Short X-Ray FEL Pulses

Investigations of the ionization and fragmentation dynamics of nano-size fullerenes subjected to ultrashort strong x-ray laser field from FELs are nascent [pub11,12]. They are important from a fundamental view point since we learn about how the deposited energy is shared within many degrees of freedom in a strongly correlated system. These investigations are also important for understanding the mechanisms of radiation damage that will benefit the development of bio-imaging techniques and radio-therapies. Recently, we reported on a multi-photon absorption and fragmentation investigation of C_{60} [pub 11,12] using intense 480 eV photons from the LCLS with 4, 30, and 90 fs pulse duration. Although the dynamics were complicated because of the number of electrons and atoms involved, the experimental results could be well reproduced by molecular dynamics (MD) modeling with electronic structure and nuclear motion taken into account [pub11,12]. To push the complexity further in our quest to understand multi-photon absorption and ionization dynamics of intermediate size molecules, we extended our multi-photon investigations to endohedral fullerenes, $\text{Ho}_3\text{N}@C_{80}$.

The experiment was carried out at the AMO hutch at the LCLS. Gas phase $\text{Ho}_3\text{N}@C_{80}$ molecules were evaporated from a heated oven and interacted with intense x-ray laser pulses. The photon energy of the x-rays was chosen at 1530 eV to optimize the ionization from the 3d shell in the Ho atoms, which were encapsulated in C_{80} cages along with a nitrogen atom in the center. The pulse duration of the FEL was set to 80 fs and the pulse energy was nominally 2.2 mJ. The x-rays

were focused to a spot approximately $5\mu\text{m}\times 5\mu\text{m}$ which delivered less fluence than in the case of the C_{60} experiment [pub11,12]. Parent ions up to quintuply charged $\text{Ho}_3\text{N}@C_{80}^{5+}$ were observed, suggesting a stable structure even with 5 charges on the parent molecule. Atomic Ho^+ ions, originating from the encapsulated Ho_3N molecule, were observed with the highest yield compared to other fragments and parent ions.

The present analysis of the data seems to indicate that additional fragmentation mechanisms occur either sequentially or simultaneously because we also observed the parent molecule multiply ionized, having lost C atoms. We measured $\text{Ho}_3\text{N}@C_m^{n+}$; $n=2,3$ and $m=78, 76, 70$ and 50 . These weak fragments most probably lost C dimers, similarly to what has been observed in previous intense IR laser work [a]. We also observed weak mixed molecular fragment indicating that the Ho atom formed carbon and nitrogen bonds since we observe HoCN^+ , HoC_2^+ , HoC_4^+ , and HoC_3N^+ albeit in small quantities. The fragmentation dynamics observed is unlike the case of the C_{60} experiment. This leads us to believe that under the present experimental conditions, only a few multiphoton ionization cycles led to the Ho_2^+ and C_3^+ charge states as well as carbon ion chains indicative of low fluence ionization. This multiphoton ionization regime is quite different from the near-complete atomization occurring at high-fluence short-pulse conditions [pub11,12]; here one observes a more intricate dynamics with bonds breaking (Ho-N, C-C) and new bond forming (Ho-C₂, HoCN, HoC₄, HoC₃N) [pub 1]. We are planning a follow up experiment to understand in details, as a function of fluence, the time-resolved ionization dynamics of this molecule.

2) Inner-shell photodetachment from carbon chain negative ions

Studies of single-photon inner-shell photodetachment of carbon chain negative ions are intriguing because anions are strongly correlated systems. The role of the extra electron can be examined as a function of the cluster size and of the chosen ionized inner shell. This work challenges theories but is also relevant to applications in astrophysics, material science and the biosciences. Recent observations of carbon chains in the interstellar medium and renewed interest in carbon materials have led to multiple theoretical studies of homonuclear carbon chains as well as their ionic forms.

We have carried out x-ray photodetachment from C_n^- with $n = 2 - 10$ for K-shell electrons using 274-296 eV photons from the ALS and inner valence photodetachment with 25-90 eV photons energy. Carbon chain anions were produced in a SNICS II negative ion source and mass analyzed. The collimated ion beam was then overlapped with the photon beam at Beamline 10.0.1 and 8.0.1 at the ALS. The resulting positive ions were collected and analyzed to get both absolute cross sections and branching ratios for the dissociation products. Comparisons of the new carbon chain data show similar resonance features to the atomic carbon negative ion shape resonance that we observed just above the K-shell photodetachment threshold near 282 eV [b, c]. In addition to the resonance features seen in the singly charged positive ion channel, we observed the doubly-charged positive chains C_3^{2+} and C_5^{2+} . We believe these to be the first observations of photon induced triple-detachment producing such small, stable molecular products. The C_3^{2+} product must have a lifetime of at least 13 fs in order to be observed in our experiment. The C_5^{2+} product is believed to be the smallest stable carbon dication [d]. Single-photon ejection of three electrons producing small doubly charged anions has not been expected and further theoretical and experimental investigations are needed for this system. This data is presently being analyzed.

References

[a] O. Johansson, et al., *J. Chem. Phys.* **139**, 084309 (2013)

[b]N. D. Gibson et al., N. Berrah *Phys. Rev. A* **67** 030703(R) (2003)

[c] C. W. Walter et al., N. Berrah, *Phys. Rev. A* **73** 062702 (2006)

[d] D. Tendero et al 2006 *Brazilian J. Phys.* **36** 529 (2006)

Future Plans.

The principal areas of investigation planned for the coming year are:

1) Prepare the approved LCLS experiment scheduled for February 2016. 2) Finish writing the paper resulting from the x-ray split and delay (XRSD) instrument commissioning data collected during our LCLS beamtime. 3) Finish writing the paper from the LAMP LCLS instrument commissioning beamtime. 4) Start writing the paper from the analyzed ALS K-shell photodetachment data in C_{60}^- . 5) Analyze the new data we generated during the summer of 2015 when we conducted the K-shell photodetachment experiments of the carbon anions chain (C_2^- - C_{12}^-) at the ALS.

Publications from DOE Sponsored Research

1. N. Berrah, B. Murphy, H. Xiong, L. Fang, T. Osipov, E. Kukkk, M. Guehr, R. Feifel, V. S. Petrovic, K. R. Ferguson, J. D. Bozek, C. Bostedt, L. J. Frasinski, P. H. Bucksbaum and J. C. Castagna, "Femtosecond x-ray induced fragmentation of fullerenes" *J. of Mod. Opt.* (in press 2015).
2. N. Berrah and P. H. Bucksbaum, Update on "The Ultimate X-ray Machine" *Scientific American* Special Issue, devoted to Physics, 112 pages that include about 15 of the most intriguing physics articles that *Scientific American* has published in recent years, (in Press, 2015).
3. P. Bucksbaum and N. Berrah, *Physics Today*, **68** (7), 26 July 2015.
4. N. Berrah and L. Fang "Chemical Analysis: Double Core-Hole Spectroscopy with Free-Electron Lasers" *J. Electr. Spect. And Rel. Phenom.* (in press, 2015)
5. C. E. Liekhus-Schmaltz, I. Tenney, T. Osipov, A. Sanchez-Gonzalez, N. Berrah, R. Boll, et al., P.H. Bucksbaum, V. Petrovic et al., "Ultrafast Isomerization Initiated by X-Ray Core Ionization" (*Nature Commun.* Accepted).
6. M. Mucke, V. Zhaunerchyk, L.J. Frasinski, R.J.Squibb, M. Siano, J.H.D. Eland, P. Linusson, P. Salen, P. v.d. Meulen, R.D. Thomas, M. Larsson, L. Foucar, J. Ullrich, K. Motomura, S. Mondal, K.Ueda, T. Osipov, L. Fang, B.F. Murphy, N Berrah, et al., and R. Feifel, "Covariance mapping of two-photon double core hole states in C_2H_2 and C_2H_6 produced by an X-ray free electron laser" *New Journal of Physics (IOP)* (in press 2015).
7. F. Penent, M. Nakano, M. Tashiro, T. P. Grozdanov, M. Žitnik, K. Bucar, S. Carniato, P. Selles, L. Andric, P. Lablanquie, J. Palaudoux, E. Shigemasa, H. Iwayama, Y. Hikosaka, K. Soejima, I.H. Suzuki, N. Berrah, A. Wuosmaa, T. Kaneyasu and K. Ito, "Double core hole spectroscopy with synchrotron radiation" *J. Electr. Spect. and Relat. Phenom.* (in press 2015).
8. A. Dubrouil, M. Reduzzi, M. Devetta, C. Feng, J. Hummert, P. Finetti, O. Plekan, C. Grazioli, M. Di Fraia, V. Lyamayev, A. La Forge, R. Katzy, F. Stienkemeier, Y. Ovcharenko, M. Coreno, N. Berrah, et al., and G. Sansone, "Nonlinear resonant excitation of interatomic Coulombic decay in neon dimers", Special issue in *JPB "Frontiers of Free-Electron Laser (FEL) Science-II"* (accepted, 2015).
9. L Fang, Z Jurek, T Osipov, B F Murphy, R Santra, and N Berrah, "Investigating Dynamics of Complex System Irradiated by Intense X-ray Free Electron Laser Pulses", *Journal of Physics: Conference Series* **601**, 012006 (2015).
10. Marc. Humphrey, Paul V. Pancella and Nora Berrah, "Idiots Guides for Quantum Physics", ALPHA Books publishing, ISBN 97781615643172, Jan 6, 2015.
11. B. F. Murphy, T. Osipov, Z. Jurek, L. Fang, S.-K. Son, L. Avaldi, P. Bolognesi, C. Bostedt, J. Bozek, R. Coffee, J. Eland, M. Guehr, J. Farrell, R. Feifel, L. Frasinski, J. Glowina, D.T. Ha, K.

- Hoffmann, E. Kukk, B. McFarland, C. Miron, M. Mucke, R. Squibb, K. Ueda, R. Santra, and N. Berrah “Bucky ball explosion by intense femtosecond x-ray pulses: a model system for complex molecules”, *Nature Communication*, **5**, 4281, doi:10.1038/ncomms 5281 (2014)
12. N. Berrah, L. Fang, T. Osipov, Z. Jurek, B. F. Murphy, and R. Santra, *Faraday Discussion*, “Emerging photon technologies for probing ultrafast molecular dynamics” *Faraday Discuss.*, **171**, 471 (2014)
 13. N. Berrah and P. H. Bucksbaum, “The Ultimate X-ray Machine” *Scientific American*, **310**, 64, January 2014.
 14. B. K. McFarland, J. P. Farrell, S. Miyabe, F. Tarantelli, A. Aguilar, N. Berrah, C. Bostedt, J. Bozek, P.H. Bucksbaum, J. C. Castagna, R. Coffee, J. Cryan, L. Fang, R. Feifel, K. Gaffney, J. Glownia, T. Martinez, M. Mucke, B. Murphy, A. Natan, T. Osipov, V. Petrovic, S. Schorb, Th. Schultz, L. Spector, M. Swiggers, I. Tenney, S. Wang, W. White, J. White and M. Gühr “Delayed Ultrafast X-ray Auger Probing (DUXAP) of Nucleobase Ultraviolet Photoprotection”, *Nature Communication*, **5**, 4235, doi:10.1038/ncomms5235 (2014)
 15. L. Fang, D. Rolles, A. Rudenko, V. Petrovich, C. Bostedt, J. D. Bozek, P. Bucksbaum and N. Berrah “Probing ultrafast electronic and molecular dynamics with free electron lasers” *J. Phys. B: At. Mol. Opt. Phys.* **47** 124006 (2014) doi:10.1088/0953-4075/47/12/124006
 16. M. Mucke, V. Zhaunerchyk, R.J. Squibb, M. Kamiska, J.H.D. Eland, P. v.d.Meulen, P. Salén, P. Linusson, R.D. Thomas, M. Larsson, L.J. Frasinski, M. Siano, T. Osipov, L. Fang, B. Murphy, N. Berrah, et al., and R. Feifel, “Mapping the decay of double core hole states of atoms and molecules”, *Journal of Physics: Conference Series* **488**, 032021 (2014).
 17. N. Berrah, L. Fang, T. Osipov, B. Murphy, C. Bostedt, and J.D. Bozek, “Multiphoton Ionization and Fragmentation of Molecules with the LCLS X-Ray FEL” *J. Elec. Spect. And Rela. Phen.*, **196**, 34-37, doi:10.1016/j.elspec.2013.10.009 (2014).
 18. B.K. McFarland, N. Berrah, C. Bostedt, J. Bozek, P. H. Bucksbaum, et al., and M Gühr, “Experimental strategies for optical pump – soft x-ray probe experiments at the LCLS” *J. Phys.: Conf. Ser.* **488** 012015 doi:10.1088/1742-6596/488/1/012015(2014).
 19. R. C. Bilodeau, N. D. Gibson, C. W. Walter, D. A. Esteves-Macaluso, S. Schippers, A. Muller, R. A. Phaneuf, A. Aguilar, M. Hoener, J. M. Rost, and N. Berrah, “Single-Photon Multiple-Detachment in Fullerene Negative Ions: Absolute Ionization Cross Sections and the Role of the Extra Electron”, *Phys. Rev. Lett.* **111**, 043003 (2013).
 20. L.J. Frasinski, V. Zhaunerchyk, M. Mucke, R.J. Squipp, M. Siano, J.H.D. Eland, P. Linusson, P.v.d. Meulen, P. Salén, R.D. Thomas, M. Larsson, L. Foucar, J. Ullrich, K. Motomura, S. Mondal, K. Ueda, T. Osipov, L. Fang, B.F. Murphy, N. Berrah, C. Bostedt, et al., and R. Feifel *Phys. Rev. Lett.* **111**, 073002 (2013).
 21. V. Zhaunerchyk, M. Mucke, P. Salén, P.v.d. Meulen, M. Kaminska, R.J. Squipp, L.J. Frasinski, M. Siano, J.H.D. Eland, P. Linusson, R.D. Thomas, M. Larsson, L. Foucar, J. Ullrich, K. Motomura, S. Mondal, K. Ueda, T. Osipov, L. Fang, B.F. Murphy, N. Berrah, C. Bostedt, et al., and R. Feifel *J. Phys. B: At. Mol. Opt. Phys.* **46**, 164034 (2013).
 22. C. Bostedt, J. D. Bozek, P. H. Bucksbaum, R. N. Coffee, J. B. Hastings, Z. Huang, R. W. Lee, S. Schorb, J. N. Corlett, P. Denes, P. Emma, R. W. Falcone, R. W. Schoenlein, G. Doumy, E. P. Kanter, B. Kraessig, S. Southworth, L. Young, L. Fang, M. Hoener, N. Berrah, C. Roedig, and L. F. DiMauro, *J. Phys. B: At. Mol. Opt. Phys.* **46**, 164003 (2013).
 23. T Osipov, L Fang, B Murphy, F Tarantelli, E R Hosler, E Kukk, J D Bozek, C Bostedt, E P Kanter and N Berrah, ” Multiphoton ionization and fragmentation of SF₆ induced by intense free electron laser pulses”, *J. Phys. B: At. Mol. Opt. Phys.* **46**, 164032 (2013).
 24. M. Larsson, P. Salén, P. van der Meulen, H. T. Schmidt, R. D. Thomas, R. Feifel, L. Fang, B. Murphy, T. Osipov, N. Berrah, et al., and K. C. Prince, “Double core-hole formation in small molecules at the LCLS free electron laser” *J. Phys. B: At. Mol. Opt. Phys.* **46**, 164030 (2013).
 25. J.C. Castagna, B. Murphy, J. Bozek, and N. Berrah, “X-ray split and delay for soft x-rays at LCLS”, *Journal of Physics:Conference Series* **425** 152021, (2013).

Ultrafast Electron Diffraction from Aligned Molecules

Martin Centurion

Department of Physics and Astronomy, University of Nebraska, Lincoln, NE 68588-0299
mcenturion2@unl.edu

Program Scope

The aim of this project is to capture the three-dimensional structure of isolated molecules during an ultrafast reaction using electron diffraction. A femtosecond laser pulse triggers the dynamics and a femtosecond electron pulse scatters from the sample and produces a diffraction pattern in a laser-pump electron-probe configuration. The structural information is retrieved from the diffraction patterns. If the molecules are pre-aligned with a laser pulse, the three-dimensional structure of the molecule can be retrieved with sub-Angstrom resolution.

Introduction

The majority of known molecular structures have been determined using either x-ray diffraction for crystallized molecules or Nuclear Magnetic Resonance (NMR) spectroscopy for molecules in solution. However, for isolated molecules there has been no method demonstrated to measure the three dimensional structure. Electron diffraction has been the main tool to determine the structure of molecules in the gas phase [1] and also to investigate dynamics on picosecond time scales [2-4]. Diffraction patterns from randomly oriented molecules contain only one-dimensional information, and thus input from theoretical models is needed to recover the structure. The diffraction pattern is compared with a calculated structure iteratively until an appropriate match between experiment and theory is found.

We have recently demonstrated that the full molecular structure can be retrieved from diffraction patterns of aligned molecules, without any previous knowledge of the structure [5]. The molecules were impulsively aligned with a femtosecond laser pulse and probed with femtosecond electron pulses in a field-free environment at the peak alignment. This ensures that the molecules are not distorted by the laser field when the structure is probed by the electron pulse. In order to retrieve a molecular image from a single diffraction pattern the degree of alignment needed is much higher than what can be achieved experimentally. While the structure cannot be retrieved from a single pattern, we have developed a new two-step retrieval algorithm that can retrieve the structure even with a limited degree of alignment. The first step in the method is a deconvolution to retrieve the diffraction pattern corresponding to perfectly aligned molecules from multiple input diffraction patterns with partial alignment, using a genetic algorithm. The second step is to reconstruct the molecular structure from the deconvolved diffraction pattern. An iterative phase retrieval algorithm in three-dimensional (3-D) cylindrical space is used to reconstruct the full 3-D molecular structure. We have shown numerically that the

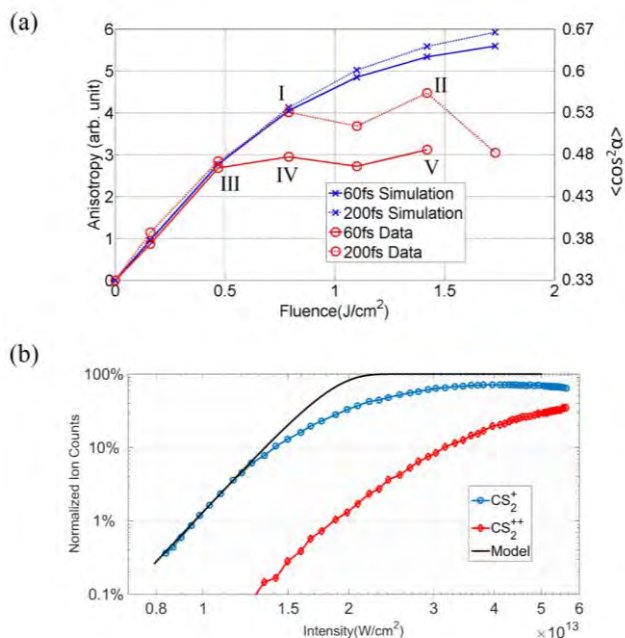


Figure 1. (a) Anisotropy/alignment parameter $\langle \cos^2 \alpha \rangle$ versus fluence. The blue curves are simulation results, and the red curves are experimental data. The solid and dashed curves represent pulse durations of 60 and 200 fs, respectively. The points labeled by roman numerals will be discussed below. (b) Number of detected singly ionized molecules, CS_2^+ (blue circles), and the doubly ionized molecules CS_2^{++} (red diamonds) as a function of laser intensity. The error bars are smaller than the symbols. To account for small pressure fluctuations, the raw counts are normalized to the average pressure for the corresponding data set. The black curve is a model for a 7-photon multiphoton ionization process that was used to fit the data

alignment continues to increase (Figure 1a). The ionization state of the sample was measured using femtosecond laser mass spectrometry, and the results showed that the saturation of alignment happens at intensities well below the ionization threshold (Figure 1b).

structure of trifluorotoluene ($C_6H_5CF_3$), an asymmetric-top molecule, can be retrieved successfully [6].

Recent Progress

We have used UED to capture the angular distribution and structural changes in molecules due to the interaction with intense laser pulses [7]. We have investigated a range of laser intensities (10^{12} - 10^{13} W/cm^2) relevant for many experimental methods that involve alignment and/or ionization of molecules. CS_2 was used a model molecule because the angular distribution and interatomic distances can be retrieved directly from the diffraction patterns without the need of iterative algorithms. This simplifies the data analysis and allows us to focus on dynamics.

From the diffraction patterns, we were able to characterize the dependence of the alignment on both the intensity and fluence of the laser pulses. We have compared the experimental results with simulations of the alignment, and seen that experimentally the alignment saturates at intensities well below 10^{13} W/cm^2 , while in the simulation the

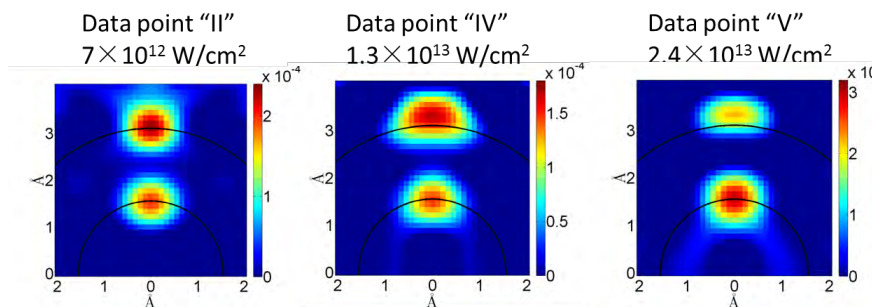


Figure 2. Molecular structure retrieved from difference diffraction patterns. The lower spot corresponds to the C-S distance, while the upper spot corresponds to the S-S distance. In the first image, the structure matches that of the ground state, while in the images at higher intensity the interatomic distances are larger, in agreement with two-photon excited states.

(approximately 1 ps after the laser). This method captures changes in the structure that take place as the intensity is increased. The changes in the structure were determined from the Fourier transform of the difference-diffraction patterns (Figure 2). The first panel in Figure 2 shows the retrieved structure corresponding to point II in Figure 1a. This structure is in good agreement with the ground state structure within the uncertainty of the measurement of 0.03 Å. For higher intensities, the bond lengths become longer than the ground state by approximately 0.1 Å. The longer bond length is consistent with two-photon excited states of CS₂. The resolution of the measurement was 1.0 ps, which prevented us from capturing the dynamics of the change in bond lengths. We also saw evidence dissociation into neutral fragments at high intensities.

We are working to improve the temporal resolution to capture the motion of the nuclei during conformation changes in molecules. We are collaborating with Xijie Wang and Markus Guehr to build a gas-phase UED experiment using the existing MeV electron gun at the Asta test facility at SLAC. This RF gun can deliver ~ 100 fs electron pulses with an energy between 2 MeV to 5 MeV. UED with relativistic electrons offers two advantages: it minimizes the velocity mismatch between laser and electrons and reduces the spreading of the pulse due to Coulomb forces. The velocity mismatch can be significant for keV electron pulses, degrading the resolution by several hundred femtoseconds, while for MeV electrons the effect is negligible. The RF gun accelerates electrons in a time-dependent electric field, so the temporal resolution is limited by both the duration of electron pulses and jitter in the time of arrival of the electrons at the sample. The project started in July of 2014, and we have finished the design and construction of an experimental chamber for gas-phase UED experiments.

The first run of experiments has finished successfully. In the first experiment, we used a laser pulse to excite a rotational wavepacket in nitrogen molecule, and used UED to follow the dynamics. The performance of the instrument was characterized and we succeeded to demonstrate a temporal resolution of 100 fs RMS (230 fs FWHM) and a spatial resolution of 0.8

We have observed a distortion of the molecular structure for intensities above 10^{13} W/cm². Difference-diffraction patterns were generated by taking the difference between patterns at high intensity and patterns at low intensity. The patterns used were captured at the time of maximum alignment

Å (a manuscript on this work has been submitted). Further experiments are currently ongoing in imaging a vibrational wavepacket in iodine, which will be the first spatially resolved imaging of coherent motion of a nuclear wavepacket.

Future Plans

We will continue to investigate molecular dynamics with UED, both in the setup in our local lab in Lincoln and at SLAC. In Lincoln, a new setup will be used to further investigate the alignment process and to capture the structure of transient intermediate states in photo-reactions. At SLAC, we are planning some improvements in the setup and a second round of experiments next year. We expect to demonstrate full three-dimensional imaging of molecules with sub-Angstrom and improved temporal resolution.

References

- [1] I. Hargittai, M. Hargittai, Stereochemical Applications of Gas-Phase Electron Diffraction, VCH Publishers Inc, New York (1988).
- [2] H. Ihee et al, Science 291, 458 (2001).
- [3] R. Srinivasan et al, Science 307, 558 (2005).
- [4] P. Reckenthaeler et al, Phys. Rev. Lett. 102, 213001 (2009).
- [5] C. J. Hensley et al, Phys. Rev. Lett. 109, 133202 (2012).
- [6] J. Yang, et al, Struct. Dyn. 1, 044101 (2014).
- [7] J. Yang et al, Nat. Commun. 6, 8172 (2015).

Publications of DOE sponsored research in the past 3 years

1. P. Hansen, C. Baumgarten, H. Batelaan, M. Centurion, "Dispersion Compensation for Attosecond Electron Pulses," Appl. Phys. Lett. **101**, 083501 (2012).
2. C. J. Hensley, J. Yang, M. Centurion., "Imaging of Isolated Molecules with Ultrafast Electron Pulses" Phys. Rev. Lett. **109**, 133202 (2012). *Featured in APS Physical Review website on 9/28/2012 as a Focus Story.*
3. J. Yang, V. Makhija, V. Kumarappan, M. Centurion, "Reconstruction of three-dimensional molecular structure from diffraction of laser-aligned molecules," Struct. Dyn. **1**, 044101 (2014).
4. J. Yang, M. Centurion, "Gas-phase electron diffraction from laser-aligned molecules" Structural Chemistry (2015) Published online: DOI 10.1007/s11224-015-0650-4.
5. S. P. Weathersby, G. Brown, M. Centurion et al, "Mega-electron-volt ultrafast electron diffraction at SLAC National Accelerator Laboratory" Rev. Sci. Inst. **86**, 073702 (2015).
6. J. Yang, J. Beck, C. J. Uiterwaal, M. Centurion, "Imaging of alignment and structural changes of carbon disulfide molecules using ultrafast electron diffraction" Nat. Commun. **6**, 8172 (2015).

Atomic and Molecular Physics in Strong Fields

Shih-I Chu
Department of Chemistry, University of Kansas
Lawrence, Kansas 66045
E-mail: sichu@ku.edu

Program Scope

In this research program, we address the fundamental physics of the interaction of atoms and molecules with intense ultrashort laser fields. The main objectives are to develop new theoretical formalisms and accurate computational methods for *ab initio* nonperturbative investigations of multiphoton quantum dynamics and very high-order nonlinear optical processes of one-, two-, and many-electron quantum systems in intense laser fields, taking into account detailed electronic structure information and electron-correlated effects. Particular attention will be paid to the exploration of the effects of electron correlation on high-harmonic generation (HHG) and multiphoton ionization (MPI) processes, multi-electron response, and underlying mechanisms responsible for the strong-field ionization of diatomic and small polyatomic molecules, as well as the development of new time-frequency transform, and optimal control algorithms for the coherent control of HHG processes for the generation of shorter and stronger attosecond laser pulses.

Recent Progress

1. Subcycle Transient HHG Dynamics and Spectroscopy in the Attosecond Time Domain

The recent development of attosecond metrology has enabled the real-time experimental observation of ultrafast electron dynamics and transient sub-cycle spectroscopy in atomic and molecular systems. While there are some recent experimental and theoretical studies of subcycle transient absorption, there has been no study of the subcycle transient behavior of the harmonic emission. We have recently initiated such a direction by extending the *self-interaction-free* TDDFT [1,2] with proper exchange-correlation (xc) energy functional, allowing the correct long-range asymptotic behavior, and the time-dependent generalized pseudospectral (TDGPS) method [1,3] for the first *ab initio* study of the subcycle HHG dynamics of He atoms [1]. We explored the dynamical behavior of the subcycle HHG for transitions from the excited states to the ground state and found oscillation structures with respect to the time delay between the single extreme ultraviolet (XUV) attosecond pulse (SAP) and near-infrared (NIR) fields. The oscillatory pattern in the photon emission spectra has a period of ~ 1.3 fs which is half of the NIR laser optical cycle, similar to that recently measured in the experiments on transient absorption of He [4]. We present the photon emission spectra from $1s2p$, $1s3p$, $1s4p$, $1s5p$, and $1s6p$ excited states as functions of the time delay. We explore the subcycle a. c. Stark shift phenomenon in NIR fields and its influence on the photon emission process. Our analysis uncovers the mechanisms responsible for the observed peak splitting in the photon emission spectra.

More recently, we have further extended the *subcycle* HHG study to the Ar atoms [5]. We present and analyze the harmonic emission spectra from $3snp_0$, $3p_0ns$, $3p_1nd_1$, $3p_1np_1$, $3p_0nd_0$, $3p_0np_0$, and $3p_0ns$ excited states and the $3p_04p_0^-$ virtual state as functions of the time delay. In addition, we explore the subcycle a.c. Stark shift phenomenon in NIR fields and its influence on the harmonic emission process. Our analysis reveals several novel features of the subcycle HHG dynamics and spectra as well as temporal energy level shift.

2. Subcycle Transient Multiphoton Ionization in the Attosecond Time Domain

In early experiments on multiphoton ionization (MPI) and above-threshold ionization (ATI), research has focused on the properties of the emitted electrons in the *energy* domain (electron energy spectra, which manifest the famous ATI peak structure). However, recent advances in laser technology opened the possibility of clocking

the electron dynamics on an attosecond scale in the *time* domain. The time-domain analysis can uncover novel new and unexplored features in the well-researched phenomenon of MPI/ATI. In a recent work, we have performed the first fully *ab initio* exploration of the *subcycle* transient MPI dynamics of atomic and molecular systems subject to intense near-IR fields on the sub-femtosecond time scale [6]. MPI bursts within a single optical cycle are found in the time-dependent ionization rates not only for diatomic molecules H_2^+ and HHe^{2+} , but also for the H atom. The analysis of the electron density reveals that several distinct density portions can be shaped and detached from the target within a half cycle of the laser field. We note that the structures of the MPI rates in the time domain discussed in this paper are not related to the above-threshold peak structures of the electron spectra in the energy domain. When created under the influence of the external field, the portions of the outgoing wave packet are localized in space and time but contain various energy contributions. That is why the shape of the structure is changed as the outgoing wave packet moves away from the core. The structures described above can be observed on the nanometer length scale.

3. High Precision Study of HHG of H_2^+ in Intense Elliptically Polarized Laser Fields

We present an *ab initio* 3D precision calculation and analysis of HHG of the hydrogen molecular ion subject to intense elliptically polarized laser pulses by means of the time-dependent generalized pseudospectral method in two-center prolate spheroidal coordinates [7]. The calculations are performed for the ground and first excited electronic states of H_2^+ at the equilibrium internuclear separation $R = 2$ a.u. as well as for the stretched molecule at $R = 7$ a.u. The spectral and temporal structures of the HHG signal are explored by means of the wavelet time-frequency analysis. Several novel aspects of ellipticity-dependent dynamical behaviors are uncovered. We found that the production of above-threshold harmonics for nonzero ellipticity is generally reduced, as compared with linearly polarized fields. However, below-threshold harmonics still appear quite strong except when the polarization plane is perpendicular to the molecular axis. Weak even harmonics are detected in the HHG spectra of stretched molecules. This effect can be explained by the broken inversion symmetry due to dynamic localization of the electron density near one of the nuclei. Multiphoton resonance and two-center interference effects are analyzed for the exploration of the quantum origin of the predicted HHG spectral and dynamical behavior [7].

4. Coherent Phase-Matched VUV Generation by Field-controlled Bound States and Dynamical Origin of Near- and Below-Threshold Harmonic Generation of Atoms in an Intense Mid-IR Laser Field

HHG has been the enabling technology for ultrafast science in the VUV and soft-X-ray spectral regions. Recently, ultrafast sources of below-threshold harmonics, with photon energies below the target ionization potential, have been demonstrated. Such harmonics are critical to the extension of time-resolved photoemission spectroscopy to megahertz repetition rates and to the development of high-average-power VUV sources, because they can be generated with relatively low driving laser intensities ($\sim 1 \times 10^{13}$ W/cm²). Ultrafast VUV sources of low-order harmonics are also critical tools for studying wave packet dynamics in bound states of atoms and molecules. However, compared to the high-order above-threshold harmonics, which have been extensively studied, little attention has been devoted to the development and characterization of below-threshold harmonic sources. Recently in collaboration with the experimental group led by Dr. Z. Chang in UCF, we extend our *self-interaction-free* time-dependent density functional theory (TDDFT) [1,2] and generalized Floquet formalism [8] and demonstrate a new regime of phase-matched below-threshold harmonics generation, for which the generation and phase matching is enabled only near Stark-shifted resonance structures of the atomic target [9]. The coherent VUV line emission exhibits sub-100 meV linewidth, low divergence and quadratic growth with increasing target density, and can be controlled by the sub-cycle field of a few-cycle driving laser with intensity of only 10^{13} W/cm², which is achievable directly from few-cycle femtosecond oscillators with nano Joule energy. This work opens the door to the future development of compact, high flux and ultrafast VUV light sources without the need for cavity or nanoplasmonic enhancement. This work has been recently published in Nature Photonics [9].

More recently we have presented an *ab initio* investigation of the below-threshold harmonics (BTHs) of

helium atoms in few-cycle IR laser fields by accurately solving the time-dependent Schrödinger equation and Maxwell's equation simultaneously [10]. We find that the enhancement of the BTH can occur only near the resonance structure of He, for which this mechanism is in agreement with the recent experimental study [9]. Moreover, we introduce a new time-frequency method, the *synchrosqueezed transform* (SST) [11], for the accurate analysis of the time-frequency HHG spectrum below the threshold. Our results uncover the dynamical origin of near- and below- threshold harmonics as well as the role of multi-rescattering trajectories to the resonance-enhanced BTH [10].

5. Sub-cycle Oscillations in Virtual States Brought to Light

Understanding and controlling the dynamic evolution of electrons in matter is among the most fundamental goals of attosecond science. While the most exotic behaviors can be found in complex systems, fast electron dynamics can be studied at the fundamental level in atomic systems, using moderately intense ($\leq 10^{13}$ W/cm²) lasers to control the electronic structure in proof-of-principle experiments. In cooperation with the UCF experimental group, we probe the transient changes in the absorption of an isolated attosecond extreme ultraviolet (XUV) pulse by helium atoms in the presence of a delayed, few-cycle near infrared (NIR) laser pulse, which uncovers absorption structures corresponding to laser-induced “virtual” intermediate states in the two-color two-photon (XUV + NIR) and three-photon (XUV + NIR + NIR) absorption process [4]. These previously unobserved absorption structures are modulated on half-cycle (~ 1.3 fs) and quarter-cycle (~ 0.6 fs) time scales, resulting from quantum optical interference in the laser-driven atom.

6. Coherent Control of the Electron Quantum Paths for the Optimal Generation of Single Ultrashort Attosecond Laser Pulse

We recently report a new mechanism and experimentally realizable approach for the coherent control of the generation of an isolated and ultrashort attosecond (*as*) laser pulse from atoms by means of the optimization of the two-color [12] and three-color [13] laser fields with proper time delays. Optimizing the laser pulse shape allows the control of the electron quantum paths and enables high-harmonic generation from the long- and short-trajectory electrons to be enhanced and split near the cutoff region. Then we further investigated the effect of macroscopic propagation on the supercontinuum harmonic spectra and the subsequent attosecond-pulse generation [14]. The effects of macroscopic propagation are investigated in near and far field by solving Maxwell's equation. The results show that the contribution of short-trajectory electron emission is increased when the macroscopic propagation is considered. However, the characteristics of the dominant long-trajectory electron emission (in the single-atom response case) are not changed, and an isolated and shorter *as* pulse can be generated in the near field. Moreover, in the far field, the contribution of long-trajectory electron emission is still dominant for both on-axis and off-axis cases. As a result, an isolated and shorter *as* pulse can be generated directly.

More recently, we propose an efficient method for the generation of ultrabroadband supercontinuum spectra and isolated ultrashort attosecond laser pulses from He atoms with two-color mid-infrared laser fields [15]. An accurate model potential is constructed which reproduces ground and high-lying singly excited states as well as oscillator strength of the He atom to a high precision. We found that the optimizing two-color mid-IR laser pulse allows the HHG cutoff to be significantly extended, leading to the production of an ultrabroadband supercontinuum. As a result, an isolated 18-attosecond pulse can be generated directly by the superposition of the supercontinuum harmonics.

7. We have completed several invited review articles on the recent development of *self-interaction-free* time dependent density functional theory (TDDFT) for the nonperturbative treatment of atomic and molecular multiphoton processes in intense ultrashort laser fields in the past 3 years [16-19].

Future Research Plans

In addition to continuing the ongoing researches discussed above, we plan to initiate the following several new project directions: (a) Extension of the exploration of the coherent control and giant enhancement of MPI and HHG driven by intense frequency-comb laser fields [20, 21] to rare gas atoms. (b) Extension of the TDGPS method in momentum space [22, 23] to the study of HHG/ATI processes in intense free electron x-ray laser fields. (c) Development of Bohmian mechanics approach [24] for the exploration of the electron quantum dynamics associated with HHG/MPI processes. (d) Development of nonperturbative methods for the accurate treatment of transient absorption and subcycle HHG dynamics in NIR+ XUV attosecond pulses. (e) Development of new time-frequency method, the *synchrosqueezing transform* (SST) [10, 11], for the exploration of the novel quantum dynamics for below- and near- threshold harmonics of diatomic molecules.

References Cited (* Publications supported by the DOE program in the period of 2012-2015).

- *[1] J. Heslar, D. A. Telnov, and S. I. Chu, Phys. Rev. A **89**, 052517 (2014).
- [2] S. I. Chu, J. Chem. Phys. **123**, 062207 (2005).
- [3] X. M. Tong and S. I. Chu, Chem. Phys. **217**, 119–130 (1997).
- *[4] M. Chini, X. Wang, Y. Cheng, Y. Wu, D. Zhao, D. A. Telnov, S. I. Chu, and Z. Chang, Sci. Rep. **3**, 1105 (2013).
- *[5] J. Heslar, D.A. Telnov, and S. I. Chu, Phys. Rev. A **91**, 023420 (2015).
- *[6] D.A. Telnov, K.N. Avanaki, and S. I. Chu, Phys. Rev. A **90**, 043404 (2014).
- *[7] K.N. Avanaki, D.A. Telnov, and S. I. Chu, Phys. Rev. A **90**, 033425 (2014).
- [8] S. I. Chu and D. A. Telnov, Phys. Rep. **390**, 1-131 (2004).
- *[9] M. Chini, X. Wang, Y. Cheng, H. Wang, Y. Wu, E. Cunningham, P.-C. Li, J. Heslar, D.A. Telnov, S.I. Chu, and Z. Chang, Nature Photonics **8**, 437 (2014).
- *[10] P. C. Li, Y. L. Sheu, C. Laughlin, and S. I. Chu, Phys. Rev. A **90**, 041401(R) (2014)
- *[11] Y.L. Sheu, L.Y. Hsu, H.T. Wu, P. C. Li, and S.I. Chu, AIP Advances **4**, 117138 (2014)
- *[12] I. L. Liu, P. C. Li, and S. I. Chu, Phys. Rev. A **84**, 033414 (2011).
- *[13] P. C. Li, I. L. Liu, and S. I. Chu, Opt. Express **19**, 23857 (2011).
- *[14] P. C. Li and S.I. Chu, Phys. Rev. A **86**, 013411 (2012).
- *[15] P. C. Li, C. Laughlin, and S. I. Chu, Phys. Rev. A **89**, 023431 (2014).
- *[16] S. I. Chu and D. A. Telnov, in *Computational Studies of New Materials II: From Ultrafast Processes and Nanostructures to Optoelectronics, Energy Storage and Nanomedicine*, edited by T.F. George, D. Jelski, R.R. Letfullin, and G. Zhang (World Scientific, 2011), pp. 75–101.
- *[17] D. A. Telnov, J. Heslar, and S.I. Chu, in *Theoretical and Computational Developments in Modern Density Functional Theory*, edited by Amlan K. Roy (Nova Science Publishers, Inc., Hauppauge, NY (USA), 2012), pp. 357- 390.
- *[18] J. Heslar, D. A. Telnov, and S. I. Chu, in *Concepts and Methods in Modern Theoretical Chemistry: Statistical Mechanics*, Volume 2, edited by S.K. Ghosh and P.K. Chattaraj (Taylor & Francis Inc., Boca Roca, USA, 2013), pp. 37-55.
- *[19] J. Heslar, D.A. Telnov, and S. I. Chu, Chinese J. Phys. **52**, 578 (2014).
- *[20] D. Zhao, F. I. Li, and S. I. Chu, Phys. Rev. A **87**, 043407 (2013).
- *[21] D. Zhao, F. I. Li, and S. I. Chu, J. Phys. B: At. Mol. Opt. Phys. **46**, 145403 (2013).
- *[22] Z. Y. Zhou and S. I. Chu, Phys. Rev. A **83**, 013405 (2011).
- *[23] Z. Y. Zhou and S. I. Chu, Phys. Rev. A **87**, 023407 (2013).
- *[24] H.Z. Jooya, D.A. Telnov, P. C. Li, and S. I. Chu, Phys. Rev. A **91**, 063412 (2015).

Formation of Ultracold Molecules

Robin Côté

Department of Physics, U-3046
University of Connecticut
2152 Hillside Road
Storrs, Connecticut 06269

Phone: (860) 486-4912
Fax: (860) 486-3346
e-mail: rcote@phys.uconn.edu
URL: <http://www.physics.uconn.edu/~rcote>

Program Scope

The original aims of this Research Program were to identify efficient approaches to obtain ultracold molecules, and to understand their properties. This scope has evolved in the last year to cover the effect of dressed interactions on molecular dynamics. In both cases, we often need to calculate the electronic properties (energy surfaces, dipole and transition moments, etc.), as well as the interaction of the molecules with their environment (*e.g.*, external fields).

Recent Progress

During FY 2015, we have made progress on 4 main axes of research: 1) Structure calculations, molecular properties, and reactions, 2) Inter-molecular long-range interactions, 3) Dressed and Rydberg states, and 4) Formation of molecules. Below, we refer to DOE supported articles during the last four years only; new articles published since the last annual report filing (August 2014) are listed as [N...], while those of the prior years since October 31st 2011 by [P...].

1) Structure calculations, molecular properties, and reactions

A continuing effort of our group involves calculations of potential energy surfaces (PESs). For example, we expanded our work on the $1^2A'$ [J.N. Byrd *et al.*, Int. J. of Qu. Chem., **109**, 3112 (2009)] and $2^2A''$ [J.N. Byrd *et al.*, Int. J. of Qu. Chem **109**, 3626 (2009)] PESs of Li_3 , to *ab initio* calculations of the long-range PES of its ground state X^2A' , including van der Waals coefficients and three-body dispersion damping terms for the atom-diatom dissociation limit [P1]. We also extended our work on K_2Rb_2 relevant to $\text{KRb}+\text{KRb}$ scattering [J.N. Byrd *et al.*, PRA **82**, 010502 (2010)] to all alkali tetramers formed from $\text{X}_2+\text{X}_2 \rightarrow \text{X}_4$, $\text{X}_2+\text{Y}_2 \rightarrow \text{X}_2\text{Y}_2$, and $\text{XY}+\text{XY} \rightarrow \text{X}_2\text{Y}_2$ association reactions [P2], and found two stable tetramer structures, rhombic (D_{2h}) and planar (C_s), with barrier-less pathways for dimer association reactions. We are now investigating the interaction between two RbCs molecules in their ro-vibrational ground state, taking into account spin-orbit coupling [N1], which will be important to understand the possible formation of $(\text{RbCs})_2$.

Building on our experience on atom-molecule scattering, *e.g.* in non-reactive $\text{OH}+\text{He}$ [T. V. Tscherbul *et al.*, PRA **82**, 022704 (2010)] or reactive $\text{D} + \text{H}_2$ [P3] systems, we investigated resonances near the scattering threshold in the reactive benchmark system H_2+Cl [P4]. We found that the inelastic cross section scales as k^{-3} in the *s*-wave regime, due to the proximity of a pole in the complex *k*-plane. We extended the study to H_2+F and gave an explanation based on the properties of the Jost function in [N2]. We also explored the effect of nuclear spin symmetry in reactions of D with para/ortho- H_2 [N3], comparing our quantum calculations with a statistical model.

Finally, we kept working on molecular ions: previously, we reported *ab initio* calculations of the $X^2\Sigma_u^+$ and $B^2\Sigma_g^+$ states of Be_2^+ , and predicting two local minima separated by a large barrier in $B^2\Sigma_g^+$ [S. Banerjee *et al.*, CPL **496**, 208211 (2010)]. We extended this work to Ca_2^+ in [P5]. We are in the process to complete two other systems: Mg_2^+ [N4] and Sr_2^+ [N5]. More recently, we helped analyzing experimental results on NaCa^+ [P6]. We are now extending this work to find a path leading to the formation of ultracold NaCa^+ in its ro-vibrational ground state using photoassociation to various excited states [N6].

2) Inter-molecular long-range interactions

In our previous work on K_2Rb_2 [J.N. Byrd *et al.*, PRA **82**, 010502 (2010)], we calculated the minimum energy path for the reaction $KRb+KRb\rightarrow K_2+Rb_2$ and found it to be barrierless. However, we recently showed that long-range barriers originating from the anisotropic interaction due to higher electrostatic, induction, and dispersion contributions could exist and stabilize a molecular sample [P7]. In addition, we showed that by changing the orientation of the molecules using an external DC electric field, and by varying its strength F , one could control the effective inter-molecular interaction. We generalized our treatment to homonuclear alkali dimers [P8], where there are still anisotropic interactions, and extended it to the case of heteronuclear diatomic alkali molecules [P9]; in addition to the multipole expansion and van der Waals terms, we also give an analytic expression for molecules in an external (weak) DC electric field. Some of this work is summarized in a book chapter on polar molecules for quantum information processing [P10]. Using those results, we are studying the possible formation on weakly bound tetramers via photoassociation of oriented ultracold diatomic molecules by external fields [N7].

3) Dressed and Rydberg states

We continued our initial work on interactions near the $69p + 71p$ [J. Stanojevic *et al.*, EPJD **40**, 3 (2006)] and $69d + 70s$ [J. Stanojevic *et al.*, PRA **78**, 052709 (2008)] asymptotes of ^{85}Rb , and its extension to study potential wells of doubly-excited atoms (macrodimers) due to ℓ -mixing [P11,P12], to explore metastable long-range *macrotrimers* made of three Rydberg atoms [P13]. We found shallow (~ 20 MHz deep) long-range wells for linear trimers. We also predicted the formation of bound states between two Rydberg atoms in an atomic condensate due to phonon exchange [N8].

We recently investigated Rydberg-dressed interactions in H_2+D [N9], using

$$\hat{H} = \begin{pmatrix} -C_6^{(g)}/R^6 & \hbar\Omega/2 \\ \hbar\Omega^*/2 & -\hbar\delta - C_6^{(r)}/R^6 \end{pmatrix}.$$

This dressed Hamiltonian, within the rotating wave approximation (RWA), describes the interaction of H_2 with D with its ground state g dressed with a Rydberg state r by a laser detuned by δ and Rabi frequency Ω . We showed in [N9] that Rydberg-dressed interactions could be used to tune $H_2+D\rightarrow HD+H$ chemical reactions. We are now investigating a possible new chemical bound between ground state atoms using Rydberg dressing of the atoms [N10]. The molecular bound states would be extremely long-range, roughly 500 bohr radii, and very weakly bound.

4) Formation of molecules

In previous papers sponsored by DOE [E. Juarros *et al.*, PRA **73**, 041403(R) (2006); E. Juarros *et al.*, JPB **39**, S965 (2006); N. Martinez de Escobar *et al.*, PRA **78**, 062708 (2008)], we explored the formation of diatomic molecules in their ground electronic state from one- and two-photon photoassociative processes [E. Juarros *et al.*, PRA **81**, 060704 (2010)]. We also worked on using many coherent laser pulses [E. Kuznetsova *et al.*, PRA **78**, 021402(R) (2008)], and Feshbach resonances [P. Pellegrini *et al.*, PRL **101**, 053201 (2008)] to increase the formation rate of ultracold diatomic molecules [P. Pellegrini, and R. Côté, NJP **11**, 055047 (2009); E. Kuznetsova *et al.*, NJP **11**, 055028 (2009); J. Deiglmayr, *et al.*, NJP **11**, 055034 (2009)].

We recently explored how Feshbach resonances could enhance a pump-dump scheme to produce ground state LiRb molecules [P14], starting from the mixed $X^1\Sigma^+$ and a $^3\Sigma^+$ states at the Feshbach resonance being excited to $B^1\Pi$ by a pump pulse followed by a dump pulse into a target rovibrational level in the $X^1\Sigma^+$ ground state. To describe the transitions between $X^1\Sigma^+$ and $B^1\Pi$,

we used the Hamiltonian (assuming RWA and dipole approximation)

$$\hat{\mathbf{H}} = \begin{pmatrix} \hat{\mathbf{T}} + V_{X^1\Sigma^+}(R) & \vec{\mu}(R) \cdot \vec{E}(t) \\ \vec{\mu}(R) \cdot \vec{E}(t) & \hat{\mathbf{T}} + V_{B^1\Pi}(R) - \hbar\omega_L \end{pmatrix},$$

where $\hat{\mathbf{T}}$ is the kinetic energy operator and $V_i(R)$ are the respective potential energy curves. We simulated the pump-dump PA process using a time-dependent wave packet approach (TDWP), assuming the laser pulse to be transform-limited $\vec{E}(t) = \vec{E}_0 f(t) \cos(\omega_L t)$ with a gaussian profile $f(t) = \exp[-\alpha(t-t_c)^2]$. We represented $\hat{\mathbf{H}}$ on a Fourier grid with a variable grid step, and solved the time-dependent Schrödinger equation ($i\hbar \frac{\partial}{\partial t} \Psi(t) = \hat{\mathbf{H}}(t)\Psi(t)$), by expanding the evolution operator ($\exp[-i\hat{\mathbf{H}}t/\hbar]$) in terms of Chebyshev polynomials. We found that an increase of up to three orders of magnitude in the absolute number of molecules produced is attainable for deeply bound vibrational levels.

In a previous study on RbOH^- and RbOH [P15], we computed the PES to model the associative detachment reaction $\text{Rb} + \text{OH}^-(v, j) \rightarrow \text{RbOH} + e^-$, paying special attention to the angular dependence of the PES, and found the rate to strongly vary with the ro-vibrational state of OH^- due to a curve-crossing at short-range, pointing to an interesting inter-dependence of the electronic and nuclear motion. We are now building on our recent experience on dressed interactions [N9,N10] and time-dependent pulses [P14] to study how nuclear motion and electronic motion can exhibit non-trivial behavior in molecular dynamics. In preliminary studies on Be_2^+ , we find that one could move the $v = 4$ bound state from an inner to an outer well of the molecular PES using ultra-short pulses by taking advantage of multiple light-induced conical intersections [N11].

Future Plans

In the coming year, we expect to extend our work on the effect of dressed interactions on molecular dynamics. For this purpose, we will continue and extend our work on computing electronic properties of molecules (PES and moments), especially for the molecular ions, where not much is available. We will use these results as input for simple diatomic molecular systems, and identify cases where complex Light Induced Conical Intersection (LICI) structures exist. By exploring such systems, we hope to gain a better understanding of the LICI framework and its application, and use it as a guide for future experiments probing the dynamics near conical intersections.

New DOE sponsored publications since August 2013

- N1. J.N. Byrd, S. Ghosal, and R. Côté, *Long-range interaction between two RbCs diatomic molecules*. In preparation for Phys. Rev. A).
- N2. Ionel Simbotin and Robin Côté, *Jost function description of near threshold resonances for coupled-channel scattering*. Chemical Physics (In Press, available on line July 2 2015): [arXiv:1505.03170](https://arxiv.org/abs/1505.03170).
- N3. Ionel Simbotin and Robin Côté, *Effect of nuclear spin symmetry in cold and ultracold reactions: D + para/ortho-H₂*. New J. Phys. **17**, 065003 (2015).
- N4. Sandipan Banerjee, John A. Montgomery, Jr., H. Harvey Michels, and Robin Côté, *Comparison of the Alkaline Earth diatomic homonuclear molecular ions*. In preparation for J. Chem. Phys.
- N5. Sandipan Banerjee, John A. Montgomery, Jr., H. Harvey Michels, and Robin Côté, *Ab initio potential curves for the X ²Σ_u⁺, A ²Π_u, and B ²Σ_g⁺ states of Sr₂⁺*. In preparation for Chem. Phys. Lett.
- N6. Marko Gacesa, John A. Montgomery, Jr., H. Harvey Michels, and Robin Côté, *Creation of ultracold NaCa⁺ molecular ion via photoassociation*. In preparation for Phys. Rev. A.

- N7. J.N. Byrd, M. Gacesa, and R. Côté, *The formation of tetramers of alkali metals by controlling inter-molecular interactions*. In preparation for Phys. Rev. Lett.
- N8. Jia Wang, Marko Gacesa, and Robin Côté, *Rydberg Electrons in a Bose-Einstein Condensate*. Phys. Rev. Lett. **114**, 243003 (2015).
- N9. Jia Wang, Jason N. Byrd, Ion Simbotin, and Robin Côté, *Tuning ultracold chemical reactions via Rydberg-dressed interactions*. Phys. Rev. Lett. **113**, 025302 (2014).
- N10. Jia Wang and Robin Côté, *A new long-range chemical bound using Rydberg-dressing*. In preparation for Phys. Rev. Lett.
- N11. M. Gacesa, I. Simbotin, D. Shu, and R. Côté, *Using multiple light-induced conical intersections to shape a molecular wave packet*. In preparation for Phys. Rev. Lett.

Prior DOE sponsored publications since 2010

- P1. Jason N. Byrd, H. Harvey Michels, John A. Montgomery, Jr., and Robin Côté, *Long-range three-body atom-diatom potential for doublet Li_3* , Chem. Phys. Lett. **529**, 23 (2012).
- P2. Jason N. Byrd, H. Harvey Michels, John A. Montgomery, Robin Côté, and William C. Stwalley, *Structure, energetics, and reactions of alkali tetramers*, J. Chem. Phys. **136**, 014306 (2012).
- P3. Ion Simbotin, Subhas Ghosal, and Robin Côté, *A case study in ultracold reactive scattering: $D + H_2$* , Phys. Chem. Chem. Phys. **13**, pp. 19148-19155 (2011).
- P4. Ion Simbotin, Subhas Ghosal, and Robin Côté, *Threshold resonance effects in reactive processes*, Phys. Rev. A **89**, 040701(R) (2014).
- P5. Sandipan Banerjee, John A. Montgomery, Jr., Jason N. Byrd, H. Harvey Michels, and Robin Côté, *Ab initio potential curves for the $X^2\Sigma_u^+$, $A^2\Pi_u$, and $B^2\Sigma_g^+$ states of Ca_2^+* , Chem. Phys. Lett. **542**, 138-142 (2012).
- P6. W. W. Smith, D.S. Goodman, I. Sivarajah, J.E. Wells, S. Banerjee, R. Côté, H.H. Michels, J.A. Montgomery Jr., and F.A. Narducci, *Experiments with an ion-neutral hybrid trap: cold charge-exchange collisions*, Appl. Phys. B **114**, 75 (2014).
- P7. Jason N. Byrd, John A. Montgomery, and Robin Côté, *Controllable Binding of Polar Molecules and Metastability of One-Dimensional Gases with Attractive Dipole Forces*, Phys. Rev. Lett. **109**, 083003 (2012).
- P8. Jason N. Byrd, Robin Côté, and John A. Montgomery, *Long-range interactions between like homonuclear alkali metal diatoms*, J. Chem. Phys. **135**, 244307 (2011).
- P9. Jason N. Byrd, John A. Montgomery, and Robin Côté, *Long-range forces between polar alkali-metal diatoms aligned by external electric fields*, Phys. Rev. A **86**, 032711 (2012).
- P10. Robin Côté, *Ultracold molecules: their formation and application to quantum computing*. Advances in Chemical Physics **154**, Chap. 7, pp. 403-448, John Wiley and Sons (New York) (2014).
- P11. N. Samboy, J. Stanojevic, and R. Côté, *Formation and properties of Rydberg macrodimers*, Phys. Rev. A **83**, 050501(R) (2011).
- P12. Nolan Samboy and Robin Côté, *Rubidium Rydberg macrodimers*, J. Phys. B **44**, 184006 (2011).
- P13. Nolan Samboy and Robin Côté, *Rubidium Rydberg linear macrotrimers*. Phys. Rev. A **87**, 032512 (2013).
- P14. M. Gacesa, S. Ghosal, J.N. Byrd, and R. Côté, *Feshbach-optimized photoassociation of ultracold $^6Li^87Rb$ molecules with short pulses*, Phys. Rev. A **88**, 063418 (2013).
- P15. Jason N. Byrd, H. Harvey Michels, John A. Montgomery, Jr., and Robin Côté, *Associative detachment of rubidium hydroxide*. Phys. Rev. A **88**, 032710 (2013).

Optical Two-Dimensional Spectroscopy of Disordered Semiconductor Quantum Wells and Quantum Dots

Steven T. Cundiff

Department of Physics, University of Michigan, Ann Arbor, MI 48109
cundiff@umich.edu

September 15, 2015

Program Scope: The goal of this program has been to implement optical 2-dimensional coherent spectroscopy and apply it to electronic excitations, including excitons, in semiconductors. Specifically of interest are epitaxially grown quantum wells that exhibit disorder due to well width fluctuations and quantum dots. In both cases, 2-D spectroscopy provides information regarding coupling among excitonic localization sites. During the last year we have begun applying this method to colloidal quantum dots in addition to epitaxially grown materials.

Progress: This project has been under a no-cost extension for the current grant year, which has limited progress. In addition, the PI is in the process of moving from University of Colorado to University of Michigan.

Quantum dots are often described as “artificial atoms” because they have discrete energy levels. However, quantum dots have an important distinction from atoms, namely they have degrees of freedom associated with motion of the constituent atoms relative to their equilibrium position, i.e., vibrational degrees of freedom, which in the case of epitaxial dots corresponds to phonons. In this way, they are more like molecules than atoms. As a consequence, many applications of InAs quantum dots require low temperatures to eliminate decoherence due to the phonons.

The interaction of an exciton confined in an InAs epitaxially grown dot with acoustic phonons can be described in a picture similar to that used for molecular vibrations. The equilibrium position of the excited state within the quantum dot is slightly displaced with respect to the ground state. For a phonon of a given energy, there is a series of vibrational bands in each state, corresponding to the number of phonons. The zero-phonon line is an optical transition between ground and excited states with the same number of phonons. Transitions between states with differing number of phonons results in emission or absorption with an energy difference corresponding to the phonon energy. If the phonon energy were discrete, as for optical phonons, or molecular vibrations, well resolved satellites would result. However, acoustic phonons have a continuous distribution of phonon energies and thus smooth phonon sidebands occur. At low temperature, i.e., around 5 K, the zero phonon line dominates. As the temperature is increased, the phonon sidebands become prominent.

The dephasing of the ground state transition of InAs quantum dots was studied using photon echo spectroscopy. These measurements showed a remarkably long dephasing time, on the order of a nanosecond, which triggered interest in using InAs quantum dots as qubits. At elevated temperature, the phonon sidebands were observed. Since these measurements were based on photon echoes, they provide an ensemble averaged value and no information about how/if the phonon-exciton interactions vary with dot size. In addition, these studies did not provide any information on the dephasing of the excited state transitions.

Self-organized InAs quantum dots have attracted a lot of attention as a possible solid state realization of a qubit for quantum information applications. This application requires that the exciton can undergo a Rabi

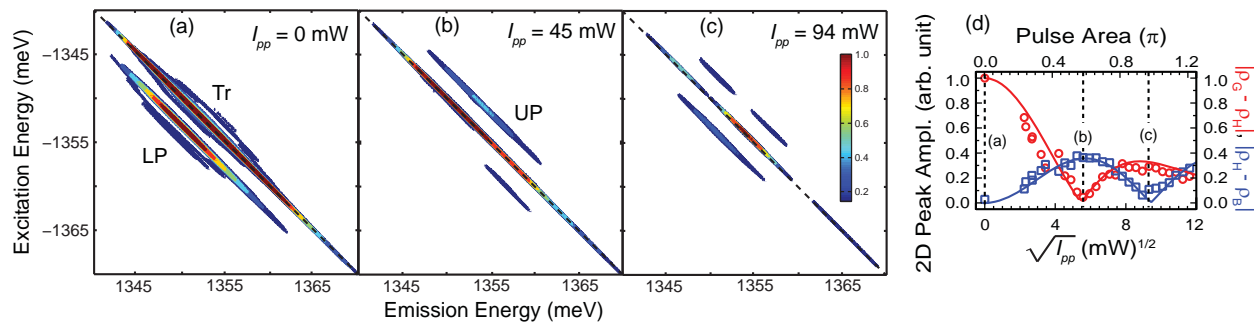


Figure 1: 2D rephasing amplitude spectra for InAs self-organized using prepulse powers of (a) 0, (b) 45 and (c) 109 mW demonstrating Rabi flopping by the prepulse. The delay between the prepulse and 2D beams is 15 ps. The Trion (Tr), lower (LP) and upper (UP) peaks are indicated. The peak amplitude of the LP and UP are shown in (d). Solid lines are simulations for the exciton-ground state and biexciton-exciton population differences. The vertical dashed lines indicate the powers corresponding to panels (a-c).

oscillation. Because the Rabi frequency depends on the detuning, and the excitonic resonance frequency of a dot depends on its size, these measurements have been almost exclusively done on single dots. Indeed ensemble measurements of Rabi flopping showed excess damping attributed to ensemble effects. However, the ability of 2D coherent spectroscopy to make size-dependent measurements suggests that it could be used to observe Rabi oscillations in an ensemble.

We have recently demonstrated that this is true. These measurements used a prepulse to drive the quantum dot excitons into the excited states. The prepulse was followed by the pulse sequence used to produce a 2D spectrum. The results are shown in Fig. 1. Without the prepulse, peaks are observed both on the diagonal and below the diagonal. The diagonal peak is due to a combination of exciton and trion transitions (the trion binding energy is much less than the inhomogeneous distribution). The peak below the diagonal is due to absorption on the ground-state to exciton transition and emission on the exciton to biexciton transition. With the prepulse, a new peak appears above the diagonal. This peak occurs because there is already a population of excitons before the 2D pulses arrive. It corresponds to absorption on the exciton to biexciton transition and emission on the exciton to ground-state transition. As the prepulse intensity is increased, the strength of the lower sideband decreases, because the ground-state is depleted and the upper side band increases in strength as the initial population of excitons increases. The strength of the sidebands are plotted as function of prepulse power in Fig. 1(d) and compared a simulation that include Rabi-flopping on both the ground-state to exciton and exciton to biexciton transitions (both must be included). The simulation agrees very well with the experiments. A manuscript describing these results is in preparation.

This approach to studying Rabi-flopping in self-organized quantum dots has several advantages over single dot studies. A significant advantage is avoiding the technical challenges associated isolating a single dot and doing so repeatedly. Without the need to isolate a single dot removes the need to process the samples and/or use low dot density samples. Another advantage is the parallelism, dots of many sizes are accessed simultaneously, albeit with different detuning. Finally, a single laser pulse drives both transitions, whereas single dot studies typically use narrow band lasers that only overlap a single transition, thus two lasers are needed to simultaneously drive both transitions.

During the last grant cycle, we began working on obtaining 2D coherent spectra of colloidal quantum dots. As colloidal quantum dots are a substantially different system than the epitaxially grown quantum wells and quantum dots we have studied in the past, there was a substantial period of learning involved. As a consequence, we have not yet published a journal paper on 2D spectroscopy of colloidal quantum dots,

but have published several conference papers on the topic, for example at the 2014 Quantum Dot conference and at CLEO 2014.

The first issues were the substantial difference in wavelength as well as the much slower relaxation times due to dark states present in colloidal quantum dots. To address both of these issues, we built a second 2D spectrometer that uses an optical parametric amplifier (OPA) pumped by a regenerative ti:sapphire amplifier running at 250 kHz repetition rate.

Another issue was dealing with the different type of sample, name solution phase rather than a wafer. To make things more challenging, we wanted to go to low temperature to study phonon-carrier scattering. We tried making thin films using spin casting and drop casting, however we found that these resulted in excess scattering, which caused the 2D spectrum to be unacceptably noisy. So overcome this, we switched to using a glass-forming liquid, namely heptamethylnonane. After some trial and error, we were able to get acceptable sample quality at low temperature. A series of 2D spectra at 10 K as function of waiting time, T , are shown in Fig. 2. This spectrum clearly shows strong elongation along the diagonal due to inhomogeneous broadening from the size dispersion of the dots. The cross-diagonal width gives the homogeneous width, and by taking cross-diagonal slices at different energies, it is possible to determine the size dependence of the homogeneous width. Remarkably, the strength clearly oscillates with T , as expected if there are coherences within one of the manifolds. In addition, there appear to be off-diagonal features that are parallel to the diagonal peak. These get stronger at large T . The spacing is smaller than the LO-phonon, biexciton and 1S-1P splitting, thus they have not been definitely assigned, but may be due to acoustic phonons.

Future plans: During the next grant cycle we propose to focus on exploiting the ability of 2D coherent spectroscopy to make size resolved measurements on an ensemble sample to study size dependent effects in both self-organized epitaxially grown quantum dots and colloidal quantum dots. Previously, size dependent phenomena could only be explored by single dot studies, which are challenging to perform. In addition, the process of isolating a single dot may modify the results, either through sample preparation or by choosing to work on an outlier because it is easier to isolate. Furthermore, determining trends, such as size dependence, is challenging because it requires a series of difficult measurement, thus the data sets are often small.

In general, quantum dots (of either type) show strong inhomogeneous broadening due to size dispersion because the variation in size leads to variation in the quantization energy of the electronic states. Variations in shape also contribute to inhomogeneous broadening, but to a lesser extent than size variations. The inhomogeneous broadening means that linear measurements on ensembles, such as absorption or luminescence, do not measure the properties of individual dots, but rather the properties of the ensemble. For example the width of the linear spectra are completely determined by the size fluctuations, not the linewidth of the individual dots. Furthermore, the individual dots may have multiple transitions, for example exciton and

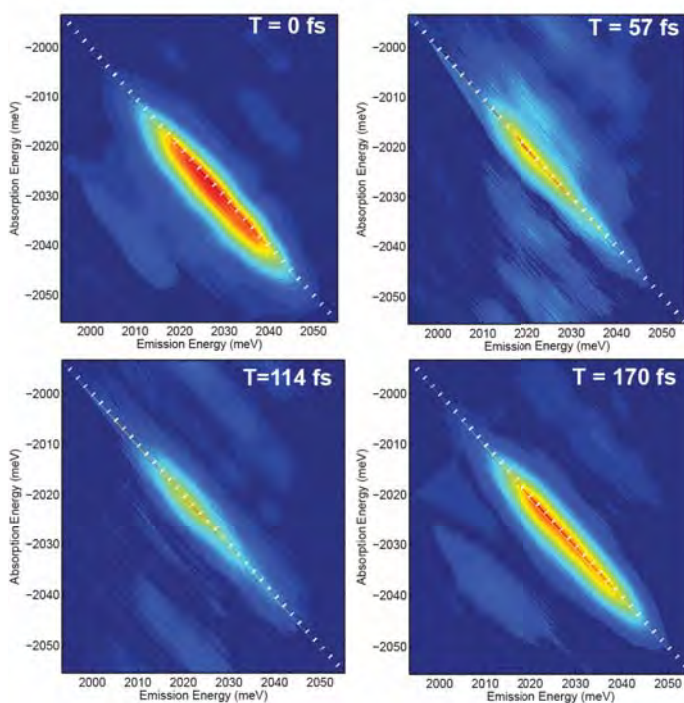


Figure 2: 2D spectrum of CdSe/ZnS core-shell colloidal quantum dots.

biexciton or fine-structure splitting, that is completely obscured by the inhomogeneity.

Traditional nonlinear spectroscopies, such as photon echoes, can observe the homogeneous linewidth even in the presence of inhomogeneous broadening. In addition, they can give evidence of multiple transitions as beating. However, photon echo measurements give an ensemble average value for the dephasing rate and for any energetic splitting. An ensemble average is problematic if the homogeneous width or an energetic splitting varies within the inhomogeneous distribution. In this case non-exponential decays are observed as well as possibly a beat frequency that varies with delay. While a photon echo signal with a non-exponential decay would indicate that the homogeneous linewidth is not constant, it does not give any information on how it is varying with transition energy, for example it does not even indicate if it is increasing or decreasing with dot size. Indeed this exact issue has been the subject of controversy for the photon echo measurements on CdSe/ZnS colloidal dots.

Two-dimensional coherent spectroscopy overcomes this limitation by correlating absorption and emission frequencies so that an inhomogeneous distribution is spread out along the diagonal. It is then possible to measure the homogeneous width, which is the cross diagonal width, as a function of energy. We have demonstrated this in natural quantum dots. In GaAs quantum wells, we have also observed that the biexciton binding energy varies with emission energy within the inhomogeneous distribution. In this case the inhomogeneity is due to disorder in the quantum well, so it loosely corresponds to the size of a quantum dot. But the important point is the demonstration that 2D spectroscopy can indeed measure a variation in a splitting energy within an inhomogeneous distribution.

We specifically plan to study both epitaxially grown self-organized InAs quantum dots and three types of colloidal quantum dots, CdTe/ZnS dots, PbSe/CdSe dots and Ge dots.

Publication during the the last 3 years from this project:

1. S.T. Cundiff and S. Mukamel, "Optical multidimensional coherent spectroscopy," *Physics Today* **66**, number 6, p. 44-49 (2013).
2. G. Moody, R. Singh, H. Li, I.A. Akimov, M. Bayer, D. Reuter, A.D. Wieck, A.S. Bracker, D. Gammon and S.T. Cundiff, "Biexcitons in semiconductor quantum dot ensembles," *Physica Status Solidi B* **250**, 1753-1759 (2013).
3. G. Moody, R. Singh, H. Li, I.A. Akimov, M. Bayer, D. Reuter, A.D. Wieck and S.T. Cundiff, "Correlation and dephasing effects on the non-radiative coherence between bright excitons in an InAs QD ensemble measured with 2D spectroscopy," *Solid State Commun.* **163**, 65-69 (2013).
4. G. Moody, R. Singh, H. Li, I.A. Akimov, M. Bayer, D. Reuter, A.D. Wieck and S.T. Cundiff, "Fifth-order nonlinear optical response of excitonic states in an InAs quantum dot ensemble measured with 2D spectroscopy," *Phys. Rev. B* **87**, 045313 (2013).
5. H. Li, G. Moody, S.T. Cundiff, "Reflection optical two-dimensional Fourier-transform spectroscopy," *Opt. Express* **21**, 1687-1992 (2013).
6. G. Moody, R. Singh, H. Li, I.A. Akimov, M. Bayer, D. Reuter, A.D. Wieck, A.S. Bracker, D. Gammon and S.T. Cundiff, "Influence of confinement on biexciton binding in semiconductor quantum dot ensembles measured with 2D spectroscopy," *Phys. Rev. B* **87**, 041304(R) (2013).
7. G. Nardin, G. Moody, R. Singh, T.M. Autry, H. Li, F. Morier-Genoud and S.T. Cundiff, "Coherent Excitonic Coupling in an Asymmetric Double InGaAs Quantum Well", *Phys. Rev. Lett.* **112**, 046402 (2014).
8. G. Moody, I.A. Akimov, H. Li, R. Singh, D.R. Yakovlev G. Karczewski, M. Wiaterski, T. Wojtowicz, M. Bayer and S.T. Cundiff, "Coherent Coupling of Excitons and Trions in a Photoexcited CdTe/CdMgTe Quantum Well", *Phys. Rev. Lett.* **112**, 097401 (2014).

SISGR: Understanding and Controlling Strong-Field Laser Interactions with Polyatomic Molecules

DOE Grant No. DE-SC0002325

Marcos Dantus, dantus@msu.edu

Department of Chemistry and Department of Physics and Astronomy, Michigan State University, East Lansing MI 48824

1. Program Scope

When intense laser fields interact with polyatomic molecules, the energy deposited leads to fragmentation, ionization and electromagnetic emission. The objective of this project is to determine to what extent these processes can be controlled by modifying the phase and amplitude characteristics of the laser field according to the timescales for electronic, vibrational, and rotational energy transfer. Controlling these processes will lead to order-of-magnitude changes in the outcome from laser-matter interactions, which may be both of fundamental and technical interest. The proposed work is unique because it seeks to combine knowledge from the field of atomic-molecular-optical physics with knowledge from the fields of analytical and organic ion chemistry. This multidisciplinary approach is required to understand to what extent the shape of the field affects the outcome of the laser-molecule interaction and to which extent the products depend on ion stability. The information resulting from the systematic studies will be used to construct a theoretical model that tracks the energy flow in polyatomic molecules following interaction with an ultrafast pulse.

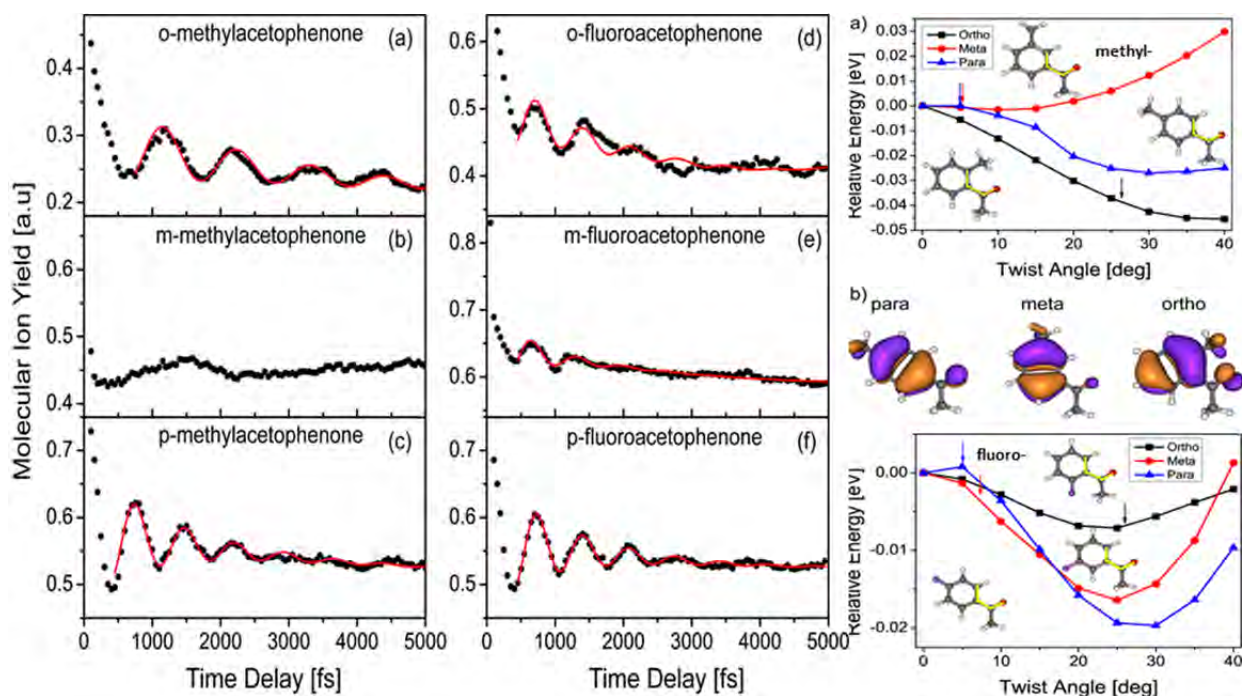
2. Recent Progress

Our interest in electronic and vibrational coherence and the development of laser pulse shaping approaches led us to some ‘model’ experiments in (a) polyatomic molecules in strong fields (b) electronic coherence in nanoparticles, and (c) electronic coherence in condensed phase.

(a) Polyatomic molecules in strong fields:

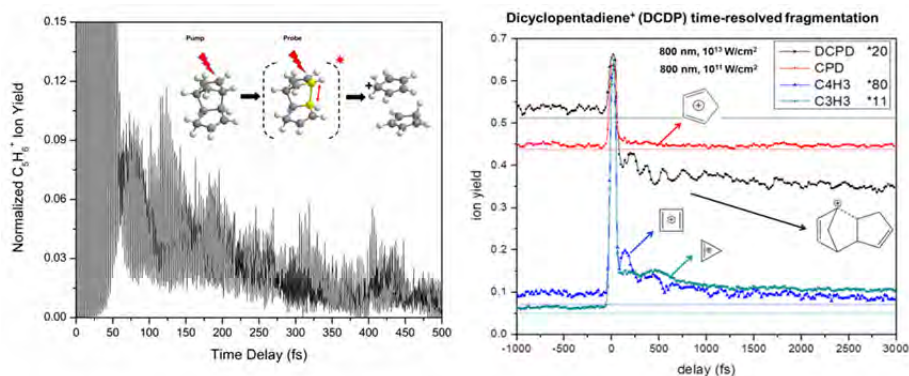
1. A. Konar, Y. Shu, V. V. Lozovoy, J. E. Jackson, B. G. Levine and M. Dantus, “Polyatomic molecules under intense femtosecond laser irradiation,” J. Phys. Chem. A, Feature Article (In press 2014).

We carried out a study to better understand the behavior of a large class of aromatic ketones when irradiated with intense femtosecond pulses and consider to what extent molecules retain their molecular identity and properties under strong field irradiation. Using time-of-flight mass spectrometry in conjunction with pump-probe techniques, we study the dynamical behavior of these molecules while monitoring the ion yield modulation caused by intramolecular motion post ionization. The large group of molecules studied is further divided into smaller subgroups depending on particular chemical changes to the backbone structure such as positional isomerism of different functional groups. We find that these changes, which energetically amount to a few meV influence the



dynamical behavior of the molecules as evident from the time-delay scans even in the presence of such high fields ($V/\text{\AA}$). The figure above shows strong-field-pump weak-field-probe time-resolved transients obtained for ortho-, meta- and para-methylacetophenone and fluoroacetophenone. The coherent oscillations correspond to motion along the twist angle of the carbonyl group with respect to the aromatic ring plane. Note that m-methylacetophenone shows no oscillations, and this is consistent with ab initio calculations (top right panel). All three isomers for fluoroacetophenone show coherent oscillations as corroborated by calculations. These results are consistent with the explanation that strong-field ionization creates a molecular ion with low internal energy. High level ab initio quantum chemical calculations were performed in order to predict molecular dynamics and single and multiphoton resonances in the neutral and ionic states. We propose that following single electron tunneling ionization, the cation is left with very little internal energy in the remaining laser field. Further fragmentation takes place as a result of both, further photon absorption modulated by one and two photon resonances and radical cation stability. The proposed hypothesis implies electron loss occurs at a rate that is faster than intramolecular vibrational relaxation and is consistent with the observation of non-statistical photofragmentation of polyatomic molecules as well as experimental results from many other research groups on different molecules and with different pulse durations and wavelengths.

2. A. Konar, Y. Shu, B. G. Levine, V. V. Lozovoy, and M. Dantus, “Electronic Coherence Mediated Quantum Control of Chemical Reactions in Polyatomic Molecules”, a manuscript being considered by Science.



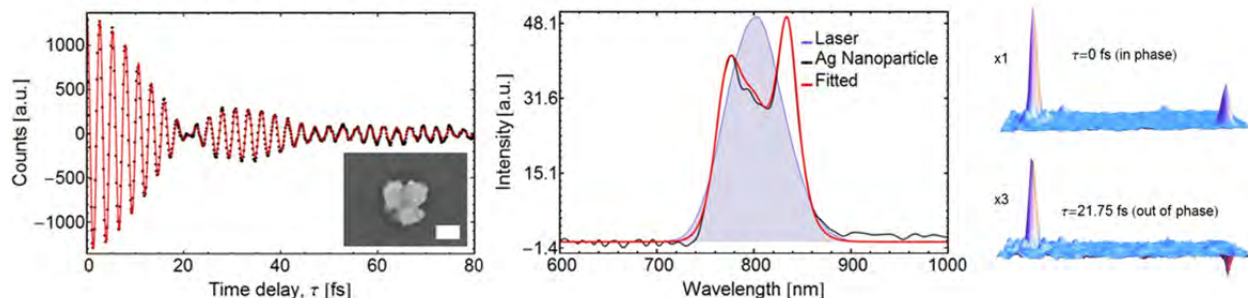
Using lasers to induce coherence onto a molecule and then using constructive or destructive interference with the mixed state to achieve quantum coherent control of its subsequent chemical transformation has been a long-standing dream. We find order-of-magnitude quantum coherent control of the yield of photofragment ions following the creation

of electronic coherence in dicyclopentadiene ($C_{10}H_{12}$) molecules using a pair of phase-locked femtosecond near-infrared laser pulses. The electronic coherence involving Rydberg states, which can preserve phase information for hundreds of femtoseconds, provides a robust platform for quantum coherent control. Control is achieved simply by changing the delay between pump and probe pulses by 400 attoseconds, even at delay times greater than 0.5 picoseconds. Our results serve as a guide on how femtosecond pulses can be used to prepare an electronic superposition intermediate state from which coherent control is possible.

(b) Electronic coherence in nanoparticles:

1. R. Mittal, R. Glenn, I. Saytashev, V. V. Lozovoy and M. Dantus, “Femtosecond Nanoplasmonic Dephasing of Individual Silver Nanoparticles and Small Clusters,” *J. Phys. Chem. Lett.* 6, 1638–1644 (2015)

We carried out experimental measurements of localized surface plasmon (LSP) emission from individual silver nanoparticles and small clusters via accurately delayed femtosecond laser pulses. Fourier transform analysis of the nanoplasmonic coherence oscillations reveals different frequency components and dephasing rates for each nanoparticle or small cluster. We find three different types of behavior: single exponential decay, beating between two frequencies, and beating among three or more frequencies. Our results provide insight into inhomogeneous and homogenous broadening mechanisms in nanoplasmonic spectroscopy that depend on morphology and nearby neighbors. In addition, we find the optical response of certain pairs of nanoparticles to be at least an order of magnitude more intense than the response of single particles. Our measurements track the linear response unlike previous measurements based on second harmonic, or photoelectron detection.

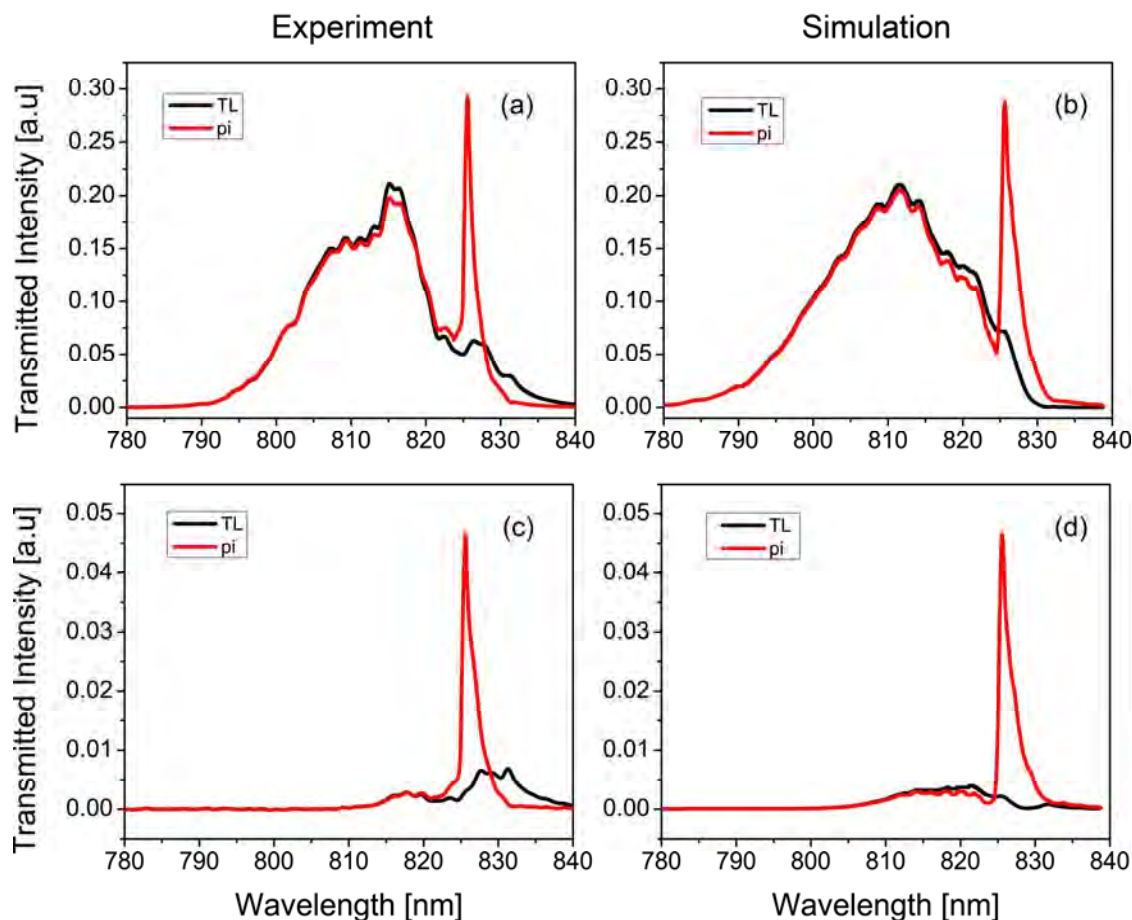


Plasmonic response of a three silver nanoparticle cluster (SEM image with 100nm scale bar) in the time and frequency domains. Shown in the frequency domain is the FT (black), the fit (red), and the laser spectrum (shaded in blue). The 3D plots show the plasmonic response from two different particles 18.6 μm apart.

(c) Electronic coherence in condensed phase:

A. Konar, V. V. Lozovoy and M. Dantus, "Stimulated Emission Enhancement using Shaped Pulses," Submitted to ACS Photonics.

Stimulated emission often competes with absorption and fluorescence under intense excitation. A π -step phase function on the excitation pulse is shown to cause greater than an order of magnitude enhancement in the stimulated emission as compared to a transform limited pulse. The results have been simulated successfully using density matrix calculations and a physical model is provided to elucidate the observed enhancement and the model is further tested experimentally using three different types of pulse shaping functions (chirp, third-order dispersion and a time-delayed probe). In the figure we show the stimulated emission due to laser pulses with a π -phase step modulation at 825.6 nm (red) compared to TL pulses (black). Experimental results are shown in panels (a) and (c) for samples having an OD~0.7 and 2.5 respectively. Numerical simulations are shown in panels (b) and (d).



3. Future Plans

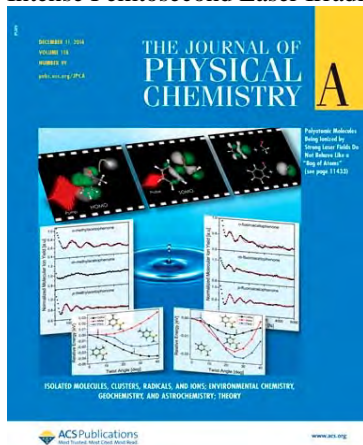
We plan to focus on understanding and controlling strong-field laser interactions with polyatomic molecules.

The proposed research addresses Grand Challenge questions related to quantum control of electrons in matter, and in particular coherent control of excited electronic states, optimal control, and control pushed to higher energy, broader bandwidth and shorter times. More specifically the goals are: (a) Assess non-adiabaticity, the nature of the nascent ion, in strong-field ionization of polyatomic molecules; (b) Develop a general understanding of strong field ionization and its dependence on molecular structure for a series of closely related aligned molecules; and (c) explore reactive pathways that generate H_3^+ from polyatomic molecules. We want to determine how the H_3^+ yield depends on molecular structure (presence or absence of methyl groups), and alignment. We hope to determine the timescale for this unusual reaction in which multiple bonds are broken and formed. Finally we want to control the yield of the reaction through pulse shaping. These projects will combine ultrafast spectroscopy, pulse shaping, molecular isomers and isotopic substitutions, knowledge of electron-impact mass spectrometry, thermochemistry, and ab initio calculations.

We also plan to reply to the reviewers of our publication on the electronic coherence involved in laser control of chemical reactions, in particular intense non-resonant fields. In terms of instrument development, we rebuilt our molecular beam and completed a PEPICO instrument that we hope to use when our grant is renewed. We have also developed new methods to quantify shot-to-shot spectral phase and amplitude noise and for identifying the presence of pre- and post-pulses from amplified ultrafast laser sources. These advancements will help our research.

4. Publications 9/15/12 to 9/13/15 last year under NCE

1. A. Konar, V.V. Lozovoy, and M. Dantus, "Solvent Environment Revealed by Positively Chirped Pulses," J. Phys. Chem. Lett. 5, 924–928 (2014)
2. A. Konar, V.V. Lozovoy, and M. Dantus, "Electronic dephasing of molecules in solution measured by nonlinear spectral interferometry," J. Spectrosc. Dyn. 4, 26 (2014). The journal was renamed and the paper reassigned to ScienceJet 4 (2015)
3. A. Konar, Y. Shu, V.V. Lozovoy, J.E. Jackson, B.G. Levine, and M. Dantus, "Polyatomic Molecules under Intense Femtosecond Laser Irradiation," J. Phys. Chem. A 118, 11433-11450 (2014)



4. R. Mittal, R. Glenn, I. Saytashev, V. V. Lozovoy and M. Dantus, "Femtosecond Nanoplasmonic Dephasing of Individual Silver Nanoparticles and Small Clusters," J. Phys. Chem. Lett. 6, 1638–1644 (2015)

SPATIAL-TEMPORAL IMAGING DURING CHEMICAL REACTIONS

Louis F. DiMauro

Co-PI: Pierre Agostini

Co-PI: Terry A. Miller

Department of Physics & Department of Chemistry

The Ohio State University

Columbus, OH 43210

dimauro@mps.ohio-state.edu

agostini@mps.ohio-state.edu

tamiller@chemistry.ohio-state.edu

1.1 PROJECT DESCRIPTION

This document describes the BES funded project (grant #: DE-FG02-06ER15833) entitled “Spatial-temporal imaging during chemical reactions” at The Ohio State University. Imaging, or the determination of the atomic positions in molecules is of central importance in physical, chemical and biological sciences. X-ray and electron diffraction are well-established method to obtain static images with sub-Angstrom spatial resolution. However their temporal resolution is limited to picoseconds. This proposal builds on the “molecule self-imaging” approach, based on bursts of strong-field driven coherent electron wave packets emitted by the molecule under interrogation. We are investigating two complementary self-imaging methods: Laser-Induced Diffraction [1] and high harmonic tomography [2, 3]. Both thrust exploit the wavelength scaling of strong-field interactions to improve the imaging capabilities.

Over the past year, our efforts have focused on several thrusts: (1) development of fixed-angle broadband laser-induced electron scattering (FABLES), (2) application of laser-induced electron diffraction (LIED) to complex molecular systems and (3) high-harmonic tomography of N₂ at mid-infrared wavelengths.

1.2 PROGRESS IN FY15: IMAGING

Fixed-angle broadband laser-driven electron scattering (FABLES). In Nature Communication [4], we introduced fixed-angle broadband laser-driven electron scattering (FABLES) as an alternative to fixed-energy, angle-swept laser-induced electron diffraction (LIED) [5]. FABLES is analogous to white light interferometry in optics, and this is the first experimental confirmation that broadband electron wave packet (EWP) can be used for imaging. In FABLES, the energy-dependent differential cross-section (DCS), $\sigma(E)$, is retrieved as compared to the angle-dependent DCS, $\sigma(\theta)$, of the LIED method. The main benefit of FABLES is a trivial retrieval of molecular structure via a simple Fourier transform (FT) with no theoretical fitting or modeling, *e.g.* no *a priori* knowledge of laser ionization. Furthermore, the method “visualizes” only bonds *parallel* to the laser polarization and has the potential for routine, real-time imaging in a pump-probe configuration. This unique aspect of FABLES combined with molecular alignment has the

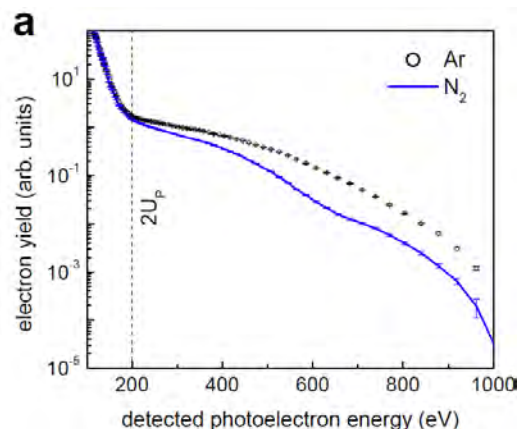


Figure 1: High-resolution photoelectron energy spectra along the laser polarization for N₂ and argon recorded at a wavelength of 2.0 μm and an intensity of 270 TW/cm². The error bars indicate the $N^{-1/2}$ Poisson statistical fluctuations for each time bin, N being the number of detected electrons. The vertical dashed line marks the $2U_p$ energy, electrons below this are direct. Above it, the long plateau corresponds to photoelectrons that are backscattered following ionization. The plateaus are a direct illustration of the broadband nature of the returning electron wave packet.

ability, according to our modelling, for a full molecular tomographic reconstruction of the molecular structure.

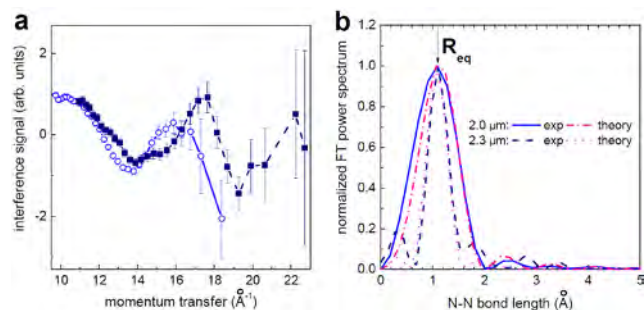


Figure 2: FABLES bond length retrieval and Fourier transform. (a) The intramolecular interference fringes extracted from the nitrogen plateau data at 2.0 μm (light blue open circles) and 2.3 μm (dark blue solid squares). The error bars represent the standard deviations of the two data sets which are calculated from measurement errors of their corresponding photoelectron energy distribution by assuming that the theoretical atomic DCS is exact. (b) The mean internuclear distance function obtained by Fourier Transform of the data in (a). The dash-dotted and dotted lines are the FT of the theoretical DCS spanning the same momentum transfer range as the experiments at 2.0 and 2.3 μm , respectively. The vertical arrow in (b) denotes the known N_2 equilibrium distance, R_{eq} . Our retrieved bond lengths deviate from R_{eq} by 0.01 \AA .

In our experiment, N_2 and Ar photoelectron spectrum were recorded under identical laser conditions using either intense 2.0 μm or 2.3 μm pulses (see Fig. 1). The detector collects electrons in a small angle (2°) along the laser polarization direction. The relevant difference between the N_2 and Ar experiment is an observed oscillation on the N_2 plateau resulting from the interference of the broadband EWP on the molecular structure. To retrieve the structural information, we adopt the mature rectification-based analysis method of conventional electron diffraction (CED). As shown in Fig. 2(a), the oscillation frequency depends upon the wavelength or in other words, on the energy of the returning EWP. Following CED's inversion procedure, a Fourier transform extracts from the momentum-space interferogram the real-space structural information. As shown in Fig. 2(b), the retrieved experimental internuclear distance peak at nearly the same position, 1.09 and 1.11 \AA for 2.0 and 2.3 μm experiments, respectively. In comparison, the known N_2 equilibrium distance, R_{eq} , is 1.10 \AA .

We believe that the FABLES is a more generally applicable method for studying nuclei molecular dynamics in a pump-probe configuration, as compared to LIED. Its advantages include: (1) no *a priori* knowledge of the angle dependent ionization, (2) the observation along one direction (polarization) is more efficient than a full momentum characterization and (3) FABLES has spatial bond selectivity. We are currently applying both LIED and FABLES to aligned molecules and more complex systems.

Current status of N_2 HHS below the AI cutoff. In the paper by Itatani *et al.* [2] high-order harmonics generation (HHG) was proposed as a means for reconstructing the Highest Occupied Molecular Orbital (HOMO) of nitrogen using a tomographic procedure. In that paper, the titanium-sapphire HHG intensity from aligned nitrogen was measured by changing the *alignment angle* that is the angle between the axis of symmetry of the molecular ensemble and the polarization of the driving field. On the contrary, the HHG phase was not measured but derived from the plane-wave approximation (PWA) dipole moment. The validity of this tomographic procedure is strongly subjected to the accuracy of PWA since it includes the Fourier-transform of the experimental recombination dipole moment (RDM). The RDM connects the neutral wave function spatial frequencies and the recombining electron momentum. Experimentally, it is obtained by normalizing out the ionization rate and the spectral amplitude of the recombining electronic wave packet from the experimental data. In 2010, Haessler *et al.* [3] reported HHG group delay measurements for ten different *alignment angles* using the RABBITT method at 0.8 μm . Later, Diveki *et al.* [6] showed that these results strongly depend on the driving laser intensity because of the contribution of both HOMO and HOMO-1 (next highest occupied molecular orbital). At 0.8 μm , ionization is not very deep into the tunneling regime and other multiphoton effects including Raman stimulated vibrational levels population [7] contribute. Furthermore, the comb density is low and not so many points are sampled. All of these factors make it very difficult to predict the phase of the attosecond emission from aligned nitrogen.

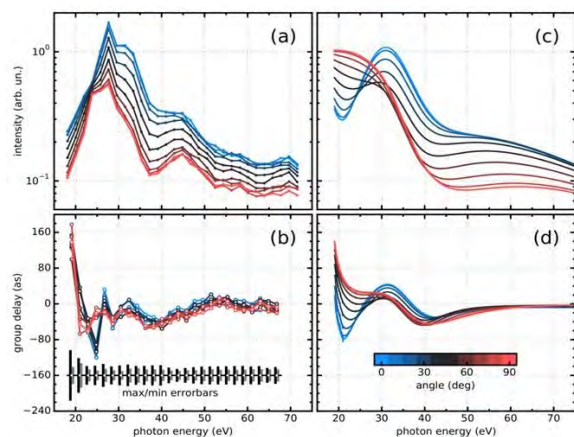


Figure 3: Experimental (a) intensity and (b) group delay of HHG in aligned nitrogen for 10 different alignment angles between 0 and 90 degrees. The experiment is compared to one orbital (HOMO) angle averaged scattering photoionization dipole moment (c) intensity and (d) GD calculated by Prof. R. Lucchese (TAMU).

resonance for molecules aligned at 0° and 30 eV. The calculations suggest that the decrease in the group delay (GD) measurement near 25 eV corresponds to the influence of the Coulomb potential. The global trend of the amplitude and phase is also well reproduced.

We find these results extremely satisfying since we are at the level of detailed comparison of high harmonic spectroscopy measurements with state-of-the-art molecular calculations. Thus we believe that the future for studying dynamics is bright. Although the agreement in Fig. 3 is encouraging there are differences between experiment and theory. For example the HHG amplitude measurement does not show the angular reversal in the emission evident in the calculation. Likewise, the decrease in GD at small angle occurs at a photon energy higher than the theory, although the general trend shows remarkable agreement. Consequently, the OSU group has begun collaborating with Dr. Lucchese. These differences can be the result of systematic errors in low electron energy RABBITT measurements or deficiencies in the theory. For example, the OSU measurements have unprecedented broad bandwidth that is not accounted for in the original Lucchese calculations, *i.e.* insufficient open channels. The OSU group and Lucchese are preparing a publication on these first results.

1.3 FUTURE PLANS

LIED and FABLES: Our current efforts are focused on both fundamental and applied tests of the LIED method: 1) the limits of spatial precision, the influence of multiple trajectories (long versus short and higher-order returns) on temporal precision, the dependence of the ionization rate on molecular alignment and the applicability of theoretical tools developed for CED analysis to LIED. 2) Applications of LIED to determine or observe structural changes in more complex systems; studies on isomeric systems and pump-probe interrogations. Larger molecules pose new challenges on experimental precision and theoretical methods in LIED. The inverse Fourier transform of the FABLES image will be further explored as an alternate structural retrieval method.

High harmonic spectroscopy: Long wavelength HHS measurements of N_2 and CO_2 are being analyzed and should provide a benchmark for future efforts. We will also perform RABBITT measurements at higher harmonic energy, >70 eV in an attempt to disentangle structural and dynamical effects. Furthermore, tuning the fundamental wavelength we also allow the assignment to resonant behavior.

In our N_2 experiment, we drive HHG using 1.3 and 2 μm pulses from an OPA. The residual depleted pump after the OPA is used to implement a 4 kick transient stacker enabling a high degree of molecular alignment. Fixing the delay to the half-revival (delay at which the angular distribution is the sharpest), we are able to control the alignment angle with a half wave plate placed after the kicker. The harmonic spectral intensity and phase are measured in our RABBITT end station. The mid-infrared HHG produce a 90 eV cutoff energy and a denser (increase by up to 2.5-times previous measurements) frequency comb.

In Fig. 3, we compared our angle-resolved HHG results to the state-of-the-art scattering wave photoionization dipole calculated by Robert Lucchese *et al.* [8]. We average the calculated dipole over a molecular ensemble estimated in a rigid rotor model. Our experimental results are in good agreement with these calculations over a large spectral bandwidth. In particular, our intensity measurements provide clear evidence of the shape

A strategy for imaging chemical dynamics using LIED and FABLES is being evaluated: the aim is to follow unimolecular dissociation using pump-probe schemes. A potential candidate is the breaking of the I-C bond in aligned ICN ($I_p = 10.8$ eV) by exciting from its ground state to its lowest excited, repulsive **A** state.

1.4 REFERENCES CITED

- [1] M. Meckel *et al.*, *Science* **320**, 1478-1482 (2008).
- [2] J. Itatani *et al.*, *Nature* **432**, 867-871 (2004).
- [3] S. Haessler *et al.*, *Nat. Phys.* **6**, 200 (2010).
- [4] Xu, J. *et al.*, *Nat Commun* **5** (2014).
- [5] C. I. Blaga *et al.*, Imaging ultrafast molecular dynamics with laser-induced electron diffraction, *Nature* **483**, 194 (2012).
- [6] Z. Diveki *et al.*, *New J. Physics* **14**, 023062 (2012).
- [7] R. E. F. Silva, F. Catoire, P. Rivière, H. Bachau & F. Martín, *Phys. Rev. Lett.* **110**, 113001 (2013).
- [8] R. R. Lucchese, G. Raseev & V. McKoy, *Phys. Rev. A* **25**, 2572 (1982).

1.5 PUBLICATION RESULTING FROM THIS GRANT SINCE 2012-2015

1. “*Diffraction using laser-driven broadband electron wave packets*”, Junliang Xu *et al.* *Nat. Comm.* **5**, 4635 (2014).
2. “*Strong-field and attosecond physics in solids*”, S. Ghimire *et al.*, *J. Phys. B* **47**, 204030 (2014).
3. “*Laser-induced electron diffraction for probing rare gas atoms*”, Junliang Xu *et al.*, *Phys. Rev. Lett.* **109**, 233002 (2012).
4. “*Imaging ultrafast molecular dynamics with laser-induced electron diffraction*”, C. I. Blaga *et al.*, *Nature* **483**, 194 (2012).
5. “*Generation and propagation of high-order harmonics in crystals*”, S. Ghimire *et al.*, *Phys. Rev. A* **85**, 043836 (2012).

1.6 REVIEW ARTICLES ACKNOWLEDGING THIS DOE AWARD

1. “*Scaling of high-order harmonic generation in the long wavelength limit of a strong laser field*”, A. D. DiChiara *et al.*, *IEEE J. Select. Topics Quan. Electro.* **18**, 419-433 (2012).
2. “*Atomic and molecular ionization dynamics in strong laser-fields: from optical to X-rays*”, P. Agostini and L. F. DiMauro, in *Atomic, Molecular, and Optical Physics*, v.61, eds. P. Berman, E. Arimondo and Chun Lin (Elsevier, Maryland Heights, 2012) pp. 117-158.
3. “*Strong-field interactions at long wavelengths*”, M. Kremer, C. I. Blaga, A. D. DiChiara, S. B. Schoun, P. Agostini, and L. F. DiMauro, in *Attosecond and XUV Physics: Ultrafast Dynamics and Spectroscopy*, eds. T. Schultz and M. Vrakking (Wiley-VCH Verlag, Weinheim, 2014), Chapter 11.

PROGRAM TITLE: ATTOSECOND AND ULTRA-FAST X-RAY SCIENCE

Louis F. DiMauro
 Co-PI: Pierre Agostini
 Department of Physics
 The Ohio State University
 Columbus, OH 43210
dimauro@mps.ohio-state.edu
agostini@mps.ohio-state.edu

1.1 PROJECT DESCRIPTION

Attosecond light pulses from gases offer a transition to a new time-scale and open new avenues of science while complementing and directly contributing to the efforts at the LCLS XFEL. An objective of this grant (DE-FG02-04ER15614) is the development of competency in generation and metrology of attosecond pulses using mid-infrared drivers and a strategy of employing these pulses for studying multi-electron dynamics in atomic systems. It concentrates on two approaches (1) attosecond spectroscopy: the application of a well characterized, phase-matched, Fourier-synthesized high harmonic attosecond source for inducing a 1-photon transition in an atom/molecule of interest in a downstream end-station and (2) high harmonic spectroscopy (HHS): the analysis of the emission of high harmonic radiation generated from an atom/molecules of interest. In HHS, the information is conveyed via the 1-photon recombination electric dipole matrix elements (RDM) between the continuum EWP and the initial state. The grant has also a complementary thrust at the LCLS XFEL for studying the scaling of strong-field interactions into a new regime of x-ray science and the metrology of ultra-fast x-ray pulses.

Progress over the past year includes (1) measurement of the atomic phase near the Cooper minimum in argon atoms, (2) study of the Wigner delay in photoionization of inert gas atoms, (3) a study to examine near threshold atomic effects in RABBITT measurements in collaboration with Prof. Robert Jones (UVa) and (4) measurement of few femtosecond x-ray pulses from the LCLS.

1.2 PROGRESS IN FY15: THE ATTOSECOND PROGRAM

The technical approach of the Ohio State University (OSU) group is the use of long wavelength ($\lambda > 0.8 \mu\text{m}$) driving lasers for harmonic and attosecond generation. Through support of this program, the long wavelength approach has been successful and adopted by many groups world-wide. Our program over the last two years has focused on using these long wavelength generated harmonics for measurements, ultimately of dynamics. We are interested in addressing two basic questions related to attosecond physics. First, can high harmonic and attosecond spectroscopy extract detailed atomic/molecular structure and second, what is really being measured.

Attosecond pulse shaping around a Cooper minimum. In this study we examined the ability of HHS for extracting atomic information from the generation atom. Although HHG process occurs in an intense laser field, the quantitative rescattering (QRS) theory suggests that the field-free recombination dipole moment (RDM) [1,2] can be factorized independent of the external field. In our study, we applied the RABBITT method to extract the amplitude and phase of the argon atom emitter near the Cooper minimum ($\sim 50 \text{ eV}$). The Cooper minimum (CM) in photoabsorption is caused by a sign change, equivalent to a π -phase jump, in the bound-free transition dipole of one angular momentum channel at a fixed energy [3]. The CM has been extensively studied using traditional photoionization spectroscopy but the phase of the total transition dipole is not directly accessible, although it strongly influences the measured electron angular distribution and spin polarization [4,5]. Previous HHS studies have observed the CM feature in the frequency spectrum of the emitted argon harmonic comb, but not the spectral phase. Amplitude measurements are problematic for several reasons. First, HHG from a NIR driver produces an argon harmonic cutoff near the CM energy. This is further exasperated by the low sampling frequency in the measurement. Second, phase-matching effects near the cutoff significantly alter the spectral shape depending on experimental conditions. Thus the CM in argon became an excellent benchmark for examining the viability of HHS at long wavelengths.

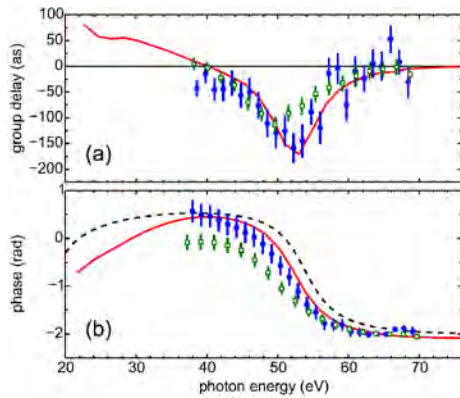


Figure 1: The group delay and phase near the Cooper minimum in argon. High harmonic radiation generated from argon atoms excited by 1.3 μm (green) and 2 μm (blue) pulses are used in the measurements. The total RDM phase evolves by 1.8–2.6 radians over a 20 eV spectral range, even though the d -channel RDM undergoes a sharp π phase shift. The solid line results from calculations performed using the TDSE-MWE method (Gaarde and Schafer). The dashed line is calculated using a simple analytical model.

of atomic and molecular dynamics. This work is a collaborative effort with Profs. Ken Schafer and Mette Gaarde (LSU) and is published in PRL.

Attosecond spectroscopy and interpreting the Wigner delay. Photoionization is the process by which an atom in a bound state absorbs a photon and makes a transition to a continuum state and there is a finite probability to detect the electron at macroscopic distances from the nucleus. Photoionization can be regarded as a quantum jump, which occurs instantaneously at any moment in the field. While there is no such thing as a time operator in quantum mechanics, the delay in photoionization can be a quantum dynamical observable when it is understood as the temporal shift in the departure of the outgoing electron wave packet relative to the arrival of the XUV pulse or when it is treated as the energy-derivative of the time-dependent quantum phase. This is the so-called Wigner delay [6].

In attosecond spectroscopy, photoionization by an XUV pulse train in the presence of an infrared reference pulse (RABBITT or Streaking methods) measures the group delay dispersion (GDD). While none of these, strictly speaking, provide an absolute photoionization delay, previous studies have observed a differential delay between the simultaneous photoemission from different atomic orbitals [7-9] within the same atom, specifically neon and argon. Various theoretical approaches that have been used to model these measurements and the results have varied from good to poor. Consequently, there is a need for more delay measurements over a broad energy range where inter-shell correlation effects are marginal and where various models can be more easily tested.

Our experiment is performed by comparing various inert gas atoms over a broader energy range than previous reports using the RABBITT measurement. In principle, the Wigner delay of the ionized atom/molecule can be extracted by eliminating GDD contributions from the source, filters and the RABBITT measurement. The attosecond pulse train (APT) is generated in neon gas and the inert gas are ionized downstream in the presences of a weak fundamental field. In principle, an ideal experiment would expose a gas mixture to the same APT but this is not practical for technical reasons. Instead, we use a differential method by conducting successive measurements on different target gases for nearly identical APT. Our approach takes the difference of the spectral delays between pairs of rare gases (Ar,He), (Kr,He) and (Ne,He), thus it is possible to eliminate in each case the larger group delay (attochirp)

The HHG photo-recombination process is the inverse of broadband photoionization: an electron wave packet (EWP) promoted and accelerated in the continuum by an intense optical pulse, returns to the core and emits XUV radiation. According to QRS theory, the EWP acts as a self-probe of the laser-free complex RDM, whose amplitude and phase can be measured by the RABBITT method. We have investigated over a broad spectral range the phase modification in the high harmonic emission induced by the $3p$ Cooper minimum of argon. The measurement is performed at two drive wavelengths, 1.3 μm and 2 μm , which produce HHG cutoff energies of 100 eV and 200 eV, respectively. Thus, the 50 eV CM is well within the HHG plateau. The measured RDM phase and amplitude agrees well with predictions based on the scattering phases and amplitudes of the interfering s - and d -channel contributions to the complementary photoionization process (see Fig. 1). The reconstructed attosecond bursts that underlie the HHG process show that the derivative of the RDM spectral phase, the group delay, does not have a straight-forward interpretation as an emission time, in contrast to the usual attochirp group delay. Instead, the rapid RDM phase variation caused by the CM reshapes the attosecond bursts. Most importantly, our results unequivocally establish that direct measurement of the RDM phase near a CM can be precisely extracted from RABBITT.

This provides a foundation for future HHS studies as a probe

associated with the APT itself and obtain the Ar, Kr and Ne “effective” Wigner delays referenced to calculated He delay. Over the energy range of our experiments the calculated He delay is a reasonably precise reference. Our extracted delays have been compared with several theoretical predictions and the results are consistent within 30 *as* over the energy range from 10-50 eV. Of particular interest are slight deviations which may be potential signatures of resonances, this is the subject of future investigations. Two technical improvements are currently underway to enhance the long-term stability and precision of these types of measurements: (1) active stabilization of our interferometer and (2) achromatic interferometric operation of the RABBITT end station. This work is published in J. Phys. B.

Measuring a few femtosecond X-ray pulse from the LCLS. One of the key characteristics of the intense X-ray pulses from the LCLS is few femtosecond operation. No measurement had succeeded in directly determining the temporal structure or even the duration of these ultrashort pulses in the few femtosecond range. In our study we used the streaking technique developed for the metrology of isolated attosecond pulses [10,11]. Like RABBITT, streaking is a two-color technique involving the process of atomic photoionization by an x-ray pulse in the presence of an intense optical reference field. Unlike RABBITT, the streaking method is non-perturbative, does not require commensurate frequencies and applicable when the X-ray pulse duration is shorter than the period of the reference field (1-10 fs), which is presumably satisfied in the “low-charge mode” LCLS operation. The major hurdle for applying this method at the LCLS is the large temporal jitter, t_j , between the X-ray and optical pulses.

The principle is that since the X-ray pulse only extends over a part of the period of the dressing field, the photoelectrons generated at different delays between the XFEL and the MIR pulse will experience redistribution in energy that depends on the magnitude of the electric field at the instant of their generation. In this way, the electron spectra are significantly altered in their final energy spread and central energy with respect to the unstreaked photoelectron burst, ϵ_c . The 2-color energy shift, $\Delta\epsilon$, is given classically as, $\Delta\epsilon(t_b) \approx -p_c A_{\text{MIR}}(t_b)$ where $p_c = (2\epsilon_c)^{1/2}$ is the unstreaked momentum in atomic units and $A_{\text{MIR}}(t_b)$ is the MIR vector potential at birth. However, the large t_j requires that the measurement be treated as a series of single shot experiments. The key is to use the spectral asymmetry that is introduced as a unique marker for each shot in the data post-processing analysis.

In our experiment a MIR laser field (2.6 μm) is coarsely synchronized and spatially overlapped with the X-ray beam in a dilute gas target. Neon gas atoms are ionized by the XFEL and the generated photoelectrons are detected with a magnetic bottle electron spectrometer (MBES) constructed by the OSU group. With an FEL photon energy of ~ 1.791 keV and a binding energy of 870 eV for the 1s electron shell in Ne, the kinetic energy of the photoelectrons in the absence of the MIR laser is distributed around a mean value of ~ 921 eV. Thus, each photoelectron can be modelled as a free wave packet, and the temporal structure of the complete photoelectron burst is a replica of the incoming XFEL pulse

We have measured that the shortest X-ray pulse durations are on average no longer than 4.4 fs. In addition, we were able to investigate the stochastic substructure of these pulses confirming the expected behavior of an underlying train of ultrashort, high-intensity spikes for SASE operation. These experiments were performed in collaboration with Prof. R. Kienberger (MPQ Garching), Dr. A. Cavalieri (CFEL Hamburg) and Dr. G. Doumy (ANL) and published in Nature Photonics.

1.3 FUTURE PLANS

In the remaining few months (March 1 end date) we will continue to investigate the applications of high harmonic and attosecond spectroscopy. First, collaboration with Prof. Robert Jones (UVa) aims at measuring the high harmonic group delay (GD) near and below threshold using RABBITT. The quasi-classical model predicts the GD obtains a universal value of zero at threshold. However, the influence of the atomic potential cannot be neglected and should be apparent in the experiment by comparing differences between atoms at fixed frequency. The measurements are complete and we are in the process of analyzing the results. Preliminary analysis seems to show this non-zero behavior at threshold.

Double ionization is a paradigm for understanding many-body effects. As part of our plans, we will use a tunneling simulator to time-resolved double ionization of helium atoms. In the experiment, attosecond pulses will photoionize helium above the 1e threshold (>24 eV) in the presence of an intense dressing field. The linearly polarized dressing field will quiver the electron in a manner similar to the

step-2 in the rescattering model. In this scenario the attosecond photoionization replaces tunnel ionization in a strong low-frequency field while the dressing field acts as the driver of the electron wave packet (EWP). Subsequent interaction of the EWP with the helium core will promote, among others, the $(e,2e)$ process. The requirement is that $3U_p \geq 54$ eV (He^+ ionization potential) and that the dressing field does not ionize helium. Simple estimates show that this is only possible with mid-infrared dressing fields. If successful, the tunnel simulator will allow exquisite control over the $(e,2e)$ process. We are currently finalizing the technical issues associated with this experiment.

Finally, we were awarded LCLS beam time in March 2015 to explore chemical sensitivity of Auger decay by observing Carbon 1s Auger electrons originating from CO, a simple diatomic molecule as well as from CF_4 , a more complicated yet symmetric system. The results of this run are currently being analyzed. This collaboration was with Dr. A. Cavalieri (CFEL Hamburg) and Dr. G. Doumy (ANL).

1.4 REFERENCES CITED

- [1] Z. Chen, A.T. Le, T. Morishita and C.D. Lin, *Phys. Rev. A* **79**, 033409 (2009).
- [2] C.D. Lin, A.T. Le, Z. Chen, T. Morishita and R. Lucchese, *J. Phys. B* **43**, 122001 (2010).
- [3] J. W. Cooper, *Phys. Rev.* **128**, 681 (1962).
- [4] K. N. Huang, W. R. Johnson and K. T. Cheng, *Atomic Data & Nuclear Data Tables* **26**, 33 (1981).
- [5] N. A. Cherepkov, *Zh. Eksp. Teor. Fiz.* **65**, 933 (1973).
- [6] E. P. Wigner, *Phys. Rev.* **98**, 145 (1955).
- [7] D. Guenot *et al.*, *Phys. Rev. A* **85**, 053424 (2012).
- [8] K. Klunder *et al.*, *Phys. Rev. Lett.* **106**, 143002 (2011).
- [9] M. Schultze *et al.*, *Science* **328**, 1658 (2010).
- [10] J. Itatani, F. Quere, G. L. Yudin *et al.*, *Phys. Rev. Lett.* **88**, 173903 (2002).
- [11] R. Kienberger, E. Goulielmakis, M. Uiberacker *et al.*, *Nature* **427**, 817 (2004).

1.5 PUBLICATION RESULTING FROM THIS GRANT FROM 2013-2015

1. “*Attosecond Pulse Shaping around a Cooper Minimum*”, S.B. Schoun, R. Chirla, J. Wheeler, C. Roedig, P. Agostini, L.F. DiMauro, K.J. Schafer, and M.B. Gaarde, *Phys. Rev. Lett.* **112**, 153001 (2014).
2. “*Atomic delay in helium, neon, argon and krypton*”, C. Palatchi, J. Dahlstrom, A. S. Kheifets, I. A. Ivanov, D. M. Canaday, P. Agostini and L. F. DiMauro, *J. Phys. B* **47**, 245003 (2014)..
3. “*Measuring the temporal structure of few-femtosecond free-electron laser X-ray pulses directly in the time domain*”, W. Helml *et al.*, *Nat. Photonics* **8**, 950 (2014).
4. “*Ultra-fast and ultra-intense X-ray sciences: first results from the Linac Coherent Light Source free-electron laser*”, C. Bostedt *et al.*, *J. Phys. B* **46**, 164003 (2013).

1.6 REVIEW ARTICLES ACKNOWLEDGING THIS DOE AWARD

1. “*Strong-field interactions at long wavelengths*”, M. Kremer, C. I. Blaga, A. D. DiChiara, S. B. Schoun, P. Agostini, and L. F. DiMauro, in *Attosecond and XUV Physics: Ultrafast Dynamics and Spectroscopy* eds. T. Schultz and M. Vrakking (Wiley-VCH Verlag, Weinheim, 2014), Chapter 11.
2. “*Strong-field atomic physics in the x-ray regime*”, L. F. DiMauro and C. A. Roedig, in *Progress in Ultrafast Intense Laser Science X*, Springer Series in Chemical Physics 106, eds. K. Yamanouchi (Springer Publishing, Geneva, 2014), pp. 65-76.

High Intensity Femtosecond XUV Pulse Interactions with Atomic Clusters

Project DE-FG02-03ER15406

Principal Investigator:

Todd Ditmire

Co-Investigator

John Keto

The Texas Center for High Intensity Laser Science

Department of Physics

University of Texas at Austin, MS C1600, Austin, TX 78712

Phone: 512-471-3296

e-mail: tditmire@physics.utexas.edu

Program Scope:

The nature of the interactions between high intensity infrared laser pulses and atomic clusters of a few hundred to a few thousand atoms have been well studied. Such studies have found that these interactions are more energetic than interactions with either single atoms or solid density plasmas and that the clusters explode with substantial energy. Under the previous phases of BES funding we extended investigation in this interesting area by undertaking a study of the interactions of intense extreme ultraviolet (XUV) pulses with atomic clusters, and more recently, interactions with intense x-ray pulses from the Linac Coherent Light Source (LCLS). Our current work builds on our previous work with femtosecond XUV pulses produced by high harmonic generation (HHG). We are now studying interactions at 100 times larger XUV intensity than we obtained earlier. This was accomplished by upgrading our HHG beam line to much higher drive energies on the upgraded THOR laser, and we will increase the intensity further by increasing the phase matching length. We also plan new target clusters, pulse-probe experiments and XUV fluorescence.

Our studies with XUV light are designed to illuminate the mechanisms for intense pulse interactions in the regime of high intensity but low ponderomotive energy by measurement of electron and ion spectra. This regime of interaction is very different from interactions of intense IR pulses with clusters where the laser ponderomotive potential is significantly greater than the binding potential of electrons in the cluster.

We have designed experiments using new targets to confirm our hypothesis about the origin of the high charge states in these exploding clusters, an effect which we ascribed to plasma continuum lowering (ionization potential depression) in a cluster nanoplasma. This effect, which is well known in plasma physics, leads to a depression of the ionization potential enabling direct photo-ionization of ion charge states which would otherwise have ionization energies which are above the photon energy employed in the experiment. To do this we will perform experiments in which XUV pulses of carefully chosen wavelength irradiate clusters composed of only low-Z atoms and clusters with a mixture of this low-Z atom with higher Z atoms (eg. SiO₂ and SnO₂). Experiments on clusters from solids will be enabled by development during the past grant period in which we constructed and tested a cluster generator based on the Laser Ablation of Microparticles (LAM) method. Using a LAM device we will explore oxide clusters as well as metal clusters chosen such that the intense XUV pulse rests at a wavelength that coincides with the giant plasma resonance of the metallic cluster. The latter clusters will exhibit higher electron densities and will serve to lower the ionization potential further than in the clusters composed only of low Z atoms. This should have a significant effect on the charge states produced in the exploding cluster.

We will also explore the transition of explosions in these XUV irradiated clusters from Coulomb to hydrodynamic expansion. We observed hints of this transition in our recent work on THOR in which we compared explosions of Xe and Ar clusters irradiated at 38 nm. The work to be performed with the upgraded beamline has now explored clusters of a wide range of constituents, including not only clusters from gases (Xe, Ar, N₂, CH₄, and Xe doped CH₄) but also clusters from solids. In particular we are currently studying CH₄ and mixed Xe/CH₄ clusters to compare with previous studies at LCLS [Pub. 6, 7] and studies of oxide clusters in gases (O₂ and CO₂) preliminary to experiments with metal oxide nanoparticles to measure the electron density dependence of continuum lowering. We have also irradiated nanoparticles produced by LAM at 800 nm.

Progress During the Past Year

In our past experiments on XUV irradiation of noble gas clusters we produced harmonic radiation by loosely focusing 40 fs pulses with a MgF $f\#/60$ lens from our THOR Ti:sapphire laser into an Ar gas jet.¹ These data showed that we were able to produce an 8 μ m spot dia. with the 38 nm pulse, yielding a focal intensity of $\sim 5 \times 10^{11}$ W/cm² assuming an XUV pulse duration of 10 fs. These harmonics were then focused into the plume of a second, low density cluster jet. The main limitation of this apparatus was that the drive laser pulse energy was limited to ~ 60 mJ by the use of lens and focal geometry constrained by the lab space. This limited the XUV energy per pulse to ~ 0.5 nJ/pulse in the 21st harmonic.

We have now improved this beam line in new expanded lab space. The new beam line employs all-reflective optics which loosely-focuses ($f/100$) the full energy of THOR (0.6J after the compressor) into a gas jet. The XUV is sent to the interaction chamber where one of the harmonics is selected and focused using a Sc/Si mirror into gas clusters or nanoparticles for HED studies. The beamline is divided in three stages: 1- Focusing, 2- HHG, 3-XUV interaction. In the first stage, the compressed 4 cm diameter beam is steered 90° in the focusing chamber, sent to a 0° mirror in the retro chamber. There the beam reflects back onto a $f/l = 5.50$ m, concave spherical mirror that focuses the beam under a rectangular shaped (~ 0.5 mm x 5 mm) conical, gas jet in the HHG stage at laser intensities up to 3×10^{15} W/cm². The jet is moved upstream of the focus to optimize harmonic conversion efficiency. Two stages of differential pumping are used upstream of the harmonic nozzle to limit the pressure to below 10^{-5} Torr in the compressor. Three stages of differential pumping are used downstream to limit the pressures to less than 10^{-7} Torr.

Separation of the XUV pulses from the fundamental and low order harmonics is done in a two-step process. Initially, the pulse before leaving the compressor traverses a 1 cm diameter mirror (reflective mask) in the center of the beam that creates a donut shaped, spatial beam profile. The mask is at approximately two focal lengths upstream from the focusing mirror and its image is located at two focal lengths downstream. At this location, right before entering the interaction chamber, an aperture with the size of the circular disk blocks most of the infrared donut shaped profile. The XUV, having a much shorter wavelength and divergence propagates through the center of the aperture with a small fraction of the fundamental light that was scattered by the gas jet. Following the aperture, a 200 nm aluminum foil (Luxel Corp.), with approximately 20-50% transmission in the XUV range, blocks the remaining fundamental light and harmonics with $\lambda > 70$ nm. Optimization of the HHG yield is achieved by observing the harmonic spectrum using a grazing incident spectrograph with a multichannel plate detector, phosphor plate, and CCD camera. We optimized the HHG production as a function of jet pressure, x,y and z position of the jet relative to the focus, pulse width of the laser (optimum at minimum pulse width), and laser energy (optimum at maximum fundamental energy). Using an XUV calibrated photodiode (AXUV100, Opto Diode Corp.) we measured the total energy on target in the 21st harmonic (38 nm) to be ~ 10 nJ. This is a factor of 20 times greater than measured for the previous beam line. We performed a knife edge measurement of the XUV focus for the Si/Sc mirror which is consistent with a spot diameter of 4 μ m at $1/e^2$ and a peak laser fluence of 80 mJ/cm². Because of the greater bandwidth of the OPCPA in the upgraded THOR laser, we achieved an IR laser pulse width of 25 fs.

Gas Cluster Explosion Dynamics Using XUV light

Our previous experiments on the interaction of intense near-infrared laser pulses with noble gas clusters have shown the ejection of anomalously high ion charge states, and revealed that the clusters' explosion mechanism (either Coulombic or hydrodynamic) depends on the cluster size and Z constitution². While the interaction of these clusters with infrared has been extensively explored, the effects of shorter wavelengths like extreme ultraviolet (XUV) have not. In this regime individual photons carry enough energy to eject bound atomic electrons via photoionization. We have used the newly constructed THOR-XUV beamline to study the explosion dynamics of Ar and Xe clusters to compare with our previous XUV experiments and for CH₄ and Xe doped CH₄ to compare with our data from the LCLS experiments. We have also completed preliminary experiments on Van der Waals clusters of O₂ and CO₂ to compare with the planned experiments measuring the ionization potentials of oxygen ions in crystalline oxide nanoparticles.

¹ K. Hoffmann, B. Murphy, N. Kandadai, B. Erk, A. Helal, J. Keto, and T. Ditmire, "Rare gas Cluster Explosions with intense short pulse XUV Light," *Phys. Rev. A* **83**, 43203-212(2011).

² B. Erk, K. Hoffmann, B. F. Murphy, N. Kandadai, A. Helal, J. Keto, and T. Ditmire, "Observation of shells in Coulomb explosion of rare-gas clusters", *Physical Review A* **83**, 043201 (2011).

Our new data for Xe clusters reproduced the previously observed charge states above Xe^{3+} , which would be expected for ionization of atoms ($\text{IP Xe}^{3+}\text{-Xe}^{4+} = 40.9 \text{ eV}$). We previously saw up to Xe^{8+} with a sharp drop in the intensities above Xe^{5+} . This is again observed in new experiments shown in Fig.1. Our previous estimates for continuum lowering predict single photon ionization of Xe^{4+} but not for production of charge states above $Z=5+$. While these charge states were observed in FEL experiments for similar intensities ($\sim 10^{13} \text{ Wcm}^{-2}$), the fluences in the FEL experiments were $\sim 10^2$ larger than even our current ones (7 J/cm^2 vs 80 mJ/cm^2) and a factor of 10^3 larger than our previous experiments.³ We have now reproduced our previous observations with significantly different laser and XUV beam line conditions. We verified in both the previous and current experiments that IR light, suggested by others to be leaking through pinholes in the Al filter, did not contribute to cluster heating. A glass slide was translated into the XUV beam following the Al filter. The slide completely blocks high harmonics but would transmit stray IR light and low harmonics potentially not blocked by the filter. The slide completely extinguished both the TOF signal and the signal on the XUV diode. We reproduced our current XUV total energy measurements after the interaction zone ($\sim 10 \text{ nJ}$) with XUV diodes of different areas and capacitance.

While we have observed the same ion states as in FEL experiments, the intensities observed are very different. We observe a $\text{Xe}^+/\text{Xe}^{2+}$ ratio of nearly 10, with factors of ~ 2 further decrease in population with each increasing charge state. The largest charge states have an area a factor $\sim 3 \times 10^4$ smaller than Xe^+ . Because of the larger fluence in FEL experiments, depletion of neutral and lower charge state ions occurs such that at a cluster size of 30,000 atoms the population of Xe^{2+} is twice that of Xe^+ , with only 20% decreases between charge states for more highly charged ions. This production of ions is supported by recent theory which includes continuum lowering, ionization from excited states of ions and atoms, and collisional ionization.⁴

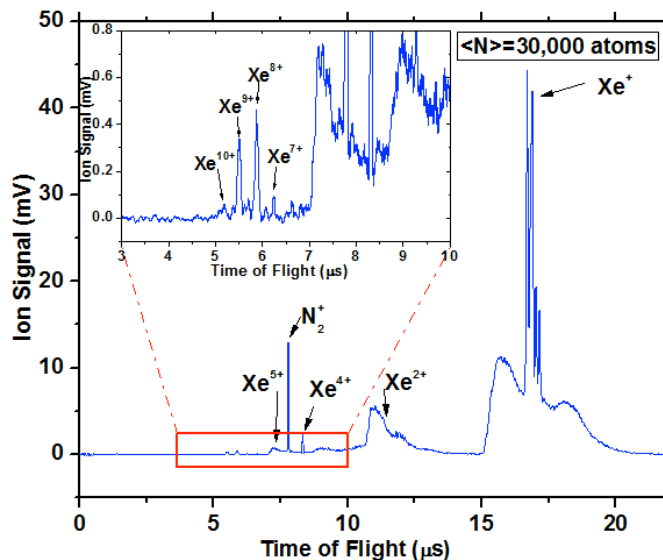


Fig. 1. New data show charge states $Z = 10+$.

The confirmation of previous results is important because recent studies of XUV heating of clusters using harmonic light failed to observe charge states above Xe^{2+} .⁵ Because of the high contrast of THOR after the upgrade, there is no possibility of preheating of the clusters by prepulses in the laser. These would not produce harmonics. The XUV intensities and fluences between the two labs are very similar, but the Xe TOF spectrum reported was excited by the 13th and 15th harmonics with a S/N of ~ 50 , which is insufficient to observe the higher ion states observed in Fig. 1. Our experiments were conducted for predominantly the 21st harmonic (25% 19th and 23rd observed) where we expected and observed production of Xe^{3+} in atomic jets (eg. $\langle N \rangle = 1$). Since the apparatus for the two experiments were similar, with similar fluences in the two experiments, we would expect similar results.

At the increased XUV intensity ($\times 200$) compared to our previous experiments, we have begun to observe effects which might be from multiphoton absorption of XUV light. In earlier experiments measuring the TOF spectrum for free electrons emitted by the exploding cluster, we saw sharp peaks consistent with direct photoionization of atoms within the cluster by the XUV light.¹ These electrons were observed for each of the harmonics at electron energies $h\nu\text{-IP}$. At the higher intensity, we have observed sharp peaks in the electron TOF spectra from Ar and CH_4 clusters at energies near 54 eV corresponding to the production of photoelectrons at energies of $2h\nu\text{-IP}$. We are investigating the origin of these electron features.

³ H. Wabnitz, et al., "Multiple ionization of atomic clusters by intense soft x-rays from a free electron laser, *Nature* **420**, 482(2002).

⁴ E. Ackad, N. Bigaouette, K. Briggs, and L. Ramunno, "Clusters in Intense XUV pulses: Effects of cluster size on expansion of dynamics and ionization," *Phys. Rev. A* **83**, 063201(2011).

⁵ B. Shutte, M. Arbeiter, Th Fennel, M.J.J. Vrakking, and A. Rouzee, "Rare-gas Clusters in Intense Extreme-Ultraviolet Pulses from a High-Order Harmonic Source," *Phys. Rev. Lett.* **112**, 073003(2014).

We have made extensive studies of methane clusters with XUV in order to compare with the previous results in SLAC experiments at photon energies of 800 and 2000 eV. [Pub. 5] The most dramatic difference between the two experiments is the intensity of the proton peak, which is 3 times brighter than the hydrocarbon peaks when exciting with 800 eV x-rays at LCLS. For XUV light, the hydrogen fragmentation is three times smaller than for the hydrocarbon peaks. We observe CH_5^+ and larger cluster ions in both experiments, and the peak intensity increases with cluster size. For both experiments the cluster explosion is more energetic as observed by the increased peak widths as the cluster size increases. Finally, we see that the height of the proton and CH_5^+ peaks generated during the cluster explosion increases until a cluster size of $\sim 30,000$ molecules, and then decrease. In the ion energy spectra we observe a transition between Coulomb and hydrodynamic explosion of the clusters at approximately the same cluster size.

Future Research Plans

Our future plans involve studying continuum lowering in mixed species clusters. We have finished the construction of a laser ablation of micro-particle LAM nanoparticle source to be installed on the XUV beam line. We have now observed the explosion of silver nanoparticles and microparticles produced by using the central zone ($\sim 10\%$) of the THOR laser beam at 800 nm. Experiments on oxide nanoparticles such as SiO_2 , TiO_2 , and ZrO_2 will measure continuum lowering in mixed low and high Z clusters.

Refereed papers published or submitted on work supported by this grant during the past three years

- 1) W. Bang, M. Barbui, A. Bonasera, G. Dyer, H. J. Quevedo, K. Hagel, K. Schmidt, F. Consoli, R. De Angelis, P. Andreoli, E. Gaul, A. C. Bernstein, M. Donovan, M. Barbarino, S. Kimura, M. Mazzocco, J. Sura, J. B. Natowitz, and T. Ditmire, "Temperature Measurements of Fusion Plasmas Produced by Petawatt-Laser-Irradiated $\text{D}_2\text{-He}^3$ or $\text{CD}_4\text{-He}^3$ Clustering Gases" *Phys. Rev. Lett.* **111**, 055002 (2013).
- 2) W. Bang, G. Dyer, H. J. Quevedo, A. C. Bernstein, E. Gaul, M. Donovan, and T. Ditmire, "Optimization of the neutron yield in fusion plasmas produced by Coulomb explosions of deuterium clusters irradiated by a petawatt laser" *Phys. Rev. E* **87**, 023186 (2013).
- 3) W. Bang, H. J. Quevedo, G. Dyer, J. Rougk, I. Kim, M. McCormick, A. C. Bernstein, A. and T. Ditmire, "Calibration of the neutron detectors for the cluster fusion experiment on the Texas Petawatt Laser" *Rev. Sci. Instruments* **83**, 063504 (2012).
- 4) H. Thomas, N. Kandadai, K. Hoffmann, A. Helal, J. Keto, B. Iwan, N. Timneanu, J. Andreasson, M. Seibert, D. van der Spoel, J. Hajdu, S. Schorb, T. Gorkhover, D. Rupp, M. Adolph, T. Möller, G. Doumy, L.F. DiMauro, C. Bostedt, J. Bozek, M. Hoener, B. Murphy, N. Berrah and T. Ditmire "Explosions of Xe-clusters in ultra-intense femtosecond x-ray pulses from the LCLS X-ray Free Electron Laser" *Phys. Rev. Lett.* **108**, 133401 (2012).
- 5) N. Timneanu, B. Iwan, J. Andreasson, M. Bergh, M. Seibert, C. Bostedt, S. Schorb, H. Thomas, D. Rupp, T. Gorkhover, M. Adolph, T. Möller, A. Helal, K. Hoffmann, N. Kandadai, J. Keto, T. Ditmire, "Fragmentation of clusters and recombination induced by intense ultrashort X-ray laser pulses," Proc. SPIE Vol. 8777, p. 87770J1-J7, (2013).
- 6) N. Kandadai, H. Thomas, K. Hoffmann, A. Helal, J. Keto, T. Ditmire, B. Iwan, N. Timneanu, J. Andreasson, M. Seibert, D. van der Spoel, J. Hajdu, S. Schorb, T. Gorkhover, D. Rupp, M. Adolph, T. Möller, G. Doumy, L.F. DiMauro, C. Bostedt, J. Bozek, M. Hoener, B. Murphy, N. Berrah, "Explosion of Methane clusters in ultra-intense femtosecond x-ray pulses from the free-electron-laser LCLS", to be published *Phys. Rev. Lett.*
- 7) N. Kandadai, et. al., "Explosion of Xe doped CH_4 clusters in intense femtosecond x-ray pulses", submitted *Phys. Rev. Lett.*

Electron Correlation in Strong Radiation Fields

J. H. Eberly
Department of Physics and Astronomy
University of Rochester, Rochester, NY 14627
eberly@pas.rochester.edu

Introduction

We are interested to understand how very intense laser pulses excite electrons in atoms and molecules, with intensities in the range $I \geq 0.1 \text{ PW/cm}^2$. This is the trigger for all high-field physics effects of recent and current interest, from multi-electron ejection to high-harmonic generation to the newly emergent area of atto-science. The combination of phase-coherent character and short-time nature of laser pulses in experimental use creates substantial challenges to theoretical study in this domain. We have listed the existing challenges and discussed the successes in an invited review [1]. The intensities are high enough to mandate development of non-perturbative approaches and this has led to several partially conflicting and partially overlapping theoretical methods. We are currently extending [2] to a full range of ellipticities the success reported previously [3] with application of the so-called SENE method, and continue to pursue when resources are available an application of the powerful Schmidt decomposition, appropriate to TDSE wave functions that must contend with strongly conditional behavior in breakup processes. High-field ionization is a very relevant example.

Research Summary and in Progress

In 2013 and 2014 we introduced the new SENE approach [3] to theoretical analysis of high-field ionization events, building on our leading studies of angular and linear momentum distributions arising from single and double ionization under elliptical polarization [4, 5, 6, 7, 8, 9, 10], with continuing DOE-BES support. The new method combines short-range solutions of the time-dependent Schrödinger equation (TDSE) with long-range solutions of time-dependent Newton equations (TDNE). The key feature of the approach is detection of the wave function by purely numerical ‘detectors’ around a ring surrounding the ion at a radius of about 10-20 a.u. [11]. Rapid numerical analysis yields the electron momenta on the ring without in any way disturbing the evolving wave function. These momenta become the initial conditions for particle trajectories via the TDNE. This exploits the strong points of both the TDSE (capturing quantum features accurately from the ionization onset) and the TDNE (efficient calculation of propagation following electron release). In particular, the initial momenta are (i) independent of intuition associated with tunneling, which is avoided altogether, and (ii) are developed further under the full influences of both the laser field and the ion’s Coulomb force. In 2015 we have extended [2] our application of the method to a wide range of ellipticities, comparing well with experimental reports.

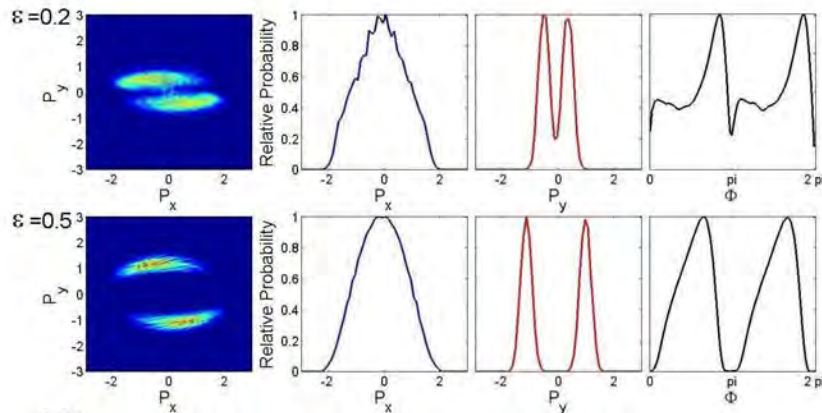


Figure 1: Ionized electron momentum distributions obtained with the SENE method. Strong similarities can be seen with experimental data reported for high-field helium ionization by Pfeiffer, et al. [12].

The numerical detector SENE method has obvious attractive features, but substantial development of it is required. Results have been reported only for high ellipticity, and for a single electron. This was suitable for a successful comparison [3] to existing experimental data. Low and mid-range ellipticities are currently being tested [2], so far successfully, as shown in Fig. 1. We note that the asymmetry of the SENE result here in Fig. 1 for $\varepsilon = 0.2$ is strongly confirmed by the similar asymmetry in the experimental record on helium for $\varepsilon = 0.3$ in Fig. 2b of Pfeiffer, et al. [12].

Our plan is to further extend its range of applicability in order to attack, with a short-range wave function calculation and subsequent SENE momentum analysis (longitudinal and transverse, average and variance) of an ionizing electron in the vicinity of the semi-fictional ionization ‘exit point’ of tunneling theory. This is an important missing link needed for systematic comparison of quantified tunneling theory with current experiments. It is the source of current controversy and an issue that was waiting to become recognized (see Pfeiffer, et al. [12], Shafir, et al. [13], Hoffman, et al. [14], and Sun, et al. [15]).

The origin of the confusion, or controversy or whatever term is best, was well anticipated in an overview a decade earlier by Ivanov, Spanner and Smirnova. As they said [16]: “Identifying the wavepacket dependence on v_x is much harder. The crucial difficulty stems from the fact that the laser field accelerates the electron while it tunnels out. The velocity distribution along the field is changed continuously during tunneling. . . . Uncertainty in the moment of tunneling, which is responsible for the uncertainty in the initial velocity, also means that it is virtually impossible to separate the initial velocity distribution from the distortions caused by the electric field during this temporal uncertainty.”

As resources permit, we will also continue to extend our work on entanglement and momentum conditionality in the ionization process. This will provide systematic and normalized evaluations of the purely quantum contribution to correlation in multi-electron ionization. The benefit will be creation of a previously unavailable feedback route able to manage theoretical assessments of the true quantum components of correlation in outgoing electron momenta, and coordinate them with experimental results. We expect this will also allow two-way exchange of information for a new form of experimental guidance.

The citations of publications that were supported by DOE Grant DE-FG02-05ER15713 in the most recent grant period are marked with *** in the listing below.

References

- [1] ***W. Becker, X.J. Liu, P.J. Ho and J.H. Eberly, “Theories of Photo-Electron Correlation in Laser-Driven Multiple Atomic Ionization,” *Rev. Mod. Phys.* **84**, 1011 (2012).
- [2] ***Justin Tian and J.H. Eberly (testing underway 2015, see Fig. 1)
- [3] ***X. Wang, J. Tian and J.H. Eberly, “Extended Virtual Detector Theory for Strong-Field Atomic Ionization,” *Phys. Rev. Lett.* **110**, 243001 (2013).
- [4] ***Justin Tian, Xu Wang and J.H. Eberly, Extended Breakdown of the Simpleman Approximation, *Chin. Opt. Lett.* **11**, 010001 (2013).
- [5] *** Xu Wang, Justin Tian and J.H. Eberly, “Angular correlation in strong-field double ionization under circular polarization,” *Phys. Rev. Lett.* **110**, (7) 073001 (2013).
- [6] ***X. Wang and J.H. Eberly, “Nonadiabatic Theory of Strong-Field Atomic Effects under Elliptical Polarization”, *J. Chem. Phys.* **137**, 22A542 (2012).
- [7] ***Xu Wang and J.H. Eberly, “Classical theory of high-field atomic ionization using elliptical polarization,” *Phys. Rev. A* **86**, 013421 (2012).
- [8] Xu Wang and J.H. Eberly, “Elliptical Polarization and Probability of Double Ionization,” *Phys. Rev. Lett.* **105**, 083001 (2010).
- [9] Xu Wang and J.H. Eberly, “Elliptical Trajectories in Nonsequential Double Ionization,” *New J. Phys.* **12**, 093047 (2010).
- [10] Xu Wang and J.H. Eberly, “Effects of Elliptical Polarization on Strong-Field Short-Pulse Double Ionization,” *Phys. Rev. Lett.* **103**, 103007 (2009).
- [11] Our virtual detectors were inspired by B. Feuerstein and U. Thumm, in *J. Phys. B* **36**, 707 (2003). Ours encircle the real two-dimensional ‘ionization space’ of the electron all the time it is interacting with an elliptically polarized laser pulse. The original Feuerstein-Thumm virtual detectors intercepted ionic fragments of a one-dimensional model dissociation of He_2^+ .
- [12] “... we study the longitudinal momentum spread of the electronic wave packet at the tunnel exit point, a quantity that has raised substantial interest and controversy.” A.N. Pfeiffer, C. Cirelli, A.S. Landsman, M. Smolarski, D. Dimitrovski, L.B. Madsen and U. Keller, *Phys. Rev. Lett.* **109**, 083002 (2012).
- [13] “We find a surprisingly sensitive dependence of Coulomb focusing on the initial transverse momentum distribution, i.e., the momentum at the moment of birth of the photoelectron.” D. Shafir, H. Soifer, C. Vozzi, A. S. Johnson, A. Hartung, Z. Dube, D. M. Villeneuve, P. B. Corkum, N. Dudovich, and A. Staudte, *Phys. Rev. Lett.* **111**, 023005 (2013).
- [14] “... there is no clear way of calculating the longitudinal momentum spread at the exit point from tunneling models.” C. Hofmann, A. S. Landsman, C. Cirelli, A. N. Pfeiffer, and U. Keller, *J. Phys. B* **46**, 125601 (2013).
- [15] “Much effort has been concentrated on exploring the initial longitudinal momentum spread, but it is still controversial.” X. F. Sun, M. Li, J. Z. Yu, Y. K. Deng, Q. H. Gong, and Y. Q. Liu, *Phys. Rev. A* **89**, 045402 (2014).
- [16] M. Y. Ivanov, M. Spanner, and O. Smirnova, *J. Mod. Opt.* **52**, 165 (2005).

Page is intentionally blank.

Image Reconstruction Algorithms

Office of Basic Energy Sciences
Division of Chemical Sciences, Geosciences, and Biosciences
Program in Atomic, Molecular, and Optical Sciences

Veit Elser, Department of Physics
PSB 426, Cornell University
Ithaca, NY 14853
(607) 255-2340
ve10@cornell.edu
uuuuuu.lassp.cornell.edu

Program Scope

The many-orders-of-magnitude gains in X-ray brightness achieved by free-electron laser sources such as the LCLS are driving a fundamental review of the data analysis methods in X-ray science. It is not just a question of doing the old things faster and with greater precision, but doing things that previously would have been considered impossible. Our group at Cornell is working closely with experimental groups at LCLS and elsewhere to develop data analysis tools that exploit the full range of opportunities made possible by the new light sources. We also provide imaging expertise to David Mueller's electron microscopy group and Sol Gruner's detector group, both at Cornell.

Sparse data crystallography

What makes crystallography with small crystals at synchrotrons so difficult is the weakness of the diffraction signal. Building on earlier proof-of-principle experiments with the Gruner group, we have now shown that structures can be determined even when the number of photons collected in each data frame is so small — a few hundred — that there are no identifiable Bragg peaks that serve, as in traditional crystallography, to establish the crystal orientation. This work resulted in two publications. One paper[7] demonstrates the first reconstruction of a molecular crystal (1.35 kDa) from sparse data; the second[8] does this for the first protein crystal (hen egg white lysozyme). Typical data frames from the second experiment are shown in Figure 1; the reconstructed intensity in Figure 2. In these studies we were limited by the experiment to rotations about a single axis. A third experiment was completed recently where this restriction was relaxed. Results of that reconstruction are being prepared for publication.

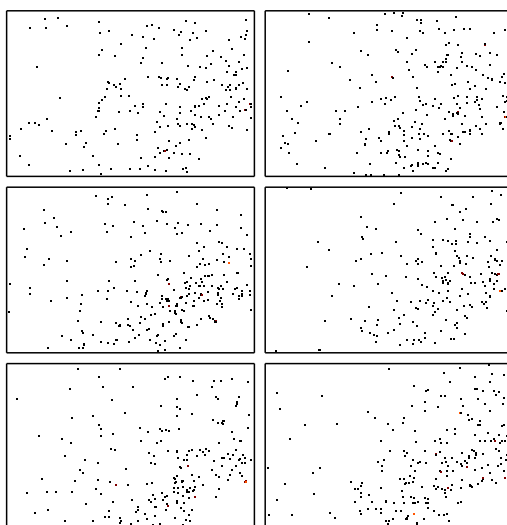


Figure 1: Random selection of six data frames from the lysozyme experiment[8]. The direct beam is incident normally at the lower right region of the detector, which is blocked by the beamstop. About 8 million unoriented sparse data frames such as these were used to reconstruct the high quality intensity shown in Figure 2.

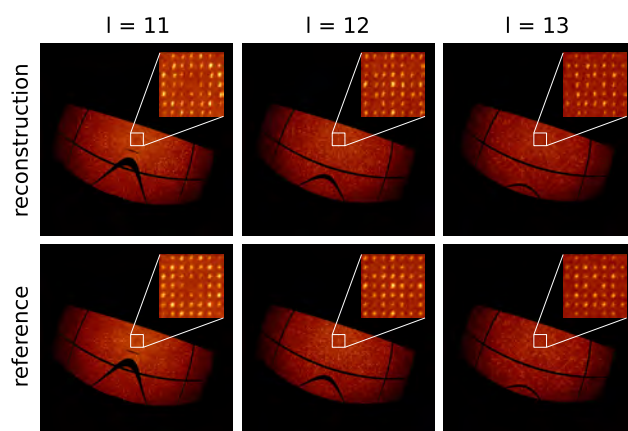


Figure 2: Reconstructed slices of the lysozyme intensity compared with the true intensity (reference). The EMC reconstruction algorithm received 8 million data frames such as those in Figure 1 as input, all with an unknown rotation angle about a single axis.

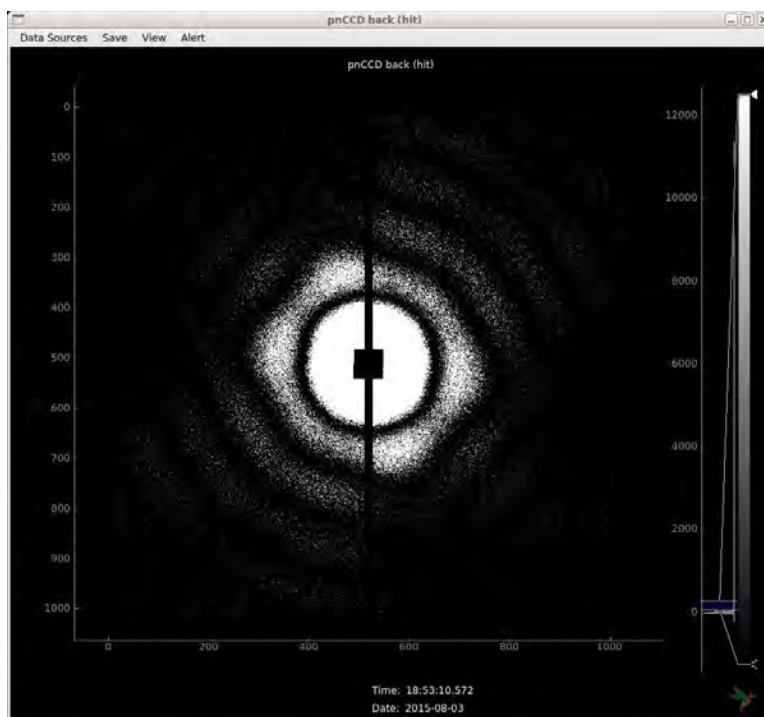


Figure 3: Rice dwarf virus diffraction pattern obtained at the LCLS-AMO beamline in August 2015.

Single particle imaging

2015 may be the year that single particle imaging (SPI) becomes a reality. The PI was fortunate to have had the opportunity to spend the first half of his 2015 sabbatical at LCLS. The timing couldn't have been better, because in March the SPI collaboration had its first beamtime at the CXI endstation. In addition to seeing the operation of the facility on a daily basis and becoming acquainted with all facets of the experiment, the PI and student Ti-Yen Lan played a leading role in selecting the targets. The rice dwarf virus (RDV) rose to the top of the list and was delivered via aerosol injector into the 100 nm focus configuration of CXI. About 200 good hits were obtained in this first experiment. A second experiment, also with RDV, was performed at the AMO endstation in August. About 10^4 hits were recorded in that experiment. Reconstruction of the virus from these diffraction data is currently underway. A sample diffraction pattern is shown in Figure 3.

Publications

- [1] H.T. Philipp, K. Ayer, M.W. Tate, V. Elser & S.M. Gruner, *Solving structure with sparse, randomly-oriented x-ray data*, Opt. Express **20** 13129-13137 (2012).
- [2] V. Elser, *Direct phasing of nanocrystal diffraction*, Acta Cryst. A **69** 559-569 (2013).
- [3] H. J. Park *et al.*, *Toward unsupervised single-shot diffractive imaging of heterogeneous particles using X-ray free-electron lasers*, Opt. Express **21** 28729-28742 (2013).
- [4] K. Ayer, H.T. Philipp, M.W. Tate, V. Elser & S.M. Gruner, *Real-Space x-ray tomographic reconstruction of randomly oriented objects with sparse data frames*, Opt. Express **22** 2403-2413 (2014).

- [5] H.T. Philipp, K. Ayyer, M.W. Tate, V. Elser & S.M. Gruner, *Recovering structure from many low-information 2-D images of randomly-oriented samples*, J. Phys. Conference Series **425** 192016-192019 (2013).
- [6] R. Hovden *et al.*, *Breaking the Crowther limit: Combining depth-sectioning and tilt tomography for high-resolution, wide-field 3D reconstructions*, Ultramicroscopy **140** 26-31 (2014).
- [7] K. Ayyer, H.T. Philipp, M.W. Tate, J.L. Wierman, V. Elser & S.M. Gruner, *Determination of crystallographic intensities from sparse data*, IUCrJ **2** 29-34 (2015).
- [8] J.L. Wierman, T.-Y. Lan, M.W. Tate, H.T. Philipp, V. Elser & S.M. Gruner, *Protein crystal structure from non-oriented, single-axis sparse x-ray data*, to appear in IUCrJ.

Collective Coulomb Excitations and Reaction Imaging

Department of Energy 2014-2015

James M Feagin

*Department of Physics
California State University–Fullerton
Fullerton CA 92834
jfeagin@fullerton.edu*

This progress report describes our ongoing DOE work to extract basic understanding and quantum control of few-body microscopic systems based on our long-time experience with more conventional studies of correlated electrons and ions.

Quantum Imaging

Modern time of flight (TOF) measurement with COLTRIMS and related reaction microscopes distinguishes particle arrivals across the face of a detector plate as a function of time. Generally, uniform electric and magnetic fields are used in the extraction process. From these measurements classical momentum distributions are inferred based on the tacit assumption that the motion of extracted particles is classical outside the microscopic reaction volume. These distributions are then compared to predicted momentum differential cross-sections defined by *quantum* scattering theory.

Historically, almost all calculations of scattering processes have used some approximate form of the T-matrix element (or its time-independent equivalent) as a starting point, since the exact form of the wavefunction $\Psi(t)$ is usually unknown and resort is made to approximations. More recently, increased computing power has enabled direct numerical evaluation of $\Psi(t)$ for many-particle fragmentation cross sections as pioneered by our colleagues in BES, including C. W. McCurdy and T. N. Rescigno,¹ and F. Robicheaux.² Then a projection of the measured final state at large times becomes a practical way of calculating fragmentation amplitudes from $\Psi(t)$. This approach has been recently reviewed by J. Macek.³

In a recent paper,⁴ we have shown how the fully time-independent scattering theory leads to the definition of a classical time outside the microscopic dimensions of the interaction zone and how quantum position variables can be used to define classical momenta. Then, time-dependent quantum propagation applies in this far zone. In the case of free motion, this quantum propagation leads to the *imaging theorem* (IT),³ an aspect we analyzed in detail in another recent paper⁵ restricting to field-free detection to equate the asymptotic spatial wavefunction to the quantum scattering amplitude. In a third recent paper,⁶ we have generalized the IT to uniform electric and magnetic field extraction and COLTRIMS detection.

It has become widely accepted that the reason we observe a classical world, although the motion of particles is governed by a quantum description, can be attributed to the phenomenon of decoherence. This is the change in the wave function of a quantum system due to interaction with a quantum environment, variously taken to be the ambient surroundings, a measuring ap-

¹ W. Vanroose, F. Martin, T. N. Rescigno, and C. W. McCurdy, Phys. Rev. A **70**, 050703 (R) (2004); Science **310**, 1787 (2005).

² J. Colgan, M. S. Pindzola and F. Robicheaux, J. Phys. B: At. Mol. Opt. Phys. **37**, L377 (2004); Phys. Rev. Lett. **98**, 153001 (2007).

³ J. H. Macek in *Dynamical Processes in Atomic and Molecular Physics*, (Bentham Science Publishers, ebook.com, 2012), G. Ogurtsov and D. Doweck, eds.

⁴ J. S. Briggs and J. M. Feagin, Phys. Rev. A **90**, 052712 (2014).

⁵ J. S. Briggs and J. M. Feagin, J. Phys. B: At. Mol. Opt. Phys. **46**, 025202 (2013).

⁶ J. M. Feagin and J. S. Briggs, J. Phys. B: At. Mol. Opt. Phys. **47**, 115202 (2014).

paratus, or a combination of both. One change necessary to achieve a classical status is shown to be the transition from an entangled and delocalized state to an incoherent superposition of probabilities, rather than a coherent superposition of amplitudes. To represent a spatially localized classical particle, the wave function must become extremely narrow so that the probability to detect the particle becomes correspondingly localized. Even though a particle may travel macroscopic distances before detection, it is necessary that the localization due to decohering interaction overcomes the natural spreading of the wave function. It is assumed that spatial localization of a wave function is a prerequisite for classical behavior, and this is achieved by environmental decoherence.

The deterministic propagation of the quantum system under the sole influence of its own Hamiltonian is generally considered not to lead to classical behavior. This past year we have been able to demonstrate generally that features of the transition to classical motion do appear from such propagation, including that due to applied external fields, typically over times and distances which are microscopic. In particular, we have shown in a very recent paper⁷ that the locus of points of equal quantum probability defines a classical trajectory. Hence classical motion will be inferred at all distances at which particle detection is made in practical experiments. Thus we have demonstrated that aspects of the quantum to classical transition do indeed arise from the undisturbed Schrödinger propagation of the system wave function without coupling to a quantum environment. After propagation to distances which are still on the nanoscale, we show that classical motion is encoded in the wave function itself in that *each and every point* of the wave function at different times are connected by a classical relation between coordinates and momenta. This is a far more powerful statement than Ehrenfest's theorem involving only averages.

The essential ingredient of our proof is simply to unify two well-known aspects of quantum dynamics whose connection previously has not been fully appreciated. The first is that classical motion arises simply as a result of deterministic Schrödinger propagation in that, for large asymptotic times and distances, the quantum propagator can be approximated by its semiclassical form. This form is decided purely by classical mechanics through the classical action function; the techniques are well developed and basic to the whole field of semiclassics and quantum chaos. The second aspect is the IT.

We have combined these two aspects in that we use the results of semiclassical quantum theory to generalize the IT to (nonrelativistic) motion under the influence of arbitrary external laboratory fields and particle interactions. Our generalized IT shows that the spatial wave function of any quantum system of particles propagating over macroscopic distances and times becomes proportional to the initial momentum wave function, *where the position and momentum coordinates are related by classical mechanics*. Most importantly, this implies that the probability to measure a particle at a given position at a certain time is identically equal to the probability that it started with a given momentum at an earlier time and has moved according to a classical trajectory. If an experiment is designed to define a final position *and* momentum the trajectory is unique. If only position is measured then more than one trajectory can contribute to the wave function and give rise to interference, as is well documented with neutron and atom interferometry and beautifully demonstrated recently with a single cold helium atom.⁸ Hence, a detection, whether showing interference or not, will infer classical behavior of the quantum system *without any environmental interaction whatsoever*, which would lead to decoherence. In short, an observer would conclude that the motion is classical despite it being governed by the Schrödinger equation. There is no change in the wave function apart from that due to external forces deciding the particles' quantum motion.

⁷ J. M. Feagin and J. S. Briggs, Phys. Rev. Lett., in review (September, 2015).

⁸ A. G. Manning, R. I. Khakimov, R. G. Dall, and A. G. Truscott, Nature Physics **11**, 539 (2015).

Transverse Coherence and Molecular Multi-Center Interference

Schulz and coworkers⁹ have measured in a precision experiment the transverse coherence length of a nearly monochromatic beam of protons, de Broglie wavelength λ , passing through a collimator aperture and scattered by a crossed beam of molecular hydrogen. The two-center nature of the molecular scattering gives rise to a well-established “double-slit interference” effect, which the authors were able to suppress by reducing the distance L of the reaction volume to the collimator aperture. A decrease in L increases the angular width $\alpha \simeq a/L$ the collimator aperture subtends at the target, where $a \ll L$ is the aperture width in the scattering plane. They found that the corresponding decrease in the transverse coherence length λ/α of the scattered protons relative to the two-center molecular bond length suppresses as expected the observed interference effects in the scattering cross section.

A sampling of their results is shown in Fig. 1 along with the theoretical cross-sections of Madison and coworkers.¹⁰ The measurements involved 75 keV incident protons, monochromatic to less than 1 eV, scattered at extraordinarily small angles of less than 1 mrad in 0.1 mrad bins. With an aperture width of $a = 0.15$ mm in the scattering plane, they varied the distance to the reaction volume from $L = 50$ cm down to $L = 6.5$ cm and thereby increased the collimator angular width from $\alpha = 0.30$ mrad to $\alpha = 2.3$ mrad. Thus, with a de Broglie wavelength of $\lambda = 0.10$ pm, they reported a corresponding decrease in the transverse coherence length of the incident beam from $\lambda/\alpha \simeq 6.6$ a.u. at $L = 50$ cm to $\lambda/\alpha \simeq 0.86$ a.u. at $L = 6.5$ cm, and therefore a change in λ/α from greater to smaller than the “two-slit” intermolecular separation $D = 1.6$ a.u. of the molecular hydrogen. They thus accounted for their observed loss at $L = 6.5$ cm of the interference dip evident in the cross section around 0.8 mrad for large L .

While we feel these experiments demonstrate the role of transverse coherence in establishing interference effects, we disagreed in a recent paper¹¹ with the conclusions of Schulz et al. that

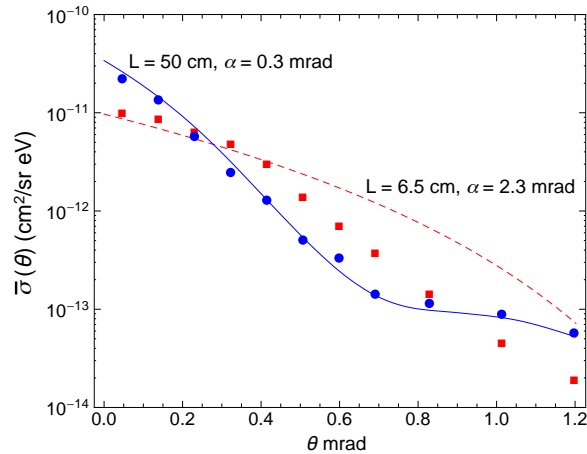


FIG. 1: The proton scattering cross section for ionization of H_2 as a function of proton scattering angle as in Fig. 1 of Schulz et al. The round (blue) and square (red) points are the $L = 50$ cm and $L = 6.5$ cm measurements, respectively, while the solid (blue) and the dashed (red) curves show the calculated cross section of Madison and coworkers *averaged* according to our derived result. The size of the data points corresponds roughly to the error bars in the data, and differences in the blue and red measurements are well outside the statistical error.

⁹ K. N. Egodapitiya, S. Sharma, A. Hasan, A. C. Laforge, D. H. Madison, R. Moshhammer, and M. Schulz, Phys. Rev. Lett. **106**, 153202 (2011).

¹⁰ U. Chowdhury, M. Schulz, and D. H. Madison, Phys. Rev. A **83**, 032712 (2011).

¹¹ J. M. Feagin and L. Hargreaves, Phys. Rev. A **88**, 032705 (2013).

the variable collimation somehow affects the incident beam in a fundamental quantum way. We used an S -matrix momentum formulation of scattering theory to average the cross section in a general way over a statistical ensemble of arbitrary incident-beam *wavepackets*.

Fig. 1 compares our derived beam-averaged cross section $\bar{\sigma}(\theta_f)$ with the data of Schulz et al. for two angular widths α . At $L = 50$ cm with $a = 0.15$ mm, we have $\alpha = 0.3$ mrad and find that $\bar{\sigma}(\theta_f)$ is virtually indistinguishable from the theoretical cross section $\sigma(\theta_f)$ calculated by Madison and coworkers, the $L \rightarrow \infty$ limit. At $L = 6.5$ cm, we have $\alpha = 2.3$ mrad so that the integration range in our expression now covers the entire plot range and the interference dip around 0.8 mrad washes out completely. We conclude it is the weakened beam collimation at $L = 6.5$ cm and the consequent bundle of off-axis incident-wavepacket trajectories that averages out the two-center interference in the molecular scattering.

Our conclusions are analogous to ones derived some time ago in connection with the notion of lost wavepacket coherence in neutron diffraction. Thus we show that the static energy-conserving scattering reactions with steady beam currents considered here will distinguish neither wavepacket structure nor coherence in the incident beam. Instead, we account for the loss of interference observed by Schulz et al. as simply an incoherent average over the poorly collimated ensemble of incident-beam momenta.

Publications

The generalized Imaging Theorem: Quantum to Classical Transition without Decoherence, J. S. Briggs and J. M. Feagin, Phys. Rev. Lett., in review (September, 2015).

Scattering Theory, Multi-Particle Detection and Time, J. S. Briggs and J. M. Feagin, Phys. Rev. A **90**, 052712 (2014).

Reaction Imaging in Uniform Electric and Magnetic Fields, J. M. Feagin and J. S. Briggs, J. Phys. B: At. Mol. Opt. Phys. **47**, 115202 (2014).

Momentum and Spatial Imaging of Multi-Fragment Dissociation Reactions, J. S. Briggs and J. M. Feagin, J. Phys. B: At. Mol. Opt. Phys. **46**, 025202 (2013).

Loss of Wavepacket Coherence in Stationary Scattering Experiments, J. M. Feagin and L. Hargreaves, Phys. Rev. A **88**, 032705 (2013).

Vortex Kinematics of a Continuum Electron Pair, J. M. Feagin, J. Phys. B: At. Mol. Opt. Phys. **44**, 011001 (2011).

Electron-Pair Excitations and the Molecular Coulomb Continuum, J. M. Feagin, J. Colgan, A. Huetz, and T. J. Reddish, Phys. Rev. Lett. **103**, 033002 (2009).

Studies of Autoionizing States Relevant to Dielectronic Recombination

T.F. Gallagher
Department of Physics
University of Virginia
P.O. Box 400714
Charlottesville, VA 22904-4714
tfg@virginia.edu

Initially this research program was focused on doubly excited autoionizing atomic states, with the goal of providing a better understanding of the inverse process, dielectronic recombination (DR), the recombination of ions and electrons via intermediate autoionizing states. DR's importance is that it provides an efficient recombination mechanism for ions and electrons in astrophysical and laboratory plasmas.¹⁻⁴ In fusion plasmas impurity ions from the wall of the containment vessel capture electrons and radiate power from the plasma, negating efforts to heat the plasma. The most important pathway for DR is through the autoionizing Rydberg states converging to the lowest lying excited states of the parent ion. Because Rydberg states are involved, DR rates are profoundly influenced by other charged particle collision processes and any small electric and magnetic fields in the plasma.^{5,6} Consequently, a major thrust of this program has been understanding how autoionization rates, and thus DR rates, are affected by collisions and external fields. The way we mimicked the rapidly varying fields of electron collisions was to use microwave fields. Although we started to use the microwave field to mimic electron collisions, the experiments are, in essence, laser photoionization of atoms in the presence of a strong microwave field. An atom in a strong microwave field exposed to visible radiation is very similar to an atom in an intense infrared field exposed to a train of attosecond xuv pulses, a problem under investigation by many research groups.⁷⁻¹¹ More generally, a microwave field strong enough to ionize atoms leaves atoms in highly excited states, a phenomenon also observed in recent laser ionization experiments.¹²

The isolated core excitation (ICE) method we have used to study autoionizing states also provides a new tool for the spectroscopy of the bound high angular momentum states of alkaline earth atoms. To be specific, it allows us to detect transitions between them. From their energy separations one can determine the polarizabilities and radial matrix elements of the ionic cores.¹³⁻¹⁵ The polarizabilities are important in determining the blackbody frequency shifts of trapped ion based clocks and for parity nonconservation measurements.¹⁶

During the past year we have worked on two projects. First, we have brought into operation an experiment to excite Li atoms in the presence of a strong microwave field phase locked to an amplitude modulated laser field. This experiment is motivated by experiments done with a combined xuv attosecond pulse train (APT) and infrared laser field^{7,8} and our experiments in which we excited atoms in a microwave field phase locked to a mode locked laser producing ps pulses^{17,18} In these experiments the sign and the amount of energy transfer to the electron produced by the xuv or ps laser pulse was dependent on the phase of the low frequency field at which the laser excitation occurred.^{7,8,17,18} According to the theoretical analysis, the large magnitude of the phase dependent ionization signal, 35%, is due to the coherent effect of the

multiple pulses in the APT.⁷ However, an experiment with a single attosecond pulse was not done. In our experiments with a single ps pulse we observed a markedly smaller phase dependence, $\sim 0.1\%$, perhaps due to the absence of coherence over multiple microwave cycles, as earlier asserted.⁷ In the present experiment we have introduced the phase coherence by replacing the ps laser excitation by amplitude modulated laser excitation phase locked to the microwave field. Specifically, we produce an 819 nm laser beam amplitude modulated, at 28 GHz, by combining the beams from two 819 nm diode lasers with frequencies 28 GHz apart. We phase lock the 28 GHz beat note between the two 819 nm lasers to the second harmonic of a 14 GHz microwave oscillator which provides the microwave field in the Fabry-Perot microwave cavity in which the atoms are excited by the laser.

When the laser is tuned above the limit we have observed a 10% modulation in the number of atoms which are recombined into bound states as we vary the phase of the microwave field at which laser excitation occurs. Similarly, when the laser is tuned below the limit, we observe a 10% variation in the number of atoms which are ionized as the phase is varied. There is a one hundred fold increase in the modulation over that observed with single ps laser pulse excitation, as suggested by the original theoretical work. There are three other interesting aspects to this work. The first is that we observe the onset of the recombination at a lower field than expected on the basis of a classical model, indicating that the effect is quantum mechanical in nature. Second, changing the phase of the microwave field at which excitation occurs is equivalent to changing the relative phase of the two 819 nm laser fields, suggesting that are exciting Floquet states. Finally, we are able to see energy transfer to both higher and lower energies. A report of this work has been submitted for publication.

We are presently examining the phase dependence when the microwave frequency is equal to the modulation frequency in the presence of a small static field. In the absence of a static field there is no phase dependent signal, but there is in the presence of a small, ~ 0.4 V/cm, static field. Many laser experiments are conducted in the presence of similar static fields in reaction microscopes, so we expect our results to have wide applicability. Our longer term plans are to replace the two laser arrangement with a single laser which is phase modulated at a frequency of up to 40 GHz, generating sidebands at multiples of 40 GHz. The phase modulated beam is easily converted to amplitude modulation, allowing us to use a higher modulation frequency, the attraction being that experiments done at higher frequencies are less affected by stray electric fields, allowing more quantitative experiments. In addition, having a phase, or frequency modulated, laser provides us with a direct way of testing whether or not the microwave field converts the atoms into Floquet states, which are, in essence, frequency modulated states.

We have published a report of microwave resonance measurements of the Ca $4s_{nf}-4s_{ng}-4s_{nh}-4s_{ni}-4s_{nk}$ intervals, In this case we have used the fact that the lifetimes of the higher ℓ states are longer than the lifetimes of the $4s_{nf}$ states to detect the $4s_{nf}-4s_{n\ell}$ microwave transitions. Using a core polarization model we have obtained the values $\alpha_d=80.0(1) a_0^3$ and $\alpha_q=228(12) a_0^5$ for the Ca^+ dipole and quadrupole polarizabilities. Our value for the dipole polarizability is much closer to the theoretical value than the previous measurement,^{19,20} but α_q is half the theoretical value.²⁰ The theoretical value for α_q is in agreement with measurements of the Ca^+ 3d lifetimes, so it appears to be correct. These Ca measurements and similar results for Ba

and Mg indicate that the core polarization models need to be re-examined. We have discussed this problem with M. Safronova, who suggested that core penetration of higher ionic states might be the problem. We are currently carrying out calculations to explore this notion.

We have started microwave resonance measurements with Yb. Yb is not only a clock candidate, but it is also being used in cold atom experiments with the goal of using the ICE transition to manipulate the cold Rydberg atoms. We have observed the $(n+3)d$ to ng transitions for $29 < n < 35$, and we are planning to use adiabatic rapid passage to move population excited by the laser to the $(n+3)d$ states to the ng states and then observe transitions to the higher ℓ states.

References

1. A. Burgess, *Astrophys. J.* **139**, 776 (1964).
2. A.L. Merts, R.D. Cowan, and N.H. Magee, Jr., Los Alamos Report No. LA-62200-MS (1976).
3. S. B. Kraemer, G. J. Ferland, and J. R. Gabel, *Astrophys. J.* **604** 556 (2004).
4. N. R. Badnell, M. G. O'Mullane, H. P. Summers, Z. Altun, M. A. Bautista, J. Colgan, T. W. Gorczyca, D. M. Mitnik, M. S. Pindzola, and O. Zatsarinny, *Astronomy and Astrophysics*, **406**, 1151 (2003).
5. A. Burgess and H. P. Summers, *Astrophysical Journal* **157**, 1007 (1969).
6. V. L. Jacobs, J. L. Davis, and P. C. Kepple, *Phys. Rev. Lett.* **37**, 1390 (1976).
7. P. Johnsson, R. Lopez-Martens, S. Kazamias, J. Mauritsson, C. Valentin, T. Remetter, K. Varju, M. B. Gaarde, Y. Mairesse, H. Wabnitz, P. Salieres, Ph. Balcou, K. J. Shafer, and A. L'Huillier, *Phys. Rev. Lett.* **95**, 013001 (2005).
8. P. Ranitovic, X. M. Tong, B. Gramkow, S. De, B. DePaola, K. P. Singh, W. Cao, M. Magrakelidze, D. Ray, I. Bocharova, H. Mashiko, A. Sandhu, E. Gagnon, M. M. Murnane, H. C. Kapteyn, I. Litvinyuk, and C. L. Cocke, *New J. Phys.* **12**, 013008 (2010).
9. P. Johnsson, J. Mauritsson, T. Remetter, A. L'Huillier, and K. J. Schafer, *Phys. Rev. Lett.* **99**, 233001 (2007).
10. X. M. Tong, P. Ranitovic, C. L. Cocke, and N. Toshima, *Phys. Rev. A* **81**, 021404 (2010).
11. P. Riviere, O. Uhden, U. Saalman, and J. M. Rost, *New J. Phys.* **11**, 053011 (2009).
12. T. Nubbemeyer, K. Gorling, A. Saenz, U. Eichmann, and W. Sandner, *Phys. Rev. Lett.* **101**, 233001 (2008).
13. J. E. Mayer and M. G. Mayer, *Phys. Rev.* **431**, 605 (1933).
14. J. H. Van Vleck and N. G. Whitelaw, *Phys. Rev.* **44**, 551 (1933).
15. S. R. Lundeen, in *Advances in Atomic, Molecular, and Optical Physics*, edited by P. Berman and C. Lin (Elsevier Academic Press, San Diego, 2005).
16. M. S. Safronova and U. I. Safronova, *Phys. Rev. A* **83**, 013406 (2011).
17. K. R. Overstreet, R. R. Jones, and T. F. Gallagher, *Phys. Rev. Lett.* **106**, 033002 (2011).
18. K. R. Overstreet, R. R. Jones, and T. F. Gallagher, *Phys. Rev. A* **85**, 055401 (2012).
19. A. G. Vaidyanathan, W. P. Spencer, J. R. Rubbmark, H. Kuiper, C. Fabre, D. Kleppner, and T. W. Ducas, *Phys. Rev. A* **26**, 3346 (1982).
20. U. I. Safronova and M. S. Safronova, *Phys. Rev. A* **79**, 022512 (2009).

Publications 2012-2015

1. J. Nunkaew and T. F. Gallagher, "Spectroscopy of barium $6p_{1/2}nk$ autoionizing states in a weak electric field," *Phys. Rev. A* **86**, 013401 (2012).
2. E. G. Kim, J. Nunkaew, and T. F. Gallagher, "Detection of Ba $6sng \rightarrow 6snh$, $6sni$, and $6snk$ microwave transitions using selective excitation to autoionizing states," *Phys. Rev. A* **89**, 062503 (2014).
3. J. Nunkaew and T. F. Gallagher, "Microwave spectroscopy of the Ca $4snf \rightarrow 4s(n+1)d$, $4sng$, $4snh$, $4sni$, and $4snk$ transitions," *Phys. Rev. A* **91**, 042503 (2015).

Experiments in Ultracold Molecules

Phillip L. Gould
Department of Physics U-3046
University of Connecticut
2152 Hillside Road
Storrs, CT 06269-3046
<phillip.gould@uconn.edu>

Program Scope:

Recent years have witnessed a great deal of progress in the production and manipulation of ultracold atoms and molecules. These advances have unquestionably benefited atomic, molecular and optical (AMO) physics, but they have also impacted a variety of other fields, including quantum information, condensed-matter physics, plasma physics, fundamental symmetries, and chemistry. Molecules, with their much richer level structure, are more difficult to cool and manipulate than atoms. However, these multiple degrees of freedom, including electronic state, vibration, rotation, electron spin, and nuclear spin, have their positive side - they span a wide range of energy scales, allowing interactions with a variety of other systems. Furthermore, heteronuclear molecules can exhibit permanent electric dipole moments, whose long-range and anisotropic potentials lead to novel and useful interactions. Molecule cooling techniques fall into two general categories: 1. “direct”, such as buffer gas cooling, electrostatic slowing, and laser cooling; and 2. “indirect”, such as photoassociation and magnetoassociation, where the molecules are assembled from already ultracold atoms. Once produced, samples of ultracold molecules can be confined and compressed in various optical, magnetic, and electrostatic traps. The numerous applications of ultracold molecules include: ultracold chemistry and collisions; quantum computation; simulations of condensed-matter systems; quantum degenerate gases; novel quantum phases of dipolar gases; and tests of fundamental symmetries and fundamental constants. Recently, the main thrust of our experimental program has been to coherently produce and manipulate ultracold molecules using pulses of frequency-chirped light on the nanosecond time scale.

Our experiments employ laser-cooled Rb atoms confined in a magneto-optical trap (MOT). Rubidium has a number of practical advantages: 1) its D_2 and D_1 resonance lines, at 780 nm and 795 nm, respectively, are conveniently matched to available diode lasers; 2) it has two naturally occurring isotopes, ^{85}Rb and ^{87}Rb ; 3) ^{87}Rb is the workhorse atom for BEC studies; and 4) the photoassociative formation of Rb_2 formation, as well as its state-selective ionization detection, have been extensively investigated here at UConn and elsewhere. In our experiments, we load a phase-stable MOT with cold atoms from a low-velocity intense source (LVIS). In order to make ultracold molecules, the atoms in the MOT are illuminated with a sequence of pulses of frequency-chirped light. These pulses are as short as 15 ns FWHM and the chirp rates as fast as 2 GHz in 38 ns. The ground-state Rb_2 molecules thus formed are detected by resonance-enhanced multiphoton ionization (REMPI) with a tunable pulsed dye laser. The resulting molecular ions are distinguished from background atomic ions by their time of flight to the detector.

Recent Progress:

We have made significant progress in several of areas: formation and detection of ultracold ground-state molecules by photoassociation with frequency-chirped light; enhancement of molecular formation using shorter pulses, faster chirps, and shaped chirps; production of intensity pulses and frequency chirps on faster time scales using intensity and phase modulators in conjunction with with a double-pass tapered amplifier; and quantum simulations of chirped photoassociation on various time scales and with shaped frequency chirps.

We have been using photoassociation with pulses of frequency-chirped light to form ultracold molecules in high vibrational levels of the $a^3\Sigma_g^+$ triplet ground state. In these experiments, the chirp is centered on a photoassociation resonance located 7.8 GHz below the $5S_{1/2} + 5P_{3/2}$ asymptote. Molecules ending up in the $a^3\Sigma_g^+$ state are detected by REMPI with a pulsed dye laser at ~ 600 nm. In earlier work using 40 ns FWHM pulses and linear chirps of 1 GHz in 100 ns, we found that, with all other parameters fixed, a positive linear chirp produced more molecules than a negative linear chirp, but less than an unchirped pulse. More recently, we are using an electro-optical modulator in a fiber loop to produce more rapid chirps (2 GHz in 38 ns) and shorter pulses (15 ns FWHM), and to incorporate shaping into the frequency chirps. As a result, we see a dramatic improvement in the molecule formation rate. The most efficient chirp shape is a piecewise positive linear (PPL) chirp, where the beginning and ending portions have a small slope, while the central portion has a large slope.

In order to understand the dependence on chirp parameters, we perform, in collaboration with Shimshon Kallush at ORT Braude and Ronnie Kosloff at Hebrew University (both in Israel), quantum simulations of the molecule formation process. We include the bound vibrational levels in both the ground-state ($a^3\Sigma_g^+$) and excited-state (0_g^- and 1_g^-) molecular potentials, as well as the ground-state continuum. The chirp first populates various excited states, and these can in turn populate high vibrational levels of the ground state, either by spontaneous (incoherent) or stimulated (coherent) emission. By following the temporal evolution of the various state populations, we learn how to optimize the formation rate. The reason that positive chirps outperform negative chirps is as follows. A positive chirp first passes through a photoassociation (free-bound) resonance, producing excited molecules from free atoms, and then through a bound-bound resonance, causing stimulated emission of the excited-state molecules into a ground-state vibrational level. This sequence is in the wrong order for a negative chirp, thereby reducing the efficiency. The simulations also tell us why the PPL chirp does so well. The slow portions of the chirp occur near the photoassociation and stimulated emission resonances, making these transitions more adiabatic, and therefore more efficient. The fast central portion of the chirp minimizes the time spent in the excited state, thereby reducing the effects of spontaneous emission. This general chirp shape, slow-fast-slow, emerged when we used local control of the phase for optimization in the simulations. Local control is a unidirectional and non-iterative time propagation scheme which adjusts the field, in our case the phase, at each instant of time in order to optimize the target at the next time step.

In order to produce even faster chirped pulses and to be able to shape them arbitrarily, we are using fiber-based electro-optic phase and intensity modulators driven

by a 4 GHz arbitrary waveform generator (AWG). With this scheme, we have been able to produce intensity pulses as short as 0.15 ns and chirps as fast as 5 GHz in 2.5 ns. To boost peak powers to several hundred mW, we are using a tapered amplifier in a delayed double-pass geometry.

Future Plans:

We will incorporate our faster chirp technology to further improve our molecular formation. We will also use a quasi-cw laser to irreversibly pump chirp-produced molecules into a different target state, thereby allowing population to accumulate there without being subject to photodestruction by subsequent chirped pulses. We will begin developing a multi-pass Ti:sapphire amplifier, which will allow us to increase our chirped-pulse intensities by several orders of magnitude. Such intensities will be necessary for experiments on an optical centrifuge for ultracold molecules. Chirped light will be used to spin up molecules, already in states of high vibration, into states of high rotation as well. Optical centrifuges for low vibrational states require huge chirps, which have been realized in the ultrafast regime. Molecules in high vibrational states, such as those we produce, are at large internuclear separations, and therefore have small rotational constants, allowing them to be spun up with chirps of several GHz in a few ns, well within the capabilities of our chirped pulse system. These molecules with large amounts of internal energy (both vibrational and rotational) and angular momentum will have interesting interaction properties.

Recent Publications:

“Quantum Dynamical Calculations of Ultracold Collisions Induced by Nonlinearly Chirped Light,” J.L. Carini, J.A. Pechkis, C.E. Rogers III, P.L. Gould, S. Kallush, and R. Kosloff, *Phys. Rev. A* **85**, 013424 (2012).

“Production of Ultracold Molecules with Chirped Nanosecond Pulses: Evidence for Coherent Effects,” J.L. Carini, J.A. Pechkis, C.E. Rogers III, P.L. Gould, S. Kallush, and R. Kosloff, *Phys. Rev. A* **87**, 011401(R) (2013).

“Population Inversion in Hyperfine States of Rb with a Single Nanosecond Chirped Pulse in the Framework of a Four-Level Atom,” G. Liu, V. Zakharov, T. Collins, P. Gould, and S.A. Malinovskaya, *Phys. Rev. A* **89**, 041803(R) (2014).

“Enhancement of Ultracold Molecule Formation by Local Control in the Nanosecond Regime,” J.L. Carini, S. Kallush, R. Kosloff, and P.L. Gould, *New J. Phys.* **17**, 025008 (2015).

“Enhancement of Ultracold Molecule Formation Using Shaped Nanosecond Frequency Chirps,” J.L. Carini, S. Kallush, R. Kosloff, and P.L. Gould, submitted for publication.

Page is intentionally blank.

Physics of Correlated Systems

Chris H. Greene

Department of Physics & Astronomy, Purdue University, West Lafayette, IN 47907-2036

chgreene@purdue.edu

Program Scope

Some of the most interesting phenomena, including all reactive physics, hinges on the coupling or correlation of multiple degrees of freedom in the system. Yet the bulk of our intuitive understanding of atomic and molecular systems and their response to applied external fields or photon sources has emerged from uncorrelated theoretical treatments of the particles. In this context, the word “uncorrelated” means that a separable wavefunction structure has been assumed, even when this is generalized in many cases to a Slater determinant when identical fermions are involved which require antisymmetrization as in Hartree-Fock theory. Many correlated phenomena can be handled simply within these simpler frameworks, such as simple configuration interaction methods for bound states which superpose Slater determinants for a few dominant electronic configurations in atomic or molecular structure calculations. As our control of quantum systems becomes increasingly refined, and as the observable phenomena become correspondingly richer and more complex, it is increasingly paramount to develop non-perturbative theoretical techniques that begin from a correlated viewpoint and yield both insight and quantitative accuracy in describing such phenomena. The emphasis of this project is on developing and improving such theoretical tools that describe correlated few-body phenomena at the atomic and molecular level, in particular striving to describe either existing experiments or else to make predictions of new phenomena that are experimentally feasible to test.

The publications listed below [1-15] are the papers that have been supported primarily by this project.

Recent Progress and Immediate Plans

(i) Few-body collisions from low energy up to chemically interesting temperatures

The chemical three-body recombination reaction starts from three initially free atoms or molecules which simultaneously collide and react to form two bound fragments. During the past year postdoctoral associate Jesus Perez-Rios has made substantial headway in understanding the properties of this reaction in the case where one of the species has a positive charge.[1] In this case the interactions are dominated at long range by the polarization potential, for the case we have treated in which the neutral species have no permanent dipole moment. It should not be surprising that Newtonian mechanics for the nuclear motion combined with a quantum calculation of the Born-Oppenheimer surface for the triatomic system should be quite accurate at high temperatures. But surprisingly, our first treatment of this system shows that it can be treated using classical mechanics down to surprisingly low temperatures. For instance, we show in [1] that the reaction $\text{Ba}^+ + \text{Rb} + \text{Rb} \rightarrow (\text{BaRb})^+ + \text{Rb}$ or $(\text{Rb}_2) + \text{Ba}^+$ can be treated classically not only up in the range from a few to several thousand Kelvin as would normally be expected, but because so many partial waves contribute under the influence of the long range polarization interaction, classical methods are predicted to be adequate even down to a few hundred nanoKelvin. Our first treatment of this problem predicts the low energy threshold law for the rate coefficient in the range where classical physics is still adequate, and our detailed

calculations also suggest a strong propensity for forming bound molecular ions rather than neutral dimers in this reaction. In the coming year we plan to continue this exploration of reactive ion physics, and we are working with experimental groups to develop a quantitative test of theory.

Another area we have investigated is a system of four equal mass charged particles, two positive and two negative, as a prototype system where the Born-Oppenheimer approximation would be unlikely to be useful in its usual form, but which remain amenable to a hyperspherical coordinate formulation. This DOE project supported part of our effort, which culminated in our first studies of the $e^+e^+e^-e^-$ and analogous systems,[5,6] and computed the first charge-exchange scattering information on this system. Our treatment of this system should serve as a prototype of this process which can occur in other chemically-interesting systems with two positive and two negative ions.

(ii) Atomic and molecular electron dynamics in internal and external fields

One of the most important developments in theoretical atomic and molecular physics in the past several decades has been the development and maturation of the technique called frame transformation theory. Some of the key early successes of this technique include its ability to quantitatively describe multichannel Rydberg physics in H_2 , H_3 , and many other molecular systems, and in numerous atomic systems as well such as the rare gas atoms, the halogens, and the alkaline earth metal atoms. In all of those systems just mentioned, there is no external field applied to the system, except for a weak radiative probe that can be treated perturbatively. An important generalization of the theory to handle nonperturbative external field effects was developed in the early 1980s, initially by Fano and Harmin, with subsequent extensions by other researchers. The resulting Stark theory of Rydberg states of atoms and molecules was a particularly powerful combination of quantum defect ideas and local coordinate transformations that is now called local frame transformation theory (LFT).

Despite its remarkable successes for a number of atoms and molecules, the LFT has been subjected to increasingly careful and quantitative scrutiny over the years, and a few examples from careful experiment and theory have suggested that it has inaccuracies which limit its usefulness in some regimes. One example is the Stark effect for lithium Rydberg states, studied carefully in 1996 by Bergeman, Metcalf, and coworkers, which found errors in the LFT calculated resonance energies ranging from 50 to a few thousand parts per million. And while the LFT has determined total photoionization cross sections to quantitative accuracy, a 2012 study by Zhao, Fabrikant, Du, and Bordas claimed that other observables such as the photoionization microscopy differential cross section are inaccurate in the LFT. Because the LFT has emerged as a major tool for theoretical physics, we have revisited the fundamental underpinnings of the LFT approximation, spearheaded by postdoctoral associate Panos Giannakeas and in collaboration with Francis Robicheaux. The careful reformation of the LFT presented in [2,3] demonstrates that the basic Harmin-Fano Stark LFT is basically correct and does not have the major flaws claimed by Zhao et al. However, the qualitative points raised by the Zhao et al. paper do suggest areas where improvements of the LFT are desirable, and this has led to a first long paper describing a treatment based on the Schwinger variational principle [4] which shows a way to implement LFT with more accuracy and reliability. In the next year of funding for this project, we plan to implement these improvements in the atomic Stark effect problem and test the improved theory against both experiment and conventional calculations that

are more exact (but more expensive). A subsequent goal is to apply the theory to other problems such as strong-field ionization of an atom or molecule by a powerful short pulse laser.

(iii) Implosive interactomic Coulombic decay processes

Most ICD processes produce a double positively-charged system is formed during the decay, which subsequently undergoes a Coulomb explosion. We have been focusing on a different class where the products formed in the decay experience an attractive interaction. The differences and similarities with the more typical type of explosive ICD process are still being explored and should come to fruition during the coming year of this project.

Papers published since 2013 that were supported by this grant.

- [1] *Communication: Classical threshold law for ion-neutral-neutral three-body Recombination*, J Pérez-Ríos and C H Greene, J. Chem. Phys. **143**, 041105-1 to -3 (2015).
- [2] *Photoionization microscopy in terms of local-frame-transformation theory*, P. Giannakeas, F. Robicheaux, and Chris H. Greene, Phys. Rev. A **91**, 043424-1 to -14 (2015).
- [3] *Comment on “Test of the Stark-effect theory using photoionization microscopy”*, P. Giannakeas, F. Robicheaux, and Chris H. Greene, Phys. Rev. A **91**, 067401-1 to -4 (2015).
- [4] *Schwinger-variational-principle theory of collisions in the presence of multiple potentials*, F. Robicheaux, P. Giannakeas, and Chris H. Greene, Phys. Rev. A **92**, 022711-1 to -21 (2015).
- [5] *Hyperspherical asymptotics of a system of four charged particles*, K. M. Daily, Few Body Systems, online publication 2015, pp 1-14, DOI 10.1007/s00601-015-0979-7.
- [6] *Scattering properties of the $2e^-2e^+$ polyelectronic system*, K. M. Daily, J. von Stecher, and C. H. Greene, Phys. Rev. A **91**, 012512-1 to -7 (2015).
- [7] *Two-photon total annihilation of molecular positronium*, J Pérez-Ríos, S. T. Love, and C. H. Greene, Europhys. Lett. **109**, 63002-1 to -4 (2015).
- [8] *Adiabatic hyperspherical analysis of realistic nuclear potentials*, K. M. Daily, A. Kievsky, and C. H. Greene, Few Body Systems, online publication 2015, pp 1-7, DOI 10.1007/s00601-015-1012-x.
- [9] *Comparison of classical and quantal calculations of helium three-body recombination*, J Pérez-Ríos, S Ragole, J Wang, and C H Greene, J. Chem. Phys. **140**, 044307-1 to -12 (2014).
- [10] *What will it take to observe processes in ‘real time’?*, S R Leone, C W McCurdy, J Burgdörfer, L S Cederbaum, Z Chang, N Dudovich, J Feist, C H Greene, M Ivanov, R Kienberger, U Keller, M F Kling, Z-H Loh, T Pfeifer, A N Pfeiffer, R Santra, K Schafer, A Stolow, U Thumm and M J J Vrakking, Nature Photonics **8**, 162-166 (2014).

- [11] *Analyzing Feshbach resonances: A ${}^6\text{Li}$ - ${}^{133}\text{Cs}$ case study*, R. Pires, M. Repp, J. Ulmanis, E. D. Kuhnle, and M. Weidemüller, T. G. Tiecke, C H Greene, B P Ruzic, J L Bohn, and E Tiemann Phys. Rev. A **90**, 012710-1 to -14 (2014).
- [12] *Low-energy electron collisions with O_2 : Test of the molecular R-matrix method without diagonalization*, M Tarana and C H Greene, Phys. Rev. A **87**, 022710-1 to -13 (2013).
- [13] *Rydberg states of triatomic hydrogen and deuterium*, Jia Wang and C H Greene, J. Phys. Chem. A **117**, 9761-9765 (2013). DOI: 10.1021/jp312462a
- [14] *Quantum defect theory for high-partial-wave cold collisions*, B P Ruzic, C H Greene and J L Bohn, Phys. Rev. A **87**, 032706-1 to -14 (2013).
- [15] *Lorentz Meets Fano in Spectral Line Shapes: A Universal Phase and Its Laser Control*, C Ott, A Kaldun, P Raith, K Meyer, M Laux, J Evers, C H Keitel, C H Greene, and T Pfeifer, Science **340**, 716-720 (2013).

Using Strong Optical Fields to Manipulate and Probe Coherent Molecular Dynamics

Robert R. Jones, Physics Department, University of Virginia
382 McCormick Road, P.O. Box 400714, Charlottesville, VA 22904-4714
bjones@virginia.edu

I. Program Scope

This project focuses on the exploration and control of dynamics in atoms and small molecules driven by strong laser fields. Our goal is to exploit strong-field processes to implement novel ultrafast techniques for manipulating and probing coherent electronic and nuclear motion within atoms, molecules, and on surfaces. Ultimately, through the application of these methods, we hope to obtain a more complete picture of correlated multi-particle dynamics in molecules and other complex systems.

II. Recent Progress and Results

During the current funding year we have: (i) continued our investigation of THz-induced, electron field-emission from nano-structured metals and the accompanying large energy transfer to the ejected electrons in the locally enhanced THz field; (ii) worked in collaboration with the DiMauro/Agostini group at OSU, employing the RABITT method to obtain time-resolved information about the effective binding potential experienced by low-energy photo-electrons as they leave their parent ion; and (iii) made technical improvements to extend our work on THz induced, transient field-free orientation of polar molecules;

Two of these projects involve the use of intense, single-cycle THz pulses which are produced via optical rectification of tilted pulse-front, 50-150 fs, 790nm laser pulses in MgO doped stoichiometric Li:NbO₃ [1,2]. Such pulses are interesting in the context of strong-field and ultrafast physics for several reasons. First, the broad frequency spectrum and large field strengths allow for direct rotational excitation of molecules, enabling the creation of controllable, mixed parity rotational wavepackets without electronic excitation, ionization, or strong static fields. Second, the long oscillation period of the field makes it possible to drive free, or quasi-free, electrons to large energies (> 100 eV) without influencing the tightly bound electrons in atoms, molecules, or condensed systems. Accordingly, these pulses can be used as time-resolved probes of photoionization times with a temporal resolution approaching a few or few tens of femtoseconds. Third, the passively CE-phase locked, true single-cycle pulses allow us to explore various strong field phenomena in a regime that has yet to be realized at visible and higher frequencies.

i) THz-Induced Electron Field Emission from Nano- and Micro-Structured Metal Wires

Due to the wavelength scaling of the pondermotive potential, electrons that are free to move over large distances can attain energies exceeding 100 eV directly from intense single-cycle THz pulses with peak fields approaching 0.5 MV/cm [ii]. Therefore, in principle, such pulses might be useful for high-energy streaking of photo-electrons from condensed matter targets, providing a time-resolved probe of electron emission without causing permanent sample damage. In addition, electron emission from a scanning probe tip, induced by non-damaging ultrashort THz pulses, might enable time-resolved electron microscopy. Indeed, THz pulses were recently

employed to gate the tunnel current in a STM [3] as well as optical field emission from metal nano-tips [4]. Some applications might also benefit from direct field emission induced by THz pulses alone. Unfortunately, the < 1 MV/cm field strengths available from typical laser-based THz sources are two to three orders of magnitude too small to induce tunneling ionization from bulk metals [5]. However, we and others [6,7] have recently observed THz-induced field-emission from nano- and micro-structured metals by exploiting the substantial field enhancements near the surface of these structures.

We find that we can generate high-energy electrons (> 5 keV) by focusing intense THz pulses with peak field strengths of ~ 400 kV/cm on unbiased single nano- and micro-tipped tungsten wires. These energies exceed, by more than an order of magnitude, those previously produced via field-emission in THz [6], infrared [7] or optical fields [8] alone. In general, the energy distributions are characterized by a sharp high-energy cutoff with a broad maximum and low energy tail, and are similar to those observed by other groups [6]. For large THz fields, the FWHM of the distribution is roughly 20% of the energy at its peak. Interestingly, the peak and high-energy cutoff scale *linearly* with the applied field. Also, despite the significant reduction in the enhanced field expected for blunter tips, the maximum energy transfer for a given THz field differs by only a factor of 2 for wires with tip radii varying over a factor of 50.

The non-pondermotive, linear dependence of the maximum electron energy with applied field is perhaps unexpected, and the magnitude of the maximum energy is striking. Indeed, the measurements suggest an underlying physical mechanism that is substantially different from the simpleman's model for energy transfer in an oscillating field. Instead, our observations are consistent with a different model [8] which assumes that the energy acquired by the electron takes place over a fraction of the field cycle. As such, it depends on the magnitude of the locally enhanced *field* at the instant of emission, rather than on the vector potential (which reflects the *time-integral* of the field after emission). In this regime, the energy transfer is equal to the work done by the approximately static, enhanced field as the electron travels over a short distance comparable to the tip radius. Interestingly, this model predicts that the maximum energy transfer should be independent of the tip radius, R , similar to what we observe.

We have performed numerical simulations of the energy transfer process, including the time-dependent tunneling probability, the spatial distribution of the enhanced field, and the time dependence of the applied field. The simulated energy distributions exhibit sharp high-energy cutoffs and low energy tails similar to the measurements, but have narrower energy widths. This may be the result of neglecting space charge effects that likely play a role in the experiments. The simulations are also consistent with our observation that the maximum electron energy has only a very weak dependence on tip radius. A manuscript describing this work is in preparation.

(ii) Near Threshold Energy Transfer to Attosecond Photoelectrons

In collaboration with the DiMauro/Agostini group at OSU, we have used attosecond pulse trains to photoionize noble gas atoms near threshold in the presence of a moderately intense, 1.3 micron, infrared dressing laser. As in the standard RABITT technique, which is typically used to reconstruct the field in attosecond pulse trains, we monitor the amplitude and phase of photoelectron sidebands. These sidebands are produced via energy transfer between the dressing field and the photoelectrons produced directly by the XUV harmonic radiation. By comparing

the amplitudes and phases of the low-energy sidebands for different atoms we can extract time-resolved information regarding the differences in the binding potentials experienced by the photoelectrons during the first 1 fs or so following their birth. In principal, a variant of these measurements might provide time-resolved information on changes in an atomic/molecular potential due to an external stimulus.

(iii) Transient Field-Free Orientation of Polar Molecules using Intense Single-Cycle THz Pulses
Following the first demonstration of field-free orientation of polar molecules by intense THz pulses [10], we showed that the degree of achievable orientation could be substantially improved by coherently preparing the molecules in rotational superposition states, via Raman transitions in a short optical pulse, prior to their exposure to the THz radiation [i]. Our initial measurements were performed at a low (15 Hz) repetition rate using 20 mJ optical pulses to generate as much THz radiation as possible. We have now rebuilt our molecular beam and detection apparatus, implementing an improved THz and optical beam geometry. In addition, we are in the process of upgrading our 1.5 mJ Ti:Sapphire amplifier to 5 mJ. This should enable us to produce comparable or greater levels of orientation at a 1 kHz repetition rate, allowing for future studies of high-harmonic generation from oriented molecules.

III. Future Plans

We will continue with the projects described in the preceding section. First, we plan to further characterize the THz-induced field emission from nano-tips (e.g. angular and temporal distributions) as a potential source of short electron bursts for initiating and probing molecular dynamics. In addition, we intend on exploiting the enhanced THz field in the vicinity of micro-tipped wires to manipulate laser-driven tunneling ionization and electron recollisions, and perhaps improve THz-based field-free molecular orientation. Second, we hope to soon have improved RABITT data at a longer dressing wavelength (1.8 microns). This will allow us reduce the uncertainties in the time-resolved information that we are able to extract regarding the effective binding potential seen by the departing electron immediately following ionization. Third, we plan to test our improved apparatus for enabling THz-induced field-free molecular orientation at kHz repetition rates.

In addition to these continuing projects, we are working to improve our experimental capabilities to revisit a problem that we have been studying for several years, namely the coupled dynamics of electrons and nuclei during asymmetric strong-field multi-electron dissociative ionization. Two recent experiments [12,iii] have offered conflicting views as to the importance of multi-electron processes during enhanced ionization. We are attempting to reduce the duration of the laser pulses available from our hollow-core-fiber compressor to < 7 fs to perform 2-color pump probe experiments in an attempt to resolve that conflict.

IV. DOE Sponsored Publications from the Last 3 Years

[i] K. Egodapitiya, Sha Li, and R.R. Jones, “THz Induced Field-Free Orientation of Rotationally Excited Molecules,” *Physical Review Letters* **112**, 103002 (2014).

[ii] Sha Li and R.R. Jones, “Ionization of Excited Atoms by Intense Single-Cycle THz Pulses,” *Physical Review Letters* **112**, 143006 (2014).

[iii] X. Gong, M. Kunitski, K.J. Betsch, Q. Song, L. Ph. H. Schmidt, T. Jahnke, Nora G. Kling,

O. Herrwerth, B. Bergues, A. Senftleben, J. Ullrich, R. Moshhammer, G.G. Paulus, I. Ben-Itzhak, M. Lezius, M.F. Kling, H. Zeng, R.R. Jones, and J. Wu, "Multielectron Effects in Strong-field Dissociative Ionization of Molecules," *Physical Review A* **89**, 043429 (2014).

[iv] M. Kubel, Nora G. Kling, K. J. Betsch, N. Camus, A. Kaldun, U. Kleineberg, I. Ben-Itzhak, R.R. Jones, G.G. Paulus, T. Pfeifer, J. Ullrich, R. Moshhammer, M.F. Kling, and B. Bergues, "Non-Sequential Double-Ionization of N₂ in a Near Single-Cycle Laser Pulse," *Physical Review A* **88**, 023418 (2013).

[v] K. J. Betsch, Nora G. Johnson, B. Bergues, M. Kubel, O. Herrwerth, A. Senftleben, I. Ben-Itzhak, G. G. Paulus, R. Moshhammer, J. Ullrich, M. F. Kling, and R. R. Jones, "Controlled directional ion emission from the dissociative ionization of CO over multiple charge states in a few-cycle laser field," *Physical Review A* **86**, 063403 (2012).

V. References

[1] Janos Hebling, Ka-Lo Yeh, Matthias C. Hoffman, Balazs Bartal, and Keith A. Nelson, "Generation of High-Power Terahertz Pulses by Tilted-Pulse-Front Excitation and Their Application Possibilities," *J. Opt. Soc. Am. B* **25**, B6 (2008).

[2] H. Hirori, A. Doi, F. Blanchard, and K. Tanaka, "Single-cycle Terahertz Pulses with Amplitudes Exceeding 1MV/cm Generated by Optical Rectification in LiNbO₃," *Appl. Phys. Lett.* **98**, 091106 (2011).

[3] Tyler L. Cocker *et al.*, "An ultrafast terahertz scanning tunnelling microscope," *Nat. Photonics* **7**, 620 (2013).

[4] L. Wimmer, G. Herink, D. R. Solli, S. V. Yalunin, K. E. Echternkamp and C. Ropers, "Terahertz control of nanotip photoemission," *Nat. Physics* **10**, 432 (2014).

[5] R. H. Fowler, L. Nordheim, "Electron Emission in Intense Electric Fields," *Proc. Roy. Soc. A* **119**, 173 (1928).

[6] G. Herink, L. Wimmer and C. Ropers, "Field emission at terahertz frequencies: AC-tunneling and ultrafast carrier dynamics," *New J. Phys.* **16**, 123005 (2014).

[7] Krzysztof Iwaszczuk, Maksim Zalkovskij, Andrew C. Strikwerda, and Peter U. Jepsen, "Nitrogen plasma formation through terahertz-induced ultrafast electron field emission," *Optica* **2**, 116 (2015).

[8] G. Herink, D. R. Solli, M. Gulde, and C. Ropers, "Field-driven photoemission from nanostructures quenches the quiver motion," *Nature* **483**, 190 (2012).

[9] M. Kruger, M. Schenk, M. Forster and P. Hommelhoff, "Attosecond physics in photoemission from a metal nanotip," *J. Phys. B: At. Mol. Opt. Phys.* **45**, 074006 (2012).

[10] Sharly Fleischer, Yan Zhou, Robert W. Field, and Keith A. Nelson, "Molecular Orientation and Alignment by Intense Single-Cycle THz Pulses," *Phys. Rev. Lett.* **107**, 163603 (2011).

[11] T. Wittman *et al.*, "Single-shot Carrier-Envelope Phase Measurement of Few-Cycle Laser Pulses," *Nat. Phys.* **5**, 357 (2009).

[12] V. Tagliamonti, H. Chen, and G. N. Gibson, "Multielectron Effects in Charge Asymmetric Molecules Induced by Asymmetric Laser Fields," *Phys. Rev. Lett.* **110**, 073002 (2013).

Quantum Dynamics Probed by Coherent Soft X-Rays

Henry C. Kapteyn and Margaret M. Murnane

JILA and Department of Physics, University of Colorado at Boulder

Phone: (303) 492-8198; FAX: (303) 492-5235; E-mail: kapteyn@jila.colorado.edu

The goal of this work is to develop novel short wavelength probes of molecules and to understand the response of atoms, molecules and nanosystems to strong laser fields. We made exciting advances in several areas since 2013.[1-10] Recent highlights include –

Angularly separated beams of circularly polarized high harmonics [1]: In work soon to be published in Nature Photonics, we generated isolated beams of circularly polarized high harmonics (HHG) using noncollinear counter-rotating driving lasers. This allows us to control the direction and polarization of HHG beams using visible lasers. This new scheme has many advantages - including separating the HHG beams from the laser beam without using filters or optics, the production of both left and right circularly polarized HHG at each wavelength, and the ability to separate different HHG orders without using a spectrometer. This approach is also the only way to generate isolated attosecond bursts of circularly polarized HHG, and enables precision differential measurements of ultrafast XMCD simultaneously at each HHG order. This work was done at JILA in collaboration with Charles Durfee from the Colorado School of Mines, who spent a sabbatical year at JILA.

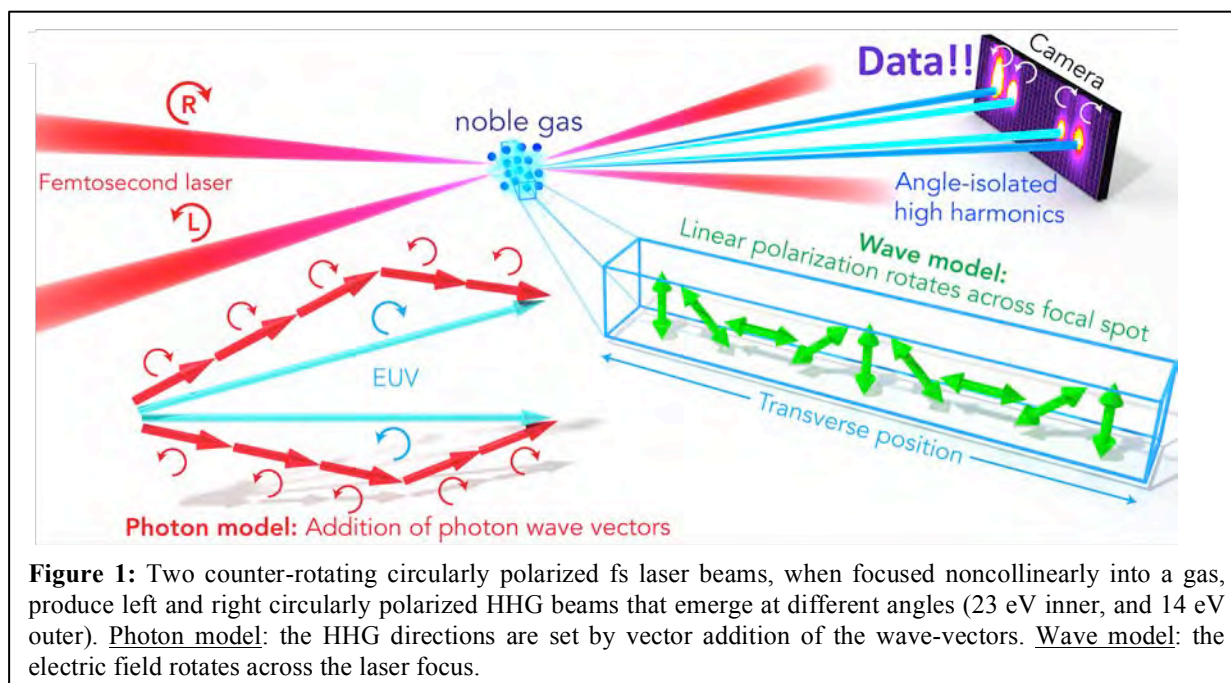


Figure 1: Two counter-rotating circularly polarized fs laser beams, when focused noncollinearly into a gas, produce left and right circularly polarized HHG beams that emerge at different angles (23 eV inner, and 14 eV outer). Photon model: the HHG directions are set by vector addition of the wave-vectors. Wave model: the electric field rotates across the laser focus.

Solvents Effects on Charge Transfer from Quantum Dots [3]: In work recently published in JACS, we explored the influence of the solvent through a comparison of quantum dot charge transfer processes occurring in both liquid phase and in vacuum. By comparing solution phase transient absorption spectroscopy and gas-phase photo- electron spectroscopy, we show that hexane, a common nonpolar solvent for quantum dots, has negligible influence on charge transfer dynamics. Our experimental results, supported by insights from theory, indicate that the

reorganization energy of nonpolar solvents plays a minimal role in the energy landscape of charge transfer in quantum dot devices. Thus, this study demonstrates that measurements conducted in nonpolar solvents can indeed provide insight into nanodevice performance in a wide variety of environments. This is important in order to predict and understand the performance of nanodevices in different environments.

Observation of a new regime of collective nanoscale thermal transport [2]: A great challenge in the semiconductor and electronics industries is that as nanoscale features get smaller and processes get faster, significant amounts of heat need to be quickly carried away from the nanostructures. In collaboration with Lawrence Berkeley National Laboratory, we made a counter-intuitive discovery - it is much easier to cool hot nanostructures when they are arranged closely together rather than far apart. This result is exciting for the field of thermal transport because in 2010 we showed that small, isolated hotspots are, in fact, quite challenging to cool.

In our experiments, we patterned an array of nanostructures on different materials. When the nanostructures were heated with an infrared laser, they emit phonons (lattice vibrations), which travel into the substrate and collide with other phonons, carrying away the heat. When the nanostructures are placed close together, cooling is enhanced because it does not matter whether the colliding phonons come from the same hot nanostructure or neighboring hot nanostructures.

Thus, paradoxically, arranging the hot nanostructures more closely together actually enhanced heat dissipation. Moreover, we were able to extract which lattice vibrations carry heat away from a hot region and also predict new ways to engineer the cooling rate in a material. This work is already generating much interest from industry, because it can inform smart designs of heat dissipation in nanostructures such as integrated circuits, thermoelectric devices, heat therapies mediated via nanoparticles, and nanoenhanced solar cells used in clean energy technologies.

Electron-Ion Rescattering in Polarization-Shaped Light Fields [4]: A remarkable ability of intense bursts of femtosecond laser light is to pluck electrons from atoms and molecules, accelerate them to high energy, and then scatter them from the same atom or molecule from which it originated. These laser-driven electrons are very useful – for example, they can emit laser-like beams of X-rays if they recombine with their parent ions. Alternatively, like a super-powered electron microscope, an electron can scatter from the ion, providing structural information on sub-Ångström spatial scales and sub-femtosecond times scales.

Typically, when electrons are driven with linearly polarized lasers, they travel in one-dimensional trajectories and produce patterns that are so complicated that it is difficult to extract structural information. In recent work, we used two-color circularly polarized laser fields to

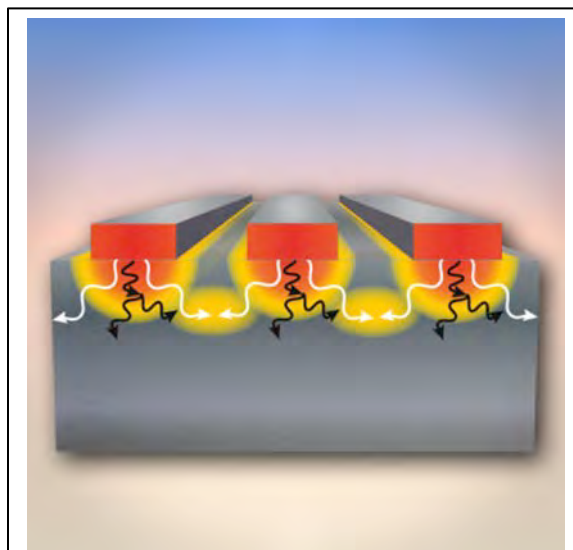
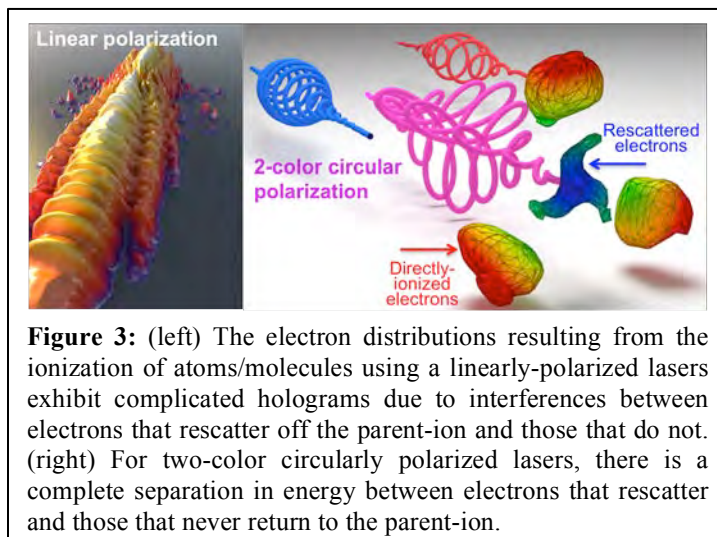


Figure 2: Hot nanowires emit phonons into underlying materials. When closely packed, these phonons collide and efficiently transport heat away.

drive electrons in two-dimensional trajectories before they rescatter off the parent-ion. This feature, coupled with the fact that rescattered electrons are well separated from those that do not rescatter, should offer the ability for multi-dimensional imaging of molecules. Moreover, this work also provides the first experimental verification of the theoretical model describing how these laser fields can be used to generate bright, circularly polarized extreme ultraviolet light.



Future work: First, we are using ultra-broad bandwidth, ultrafast HHG soft X-rays to capture NEXAFS over hundreds of electron volt energies simultaneously. To implement dynamic NEXAFS, gas, solid and liquid-phase samples will be excited using mid-IR – UV light, and then probed using soft X-ray HHG supercontinua. Second, we will capture orbital dynamics in molecules and nanosystems using photoelectron spectroscopy. Finally we will characterize circularly and linearly polarized attosecond pulses in the EUV and soft x-ray regions.

Publications from DOE AMOS support in past 3 years

1. D. Hickstein, F. Dollar, P. Grychtol, J. Ellis, R. Knut, C. Hernández-García, C. Gentry, D. Zusin, J. Shaw, T. Fan, K. Dorney, A. Becker, A. Jaroń-Becker, H. Kapteyn, M. Murnane, C. Durfee, “Angularly separated beams of circularly polarized high harmonics,” in press, *Nature Photonics* (2015).
2. K.M. Hoogeboom-Pot, J.N. Hernandez-Charpak, T. Frazer, E.H. Anderson, W. Chao, R. Falcone, X. Gu, R. Yang, M.M. Murnane, H.C. Kapteyn, D. Nardi, “A new regime of nanoscale thermal transport: collective diffusion increases dissipation efficiency”, *PNAS* **112**, 4846–4851 (2015).
3. Jennifer L. Ellis, Kyle J. Schnitzenbaumer, Daniel Hickstein, Molly B. Beernink, Brett B. Palm, Jose L. Jimenez, Gordana Dukovic, Henry C. Kapteyn, Margaret M. Murnane, Wei Xiong, “Revealing solvent effects on charge transfer between quantum dots and surface adsorbates”, *JACS* **137** (11), 3759–3762 (2015).
4. Chris Mancuso, Daniel D. Hickstein, Patrick Grychtol, Ronny Knut, Ofer Kfir, Xiao-Min Tong, Franklin Dollar, Dmitriy Zusin, Maithreyi Gopalakrishnan, Christian Gentry, Emrah Turgut, Jennifer L. Ellis, Ming-Chang Chen, Avner Fleischer, Oren Cohen, Henry C. Kapteyn, and Margaret M. Murnane, “Observation of photoelectron distributions resulting from strong field ionization from two-color circularly polarized laser fields using tomographic methods”, *Physical Review A* **91**, 031402(R) (2015).
5. Damiano Nardi, Marco Travaglini, Margaret M. Murnane, Member, Henry C. Kapteyn, Gabriele Ferrini, Claudio Giannetti, Francesco Banfi, “Impulsively Excited Surface Phononic Crystals: a Route towards Novel Sensing Schemes”, *IEEE Sensors Journal* **15**, 5142 (2015).
6. M.-C. Chen, C. Hernández-García, C. Mancuso, F. Dollar, B. Galloway, D. Popmintchev, P.-C. Huang, B. Walker, L. Plaja, A. Jaron-Becker, A. Becker, T. Popmintchev, M.M. Murnane, H. C. Kapteyn, “Generation of Bright Isolated Attosecond Soft X-Ray Pulses Driven by Multi-Cycle Mid-Infrared Lasers”, *PNAS* **111** (23) E2361-E2367 (2014).

7. Chengyuan Ding, Wei Xiong, Tingting Fan, Daniel D. Hickstein, Tenio Popmintchev, Xiaoshi Zhang, Mike Walls, Margaret M. Murnane, and Henry C. Kapteyn, "High flux coherent supercontinuum soft X-ray source driven by a single-stage 10 mJ, kHz, Ti:sapphire laser amplifier," *Optics Express* **22**(5), 6194-6202 (2014).
8. X.-M. Tong, P. Ranitovic, D. D. Hickstein, M. M. Murnane, H. C. Kapteyn, and N. Toshima, "Enhanced multiple-scattering and intra-half-cycle interferences in the photoelectron angular distributions of atoms ionized in midinfrared laser fields," *Physical Review A* **88**(1), 013410 (2013).
9. W. Xiong, D. D. Hickstein, K. J. Schnitzenbaumer, J. L. Ellis, B. B. Palm, K. E. Keister, C. Ding, L. Miaja-Avila, G. Dukovic, J. L. Jimenez, M. M. Murnane, and H. C. Kapteyn, "Photoelectron Spectroscopy of CdSe Nanocrystals in the Gas Phase: A Direct Measure of the Evanescent Electron Wave Function of Quantum Dots," *Nano Letters* **13**(6), 2924-2930 (2013).
10. T. Popmintchev, M. Chen, A. Bahabad, M. Murnane, H. Kapteyn, "Method for phase-matched generation of coherent soft and hard x-rays using IR lasers," US Patent # 20110007772, Notice of Allowance 2013.

Imaging Multi-particle Atomic and Molecular Dynamics

Allen Landers

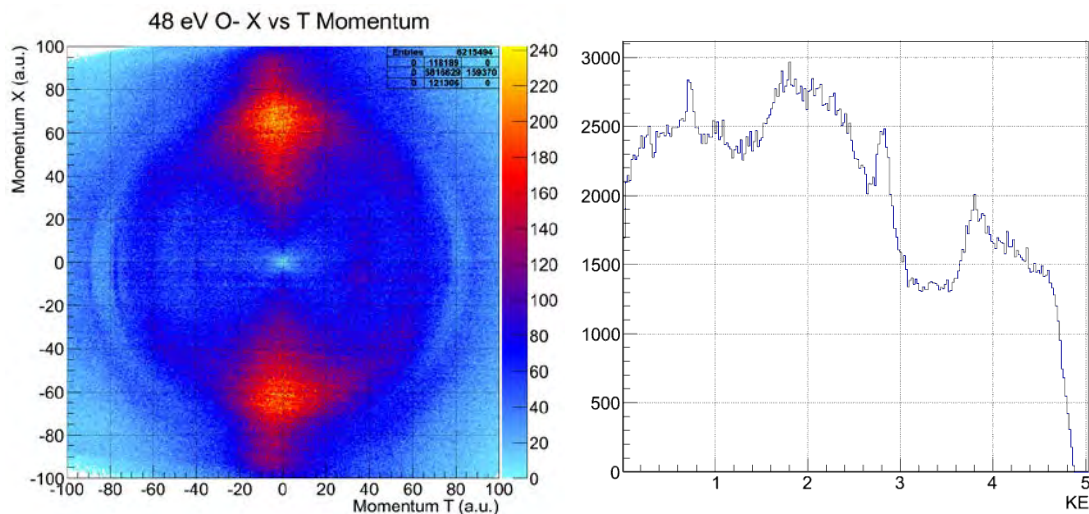
landers@physics.auburn.edu

Department of Physics
Auburn University
Auburn, AL 36849

Program Scope: We are investigating phenomena associated with ionization of an atom or molecule by single photons (weak field) or low energy electrons with an emphasis on ionization-driven atomic and molecular dynamics. Of particular interest is untangling the complicated electron-correlation effects and molecular decay dynamics that follow an initial photoionization or electron attachment event. We perform these measurements using variations on the well-established COLTRIMS technique. The experiments take place at the Advanced Light Source at LBNL as part of the ALS-COLTRIMS collaboration with the groups of Reinhard Dörner at Frankfurt and Thorsten Weber at LBNL and at Auburn University in collaboration with Prof. Mike Fogle. Because the measurements are performed in “list mode” over a few days where each individual event is recorded to a computer, the experiments can be repeated virtually with varying gate conditions on computers at Auburn University months following the measurements. We continue to collaborate closely with theoreticians also funded by DOE-AMOS including the groups of C.W. McCurdy, T. Resigno, A. Orel, and D. Haxton. Below are two brief examples of recent results (submitted or to be submitted for publication).

Recent Progress:

Electron driven Molecular Dynamics:



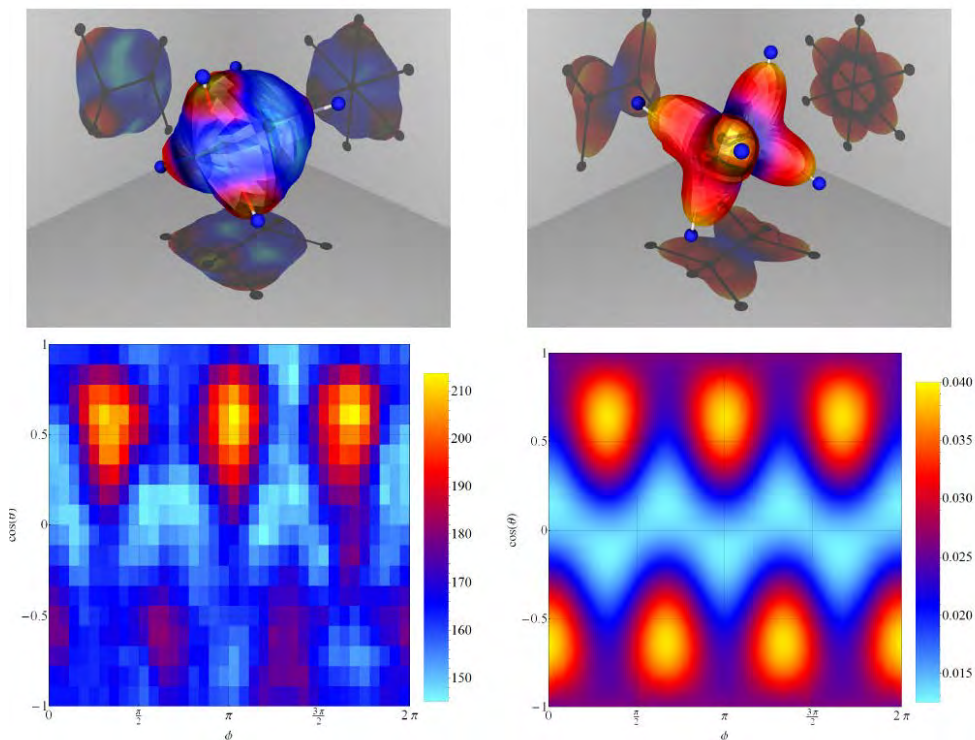
Left: O^- momentum distribution following interaction with a 48 eV electron (electron beam direction is up in the figure). Right: Associated Kinetic Energy distribution for the momentum distribution at left. Note the multiple sharp peaks, corresponding to excitations that decay through ion-anion pair production.

We have performed a number of dissociative electron attachment measurements on small molecules in collaboration with Prof. Mike Fogle at Auburn, where we have used momentum imaging of the resulting anion in order to explore the dissociation dynamics. Recently, we have

employed a momentum imaging technique to measure the electron impact anion production far above the dissociative ionization threshold for number of small molecules including O_2 . By measuring the momentum distribution of the anion produced we are able to determine the kinetic energy release in the reaction as a function of emission angle over the full 4π solid angle of acceptance. We have found that the high angular resolution of our supersonic crossed-beam experiment has provided new insights into previous measurements of some systems, and we anticipate additional fruitful collaboration with the LBNL theoretical (listed above) and experimental group (Belkacem and Slaughter) also funded within the DOE-AMOS program.

One such example is shown in the figure on the previous page showing recent results for dissociative electron excitation at 48eV electron energy resulting in O^- fragments. Although well above the dissociative attachment energies, we find a substantial number of anions formed through excitations that decay through ion-anion pair production. Currently we are working to identify individual states populated, determine their relative production fractions, and individual angular distributions. Theory support for these experiments is greatly needed.

Photoionization experiments at ALS:



MFPAD for C_2H_6 at 4.5 eV above the C 1s threshold from analysis of the experimental data assuming the three protons in the breakup channel $C_2H_6 + h\nu \rightarrow H^+ + H^+ + H^+ + neutrals + 3e^-$ originated from the same carbon atom (left column) and complex Kohn calculations at 4.35 eV (right column).

Auburn has continued participating in the collaboration with the University of Frankfurt and LBNL groups in COLTRIMS experiments at the Advanced Light Source at LBNL. The most recent example resulting from this joint effort is a work led by Joshua Williams and the McCurdy group recently submitted to *Journal of Physics B*.

We measured molecular frame photoelectron angular distributions (MFPADs) in electron-ion momentum imaging experiments and compared these with complex Kohn variational calculations (LBNL, McCurdy group) for carbon K-shell ionization of CF_4 , C_2H_6 (shown above) and $\text{C}_2\text{H}_2\text{F}_2$. While in ethane the polarization averaged MFPADs show a tendency at low energies for the photoelectron to be emitted in the directions of the bonds, the opposite effect is seen in CF_4 . A combination of these behaviors is seen in difluoroethylene where ionization from the two carbons can be distinguished experimentally because of their different K-shell ionization potentials. Excellent agreement is found between experiment and theoretical calculations performed by Cynthia Trevisan and the LBNL theory group.

Future Plans:

We intend to pursue additional experiments as part of our work within the ALS-COLTRIMS collaboration and expand our efforts at Auburn to study electron driven phenomena. Here are some examples:

- Extend electron driven dynamics measurements to include liquid and complex targets (e.g. alcohols, formic acid, clusters)
- Study core-photoionization in similar systems to methane to explore whether or not the imaging effect observed in methane occurs elsewhere (e.g. H_2O , NH_3).
- Measure the Auger electrons in coincidence with fragments to produce molecular frame angular distributions for Auger electrons in order to better identify dissociative pathways following photoionization.
- Use larger polyatomic molecules (e.g. allene) to probe the limits of extending these measurements to systems of increasing complexity.
- Continue to be guided by and partner with theoreticians to study these fundamental processes.

Refereed Publications: Supported by most recent DOE-AMOS funding (2011-2015)

1. **Molecular frame photoelectron angular distributions for core ionization of ethane, carbon tetrafluoride and 1,1-difluoroethylene** A. Menssen, C.S. Trevisan, M.S. Schöffler, T. Jahnke, I. Bocharova, F. Sturm, N. Gehrken, B. Gaire, H. Gassert, S. Zeller, J. Voigtsberger, A. Kuhlins, A. Gatton, J. Sartor, D. Reedy, C. Nook, B. Berry, M. Zohrabi, A. Kalinin, A. Belkacem, R. Dörner, Th. Weber, A.L. Landers, T.N. Rescigno, C.W. McCurdy, J.B. Williams, (submitted to *J Phys B*)
2. **Hydrogen and fluorine migration in photo-double-ionization of 1,1-difluoroethylene ($1,1\text{-C}_2\text{H}_2\text{F}_2$) near and above threshold** B. Gaire, I. Bocharova, F. P. Sturm, N. Gehrken, J. Rist, H. Sann, M. Kunitski, J. Williams, M. S. Schöffler, T. Jahnke, B. Berry, M. Zohrabi, M. Keiling, A. Moradmand, A. L. Landers, A. Belkacem, R. Dörner, I. Ben-Itzhak, and Th. Weber, *Phys Rev A* **89** 043423 (2014).
3. **Photo-double-ionization of ethylene and acetylene near threshold** B Gaire, SY Lee, DJ Haxton, PM Pelz, I Bocharova, FP Sturm, N Gehrken, M Honig, M Pitzer, D Metz, H-K Kim, M Schöffler, R Dörner, H Gassert, S Zeller, J Voigtsberger, W Cao, M Zohrabi, J Williams, A. Gatton, D Reedy, C Nook, Thomas Müller, AL Landers, CL Cocke, I Ben-Itzhak, T Jahnke, A Belkacem, Th Weber, *Phys Rev A* **89** 013403 (2014).
4. **Resonant Auger decay driving intermolecular Coulombic decay in molecular dimers**, F Trinter, MS Schöffler, H-K Kim, FP Sturm, K Cole, N Neumann, A Vredenburg, J Williams, I Bocharova, R Guillemin, M Simon, A Belkacem, AL Landers, Th Weber, H Schmidt-Böcking, R Dörner, T Jahnke, *Nature* **505** 664-666 (2014).

5. **Dissociative electron attachment to carbon dioxide via the $^2\Pi_u$ shape resonance**, A. Moradmand, D.S. Slaughter, D.J. Haxton, A.L. Landers, C.W. McCurdy, T.N. Rescigno, M. Fogle, A. Belkacem *Phys. Rev. A* **88** 032703 (2013).
6. **Dissociative-electron-attachment dynamics near the 8-eV Feshbach resonance of CO₂**, A. Moradmand, D. Slaughter, A.L. Landers, M. Fogle, *Phys. Rev. A* **88** 022711 (2013).
7. **Momentum imaging of dissociative electron attachment to N₂O**, A. Moradmand, A.L. Landers, M. Fogle, *Phys. Rev. A* **88** 012713 (2013).
8. **Momentum-imaging apparatus for the study of dissociative electron attachment dynamics** A. Moradmand, J. Williams, A. Landers, M. Fogle, *Review of Scientific Instruments* **84**, 033104 (2013).
9. **Ejection of quasi free electron pairs from the helium atom ground state by a single photon**, M. S. Schöffler, C. Stuck, M. Waitz, F. Trinter, T. Jahnke, U. Lenz, M. Jones, A. Belkacem, A.L. Landers, C.L. Cocke, J. Colgan, A. Kheifets, I. Bray, H. Schmidt-Böcking, R. Dörner, and Th. Weber *Phys. Rev. Lett.*, **111** 013003 (2013).
10. **Probing the Dynamics of Dissociation of Methane Following Core Ionization Using Three-Dimensional Molecular Frame Photoelectron Angular Distributions**, J. B. Williams, C. S. Trevisan, M. S. Schöffler, T. Jahnke, I. Bocharova, H. Kim, B. Ulrich, R. Wallauer, F. Sturm, T. N. Rescigno, A. Belkacem, R. Dörner, Th. Weber, C. W. McCurdy, and A.L. Landers, *J. Phys. B: At. Mol. Opt. Phys.*, **45** 194003 (2012).
11. **Calculated and measured angular correlation between photoelectrons and Auger electrons from K-shell ionization**, F. Robicheaux, M. P. Jones, M. S. Schöffler, T. Jahnke, K. Kreidi, J. Titze, C. Stuck, R. Dörner, A. Belkacem, Th. Weber, and A.L. Landers *J. Phys. B: At. Mol. Opt. Phys.*, **45** 175001 (2012).
12. **Multi fragment vector correlation imaging - A proposal to search for hidden dynamical symmetries in many-particle molecular fragmentation processes**, F. Trinter, L. Ph. H. Schmidt, T. Jahnke, M. S. Schöffler, O. Jagutzki, A. Czasch, J. Lower, T. A. Isaev, R. Berger, A. L. Landers, Th. Weber, R. Dörner, H. Schmidt-Böcking *Molecular Physics* **110** 1863 (2012).
13. **Imaging polyatomic molecules in three dimensions using molecular frame photoelectron angular distributions**, J. B. Williams, C. S. Trevisan, M. S. Schöffler, T. Jahnke, I. Bocharova, H. Kim, B. Ulrich, R. Wallauer, F. Sturm, T. N. Rescigno, A. Belkacem, R. Dörner, Th. Weber, C. W. McCurdy, and A.L. Landers, *Phys. Rev. Lett.* **108** 233002 (2012).
14. **Dynamic modification of the fragmentation of autoionizing states of O+2**, W. Cao, G. Laurent, S. De, M. Schöffler, T. Jahnke, A. S. Alnaser, I. A. Bocharova, C. Stuck, D. Ray, M. F. Kling, I. Ben-Itzhak, Th. Weber, A. L. Landers, A. Belkacem, R. Dörner, A. E. Orel, T. N. Rescigno, and C. L. Cocke, *Phys. Rev. A* **84** 053406, (2011).
15. **Matter wave optics perspective at molecular photoionization: K-shell photoionization and Auger decay of N₂**, M. Schöffler, T. Jahnke, J. Titze, N. Petridis, K. Cole, L. Ph. H. Schmidt, A. Czasch, O. Jagutzki, J.B. Williams, C.L. Cocke, T. Osipov, S. Lee, M.H. Prior, A. Belkacem, A.L. Landers, H. Schmidt-Böcking, R. Dörner, and Th. Weber, *New Journal of Physics* **13** 095013 (2011).
16. **Production of excited atomic hydrogen and deuterium from H₂, HD and D₂ photodissociation** R Machacek , V M Andrianarijaona , J E Furst , A L D Kilcoyne , A L Landers , E T Litaker , K W McLaughlin and T J Gay *J. Phys. B: At. Mol. Opt. Phys.* **44** 045201 (2011).

Exploiting Non-equilibrium Charge Dynamics in Polyatomic Molecules to Steer Chemical Reactions

Wen Li, Wayne State University (wli@chem.wayne.edu)

Raphael D. Levine, University of California-Los Angeles (rafi@chem.ucla.edu)

Henry C. Kapteyn, University of Colorado at Boulder (henry.kaptyen@colorado.edu)

H. Bernhard Schlegel, Wayne State University (hbs@chem.wayne.edu)

Françoise Remacle, University of Liège, Belgium (FRemacle@ulg.ac.be)

Margaret M. Murnane, University of Colorado at Boulder
(Margaret.murnane@colorado.edu)

Program Scope

The project has two aims: (1) Creating and probing photoinduced charge migration dynamics of pure electronic origin on the attosecond to few femtoseconds time scales and studying the role of non-equilibrium charge distributions in inducing selectivity of chemical reactions in polyatomic molecules. (2) Achieving mode-selective chemistry in polyatomic molecules using intense ultrashort mid-infrared pulses. In the past year, we have achieved significant progress with both goals, experimentally and theoretically.

Recent Progress and Future Plans

Attosecond-Resolved Electron Correlation in Benzene (Wen Li, Raphael Levine, Françoise Remacle and H. Bernhard Schlegel)

The Li group recently developed a novel 3D coincidence imaging system capable of highly efficient electron-electron coincidence detection. Such a capability is critical for probing coherent electronic dynamics. Exploiting this capability and the principle of angular streaking, we implemented a universal probe of attosecond electronic dynamics with a time range from zero attosecond to a few femtoseconds with a resolution of tens of attoseconds. By implementing both triple and quadruple coincidence measurements, we were also able to study the state-resolved electron momentum correlation for the first time. Strong field double ionization of benzene was chosen as the first case study system, focusing on time-resolved double ionization rate. The preliminary result is exciting and promising: the double ionization rate decays as the time separation between the two electron ionization increases from zero attosecond to one femtosecond. The measurement was further supported by the decay of electron repulsion in the direction perpendicular to the polarization plane. This is the first clear evidence that the correlated electron motion promotes double ionization in attosecond time scale. Currently both the Schlegel group and the UCLA-ULg groups are helping to further understand this result. Experiments on other large aromatic and non-aromatic molecules such as furan, pyrrole, cyclohexadiene are on-going. Future development of this technique will be to use few-cycle mid-IR pulse to extend the time range to tens of femtoseconds, which will be especially suitable for studying coupled electronic and nuclear wave packet dynamics.

Strong Field Dissociation Dynamics by Circularly Polarized Mid-IR pulse (H. Bernhard Schlegel and Wen Li)

The Schlegel group is currently studying the effect of intense circularly polarized mid-IR laser fields on the fragmentation of different molecular systems. Lower intensities of circularly polarized light are needed to obtain the same degree of fragmentation, which is favorable for avoiding ionization implications. When the propagation of light is perpendicular to the plane of the molecule, the dissociation is almost entirely in the plane of the molecule. In formyl chloride, the branching ratios for circularly polarized light, $\text{H}+\text{ClCO}^+ > \text{Cl}+\text{HCO}^+ > \text{HCl}^++\text{CO}$, are different than for linearly polarized light averaged over the corresponding angles, $\text{Cl}+\text{HCO}^+ > \text{H}+\text{ClCO}^+ > \text{HCl}^++\text{CO}$. While the total angular momentum of the system after the pulse is the same for right and left circularly polarized light, it is surprising to see the components of angular momentum of the fragments differ in sign and magnitude for right and left circularly polarized light. This suggests the possibility of using the helicity of laser pulses as a new “knob” to control chemical reactions.

Development and Application of Mid-IR Light Sources for Mode Selective Chemistry (Henry Kapteyn and Margaret Murnane)

At JILA, the focus in the first year has been on developing the experimental capabilities necessary for the project. First, we developed a mid-IR laser system using a combination of Yb:YAG pump lasers and parametric amplification (OPCPA) using periodically-poled nonlinear materials, that is operating in the parameter range of interest: kHz repetition-rate, 1 mJ pulse energy at 3.1 micron wavelength, and sub-100-fs pulse duration. For experiments requiring longer mid-IR wavelengths, we have also designed and recently received custom-fabricated ZGP crystals from BAE systems that is allowing us to use the OPCPA laser (and a Ti:sapphire-pumped OPA) as a pump source for generating 4 μm and even longer-wavelength pulses in the 6-8 μm spectral region, with pulse duration of ≈ 5 cycles. This provides the team with truly unique experimental capabilities to test the Wayne State prediction that long wavelength driving lasers will enable increased molecular fragmentation. The molecular dynamics studies are being done using novel coincidence-capable time-of-flight velocity map imaging techniques pioneered at Wayne State by the Li group. At JILA, we implemented this technique in one of the two VMI setups. Finally, we are using UV pump pulses to selectively excite coupled electronic and nuclear dynamics in small molecules, by ionizing from different states.

Time-Resolved Charge migration (Raphael Levine and Francoise Remacle)

The UCLA-ULg groups started investigating the role of non-equilibrium electronic density on the nuclear motion on a diatomic molecule, N_2 (UCLA) and on larger medium size polyatomic molecules (ULg), PENNA ($\text{C}_{10}\text{H}_{15}\text{N}$) and ABCO ($\text{C}_7\text{H}_{13}\text{N}$). These molecules were chosen after discussion with the Li group, who simultaneously started to plan the experiments on N_2 and on ABCO. We are developing and applying approximate methodologies for PENNA and ABCO. In the case of PENNA, we first determined which internal nuclear degrees of freedom were involved in the charge-migration-

fragmentation channel. Two conical intersections were identified coupling the 3 lowest electronic states of the cation and the PES were computed for the two internal coordinates, C-C bond between the two moieties and dihedral puckering angle of the amine end, involved in these intersections. At the same time, surface hopping dynamics for the entire number of internal degrees of freedom was run on the fly on the three lowest states of the cation. In the next few months, fully quantum dynamics will be run on the 2D PES and the results compared with the surface hopping ones to assess the role of coherence. In the case of ABCO, the excited states of the neutral and the cation were computed. Following consultation with the Li group, electronic dynamics was then run for frozen nuclei for UV fs pulses with a 200 and 400 nm carrier frequency. The next step here is to compute the initial response of the nuclei by computing the force due to the non-stationary electron density. Preliminary steps have been made and will be pursued in the coming months. For N₂ we are using the pulse parameters of the Li group to excite the molecule while retaining a full description of the nuclear motion. In particular the dipole response exhibits clear evidence for nonadiabatic coupling in the nuclear motion starting at about 10 fs following excitation.

Publications from DOE-funded research (the first year)

(none yet)

Page is intentionally blank.

Probing electron-molecule scattering with HHG: Theory and Experiment

Robert R. Lucchese, Department of Chemistry, Texas A&M University, College Station, TX, 77843, lucchese@mail.chem.tamu.edu

Erwin Poliakoff, Department of Chemistry, Louisiana State University, Baton Rouge, LA 70803, epoliak@lsu.edu

Program Scope

Understanding electron-molecular scattering dynamics is the overall theme of our program. Until a few years ago, our primary focus was on one-photon molecular ionization and the coupling between vibrational and electronic motion. Recently, we have begun to study electron-molecule collisions that occur in high-field processes such as high harmonic generation (HHG) and recollision spectroscopy. Both experimentally and theoretically, this work is being performed in collaboration with the McDonald Laboratory at Kansas State University. Additionally, we have begun a collaboration with the Atomic, Molecular, and Optical Theory group at Lawrence Berkeley National Laboratory (LBNL) to develop next generation computational tools for studying electron-molecule collisions. All of these research efforts benefit the Department of Energy because the results elucidate structure/spectra correlations that will be indispensable for probing complex and disordered systems of interest to DOE such as clusters, catalysts, reactive intermediates, transient species, and related species.

Recent Progress

High Resolution Photoelectron Spectroscopy

As larger systems are considered, the experimental study of vibrationally resolved photoionization cross sections is limited by the increase in the density of states that makes the extraction of vibrationally specific cross sections difficult. This is caused by the number of thermally accessible low-lying tautomers in large molecules, the increase in the density of electronic states of the molecular ion, and to the increase in the density of vibrational states. These limitations are seen in our recent study of the high resolution photoelectron spectrum with partial vibrational resolution of a series of pyrimidine-type nucleobases: thymine, uracil and cytosine. The improved resolution allowed us to identify the electronic origins for the outermost valence electronic states. In the case of cytosine, there has also been much disagreement over which tautomers exist in the gas phase. Better resolution combined with recently published calculated spectra of cytosine tautomers gave insight into which cytosine tautomers exist in the gas phase. Striking similarities in the spectral features of all three pyrimidine-type nucleobases led us to conclude that the features in the cytosine photoelectron spectrum are not due to contributions from multiple tautomers but instead are from unresolved vibrational progressions. Since these features are practically the same in the spectra for all three molecules, we further conclude that the dominant vibrational progressions must be due to the pyrimidine back-bone, which all three molecules have in common

Correlation and Vibrational Effects in One-Photon Ionization

As preparation for studying HHG with SF₆ as a target molecule, we have completed some preliminary studies of one-photon ionization of this molecule to understand in greater detail the

electron scattering dynamics for low-lying ion states of SF₆. Of particular interest is the relative importance of multichannel scattering effects and the effects of molecular vibrations in the description of the narrow shape resonances which occur in the one-photon ionization of SF₆. These resonances are very prominent in the fixed-nuclei single channel photoionization calculations. When compared to the results of one-photon ionization experiments these calculations yielded resonance peaks that are much larger than those found in the experiment. An example of the effects of correlation as treated by channel coupling is the ionization from the 5t_{1u} orbital where we found that the computed peak value of the cross section of a low energy k t_{2g} resonance is reduced by a factor of two by coupling to the other open ionization channels, in much better agreement with experiment. In contrast, a high energy 5t_{1u} → k e_g resonance was not substantially affected by such coupling. This led us to consider the effects of the different geometries that are sampled by the ground vibrational state. Using the adiabatic approximation, we found that the symmetric stretching mode had only a minor effect on the total cross sections in the 5t_{1u} → k e_g channel. However, averaging over non-symmetric geometries sampled by the asymmetric stretching mode led to a significant reduction in the resonance peak and a broadening of the resonance feature, in much better agreement with experimental data. This can be understood by the fact that the asymmetric stretch leads to symmetry breaking and thus the single resonance in the degenerate e_g symmetry is split into two resonances at different, shifted energies, thus reducing and broadening the peak in the total cross section.

Atomic HHG

With respect to high harmonic spectra, we have worked on both atomic and molecular targets. In particular, we have worked with Tony Starace at the University of Nebraska and his collaborators in order to develop methods for extracting photoionization data quantitatively from HHG spectra via ellipticity measurements. More specifically, we have shown that it is possible to extract photoionization asymmetry parameters via measurements of the ellipticity dependence of HHG spectra of Ar.

Molecular Aspects of HHG

We have made considerable progress, in collaboration with Profs. Trallero and Lin at the McDonald Laboratory in the study of molecular HHG. We have studied HHG in relatively complex molecules. In the HHG spectrum SF₆ we observed noticeable structure in the experimental spectrum. Changing the gas jet position changes the macroscopic propagation and the effective trajectories of the returning electron. The one feature that is consistently present in the experimental data is the minimum in the HHG spectrum at the 17th harmonic (~26 eV), with a corresponding peak at lower energy (~23 eV). In the theory we have applied the quantitative rescattering (QRS) theory to isolated molecules and considered the ionization of the electrons from the three most weakly bound orbitals, i.e. the highest occupied molecule orbital (HOMO), the HOMO-1, and the HOMO-2. These three orbitals have ionization potentials that are all within 1.5 eV of each other.

The theoretical calculations were performed using relatively simple single-channel static-exchange type calculations for the recombination step in the three step model which is the basis of the QRS. Using the form of QRS where the rescattered wave is modeled using a reference pseudo hydrogen atom (QRS2) we found that we could model the main features of the observed HHG spectrum, i.e. the narrow peak at 23 eV and the broad peak centered at 35 eV. These

features can be explained as being due to shape resonances in ionization from the HOMO ($1t_{1g}$) and HOMO-1 ($5t_{1u}$) orbitals, either directly or through inter-channel coupling.

Grid Based Electron-Molecule Scattering Calculations

Another component of our research program is the development of a next-generation electron-molecule scattering code. This work is being done in collaboration with Bill McCurdy of the Atomic, Molecular, and Optical Theory group at LBNL. This code will be based on the complex Kohn approach with a numerical grid-based representation of the scattering wave functions. Additionally, we have analyzed the methods for implementing an overset grid representation where centered on each nucleus in a molecule there is a local grid which has spherical symmetry around that center. Additionally, these atomic centered grids are combined with an encompassing grid which connects the molecular region and asymptotic regions. These different grids are partially overlapping, thus they are referred to as overset grids. We have developed an iterative approach for solving the complex Kohn scattering equations. This approach starts with free-particle solutions and forms iterates by computing $G_0(E-H)$ repeatedly on each free particle function. This approach leads to an iterative subspace of the full scattering problem that has been found in model problems to give very rapidly convergent scattering matrices.

Future Plans

Theoretically, we will consider the effects of correlation and vibrational averaging on the recombination step of HHG within the QRS model. We will also explore the effects of resonances and electron correlation on the ellipticity of the light generated in the HHG process from aligned molecules. We have begun to implement the overset-grid iterative complex-Kohn scheme on general polyatomic systems using some of the framework that has been developed in the single-center expansion ePolyScat code. The near-term goal is the computation of electron scattering dynamics at the static-exchange level for molecular systems with up to ~ 20 atoms. Subsequently, correlation effects will be incorporated into the new code.

Publications in 2013-2015 Acknowledging Support from DOE

1. M. C. H. Wong, A.-T. Le, A. F. Alharbi, A. E. Boguslavskiy, R. R. Lucchese, J.-P. Brichta, C.D.Lin, and V.R.Bhardwaj, High Harmonic Spectroscopy of the Cooper Minimum in Molecules, *Phys. Rev. Lett.* **110**, 033006:1-5 (2013).
2. Anh-Thu Le, R. R. Lucchese, and C. D. Lin, Quantitative rescattering theory of high-order harmonic generation for polyatomic molecules, *Phys. Rev. A* **87**, 063406:1-9 (2013).
3. Ralph Carey, Robert R. Lucchese, and F. A. Gianturco, Electron scattering from gas phase cis-diamminedichloroplatinum(II): quantum analysis, *J. Chem. Phys.* **138**, 204308:1-10 (2013).
4. S. Marggi Poullain, K. Veyrinas, P. Billaud, M. Lebech, Y. J. Picard, R. R. Lucchese and D. Dowek, The role of Rydberg states in Photoionization of NO_2 and $(\text{NO}^+, \text{O}^-)$ Ion Pair Formation induced by One VUV Photon, *J. Chem. Phys.* **139**, 044311:1-12 (2013).
5. Anh-Thu Le, R. R. Lucchese, and C. D. Lin, High-order-harmonic generation from molecular isomers with midinfrared intense laser pulses, *Phys. Rev. A* **88**, 021402:1-5(R) (2013).
6. J. Jose and R. R. Lucchese, Study of resonances in the photoionization of $\text{Ar}@C_{60}$ and C_{60} , *J. Phys. B* **46**, 215103:1-7 (2013).

7. K. Veyrinas, C. Elkharrat, S. Marggi Poullain, N. Saquet, D. Dowek, R. R. Lucchese, G. A. Garcia and L. Nahon, Molecular polarimetry: accurate full polarization ellipse determination by electron-ion vector correlations, *Phys. Rev. A* **88**, 063411:1-5 (2013).
8. J. Jose, R. R. Lucchese, and T. N. Rescigno, Interchannel coupling effects in the valence photoionization of SF₆, *J. Chem. Phys.* **139**, 204305:1-10 (2014).
9. S. Marggi Poullain, C. Elkharrat, W. B. Li, K. Veyrinas, J.C. Houver, C. Cornaggia, T. N. Rescigno, R. R. Lucchese and D. Dowek, Recoil frame photoemission in multiphoton ionization of small polyatomic molecules: Photodynamics of NO₂ probed by 400 nm femtosecond pulses, *J. Phys. B* **47**, 124024:1-18 (2014).
10. M. Okunishi, R. R. Lucchese, T. Morishita, and K. Ueda, Rescattering photoelectron spectroscopy of small molecules, *J. Electron Spectrosc. Relat. Phenom.* **195**, 313-319 (2014).
11. Jesús A. López-Domínguez, Robert R. Lucchese, K. D. Fulfer, David Hardy, E. D. Poliakoff, and A. A. Aguilar, Vibrationally specific photoionization cross sections of acrolein leading to the \tilde{X}^2A' ionic state, *J. Chem. Phys.* **141**, 094301:1-7 (2014).
12. U. Jacovella, D. M. P. Holland, S. Boyé-Péronne, D. Joyeux, L. E. Archer, N. de Oliveira, L. Nahon, R. R. Lucchese, Hong Xu, and S. T. Pratt, High-resolution photoabsorption spectrum of jet-cooled propyne, *J. Chem. Phys.* **141**, 114303:1-14 (2014).
13. J. Jose and R. R. Lucchese, Vibrational effects in the shape resonant photoionization leading to the A^2T_{1u} state of SF₆⁺, *Chem. Phys.* **447**, 64-70 (2015).
14. U. Jacovella, D. M. P. Holland, S. Boyé-Péronne, B. Gans, N. de Oliveira, D. Joyeux, L. E. Archer, R. R. Lucchese, H. Xu, and S. T. Pratt, High-resolution vacuum-ultraviolet photoabsorption spectra of 1-butyne and 2-butyne, *J. Chem. Phys.* **143**, 034304:1-14 (2015).
15. K. D. Fulfer, D. Hardy, A. A. Aguilar, and E. D. Poliakoff, High resolution photoelectron spectroscopy of the pyrimidine-type nucleobases, *J. Chem. Phys.* **142**, 224310:1-9 (2015).

Photoabsorption by Free and Confined Atoms and Ions

Steven T. Manson, Principal Investigator

Department of Physics and Astronomy, Georgia State University, Atlanta, Georgia 30303
(smanson@gsu.edu)

Program Scope

The goals of this research program are: to provide theoretical support to, and collaboration with, various experimental programs that employ latest generation light sources, particularly ALS, APS and LCLS; to further our understanding of the photoabsorption process; and to study the properties (especially photoabsorption) of confined atoms and ions. Specifically, calculations are performed using and upgrading state-of-the-art theoretical methodologies to help understand the physics of the experimental results; to suggest future experimental investigations; and seek out new phenomenology, especially in the realm of confined systems. The primary areas of programmatic focus are: nondipole and relativistic effects in photoionization; photoabsorption of inner and outer shells of atoms and atomic ions (positive and negative); dynamical properties of atoms endohedrally confined in buckyballs, primarily C₆₀; studies of time delay on the attosecond scale in photoionization of free and confined atomic systems. Flexibility is maintained to respond to opportunities.

Highlights of Recent Progress

The study of confined atoms is fairly new. There are a number of theoretical investigations of various atoms endohedrally confined in C₆₀ [1,2], but experimental studies are sparse [3-5]. Our theoretical program, at various levels of approximation, is aimed at delineating the properties of such systems, especially photoionization, to guide experiment and uncover new phenomena. Among our major results, we have found that a huge transfer of oscillator strength from the C₆₀ shell, in the neighborhood of the giant plasmon resonance, to the encapsulated atom for both Ar@C₆₀ [6] and Mg@C₆₀ [7]. In addition, confinement resonances [8], oscillations in the photoionization cross section of an endohedral atom due to the interferences of the photoelectron wave function for direct emission with those scattered from the surrounding carbon shell have been predicted in a broad range of cases; recently, their existence has been confirmed experimentally [4,5]. Further, in the photoionization of endohedral atoms within nested fullerenes, has shown that, as a result of the multi-walled confining structures, the confinement resonances become considerably more complicated [9]. And we have shown that confinement resonances induce rather significant resonances in the attosecond time-delay of photoelectron emission [10], which suggests that time-domain spectroscopy might be efficacious in the study of electron dynamics in endohedral systems and clusters.

Considering Xe confined in C₆₀ the formation of a new type of atom-fullerene hybrid state was discovered [11]. These dimer-type states arise from the near-degeneracy of inner levels of the confined atom and the confining shell, in contrast to the known overlap-induced hybrid states around the Fermi level of smaller compounds, and are found to occur in confined noble gas, alkali-earth atoms [12] and the Zn series [13,14]. The photoionization cross sections of these hybrid states exhibit rich structures and are radically different from the cross sections of free atomic or fullerene states. This also

occurs in buckyonions, nested fullerenes [15] which suggests the possibility of creating buckyonions with plasmons of specified character, i.e., *designer resonances*.

We have also explored the interatomic Coulomb decay (ICD) phenomenon in confined atoms and found, owing to hybridization between atomic and shell orbitals, that ICD occurs both ways, from atom to shell and shell to atom, and the rates (widths) are often much larger than the ordinary Auger rates [16].

To treat endohedrals accurately, we have embarked upon an initiative to include the geometry of an atom in a buckyball essentially exactly using fully molecular bases and codes. Using the exact geometry, our results on Ar@C₆₀ [17] exhibited confinement resonances, but with differences from the “spherical potential” models at low photoelectron energy where our calculation showed much sharper resonances. We have also studied the effects of the interchannel coupling of the carbon 1s channels from the C₆₀ shell on the atomic cross sections in the vicinity of the carbon 1s thresholds. Since the shell cross section is about 60 Mb at the 1s threshold, much larger than the atomic cross sections at that energy, there was a possibility of significant interchannel coupling. Our results showed that interchannel coupling was miniscule because the interchannel coupling matrix element between shell and atomic channels is tiny as the overlap between shell and atomic bound states is so small; they exist in different regions of space.

A relativistic random phase approximation study has explained the significant structure in subshell photoionization cross sections many keV above their thresholds found experimentally in Ag [18]; the structure is nonresonant and about 50 eV wide. It was found to be induced by interchannel coupling with inner-shell ionization channels, in the vicinity of the inner-shell thresholds. Of significance is that this kind of structure should be a general phenomenon in photoionization throughout the Periodic Table.

Several aspects of attosecond time delay were explored. Time delay of photoemission from valence subshells of noble-gas atoms were theoretically scrutinized within the framework of the dipole relativistic random phase approximation [19] with a focus on the variation of time delay in the vicinity of the Cooper minima where the corresponding dipole matrix element changes its sign while passing through a node. It was found that the presence of the Cooper minimum in one photoionization channel has a strong effect on time delay in other channels owing to interchannel coupling, and that relativistic effects affect time delay significantly in Regions of Cooper minima. A study of time delay in Mn photoionization in the region of the 3p→3d giant resonance showed the dramatic effect of the resonance on the time delay of photoemission from the 3d and 4s valence subshells of the Mn atom [20]. It was shown that photoionization time delay in the autoionizing resonance region is explicitly associated with the resonance lifetime, which can, thus, be directly measured in attosecond time-delay experiments. Similar features are expected to emerge in photoionization time delays of other transition-metal and rare-earth atoms with half-filled subshells that possess giant autoionization resonances as well.

Future Plans

Our future plans are to continue on the paths set out above. In the area of confined atoms, expand on our studies of interatomic Coulomb decay (ICD) of resonances. We will also work on ways to enhance the time-dependent local-density approximation to make it more accurate in our calculations of confined atoms. In

addition, we shall work towards upgrading our theory to include relativistic interactions to be able to deal with heavy endohedrals with quantitative accuracy. We will also look at the attosecond time delay in photoionization that has been found in various experiments, and we work to further our understanding of how confinement might affect this time delay. In addition, the search for cases where nondipole effects are likely to be significant, as a guide for experiment, and quadrupole Cooper minima, will continue. And we shall respond to new experimental results as they come up.

Publications over the Past 3 Years Citing DOE Support

- “Photoionization of ground and excited states of Ca^+ and comparison along the isoelectronic sequence,” A. M. Sossah, H.-L. Zhou, S. T. Manson, *Phys. Rev. A* **86**, 023403-1-10 (2012).
- “Photoionization of Endohedral Atoms Using R-matrix Methods: Application to $\text{Xe}@C_{60}$,” T. W. Gorczyca, M. F. Hasoğlu, and S. T. Manson, *Phys. Rev. A* **86**, 033204-1-9 (2012).
- “Atom-fullerene hybrid photoionization mediated by coupled d -states in $\text{Zn}@C_{60}$,” Jaykob N. Maser, Mohammad H. Javani, Ruma De, Mohamed E. Madjet, Himadri S. Chakraborty, and Steven T. Manson, *Phys. Rev. A* **86**, 053201-1-5 (2012).
- “Photoionization of Confined Ca in a Spherical Potential Well,” M. F. Hasoğlu, H.-L. Zhou, T. W. Gorczyca, and S. T. Manson, *Phys. Rev. A* **87**, 013409-1-5 (2013).
- “Core Correlation Effects in the Valence Photodetachment of Cu^- ,” J. Jose, H. R. Varma, P. C. Deshmukh, S. T. Manson, and V. Radojević, *Proceedings of the 26th Summer School and International Symposium on the Physics of Ionized Gases (SPIG 2012), 27th-31st August 2012, Zrenjanin, Serbia, Book of Contributed Papers & Abstracts of Invited Lectures and Progress Reports*, editors: M. Kuraica and Z. Mijatović (University of Novi Sad, Novi Sad, Serbia, 2012), pp. 39-42.
- “Photoionization of Endohedrally Confined Ca ($\text{Ca}@C_{60}$),” M. F. Hasoglu, P. Prabha, M. H. Javani, H. L. Zhou, and S. T. Manson, *J. Phys. Conf. Ser.* **388**, 022026 (2012).
- “Dipole and Quadrupole Photoionization of Intermediate Subshells of Atomic Mercury,” T. Banerjee, Hari R. Varma, P. C. Deshmukh, and S. T. Manson, *J. Phys. Conf. Ser.* **388**, 022076 (2012).
- “Dipole and quadrupole photodetachment/photoionization studies of the Ar isoelectronic sequence,” J. Jose, G. B. Pradhan, V. Radojević, S. T. Manson and P. C. Deshmukh, *J. Phys. Conf. Ser.* **388**, 022098 (2012).
- “Effect of Interchannel Coupling and Confinement on the Photoionization of Kr,” J. George, Hari R. Varma, P. C. Deshmukh and S. T. Manson, *J. Phys. Conf. Ser.* **388**, 022009 (2012).
- “Pronounced Effects of Interchannel Coupling In High-Energy Photoionization,” W. Drube, T.M. Grehk, S. Thiess, G. B. Pradhan, H. R. Varma, P. C. Deshmukh and S. T. Manson, *J. Phys. B* **46**, 245006-1-6 (2013).
- “Positron differential studies: Comparison to photoionization,” A. C. F. Santos, R. D. DuBois and S. T. Manson, *AIP Conference Proceedings* **1525**, 441-443 (2013).
- “Innershell Photoionization of Atomic Chlorine,” W. C. Stolte, Z. Felfli, R. Guillemin, G. Ohrwall, S.-W. Yu, J. A. Young, D. W. Lindle, T. W. Gorczyca, N. C. Deb, S. T. Manson, A. Hibbert, and A. Z. Msezane, *Phys. Rev. A* **88**, 053425-1-11 (2013).
- “Photoionization of the 5s subshell of Ba in the region of the second Cooper minimum: cross sections and angular distributions,” A. Ganesan, S. Deshmukh, G. B. Pradhan, V. Radojevic, S. T. Manson and P. C. Deshmukh, *J. Phys. B* **46**, 185002-1-5 (2013).
- “Probing confinement resonances by photoionizing Xe inside a C_{60}^+ molecular cage,” R. A. Phaneuf, A. L. D. Kilcoyne, N. B. Aryal, K. K. Baral, D. A. Esteves-Macaluso, C. M. Thomas, J. Hellhund, R. Lomsadze, T. W. Gorczyca, C. P. Ballance, S. T. Manson, M. F. Hasoglu, S. Schippers, and A. Müller, *Phys. Rev. A* **88**, 053402-1-7 (2013).
- “A Comprehensive X-ray Absorption Model for Atomic Oxygen,” T. W. Gorczyca, M. A. Bautista, M. F. Hasoglu, J. Garcia, E. Gatuzz, J. S. Kaastra, T. R. Kallman, S. T. Manson, C. Mendoza, A. J. J. Raassen, C. P. de Vries and O. Zatsarinny, *Astrophys. J.* **779**, 78-1-11 (2013).
- “Photoionization study of Xe 5s: Ionization Cross Sections and Photoelectron Angular Distributions,” G. Aarthi, J. Jose, S. Deshmukh, V. Radojević, P. C. Deshmukh and S. T. Manson, *J. Phys. B* **47**, 025004-1-5 (2014).
- “Valence Photoionization of Noble Gas Atoms Confined in the Fullerene C_{60} ,” M. H. Javani, H. S. Chakraborty, and S. T. Manson, *Phys. Rev. A* **89**, 053402-1-12 (2014).
- “Resonant Auger-intersite-Coulombic hybridized decay in the photoionization of endohedral fullerenes” by M. H. Javani, J. B. Wise, R. De, M. E. Madjet, H. S. Chakraborty, and S. T. Manson, *Phys. Rev. A* **89**, 063420-1-4 (2014).

- “Attosecond time delay in the photoionization of endohedral atoms $A@C_{60}$: A new probe of confinement resonances,” P. C. Deshmukh, A. Mandal, S. Saha, A. S. Kheifets, V. K. Dolmatov and S T Manson, *Phys. Rev. A* **89**, 053424-1-4 (2014).
- “Photoionization of Ca 4s in a spherical attractive well potential: dipole, quadrupole and relativistic effects,” A. Kumar, G. B. Pradhan, H. R. Varma, P. C. Deshmukh and S. T. Manson, *J. Phys. B* **47**, 185003-1-8 (2014).
- “Photoionization of bonding and antibonding-type atom-fullerene hybrid states in $Cd@C_{60}$ vs $Zn@C_{60}$,” M. H. Javani, R. De, M. E. Madjet, S. T. Manson and H. S. Chakraborty, *J. Phys. B* **47**, 175102-1-7 (2014).
- “Empirical Formulae for Direct Double Ionization by Bare Ions: $Z = -1$ to $+92$,” A. C. F. Santos, R. D. DuBois and S. T. Manson, *Phys. Rev. A* **90**, 052721-1-10 (2014).
- “Relativistic effects in photoionization time delay near the Cooper minimum of noble gas atoms,” S. Saha, J. Jose, S. Saha, H. R. Varma, P. C. Deshmukh, A. S. Kheifets, V. K. Dolmatov and S. T. Manson, *Phys. Rev. A* **90**, 053406-1-7 (2014).
- “Fano shape analysis of autoionization resonances in neon isoelectronic sequence using relativistic multichannel quantum defect theory,” M. Nrisimhamurty, G. Aravind, P. C. Deshmukh and S. T. Manson, *Phys. Rev. A* **91**, 013404-1-12 (2015).
- “Attosecond time delay in the photoionization of Mn in the $3p \rightarrow 3d$ giant resonance region,” V. K. Dolmatov, A. S. Kheifets, P. C. Deshmukh and S. T. Manson, *Phys. Rev. A* **91**, 053415-1-7 (2015).
- “Photoabsorption studies of some closed-shell ions in the La isonuclear sequence,” S. Kalyadan, H. R. Varma, P. C. Deshmukh, J. T. Costello, P. Hayden and S. T. Manson, *Phys. Rev. A* (in press).
- “Photoionization of Endohedral Atoms: Molecular and Interchannel Coupling Effects” A. Ponzi, P. Decleva and S. T. Manson, *Phys. Rev. A* **92**, 023405-1-7 (2015).
- “Jellium Model Potentials for the C_{60} Molecule and the Photoionization of Endohedral Atoms, $A@C_{60}$,” A. S. Baltenkov, S. T. Manson S. T. and A. Z. Msezane, *J. Phys. B* **48**, 185103 (2015).

References

- [1] V. K. Dolmatov, A. S. Baltenkov, J.-P. Connerade and S. T. Manson, *Radiation Phys. Chem.* **70**, 417 (2004) and references therein.
- [2] V. K. Dolmatov, *Advances in Quantum Chemistry*, **58**, 13 (2009) and references therein.
- [3] A. Müller *et al*, *Phys. Rev. Lett.* **101**, 133001 (2008).
- [4] A. L. D. Kilcoyne, A. Aguilar, A. Müller, S. Schippers, C. Cisneros, G. Alna'Washi, N. B. Aryal, K. K. Baral, D. A. Esteves, C. M. Thomas, and R. A. Phaneuf, *Phys. Rev. Lett.* **105**, 213001 (2010).
- [5] R. A. Phaneuf, A. L. D. Kilcoyne, N. B. Aryal, K. K. Baral, D. A. Esteves-Macaluso, C. M. Thomas, J. Hellhund, R. Lomsadze, T. W. Gorczyca, C. P. Ballance, S. T. Manson, M. F. Hasoglu, S. Schippers, and A. Müller, *Phys. Rev. A* **88**, 053402-1-7 (2013).
- [6] M. E. Madjet, H. S. Chakraborty and S. T. Manson, *Phys. Rev. Letters* **99**, 243003 (2007).
- [7] M. E. Madjet, H. S. Chakraborty, J. M. Rost and S. T. Manson, *Phys. Rev. A* **78**, 013201 (2008).
- [8] V. K. Dolmatov and S. T. Manson, *J. Phys. B* **41**, 165001 (2008).
- [9] V. K. Dolmatov and S. T. Manson, *J. Phys. Rev. A* **78**, 013415 (2008).
- [10] P. C. Deshmukh, A. Mandal, S. Saha, A. S. Kheifets, V. K. Dolmatov and S T Manson, *Phys. Rev. A* **89**, 053424 (2014).
- [11] H. S. Chakraborty, M. E. Madjet, T. Renger, J.-M. Rost and S. T. Manson, *Phys. Rev. A* **79**, 061201(R) (2009).
- [12] M. H. Javani, M. R. McCreary, A. B. Patel, M. E. Madjet, H. S. Chakraborty and S. T. Manson, *Eur. Phys. J. D* **66**, 189 (2012).
- [13] J. N. Maser, M. H. Javani, R. De, M. E. Madjet, H. S. Chakraborty and S. T. Manson, *Phys. Rev. A* **86**, 053201 (2012).
- [14] M. H. Javani, R. De, M. E. Madjet, S. T. Manson and H. S. Chakraborty, *J. Phys. B* **47**, 175102 (2014).
- [15] M. A. McCune, R. De, M. E. Madjet, H. S. Chakraborty, and S.T. Manson, *J. Phys. B* **44**, 241002 (2011).
- [16] M. H. Javani, J. B. Wise, R. De, M. E. Madjet, H. S. Chakraborty, and S. T. Manson, *Phys. Rev. A* **89**, 063420 (2014).
- [17] A. Ponzi, P. Decleva and S. T. Manson, *Phys. Rev. A* **92**, 023405 (2015).
- [18] W. Drube, T.M. Grehk, S. Thiess, G. B. Pradhan, H. R. Varma, P. C. Deshmukh and S. T. Manson, *J. Phys. B* **46**, 245006 (2013).
- [19] S. Saha, J. Jose, S. Saha, H. R. Varma, P. C. Deshmukh, A. S. Kheifets, V. K. Dolmatov and S. T. Manson, *Phys. Rev. A* **90**, 053406 (2014).
- [20] S. Saha, J. Jose, S. Saha, H. R. Varma, P. C. Deshmukh, A. S. Kheifets, V. K. Dolmatov and S. T. Manson, *Phys. Rev. A* **90**, 053406 (2014).

ABSTRACT

ELECTRON-DRIVEN PROCESSES IN POLYATOMIC MOLECULES

Investigator: Vincent McKoy

A. A. Noyes Laboratory of Chemical Physics

California Institute of Technology

Pasadena, California 91125

email: mckoy@caltech.edu

PROJECT DESCRIPTION

The focus of this project is the development and application of accurate, scalable methods for computational studies of low-energy electron–molecule collisions, with emphasis on larger polyatomics relevant to electron-driven chemistry in biological and materials-processing systems. Because the required calculations are highly numerically intensive, efficient use of large-scale parallel computers is essential, and the computer codes developed for the project are designed to run both on tightly-coupled parallel supercomputers and on workstation clusters.

HIGHLIGHTS

In the past year we completed some major projects and initiated new lines of research. Collaboration with experimental groups having complementary interests continues to be central to our work. Highlights include:

- Carried out initial, exploratory calculations using localized-orbital methods to address the scaling problem in accurate electron-collision calculations on larger molecules
- Completed and published a joint experimental-theoretical study of electron-impact excitation of the simplest alcohol, methanol
- Completed joint experimental-theoretical studies of elastic electron scattering by the two prototypical halogenated alkanes, chloromethane and chloroethane

ACCOMPLISHMENTS

We have begun exploring the use of localized molecular orbitals in electron-molecule collision calculations. Accurate calculations at low energies require a representation of the target molecule's response to the projectile electron during the collision (the polarization effect). In our Schwinger multichannel (SMC) approach, that response is accounted for by including configurations built upon excited states of the target molecule in the variational basis set that represents the many-electron wave function of the electron–molecule system. Although this approach is more fundamental and flexible than using a local “polarization potential,” as is done in some other approaches, it comes at the cost of a rapid scaling with molecular size: the number of configurations needed to achieve results of a given quality increases roughly as the third power of the number of electrons in the molecule, and the computational cost increases even faster.

To improve on that scaling and so enable accurate scattering calculations on larger systems, we have borrowed a technique from bound-state electronic structure calculations, where an analogous scaling problem arises in configuration-interaction calculations that attempt to account for dynamic electron correlation. The underlying physical idea is that correlation (in our case, the response of the target molecule's charge density to the presence of the projectile) is primarily a local phenomenon; that is, the change in electron density in one part of a large molecule is largely independent of what is happening in distant parts of the molecule. To take advantage of this fact, we make a unitary transformation from the commonly used canonical molecular orbitals, which are delocalized across the whole molecule, to localized orbitals. We then restrict the variational space for the scattering calculation so that only excitations between orbitals located in the same part of the molecule are included when forming configurations representing polarization. The overall scaling of the scattering calculation is thereby reduced from cubic to quadratic in molecular size.

The initial, trial applications that we have carried out are highly promising. We have verified that physically reasonable and apparently well-converged results can be obtained for medium-sized test molecules. We have begun additional exploratory work on larger target systems, including the uracil-adenine base pair, which would be difficult to treat accurately in any other way.

During the year we also completed and published our work on electron-impact excitation of low-lying electronic states of methanol [1]. This work was done in collaboration with experimentalists at California State University, Fullerton, led by Profs. Murtadha Khakoo and Leigh Hargreaves, and with two theorists, Dr. Thomas Rescigno (LBL) and Prof. Ann Orel (University of California, Davis), who used the complex Kohn variational approach to treat the scattering. We found generally good qualitative and often quantitative agreement between our SMC results and the Kohn results. Agreement between the calculated cross sections and the measurements was less good, especially for the triplet excitation channels. Interestingly, the patterns of both agreement and disagreement generally mirror those we saw in excitation of water [2,3].

As part of our ongoing collaboration with the experimental electron-molecule collision program at California State University, Fullerton, we completed studies of two small alkyl halides, chloromethane (CH_3Cl) and chloroethane ($\text{C}_2\text{H}_5\text{Cl}$). These molecules are analogues of the alcohols that we have studied previously and also prototypes of halogenated organic molecules, where the low-lying antibonding (σ^*) orbital associated with the carbon-halogen bond is known to play an important role in capturing electrons to drive vibrational excitation and dissociative attachment. Our computed and measured results for chloromethane were in generally good agreement with each other and with available literature data. Chloroethane is much less well studied, and our results added new information about its differential scattering cross sections in the 1 to 30 eV energy range while confirming that the C-Cl σ^* resonance falls significantly lower in energy, at roughly 2.5 eV vs. 3.3 eV in chloromethane. Results for chloromethane were recently published [4], and those for chloroethane are in press.

PLANS FOR COMING YEAR

In the coming year we will continue to gain experience using localized orbitals for high-level scattering calculations on large target systems. We intend to complete studies of one or more nucleobase pairs using this approach, with the goal of understanding how the energies and widths of the low-energy resonances responsible for dissociative electron attachment (and thus electron-driven DNA damage) may differ in a more realistic setting from those that have been obtained by existing calculations and gas-phase measurements on isolated single molecules.

We also plan to continue work on angle-resolved dissociative-attachment studies in collaboration with Drs. Daniel Slaughter and Ali Belkacem of LBL, following up our recent study of the RNA base uracil [5]. Preliminary data from LBL indicate that a similar mechanism for H^- loss may operate in the DNA base thymine (5-methyl uracil). We are initiating electronic structure calculations to identify a candidate Feshbach resonance and will follow that work up with electron-collision calculations to obtain entrance amplitudes for the dissociative-attachment process.

We further plan to carry out calculations on vibrational excitation of chloromethane by electron impact, in collaboration with the Khakoo and Hargreaves experimental groups at California State University, Fullerton. This work is a natural follow-on to our study of elastic scattering and, more importantly, a lead-in to future computational studies of dissociative attachment dynamics.

REFERENCES

- [1] K. Varela, L. R. Hargreaves, K. Ralphs, M. A. Khakoo, C. Winstead, V. McKoy, T. N. Rescigno, and A. E. Orel, *J. Phys. B* **48**, 115208 (2015).
- [2] K. Ralphs, G. Serna, L. R. Hargreaves, M. A. Khakoo, C. Winstead, and V. McKoy, *J. Phys. B* **46**, 125201 (2013).
- [3] T. N. Rescigno and A. E. Orel, *Phys. Rev. A* **88**, 012703 (2013).

- [4] C. Navarro, A. Sakaamini, J. Cross, L. R. Hargreaves, M. A. Khakoo, Kamil Fedus, C. Winstead, and V. McKoy, *J. Phys. B* **48**, 195202 (2015).
- [5] Y. Kawarai, Th. Weber, Y. Azuma, C. Winstead, V. McKoy, A. Belkacem, and D. S. Slaughter, *J. Phys. Chem. Lett.* **5**, 3854 (2014).

PROJECT PUBLICATIONS AND PRESENTATIONS, 2013–2015

1. “Low-Energy Elastic Electron Scattering by Acetylene,” A. Gauf, C. Navarro, G. Balch, L. R. Hargreaves, M. A. Khakoo, C. Winstead, and V. McKoy, *Phys. Rev. A* **87**, 012710 (2013).
2. “Excitation of the 6 Lowest Electronic Transitions in Water by 9 to 20 eV Electrons,” K. Ralphs, G. Serna, L. R. Hargreaves, M. A. Khakoo, C. Winstead, and V. McKoy, *J. Phys. B* **46**, 125201 (2013).
3. “Low-Energy Elastic Electron Scattering by Acetaldehyde,” A. Gauf, C. Navarro, G. Balch, L. R. Hargreaves, M. A. Khakoo, C. Winstead, and V. McKoy, *Phys. Rev. A* **89**, 022708 (2014).
4. “Low-Energy Elastic Electron Scattering from Isobutanol and Related Alkyl Amines,” K. Fedus, C. Navarro, L. R. Hargreaves, M. A. Khakoo, F. M. Silva, M. H. F. Bettiga, C. Winstead, and V. McKoy, *Phys. Rev. A* **90**, 032708 (2014).
5. “Excitation of the 4 Lowest Electronic Transitions in Methanol by Low-Energy Electrons,” K. Varela, L. R. Hargreaves, K. Ralphs, M. A. Khakoo, C. Winstead, V. McKoy, T. N. Rescigno, and A. E. Orel, *J. Phys. B* **48**, 115208 (2015).
6. “Low-energy elastic electron scattering from chloromethane, CH_3Cl ,” C. Navarro, A. Sakaamini, J. Cross, L. R. Hargreaves, M. A. Khakoo, Kamil Fedus, C. Winstead, and V. McKoy, *J. Phys. B* **48**, 195202 (2015).
7. “Low-Energy Elastic Scattering and Electronic Excitation of Water and Methanol by Electron Impact,” M. A. Khakoo, L. R. Hargreaves, K. Varela, K. Ralphs, C. Winstead, and V. McKoy, XVIII International Symposium on Electron-Molecule Collisions and Swarms, Kanazawa, Japan, July 19–21, 2013.

Page is intentionally blank.

ELECTRON/PHOTON INTERACTIONS WITH ATOMS/IONS

Alfred Z. Msezane (email: amsezane@cau.edu)

Clark Atlanta University, Department of Physics and CTSPS, Atlanta, Georgia 30314

PROGRAM SCOPE

The project's primary objective is to gain a fundamental understanding of the near-threshold electron attachment mechanism in low-energy electron scattering from atoms. Creatively, we have used our complex angular momentum (CAM) method to link low-energy electron scattering resonances with chemical reaction dynamics and extracted accurate atomic electron affinities (EAs). These EAs have been used to develop a fundamental theory of negative ion catalysis. Very recently, the CAM method has been used to demonstrate that relativity contributes insignificantly to the calculation of atomic EAs, even in the heavy At atom [1]. Results from selected Transition Metals [Zn, Cd, Au, Mg] will benefit directly the DOE EFRC Center for Atomic-Level Catalyst Design at LSU and the LBL's Advanced Light Source studies of Photoionization of Au positive ions and developments in the synthesis of the endohedral metallofullerene Au@C₆₀⁺.

CONTINUING RESEARCH

The time-dependent-density-functional theory is utilized to investigate the photoabsorption spectra of encapsulated atoms [Zn, Cd, Au, Mg], focusing on the confinement resonances. Their photoionization cross sections and electron differential cross sections (DCSs) are also calculated. Regge Trajectories are employed to probe at the fundamental level electron attachment in multielectron systems (transition metal atoms and fullerenes), yielding ground and excited anions as Regge resonances. Benchmark binding energies of these anions will be extracted from the calculated electron elastic total cross sections (TCSs) using the CAM method. Standard structure-type methods such as CIV3, GRASP and MCHF will be used to calculate the additional energy levels and construct the attendant configurational wave functions for negative ion inner-shell studies.

We also continue our investigations of low-energy electron scattering from simple and complex atoms such as listed above (and the hotly debated La, Ce, Yb) to obtain new accurate EAs and identify possible anionic catalysts. The CAM method is being extended to investigate Feshbach resonances. R-matrix calculations continue of the computationally exacting inner-shell photoionization of Cl.

SUMMARY OF RECENT RESEARCH ACCOMPLISHMENTS

I. Core-Polarization and Relativistic Effects in Electron Affinity Calculations for Atoms:

A Complex Angular Momentum Investigation

Regge poles are singularities of the S-matrix; therefore, they rigorously define resonances. Of crucial importance in the complex angular momentum (CAM) method are the Regge trajectories that probe electron attachment at the fundamental level near threshold; they penetrate the atomic core, thereby allow the determination of reliable electron affinities (EAs) of complex atomic and molecular systems.

Here core-polarization interactions have been investigated in low-energy electron elastic scattering from the atoms In, Sn, Eu, Au and At through the calculation of their EAs [1]. The CAM method wherein is embedded fully the vital electron-electron correlations has been used. The core-polarization effects have been studied through the well investigated rational function approximation of the Thomas-Fermi potential, which can be analytically continued into the complex plane. The EAs are extracted from the large resonance peaks in the CAM calculated low-energy electron -atom scattering total cross sections and compared with those from measurements and sophisticated theoretical methods. When the electron correlation and core polarization effects are accounted for adequately our novel approach is able to assess the importance of relativity on the calculation of the EAs of atoms and determine the accurate binding energies of low-lying excited anionic states.

When our EAs for these atoms are compared with those from measurements and sophisticated relativistic calculations, it is concluded that relativity contributes less than about 3.6% to the calculation of their EAs, even in the heavy At atom [1, 2]. This is consistent with our conclusion from nanoscale catalysis using the Au⁻ anion [3], where relativistic effects were found to contribute less than 2.3%.

II. Photon Interactions with Atoms and Fullerenes

II.1 Lorentz-bubble potential for C_{60} and photoionization of $H@C_{60}$

The experimental discovery of confinement resonances in the photoionization of the $4d$ subshell of Xe atom in molecular $Xe@C_{60}^+$ [4] stimulated a number of theoretical investigations, see references in [5]. While some attempted to understand the predicted distortion of the $4d$ giant resonance caused by the confinement resonances, others tried to describe the experimental results by varying the parameters of the phenomenological square well potential. Very recently, Baltenkov et al [5] investigated, within the framework of the Jellium model, the simple model potentials of the C_{60} shell, widely used to describe the interaction of electrons/photons with fullerene-like molecular systems to gain a deeper insight into their physical content. Paper [5] concluded that the phenomenological potentials used to simulate the C_{60} shell should belong to a family of potentials with a non-flat bottom and non-parallel potential walls similar to the Lorentz-bubble potential [6, 7] (see also Ref. [5]); these potentials lead to unphysical charge densities.

The parameters of the Lorentz-bubble potential (depth and thickness) have been determined such that in the potential well an electronic level exists with the experimental EA of the C_{60} molecule. The Lorentz-bubble potential has been used very recently to investigate the photoionization cross sections of $H@C_{60}$ [5]. The resultant confinement resonances in the cross sections were found to be essentially the same as those obtained within the framework of the potential wells with well-defined borders (parallel walls). The paper [5] concluded that the inherent characteristic distances of the potential are not necessary to produce confinement resonances in atoms or molecules confined in near-spherical fullerenes.

II.2 Existence of the C_{60}^{2-} anion and its photodetachment cross sections

II.2.1 Existence of the C_{60}^{2-} anion

The existence of the endohedral anions $A@C_{60}^{z-}$, with the charge z varying from 0 through 5, has been investigated, including the photoionization of the atom A inside. Due to the Coulomb repulsion of the extra electrons whose wave functions have the parent atomic nucleus as the center, atomic multiply-charged ions (even for $z=2$) are generally unstable systems with lifetimes of 10^{-6} – 10^{-7} s. Conceivably, under appropriate conditions the existence of multiply-charged anions C_{60}^{z-} could become more favorable.

Here we have begun and continue the investigation of the electronic structure of the negative ion C_{60}^{2-} and preliminary results appear in our paper [6]. The results were obtained within the Dirac- and Lorentz-bubble potential models, using a variational method [6, 7]. The same study concluded that the multiply-charged anions C_{60}^{z-} (with $z=3, 4, 5$) are unlikely to exist in a stable state, but only the $z=2$ and 1 anions are stable.

II.2.2 Photoionization of the C_{60}^{2-} anion

Additional important information on the electronic structure of anions can be obtained by the method of photoelectron spectroscopy. However, a problem with the C_{60}^{2-} anion is whether its ground state is s-state or p-state. This is important in the determination of the parameters of the Lorentz-bubble potential. So, in [6, 7] the photodetachment cross section of the C_{60}^{2-} anion was investigated near the photodetachment thresholds and continues.

Preliminary results indicate the presence of two thresholds, each with the appropriate EA. Due to the Coulomb interaction of the electrons the cross section for the reaction $C_{60}^{2-} + \hbar\omega = C_{60}^- + e$ ($\hbar\omega$ is the photon energy) was found to vanish exponentially for $(\omega - J_1) \rightarrow 0$ ($J_1 = \epsilon_2$ corresponds to the photodetachment energy of the doubly-charged anion). The photodetachment cross section of the singly-charged anion near the threshold of the reaction $C_{60}^- + \hbar\omega = C_{60} + e$ is proportional to $(\omega - J_2)^{3/2}$, consistent with the Wigner threshold law. According to [6] the first detachment energy of the doubly-

charged C_{60}^{2-} anion is $J_1 = 1.061 \text{ eV}$ while $J_2 = 2.65 \text{ eV}$ is the photodetachment energy of the singly-charged anion. Since the $J_1 = 1.061 \text{ eV}$ value depends on the J_2 value, it requires verification.

III. Photoabsorption spectra of Xe atoms encapsulated inside fullerenes

The photoabsorption spectra of Xe atoms encapsulated inside C_{180} and C_{240} have been investigated using the time-dependent density-functional theory (TDDFT) and compared with the result of our short range spherical well [8]. The calculations were performed in the energy region of the Xe 4d giant resonance and assumed the central location of the Xe atom inside the fullerenes. The Xe- C_{180} and Xe- C_{240} binding energies along some high symmetry directions have been evaluated as well. The obtained curves show the possibility of other Xe positions. The main features of the confinement resonances for the Xe atoms inside C_{180} and C_{240} may be predicted by the formula $E(\text{eV}) = 67.55 + (12.25n/2r)^2$, where r is the radius in \AA of the fullerene, n is the integer 2,3,4,5 · · ·, and $E(\text{eV})$ is the location of a confinement peak.

The calculations indicate that if the radius of a fullerene equals an integer (≥ 2) \times the half wave length of the photoelectron, then at this photon energy we may observe a confinement peak. The photoabsorption spectra of Xe atoms encaged inside C_{58} , C_{56} and C_{54} have also been studied. The results demonstrate that, except for the Xe atom inside C_{58} , which has similar confinement resonances as those of the Xe atom inside C_{60} , the Xe atoms inside C_{54} and C_{56} have completely different spectra. It is concluded that the quantum confinement resonances will be destroyed if the shape of the fullerene is deformed significantly from a sphere.

References and some publications acknowledging the DOE grant

- [1] “Core-Polarization and Relativistic Effects in Electron Affinity Calculations for Atoms: A Complex Angular Momentum Investigation”, Z. Felfli and A. Z. Msezane, Phys. Rev. A, Submitted (2015)
- [2] J. Li, Z. Zhao, M. Andersson, X. Zhang, and C. Chen, J. Phys. B **45**, 165004 (2012)
- [3] “Atomic Gold and Palladium Negative-ion Catalysis of Light, Intermediate, and Heavy Water to Corresponding Peroxides”, A. Tesfamichael, K. Suggs, Z. Felfli, X.-Q. Wang and A. Z. Msezane, J. Phys. Chem. C **116**, 18698 (2012)
- [4] A. L. D. Kilcoyne *et al.*, Phys. Rev. Lett. **105**, 213001 (2010)
- [5] “Jellium Model Potentials for the C_{60} Molecule and the Photoionization of Endohedral Atoms, A@C60”, A. S. Baltenkov, S. T. Manson and A. Z. Msezane, J. Phys. B **48**, 185103 (2015).
- [6] A. S. Baltenkov and A. Z. Msezane, *Proceedings of Dynamic Systems and Applications*, **7** (Dynamic Publishers, Atlanta, Georgia, 2015), in press
- [7] “Doubly-charged negative ion of C_{60} ”, A. S. Baltenkov and A. Z. Msezane, ICPEAC, Abstracts TU-047 (2015)
- [8] “Photoabsorption spectra of Xe atoms encapsulated inside fullerenes”, Z. Chen and A. Z. Msezane, Eur. Phys. J. D **69**, 88 (2015)

SOME RESEARCH PUBLICATIONS 2012-2015 (Refereed Physics Journals)

- [1] “Slow electron elastic scattering cross sections for In, Tl, Ga and At atoms”, Z. Felfli, A.Z. Msezane and D. Sokolovski, J. Phys. B **45**, 045201 (2012)
- [2] “Self-intersecting Regge trajectories in multi-channel scattering”, D. Sokolovski, Z. Felfli, A.Z. Msezane, Physics Letters A **376**, 733-736 (2012)
- [3] “Photoabsorption spectrum of the Xe@C60 endohedral fullerene”, Zhifan Chen and Alfred Z. Msezane, Euro. Phys. J. D **66**, 184, (2012)
- [4] “Interference in Molecular Photoionization and Young’s Double-Slit Experiment”, A. S. Baltenkov, U. Becker, S. T. Manson and A. Z. Msezane, J. Phys. B **45**, 035202 (2012)
- [5] “Identification of strongly correlated spin liquid in Herbertsmithite”, V. R. Shaginyan, A. Z. Msezane, K. G. Popov, G. S. Japaridze and V. A. Stephanovich, Euro. Phys. Lett. **97**, 56001 (2012)
- [6] “A Mathematical Model of Negative Molecular Ion”, A. S. Baltenkov, S. T. Manson, and A. Z. Msezane, Proc. Dynamic Systems and Appl. **6** (Dynamic Publishers, Atlanta, Georgia, 2012), pp. 53-57
- [7] “Fine-Structure energy levels, radiative rates and lifetimes in Si-like Nickel”, G. P. Gupta

- and A. Z. Msezane, *Phys. Scripta* **86**, 015303 (2012)
- [8] “Gold anion catalysis of methane to methanol”, A. Z. Msezane, Z. Felfli, A. Tesfamichael, K. Suggs, and X.-Q. Wang, *Gold Bulletin* **45**, Issue 3, pp 127-1357 (2012)
- [9] “Atomic Gold and Palladium Negative Ion-Catalysis of Water to Peroxide: Fundamental Mechanism”, A. Tesfamichael, K. Suggs, Z. Felfli, Xiao-Qian Wang and A. Z. Msezane, *J. Nanoparticles Research* **15**, 1333 (2013)
- [10] “Photoabsorption spectrum of the Sc₃N@C₈₀ molecule”, Zhifan Chen and Alfred Z. Msezane, *J. Phys. B* **45**, 235205 (2012)
- [11] “Nature of the Quantum Critical Point As Disclosed by Extraordinary Behavior of Magnetotransport and the Lorentz Number in the Heavy Fermion Metal YbRh₂Si₂”, V. R. Shaginyan, A. Z. Msezane, K. G. Popov, J. W. Clark, M. V. Zverev and V. A. Khodel, *JETP Letters*. **96**, 397–404 (2012)
- [12] “Effect of C₆₀ giant resonance on the photoabsorption of encaged atoms”, Zhifan Chen and A. Z. Msezane, *Phys. Rev. A* **86**, 063405 (2012)
- [13] “Scaling in dynamic susceptibility of herbertsmithite and heavy-fermion metals”, V. R. Shaginyan, A. Z. Msezane, K.G. Popov and V.A. Khodel, *Physics Letters A* **376**, 2622 (2012)
- [14] “Magnetic field dependence of the residual resistivity of the heavy-fermion metal CeCoIn₅”, V. R. Shaginyan, A. Z. Msezane, K. G. Popov, J. W. Clark, M. V. Zverev, and V. A. Khodel, *Phys. Rev. B* **86**, 085147 (2012)
- [15] “Slow electron scattering from Ag, Pd, Pt, Ru and Y atoms: Search for nanocatalysts”, A. Z. Msezane, Z. Felfli, and D. Sokolovski, *Journal of Physics: Conference Series* **388**, 042002 (2012)
- [16] “Fine-structure energy levels, radiative rates and lifetimes in Fe XIII”, Vikas Tayal, G. P. Gupta, and A. Z. Msezane, *Journal of Physics: Conference Series* **388**, 042012 (2012)
- [17] “Methane Oxidation to Methanol without CO₂ Emission: Catalysis by Atomic Negative Ions”, A. Tesfamichael, K. Suggs, Z. Felfli, and A. Z. Msezane, <http://arxiv.org/abs/1403.0597> (2014)
- [18] “Excitation energies, oscillator strengths and lifetimes in Mg-like Vanadium”, G. P. Gupta and A. Z. Msezane, *Phys. Scr.* **88**, 025301 (2013)
- [19] “Energy levels and radiative rates for transitions in Ti VI”, K M Aggarwal, F P Keenan and A Z Msezane, *Phys. Scr.* **88**, 025302 (2013)
- [20] “Common quantum phase transition in quasicrystals and heavy-fermion metals”, V. R. Shaginyan, A. Z. Msezane, K. G. Popov, G. S. Japaridze, V. A. Khodel, *Phys. Rev. B* **87**, 245122 (2013)
- [21] “Flat Bands and Enigma of Metamagnetic Quantum Critical Regime in Sr₃Ru₂O₇”, V. R. Shaginyan, A. Z. Msezane, K. G. Popov, J. W. Clark, M. V. Zverev, and V. A. Khodel, *Physics Letters A*, Volume **377**, Issue 39, p. 2800-2805 (2013)
- [22] “Photoabsorption spectra of the Ce atom encapsulated inside a C₈₂ fullerene”, Zhifan Chen and A. Z. Msezane, *PHYSICAL REVIEW A* **88**, 043423 (2013)
- [23] “Innershell Photoionization of Atomic Chlorine,” W. C. Stolte, Z. Felfli, R. Guillemin, G. Ohrwall, S.-W. Yu, J. A. Young, D. W. Lindle, T. W. Gorczyca, N. C. Deb, S. T. Manson, A. Hibbert, and A. Z. Msezane, *Phys. Rev. A* **88**, 053425 (2013).
- [24] “Off-center effect on the photoabsorption spectra of encapsulated Xe atoms”, Zhifan Chen and A. Z. Msezane, *Phys. Rev. A* **89**, 025401 (2014)
- [25] “General properties of phase diagrams of heavy-fermion metals”, V.R. Shaginyan, A.Z. Msezane, K.G. Popov, G.S. Japaridze and V.A. Khodel, *EPL (European Phys. Letters)* **106**, 37001 (2014)
- [26] “Near-threshold electron elastic scattering cross sections for Ta, W, Re, Mo, Tc and Rh atoms: Determination of electron affinities and Ramsauer-Townsend minima”, Zineb Felfli, Alfred Msezane, and Dmitri Sokolovski, *Journal of Physics: Conference Series* **488**, 042019 (2014)
- [27] “Heavy fermion spin liquid in herbertsmithite”, V.R. Shaginyan, M.Ya. Amusia, A.Z. Msezane, K.G. Popov, V.A. Stephanovich, *Phys. Lett. A* **379**, 2092-2096 (2015)
- [28] “Nelson Mandela’s Leadership”, A. Z. Msezane and S. K. Mtingwa, *The Back Page-American Physical Society*, <http://www.aps.org/publications/apsnews/201405/backpage.cfm> (2014)
- [29] “Model potentials for a C₆₀ shell.” A. S. Baltakov, S. T. Manson and A. Z Msezane, *Proceedings of Dynamic Systems and Applications* **7** (Dynamic Publishers, Atlanta, Georgia, 2015), in press.

Theory and Simulation of Nonlinear X-ray Spectroscopy of Molecules

Shaul Mukamel

University of California, Irvine, CA 92697

Progress Report September 2015

DOE DE-FG02-04ER15571

Program Scope

Nonlinear X-ray spectroscopy experiments, which use sequences of coherent broadband X-ray pulses, are made possible by new X-ray free electron laser (XFEL) and high harmonic generation (HHG) sources. These techniques provide a unique window into the motions of electrons and nuclei in molecules and materials and novel probes for electron and energy transfer in molecular complexes. This program is aimed at the design of X-ray pulse sequences for probing core and valence electronic excitations, and the development of effective simulation protocols for describing multiple-core excited state energetics and dynamics. Applications are made to time-resolved photoelectron spectroscopy, detecting electronic coherence by multidimensional broadband stimulated x-ray Raman signals, long range electron transfer in metalloproteins, and capturing transient intermediates in bio-catalytic reactions.

Recent Progress

Computational protocols for multiple core excitations in molecules were developed and benchmarked. Several effects associated with the optical response of systems prepared in a nonequilibrium state by impulsive excitations were predicted. The linear response depends on the phase of the electric field even if the initial nonequilibrium state has only populations, no coherences. Initial electronic coherences created by x-ray pulses induce additional phase dependence, and show new resonances in nonlinear wave mixing.

Long-range electron transfer (ET) in proteins is essential in many energy conversion processes and biological redox reactions in living organisms. Conventional time-resolved infrared (IR) and UV-vis spectroscopic techniques cannot pinpoint the electron transfer dynamics due to the inability to prepare and detect localized states. In addition, different ET pathways are difficult to resolve. X-ray spectroscopy has unprecedented spatial and temporal resolution for studying ET. We showed that X-ray pulses can directly probe the evolving oxidation states and the electronic structure around selected atoms with detail via a stimulated Raman process. In a multi-step ET, all units along the ET pathway including the donor, the intermediate bridge and the acceptor, can be selectively detected. This was demonstrated in a simulation study of the stimulated X-ray Raman spectroscopy (SXRS) signals in Re-modified azurin, which serves as a benchmark system for photoinduced ET in proteins. In Fig. 1 we show the signals at different times and the corresponding evolving electron density differences. These signals offer a direct window into the long-range ET mechanism.

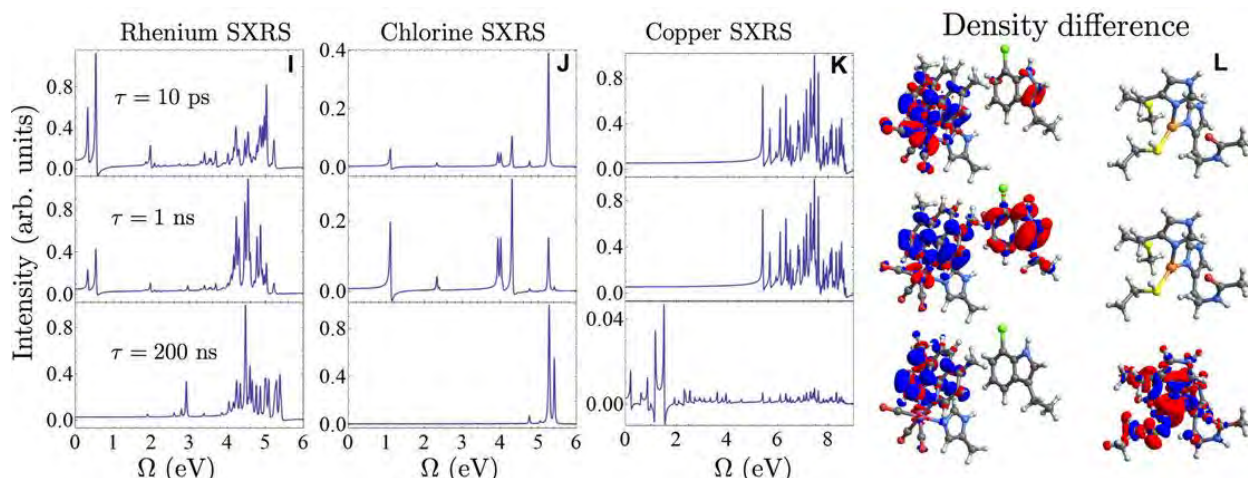


Fig. 1: Time-dependent SXRS signals for Azurin. (I) Time-dependent *Re* L-edge SXRS signals for the three snapshots indicated in the figure. (J) Same as panel I, but for the *Cl* L-edge SXRS signals. (K) Same as panel I, but for the *Cu* L-edge SXRS signals. (L) Three snapshots, with the delay between the initiation and the Raman pulses set to 10 ps, 1 ns, and 200 ns from top to bottom, of the evolving electron density difference of the system (excited state density minus ground state density). Red denotes a negative sign (hole) and blue denotes a positive sign (electron). Rhenium is in pink, chlorine is in green, copper is in orange, nitrogen is in blue, oxygen is in red, carbon is in gray, and hydrogen is in white. [P2]

Cytochrome P450 enzymes (CYPs) are important biocatalysts. They oxidize the chemically inert C-H bonds and account for most of the drug metabolism. The key reaction intermediates in the CYP catalytic cycle are not completely understood. The most important reaction intermediates are P450 Compound I (Cpd-I) and II (Cpd-II). We simulated X-ray spectroscopy signals including X-ray absorption near-edge structure (XANES), resonant inelastic X-ray scattering (RIXS), and stimulated X-ray Raman spectroscopy (SXRS) of the low- and high-spin states of Cpd-I and II. Characteristic peak patterns are found and connected to the corresponding electronic structures, as shown in Fig. 2. Two-color SXRS, can help identify transient species along the CYP catalytic reaction path.

Future Plans

Non-stationary molecular states which contain electronic coherences can be impulsively created and manipulated by using ultrashort X-ray pulses via photoexcitation, photoionization and Auger processes. Stimulated-Raman detection schemes that can monitor the phase-sensitive electronic and nuclear dynamics will be explored.

More accurate simulation protocols for multiple core excitations will be developed and pulse shaping coherent control schemes for x-ray pulses including frequency combs will be explored to optimize the signals. Applications will be made to detecting electronic coherence by multidimensional broadband stimulated x-ray Raman signals.

We will continue to explore the application of X-ray pulses to probe electron transfer. Manipulating ET through external factors has many potential applications to solar cells. In a

donor/bridge/acceptor scheme we propose to move electrons between the bridge valence orbitals through an X-ray Raman process, in order to facilitate the electron flow from the donor to the bridge, or from the bridge to the acceptor. The resulting ET dynamics can be detected by other X-ray pulses. Compared to IR or UV-vis pulses, X-ray pulses can selectively excite different units in a ET system. Core excitations induced by X-ray pulses significantly affect the local electronic structures and lead to large effects. Model systems will be studied for illustrating the principles and real molecular systems will be explored for applications.

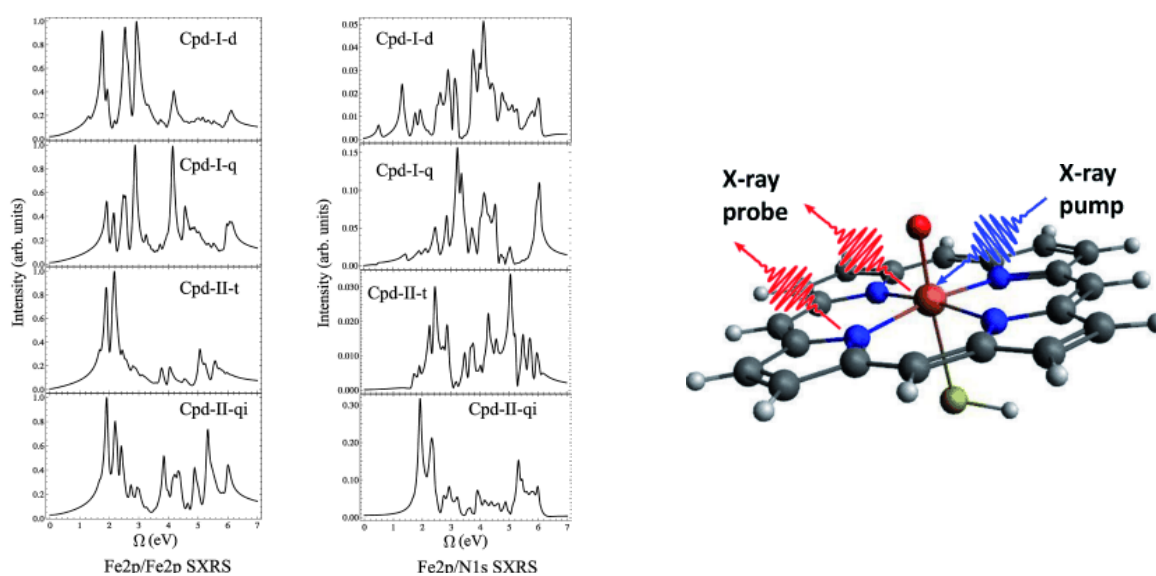


Fig. 2: Modulus one-color ($Fe2p$ pump and $Fe2p$ probe, $Fe2p/Fe2p$), and two-color ($Fe2p$ pump and $N1s$ probe, $Fe2p/N1s$) I²P-SXRS signals of the four studied species, obtained at iron core excitation edges of 698.913, 698.906, 698.387, and 696.630 eV for Cpd-I-d, Cpd-I-q, Cpd-II-t, and Cpd-II-qi, respectively. The scheme in the right illustrate the spectroscopic technique. The molecular model of CYP is shown in the right panel.[P8]

Publications Resulting from the Project

- P1. "Three-Dimensional Attosecond Resonant Stimulated X-Ray Raman Spectroscopy of Electronic Excitations in Core-ionized Glycine", Y. Zhang, J.D. Biggs, W. Hua, K.E. Dorfman, and S. Mukamel. *PCCP*, 16,24323-24331 DOI: 10.1039/C4CP03361B (2014)
- P2. "Monitoring Long-range Electron Transfer in Proteins by Stimulated Broadband X-Ray Raman Spectroscopy", Yu Zhang, J.D. Biggs, Niri Govind, and Shaul Mukamel. *JPC Lett*, 5, 3656-3661 (2014)
- P3. "Probing Chirality Fluctuations in Molecules by Nonlinear Optical Spectroscopy", N. Mann, P. Nalbach, S. Mukamel, and M. Thorwart. *JCP*, 141, 234305 (2014)

- P4. "Evaluation of Optical Probe Signals from Nonequilibrium Systems", B. K. Agarwalla, K.E. Dorfman, and S. Mukamel. *PRA*, 91, 052501(2015)
- P5. "Nonlinear Spectroscopy of Core and Valence Excitations Using Short X-ray Pulses: Simulation Challenges", Y. Zhang, W. Hua, K. Bennett, and S. Mukamel. *Topics in Current Chemistry*, 2015, DOI: 10.1007/128_2014_618
- P6. "Nonlinear fluctuations and dissipation in matter revealed by quantum light", S. Mukamel and K.E. Dorfman. *Phys. Rev. A* 91, 053844 (2015) DOI: 10.1103/PhysRevA.91.053844
- P7. "Energy flow between of spectral components in 2D Broadband Stimulated Raman Spectroscopy", G. Batignani, G. Fumero, S. Mukamel, and T. Scopigno. *Physical Chemistry Chemical Physics*, 2015, DOI: 10.1039/C4CP05361C
- P8. "Characterizing the Compound I and II Intermediates in the Cytochrome P450 Catalytic Cycle with Nonlinear X-ray Spectroscopy: A Simulation Study", Yu Zhang, Jason D. Biggs, and Shaul Mukamel. *Chem Phys Chem* (2015) DOI: 10.1002/cphc.201500064
- P9. "Multidimensional Characterization of Stochastic Dynamical Systems Based on Multiple Perturbations and Measurements", Maksym Kryvohuz and Shaul Mukamel. *Journal of Chemical Physics*, 142, 212430 (2015); doi: 10.1063/1.4917527
- P10. "Detecting Modes of Electronic Coherence in Multidimensional Broadband Stimulated X-ray Raman Signals; A Comparative Study", Konstantin E. Dorfman, Kochise Bennett, and Shaul Mukamel. *PRA* (Accepted, 2015)

Revealing Nanoscale Energy Flow Using Ultrafast THz to X-ray Beams

Keith A. Nelson
Department of Chemistry
Massachusetts Institute of Technology
Cambridge, MA 02139
Email: kanelson@mit.edu

Margaret M. Murnane
JILA
University of Colorado and National Institutes of Technology
Boulder, CO 80309
E-mail: murnane@jila.colorado.edu

Program Scope

We are developing novel spectroscopic methods and making use of them to study energy flow on nanometer length scales and ultrafast time scales. Access to short length scales is provided through the use of light beams with short wavelengths (EUV through hard x-ray spectral ranges) and/or fabricated structural elements with nanometer dimensions. Recent advances in tabletop high harmonic generation of extreme ultraviolet (EUV) pulses are exploited to measure thermal transport and acoustic vibrations using time-resolved diffraction from photoexcited periodic nanostructures, revealing new physics that arises at length scales of tens to hundreds of nm. A key further step is to employ coherent diffractive imaging to make possible detailed visualization of thermoelastic responses from a single heated nanostructure or an irregular nanostructural pattern. Even shorter (x-ray) wavelengths from free-electron laser (FEL) facilities at the Stanford Linear Accelerator (SLAC) and ELETTRA in Trieste will be used to detect thermoelastic responses of materials on the shortest length scales. The tabletop EUV sources and the ELETTRA FEL soft x-ray pulses will also be used to generate as well as measure nanoscale thermoelastic responses without the need for patterned nanostructures, with the short length scale coming from optical interference patterns formed by crossing pairs of beams in transient grating experiments. Finally, we will use light at optical and terahertz frequencies to excite and monitor ultrahigh-frequency acoustic waves at ultraflat interfaces and multilayer structures, extending our recent measurements of the highest-frequency coherent acoustic waves observed to date. Our measurements of acoustic properties will allow direct calculation of thermal conductivities which will be compared with our measurements of thermal transport and with first-principles calculations. Terahertz-frequency acoustic measurements will also be used to reveal complex relaxation dynamics in glass-forming liquids and partially disordered solids. The methods we develop have broad fundamental applications and may also enable new practical metrology for use in nanoelectronics, just as earlier methods we developed have found commercial applications in microelectronics metrology.

Recent Progress

First Experimental Phonon Mean Free Path Spectroscopy Capability

In recent work we demonstrated the only experimental approach for phonon mean free path (MFP) spectroscopy that allows us to extract differential conductivity as a function of phonon mean free path in materials [1,2]. In our experiment, arrays of nickel nanowires were heated by an ultrafast laser and their expansion and cooling was then probed using EUV high harmonic probe beams. The nanogratings were fabricated by LNBL on the surface of sapphire and silicon substrates. The nanowire linewidths L range from 750 nm down to 30 nm, with period $P = 4L$ and a rectangular profile height of ~ 13.5 nm. The use of nano-patterned structures rather than optical absorption allows us to explore the dynamics of heat sources much smaller than the diffraction limit of visible light. Moreover, because the linewidth and period set the location and width of an effective notch filter in the phonon MFP spectrum, each grating structure uniquely samples the contribution to thermal conductivity of different MFP ranges of phonon modes, with a resolution controlled primarily by the number of configurations tested. The larger the resistivity

correction needed for a given nano-grating, the stronger the conductivity contribution of phonon modes which were suppressed.

Although the number of experimental data points (gratings) limits our resolution, we can still see in Fig. 1 that for sapphire, both calculations and experimental data imply that phonons with MFPs shorter than 1 μm are responsible for > 95% of the thermal conductivity, so the cumulative thermal conductivity curves approach unity at 1 μm . For silicon, our data are consistent with large contributions from longer MFPs.

There are two significant advantages of our EUV-based technique compared with previously reported MFP spectroscopy techniques. First, our approach that combines nano-heaters with the phase sensitivity of short-wavelength provides a way to experimentally access dimensions far below 100 nm in order to directly resolve the contributions of phonons with MFP down to 14 nm. Other spectroscopic approaches for samples with macroscopic dimensions such as our substrates require numerical extrapolation techniques and interpretation, which are still being developed. Second, we can probe arbitrary segments of the MFP spectrum for any novel material, even where predictions do not yet exist.

Extracting Nanoscale Mechanical Properties

In other work, our team used the same setup to extend photoacoustic spectroscopy into the extreme ultraviolet (EUV) region [2-5]. Using the setup to measure the characteristic longitudinal and surface acoustic waves from which longitudinal and transverse acoustic velocities can be determined, we can extract the Young's modulus and Poisson ratio (and the full elastic tensor) of ~ 10 -100 nm dielectric thin films, that cannot be accessed using other approaches. As shown in Fig. 2, we observed a deviation from the expected macroscale elastic behavior in very soft films that is likely due to their growth method.

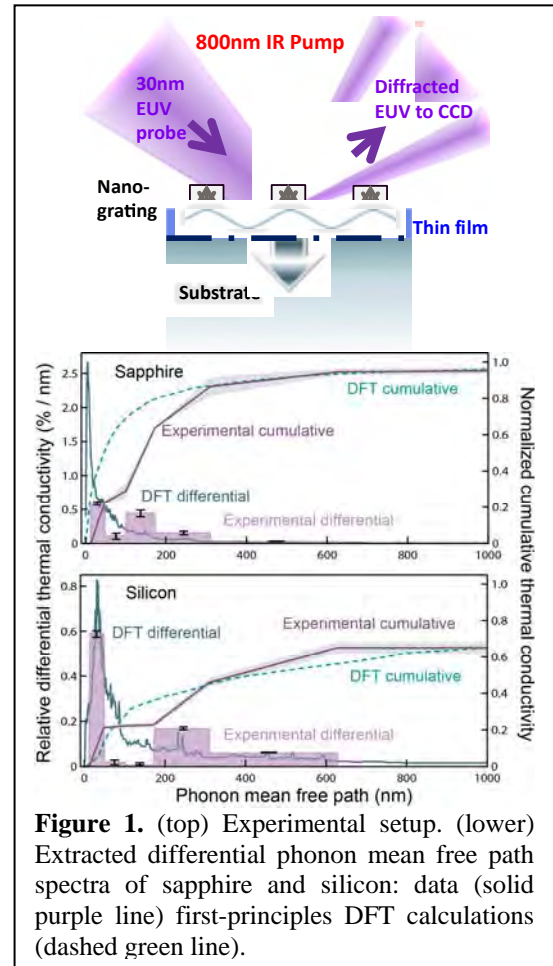
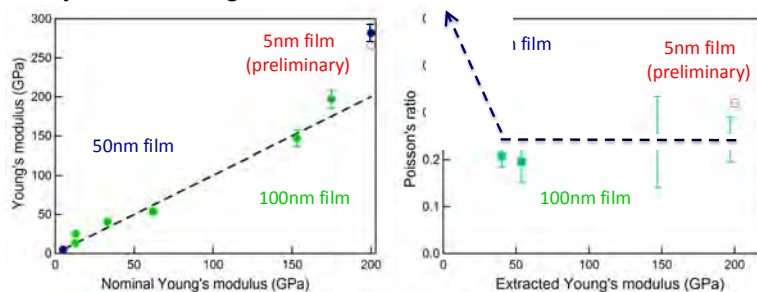


Figure 1. (top) Experimental setup. (lower) Extracted differential phonon mean free path spectra of sapphire and silicon: data (solid purple line) first-principles DFT calculations (dashed green line).

Figure 2. (left) First measurements of the Young's modulus and Poisson ratio of very thin 10 – 100 nm soft and stiff low-k dielectric SiC:H films, where the Young's modulus was adjusted by varying the extent of hydrogenation. (right) For very soft thin films, the Poisson's ratio deviates dramatically from the macroscale expectation of constant values.

Optical measurements of THz acoustic waves

Recently we demonstrated optical generation of the highest-frequency coherent acoustic phonons ever observed, up to 2.5 THz [6]. Since then we have moved from the “demonstration” phase to measurement of THz phonon mean free paths and acoustic spectroscopy nanometer structural features, moving well beyond our earlier GHz results [7,8]. We have used InGaN/GaN superlattice (SL) structures whose differential absorption of a femtosecond pump pulse leads to spatially periodic excitation and generation of acoustic waves with wavelengths (and corresponding frequencies) given by the SL periods. We

measure the acoustic waves in the SLs (through acoustically modulated SL absorption of probe light) initially upon generation and, in some cases, after propagation in an adjacent region of bulk GaN. Figure 3 shows a schematic illustration of acoustic wave generation in a 25-period SL, propagation through 150 nm of GaN to a free surface, reflection from the interface, and propagation back to the SL. The data are from measurements made initially (at times $t = 0-20$ ps, with signal diminishing as the acoustic wave leaves the SL) and after acoustic wave return to the SL (35-75 ps as the acoustic wave returns to and passes through the SL). The measurement allows assessment of the interface specularity, a property that is important in nanostructure thermal transport as well as acoustic wave behavior. The acoustic frequencies are centered at ~ 1.0 THz, which corresponds to an acoustic wavelength of 8.0 nm (the SL period). For such short wavelengths, surface roughness on the order of 1 nm leads to significant scattering and dephasing, reducing the coherent acoustic amplitude and bandwidth after reflection.

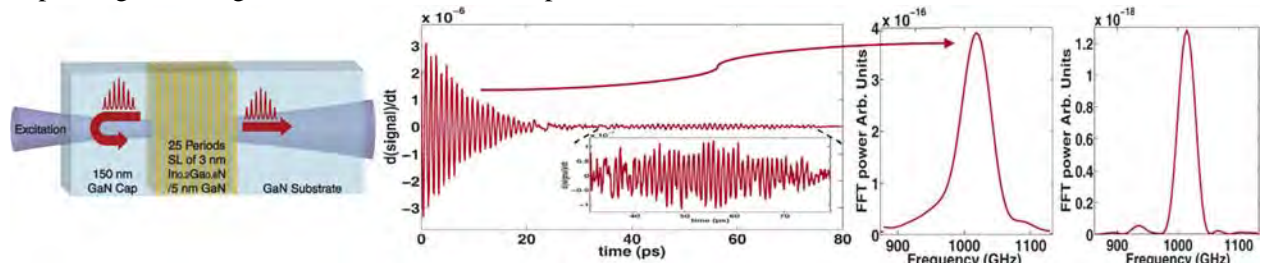


Figure 3. Measurement of surface specularity through reflection of an acoustic wave with 8-nm wavelength.

Figure 4 shows measurements from within two 100-period SL structures whose SEM images reveal very different degrees of interface roughness. The very different acoustic dephasing times of ~ 30 ps and 5 ps demonstrate that the measurement provides a simple, noncontact optical diagnostic for SL quality, with potential applications in assessment of periodic nanostructures in electronics as well as thermoelectrics and other areas in which thermal transport plays an important role.

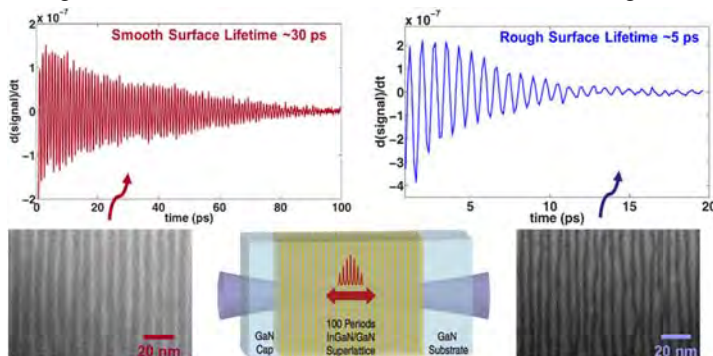


Figure 4. SEM images and acoustic wave data from SL structures of different quality.

Figure 5 shows data recorded from acoustic waves upon their generation initially in a pair of SL structures and again after their propagation through a GaN layer and arrival at the opposite SLs. The measurements are continuing with various GaN thicknesses in order to determine phonon mean free paths at frequencies (to date) up to 1.4 THz. The results will allow incisive comparison to thermal transport data from which phonon mean free path distributions are inferred as discussed above. Similar measurements will permit assessment of the nature and extent of disorder in glasses and partially disordered crystals, and may allow study of viscoelastic behavior beyond the 200 GHz range that we reached previously [9].

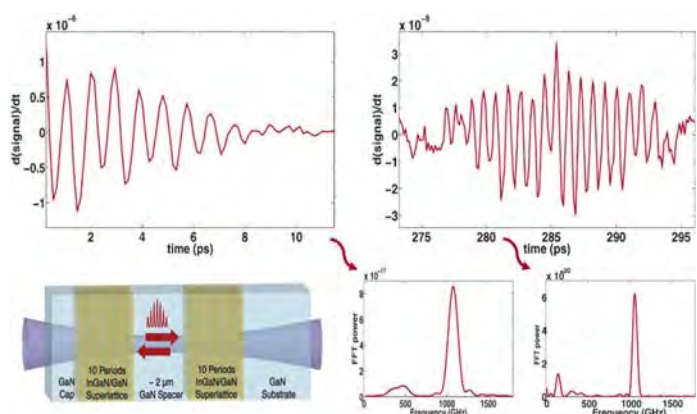


Figure 5. Acoustic waves measured upon generation (0-10 ps) in each of two SL structures and in the same two SL structures (275-295 ps) after traversal across an intermediate 2.0 μm thick GaN layer.

Nonlinear GHz-frequency viscoelasticity

We have measured amplitude-dependent velocities of 20-GHz acoustic waves in both glassy and viscous liquid states of the organic glass former tetramethyl-tetraphenyl-trisiloxane (trade name DC704) [10]. The nonlinear acoustic behavior informs us about the dynamics of excursions farther from local equilibrium than those that we have probed earlier [ref] in the linear response regime. Large-amplitude local structural rearrangements play key roles in liquid flow and other phenomena of central interest. The nonlinearity was constant at temperatures below T_g , the glass transition temperature, but increased monotonically at $T > T_g$. This cannot be explained by linear relaxation dynamics which show no T -dependent 20-GHz features because they are on time scales of seconds, not picoseconds, near T_g ! We believe the nonlinearity indicates far faster motions that become possible once local intermolecular geometries are disrupted.

Future Plans

We are further refining our capabilities for direct measurement of nanoscale thermal transport and the acoustic phonon mean free paths that mediate it as well as nanoscale mechanical properties and high-frequency viscoelastic behavior. The same efforts will continue to demonstrate potential applications of our novel measurement methods in nanoscale thermal management and noncontact characterization of nanostructures. Several additional experimental components are planned. These include coherent diffraction imaging of nanoscale thermoelastic responses using tabletop high harmonic generation; EUV transient grating measurements, with beamtime scheduled at ELETTRA; and diffuse x-ray scattering from squeezed high-wavevector acoustic phonons, in collaboration with Stanford Professor David Reis who pioneered the technique, with beamtime scheduled at the LCLS.

References and Selected Additional Publications (all from DOE AMOS Support)

1. K.M. Hoogeboom-Pot, J.N. Hernandez-Charpak, T. Frazer, E.H. Anderson, W. Chao, R. Falcone, X. Gu, R. Yang, M.M. Murnane, H.C. Kapteyn, D. Nardi, "A new regime of nanoscale thermal transport: collective diffusion increases dissipation efficiency", *PNAS* **112**, 4846 (2015).
2. K. Hoogeboom-Pot, J. Hernandez-Charpak, T. Frazer, X. Gu, E. Turgut, E. Anderson, W. Chao, J. Shaw, R. Yang, M. Murnane, H. Kapteyn, M. Nardi, "Mechanical and thermal properties of nanomaterials at sub-50nm dimensions characterized using coherent EUV beams", *SPIE Advanced Lithography* **9424**, 942417-1 (2015).
3. D. Nardi, M. Travagliati, M. Murnane, Member, H. Kapteyn, G. Ferrini, C. Giannetti, F. Banfi, "Impulsively Excited Surface Phononic Crystals: a Route towards Novel Sensing Schemes", *IEEE Sensors Journal* **15**, 5142 (2015).
4. Q. Li, K. Hoogeboom-Pot, D. Nardi, M. Murnane, H. Kapteyn, M. Siemens, E. Anderson, O. Hellwig, B. Gurney, R. Yang, K. Nelson, "Generation and Control of Ultrashort-Wavelength 2D Surface Acoustic Waves at Nano-interfaces", *Physical Review B* **85**, 195431 (2012).
5. D. Nardi, K. Hoogeboom-Pot, J. Hernandez-Charpak, M. Tripp, S. King, E. Anderson, M. Murnane, H. Kapteyn, "Probing limits of acoustic nanometrology using coherent extreme ultraviolet light", *SPIE Advanced Lithography* **8681**, 86810N (2013).
6. A.A. Maznev, K.J. Manke, K.-H. Lin, K.A. Nelson, C.-K. Sun, and J.-I. Chyi, "Broadband terahertz ultrasonic transducer based on a laser-driven piezoelectric semiconductor superlattice," *Ultrasonics* **52**, 1-4 (2012).
7. A.A. Maznev et al., "Lifetime of sub-THz coherent acoustic phonons in a GaAs-AlAs superlattice", *Appl. Phys. Lett.* **102**, 041901 (2013).
8. F. Hofmann et al., "Intrinsic to extrinsic phonon lifetime transition in a GaAs-AlAs superlattice", *J. Phys.: Condens. Matter* **25**, 295401 (2013).
9. C. Klieber et al., "Mechanical spectra of glass-forming liquids. II. Gigahertz-frequency longitudinal and shear acoustic dynamics in glycerol and DC704 studied by time-domain Brillouin scattering," *J. Chem. Phys.* **138**, 12A544-1-12 (2013).
10. C. Klieber, V.E. Gusev, T. Pezeril, and K.A. Nelson, "Nonlinear acoustics at GHz frequencies in a viscoelastic fragile glass former," *Phys. Rev. Lett.* **114**, 065701 1-5 (2015).

2015 Abstract for Program: DOE-FG02-02ER15337
“Low-Energy Electron Interactions with Complex Molecules and Biological Targets”

Thomas M. Orlando

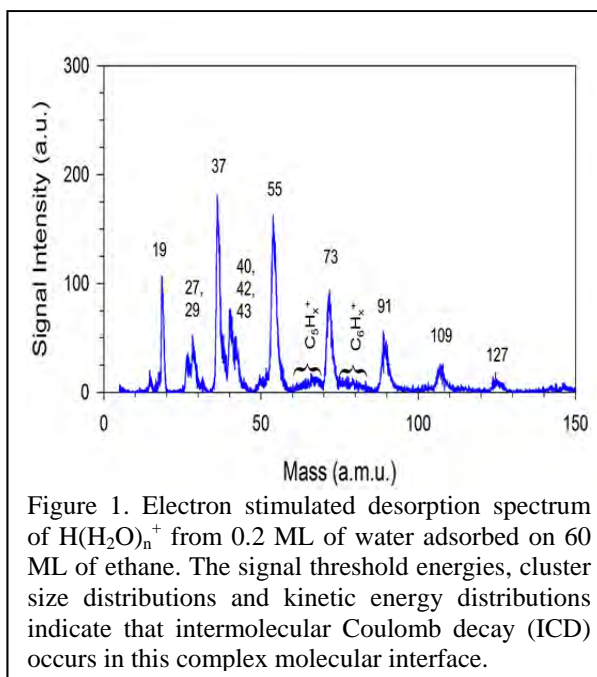
School of Chemistry and Biochemistry and School of Physics,
Georgia Institute of Technology, Atlanta, GA 30332-0400
Thomas.Orlando@chemistry.gatech.edu, Phone: (404) 894-4012, FAX: (404) 894-7452

Project Scope: The primary objectives of this program are to investigate the fundamental physics and chemistry involved in low-energy (1-250 eV) electron and soft x-ray interactions with complex targets. There is a particular emphasis on understanding correlated electron interactions and energy exchange in the deep valence and shallow core regions of the collision targets. The energy loss channels associated with these types of excitations involve ionization/hole exchange and negative ion resonances. Thus, the energy decay pathways are extremely sensitive to many body interactions and changes in local potentials. Our proposed investigations should help determine the roles of hole exchange via inter-atomic and intermolecular Coulomb decay (ICD) and energy exchange via localized shape and Feshbach resonances in the non-thermal damage of biological interfaces.

Recent Progress: We have carried out limited work on several tasks during the past year. The first task focused on intermolecular coulomb decay (ICD) at weakly interacting interfaces. The second examined low-energy electron induced damage of DNA and RNA nucleotides adsorbed on graphene. The third extended this study and probed the role of secondary electrons and substrate interactions in x-ray induced DNA and RNA nucleotide damage.

Task 1. Investigating ICD at weakly interacting molecular interfaces.

We have carried out preliminary studies which indicate that ICD may occur in complex molecular systems containing water clusters adsorbed on multilayers of ethane. As can be seen in Figure 1, the water cluster yield (0.2 ML of water adsorbed onto 60 ML of C_2H_6) is high and co-incident with the formation and release of $C_2H_5^+$ and probably $C_3H_5^+$. The water interaction with this hydrophobic surface will lead to the deposition/growth of small water clusters typically seen on rare gas layers. As shown previously, water cluster ions can be ejected by Coulomb explosions resulting from ICD; especially in the inner valence ionization energy range. The preliminary threshold energy (~ 30 eV) and kinetic energy measurements (~ 2 eV) are consistent with ICD. The water cluster ion yield is also greatly enhanced for coverages < 0.5 ML, as expected and previously observed for ICD on rare gas substrates.



Project 2. Low-energy electron induced damage of DNA and RNA nucleotides on a novel graphene platform

We have examined the low-energy electron (LEE) induced damage of DNA and more recently several nucleotides using a novel graphene-platform and Raman micro-spectroscopy approach. The single stranded DNA was shown to undergo significant damage due to the capture of electrons into primarily π^* shape resonances initially localized on the bases. Adsorption on p-doped graphene can also lead to direct capture in phosphate σ^* -type levels. Though similar processes are expected for isolated nucleotides based on gas-phase studies of the constituent sugars and bases, we only observe limited damage of the RNA constituent nucleotides following < 5 eV electron bombardment. However, significant LEE-induced damage of DNA nucleotides such as deoxyadenosine monophosphate (dAMP) occurs after bombardment of only 2 eV electrons. The much higher stability of the RNA nucleotide adenosine monophosphate (AMP) is correlated with a change in the electronic structure associated with the simple addition of an $-OH$ group to the 2'-C site on the sugar. This dramatically changes the attachment energies and lifetimes of the transient negative ion resonances. The DNA nucleotides have lifetimes long enough to allow base damage and glycosidic bond cleavage at energies < 2 eV. This is not the case for the RNA nucleotides. The general radiation stability of important RNA sub-units relative to those in DNA is consistent with an RNA or RNA-like polymer based origin of life hypothesis.

Project 3. X-ray induced damage of DNA and RNA nucleotides.

Our collaboration at Argonne National Laboratory has recently focused on examining secondary electron induced damage of DNA and RNA nucleotides using tunable x-rays. Specifically, we are examining the cross sections and rates of low-energy electron damage of dAMP and rAMP as well as dTMP and rUMP. Time dependent photoemission from C, O and P core levels are directly compared to damage measured by Raman microspectroscopy.

Future Plans.

We are particularly interested in extending our initial ICD studies to water clusters adsorbed on other weakly coupled molecular solids such as ethane (C_2H_6), acetylene (C_2H_2), and formaldehyde (HCHO). This series span the regime of essentially no coupling (C_2H_6), to weak π -interactions (C_2H_2), and hydrogen bonding (HCHO). HCHO can also be considered a building block for more complicated biomolecules and has hydrogen bonding interactions expected in biochemical systems.

We will continue LEE-induced damage studies of nucleotides using the graphene platform and Raman microspectroscopy. Nucleotides we plan to study include but are not limited to, deoxycytidine monophosphate (dCMP), cytidine monophosphate (rCMP), deoxythymidine monophosphate (dTMP), thymidine monophosphate (rTMP), deoxyuridine monophosphate (dUMP) and uridine monophosphate (rUMP). The damage probability will be studied as a function of incident electron energy, total electron dose and base identity.

Publications acknowledging support from this program

1. E. Alizadeh, T. M. Orlando and L. Sanche, "Biomolecular damage induced by ionizing radiation; The direct and indirect effects of low-energy electrons on DNA", *Ann. Rev. of Phys. Chem.* 66, 379-98 (2015).
2. R. A. Rosenberg, J. M. Symonds, V. Kalyanaraman, T.Z. Markus, T. M. Orlando and R. Naaman, "The relationship between interfacial bonding and radiation damage in adsorbed DNA", *Phys. Chem. Chem. Phys.* 2014, Advance Article DOI: 10.1039/C4CP01649A (2014).
3. R. Rosenberg, J. M. Symonds, T. Z. Markus, T. M. Orlando and R. Naaman, "The lack of spin selectivity in low-energy electron induced damage of DNA films", *J. Phys. Chem. C*. doi: 10.1021/jp402387y (2013).
4. A. N. Sidorov and T. M. Orlando, "Monolayer graphene platform for the study of DNA damage by low-energy electron irradiation", *J. Phys. Chem. Lett.*, 4 (14), 2328–2333 (2013).
5. A. N. Sidorov and T. M. Orlando, "Shape resonance induced damage of dAMP and rAMP", *in prep, Phys. Rev. Lett.*

Presentations acknowledging support from this program

1. T. M. Orlando, "Low energy (<5 eV) electron interactions with DNA and RNA nucleotides", XIX International symposium on electron-molecule collisions and swarms", July 17-20, 2015.
2. T. M. Orlando, "Very low energy electron-induced damage of DNA", Dept. of Physics, Auburn University, March 21, 2015.
3. T. M. Orlando, "Very low energy electron-induced damage of DNA", Dept. of Physics, University of Georgia, March 21, 2014.
4. T. M. Orlando, "Very low energy electron-induced damage of DNA", CUNY, Dec. 6, 2013.
5. T. M. Orlando, "A monolayer graphene: Au surface enhanced Raman micro-spectroscopy platform for DNA damage studies", SERMACS, Atlanta, GA Nov. 13, 2013.
6. T. M. Orlando, "Very low energy electron-induced damage of DNA", Dept. of Physics, Vanderbilt University, Jan. 31, 2013.

Page is intentionally blank.

Structure from Fleeting Illumination of Faint Spinning Objects in Flight

A. Ourmazd*

Dept. of Physics, University of Wisconsin Milwaukee, 3135 N. Maryland Ave,
Milwaukee, WI 53211
Ourmazd@uwm.edu

There is an urgent need for new data-analytical approaches capable of efficiently extracting reliable information from XFEL datasets in the presence of sample heterogeneity and timing uncertainty. We have developed and validated a powerful algorithmic platform for determining conformational heterogeneity, ensemble kinetics, energy landscapes, and dynamics beyond the limits set by these effects.

1. Conformations, molecular movies, and energy landscapes of nanomachines

Many functions in the cell are performed by Brownian machines, macromolecular assemblies that use energy from the thermal environment in their work cycles. We have developed a new approach capable of mapping the motions of such nanomachines along their trajectories in the free-energy landscape (*I*). The input data consist of cryo-EM snapshots of randomly oriented machines without timing information or use of templates. Application to experimental snapshots of yeast ribosome reveals a closed pathway corresponding to the elongation cycle. Our approach constitutes a universal platform for the analysis of free-energy landscapes and conformational motions of nanomachines, and their dependencies on temperature, buffer conditions, and regulatory factors. The application of this approach to other important nanomachines is underway.

2. Accurate dynamics from data with extreme timing uncertainty

Imperfect knowledge of the time-points at which “snapshots” of a system were recorded often degrades our ability to recover dynamical information, and can even scramble the sequence of events. In X-ray Free Electron Lasers (XFELs), for example, the uncertainty – the so-called timing jitter – between the arrival of an optical pump pulse and a probing X-ray pulse can exceed the X-ray pulse-length by up to two orders of magnitude (2), thus marring the otherwise exquisite time-resolution capabilities of this powerful class of instruments. The widespread notion that little information is available on timescales significantly shorter than the timing uncertainty has spawned a variety of elaborate hardware schemes to reduce timing uncertainty [see, e.g., (3-5)]. These schemes are expensive, tend to be specific to one experimental approach, and cannot be employed when the record was created under ill-defined or uncontrolled conditions, as, for example, in geological or cosmological events. We have developed a purely data-analytical approach (6) based on machine-learning (7-9), which is capable of recovering accurate histories and dynamics from noisy snapshots recorded at extremely uncertain time points. We have demonstrated the power of this approach by extracting novel dynamical information on the few-femtosecond timescale from noisy experimental XFEL data recorded with 300 fs timing uncertainty (2). This capability far exceeds what was

* In collaboration with: A. Dashti, R. Fung, A. Hosseinizadeh, P. Schwander (Univ. of Wisconsin, Milwaukee), S. Ramakrishna, T. Seideman (Northwestern University), R. Santra (CFEL, and the University of Hamburg, Germany), and the Single-Particle Initiative (SPI Collaboration, LCLS, SLAC).

previously thought possible, with potentially wide impact whenever dynamical or historical information is tainted by timing uncertainty. We plan to exploit this capability to study ultrafast dynamics on the single-femtosecond timescale in the first instance.

3. Single-particle Initiative

In 1970, Breedlove and Trammel (10), and later Solem and Baldwin (11) suggested that the problem of radiation damage in structural biology might be solved by destroying the sample with a short pulse of intense radiation, because a few photons should be scattered before the onset of radiation damage. Backed by simulations, the proposal was revived in the year 2000 (12) to use ultrashort, intense pulses of X-rays generated by X-ray Free Electron Lasers to determine the structure of biological molecules without the need for crystals. Although algorithmic solutions for three-dimensional (3D) structure recovery emerged quickly (13-17), the experimental road has proved arduous, yielding only a limited number of three-dimensional structures (18, 19), often at resolutions comparable with optical methods. The daunting experimental challenges (20) resulted in the formation of an international collaboration led by the LCLS, designed to tackle the experimental and algorithmic challenges in a systematic fashion (21). The group of this PI has been an active participant in this collaboration, with strong representation at both experimental beamtimes in 2015 and the subsequent data analysis effort. Progress has been gratifying, but many experimental and algorithmic challenges remain.

References

1. A. Dashti *et al.*, *Proc Natl Acad Sci U S A* **111**, 17492 (2014).
2. J. M. Glowacki *et al.*, *Optics Express* **18**, 17620 (2010).
3. C. Gahl *et al.*, *Nature Photonics* **2**, 165 (2008).
4. F. Lohl *et al.*, *Physical review letters* **104**, 144801 (2010).
5. M. Harmand *et al.*, *Nature Photonics* **7**, 215 (2013).
6. R. Fung, S. Ramakrishna, T. Seideman, R. Santra, A. Ourmazd, *Submitted*, (2015).
7. R. R. Coifman *et al.*, *Proc Natl Acad Sci U S A* **102**, 7426 (2005).
8. D. Giannakis, A. J. Majda, *Proc Natl Acad Sci U S A* **109**, 2222 (2012).
9. T. Berry, R. Cressman, Z. Greguric-Ferencek, T. Sauer, *SIAM J Dynamic Systems* **12**, 618 (2013).
10. J. R. Breedlove, G. T. Trammell, *Science* **170**, 1310 (1970).
11. J. C. Solem, G. C. Baldwin, *Science* **218**, 229 (1982).
12. R. Neutze, R. Wouts, D. van der Spoel, E. Weckert, J. Hajdu, *Nature* **406**, 752 (2000).
13. R. Fung, V. Shneerson, D. K. Saldin, A. Ourmazd, *Nature Physics* **5**, 64 (2009).
14. N. T. Loh, V. Elser, *Phys Rev E* **80**, 026705 (2009).
15. B. Moths, A. Ourmazd, *Acta Cryst A* **67**, 481 (2011).
16. D. Giannakis, P. Schwander, A. Ourmazd, *Optics Express* **20**, 12799 (2012).
17. P. Schwander, D. Giannakis, C. H. Yoon, A. Ourmazd, *Optics Express* **20**, 12827 (2012).
18. R. Xu *et al.*, *Nature Communications* **5**, 4061 (2014).
19. T. Ekeberg *et al.*, *Phys Rev Lett* **114**, 098102 (2015).

20. A. Hosseinizadeh, A. Dashti, P. Schwander, R. Fung, A. Ourmazd, *Structural Dynamics* **2**, 041601 (2015).
21. A. Aquila *et al.*, *Structural Dynamics* **2**, 041701 (2015).

Publications from DoE sponsored research over the past three years:

1. D. Giannakis, P. Schwander, and A. Ourmazd, Symmetries of image formation: I. Theoretical framework, *Optics Express* **20**, 12799 (2012).
2. P. Schwander, D. Giannakis, C.H. Yoon, and A. Ourmazd, Symmetries of image formation: II. Applications, *Optics Express* **20**, 12827 (2012).
3. J.M. Glowacki, A. Ourmazd, R. Fung, J. Cryan, A. Natan, R. Coffee, and P.H. Bucksbaum, Sub-cycle strong-field influences in X-ray photoionization, *CLEO Technical Digest*, QW1F.3 (2012).
4. P. Schwander, R. Fung, A. Ourmazd, Conformations of macromolecules and their complexes from heterogeneous datasets, *Phil Trans Roy Soc B* **369**, 20130567 (2014).
5. A. Hosseinizadeh, P. Schwander, A. Dashti, R. Fung, R.M. D'Souza, A. Ourmazd, High resolution structure of viruses from random snapshots *Phil Trans Roy Soc B* **369**, 20130326 (2014).
6. Tenboer *et al.*, Time-resolved serial femtosecond crystallography captures high-resolution intermediates of Photoactive Yellow Protein, *Science* **346**, 1242 (2014).
7. A. Dashti, P. Schwander, R. Langlois, R. Fung, W. Li, A. Hosseinizadeh, H.Y. Liao, J. Pallesen, G. Sharma, V.A. Stupina, A. E. Simon, J. Dinman, J. Frank, A. Ourmazd, Trajectories of a Brownian machine: the ribosome, *PNAS* **111**, 17492 (2014).
8. A. Hosseinizadeh, A. Dashti, P. Schwander, R. Fung, A. Ourmazd, Single-particle structure determination by X-ray Free Electron Lasers: Possibilities and challenges *Structural Dynamics* **2**, 041601 (2015).
9. A. Aquila *et al.*, The linac coherent light sources single particle imaging roadmap *Structural Dynamics* **2**, 041701 (2015).
10. R. Fung, S. Ramakrishna, T. Seideman, R. Santra, A. Ourmazd, Accurate dynamics from data with extreme timing uncertainty, *Submitted* (2015).

Page is intentionally blank.

Control of Molecular Dynamics: Algorithms for Design and Implementation

Herschel Rabitz and Tak-San Ho

Princeton University, Frick Laboratory, Princeton, NJ 08540

hrabitz@princeton.edu, tsho@princeton.edu

A. Program Scope:

This research is concerned with the conceptual and algorithmic developments addressing control over quantum dynamics phenomena. The research is theoretical and computational in nature, but its ultimate significance lies in the associated implications and applications in the laboratory. The goal of the research is to develop a deeper understanding of the principles of quantum control as well as to provide new algorithms to extend the laboratory control capabilities.

B. Research Progress:

In the past year, a broad variety of research topics were pursued in the general area of controlling quantum dynamics phenomena. A summary of these activities is provided below.

[1] Assessment of optimal control mechanism complexity by experimental landscape Hessian analysis: fragmentation of CH₂BrI: In this study, we introduced landscape Hessian analysis (LHA) as a practical experimental tool to aid in elucidating control mechanism insights. This technique was applied to the dissociative ionization of CH₂BrI using shaped fs laser pulses for optimization of the absolute yields of ionic fragments as well as their ratios for the competing processes of breaking the C–Br and C–I bonds. The experimental results suggested that these nominally complex problems can be reduced to a low dimensional control space with insights into the control mechanisms.

[2] Systematically altering the apparent topology of constrained quantum control landscapes: This work developed algorithms to (1) seek optimal controls under restricted resources, (2) explore the nature of apparent suboptimal landscape topology, and (3) favorably alter trap topology through systematic relaxation of the constraints. Mathematical tools were introduced to meet these needs by working directly with dynamic controls. The new tools were illustrated using few-level systems showing the capability of systematically relaxing constraints to convert an isolated trap into a level set or saddle feature on the landscape, thereby opening up the ability to find new solutions including those of higher fidelity.

[3] Exploring the complexity of quantum control optimization trajectories: This study addressed the structure of the landscape as a complement to topological critical point features. Especially, we extended the state-to-state transition probability results to the quantum ensemble and unitary transformation control landscapes. The interplay of optimization trajectories with critical saddle submanifolds was found to influence landscape structure. A fundamental relationship necessary for perfectly straight gradient-

based control trajectories was derived, wherein the gradient on the quantum control landscape must be an eigenfunction of the Hessian.

[4] Constrained control landscape for population transfer in a two-level system: This work explored the effects of constraining the control field fluence on the topology and features of the control landscape for pure-state population transfer in a two-level system through numerical simulations, where unit probability population transfer in the system was only accessible in the strong coupling regime within the model explored here. With the fluence and three phase variables used for optimization, no local optima were found on the landscape, although saddle features are widespread at low fluence values. Global landscape optima were found to exist at two disconnected regions of the fluence that possess distinct topologies and structures. Broad scale connected optimal level sets were found when the fluence is sufficiently large, while the connectivity was reduced as the fluence becomes more constrained.

[5] Topology of classical molecular optimal control landscapes for multi-target objectives: This work considered a control landscape defined in terms of multi-target (MT) molecular states and analyzed the landscape as a functional of the control field. The topology of the MT control landscape was assessed through its gradient and Hessian with respect to the control. Under particular assumptions, the MT control landscape was found to be free of traps that could hinder reaching the objective. Numerical simulations were presented to illustrate the classical landscape principles and further characterize the system behavior as the control field is optimized.

[6] Hessian facilitated analysis of optimally controlled quantum dynamics of systems with coupled primary and secondary states: This study considered a quantum system composed of coupled primary and secondary subspaces of energy levels with the initial and target states lying in the primary subspace. Important insights about the resultant dynamics in each case were revealed in the structural patterns of the corresponding Hessian. The Fourier spectrum of the Hessian was shown to be complementary to mechanistic insights provided by the optimal control field and population dynamics.

[7] Searching for quantum optimal controls under severe constraints: Using optimal control simulations, this study showed that constraints on quantities such as the number of control variables, the control duration, and the field strength were potentially severe enough to prevent successful optimization of the objective. For each such constraint, we showed that exceeding quantifiable limits can prevent gradient searches from reaching a globally optimal solution.

[8] Experimental observation of saddle points over the quantum control landscape of a two-spin system: This paper presented a systematic experimental study of quantum control landscape saddle points. Nuclear magnetic resonance control experiments were performed on a coupled two-spin system in a ^{13}C -labeled chloroform ($^{13}\text{CHCl}_3$) sample. We addressed the saddles with a combined theoretical and experimental approach, measured the Hessian at each identified saddle point, and studied how their presence can influence the search effort utilizing a gradient algorithm to seek an optimal control

outcome.

[9] Coherent revival of tunneling: This study introduced a tunneling effect by a driving field, referred to as coherent revival of tunneling (CRT), corresponding to complete tunneling (transmission coefficient = 1) that is revived from the circumstance of total reflection (transmission coefficient ≈ 0) through application of an appropriate perpendicular high-frequency ac field. To illustrate CRT, we simulated electron transport through fish-bone-like quantum-dot arrays and explored the corresponding current-field amplitude characteristics as well as current-polarization characteristics. We also discussed two practical conditions for experimental realization of CRT.

[10] Coherent light-driven electron transport through polycyclic aromatic hydrocarbon: laser frequency, field intensity, and polarization angle dependence: In this study, we simulated a phenyl-acetylene macrocycle (PAM) within a linear-polarized laser field. In the absence of the laser field, the PAM behaved as a perfect insulator due to destructive quantum interference. In the weak-field regime, field-amplitude power laws for one-, two-, and three-photon assisted tunneling were evident in the computational results. The study revealed a range of experimentally feasible field strengths for the observation of picoampere current caused by photon assisted tunneling. In addition, we found that the light-driven current is proportional to the cosine square of the polarization angle, and molecular electronic structure was revealed by the current-frequency characteristics. The computations showed that PAM-based optoelectronic switches have robust large on-off switching ratios under weak-field operating conditions, which are not sensitive to asymmetric molecule-lead couplings.

C. Future Plans:

The research in the coming year will include the following: **(1)** We plan to continue our work on landscape Hessian analysis (LHA) by combining it with judicious vibronic information about a particular molecular system to fit the Hessian data to practical models. Future works may benefit from systematically performing LHA on a series of optimal solutions at different laser energies to reveal information about the nature of the resonance transitions combined with model extraction from the data. **(2)** We plan to explore a variety of possible control variables and constraints to investigate the rich nature of constrained control landscape topology. The complex interplay between controls and constraints makes it virtually impossible to know *a priori* how to relax the constraints, especially in a minimal fashion, to achieve enhanced control performance. Specifically, we plan to explore how systematic variations of control resources affect the apparent constrained landscape topology. For example, the controls may also be expanded to include the Hamiltonian structure as resources when system engineering or manipulation is possible. Moreover, in order to fully understand the effects of constraining fluence, further investigations on a variety of quantum systems are needed, for example, including with different control field parameterizations. Here we specifically plan to examine the importance of other control resources beyond fluence in order to provide a greater understanding of the consequences of constraining necessary control resources upon the apparent control landscape. **(3)** The analysis of the classical molecular optimal control landscape rests on the nature of the objective functional, the

controllability and surjectivity of the system, and access to any desired control. As in the quantum case, we plan to investigate the fundamental and practical consequences of violating the assumptions to varying degrees. In addition, to further examining the continuous classical ensemble control, we plan to study the subtle issues of controllability and surjectivity. **(4)** We plan to continue our study on light-driven electron transport with single molecular junctions beyond (a) the wide-band limit by including the memory effects caused by the electrodes, (b) the independent electron model by including many-body effects such as electron-electron interactions and electron-photon interactions, and (c) the Huckel-type Hamiltonian by computing a more realistic molecular model, e.g., based on the density functional theory. In addition, we plan to study the interplay between the photon assisted tunneling and electronic excitation in a molecular junction. **(5)** We plan to build on our current study, in collaboration with Dr. Yuzuru Kurosaki in Japan, to form a more elaborate assessment of the prospects of performing ozone isomerization by executing OCT calculations to include rotation under the sudden approximation in order to reveal more general nature of the field resonances necessary for a learning control experiment.

D. References:

1. Assessment of optimal control mechanism complexity by experimental landscape Hessian analysis: fragmentation of CH₂BrI, X. Xing, R. Rey-de-Castro, and H. Rabitz, *New Journal of Physics* **16**, 125004 (2014).
2. Systematically altering the apparent topology of constrained quantum control landscapes, A. Donovan and H. Rabitz, *Math. Chem.* **53**, 718–736 (2015).
3. Exploring the complexity of quantum control optimization trajectories, A. Nanduri, O. M. Shir, A. Donovan, T.-S. Ho, and H. Rabitz, *Phys. Chem. Chem. Phys.*, **17**, 334 (2015).
4. Constrained control landscape for population transfer in a two-level system, K. M. Tibbetts and H. Rabitz, *Phys. Chem. Chem. Phys.*, **17**, 3164 (2015).
5. Topology of classical molecular optimal control landscapes for multi-target objectives, C. Joe-Wong, T.-S. Ho, H. Rabitz, and R. Wu, *J. Chem. Phys.* **142**, 154115 (2015).
6. Hessian facilitated analysis of optimally controlled quantum dynamics of systems with coupled primary and secondary states, C.-C. Shu, M. Edwalds, A. Shabani, T.-S. Ho, and H. Rabitz, *Phys. Chem. Chem. Phys.*, **17**, 18621 (2015).
7. Searching for quantum optimal controls under severe constraints, G. Riviello, K. M. Tibbetts, C. Brif, R. Long, R. Wu, T.-S. Ho, and H. Rabitz, *Phys. Rev. A* **91**, 043401 (2015).
8. Experimental observation of saddle points over the quantum control landscape of a two-spin system, Q. Sun, I. Pelczer, G. Riviello, R. Wu, and H. Rabitz, *Phys. Rev. A* **91**, 043412 (2015).
9. Coherent revival of tunneling, L.-Y. Hsu and H. Rabitz, *Phys. Rev. B* **92**, 035410 (2015).
10. Coherent light-driven electron transport through polycyclic aromatic hydrocarbon: laser frequency, field intensity, and polarization angle dependence, L.-Y. Hsu and H. Rabitz, *Phys. Chem. Chem. Phys.* July 2015.

“Atoms and Ions Interacting with Particles and Fields”

F. Robicheaux

Purdue University, Department of Physics, 525 Northwestern Ave, West Lafayette IN 47907
(robichf@purdue.edu)

Program Scope

This theory project focuses on the time evolution of systems subjected to either coherent or incoherent interactions represented by fields and particles, respectively. This study is divided into three categories: (1) coherent evolution of highly excited quantum states, (2) incoherent evolution of highly excited quantum states, and (3) the interplay between ultra-cold plasmas and Rydberg atoms. Some of the techniques we developed have been used to study collision processes in ions, atoms and molecules. In particular, we have used these techniques to study the correlation between two (or more) continuum electrons and electron impact ionization of small molecules.

Recent Progress 2014-2015

Single cycle ionization: The manipulation of electrons within atoms is an important objective in many groups. R.R. Jones recently published results in PRL where a single-cycle electric-field ionized highly excited atoms. Inspired by these experiments, the postdoc Baochun Yang performed systematic studies of single cycle ionization of atoms, from highly excited states down to the ground state.[16,17] The resulting dynamics depends on the binding energy of the electron and duration of the pulse. In Ref. [16], we investigated the threshold electric field needed for ionization and found that it scaled *inversely* with the binding energy when the pulse duration becomes shorter than the classical Rydberg period. We showed this behavior holds for weakly bound electrons with large principle quantum number n down to the ground electronic state. When the pulse duration is short, the effect of the single cycle pulse is to displace the electron; the ionization that results from this displacement is qualitatively different from tunneling ionization and multiphoton ionization. In Ref. [17], we investigated the energy distribution of electrons ionized by a single-cycle electric field. As seen in the experiments from R.R. Jones' group, we found that more deeply bound electrons led to *larger* ionization energy of the electron. We also described the implications of the substantial difference in the character of ionization from a single cycle pulse compared to a multicycle pulse.

Quasistable states in a strong IR field: The stabilization of atoms in strong, oscillating fields has been an important issue for ~ 20 years. In 2013, we were involved in an experimental and theoretical study with T.F. Gallagher's group of how atoms can have resonance states in extremely strong microwave fields.[10] As had been seen earlier, when atoms are exposed to intense laser or microwave pulses, $\sim 10\%$ of the atoms are found in Rydberg states subsequent to the pulse, even if it is far more intense than required for static field ionization. In Ref. [20], the graduate student Changchun Zhong performed calculations for the analogous system but for excitation in a strong IR field. Because the IR frequency is much greater than the microwave frequency, we found that the stabilized states have $n \sim 10$ in the IR field compared to $n \sim 500$ for microwaves. Although the number of resonances in the stabilized states was substantially less than for microwaves, we found a series of stabilized states that extended from below the $n=2$ state in H to above the ionization threshold. The atoms survive the strong IR field even after hundreds of IR cycles. This paper was an Editor's Choice for July, 2015.

Two electron physics: The correlated motion of two electrons is a fundamental system for atomic scattering theory. We recently developed a method for dealing with the quantum mechanics when two electrons extend over very large regions and/or interact for a long time. With the graduate student Qianxia Wang, we used our fully quantum method to test the range of validity of some of the approximations that are standard in PCI.[14] We compared our time dependent calculation to the best approximate methods for the energy and angular distributions where the two methods should agree and where they should disagree, thus demonstrating their consistency and range of accuracy. For the regions where the methods disagree, we discussed the reasons for the discrepancies and the trends in the differences. We also compared the calculations with existing experimental data as a final check on accuracy.

Fundamental investigations in scattering theory: With the postdoc Panos Giannakeas and with Chris Greene, we have embarked on a series of studies in fundamental scattering theory. The basic problem in scattering theory is to calculate the amplitude for a system to start in channel i and scatter into channel j . As a paradigm, we investigated the case where the scattering center has a small range but has a different symmetry from the channel functions.[18,19,21] In Refs. [18,19], the system is a highly excited atom in a strong electric field. Since a pure Coulomb potential plus a uniform electric field separates in parabolic coordinates, the channels are the eigenstates in parabolic coordinates while the scattering center is the non-Coulomb part of the potential (arising from core electrons) which has spherical symmetry. We used a standardized form of the local-frame-transformation and generalized quantum defect theory to study the angular distribution of outgoing electrons. Our formulation allowed us to treat the angular distribution through the local frame transformation and gave a critical test of the accuracy of frame transformations. This study is important because the frame transformation approximation underlies the treatment of several important scattering systems. In Ref. [21], we reformulated the underlying theory of the frame transformation using the Schwinger-variational-principle. This reformulation agreed in some cases with previous frame transformations but in other cases showed that previous treatments contain inherent approximations. Also, the treatment of Ref. [21] gave results without the divergences that need to be regularized in other methods. We used the method to treat photodetachment in the presence of various confining potentials, thereby highlighting effects of infinitely many closed channels. Two general features predicted were the vanishing of the *total* photoabsorption probability at *every* channel threshold and the occurrence of resonances below the channel thresholds for negative scattering length.

Neutron-impact ionization of He: The double ionization of He by photon absorption or ion impact has been extensively studied because they are simple examples of correlated electrons; although the systems are simple, the accurate calculation of the wave function is a challenge. When neutrons collide with a nucleus, the sudden change in velocity of the atom can cause one or more electrons to be shaken off the atom. We used a time-dependent close-coupling calculation to accurately calculate the neutron-impact single and double ionization cross sections for He.[13] We also investigated the ratio of double to single ionization and found a rapid rise of the ratio at high neutron energies: a trend unique to neutron-impact ionization.

Plasma with equal masses: P.L. Gould at UConn suggested the study of an ultracold plasma consisting of charged particles with opposite sign charges but the same mass. Two examples are an electron-positron plasma or a plasma consisting of A^- and A^+ ions. Ultracold plasmas could lead to strong coupling between the different species which would lead to correlated motion. With the undergrads Brian Bender and Michael Phillips, we simulated the evolution of a plasma created by the fast dissociation of a neutral particle.[15] The temperature of the plasma is

controlled by the relative energy of the dissociation. At early plasma times, we studied the temperature evolution and three body recombination for plasmas initially in the strongly coupled regime. For weakly coupled plasmas, we studied how an expanding plasma thermalizes and how the scattering affects the expansion.

Finally, this program has several projects that are strongly numerical but only require knowledge of classical mechanics. This combination is ideal for starting undergraduates on publication quality research. Since 2004, twenty-seven undergraduates have participated in this program. Most of these students have completed projects published in peer reviewed journals. Two undergraduates, Michael Wall in 2006 and Patrick Donnan in 2012, were one of the 5 undergraduates invited to give a talk on their research at the undergraduate session of the DAMOP meeting. Four publications during the past three years [6,7,11,15] had an undergraduate supported by DOE as first author or coauthor.

Future Plans

Single cycle ionization: We will continue the study of atoms interacting with single cycle electric fields started in Refs. [16,17]. One aspect of interest is the behavior of negative ions. For atoms, the single cycle led to a displacement of the electron when the duration of the pulse is less than the period of motion. These concepts become somewhat sketchy for negative ions (what corresponds to the period? what part of the wave function shifts?). We are also interested in how an electron ionized by a laser pulse would interact with a single cycle pulse. For this case, we expect that there are situations where there are two or more electron paths that can lead to the same result which would lead to interesting quantum interference.

Basic scattering theory: We will further apply the developments in Ref. [21] to understand the limitations and extend the applicability of the local frame transformation. We will attempt to extend the basic Harmin-Fano theory of the Stark effect to include the strongly closed parabolic channels. In the current theory, only weakly closed channels are included but, in Ref. [21], we found that the sum over the infinite number of strongly closed channels could lead to qualitative changes in other scattering systems. We will also try to apply the method to the complicated problem of atoms/ions in crossed electric and magnetic fields.

Strong laser physics: T.F. Gallagher's group has probed the stabilized states in a microwave field by coherently exciting the atom to the threshold region using two laser frequencies. Guided by these results, we will investigate the analogous situation but for the case where the atom is driven by a strong IR field of $\sim 1 \mu\text{m}$ wavelength. We will focus on how the total survival probability varies with the phase of the two laser photons. We will also explore whether information about the spatial asymmetry of the stabilized electron is available. Also, P.H. Bucksbaum's group recently published experiments that use two lasers with frequencies f and $f/2$ to obtain asymmetric ionization in the strong field limit. We will perform calculations to understand how the asymmetry in the direction of the electron ionization depends on properties of the system (e.g. phase shift of electron waves in zero field, strength of the lasers, frequency of the lasers etc).

DOE Supported Publications (9/2012-8/2013)

- [1] T. Topcu and F. Robicheaux, Phys. Rev. A **86**, 053407 (2012).
- [2] X. Zhang, R. R. Jones, and F. Robicheaux, Phys. Rev. Lett. **110**, 023002 (2013).

- [3] M. S. Pindzola, C. P. Balance, Sh. A. Abdel-Naby, F. Robicheaux, G. S. J. Armstrong, and J. Colgan, *J. Phys. B* **46**, 035201 (2013).
- [4] S. Cohen, M. M. Harb, A. Ollagnier, F. Robicheaux, M. J. J. Vrakking, T. Barillot, F. Lepine, and C. Bordas, *Phys. Rev. Lett.* **110**, 183001 (2013).
- [5] A. S. Stodolna, A. Rouzee, F. Lepine, S. Cohen, F. Robicheaux, A. Gijsbertsen, J. H. Jungman, C. Bordas, and M. J. J. Vrakking, *Phys. Rev. Lett.* **110**, 213001 (2013).

DOE Supported Publications (9/2013-8/2014)

- [6] G.W. Gordon and F. Robicheaux, *J. Phys. B* **46**, 235003 (2013).
- [7] P.L. Price, L.D. Noordam, H.B. van Linden van den Heuvell, and F. Robicheaux, *Phys. Rev. A* **89**, 033414 (2014).
- [8] M.S. Pindzola, Sh.A. Abdel-Naby, F. Robicheaux, and J. Colgan, *J. Phys. B* **47**, 085002 (2014).
- [9] F. Robicheaux, *Phys. Rev. A* **89**, 062701 (2014).
- [10] A. Arakelyan, T. Topcu, F. Robicheaux, and T.F. Gallagher, *Phys. Rev. A* **90**, 013413 (2014).
- [11] F. Robicheaux, M.M. Goforth, and M.A. Phillips, *Phys. Rev. A* **90**, 022712 (2014).
- [12] A.S. Stodolna, F. Lepine, T. Bergeman, F. Robicheaux, A. Gijsbertsen, J.H. Jungmann, C. Bordas, and M.J.J. Vrakking, *Phys. Rev. Lett.* **113**, 103002 (2014).

DOE Supported Publications (9/2014-8/2015)

- [13] M.S. Pindzola, T.G. Lee, Sh.A. Abdel-Naby, F. Robicheaux, J. Colgan, and M.F. Ciappina, *J. Phys. B* **47**, 195202 (2014).
- [14] Q. Wang, S. Sheinerman, and F. Robicheaux, *J. Phys. B* **47**, 215003 (2014).
- [15] F. Robicheaux, B.J. Bender, and M.A. Phillips, *J. Phys. B* **47**, 245701 (2014).
- [16] B.C. Yang and F. Robicheaux, *Phys. Rev. A* **90**, 063413 (2014).
- [17] B.C. Yang and F. Robicheaux, *Phys. Rev. A* **91**, 043407 (2015).
- [18] P. Giannakeas, F. Robicheaux, and C.H. Greene, *Phys. Rev. A* **91**, 043424 (2015).
- [19] P. Giannakeas, F. Robicheaux, and C.H. Greene, *Phys. Rev. A* **91**, 067401 (2015).
- [20] C. Zhong and F. Robicheaux, *Phys. Rev. A* **92**, 013406 (2015).
- [21] F. Robicheaux, P. Giannakeas, and C.H. Greene, *Phys. Rev. A* **92**, 022711 (2015).

Generation of Bright Soft X-ray Laser Beams

Jorge J. Rocca

Department of Electrical and Computer Engineering and Department of Physics

Colorado State University, Fort Collins, CO 80523-1373

jorge.rocca@colostate.edu

Program description

The great interest in the use of high intensity coherent soft x-ray and x-ray light motivates the development of compact sources of intense coherent soft x-ray light that can be readily accessible. The project goals are to explore amplification of atomic transitions in plasma regimes leading to compact soft x-ray lasers emitting high energy pulses of femtosecond pulsewidth at high repetition rate, and to investigate schemes that promise to increase their conversion efficiency with the ultimate goal of achieving high average powers. This research builds on recent progress in the generation of bright soft x-ray laser beams on a table-top. We have recently made use of a diode-pumped laser driver to demonstrated soft x-ray laser operation at 100 Hz repetition rate, producing a record 0.1 mW average power at 13.9 nm from a table-top laser. The project experimentally and theoretically studies the amplification of soft x-ray radiation in high plasma density regimes in which collisions broaden the laser transitions to create a gain medium with the increased bandwidth necessary to amplify femtosecond soft x-ray laser pulses. The ultrafast high energy pump laser that we are developing to enable this research will also allow us to explore lasing at wavelengths below 8 nm in transitions of Ni-like lanthanide ions. In addition, we are using hydrodynamic/atomic physics simulations and experiments to tailor the interaction between the driver laser and the target in table-top soft x-ray plasma amplifiers with the goal of obtaining a significant increase in efficiency, as part of an strategy to develop high average power table-top soft x-ray lasers. The combination of an increased efficiency with a further increase in repetition rate can be expected to yield soft x-ray laser beams with an unprecedented average power on a table-top high photon flux demanding applications.

Modeling of dense soft x-ray laser amplification media

We have used an atomic physics/hydrodynamic code to model novel atomic soft x-ray laser amplifiers based on high density plasmas. Simulations were conducted for two different type of amplifiers in which we plan to conduct experiments. The first consists in dense plasmas of lanthanide ions that are of interest to generate intense laser pulses at wavelengths shorter than 8 nm. The second concerns the generation of a super-critical density plasma generating by irradiation of arrays of aligned nanowires with high intensity femtosecond optical laser pulses. The aim in this case is to create very dense plasmas in which large collisional broadening of the atomic laser lines can support amplification of femtosecond soft x-ray pulses.

We performed a set of simulations with the goal of extending transient collisional lasers to sub-8 nm wavelengths in a plasma of Ni-like lanthanide ions. A goal is to determine efficient pumping configurations to extend these lasers to the shortest possible wavelengths. Specifically we are interested in first attempting to produce a gain saturated soft X-ray laser amplifier at $\lambda = 7.3$ nm in Ni-like samarium, and next explore soft X-ray laser amplification in the $4d \ ^1S_0-4p \ ^1P_1$ transition of Ni-like Gd at $\lambda = 6.7$ nm. We have conducted simulations to determine the optimum laser parameters for such experiments. As an example we discuss below results for lasing in Ni-like Gd at $\lambda = 6.7$ nm. Figure 1 shows the evolution of the electron temperature, ion temperature and electron density of a prospective Gd plasma soft X-ray amplifier created irradiating a Gd flat target with a sequence of a 300 ps optical laser ($\lambda = 800$ nm) pre-pulse with an intensity of 2×10^{13} W cm⁻², followed by a 3 ps duration pulse with an intensity of 1×10^{15} W cm⁻². The spatio-

temporal evolution of the gain in the 6.7 nm laser transition is shown in Fig. 1(d) to reach values of about 50 cm^{-1} . This gain coefficient is sufficient to observe strong amplification in such plasma, but is likely to be too small to allow us to reach gain saturation. We are therefore exploring optimum irradiation conditions to optimize the gain. Fig. 1(e) shows the computed gain coefficient as a function of the angle with which the short pulse impinges onto the target. The largest gain is predicted for the angle closest to normal incidence of those explored, 45 degrees. Figure 1(f) shows the dependence of the gain on time delay between the 300 ps pre-pulse and the short pulse for a configuration in which the short pulse impinges at an angle of 55 degrees respect to the target normal. Next we plan to run experiments first on samarium (laser line at $\lambda = 7.3 \text{ nm}$), and then in gadolinium (laser line $\lambda = 6.7 \text{ nm}$) and to compare the results with model the simulations.

A second set of simulations was conducted to study the possibility of amplification in super-dense plasmas. Figs. 2,3 show the results of simulations for a prospective soft x-ray laser plasma amplifier generated by irradiation of a target consisting of aligned ruthenium nanowires. The target is assumed to be irradiated by high contrast pulses of 50 fs duration at an intensity of $5 \times 10^{16} \text{ W cm}^{-2}$. Based on the results of our recent experiments with nanowire array targets the absorption depth of the laser pulse into the target is assume to be $\sim 5 \mu\text{m}$. Fig. 2(a) shows that the electron temperature is predicted to reach 500 eV over a depth $> 5 \mu\text{m}$ while ions reach a temperature of 200 eV. The electron density is computed to exceed $1 \times 10^{22} \text{ W cm}^{-3}$. The mean degree of ionization is predicted to reach a value of $Z=15$ with a density of Ni-like ions, the prospective lasing species, of $\sim 20 \%$. Fig. 2(e) shows the spatio-temporal distribution of Ni-like ions. Figures 2(f) shows the gain in the $4d \ ^1S_0-4p \ ^1P_1$ transition of Ni-like ruthenium ions at $\lambda = 16.7 \text{ nm}$. is computed to exceed 120 cm^{-1} at 400 fs after the peak of the irradiating laser pulse. Figure 3 shows the simulated bandwidth of this laser transition as a function of the electron density. The bandwidth is observed to increase with plasma density due to collisional broadening. At the predicted electron density of $1 \times 10^{22} \text{ cm}^{-3}$ the bandwidth corresponds to a transform-limited pulse width of a few femtosecond. However gain narrowing limits the amplified laser pulse bandwidth to a value corresponding to a transform limited pulse width of $\sim 50 \text{ fs}$ (Fig.(3b)).

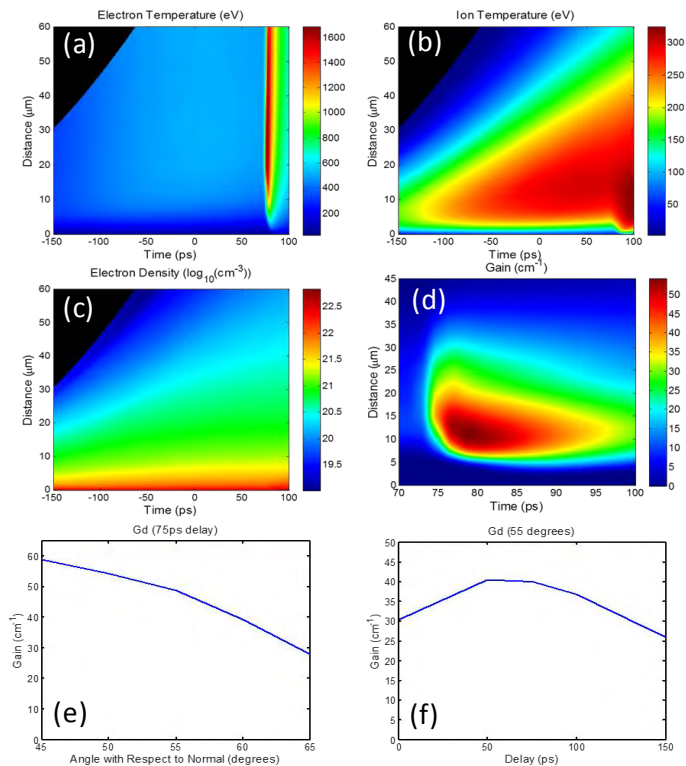


Fig.1. Simulations of plasma parameters and laser gain in the $\lambda = 6.7 \text{ nm}$ line in a Gd laser-created plasma. (a) electron temperature, (b) ion temperature, (c) electron density, (d) gain coefficient, (e) gain coefficient as a function of angle of incidence of the main excitation pulse respect to the target normal, (f) gain coefficient as a function of time delay between the pre-pulse and short pulse for a short pulse an angle of incidence of 55 degrees. The irradiation conditions are those described in the text.

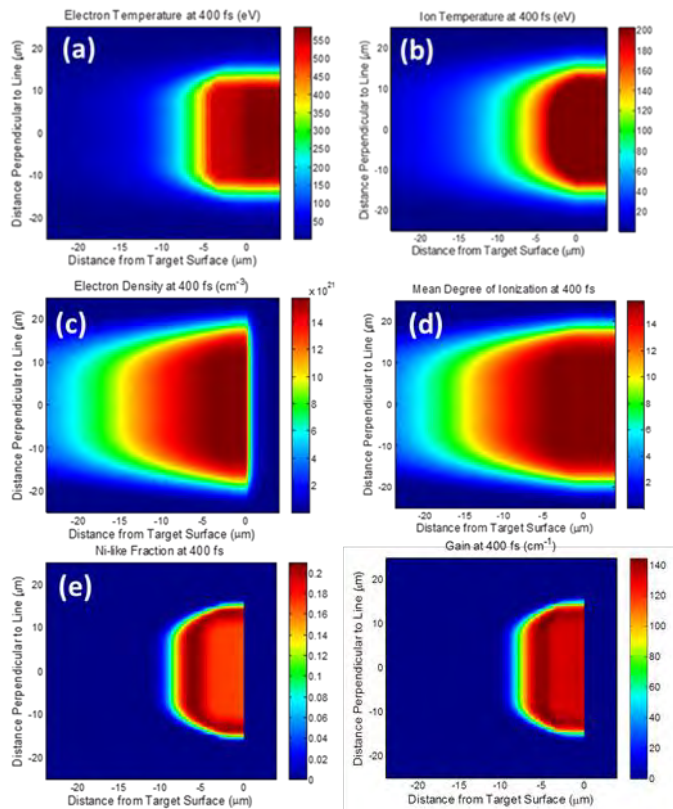


Fig. 2. Computed parameters of plasma amplifier generated by irradiation of aligned ruthenium nanowires with femtosecond laser pulses at an intensity of $5 \times 10^{16} \text{ W cm}^{-2}$ (a) electron temperature; (b) ion temperature, (c) electron density, (d) mean degree of ionization, (e) Ni-like ion fraction, (f) spatial distribution of the soft x-ray laser gain at 400 fs after the peak of the excitation pulse.

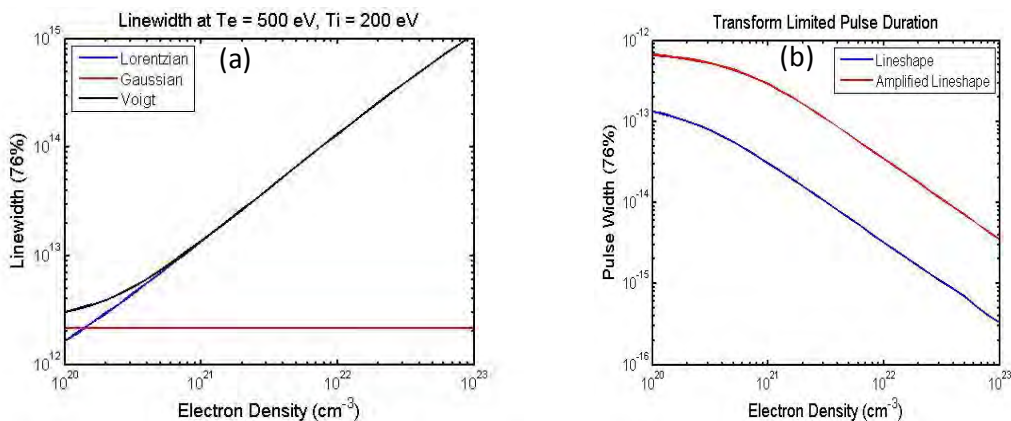


Fig 3. (a) Computed bandwidth of the amplified $4d^1S_0-4p^1P_1$ laser transition in Ni-like ruthenium as a function of electron density showing the effect of collisional broadening, and (b) corresponding bandwidth and transform of the laser pulse amplified to reach saturation taking into account the gain narrowing

Upgrade of Ti:Sapphire pump laser

During the past year we have also worked in upgrading to higher energy the Ti:sapphire laser that will be used as pump laser in a large part of the experiments. The laser, that was recently installed into a new

laboratory space, was upgraded by adding an additional amplification stage pumped by a new chain of frequency doubled Nd:glass slab amplifiers. We achieved a Ti:sapphire pulse energy of 32 J before compression. A new grating compressor was also installed to allow for the compression of higher energy pulses. The new compressor was measured to have an efficiency of ~ 70 percent, and to deliver pulses of 50fs duration. With the capability of operating at multi-Hertz repetition rate at a peak power approaching 0.5 Pw this high energy ultrashort pulse is a unique facility. Figure 4 shows a photograph of the newly upgraded laser system. New line focus optics is currently being installed to conduct the proposed experiments. Future plans includes the realization of these experiments.



Fig. 4. Wide angle view of the high energy Ti:Sapphire laser developed at Colorado State University.

Publications resulting from DOE-BES supported work (2013-2015)

1. Y. Wang, S. Wang, E. Oliva, L. Lu, M. Berrill, L. Ying, J. Nejd, B. Luther, C. Proux, T.T. Le, J. Dunn, D. Ros, P. Zeitoun, J. J. Rocca, "Gain dynamics in a soft X-ray laser amplifier perturbed by a strong injected X-ray field," *Nature Photonics* **8**, 381 (2014)
2. C. Weninger, M. Purvis, D. Ryan, R. A. London, J. D. Bozek, C. Bostedt, A. Graf, G. Brown, J. J. Rocca, N. Rohringer, "Stimulated electronic X-ray Raman scattering," *Physical Review Letters*, **111**, (2013).
3. Y. Wang, L. Yin, S. Wang, M. C. Marconi, J. Dunn, E. Gullikson, J. J. Rocca, "Single-shot soft X-ray laser linewidth measurement using a grating interferometer," *Optics Letters* **38**, 5004 (2013).
4. B. A. Reagan, W. Li, L. Urbanski, K. Wernsing, C. Salsbury, C. Baumgarten, M. Marconi, C. S. Menoni, and J. J. Rocca, "Hour-long continuous operation of a table-top soft X-ray laser at 50-100 Hz repetition rate," *Optics Express* **21**, 28320 (2013).
5. Lu Li, Y. Wang, S. Wang, E. Oliva, L. Ying, T.T. Thuy Le, S. Daboussi, D. Ross, G. Maynard, S. Sebban, B. Hu, J.J. Rocca P. Zeitoun, "Wavefront improvement in injection-seeded soft x-ray laser based on solid-target plasma amplifier" , *Optics Letters*, **38**, 4011 (2013)
6. B. A. Reagan, C. Baumgarten, K. Wernsing, H. Bravo, M. Woolston, A. Curtis, F.J. Furch, B. Luther, D. Patel, C. Menoni, J.J. Rocca, "1 Joule, 100 Hz Repetition Rate, Picosecond CPA Laser for Driving High Average Power Soft X-ray Lasers," *Proceedings Conference on Lasers and Electro-Optics (CLEO)*, Invited, 2014
7. B.A. Reagan, C. Baumgarten, K.A. Wernsing, M. Berrill, M. Woolston, L. Urbanski, W. Li, M.C. Marconi, C.S. Menoni, and J.J. Rocca, "Advances in High Average Power, 100 Hz Repetition Rate Table-top Soft X-ray Lasers), (Invited) *Proceedings of the 14th International Conference on X-Ray Lasers*. Springer , in press (2015)
8. L. Li, Y. Wang, S. Wang, E. Oliva, L. Yin, T. T. T. Le, S. Daboussi, D. Ros, G. Maynard, S. Sebban, B. Hu, J. J. Rocca, and Ph. Zeitoun, "Wave Front Study of Fully Coherent Soft X-Ray Laser Using Hartmann Sensor", *Proceedings of the 14th International Conference on X-Ray Lasers*. Springer , in press (2015)
9. S. Wang, Y. Wang, E. Oliva, L. Lu, M. Berrill, L. Yin, J. Nejd, B. Luther, C. Proux, T.T. Thuy Le, J. Dunn, D. Ros, Ph. Zeitoun, J.J. Rocca, "Gain Dynamics in Injection-seeded Soft X-ray Laser Plasma Amplifiers", *Proceedings of the 14th International Conference on X-Ray Lasers*. Springer , in press (2015)

Spatial Frequency X-ray Heterodyne Imaging and Ultrafast Nanochemistry

Christoph G. Rose-Petruck

*Department of Chemistry, Box H, Brown University, Providence, RI 02912
phone: (401) 863-1533, fax: (401) 863-2594, Christoph_Rose-Petruck@brown.edu*

1 Program Scope

The goal of this research program is the study of processes at nanometer length scales and ultrafast to slow time scales. We study the structure of nanometer-sized materials using Spatial Frequency Heterodyne Imaging (SFHI), an x-ray imaging modality developed during the past DOE funding cycle. Ultrafast dynamics of molecules in their solvation environment are studied with picosecond x-ray absorption fine structure (XAFS) spectroscopy using an endstation that we developed in collaboration with Bernhard Adams at 7ID-C of the Advanced Photon Source, Argonne National Laboratory.

1.1 SFHI of water phase transitions in carbon nanotubes

The spatial dimensions of nanomaterials bestow on them unique properties, and fluids confined at the nanoscale show properties that differ from the bulk. Evaporation and condensation of water confined to the inner cavity of carbon nanotubes (CNTs) was the focus of this study. Understanding of fluids confined to nano dimensions is necessary to facilitate widespread application of nanofluidic phenomena to fields including transmembrane transport⁴, sequestration of gases in nanoporous minerals, nanofluidic devices, chromatography, water purification but also ultrafast dynamics in nano-confined spaces.

CNTs are made of hydrophobic graphene sheets. Despite the hydrophobic nature of the grapheme sheets, experimental studies have revealed that water can be confined in CNTs. They are wetted by liquids of interfacial tension below 200 mN/m. Water has an interfacial tension of approximately 72 mN/m and therefore wets CNTs despite their insolubility in polar solvents. The acute contact angle water makes with CNT surfaces permits population of the inner cavity via capillary forces. Functionalization of the CNT surfaces by oxidation decreases the contact angle of water by addition of oxygen containing functional groups, exaggerates defect sites, and removes any hemispherical caps possibly sealing the CNTs at either end.

Capillary theory predicts a decrease in water vapor pressure within CNTs resulting from formation of an aqueous meniscus with negative radii of curvature. An increased boiling point is an immediate consequence of decreased vapor pressure. The Kelvin equation predicts the change in vapor pressure of a liquid as its free surface deviates from a planar geometry, and the Clausius-Clayperon equation yields the change in boiling point given the change in vapor pressure. Molecular dynamics simulations have also shown that pressures on the order of hundreds of bar are possible by heating water confined to a closed CNT within a few tens of degrees above its boiling point. The ability to generate such high pressures by relatively mild heating could have a dramatic impact on the high pressure chemical industry. We used Spatial Frequency Heterodyne Imaging (SFHI) developed with support from this DOE program to measure the loading and unloading of water into Carbon Nanotubes (CNTs). Our objective is to develop SFHI as an X-ray detection method suitable for studying phase transitions in nanomaterials.

SFHI is related to small angle x-ray scattering (SAXS), but simultaneously measures at thousands of points in a sample the integrals of the SAXS profiles in a single x-ray image exposure. The image data can be numerically decomposed into a pure absorption image and several images that only contain the scattered x-rays. As SAXS is particularly sensitive to the nano and mesoscopic structures of a sample, SFHI images the distribution, size, and orientation of nanostructures in a sample. Since all image points are measured simultaneously and only a single x-ray exposure is needed to obtain a complete image of the sample, ultrafast time-resolved imaging of an entire sample is possible. The imaging setup does not require any x-ray optics between the x-ray source and the sample and is equally well-suited for use with point x-ray sources as well as accelerator-based sources. This feature enables future measurements of the dynamics of nanomaterials on an ultrafast time scale with the nanometer-sensitivity typical of conventional SAXS. Here we present results for the equilibrium structure of CNTs during water loading and unloading.

Multi-wall CNTs with an inner diameter of 7 ± 2 nm, an outer diameter of 15 ± 5 nm, and a length of 1-5 μm produced by chemical vapor deposition were obtained from Nano Lab Inc. (Waltham, MA). A fraction of the multi-wall CNTs were placed in a Pyrex tube open to atmosphere and heated to 500°C for approximately 50 minutes in order to functionalize the CNTs. Heating produced a 15% mass loss.

Two functionalized (heat treated) and two as purchased 16 mg samples of multi-wall CNTs were placed in glass tubes. The CNTs were packed at one end of the glass tubes by a glass wool plug, and 250 μl of nano-pure water were added to one functionalized and one as purchased sample. All four samples were then vacuum sealed and

placed in an aluminum holder fitted with two heating elements, a thermocouple, and five sample slots. The middle slot contained an empty glass tube. The two samples that did not have water explicitly added were heated to 110°C for ten minutes while under vacuum in order to insure that all water already adsorbed into the CNTs was removed. The portions of the glass tubes containing CNTs were within the dimensions of the holder, while the empty lengths of glass tubing that remained extended beyond the holder. Extension beyond the dimensions of the aluminum holder allowed the vacant portion of the glass tubes to remain at room temperature throughout the experiment. The dry samples were therefore under vacuum while the wet samples were under a pressure equal to that of water vapor pressure at room temperature. A schematic of the holder is presented in Figure 3.

The holder was placed 1.2 m below a 12 bit RadEye 200 CMOS detector in a vertical imaging arrangement with a 1.6 m source to detector distance. The source was a True Focus X-ray tube, model TFX-3110EW with a Tungsten anode and 10 μm focus size. The tube was operated at 80 KV and 0.2 mA. The absorption grid was a two dimensional 170 μm period stainless steel wire mesh with 66 μm gauge. The grid was placed immediately below the sample holder. Only the sample volumes contained within the dimensions of the aluminum holder were in the viewing field of the imaging system. As the samples were heated a temperature gradient was established and water condensed at the room temperature end of the glass tubes out of the viewing field.

Prior to imaging the samples were situated in a vertical position to ensure contact of the CNTs with the added water. The samples were then oriented horizontally and heated to 80°C for 30 minutes to expel excess water from the samples into the region of the glass tubes outside of the viewing field. After preheating the samples were allowed to cool for four hours. The samples were heated as quickly as possible to a set point temperature that was then maintained.

Figure 1 contains the results of heating the samples to various set point temperatures. The signals depicted are the differences between the intensities measured for the samples containing water and their corresponding dry samples, so any change in intensity is due solely to the effect of added water. The abscissa was normalized to the time at which all water had been removed from the as purchased CNTs. The time in hours to which the abscissa was normalized is located next to the temperature at which images were collected.

The left ordinate is the scale for image intensities obtained from the (0,0) harmonic, so these intensities are due to changes in absorption and have been rescaled to represent the amount of water in the samples as a percentage of the initial water content. A rescaling of absorbance values is permissible because absorbance is proportional to concentration. No such rescaling is permissible for the integrated scatter intensities, whose scale is the right ordinate. Scattered intensity is only related to the number of scattering centers squared in the zero scattering angle limit. Both the scatter and absorbance intensities were offset corrected.

In each of the four graphs shown in Figure 1 the absorbance intensities decrease monotonically in accord with water leaving the viewing field. The integrated scatter intensity profiles for the functionalized and as purchased samples are qualitatively the same at each temperature with an initial increase in intensity, followed by a subsequent increase, and then decrease back to baseline. A change in integrated scatter intensity for both samples is not observed until 20 to 30% of the water has been

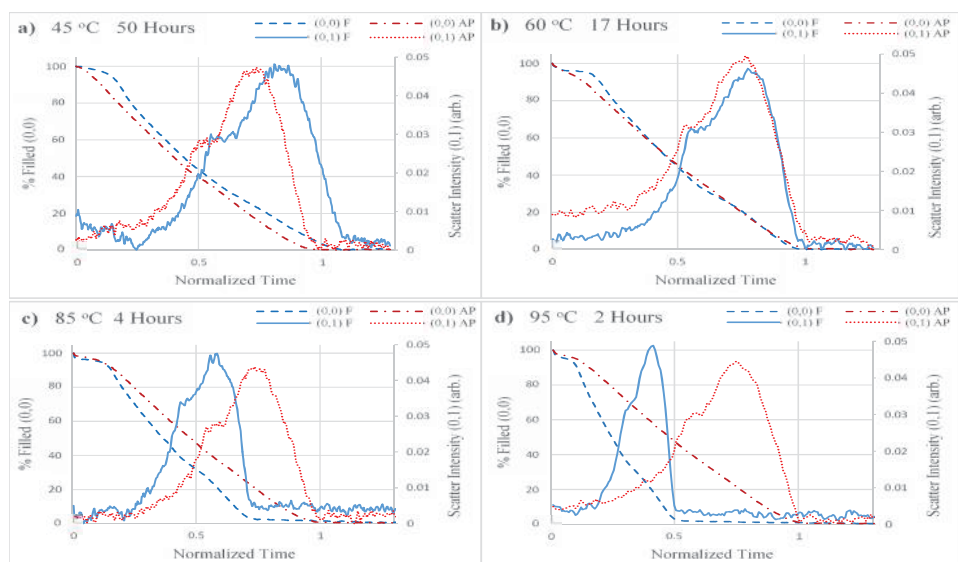


Figure 1: Temporal x-ray absorbance and scatter profile of CNTs heated to 45°C (a), 60°C (b), 85°C (c), and 95°C (d). The abscissa has been normalized to the time at which evaporation went to completion in the as purchased sample. The time to which the abscissa was normalized is located next to the temperature at which the experiment was conducted. All signals depicted are the differences between the wet samples and their corresponding dry samples. In the legends F stands for the samples that were functionalized by heat treatment, and AP stands for the as purchased samples. The relative error for a 95% confidence interval was never greater than 4% of the signal amplitude for all curves displayed.

evaporated from the CNTs, indicating that unlike absorbance the scatter intensity is not sensitive to the change in water content alone. At 45°C (Figure 1a) and 60°C (Figure 1b) water starts to evaporate from the as purchased sample at an earlier time than the functionalized sample, and at 85°C (Figure 1c) and 95°C (Figure 1d) water starts to evaporate from the as purchased and functionalized samples at about the same time. At all temperatures regardless of when evaporation begins water leaves the functionalized samples at a faster rate. The change in evaporation rates between the functionalized and as purchased samples with temperature is clearly seen in the absorbance profiles, but is also dramatized by the displacement of the scattering profiles relative to one another. At 85°C and 95°C the increased evaporation rate of water from the functionalized sample compresses the scatter intensity profiles in time relative to the as purchased sample.

In an effort to interpret the shape of the scatter intensity profiles in terms of CNT shape and water content the integrals over SAXS distributions corresponding to the four states of CNTs were calculated. Figure 2 depicts the CNT model states used to compute SAXS distributions. The series of states modeled represent different instances along the progression of capillary condensation. The CNTs were modeled as 10 nm long tubule segments with electron densities taken as that of bulk material. The integrals over SAXS distributions corresponding to CNTs of constant cross section undergoing capillary condensation, and CNTs of changing cross section without capillary condensation were also calculated. The integral of these SAXS distributions were compared to the measured scatter intensities shown in Figure 1 and found to be in qualitative agreement with the observed scatter profiles. Coincidence of the change in evaporation time scales with the boiling point predicted by the Kelvin equation and the qualitative agreement between the theoretical calculations and observed scatter intensity of the as-purchased sample during condensation establishes the applicability of thermodynamics to water confined to dimensions less than 10 nm. To our knowledge this is the first experimental verification that thermodynamics may be applied within this size regime.

1.2 Ultrafast XANES of solvation shell dynamics

The ultrafast x-ray absorption near edge spectra (UXANES) of two anionic ions, $[\text{Fe}(\text{CN})_6]^{4-}$ and MgO_4^- , in water have been measured after intense photoexcitation with 266-nm, 50-fs laser pulses. The resulting

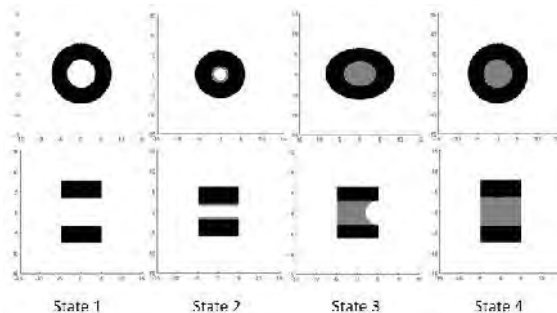


Figure 2: State 1: empty CNT with circular cross section; state 2: CNT after a 20% radial contraction caused by the formation of 1 nm thick film of water; state 3: elliptical cross section resulting from a 10% change in radius along both the semi major and minor axes, following the formation of an aqueous meniscus; state 4: CNT with its original cross section and complete filling with a planar meniscus at each end.

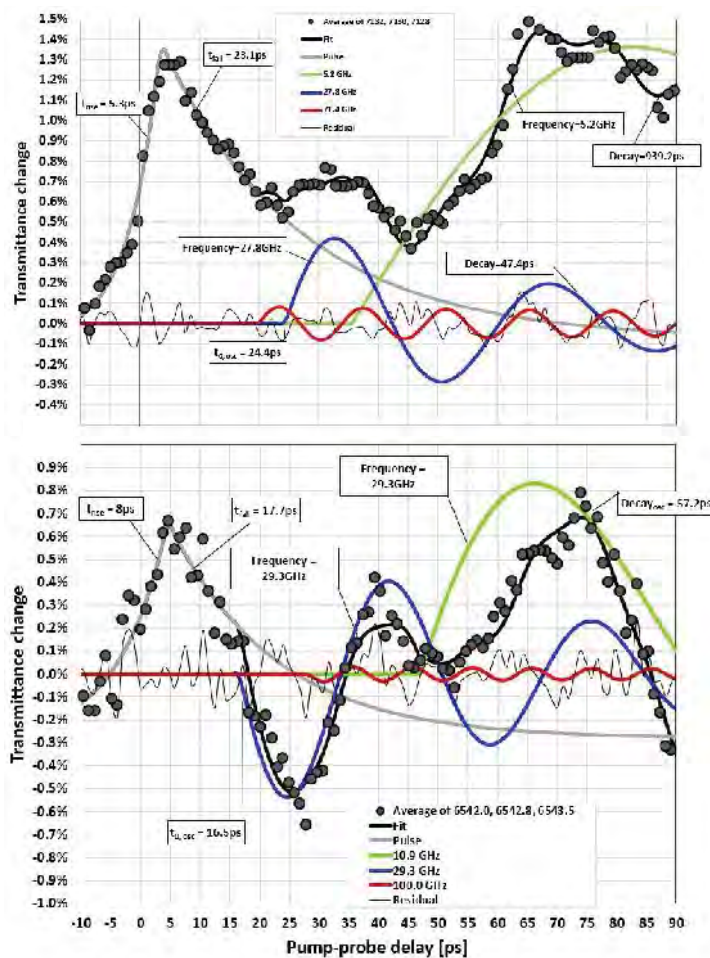


Figure 3: Decomposition of the total x-ray transmittance vs. time after excitation of $[\text{Fe}(\text{CN})_6]^{4-}$ (top) and MnO_4^- (bottom) with 50-fs, 266nm laser pulses. Fit functions are: a double-exponential function, a sigmoidal function, and a damped sinusoidal function. Relevant function parameters are indicated.

dynamics causes modulations in the UXANES. Figure 3 shows the data points and their respective fit curves. The nature of the anions is not very important; they simply act as probes of the solvation shell dynamics that results from the laser excitation. The XANES spectra were measured at 7128 eV – 7132 eV for $[\text{Fe}(\text{CN})_6]^{4-}$. This spectral range is most sensitive to changes in the solvation environment. It is also strongly changes if, for instance, reaction products are formed. Thus, from this limited range, structural details cannot be deduced. MnO_4^- was probed at 6542.8 eV, the energy of the 1s \rightarrow 3d transition of Mn. This transition is only detectable because of the tetrahedral symmetry of the complex. It vanished upon distortion of this complex or the formation of reaction products. Thus, measurements at this location will only show departure from the (pre-excitation) equilibrium structure.

Figure 3 shows the two x-ray absorption spectra measured in transmission mode. Raw data points are shown every 900 fs. The spectra are each fitted with an exponential rise and an exponential drop. The rise time constant is a few ps. There is an exponential decay on with time scales of 23 ps and 17 ps for ferrocyanide and permanganate, respectively. We attribute this decay mainly to the vibrational cooling process. At about 20 ps both measurements show oscillations (blue fitted curves) with about 30-ps oscillation periods. The green fit curves likely are the product formations. The red curves improve the fit qualities, but we do not interpret them due to their small amplitudes.

It is clear that the oscillations cannot be the consequence of molecular vibrations, because the oscillation frequencies are much too low. Instead, the oscillation periods approximately match that known from microwave data for bulk water, which is caused by the oscillations of water networks. Since x-ray spectroscopy can only probe the 1st, and perhaps the 2nd, solvation shells, the oscillation shown here cannot be caused by bulk water. We believe that the oscillations of the water in the solvation shells modulate the dielectric constant into which the anions are embedded. The XANES scatter phases, or in the case of permanganate the 3d orbital energies, are sensitive to the dielectric environment. Thus, this modulation should shift or broaden the absorption features, an effect which is detected as a modulation of the x-ray absorbance as shown in Figure 3. Since both solutes are entirely different the similarity of the frequencies supports this interpretation. Similar effect should be detectable in many other ultrafast XANES and pore-edge measurements.

2 Papers acknowledging this DOE grant^{1-14,15}

- (1) Rand, D. *et al. Scientific Reports* **2015**, *in press*.
- (2) Schunk, F. *et al. PCCP* **2015**, *submitted*.
- (3) Adams, B. *et al. Journal of Synchrotron Radiation* **2015**, *22*, 16.
- (4) Adams, B. *et al. Journal of Synchrotron Radiation* **2015**, *22*, 1022.
- (5) Jiao, Y. *et al.* **2015**, *submitted*.
- (6) Bruza, P. *et al. Applied Physics Letters* **2014**, *104*, 254101.
- (7) Rand, D. *et al. Physics in Medicine and Biology* **2014**, *60*, 769.
- (8) Rand, D. *et al. Optics Express* **2014**, *22*, 23290
- (9) Wu, B. *et al. Applied Physics Letters* **2012**, *100*, 061110.
- (10) Chollet, M. *et al. IEEE Journal of Selected Topics in Quantum Electronics* **2012**, *18*, 66.
- (11) Chollet, M. *et al. Nuclear Instruments and Methods in Physics Research A* **2011**, *649*, 70
- (12) Liu, Y. *et al. Optics Letters* **2011**, *36*, 2209.
- (13) Rand, D. *et al. NanoLetters* **2011**, *11*, 2678.
- (14) Ahr, B. *et al. PCCP* **2011**, *13* (Also PCCP Cover Page, April 2011), 5590.
- (15) Rose-Petruck, C. *et al.*, US Patent Appl. Number: 61/544,419, (2011)

3 Publications and Ph.D. theses related to this DOE grant

1. "Chemical Dynamics in the Condensed Phase: Time-resolved X-ray Imaging and Ultrafast X-ray Absorption Spectroscopy" B. Ahr, Brown University, 2011.
2. "Pulse Plasma Soft X-ray Source in Biomedical Research" P. Bruza, Czech Technical University, 2014.
3. "X-Ray Spatial Frequency Heterodyne Imaging of Hepatocellular Carcinoma Using Nanoparticle Contrast Agents" D. Rand, Brown University, 2014.
4. "A fickle molecule caught in the act," D. Bradley, 2011 Annual Report of the Advanced Photon Source (2012).

Transient Absorption and Reshaping of Ultrafast Radiation

DE-FG02-13ER16403

Kenneth J. Schafer (schafer@phys.lsu.edu)

Mette B. Gaarde (gaarde@physics.lsu.edu)

Department of Physics and Astronomy, Louisiana State University

Baton Rouge, LA 70803

September 2015

Program Scope

Our program is centered around the theoretical study of transient absorption of ultrafast extreme ultraviolet (EUV) radiation by atoms and materials interacting with a precisely synchronized near-to-mid infrared (IR) laser pulse. Transient absorption spectroscopy can in principle provide high spectral resolution and high (attosecond) time resolution simultaneously, by spectrally resolving the light transmitted through a sample as a function of delay between the dressing laser pulse and the broadband attosecond EUV probe. As in all transient absorption calculations/measurements, one of the main challenges we confront is the extraction of time-dependent dynamics from delay-dependent information. In addition, we must also account for the reshaping of the broadband XUV light in the macroscopic medium. We study attosecond transient absorption (ATA) using a versatile theoretical treatment that takes account of both the strong laser-atom interaction at the atomic level via the time-dependent Schrodinger equation (TDSE), as well as propagation of the emitted radiation in the non-linear medium via the Maxwell wave equation (MWE), in the single-active electron (SAE) approximation up to now [1]. We have now extended our SAE treatment in atoms to fully-active two electron calculations in helium, in both full and reduced dimensions. Our immediate goal is to extend our Maxwell/TDSE treatment to include multi-electron systems, beginning with reduced dimensions.

Recent Progress

In the past year we completed a number of research projects in collaboration with experimental groups carrying out attosecond transient absorption (ATA) measurements. These have now appeared or will soon appear as journal articles [R1-R4]. An Invited Topical Review to appear in *Journal of Physics B* [P2] will summarize and place in context many of the theoretical results on attosecond transient absorption that we have obtained in the course of this work.

As part of our work on the fundamental properties of ATA, we collaborated with the experimental group of Prof. G. Sansone at Politecnico Milan, Italy. We explored the dependence of broadband, attosecond XUV absorption on the relative polarizations of an isolated attosecond pulse (IAP) and an IR pulse [R4]. This *polarization control* manifests itself in the variation of the light induced states (LIS) in the transient absorption spectrum. The LISs [2], which appear when the XUV and IR pulses overlap in time, are manifestations of the strong IR-induced coupling between states that are bright (dipole allowed) or dark (dipole forbidden) with respect to the XUV absorption. When the strongly coupled bright and dark states are detuned from resonance with the IR field, the LISs can be thought of as one IR photon sidebands on the dark states. This allows the various LISs to be assigned to specific dark states, and to be labeled accordingly. While this picture makes sense, we sought experimental verification. Rotating the relative polarization of the XUV and IR pulses allowed us to prove that our picture of the LISs is correct since it allowed us to predict which LISs would survive when the polarization was rotated and which would not. The excellent agreement between experiment and theory is shown in Figure 1. This work demonstrates that the pump-probe polarization can be used to selectively turn on and off the transient processes that lead to two photon (phase sensitive Raman-like) population transfer in laser-dressed systems.

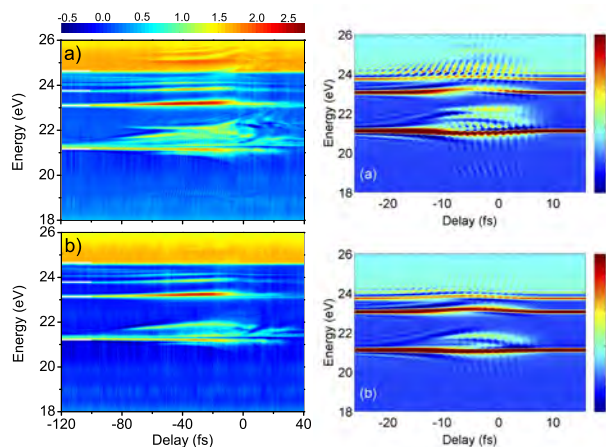


Figure 1: *Left panels:* Experimental optical densities for attosecond transient absorption in helium atoms as a function of the relative delay between the XUV and IR pulses for the XUV and IR polarizations that are (a) parallel or (b) perpendicular. In the region between 21 and 23 eV light induced states appear between the the dipole allowed $1s2p$ and $1s3p$ transitions near zero delay. More LISs appear for parallel than for perpendicular polarizations due to the presence or absence of IR-induced $s-p$ couplings. *Right panels:* TDSE calculations that mimic the experimental conditions reveal the same pattern. From M. Reduzzi, *et al.*, *Polarization-control of absorption of virtual dressed-states in helium*, Phys. Rev. A, accepted (2015).

As part of our work on the macroscopic properties of attosecond transient absorption, we collaborated with the group of Prof. A. Sandhu at the University of Arizona, Tuscon [R3]. Specifically, we studied the macroscopic propagation effects in the absorption of attosecond pulse trains (APTs) by IR-laser-dressed He atoms. Since transient absorption experiments must measure a non-zero (usually substantial) amount of absorption, it is important to understand the absorption lineshape beyond the single atom response, and in particular the interplay of microscopic and macroscopic effects. An additional motivation for this work is the great amount of interest that has been generated by the work of Thomas Pfeifer’s group on the reshaping of absorption lines in helium by a strong IR field [3]. The work of the Pfeifer group has all been in the single atom framework, ignoring collective (*i.e.*, propagation) effects.

In the LSU/UofA collaboration we studied the interplay between the IR-induced phase shift of the microscopic time-dependent dipole moment [3,4] and the resonant-propagation-induced reshaping of the macroscopic XUV pulse [5]. Our results showed that as the optical depth increases, this interplay leads initially to a broadening of the IR-modified line shape, and subsequently to the appearance of new, narrow features in the absorption line. We were able to explicitly observe its effects in attosecond transient absorption for the first time and show how the coupling between the single-atom IR-induced phase and the collective resonant pulse propagation effects manifests itself in the absorption profile. Our full TDSE-MWE calculations reproduced the experimental results quite well, and we were able to use few-state models plus propagation to understand the basic effects. An interesting extension of this work relates to the Milan polarization control experiment. Rotating the relative polarization between IR and XUV pulses will alter the IR-induced phase on the absorption line. This should be a stringent test of our understanding of the reshaping. We are currently pursuing this in collaboration with the UofA group.

Future directions

A major goal of our research program is the study of attosecond transient absorption in multi-electron systems. Our approach is to begin with two electron systems in both full dimension and in reduced dimensions. The full dimensional problem is studied in our group using an ab-initio, five-dimensional, two-electron TDSE solver for He atoms interacting with electromagnetic fields written by Dr. X. Guan (formerly of Drake University, now at the High Performance Computing Center at LSU). We are currently exploring transient absorption around the low-lying autoionizing resonances in helium. The modification of these (Fano-like)

resonance features by an IR dressing field has been extensively studied by T. Pfeifer's group [3,6]. Our work has examined the appearance of LIS in the helium attosecond transient absorption spectrum above the first ionization threshold. These LISs are manifestations of the strong IR-induced coupling between bright and dark *autoionizing states*, in contrast to our earlier work below the first ionization threshold [2]. We emphasize that it is very difficult to study the dark autoionizing states, such as the $2s^2\ ^1S^e$, $2p^2\ ^1S^e$ and $^1D^e$ states, since they do not appear in synchrotron spectra unless a static electric field is used, and the electric field of an IR laser such as those used in attosecond transient absorption experiments is thousands of times stronger than the largest static fields employed in synchrotron studies. The dark states couple strongly with bright states like the $sp_{2,2}^+$ to yield several LISs around 60 eV. The assignment of the particular bright/dark state coupling which gives rise to a particular LIS in the autoionizing region can be very difficult because so little is known about, for example, the dipole matrix elements between the autoionizing states. Our strategy in studying the LIS is to vary the wavelength of the dressing laser and observing how the features move in the delay-dependent spectrogram. The preliminary results from this strategy are very promising and this strategy seems to allow us to assign the bright/dark state couplings that give rise to a particular LIS with high confidence. In addition, we will try and demonstrate a consistent, ab-initio method for extracting the bright/dark state dipole matrix elements from the delay-dependent oscillations in the ATA spectrum. A related goal is to study the intensity dependence of the LIS in the autoionizing region.

Of course true two-electron calculations (in at least five spatial dimensions) are very expensive and so we have also initiated a program, led by a new post-doc, Dr. R. Pazourek and a graduate student Mr. Seth Camp, to study lower-dimensional models of two electron systems. Our goal is to couple these reduced-dimension helium model calculations to the MWE solver to study propagation effects around auto ionizing resonances. Initial testing of the two dimensional, two electron TDSE coupled to the MWE solver are promising and we expect that this will be a major focus in the coming year.

Cited publications

1. M. B. Gaarde *et al.*, Phys. Rev. A **82**, 023401 (2011).
2. S. Chen, et al., Phys. Rev. A **86** 063408 (2012).
3. C. Ott, *et al.*, Science **340** 716 (2013).
4. S. Chen *et al.*, Phys. Rev. A **87**, 013828 (2013).
5. U. van Burck, Hyperfine Interactions 123/124, 483 (1999).
6. A. Kaldun, *et al.*, Phys. Rev. Lett. **112**, 103001 (2014).

Publications supported by this grant:

- R1. A. R. Beck, B. Bernhardt, E. R. Warrick, M. Wu, S. Chen, M. B. Gaarde, K. J. Schafer, D. M. Neumark, and S. R. Leone, *Attosecond transient absorption probing of electronic superpositions of bound states in neon: detecting quantum beats by laser coupling of individual states*, **New Journal of Physics** **16**, 113016 (2015).
- R2. J. Herrmann, M. Lucchini, A. Ludwig, L. Kasmi, L. Gallmann, S. Chen, M. Wu, K. J. Schafer, M. B. Gaarde, and U. Keller, *Multiphoton transitions for delay-zero calibration in attosecond spectroscopy*, **New Journal of Physics** **17**, 013007 (2015).
- R3. C. T. Liao, A. Sandhu, S. Camp, K. J. Schafer, M. B. Gaarde, *Beyond the Single-Atom Response in Absorption Line Shapes: Probing a Dense, Laser-Dressed Helium Gas with Attosecond Pulse Trains*, **Phys. Rev. Lett.** **114**, 143002 (2015).
- R4. M. Reduzzi, J. Hummert, A. Dubrouil, F. Calegari, M. Nisoli, F. Frassetto, L. Poletto, S. Chen, M. Wu, M. B. Gaarde, K. J. Schafer, G. Sansone, *Polarization-control of absorption of virtual dressed-states in helium*, **Phys. Rev. A**, accepted (2015).

- R5. X. Li, D. J. Haxton, M. Gaarde, K. J. Schafer, and C. W. McCurdy, *Direct extraction of intense-field induced polarization in the continuum on the attosecond time scale from transient absorption*, **Phys. Rev. A**, submitted (2015).

Publications in preparation supported by this grant:

- P1. X. Guan, M. Wu, M. B. Gaarde, and K. J. Schafer, *Dressing wavelength dependence of correlated attosecond transient absorption in helium*, in preparation.
- P2. M. Wu, S. Chen, S. Camp, K. J. Schafer, and M. B. Gaarde, *Theory of strong-field attosecond transient absorption*, in preparation for J. Phys. B Invited Topical Review.
- P3. C. T. Liao, A. Sandhu, S. Camp, K. J. Schafer, M. B. Gaarde, *Attosecond Transient Absorption in Dense Gases: Dependence of Lineshapes on Perturbing Laser Pulse Parameters*, in preparation.

Time Resolved High Harmonic Spectroscopy: A Coherently Enhanced Probe of Charge Migration

Science Using Ultrafast Probes: DE-SC0012462

Kenneth Schafer¹, Mette Gaarde¹, Kenneth Lopata¹,
Louis DiMauro², Pierre Agostini², Robert Jones³

1) *Department of Physics and Astronomy, Louisiana State University, Baton Rouge, LA*

2) *Department of Physics, The Ohio State University, Columbus, OH*

3) *Physics Department, University of Virginia, Charlottesville, VA*

Program Scope

Understanding the quantum transport of electrons and holes, and the correlations between them, provides an avenue toward improving the efficiency of chemical processes including energy conversion and catalysis. The relevant electron dynamics evolve on exceedingly fast time scales down to the natural time scale of the electron, the attosecond. For this reason attosecond science has increasingly focused on the possibilities for measuring and controlling correlated electron motion in complex many body systems such as polyatomic molecules as one of the key applications of this new science.

There are two broad motivations for extending the measurement of electron/hole dynamics in chemical systems to the attosecond time scale. The first is the study of electron correlation itself. Though electrons interact on an attosecond time scale, currently measurements are made over much longer time scales, meaning that two and many-electron interactions are averaged over. Attosecond studies open a new perspective on these interactions beyond the mean-field picture and without time-averaging. The second motivation is the study of the earliest phase of charge transfer reactions. These reactions are among the simplest processes in chemistry yet the efficiency with which electrons move around in a molecule is one of the primary regulation mechanisms in biology. As an important example of correlated electron dynamics in many-body systems we will study ultrafast charge migration in complex chemical environments. Charge migration refers to the rapid movement (femtosecond or faster) of positively charged holes in a molecule following localized excitation or ionization.

Attosecond charge migration in molecular systems is thought to be driven by a complex interplay between many-electron correlation effects and dephasing/relaxation due to weak coupling with nuclear motion. Understanding the mechanisms of this migration, and developing experimental tools for observing this process, are crucial to advancing ultrafast science. The objective of the ATTO-CM team is to advance ultrafast science in the US both on small-scale and large-scale facilities using a concerted effort of both theorists and experimentalist solving these problems side by side. Our emphasis is to evaluate high harmonic spectroscopy as a sensitive probe for studying charge migration dynamics in chemical systems by developing a symbiotic relationship between theory and experiment. The initial experimental campaigns will be laboratory based but with the probes maturation will translate onto a large-scale facility, like LCLS, a natural progression for the science.

Recent Progress – LSU Node

The primary goal of the LSU node is to determine the sensitivity of time-resolved HHG as a probe of charge migration in strong-field ionized molecules. With the arrival of Samuel Hernandez from UCLA, the LSU effort comprises one postdoc and one student each in Chemistry and in Physics. The theoretical approach consists of modeling all three steps of the time-resolved high harmonic generation process (ionization, wave packet propagation, and electron/molecule scattering) along with the electron/hole dynamics generated on the ionized molecule. Progress this year has focused on the first-principles ionization and semiclassical wave packet propagation steps, which will form the

foundation for future TR-HHG simulations, both on model systems, and in conjunction with ongoing experimental efforts at OSU and UVa.

First-Principles Ionization Rates: For the ionization step of the process, we have recently developed a time dependent density functional theory (TDDFT) approach which uses a linear combination of atomic orbitals (LCAO) to capture strong-field ionization rates and dynamics in atoms and small molecules. The electronic density matrix is propagated in time with a time-dependent laser potential which drives ionization in the system. A space-dependent, non-Hermitian complex absorbing potential (CAP) is projected onto the atom-centered basis set(s) to remove ionized charge from the simulation. The use of an LCAO scheme enables us to use tuned range-separated functionals (e.g., LC-PBE*), which have the correct asymptotic $-1/r$ form of the potential and to significantly reduce localization errors as compared to traditional pure or hybrid DFT functionals. This prescription gives quantitative agreement with strong-field approximation calculations for simple, well-characterized diatomic molecules (e.g., N_2 in Fig. 1, left panel), it reproduces the experimentally observed ionization anisotropies (Fig. 1, right panel), and it yields molecular orbital ionization mechanisms consistent with previous studies (Fig. 2). Moreover, our atom-centered basis approach also scales to large molecules and is applicable to future core-level ionization dynamics studies, as it does not require the use of pseudo-potentials. Finally, the use of range-separated hybrid functionals is expected to yield improved electron/hole charge migration dynamics on the parent ion, whereas traditional local-density and global hybrid DFT functionals qualitatively fail to capture charge transfer excitations and are thus unsuitable for charge migration.

Wave packet Propagation: In parallel, the LSU node has also been working towards modeling the propagation of the ionized electronic wave packet. To this end we have constructed a classical trajectory Monte Carlo (CTMC) model of strong field ionization, following the general outline of the CTMC-QUEST model. We are in the process of testing this code against published results, both theoretical and experimental. Using large numbers of classical trajectories is computationally efficient even when the laser fields are complex (e.g., multiple driving fields or time-dependent polarizations).

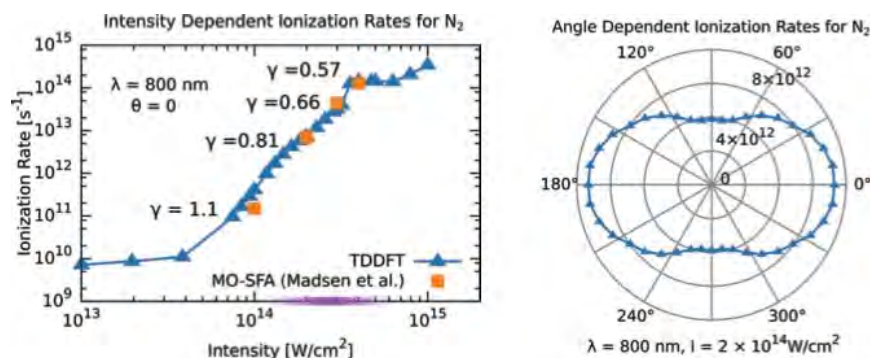


Figure 1: (left panel) Intensity-dependent ionization rates for molecular nitrogen irradiated with 800 nm light polarized parallel to the molecular axis. Tuned range-separated TDDFT (blue triangles) gives quantitative agreement with molecular-orbital strong-field approximation (MO-SFA) rates (orange squares) over the range of intensities relevant to HHG experiments (purple band). (right panel): Ionization rates for molecular nitrogen as a function of angle θ between molecular axis and light polarization. The calculated anisotropy ratio of approximately 2 is consistent with the experimentally observed ionization anisotropy.

Future Plans – LSU Node

Ionization Rates: Next, we will validate the ionization calculations against a wider range of molecules, and begin integrated work with the UVa node to compute the angle-dependent ionization rate calculations on a range of small gas phase molecules. Additionally, we will further elucidate the molecular orbital mechanisms giving rise to the ionization by going beyond a simple MO occupation picture, and instead extract the phase between the various MO channels directly from the time-dependent TDDFT density matrix. These results will then form the basis for future time-dependent scattering calculations.

Wave packet Propagation: Using the CTMC-QUEST code and assigning a quantum phase to each returning trajectory via the classical action, we can construct the returning wave packet. We will normalize the continuum wave packet using ionization rates supplied by the TDDFT simulations. We are also exploring scenarios where the classical position and momentum of the returning trajectories are taken as the peak position and momentum of a Gaussian function, which will allow us to account for the momentum spread of the returning wave packet in a natural way. Our next step will be to put together a benchmark model which includes ionization, wave packet propagation, and recombination out of and in to different molecular orbitals, for instance in N_2 . For now we will use dipole recombination matrix elements from the literature (see below).

Charge Migration and Time-Dependent Scattering Cross Sections: With the arrival of our new LSU postdoc (Samuel Hernandez) we are now ready to begin charge migration calculations by extending our real-time TDDFT ionization simulations to capture electron/hole dynamics via localization functions. Initial studies will validate TDDFT (especially the use of range separated functionals) against previous computational studies of vertical excitation-triggered charge migration in simple molecules, before moving on to ionization-triggered migration. Additionally, we will begin work towards computing the third step of the time-resolved high harmonic generation process, namely the recombination of the photoelectron with a time-dependent (non-stationary) state on the parent ion. The first stage is to compute scattering matrix elements by adapting existing technologies (*e.g.*, multi-channel scattering approaches) to a time-dependent molecular state, before attempting to extend the TDDFT formalism to directly compute the matrix elements from the time-dependent density matrix.

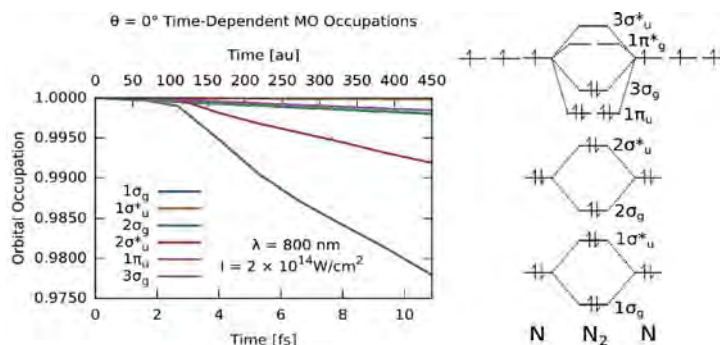


Figure 2: Molecular orbital-dependent ionization rates for on-axis strong field ionization of molecular nitrogen. The dominant contributions come from the HOMO ($3\sigma_g$) and HOMO-2 ($2\sigma_u^*$), which are the two frontier orbitals oriented along the laser polarization.

Publications During the Current Grant Period – LSU Node

A. Sissay, P. Abanador, F. Mauger, M. B. Gaarde, K. J. Schafer, and Kenneth Lopata, “Quantitative Angle-Dependent Strong-Field Molecular Ionization Rates with Tuned Range-Separated Time-Dependent Density Functional Theory”, (in preparation).

F. Mauger, P. Abanador, K. Lopata, M. B. Gaarde, and K. J. Schafer, “Semi-classical wave function perspective on high harmonic generation”, (in preparation).

Recent Progress - OSU Node

At Ohio State a team has been assembled for performing the collaborative experimental program. A 3rd year graduate student, Tim Gorman, started in March 2015 and a post-doc, Tim Scarborough, joined our group on September 1, 2015 from Prof. Zewail group at Caltech. Also, Lou Barreau (graduate student of our collaborator Dr. Pascal Salieres, Saclay) participated in RABBITT measurements at OSU during August 2015.

The emphasis at OSU has been in developing competency in performing two-source high harmonic spectroscopy on molecular systems. The technical aspects that are being addressed include (1) making the RABBITT interferometer achromatic, (2) developing a 1D imaging soft x-ray

spectrometer for the two source interferometry and (3) performing high-resolution RABBITT measurements.

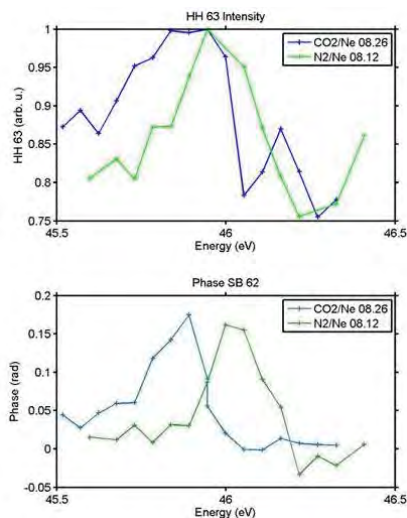


Figure 3: Top is the Fano intensity profile of neon. Each point is acquired by varying the drive wavelength around $1.72 \mu\text{m}$. Bottom is the phase variation around the Fano profile for photon energy 62-times the fundamental. The different traces are taken with N_2 and CO_2 harmonic generation source. Taken by Camper & Barreau at OSU.

detector allows measurements over a broad spectral range while observing the two source interference in the perpendicular direction.

High-resolution RABBITT measurements: In order to perform complementary RABBITT measurements to our two source spectroscopy it is necessary to increase the resolution of our magnetic bottle electron spectrometer (MBES) at high harmonic energies ($> 100 \text{ eV}$). We are implementing retardation field plates into our MBES, similar to our design used on the LCLS MBES.

Future Plans – OSU node

The priority is to implement the two source interferometry in our laboratory by the end of the calendar year. All procurement has been completed for the imaging photon spectrometer. The vacuum chamber is scheduled for delivery in mid-October 2015. This will be followed by final assembly and commissioning. The phase plates needed for producing the two source harmonic scheme are being designed and ordered by Tim Scarborough. We will initially target our design for $1.3 \mu\text{m}$ and $1.8 \mu\text{m}$ experiments. We hope to have the optics by November 2015. The first case study for the two source interferometry will use N_2 since our post-doc, Antoine Camper, performed these studies at $0.8 \mu\text{m}$ as part of his thesis work at Saclay. Of course our work will be performed in the mid-infrared. For these initial studies the OSU group will host student/post-docs from the participating institutions. Lou Barreau will return to Columbus and stay until the end of year. Prof. Jones will also send a UVa student to participate in these initial measurements and coordinate future campaigns. The LSU group will also send a student and a post-doc at this time to OSU for discussions and to become familiar with the experimental metrology. This will be an excellent opportunity for all nodes to exchange ideas and coordinate plans.

Publications During the Current Grant Period – OSU Node

None yet from the OSU node on work supported by this grant.

Achromatic RABBITT: In our N_2 high harmonic spectroscopy (HHS) studies, we have found that resonances play a critical role in identifying dynamical phase effects. This is particular evident using mid-infrared drivers which produce a high density frequency comb. Consequently, we have modified our 2-color interferometer by eliminating chromatic optical elements, e.g. transmission beam splitters, lens. In the current configuration, beam splitters have been replaced by mirrors with designed holes. The HHG generating beam and harmonic radiation transmit through the holes of the beam splitter and combiner. The mid-infrared reference beam is relay imaged as a doughnut mode, thus maximizing delivery of the pulse energy into the RABBITT magnetic bottle spectrometer detector. During Lou Barreau's visit we investigated the new capability to tune the mid-infrared driver near sharp Fano resonances. Tuning the driver around $1.7 \mu\text{m}$ will excite the argon and neon Fano resonance ($\sim 150 \text{ meV}$ width) near 26.6 eV and 45 eV , respectively. Figure 3 shows neon measurements.

1D imaging photon spectrometer: As discussed in the original proposal, we have designed and are assembling a 1D imaging spectrometer. The photon spectrometer can cover an energy range of approximately $15 - 1,240 \text{ eV}$. Two concave variable line spacing gratings (Hitachi) were chosen to cover the entire energy range: $15 - 248 \text{ eV}$ and $248 - 1,240 \text{ eV}$.

The resulting flat field image produced on a MCP/phosphor

Recent Progress - UVa Node

Although delays in receipt of funding meant that we could not bring any personnel onto this project until Summer 2015, progress has been made. First, the molecular beam apparatus that was used previously used to demonstrate THz-induced molecular orientation at a 15 Hz repetition rate [2] has been modified, and moved to a new laboratory, where we hope to soon demonstrate field-free THz orientation at kHz repetition rates. Second, an upgraded 1 kHz Ti:Sapphire amplifier, which will supply sufficient laser energy (~ 5 mJ) for the three beams required to explore THz orientation (pre-alignment, THz generation, and Coulomb explosion probe) has been constructed and will soon be commissioned. Third, we are working to improve the design of our hollow-core-fiber based HHG source, to improve reliability and reproducibility and to enhance the XUV yield. Fourth, we have installed dispersion compensation mirrors to remove high-order chirp from the amplified pulses produced by our Ti:Sapphire laser amplifier. This should allow us to produce shorter pulses from our hollow-core fiber compressor. These will be needed for producing the ~3 fs UV laser pulses which will serve as pump pulses in future charge migration studies. Fifth, preliminary concepts for the ~3fs UV pump source are under consideration.

Future Plans – UVa node

With the anticipated arrival of a post-doc this fall, we hope to begin experiments in earnest. First, we plan to measure the angular-dependence of the strong-field ionization rate for several symmetric and/or asymmetric top molecules. Following Kumarappan *et al.* [3] we will record the ionization yield as a function of the delay between a non-ionizing alignment pulse and the ionizing laser. Using the known rotational constants of the molecule, the experimental ionization rate anisotropies (angularly symmetrized versions for symmetric tops) can be determined from fits to the time-dependent yield. These experimental values will be used to test and benchmark the calculations of angular-dependent strong-field ionization rates performed by members of the LSU team. Second, we will initiate experiments aimed at demonstrating THz orientation of halogenated methanes or other symmetric top molecules of similar size and complexity. Once again, we will plan to measure strong-field ionization rate anisotropies, now with the head vs. tail ambiguity removed, as a test of theory. Third, we intend to explore HHG from aligned halogenated methanes in a hollow-core fiber. Working with the theoretical team at LSU, we hope to quantitatively assess phase-matching as a tool for coherently enhancing the observability of ionization rate anisotropies in molecular gases. Fourth, one student and/or a postdoc will visit OSU for several weeks to prepare for future collaborative experiments involving their mid-infrared lasers and attosecond beamline. Fifth, the UVa postdoc will visit LSU, or LSU postdoc(s) may visit UVa, during the analysis of the ionization rate anisotropy data, to both extract the experimental ionization rates from simulations and compare the experimental and theoretical rates.

Publications During the Current Grant Period – UVa Node

None yet from the UVa node on work supported by this grant.

References

- [1] J. Higuët, H. Ruf, N. Thire, R. Cireasa, E. Constant, E. Cormier, D. Descamps, E. Mevel, S. Petit, B. Pons, Y. Mairesse, and B. Fabre, "High-order harmonic spectroscopy of the Cooper minimum in argon: Experimental and theoretical study," *Phys. Rev. A* **83**, 053401 (2011).
- [2] K. Egodapitiya, Sha Li, and R.R. Jones, "THz Induced Field-Free Orientation of Rotationally Excited Molecules," *Physical Review Letters* **112**, 103002 (2014).
- [3] V. Kumarappan, X. Ren, A.-T. Le, and V. Makhija, "Fully angle-resolved strong-field ionization and dissociation of ethylene from rotational wavepacket dynamics," *Bulletin of the American Physical Society*, DAMOP 2015.

Page is intentionally blank.

Tamar Seideman
Department of Chemistry, Northwestern University
2145 Sheridan Road, Evanston, IL 60208-3113
t-seideman@northwestern.edu

Strong-Field Control in Complex Systems

1. Program Scope

Our AMOS-supported research can be broadly categorized into two related topics: (1) the design and control of complex material system with strong field concepts developed in our earlier AMOS work, including alignment, 3D alignment, torsional alignment and molecular focusing; and (2) the physics, theory, and potential applications of high harmonics generated from aligned molecules. Whereas the first topic is a generalization of the thrust of our original AMOS-supported research, the second has been motivated by the intense interest of the AMOS Program in attosecond science and rescattering electrons physics, and has been carried out in collaboration with AMOS experimentalists colleagues.

Our AMOS-supported research during the past year has focused primarily on the former problem, as summarized in Secs. 2.1–2.8 and includes a theory development project, three collaborative research projects with different experimental laboratories, and four concept development projects. Research in the next year on the problem of strong field coherent control in complex molecular and material systems is discussed in Sec. 3.1. Within the second part of our AMOS-supported research during the past year (2.9), we continued earlier research in collaboration with experimental AMOS colleagues on the problem of ellipticity in harmonic signals. Our plans for further research in the area of attosecond physics and high harmonic generation (HHG) during the next year is outlined in Sec. 3.2. Citations refer to the list of AMOS-supported publications from the Sept. 2013–Aug. 2015 period, Sec. 4.

2. Progress during the past year

2.1 Alignment Thresholds of Molecules

In a recently submitted letter¹ we illustrate and explore the physical origin of a new phenomenon in the adiabatic alignment dynamics of molecules, which is fundamentally interesting and has an important practical implication. Namely, the intensity dependence of the degree of adiabatic alignment exhibits a threshold behavior, below which molecules are isotropically distributed rotationally and above which the alignment is rapidly maximized. Furthermore, we show that the intensity dependence of the alignment of all molecules is universal. Finally, we illustrate that the alignment threshold occurs very generally at a lower intensity than the off-resonance ionization threshold, a numerical observation that is readily explained. This finding illustrates that nonresonant alignment of molecules is a very general method, applicable to all anisotropic molecules. The threshold behavior is attributed to a tunneling mechanism that rapidly switches off at the threshold intensity, where tunneling between the potential wells corresponding to the two orientations of the aligned molecules becomes forbidden.

2.2 Collisional Decoherence and Quasi-Revivals in Asymmetric Tops

In a collaborative research with AMOS colleague Phil Bucksbaum,² recently submitted for publication, we demonstrate the observation of quasi-periodic revivals out to 27 ps in an impulsively-aligned asymmetric-top molecule, sulfur dioxide, at high sample temperature and density. We use a linear birefringence measurement fit to a full quantum simulation of the asymmetric rotor, and are able to separately measure both the population (T1) and coherence

(T2) lifetimes of the rotational wavepacket. Additionally, we observe a high rate of elastic decoherence and attribute this to long-range interactions mediated by the permanent dipole of the SO_2 molecule. We propose the use of birefringence measurements to study intermolecular interactions in a coherent ensemble, as a step toward using field-free alignment to investigate reaction dynamics and dissipative processes.

2.3 Accurate Dynamics from Data with Extreme Timing Uncertainty

Imperfect knowledge of the time-points at which “snapshots” of a system were recorded often degrades our ability to recover dynamical information, and can even scramble the sequence of events. In collaboration with AMOS colleague Abbas Ourmazd, we present in a submitted publication³ a data-analytical approach based on machine-learning, which is capable of recovering accurate histories and dynamics from noisy snapshots recorded at extremely uncertain time points. The power of the approach is demonstrated by extracting novel dynamical information on the few-femtosecond timescale from noisy experimental XFEL data recorded with 300 fs timing uncertainty. This capability far exceeds what was previously thought possible, with potentially wide impact whenever dynamical or historical information is tainted by timing uncertainty.

2.4 Laser Alignment and Orientation of Semiconductor Nanorods

Semiconductor nanorods have a large variety of potential applications, ranging from solar cells to bio-sensors. Orientational order is important for all these applications. In a recently published article,⁴ we present the results of molecular dynamics simulations of semiconductor nanorods aligning and orienting under the combined influence of static electric and laser fields. The transformation of the isotropic ensemble into an orientationally ordered assembly is a slow (microseconds) process, but in sharp contrast to previously oriented systems yields high levels of both alignment and orientation at elevated temperatures (300 K) and rather low fields (1.4 GWcm^{-2} laser intensity and 2–4 $\text{V}\mu\text{m}^{-1}$ static field amplitude). The resulting long range orientational order could serve to control the electric, magnetic and mechanical properties of the nanorods assembly and hence assist several of its applications.

2.5 Time-Dependent, Optically-Controlled Dielectric Function

Plasmon resonances associated with metal nano-constructs, with their vast variety of applications, are sensitive to the dielectric function of the medium. In 5 we suggest optical modulation of the refractive index of a molecular monolayer adsorbed on a metal surface as a potential means of controlling plasmon resonance phenomena. The refractive index is altered using a laser pulse of moderate intensity and linear polarization to align the constituent molecules. Time-dependent, optically-controlled dielectric function is illustrated by molecular dynamics calculations.

2.6 Wigner Representation of the Rotational Dynamics of Rigid Tops

The broad rotational wavepackets associated with aligned molecules become increasingly difficult to compute quantum mechanically as the system complexity grows. Semiclassical methods make an attractive alternative that can also yield useful insight. In 6 we propose a methodology to design Wigner representations in phase spaces with nontrivial topology having evolution equations with desired mathematical properties. As an illustration, two representations of molecular rotations are developed to facilitate the analysis of laser-assisted molecular alignment, diagnostics of reaction dynamics, studies of scattering and dissipative processes.

2.7 Strong Field Coherent Control of Molecular Torsions. Analytical Models

The concept of torsional alignment, introduced in our earlier AMOS-supported research, introduces a wide variety of potential applications along with several interesting phenomena. In addition, it offers analytically soluble limits that are pedagogically useful and also assist the design

of future experiments. The latter feature is illustrated in a recent publication⁷ that introduces analytical models of torsional alignment applicable to the limiting cases of the torsional barrier heights. Using these models, we explore the role that the laser intensity and pulse duration play in coherent torsional dynamics. We also investigate several interesting torsional phenomena, including the onset of impulsive alignment of torsions, field-driven oscillations in quantum number space, and the disappearance of an alignment upper bound observed for a rigid rotor in the impulsive torsional alignment limit.

An ongoing study extends the torsional alignment concept to the case of multiple torsion angles. The latter exhibit new phenomena, including interesting chirality properties and strongly enhanced dependence of the electronic coupling on the alignment field as compared to the dimer case.

2.8 Unidirectional Electron Transfer via Torsional Control

One of the applications of torsional alignment (item 2.7) is explored in a recently submitted manuscript⁸ in collaboration with an experimental Northwestern group focused on charge transport. Specifically we suggest an approach to enhance forward electron transfer while suppressing backward electron transfer with its consequent undesired recombination events. The scheme is based on the vast laser enhancement of the electronic coupling in donor-bridge-acceptor systems where the bridging molecule exhibits one or more torsional modes. It suggests the usefulness of torsional alignment as a method to reduce undesired electron-hole recombination in applications such as solar cells and catalysis.

2.9 Ultrafast Elliptical Dichroism in High-Order Harmonics

Molecules illuminated by an elliptically polarized, high intensity laser field emit elliptically polarized high-order harmonics. In a submitted article⁹, we discuss collaborative experimental and theoretical work with AMOS colleagues Murnane and Kapteyn, where surprising experimental observations of ultrafast elliptical dichroism in the harmonic emission as the ellipticity of the driving field and the molecular alignment are scanned are explained and generalized. To that end we develop a simple model in which both the collision angle of the continuum electron with the molecule and the interference between recombination at multiple charge centers play a role. Our analysis ties the observed elliptical dichroism to the journey of the continuum electron in the field and the underlying bound state of the molecular ion. These results show how to use molecular structure and alignment to manipulate the polarization state of high-order harmonics, and also present a potential new attosecond probe of the underlying molecular system. .

3. Future Plans

3.1 Strong Field Coherent Control in Complex Material and Molecular Systems

1. An experimental realization of an ultrafast, nanoscale electron switch based on laser orientation of an organic molecule adsorbed onto a silicon surface and subject to a metal tip, which was proposed in our earlier AMOS-supported work, was recently initiated by the groups of Stelios Tzortzakis and Maria Vamvakaki in Greece. We will collaborate with the experimental groups by carrying out calculations to assist the design of the molecule and the interpretation of the results.
2. We will extend our torsional alignment research to the case of an adsorbed assembly of biphenyl derivatives. Here we expect to observe correlated torsional alignment as well as locking of the molecules in the torsionally-aligned configuration after the pulse turn-off through chemical interactions.

3. In collaboration with the group of AMOS colleague Phil Bucksbaum, we will explore the orientation of water molecules by half-cycle pulses. This work will continue our (already fruit bearing) collaborative efforts to unravel the quantum dynamics of the asymmetric top and their correlation to its classically unstable motion.

3.2: The physics, Numerical Methodology and Applications of High Harmonics from Aligned Molecules

A goal of future research, which will hopefully be largely accomplished within the next year, is to develop an approach for accurate modeling of the continuum electronic wavefunction underlying harmonic signals and combine it with our rotational theory of HHG. Our approach will be based on time-dependent density functional theory, currently being tested in our group. The method will be first applied to linear systems, but my main interest is in the case of 3D aligned (e.g., by means of an elliptically polarized field) asymmetric top molecules as targets for the recolliding continuum electron. These I expect to allow both a new view of the electronic structure and dynamics in complex polyatomic molecules and a new and interesting approach to probe the (classically unstable) rotations of asymmetric tops in the fully quantum domain.

4. Publications from DOE sponsored research(9/13–8/15, in citation order)

1. J. E. Szekely and T. Seideman, *Alignment Thresholds of Molecules*, submitted for publication in Phys. Rev. Lett.
2. I. F. Tenney, M. Artamonov, T. Seideman and P. H. Bucksbaum, *Collisional Decoherence and Rotational Quasi-Revivals in Asymmetric-Top Molecules*, submitted for publication in Phys. Rev. A.
3. R. Fung, S. Ramakrishna, T. Seideman, R. Santra and A. Ourmazd, *Accurate Dynamical Histories From Data with Extreme Timing Uncertainty*, submitted for publication in Nature
4. M. Artamonov and T. Seideman, *Alignment and Orientation of Semiconductor Nanorods with a Combination of Static and Laser Fields*, submitted for publication in NanoLett.
5. M. Artamonov and T. Seideman, *Time-Dependent, Optically-Controlled Dielectric Function*, J. Phys. Chem. Lett. **6**, 320-325 (2015).
6. D. V. Zhdanov and T. Seideman, *Wigner Representation of the Rotational Dynamics of Rigid Tops*, Phys. Rev. A. **92**, 012129, (2015).
7. B. A. Ashwell, S. Ramakrishna, and T. Seideman, *Strong Field Coherent Control of Molecular Torsions - Analytical Models*, J. Chem. Phys. **143**, 064307, (2015).
8. B. A. Ashwell, A. M. Rasmussen, E. A. Weiss and T. Seideman, *Unidirectional Electron Transfer via Torsional Control*, submitted for publication.
9. P. A. J. Sherratt, R. M. Lock, X. Zhou, H. C. Kapteyn, M. M. Murnane, and T. Seideman, *Ultra-fast Elliptical Dichroism in High-Order Harmonics as a Probe of Molecular Structure and Electron Dynamics*, submitted for publication in Phys. Rev. Lett.
10. L. S. Spector, M. Artamonov, S. Miyabe, Todd Martinez, T. Seideman, M. Guehr, and P. H. Bucksbaum, *Axis-dependence of molecular high harmonic emission in three dimensions*, Nature Communications **5**, 3190 (2013).
11. J. Wu, X. Gong, M. Kunitski, L. Ph. H. Schmidt, T. Jahnke, A. Czasch, T. Seideman, and R. Dorner, *Sequencing Strong Field Multiple Ionization of a Multicenter Multibond Molecular System*, Phys. Rev. Lett. **111**, 083003 (2013)
12. S. M. Parker, M. Smeu, I. Franco, M. A. Ratner, and T. Seideman, *Molecular Junctions: Can Pulling Influence Optical Controllability?*, NanoLett. **14**, 4587 (2014).
13. B. Ashwell, S. Ramakrishna and T. Seideman, *Laser-Driven Torsional Coherences*, J. Chem. Phys. **138**, 044310 (2013).
14. B. Ashwell, S. Ramakrishna and T. Seideman, *Dissipative Dynamics of Laser-Induced Torsional Coherences*, Special Issue of J. Phys. Chem. C **117**, 22391 (2013) (**invited**).

Inelastic X-ray Scattering Under Extreme and Transitional Conditions

Gerald T. Seidler, seidler@uw.edu,
Department of Physics
University of Washington
Seattle, WA 98195-1560

Program Scope

The goal of this program is to expand the scope and scientific potential of advanced x-ray spectroscopies, including x-ray absorption fine structure (XAFS), x-ray emission spectroscopy (XES), and time-resolved inelastic x-ray scattering (IXS). During the term of this award this effort has had several notable accomplishments, including: new insight into the energy transfer mechanisms of lanthanide-based phosphors and related luminescent materials; new theoretical and experimental methods for the study of dense plasmas, such as in the transitional, ‘warm dense matter’ regime; improved instrumentation and resulting strong collaborations focused on the time-dynamics of energy transfer in photosynthetic proteins and on the f-electron physics of lanthanide elements and compounds at high pressures; and a rejuvenation of laboratory-based XAFS and XES. This latter development is allowing for a broad range of XAFS studies in contemporary energy sciences and for new fundamental investigations of excitonic and multi-electron effects via coupled XAFS and XES studies. It is anticipated that the technology developed under this award will soon be licensed to a local startup whose mission is to enable and enlarge the community of scientists and engineers who already use or who could benefit from advanced x-ray spectroscopies.

Selected Recent Progress and Future Directions

I. A Rejuvenation of Laboratory-based High-Resolution X-ray Spectroscopies

In October 2013 we commissioned a new type of inexpensive lab-based spectrometer for high-resolution x-ray studies, including x-ray absorption fine structure (XAFS) and x-ray emission spectroscopy (XES). The startling performance of this modest instrument [Seidler, et al, RSI 2014] has garnered significant interest that, we emphasize, has been solely focused on DOE-priority research issues and that does not have the character of competition with synchrotron facilities. In addition to providing a true introductory capability that can help attract and educate entire new user communities, laboratory-based XAFS enables measurements that, for reasons of long duration, sample preparation complexity, chemical hazards, or radioisotope hazards, cannot be performed with regularity or certainty at synchrotron light sources. To this end, under funding from the University of Washington, we have used the technology developed under support from this award to build a mid-scale lab XAFS user facility for the UW Clean Energy Institute (CEI), with a highest emphasis on *in situ* battery studies. Commissioning is proceeding well, and all performance milestones for flux and energy resolution have been achieved. It is anticipated that the technology developed under this award will soon be licensed to a new start-up, *easyXAFS LLC*, that is dedicated to broadly increasing access to XAFS and XES. This goal is especially important given the decrease in ‘routine’ XAFS capability in the US after the closing of NSLS-I and also given the steadily increasing importance of XAFS in electrical energy storage research.

From the fundamental perspective, these lab instruments demonstrate some capabilities that are difficult to replicate at synchrotron beamlines. In Figures 1 and 2 we present a recent

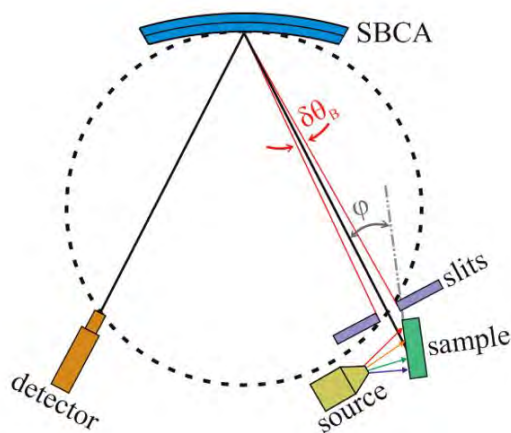


Figure 1 [From Mortensen, et al, 2015]. The lab-based Rowland-circle spectrometer. The slits in front of the sample constrain the angular width ($\delta\theta_B$) probed by the analyzer which improves energy resolution and reproducibility. The sample is slightly rotated (φ) to improve line-of-sight to the SBCA.

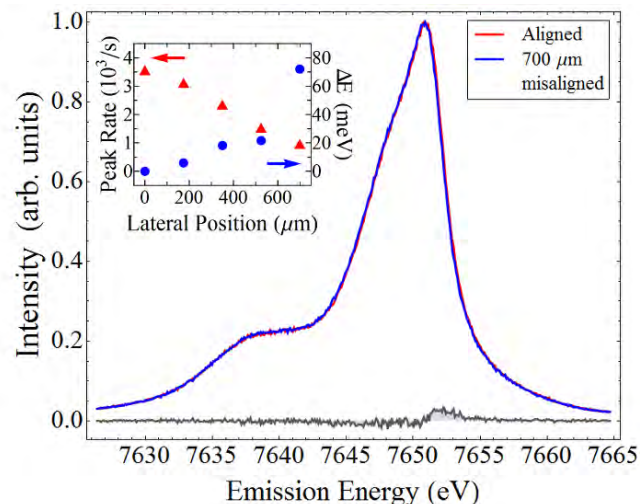


Figure 2. [From Mortensen, et al., 2015] Peak-intensity normalized CoO K β spectra measured at the aligned and the extreme misaligned location. The gray curve shows the residual between the two spectra. Inset: the peak count rate and energy shift as a function of lateral sample position.

instrument modification that results in an exceptional energy-scale stability of better than 20 meV between different samples. This same stability of energy calibration extends to XANES studies and to the consistency between XANES and XES studies with the low-powered spectrometer. This allows for unique studies of excitonic (core hole) effects, see Fig. 3.

II. X-ray Heating Studies at LCLS/MEC

The recent LD67 campaign at LCLS/MEC was led by the PI. While this beamrun emphasized laser-shock heating of multicomponent targets (supported by a grant from DOE/FES), complementary x-ray heating experiments were also performed as part of the WDM research under the present award. The results are still under analysis, but show interesting effects in the electronic structure of metallic and more complex intermediate-Z alloys and compounds. For example, the ability to compare response across multiple intermediate-Z species in alloys will allow a detailed interrogation of the correct theoretical treatment of the electronic structure of isochorically heated matter. Ideas spawned from the results of the LD67 campaign led to the successful beamtime proposal LK20, also led by the PI, that will investigate new x-ray heating target designs and their use in two-color x-ray studies aimed at testing finite-T treatments of density functional theory.

III. Time-resolved Studies of Energy Transfer and Electron Correlations

Lanthanide compounds and coordination complexes are responsible for a wide range of light-gathering and light-emitting applications, including as commercial phosphors in lighting applications, as tools to better match the solar spectrum to the function of photovoltaic devices, and as a critical component in many bioassays. In this lattermost role, an organic ‘antenna’ acts as a strong near-UV photoabsorber before nonradiatively transferring energy to a chelated,

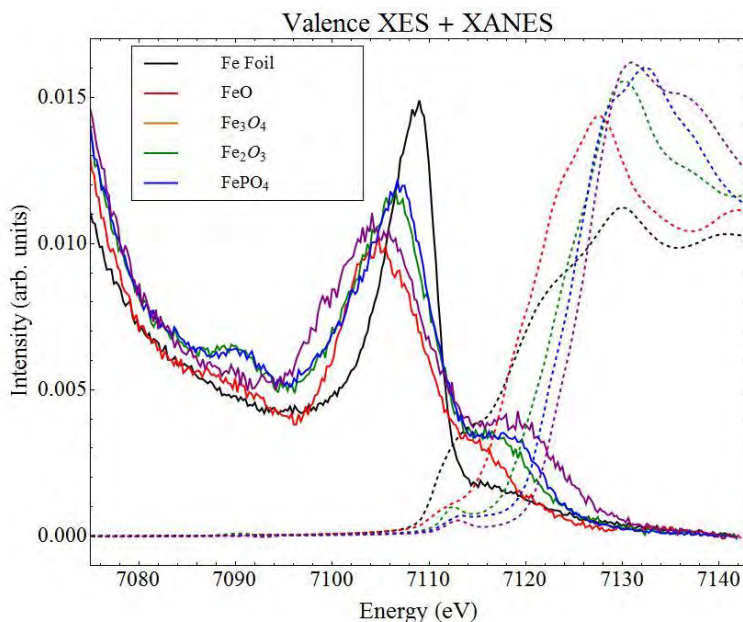


Figure 3: [From Mortensen, et al., *in prep* 2015] XES and XANES on the same energy scale, to a precision of ~ 20 meV. These results will allow new tests of the theoretical treatment of excitonic (core-hole) effects on XANES spectra. The apparently above-Fermi-level emission is due to multi-electron effects.

trivalent lanthanide ion via a 4f-4f intrashell excitation. This dipole-forbidden excitation subsequently decays through the so-called ‘hypersensitive’ pseudo-quadrupolar decay, giving light at delays of order msec after the initial excitation due to the long lifetime for the 4f excitation. This long time-delay allows simplest time-gate filtering of the emission from the luminescent lanthanide complex from that of the host biological system.

The microscopic physics underlying each step in the energy transfer pathway in the luminescent lanthanides remain incompletely understood. Our recent work at the Advanced Photon Source on luminescent lanthanide complexes demonstrate an unexpected, but clear expression of the 4f intrashell excitation in the time-resolved x-ray absorption near-edge spectrum (XANES) of the lanthanide ion.[Pacold, et al., JACS 2014] Our leading explanation requires a surprisingly dynamic coupling between the 4f and 5d orbitals of the lanthanide ion. In any event, this discovery opens up new opportunities to use the LCLS to directly monitor the energy transfer onto the lanthanide species, giving an important complement to studies of the de-excitation of multiple ligand states by transient optical absorption. We have recently extended this project with time-resolved x-ray excited optical luminescence (TR-XEOL) studies performed at the Advanced Photon Source. The high flux-density of the 20-ID microprobe endstation allowed us to reach a nonlinear XEOL regime where the time scales for different steps in the energy relaxation cascade in Bi-sensitized $\text{Y}_2\text{O}_3:\text{Eu}$ phosphors can be separated. A manuscript is in preparation.

Manuscripts and Publications in the Last 3 Years of this Award

1. G.T. Seidler, D.R. Mortensen, A. Ditter, N. Ball, and A. Remesnik, “A Modern Laboratory XAFS Cookbook,” *submitted*, Journal of Physics: Conference Series (2015).
2. D.R. Mortensen, P. Glatzel, G.T. Seidler, “Benchtop Nonresonant X-ray Emission Spectroscopy: Coming Soon to Laboratories and Beamlines Near You,” *submitted*, Journal of Physics: Conference Series (2015).
3. M.J. Lipp, J.R. Jeffries, J.-H. Park Klepies, W.J. Evans, D.R. Mortensen, G.T. Seidler, Y. Xiao, and P. Chow, “4f-electron behavior in the cerium oxides Ce_2O_3 and CeO_2 under pressure,” *submitted*, Phys. Rev. B (2015).

4. Katherine M. Davis, Brendan T. Sullivan, Mark Palenik, Lifan Yan, Vatsal Purohit, Gregory Robison, Irina Kosheleva, Robert W. Henning, Gerald T. Seidler, Yulia Pushkar, "rapid Evolution of the Photosystem II Electronic Structure during Water Splitting," *submitted*, Science (2015).
5. K. Davis, M. Palenik, Lifan Yan, P.F. Smith, G.T. Seidler, G.C. Dismukes, Y. Pushkar, "X-ray emission spectroscopy of Mn coordination complexes towards interpreting the electronic structure of the Oxygen Evolving Complex of Photosystem II," *submitted*, Chemical Communications (2015).
6. Oliver R. Hoidn and Gerald T. Seidler, "A Tender X-ray Camera Based on Mass Produced CMOS Sensors and Single-Board Computers," Review of Scientific Instruments **86**, 086107 (2015).
7. Brian A. Mattern, Gerald T. Seidler, Joshua J. Kas, "Condensed Phase Effects on the Electronic Momentum Distribution in the Warm Dense Matter Regime," *submitted*, Physical Review Letters (2013).
8. G.T. Seidler, D.R. Mortensen, A.J. Remesnik, et al., "A Laboratory-based Hard X-ray Monochromator for High-Resolution X-ray Emission Spectroscopy and X-ray Absorption Near Edge Structure Measurements," Review of Scientific Instruments **85**, 113906 (2014).
9. M.J. Lipp, D.R. Mortensen, H. Cynn, W.J. Evans, G.T. Seidler, Y. Xiao, P. Chow, "4f moment and magnetic susceptibility of cerium under pressure: Comparison with lanthanum and CeO₂," *submitted* Journal of Physics: Condensed Matter (2014).
10. Matthew Gliboff, Dana Sulas, Dennis Nordlund, *et al.*, "Direct Measurement of Acceptor Group Localization on Donor-Accepted Polymers using Resonant Auger Spectroscopy," Journal of Physical Chemistry C **118**, 5570 (2014).
11. Joseph I. Pacold, David S. Tatum, Gerald T. Seidler, et al., "Direct Observation of 4f Intrashell Excitation in Luminescent Lanthanide Complexes by Time-Resolved X-ray Absorption Near Edge Spectroscopy," Journal of the American Chemical Society **136**, 4186 (2014).
12. D.R. Mortensen, G.T. Seidler, J.A. Bradley, M.J. Lipp, W.J. Evans, P. Chow, Y.-M. Xiao, G. Boman, and M.E. Bowden, "A Versatile Medium-Resolution X-ray Emission Spectrometer for Diamond Anvil Cell Applications," Review of Scientific Instruments **84**, 083908 (2013).
13. Steven D. Conradson, *et al.*, "Bose condensate-type behavior from a collective excitation in the chemically and optically doped Mott-Hubbard system, UO_{2+x}," Physical Review B **88**, 115135 (2013).
14. K.M. Davis, I. Kosheleva, R.W. Henning, G.T. Seidler, Y. Pushkar, "Kinetic Modeling of the X-ray-induced Damage to a Metalloprotein," Journal of Physical Chemistry B **117**, 9161 (2013).
15. Matthew Gliboff, Hong Li, Kristina M. Kneeting, Anthony J. Giordano, Dennis Nordlund, Gerald T. Seidler, Jean-Luc Bredas, Seth R. Marder, and David S. Ginger, "Competing Effects of Fluorination on the Orientation of Aromatic and Aliphatic Phosphonic Acid Monolayers on ITO," Journal of Physical Chemistry C **117**, 15139 (2013).
16. Matthew Gliboff, Lingzi Sang, Kristina M. Kneeting, *et al.*, "Orientation and Order of Phenylphosphonic Acid Self-assembled Monolayers on Transparent Conductive Oxides: A Combined NEXAFS, PM-IRRAS and DFT Study," Langmuir **29**, 2166 (2013).
17. Stefan G. Minasian, *et al.*, "Covalency in Metal–Oxygen Multiple Bonds Evaluated Using Oxygen K-edge Spectroscopy and Electronic Structure Theory", J. American Chemical Society **135**, 1864 (2013).
18. Brian A. Mattern and Gerald T. Seidler, "Theoretical Treatments of the Bound-Free Contribution and Experimental Best Practice in X-ray Thomson Scattering from Warm Dense Matter," Physics of Plasmas **20**, 022706 (2013).
19. S.M. Heald, G.T. Seidler, D. Mortensen, B. Mattern, J.A. Bradley, N. Hess, M. Bowden, "Recent Tests of X-ray Spectrometers Using Polycapillary Optics," in Advances in X-Ray/EUV Optics and Components VII, edited by Shunji Goto, Christian Morawe, Ali M. Khounsary, Proc. of SPIE Vol. 8502 (2012), article number 85020I.
20. K.M. Davis, B.A. Mattern, J.I. Pacold, T. Zakharova, D. Brewé, I. Kosheleva, R.W. Henning, T.J. Graber, S.M. Heald, G.T. Seidler, Y. Pushkar, "Fast Detection Allowing Analysis of Metalloprotein Electronic Structure by X-ray Emission Spectroscopy at Room Temperature," Journal of Physical Chemistry Letters **3**, 1858 (2012).
21. B.A. Mattern, G.T. Seidler, J.J. Kas, J.I. Pacold, J.J. Rehr, "Real-Space Green's Function Calculation of Compton Profiles," Phys. Rev. B **85**, 115135 (2012).

DYNAMICS OF FEW-BODY ATOMIC PROCESSES

Anthony F. Starace, P.I.

*The University of Nebraska, Department of Physics and Astronomy
855 North 16th Street, 208 Jorgensen Hall, Lincoln, NE 68588-0299*

Email: astarace1@unl.edu

PROGRAM SCOPE

The goals of this project are to understand, describe, control, and image processes involving energy transfers from intense electromagnetic radiation to matter as well as the time-dependent dynamics of interacting few-body, quantum systems. Investigations of current interest are in the areas of strong field (intense laser) physics, attosecond physics, high energy density physics, and multiphoton ionization processes. Nearly all proposed projects require large-scale numerical computations, involving, e.g., the direct solution of the full-dimensional time-dependent or time-independent Schrödinger equation for two-electron (or multi-electron) systems interacting with electromagnetic radiation. In some cases our studies are supportive of and/or have been stimulated by experimental work carried out by other investigators funded by the DOE AMOS physics program. Principal benefits and outcomes of this research are improved understanding of how to control atomic processes with electromagnetic radiation and how to transfer energy optimally from electromagnetic radiation to matter.

RECENT PROGRESS

A. Asymmetries in Production of $\text{He}^+(n=2)$ with an Intense Few-Cycle Attosecond Pulse

By solving the two-electron time-dependent Schrödinger equation, we studied carrier-envelope-phase (CEP) effects on ionization plus excitation of He to $\text{He}^+(n=2)$ states by a few-cycle attosecond pulse with a carrier frequency of 51 eV. For most CEPs the asymmetries in the photoelectron angular distributions with excitation of $\text{He}^+(2s)$ or $\text{He}^+(2p)$ have opposite signs and are two orders of magnitude larger than for ionization without excitation. These results indicate that attosecond pulse CEP effects may be significantly amplified in correlated two-electron ionization processes. (*See reference [3] in the publication list below.*)

B. Carrier-Envelope-Phase-Induced Asymmetries in Double Photoionization of He by an Intense Few-Cycle XUV Pulse

The carrier-envelope-phase (CEP) dependence of electron angular distributions in double ionization of He by an arbitrarily-polarized, few-cycle, intense XUV pulse is formulated using perturbation theory in the pulse amplitude. Owing to the broad pulse bandwidth, interference of first and second order perturbation amplitudes produces asymmetric angular distributions that are sensitive to the CEP. Our perturbation theory parametrization is shown to be valid by comparing with results of solutions of the full-dimensional, two-electron time-dependent Schrödinger equation for the case of linear polarization. (*See reference [4] in the publication list below.*)

C. High-Order Harmonic Generation of Be in the Multiphoton Regime

The high-order harmonic generation (HHG) spectrum of Be is investigated in the multiphoton regime by solving the full-dimensional, two-active-electron, time-dependent Schrödinger equation in an intense (10^{13} W/cm²), 30-cycle laser field. As the laser frequency ω_L varies from 1.7 to 1.8 eV (which is in the tunable range of a Ti:sapphire laser), the 7th harmonic becomes resonant sequentially with the transition between the ground state and two doubly-excited autoionizing states while the 3rd harmonic becomes resonant with the 2s2p(¹P) singly-excited state. At each resonant frequency, the HHG power spectrum increases by an order of magnitude over a range of harmonics that form a plateau, extending from the resonant harmonic up to a cutoff at the 25th harmonic. In contrast to the well-known rescattering plateau cutoff law appropriate in the tunneling regime (which predicts a cutoff at the 5th or 7th harmonic), the multiphoton regime plateau we find for Be originates from atomic resonance effects. Off-resonance, the Be HHG spectrum decreases monotonically with harmonic order. By taking the ratio of the integrated harmonic power of the 7th harmonic to that of the 5th harmonic, one can isolate the resonant effects of the two doubly-excited states in the HHG spectrum from those of singly-excited resonance states. These ratios exhibit resonance profiles for driving laser pulse durations much longer than the lifetimes of these autoionizing states. The energy widths of these resonance features are comparable to the widths of the laser pulse and are much smaller than the autoionizing state widths. These results demonstrate an important role for electron correlations in enhancing harmonic generation rates in the multiphoton regime. (*See reference [5] below.*)

D. Potential Barrier Features in Three-Photon Ionization Processes in Atoms

Resonance-like enhancements of generalized three-photon cross sections for XUV ionization of Ar, Kr, and Xe have been demonstrated and analyzed within a single-active-electron, central-potential model. The resonant-like behavior is shown to originate from the potential barriers experienced by intermediate- and final-state photoelectron wave packets corresponding to absorption of one, two, or three photons. The resonance-like profiles in the generalized three-photon ionization cross sections are shown to be similar to those found in the generalized two-photon ionization cross sections [*Phys. Rev. A* **82**, 053414 (2010)]. The complexity of Cooper minima in multiphoton ionization processes is also discussed. Owing to the similar resonance-like profiles found in both two- and three-photon generalized cross sections, we expect such potential barrier effects to be general features of multiphoton ionization processes in most atoms with occupied *p*- and *d*-subshells. (*See reference [6] in the publication list below.*)

E. Nonlinear dichroism in back-to-back double ionization of He by an intense elliptically-polarized few-cycle XUV pulse

We have predicted a new dynamical effect observable in double photoionization of the He atom by an elliptically-polarized, ultrashort laser pulse: nonlinear dichroism (ND). The ND effect is exquisitely sensitive not only to electron correlations, but also to the temporal duration, the polarization, and the carrier-envelope phase (CEP) of a laser pulse. This new effect thus permits one to explore electron correlations on their natural time scale (in the case of attosecond XUV pulses), providing both dynamical and phase information on the double photoionization amplitudes involved. It also provides a new means for experiment to characterize the duration,

the polarization, and the CEP of ultrashort (attosecond) XUV pulses. Measurement of this predicted ND effect requires more intense attosecond pulses than are available currently, but great strides are being made to increase the intensity of attosecond pulses. Finally, our predictions have required us to develop theoretical tools to solve the full six-dimensional problem of the interaction of the fundamental two-electron He atom with an ultrashort, elliptically-polarized attosecond pulse. (*See reference [7] in the publication list below.*)

F. Electron Vortices in Photoionization by Circularly-Polarized Attosecond Pulses

Single ionization of He by two oppositely circularly-polarized, time-delayed attosecond pulses is shown to produce photoelectron momentum distributions in the polarization plane having helical vortex structures sensitive to the time-delay between the pulses, their relative phase, and their handedness. The matter-wave vortex patterns we predict have a counterpart in optics, in which similar vortex patterns have been produced by interference of particular kinds of laser beams. However, such vortices have never before been either observed or predicted by interference of electron matter waves. *We thus have here a dramatic example of wave-particle duality.* Results are obtained by both *ab initio* numerical solution of the two-electron time-dependent Schrödinger equation and by a lowest-order perturbation theory analysis. The energy, bandwidth, and temporal duration of attosecond pulses are ideal for observing these vortex patterns. In particular, attosecond pulse durations are required to observe the momentum space vortex patterns we predict. Our results indicate the exquisite sensitivity of the spiral vortex patterns to both the properties of the two laser pulses and the time-delay between them, thus indicating (i) that this is a new means to control electron motion with laser pulses and (ii) that this process provides a new diagnostic tool for characterizing the laser pulses and for determining the delay between them. (*See reference [8] in the publication list below.*)

G. Favorable target positions for intense laser acceleration of electrons in hydrogen-like, highly-charged ions

Classical relativistic Monte Carlo simulations of petawatt laser acceleration of electrons bound initially in hydrogen-like, highly-charged ions show that both the angles and energies of the laser-accelerated electrons depend on the initial ion positions with respect to the laser focus. Electrons bound in ions located after the laser focus generally acquire higher (\approx GeV) energies and are ejected at smaller angles with respect to the laser beam. Our simulations assume a tightly-focused linearly-polarized laser pulse with intensity of $\approx 10^{22}$ W/cm². Up to fifth order corrections to the paraxial approximation of the laser field in the focal region are taken into account. In addition to the laser intensity, the Rayleigh length in the focal region is shown to play a significant role in maximizing the final energy of the accelerated electrons. Results are presented for both Ne⁹⁺ and Ar¹⁷⁺ target ions. (*See reference [9] in the publication list below.*)

FUTURE PLANS

Our group is currently carrying out research on the following additional projects:

- We are investigating higher-order Fermat spiral vortices in single ionization of the He atom by oppositely circularly-polarized and time-delayed attosecond laser pulses.

- We are investigating the efficient production of high-energy bremsstrahlung photons and their control by means of external laser pulse fields.
- We are investigating the use of helical laser beams to accelerate electrons bound in highly-charged ions to GeV energies.
- We are investigating resonant harmonic generation with chirped laser pulses, using the chirp as a means to be on resonance with doubly-excited states of two-electron atoms such as He and Be.

PUBLICATIONS STEMMING FROM DOE-SPONSORED RESEARCH (2012 – 2015)

- [1] M.V. Frolov, D.V. Knyazeva, N.L. Manakov, A.M. Popov, O.V. Tikhonova, E.A. Volkova, M.-H. Xu, L.-Y. Peng, and A.F. Starace, “Validity of Factorization of the High-Energy Photoelectron Yield in Above-Threshold Ionization of an Atom by a Short Laser Pulse,” *Phys. Rev. Lett.* **108**, 213002 (2012).
- [2] J.M. Ngoko Djiokap, S.X. Hu, W.-C. Jiang, L.-Y. Peng, and A.F. Starace, “Enhanced Asymmetry in Few-Cycle Attosecond Pulse Ionization of He in the Vicinity of Autoionizing Resonances,” *New J. Phys.* **14**, 095010 (2012). [*Published in the Focus Issue on “Correlation Effects in Radiation Fields.”*]
- [3] J.M. Ngoko Djiokap, S.X. Hu, W.-C. Jiang, L.-Y. Peng, and A.F. Starace, “Asymmetries in Production of $\text{He}^+(n=2)$ with an Intense Few-Cycle Attosecond Pulse,” *Phys. Rev. A* **88**, 011401(R) (2013).
- [4] J.M. Ngoko Djiokap, N.L. Manakov, A.V. Meremianin, and A.F. Starace, “Carrier-Envelope-Phase-Induced Asymmetries in Double Photoionization of He by an Intense Few-Cycle XUV Pulse,” *Phys. Rev. A* **88**, 053411 (2013).
- [5] J.M. Ngoko Djiokap and A.F. Starace, “Resonant Enhancement of the Harmonic Generation Spectrum of Beryllium,” *Phys. Rev. A* **88**, 053412 (2013).
- [6] L.-W. Pi and A.F. Starace, “Potential Barrier Effects in Three-Photon Ionization Processes,” *Phys. Rev. A* **90**, 023403 (2014).
- [7] J.M. Ngoko Djiokap, N.L. Manakov, A.V. Meremianin, S.X. Hu, L.B. Madsen, and A.F. Starace, “Nonlinear dichroism in back-to-back double ionization of He by an intense elliptically-polarized few-cycle XUV pulse,” *Phys. Rev. Lett.* **113**, 223002 (2014). [*This Letter was featured in the February 2015 issue of Photonics Spectra (p. 32); the online version appears here: <http://www.photonics.com/Article.aspx?PID=5&VID=125&IID=801&Tag=Tech+Pulse&AID=56939>]*
- [8] J.M. Ngoko Djiokap, S.X. Hu, L.B. Madsen, N.L. Manakov, A.V. Meremianin, and A.F. Starace, “Electron Vortices in Photoionization by Circularly Polarized Attosecond Pulses,” *Phys. Rev. Lett.* **115**, 113004 (2015). *This work was featured on the cover of the 11 September 2015 issue of Physical Review Letters.*
- [9] L.-W. Pi, S.X. Hu, and A.F. Starace, “Favorable Target Positions for Intense Laser Acceleration of Electrons in Hydrogen-Like, Highly-Charged Ions,” *Phys. Plasmas* **22**, 093111 (2015).

FEMTOSECOND AND ATTOSECOND LASER-PULSE ENERGY TRANSFORMATION AND CONCENTRATION IN NANOSTRUCTURED SYSTEMS

DOE Grant No. DE-FG02-01ER15213

Mark I. Stockman, PI

Department of Physics and Astronomy, Georgia State University, Atlanta, GA 30303

E-mail: mstockman@gsu.edu, URL: <http://www.phy-astr.gsu.edu/stockman>

Current Year Grant Period of 2014-2015 (Publications 2013-2015)

1 Program Scope

The program is aimed at theoretical investigations of a wide range of phenomena induced by ultrafast laser-light excitation of nanostructured or nanosize systems, in particular, metal/semiconductor/dielectric nanocomposites and nanoclusters. Among the primary phenomena are processes of energy transformation, generation, transfer, and localization on the nanoscale and coherent control of such phenomena.

2 Recent Progress and Publications

Publications resulting from the grant during the period of 2013-2015 are: [1-21]. During the current grant period of 2014-2015, the following articles with this DOE support have been published [10-13]. The following articles received, as acknowledged, supplementary support of this grant during 2014-2015 [14, 15, 17-21]. Below we highlight selected articles that we consider most significant.

2.1 Strong-Field and Attosecond Physics in Solids [1]

In this article, we consider the status of strong-field and attosecond processes in bulk transparent solids near the Keldysh tunneling limit. For high enough fields and low-frequency excitations, the optical and electronic properties of dielectrics can be transiently and reversibly (adiabatically) modified within the applied pulse. One of the phenomena considered is high harmonic generation (HHG) from solids. We conclude that the solid-state HHG is significantly different from that in gases due to structural periodicity inherent in crystals. One of the consequences is that the cutoff harmonic frequency is linearly proportional to the field, instead of quadratic dependence in gases. This can be interpreted as a result of adiabatic Wannier-Stark localization and Bloch oscillations of electrons in the presence of the strong field. Other class of the considered phenomena is reversible semi-metallization of dielectric in the strong fields, which causes appearance of ultrafast electrical currents controlled by the carrier-envelope phase of the pulse.

2.2 Strong-Field Perspective on High-Harmonic Radiation from Bulk Solids [2]

In this article, mechanisms of HHG from crystals are described by treating the electric field of a laser as a quasistatic strong field. Under the quasistatic electric field, electrons in periodic potentials form dressed states, known as Wannier-Stark states. The energy differences between the dressed states, which is the Bloch frequency $\omega_B = eaF/\hbar$, where e is unit charge, a is lattice constant, and F is the electric field, determine the frequencies of the radiation. The radiation yield is determined by the magnitudes of the interband and intraband current matrix elements between the dressed states. The generation of attosecond pulses from solids is predicted. Ramifications for strong-field physics are discussed. In particular, HHG from solids may provide a pathway to creation of a nanosource of VUV and XUV radiation with pronounced application potential.

2.3 Graphene in Ultrafast and Superstrong Laser Fields [3]

For graphene interacting with a few-fs intense optical pulse, we predict unique and rich behavior dramatically different from three-dimensional solids. Quantum electron dynamics is shown to be coherent but highly nonadiabatic and effectively irreversible due to strong dephasing. This dephasing is due to the absence of the bandgap – graphene is a semimetal. Electron distribution in reciprocal space exhibits hot spots at the Dirac points and oscillations whose period is determined by nonlocality of electron response and whose number is proportional to the field amplitude. The optical pulse causes net charge transfer in the plane of graphene in the direction of the instantaneous field maximum at relatively low fields and in the opposite direction at high fields. This behavior of graphene is related to peculiarities of the Wannier-Stark states of electrons in strong fields [5]. The phenomena described in this article [3] promise ultrafast optoelectronic applications with petahertz bandwidth.

2.4 Ultrafast Field Control of Symmetry, Reciprocity, and Reversibility in Buckled Graphene-Like Materials [9]

In this article, we theoretically show that buckled two-dimensional graphene-like materials (silicene and germanene) subjected to a femtosecond strong optical pulse can be controlled by the optical field component normal to their plane. In such strong fields, these materials are predicted to exhibit nonreciprocal reflection, optical rectification, and generation of electric currents both parallel and normal to the in-plane field direction. Reversibility of the conduction band population is also field- and carrier-envelope phase controllable. There is a net charge transfer along the material plane that is also dependent on the normal field component. Thus a graphene-like buckled material behaves analogously to a field-effect transistor controlled and driven by the electric field of light with subcycle (femtosecond) speed.

3 Directions of Work for the Next Period

We will develop the present success in the optics of ultrastrong and ultrafast fields on the nanoscale. We will extend the existing theory to other dielectrics, semimetals, and metals, in particular sapphire, alkali and alkali-earth fluorides, silicene, and germanine. We will invoke more realistic models for the crystal structure of the materials involved, in particular using tight-binding model with experimentally known geometry of the unit cell and pseudopotential model. We will extend theory to describe photoelectron emission caused by the strong ultrashort pulses and probe attosecond XUV pulses in graphene. We will extend theory to describe generation of high harmonics in solids in strong ultrafast optical fields of nontrivial polarization structure. In ultrafast active plasmonics, we will study properties of the spaser with optical pumping as ultrabright label for biomedical diagnostics and laser therapy. We will extend our theory to ultrafast processes and spasing in topological insulators

4 References

1. D. Li and M. I. Stockman, *Electric Spaser in the Extreme Quantum Limit*, Phys. Rev. Lett. **110**, 106803-1-5 (2013).
2. A. Schiffrin, T. Paasch-Colberg, N. Karpowicz, V. Apalkov, D. Gerster, S. Muhlbrandt, M. Korbman, J. Reichert, M. Schultze, S. Holzner, J. V. Barth, R. Kienberger, R. Ernstorfer, V. S. Yakovlev, M. I. Stockman, and F. Krausz, *Optical-Field-Induced Current in Dielectrics*, Nature **493**, 70-74 (2013).
3. M. Schultze, E. M. Bothschafter, A. Sommer, S. Holzner, W. Schweinberger, M. Fiess, M. Hofstetter, R. Kienberger, V. Apalkov, V. S. Yakovlev, M. I. Stockman, and F. Krausz, *Controlling Dielectrics with the Electric Field of Light*, Nature **493**, 75-78 (2013).
4. M. I. Stockman, *Spaser, Plasmonic Amplification, and Loss Compensation*, in *Active Plasmonics and Tuneable Plasmonic Metamaterials*, edited by A. V. Zayats and S. Maier (John Wiley and Sons, Hoboken, NJ, 2013).

5. V. Apalkov and M. I. Stockman, *Metal Nanofilm in Strong Ultrafast Optical Fields*, Phys. Rev. B **88**, 2454381-7 (2013).
6. A. Giugni, B. Torre, A. Toma, M. Francardi, M. Malerba, A. Alabastri, R. Proietti Zaccaria, M. I. Stockman, and E. Di Fabrizio, *Hot-Electron Nanoscopy Using Adiabatic Compression of Surface Plasmons*, Nat. Nano **8**, 845-852 (2013).
7. H. K. Kelardeh, V. Apalkov, and M. I. Stockman, *Interaction of Graphene Monolayer with Ultrashort Laser Pulse*, arXiv:1401.5786 [cond-mat.mes-hall], 1-11 (2014).
8. M. I. Stockman, *Nanoplasmonics: From Present into Future*, in *Plasmonics: Theory and Applications*, edited by T. V. Shahbazyan and M. I. Stockman (Springer, Dordrecht, Heidelberg, New York, London, 2013), Vol. 15, p. 1-101.
9. V. Apalkov and M. I. Stockman, *Metal Nanofilm in Strong Ultrafast Optical Fields*, Phys. Rev. B **88**, 245438-1-7 (2013).
10. S. Ghimire, G. Ndabashimiye, A. D. DiChiara, E. Sistrunk, M. I. Stockman, P. Agostini, L. F. DiMauro, and D. A. Reis, *Strong-Field and Attosecond Physics in Solids*, Journal of Physics B: Atomic, Molecular and Optical Physics **47**, 204030-1-10 (2014).
11. T. Higuchi, M. I. Stockman, and P. Hommelhoff, *Strong-Field Perspective on High-Harmonic Radiation from Bulk Solids*, Phys. Rev. Lett. **113**, 213901-1-5 (2014).
12. H. K. Kelardeh, V. Apalkov, and M. I. Stockman, *Graphene in Ultrafast and Superstrong Laser Fields*, Phys. Rev. B **91**, 0454391-8 (2015).
13. V. S. Yakovlev, S. Y. Kruchinin, T. Paasch-Colberg, M. I. Stockman, and F. Krausz, *Ultrafast Control of Strong-Field Electron Dynamics in Solids* arXiv:1502.02180, 1-21 (2015).
14. H. K. Kelardeh, V. Apalkov, and M. I. Stockman, *Wannier-Stark States of Graphene in Strong Electric Field*, Phys. Rev. B **90**, 085313-1-11 (2014).
15. F. Krausz and M. I. Stockman, *Attosecond Metrology: From Electron Capture to Future Signal Processing*, Nat. Phot. **8**, 205-213 (2014).
16. V. Apalkov and M. I. Stockman, *Proposed Graphene Nanospaser*, Light Sci. Appl. **3**, e191-1-6 (2014).
17. Y.-J. Lu, C.-Y. Wang, J. Kim, H.-Y. Chen, M.-Y. Lu, Y.-C. Chen, W.-H. Chang, L.-J. Chen, M. I. Stockman, C.-K. Shih, and S. Gwo, *All-Color Plasmonic Nanolasers with Ultralow Thresholds: Autotuning Mechanism for Single-Mode Lasing*, Nano Lett. **14**, 4381-4388 (2014).
18. E. I. Galanzha, R. Weingold, D. A. Nedosekin, M. Sarimollaoglu, A. S. Kuchyanov, R. G. Parkhomenko, A. I. Plekhanov, M. I. Stockman, and V. P. Zharov, *Spaser as Novel Versatile Biomedical Tool*, arXiv:1501.00342, 1-33 (2015).
19. H. K. Kelardeh, V. Apalkov, and M. I. Stockman, *Ultrafast Field Control of Symmetry, Reciprocity, and Reversibility in Buckled Graphene-Like Materials*, Phys. Rev. B **92**, 045413-1-9 (2015).
20. M. I. Stockman, *Nanoplasmonics: Fundamentals and Applications*, in *Nano-Structures for Optics and Photonics*, edited by B. diBartolo and e. al. (Springer Netherlands, 2015).
21. M. I. Stockman, *Quantum Nanoplasmonics*, in *Photonics, Volume II: Scientific Foundations, Technology and Applications*, edited by D. L. Andrews (John Wiley & Sons, Inc., Hoboken, NJ, USA. , 2015), p. 85-132.

Page is intentionally blank.

Laser-Produced Coherent X-Ray Sources

Donald Umstadter

Physics and Astronomy Department

501 Building Rm 38, University of Nebraska, Lincoln, NE 68588-0207

donald.umstadter@unl.edu

Program Scope

X-ray synchrotrons and x-ray free-electron lasers have proven to be transformational technologies for physical and biological sciences. As part of this project, we developed a new type of x-ray source, one which—by virtue of its unique characteristics—may have similar transformational potential. Not only does its x-ray peak brightness and photon energy rival that of 3rd generation x-ray synchrotrons, but its femtosecond x-ray pulse duration is comparable to x-ray free-electron lasers. Moreover, the device is small enough to fit in a university laboratory.

The new light source is based on inverse Compton back-scattering (ICS), driven by two intense light pulses, each of which is amplified by a single high-power laser system. One laser pulse rapidly accelerates electrons (~ 3 GeV/cm) by means of the laser-wakefield mechanism; and the other laser pulse backscatters from the relativistic electrons. The scattered light is relativistically Doppler upshifted to high photon energy. We have demonstrated that these x-ray beams have several other unique features: narrow spectral bandwidth ($\Delta E/E \sim 50\%$), large energy-tuning range ($50 \text{ keV} \leq h\nu \leq 10 \text{ MeV}$), and small angular divergence (10-mrad) [Powers et al (2014)].

These features have advantages for x-ray science in general, and for the study of ultrafast phenomena in particular. An exceptionally large x-ray-energy tuning range can facilitate the probing of almost any element's inner-shell atomic structure. Femtosecond x-ray pulse duration, coupled to high photon energy, can enable ultrafast time-resolved studies with atomic-scale spatial and temporal resolutions. Synchronization with ultra-high-intensity laser light pulses ($\leq 10^{22} \text{ W/cm}^2$, $a_0 \sim 100$) can merge ultrafast science with ultra-high-field science.

Near-term objectives of this project include: (i) reduction of the x-ray spectral width, (ii) measurement of the x-ray pulse duration (inferred to be < 10 fs), and (iii) demonstration of an x-ray pump-probe capability.

Recent Progress

High peak power laser system

The all-solid-state DIODES laser is based on the technique of chirped-pulse amplification, a broadband amplification medium (titanium sapphire), and an oscillator with Kerr-lens mode-locking. For the experiments described here, 3-J, 35-fs, 805-nm laser pulses were produced at 10-Hz repetition rate [Liu et al. (2013)].

Recently, the laser system was modified to produce two independently controllable laser pulses, one each from two separate grating pulse compressors (as shown in Figure 1, left). The ability to use two laser pulses with independently variable parameters allows for independent optimization of both the electron acceleration and ICS, which have very different parameter requirements. For instance, second harmonic generation of the scattering laser beam, as shown in Figure 1, right [Zhao et al. (2014)], allowed us to reach an x-ray energy of 9 MeV [Liu et al. (2014)], which—by virtue of exceeding the giant dipole resonance—is sufficient for photo-nuclear active interrogation [Silano et al. (2013)] and shielded radiography [Banerjee et al. (2015)]. The production of 9-MeV x-ray photons with electrons of the same energy as used previously to produce 4.5 MeV x-rays would not have been possible without the use of phase correction of the second harmonic laser beam (as shown in Figure 1, right).

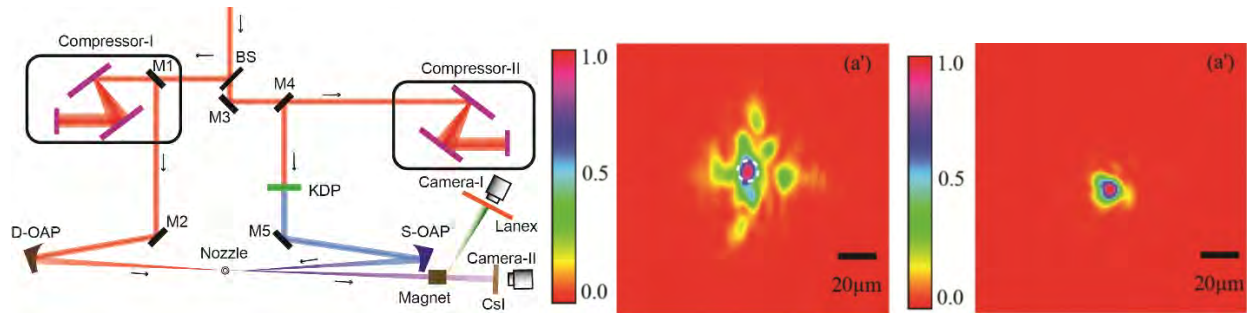


FIGURE 1: LEFT: A NOVEL LASER DESIGN WITH TWO INDEPENDENTLY ADJUSTABLE PULSE COMPRESSORS TO CREATE TWO INDEPENDENTLY ADJUSTABLE DRIVE LASER PULSES ALLOWS DIFFERENT PARAMETER OPTIMIZATION FOR ELECTRON ACCELERATION AND COMPTON SCATTERING. MIDDLE AND RIGHT: IMPROVEMENT OF SECOND-HARMONIC-GENERATED FOCUS. MIDDLE: UNCORRECTED FOCAL SPOT OF SECOND HARMONIC LIGHT (400 NM). THE PERCENTAGE ENERGY ENCLOSED IN A 10- μm FOCAL AREA IS 10.7%. FAR RIGHT: PHASE-CORRECTED FOCAL SPOT OF SECOND HARMONIC LIGHT (400 NM). THE PERCENTAGE ENERGY ENCLOSED IN A 10- μm FOCAL AREA IS 33.4%.

Laser wakefield electron accelerator

Since the x-ray beam parameters are directly dependent on the electron beam parameters, in order to generate narrow-bandwidth and tunable x-ray beams, it is necessary to generate electron beams with the same characteristics. To accomplish this, we implemented a novel dual-jet accelerator design, which allowed for independent optimization and control of electron injection and acceleration [Golovin et al. (2015)], as shown in Figure 2.

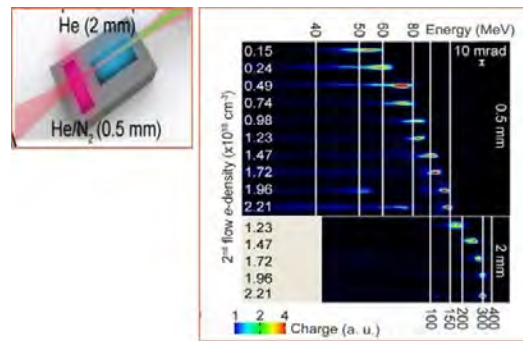


FIGURE 2: DUAL JET DESIGN FOR INDEPENDENT OPTIMIZATION AND CONTROL OF ELECTRON INJECTION AND ACCELERATION (LEFT). SPECTRA OF TUNABLE AND NARROW-BANDWIDTH ELECTRON BEAMS (RIGHT).

X-ray source based on inverse Compton scattering of laser light with laser-wakefield-accelerated electrons

In experiments conducted early in the project, two separate counter-propagating laser beams are generated from a single beam by means of an optical beam splitter. One laser beam (the scattering beam) is spatially overlapped with the electron bunch that is accelerated by the other laser beam (the drive beam). The scattering interaction occurs in vacuum just downstream from the electron accelerator. In this case, a well-collimated (10-mrad divergence angle) and high photon energy (4 MeV) x-ray beam is produced [Chen et al. (2013)].

In subsequent experiments, the monoenergetic laser-accelerated electron beams from Figure 2 were used to produce an x-ray pulse with peaked photon-number spectral density [Powers et al. (2014)]. Additionally, the x-ray photon energy was tuned over an unprecedentedly large range, extending more than an order of magnitude, from 50 keV to 1 MeV. This is accomplished by tuning the energy of the electron beam energy (from 50 MeV to 300 MeV), as in Figure 2. These results represent the first demonstration of any type of

all-laser-driven hard x-ray source with a peaked photon-number spectral density. It also demonstrated the widest tuning range of an x-ray source of any type.

Spectroscopic imaging of the x-ray beam

In the most recent experiments, the same peaked x-ray spectrum was measured by a different, more versatile and direct method. Whereas our prior x-ray spectral measurements were based on the Ross filter technique [Powers et al. (2014)], which has quite a limited range of utility, we have recently used instead single-photon counting spectroscopy. Figure 3 (a) shows the dispersed image of the electron beam used to obtain the electron spectrum [Figure 3 (b)]. The electron beam was quasi-monoenergetic, peaked at 60 ± 1 MeV and with $10 \pm 1\%$ (FWHM) spread and 2.4 ± 0.4 pC charge. The image of the x-ray beam on a CdTe detector for this shot is shown in Figure 3 (c). The pulse height information is converted to energy using the measured response function of the detector. The resulting x-ray spectrum is shown in Figure 3 (d) (red curve). The black curve in Figure 3(d) is the x-ray spectrum calculated for the measured electron spectrum. The x-ray spectrum was peaked at 85 ± 1 keV with $24 \pm 2\%$ spread (FWHM, averaged over 6-mrad cone), which is comparable to the x-ray bandwidth from conventional RF-LINAC-based Compton sources, and the narrowest yet reported from an all-laser ICS x-rays.

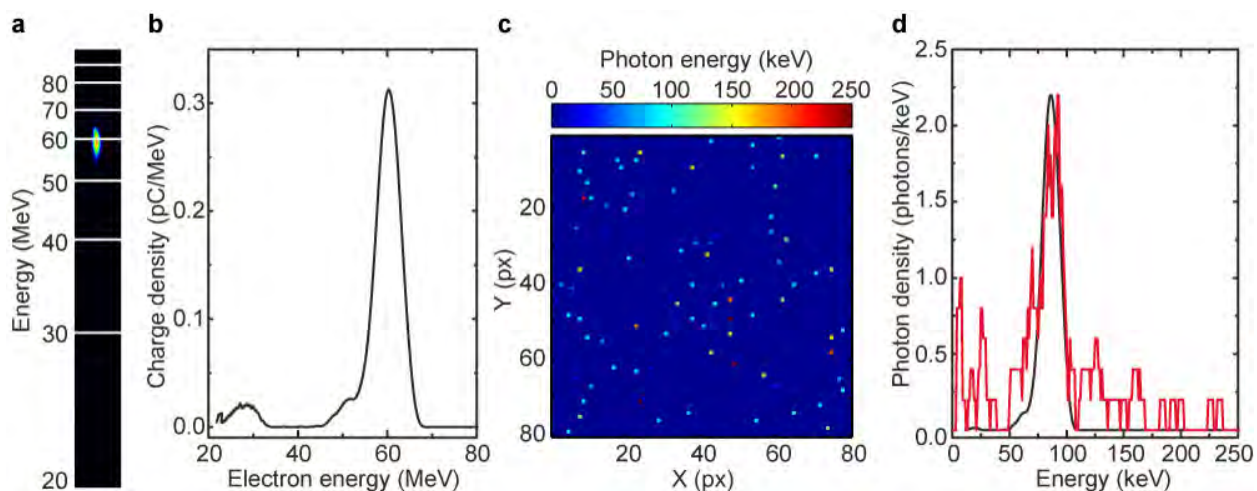


FIGURE 3. MEASURED ELECTRON AND X-RAY SPECTRUM OBTAINED USING MAGNETIC SPECTROSCOPY AND SPECTROSCOPIC X-RAY IMAGING. (A) LANEX IMAGE OF THE DISPERSED ELECTRON BEAM. (B) RECONSTRUCTED ELECTRON BEAM SPECTRUM BASED ON THE RESPONSE FUNCTION OF THE MAGNETIC SPECTROMETER. (C) MEASURED X-RAY SIGNAL ON THE CDTE DETECTOR WITH CHARGE SHARING CORRECTION. EACH DOT REPRESENTS A SINGLE PHOTON EVENT. (D) X-RAY SPECTRUM, MEASURED WITH THE CDTE DETECTOR (RED) AND SIMULATED SPECTRUM BASED ON THE ELECTRON BEAM SPECTRUM (BLACK).

Future Plans

We are increasing the number of x-ray photons generated per pulse by three orders-of-magnitude by increasing the field of the scattering laser light pulse from $a_0 \sim 0.7$ to $a_0 \sim 15$. This increased x-ray flux will enable femtosecond time-resolved x-ray pump-probe studies of ultrafast phenomena.

Publications supported in part by this DOE grant (published within last three years)

1. D. Umstadter, "Hard x-rays from a tabletop all-laser-driven synchrotron light source," Proc. SPIE **9590**, Advances in Laboratory-based X-Ray Sources, Optics, and Applications IV, 959002 (August 26, 2015); doi:10.1117/12.2196369.

2. D. Umstadter, "Narrow bandwidth and tunable hard x-rays from an all-laser-driven Thomson light source," Proc. SPIE **9509**, Relativistic Plasma Waves and Particle Beams as Coherent and Incoherent Radiation Sources, 95090A (May 12, 2015); doi:10.1117/12.2182696.
3. S. Banerjee, G. Golovin, P. Zhang et al., "Photonuclear and radiography applications of narrowband, multi-MeV all-optical Thomson x-ray source," Proc. SPIE **9515**, Research Using Extreme Light: Entering New Frontiers with Petawatt-Class Lasers II, 95151C (May 1, 2015); doi:10.1117/12.2183401.
4. G. Golovin, S. Chen, N. Powers et al., "Independent control of laser-wakefield--accelerated electron-beam parameters," Proc. SPIE **9514**, Laser Acceleration of Electrons, Protons, and Ions III; and Medical Applications of Laser-Generated Beams of Particles III, 951405 (May 14, 2015); doi:10.1117/12.2182707.
5. G. Golovin, S. Banerjee, J. Zhang et al., "Tomographic imaging of non-symmetric multi-component tailored supersonic flows from structured gas nozzles," Applied Optics **54**, 3491-3497 (2015).
6. S. Banerjee, S. Chen, N. Powers et al., "Compact source of narrowband and tunable x-rays for radiography," Nuclear Instruments and Methods in Physics Research Section B **350**, 106-111 (2015).
7. D. Umstadter, "All-laser-driven Thomson x-ray sources," Contemporary Physics; doi: 10.1080/00107514.2015.1023519 (2015).
8. G. Golovin, S. Chen, N. Powers et al., "Tunable monoenergetic electron beams from independently controllable laser-wakefield acceleration and injection," Phys. Rev. STAB **18**, 011301 (2015).
9. B. Zhao, J. Zhang, S. Chen, et al., "Wavefront-correction for nearly diffraction-limited focusing of dual-color laser beams to high intensities," Optics Express **22**, 22, 26947-26955 (2014).
10. C. Liu, G. Golovin, S. Chen et al., "Generation of 9-MeV γ -rays by all-laser-driven Compton scattering with second-harmonic laser light," Opt. Lett. **39**, 14, 4132-4135 (2014).
11. C. Liu, J. Zhang, S. Chen et al., "Adaptive-feedback spectral-phase control for interactions with transform-limited ultra-short high-power laser pulses," Opt. Lett. **39**, 1, 80-83 (2014).
12. N. D. Powers, I. Ghebregziabher, G. Golovin et al., "Tunable and quasi-monoenergetic x-rays from a laser-driven Compton light source," Nat. Photonics **8**, 28-31 (2014).
13. S. Chen, N. D. Powers, I. Ghebregziabher et al., "MeV-energy x-rays from inverse Compton scattering with laser-wakefield accelerated electrons," Phys. Rev. Lett. **110**, 155003 (2013).
14. S. Banerjee, S. Y. Kalmykov, N. D. Powers et al., "Stable, tunable, quasi-monoenergetic electron beams produced in a laser wakefield near the threshold for self-injection," Phys. Rev. ST Accel. Beams **16**, 031302 (2013).
15. I. Ghebregziabher, B. A. Shadwick and D. Umstadter, "Spectral bandwidth reduction of Thomson scattered light by pulse chirping," Rev. ST Accel. Beams **16**, 030705 (2013).
16. J. Silano S. Clarke, S. Pozzi et al., "Selective activation with all-laser-driven Thomson γ -rays," Proceedings of the 2013 *IEEE* International Conference on Technologies for Homeland Security, 429 - 434 (Waltham, MA, 2013).
17. S. Banerjee, N. D. Powers, V. Ramanathan et al., "Generation of tunable, 100-800 MeV quasi-monoenergetic electron beams from a laser-wakefield accelerator in the blowout regime," Phys. Plasmas **19**, 056703 (2012).
18. B. M. Cowan, S. Y. Kalmykov, A. Beck et al., "Computationally efficient methods for modeling laser wakefield acceleration in the blowout regime," J. Plasma Phys. **78**, 469 (2012).

Combining High Level *Ab Initio* Calculations with Laser Control of Molecular Dynamics

Thomas Weinacht
Department of Physics and Astronomy
Stony Brook University
Stony Brook, NY
thomas.weinacht@stonybrook.edu

Spiridoula Matsika
Department of Chemistry
Temple University
Philadelphia, PA
smatsika@temple.edu

1 Program Scope

We use intense, shaped, ultrafast laser pulses to follow and control molecular dynamics and high level *ab initio* calculations to interpret the dynamics and guide the control.

2 Recent Progress

2.1 Photoelectron Spectrum and Dynamics of the Uracil Cation

A focus of the theoretical part of this project for the past year has been understanding better dynamics of radical cations formed during strong field ionization, and how they proceed to fragmentation. Ionization processes can lead to the formation of radical cations with population in several ionic states. An important question is whether fragmentation occurs on the excited ionic states or very fast relaxation to the ground ionic state occurs first followed by fragmentation.

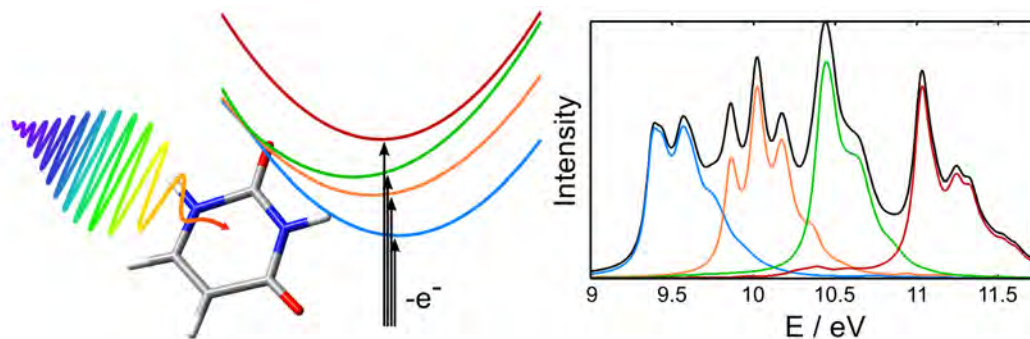


Figure 1: *The photoelectron spectrum of uracil is shown as calculated using MCTDH. The first four ionic states contribute to the spectrum up to 12 eV.*

The first approach we used to explore the above questions was multiconfigurational time-dependent Hartree (MCTDH) method. The photoelectron spectrum of uracil and the molecular dynamics of its radical cation were investigated using MCTDH. For this aim, the vibronic coupling model Hamiltonian was used including up to ten important a' modes. Moreover, to account for coupling through conical intersections between states of different symmetry in the system, coupling constants of two a'' modes had to be taken into account. The parameters used in the model were obtained by fitting to *ab initio* data obtained with extensive EOM-IP-CCSD calculations. The first four cationic states were investigated, which are either of A'' (hole in a π orbital) or A' (hole in a n_O orbital) symmetry. The results of the wavepacket propagations were used to calculate the corresponding photoelectron spectrum and compare to the experimental spectrum (see Figure 1). The MCTDH simulations reproduce the experimental spectrum well. The dynamics starting from the D2 and D3 ionic states show a fast relaxation to the cationic ground state often involving direct $D2 \rightarrow D0$ or $D3 \rightarrow D1$ transitions.

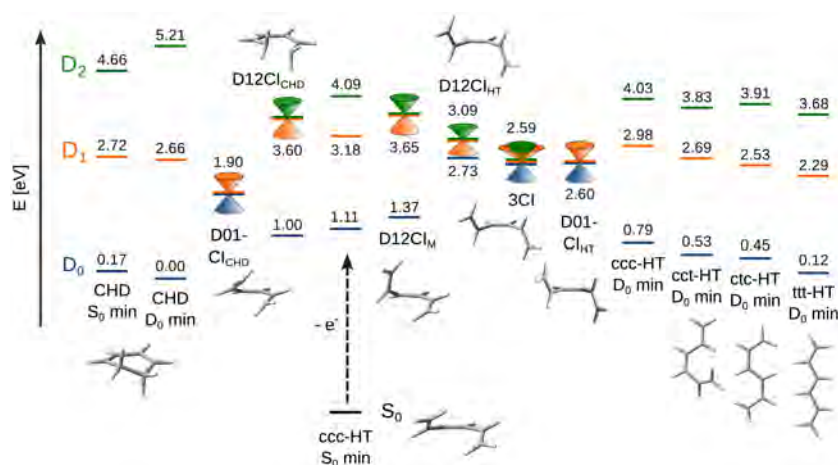


Figure 2: *Energies of the cationic states in the CHD-HT system at important geometries. All energies are given in eV at CASSCF(5,6)/cc-pVDZ level of theory relative to the energy of D_0 at its minimum. Geometries are optimized at the CASSCF level except the S_0 and D_0 minima which are optimized at the B3LYP level.*

2.2 Surface hopping investigation of the relaxation dynamics in radical cations

In this study we examined the dynamics of three radical cations starting from an excited ionic state using trajectory surface hopping dynamics in combination with multiconfigurational electronic structure methods. The competition between relaxation to the ground state and fragmentation was examined. The potential energy surfaces of the cations can be complicated involving multiple conical intersections, as is illustrated in Figure 2 for the cyclohexadiene/hexatriene system. The results on cyclohexadiene, hexatriene and uracil indicate that relaxation to the ground ionic state is very fast in these systems, while fragmentation before relaxation is rare. Ultrafast relaxation is facilitated by the close proximity of electronic states and the presence of two- and three-state conical intersections. Examining the properties of the systems in the Franck-Condon (FC) region can give some insight into the subsequent dynamics.

2.3 Velocity map imaging studies of molecular cation dynamics

An important aspect of our project has been the dynamics of molecular cations in strong laser fields. As discussed above, we have devoted considerable effort to calculating the dynamics of molecules in excited cationic states, with an aim toward understanding how relaxation competes with dissociation. As part of our experimental efforts along these lines, we made detailed measurements of dissociative ionization of cyclohexadiene. The original idea was to use our coincidence velocity map imaging measurements to establish which ionic states are populated via strong field ionization, and then study the kinetic energy release (KER) of the fragments in conjunction with theory to see whether molecules ionized to excited states dissociated before internal conversion.

We specifically looked to fragments ejected with nonzero kinetic energy to see evidence of dissociation on the ground state after internal conversion from an excited state of the cation. The most striking feature we found in our momentum resolved fragment ion measurements was evidence of significant double ionization at intensities where we did not expect to see any. We found peaks in the fragment ion KER spectrum which always corresponded to a total dissociation energy of about 5 eV when considering two body dissociation in the axial recoil approximation. This energy corresponds to the kinetic energy one would expect for the dissociation of a doubly charged cation with an initial separation of the ring diameter.

In order to test our hypothesis that these high energy fragments were a result of double ionization, we devised a coincidence measurement, in which we measured the momentum resolved spectrum of fragments measured in coincidence from a single molecule. In other words, we reduced the gas

density such that each laser shot on average ionized less than one molecule. We then recorded the spectrum of fragments for each laser shot whose vector momentum added to zero. The spectrum measured in this fashion corresponds to the spectrum for double ionization, and overlapped very well with the 5 eV peak which we found in the non-coincidence measurements.

We feel that these coincidence measurements conclusively establish their origin as being double ionization, and we are currently in the process of interrogating the mechanism for this double ionization at low intensities. Measurements as a function of pulse duration indicate that there is roughly as much double ionization for a 10 fs pulse as a 30 fs pulse with comparable peak intensity. Our current working hypothesis is that the double ionization is due to enhanced ionization. While enhanced ionization in diatomic molecules typically occurs away from the Franck Condon region at bond lengths of roughly 6 atomic units ($\sim 3\text{\AA}$), the case of ring molecules such as cyclohexadiene is interesting because already at the equilibrium geometry, the ring diameter roughly corresponds to this distance.

2.4 UV pump VUV probe measurements of excited state dynamics

We have been working over the past two years to develop a femtosecond VUV source as a probe for following excited state dynamics such as internal conversion and dissociation. Our aim was to develop a femtosecond probe pulse with a photon energy of 8 eV ($\lambda_0 = 160$ nm), since this is in many ways the perfect probe of excited state dynamics: it is capable of ionizing from almost anywhere in any molecular excited state, but not capable of ionizing ground state molecules, ensuring a probe which can follow the evolution of the wave packet throughout the excited state surface, without having any background ionization of ground state molecules. We demonstrated the generation of VUV pulses about a year ago, with sufficient pulse energy to produce several ions per laser shot when ionizing a special sample chosen to have an ionization potential below the photon energy. Very recently we have been able to carry out first pump probe experiments, using a UV pump ($\lambda_0 = 260$ nm), and a VUV probe. Figure 3 illustrates how the UV/VUV experiments can probe excited state dynamics and also shows some of our initial pump probe results for cyclohexadiene. While the time resolution is still quite poor (with an impulse response function of 300-400 fs) already the measurements are quite interesting as we see a marked asymmetry in the yields for large positive and negative delays, despite the fact that cyclohexadiene is understood to undergo rapid internal conversion after excitation in the UV, with 100 % of the excited state population making it down to the ground state in less than 200 fs. We are currently working on improving the time resolution by an order of magnitude by reducing the dispersion in the pump and probe paths. Additionally, we are modifying our apparatus to handle solid samples (such as DNA/RNA bases), and within the next year or so, we plan on adding velocity map imaging capability to the detection.

3 Future Plans

We have several goals for the immediate future:

1. We plan on using our UV pump VUV probe apparatus to study internal conversion and isomerization dynamics in several molecules of interest, including uracil, cytosine, adenine and cyclohexadiene. We will also use this apparatus to compare strong and weak field ionization of molecular excited states to test many basic aspects of strong field ionization.
2. We will follow up calculations of excited cationic dynamics with velocity map imaging studies of excited molecular cations produced via strong field ionization. A molecule of particular interest is hexatriene, for which extensive calculations have been carried out, but which needs to be produced in our lab as it is not commercially available. We plan on producing it from cyclohexadiene using deep UV laser pulses in our laboratory.

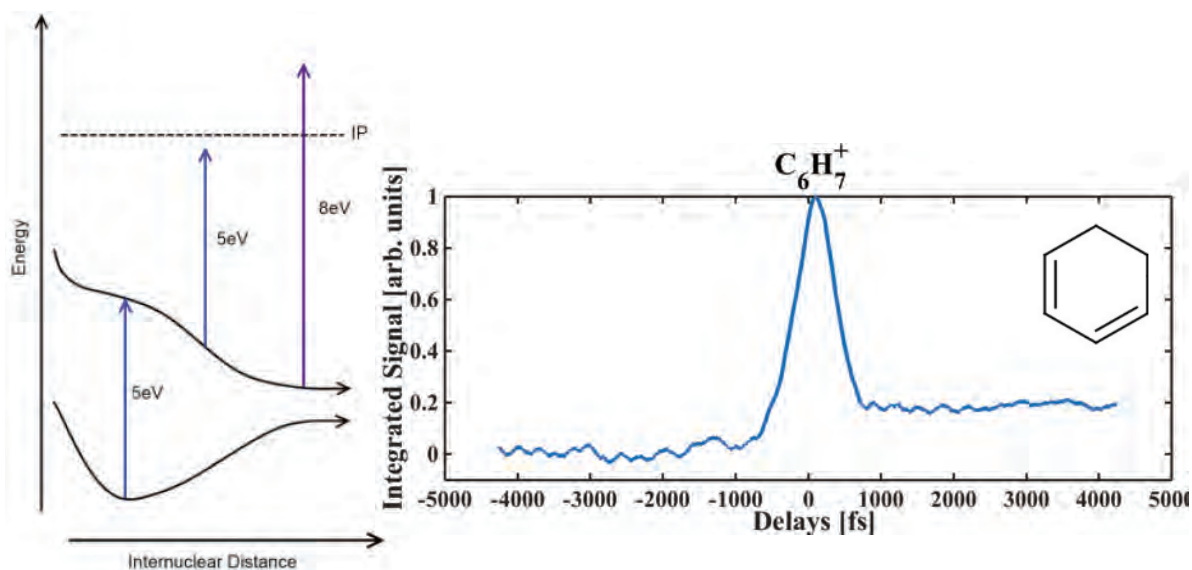


Figure 3: A cartoon illustrating UV pump VUV probe experiments (left). Initial measurements for cyclohexadiene excited showing the ion yield as a function of pump probe delay.

3. We plan on completing our study of strong field double ionization of cyclohexadiene. In particular, we would like to test the hypothesis that the double ionization is driven by enhanced ionization of the singly ionized cation.

4 Publications of DOE Sponsored Research

- “Field Dressed Orbitals in Strong Field Molecular Ionization”, Robert Siemering, Oumarou Njoya, Thomas Weinacht, Regina de Vivie-Riedle, *Phys. Rev. Lett.*, submitted (2015)
- “Surface hopping investigation of the relaxation dynamics in radical cations”, Mariana Assmann, Thomas Weinacht, and Spiridoula Matsika, *J. Chem. Phys.*, submitted (2015)
- “Photoelectron spectrum and dynamics of the uracil cation”, Mariana Assmann, Horst Köppel and Spiridoula Matsika, *J. Phys. Chem. A*, **119**, 866-875, (2015)
- “Modified Nucleobases”, S. Matsika, “Topics in Current Chemistry - Photoinduced Phenomena in Nucleic Acids” (DOI:10.1007/128_2014_532), **355**, 209-243, (2015)

List of Participants

Page is intentionally blank.

Andreas Becker
JILA /University of Colorado
440 UCB
Boulder, CO 80309-0440
Phone:

Ali Belkacem
Lawrence Berkeley National Laboratory
1 Cyclotron road
Berkeley, CA 94720
Phone: 510-486-6382

Itzik Ben-Itzhak
J.R. Macdonald Laboratory, KSU
116 Cardwell Hall, Physics Department
Manhattan, KS 66506
Phone: 785-532-1636

Nora Berrah
University of Connecticut
Physics Department
Storrs, CT 6268
Phone: 860-486-0639

Christoph Bostedt
Argonne National Laboratory
9700 South Cass Avenue
Lemont, IL 60439
Phone: 630-252-1268

Philip Bucksbaum
SLAC National Accelerator Lab - PULSE
2575 Sand Hill Road
Menlo Park, CA 94025
Phone: 650-926-5337

Martin Centurion
University of Nebraska
Jorgensen Hall, 855 North 16th Street
Lincoln, NE 68588
Phone: 402-472-5810

Shih-I Chu
University of Kansas
Dept. of Chemistry
Lawrence, KS 66045
Phone:

Robin Cote
University of Connecticut
2152 Hillside Road
Storrs, CT 6269
Phone: 860-486-4912

Scott Crooker
Los Alamos National Laboratory
Mail Stop E536
Los Alamos, NM 87545
Phone: 505-665-7595

James Cryan
SLAC National Accelerator Laboratory
2575 Sand Hill Rd.
Menlo Park, CA 94025
Phone: 650-926-3290

Steven Cundiff
University of Michigan
450 Church St.
Ann Arbor, MI 48109
Phone: 734-647-3343

Marcos Dantus
Michigan State University
578 S. Shaw Lane, Room 58
East Lansing, MI 48824
Phone: 517-355-9715

Louis DiMauro
The Ohio State University
1910 West Woodruff Avenue
Columbus, OH 43210
Phone: 614-688-5726

Todd Ditmire
University of Texas, Austin
2515 Speedway Stop C1600
Austin, TX 78712
Phone: 512-471-3296

Gilles Doumy
Argonne National Laboratory
9700 S. Cass Ave.
Argonne, IL 60439
Phone: 630-252-2588

Robert Dunford
Argonne National Laboratory
9700 S. Cass Ave
Lemont, IL 60439
Phone: 630-252-4052

Joseph Eberly
University of Rochester
600 Wilson Blvd.
Rochester, NY 14627
Phone: 585-275-4351

Veit Elser
Cornell University
PSB 426
Ithaca, NY 14853
Phone: 607-255-2340

Brett Esry
J.R. Macdonald Laboratory, KSU
Dept. of Physics, 116 Cardwell Hall
Manhattan, KS 66506
Phone:

Roger Falcone
University of California, Berkeley
One Cyclotron Rd., Mailstop 80R0114
Berkeley, CA 94720
Phone: 510-486-6692

Jim Feagin
California State University, Fullerton
800 N State College Ave
Fullerton, CA 92834
Phone: 657-278-4827

Mette Gaarde
Louisiana State University
Department of Physics and Astronomy, LSU
Baton Rouge, LA 70803-4001
Phone: 225-578-0889

Kelly Gaffney
SLAC National Accelerator Laboratory
2575 San Hill Road
Menlo Park, CA 94025
Phone: 650-926-2382

Thomas Gallagher
University of Virginia
Department of Physics
Charlottesville, VA 22904
Phone: 434-924-6817

Oliver Gessner
Lawrence Berkeley National Laboratory
1 Cyclotron Rd
Berkeley, CA 94720
Phone: 510-486-6929

Shambhu Ghimire
SLAC National Accelerator Laboratory
2575 Sand Hill Rd
Menlo Park, CA 94306
Phone: 650-926-2071

Phillip Gould
University of Connecticut
Physics Dept. U-3046, 2152 Hillside Rd.
Storrs, CT 06269-3046
Phone: 860-486-2950

Chris Greene
Purdue University
525 Northwestern Ave
West Lafayette, IN 47906
Phone:

Markus Guehr
SLAC National Accelerator Laboratory
2575 Sand Hill Road
Menlo Park, CA 94025
Phone: 650-926-5550

Daniel Haxton
Lawrence Berkeley National Laboratory
PO Box 1579
El Cerrito, CA 94530
Phone: 510-495-2508

Tony Heinz
SLAC National Accelerator Laboratory
2575 Sand Hill Road
Menlo Park, CA 94025
Phone: 650-723-1810

Phay Ho
Argonne National Laboratory
9700 South Cass Ave
Lemont, IL 60439
Phone: 630-252-1257

Robert Jones
University of Virginia
Department of Physics, 382 McCormick Rd
Charlottesville, VA 22904-4714
Phone: 434-924-3088

Elliot Kanter
Argonne National Laboratory
9700 S. Cass Ave.
Argonne, IL 60439
Phone: 908-617-1622

Henry Kapteyn
JILA/University of Colorado
440 UCB
Boulder, CO 80309
Phone: 303-492-6763

Bertold Kraessig
Argonne National Laboratory
437 7th Avenue
La Grange, IL 60525
Phone: 708-482-3891

Jeffrey Krause
U.S. Department of Energy
19901 Germantown Rd.
Germantown, MD 20874
Phone: 301-903-5827

Vinod Kumarappan
James R. Macdonald Laboratory, KSU
328 Cardwell Hall
Manhattan, KS 66506
Phone: 785-532-3415

Allen Landers
Auburn University
206 Allison Lab
Auburn, AL 36849
Phone: 334-844-4048

Anh-Thu Le
Kansas State University
Department of Physics, 116 Cardwell Hall
Manhattan, KS 66506
Phone: 785-532-1635

Stephen Leone
LBNL/University of California
Dept of Chemistry
Berkeley, CA 94720
Phone: 510-643-5467

Raphael Levine
University of California, Los Angeles
Los Angeles, CA 90095
Phone: 310-206-0476

Wen Li
Wayne State University
5101 Cass ave.
Detroit, MI 48202
Phone: 313-577-8658

Chii-Dong Lin
Kansas State University
2101 Hillview Dr
Manhattan, KS 66502
Phone: 785-532-1617

Kenneth Lopata
Louisiana State University
742 Choppin Hall
Baton Rouge, LA 70808
Phone: 225-578-2063

Robert Lucchese
Texas A&M University
Department of Chemistry
College Station, TX 77843-3255
Phone: 979-845-0187

Steven Manson
Georgia State University
Dept. of Physics & Astronomy
Atlanta, GA 30303
Phone: 404-413-6046

Diane Marceau
U.S. Department of Energy
19901 Germantown Road
Germantown, MD 21702
Phone:

Todd Martinez
SLAC National Accelerator Laboratory
2575 Sand Hill Rd
Menlo Park, CA 94025
Phone: 650-417-4612

Spiridoula Matsika
Temple University
Department of Chemistry
Philadelphia, PA
Phone:

William McCurdy
Lawrence Berkeley National Laboratory
One Cyclotron Road
Berkeley, CA 94720
Phone: 510-486-4283

Terry Miller
Ohio State University
100 W. 18ths
Columbus, OH 43210
Phone: 614-292-2569

Alfred Z Msezane
Clark Atlanta University
223 James P. Brawley Drive SW
Atlanta, GA 30314
Phone: 404-880-8663

Shaul Mukamel
University of California, Irvine
1102 Natural Sciences II
Irvine, CA 92697-2025
Phone: 949-824-7600

Margaret Murnane
JILA/University of Colorado
440 UCB
Boulder, CO 80309
Phone: 303-492-6763

Keith Nelson
Massachusetts Institute of Technology
77 Massachusetts Ave., Room 6-235
Cambridge, MA 2139
Phone: 617-253-1423

Daniel Neumark
University of California, Berkeley
Department of Chemistry
Berkeley, CA 94720
Phone: 510-642-3502

Thomas Orlando
Georgia Institute of Technology
901 Atlantic Dr.
Atlanta, GA 30332
Phone: 404-894-4012

Abbas Ourmazd
University of Wisconsin, Milwaukee
3135 N Maryland Ave
Milwaukee, WI 53211
Phone: 414-229-2610

Enrique Parra
Air Force Office of Scientific Research
875 N. Randolph Street Suite 325
Arlington, VA 22203
Phone: 703-696-8571

Tanja Pietrass
U.S. Department of Energy
1000 Independence Ave
Washington, DC
Phone: 301-903-8165

Herschel Rabitz
Princeton University
Frick Chemistry Lab, Washington Road
Princeton, NJ 8544
Phone: 609-258-3917

David Reis
SLAC National Accelerator Laboratory
2575 Sand Hill Rd
Menlo Park, CA 94025
Phone: 650-926-4192

Francoise Remacle
University of Liege
Department of Chemistry
Liege, Belgium, 4000
Phone:

Thomas Rescigno
Lawrence Berkeley National Laboratory
1 Cyclotron Rd MS 2-100
Berkeley, CA 94720
Phone: 510-486-8652

Francis Robicheaux
Purdue University
525 Northwestern Avenue
West Lafayette, IN 47907
Phone: 765-494-3029

Jorge Rocca
Colorado State University
Electrical and Computer Engineering
Fort Collins, CO 80523
Phone: 970-491-8371

Daniel Rolles
JRML, Kansas State University
327 Cardwell Hall
Manhattan, KS 66506
Phone: 785-532-1615

Christoph Rose-Petruck
Brown University
324 Brook Str
Providence, RI 2912
Phone: 401-863-1533

Artem Rudenko
Kansas State University
116 Cardwell Hall
Manhattan, KS 66503
Phone: 785-532-4470

H. Bernhard Schlegel
Wayne State University
5101 Cass Ave.
Detroit, MI 48202
Phone: 313-577-2546

Robert Schoenlein
SLAC National Accelerator Laboratory
2575 Sand Hill Rd.
Menlo Park, CA 94025
Phone: 650-926-5155

Tamar Seideman
Northwestern University
2145 Sheridan Road
Evanston, IL 60208-3113
Phone: 847-467-4979

Gerald Seidler
University of Washington
3910 15th Ave. NE, Physics C121
Seattle, WA 98195-1560
Phone: 206-427-8045

Tom Settersten
U.S. Department of Energy
19901 Germantown Road, SC-22.1
Germantown, MD 20874
Phone: 301-903-8428

Daniel Slaughter
Lawrence Berkeley National Laboratory
1 Cyclotron Rd
Berkeley, CA 94720
Phone: 510-486-4847

Steve Southworth
Argonne National Laboratory
Bldg. 401
Lemont, IL 60439
Phone: 630-252-3894

Claudiu Stan
SLAC National Accelerator Laboratory
2575 Sand Hill Road
Menlo Park, CA 94025
Phone: 650-926-5306

Anthony F Starace
University of Nebraska, Lincoln
855 North 16th Street, 208 Jorgensen Hall
Lincoln, NE 68588-0299
Phone: 402-472-2795

Mark Stockman
Georgia State University
29 Peachtree Center Ave
Atlanta, GA 30303
Phone: 678-457-4739

Uwe Thumm
Kansas State University
116 Cardwell Hall
Manhattan, KS 66506
Phone:

Carlos A Trallero
James R. Macdonald Laboratory
116 Cardwell Hall
Manhattan, KS 66506
Phone: 785-532-0846

Donald Umstadter
University of Nebraska, Lincoln
501 Stadium Dr. Room 38
Lincoln, NE 68588
Phone: 402-472-8115

Thorsten Weber
Lawrence Berkeley National Laboratory
1 Cyclotron Road
Berkeley, CA 94720
Phone: 510-486-5588

Thomas Weinacht
Stony Brook University
Dept of Physics
Stony Brook, NY 11794-3800
Phone: 631-632-8163

Thomas Wolf
SLAC National Accelerator Laboratory
2575 Sand Hill Road
Menlo Park, CA 94025-7015
Phone: 650-926-2533

Linda Young
Argonne National Laboratory
9700 S. Cass Ave
Argonne, IL 60439
Phone: 630-252-8878

Page is intentionally blank.